

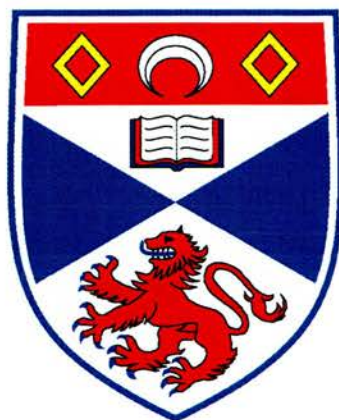
University of St Andrews



Full metadata for this thesis is available in
St Andrews Research Repository
at:

<http://research-repository.st-andrews.ac.uk/>

This thesis is protected by original copyright



A Study of Minimal Self-Replicating Systems

By

Julie M Quayle MChem (Hons)

A Thesis Presented for the Degree of

Doctor of Philosophy

in the

School of Chemistry

University of St Andrews

St Andrews

September 2002



The E260

(i) I, Julie Quayle, hereby certify that this thesis, which is approximately 72 000 words in length, has been written by me, that it is the record of work carried out by me and that it has not been submitted in any previous application for a higher degree.

Signature of candidate .

Date ..12.11.02

(ii) I was admitted as a research student in September 2000, and as a candidate for the degree of Doctor of Philosophy in September 2000; the higher study for which this is a record was carried out in the University of St Andrews between 2000 and 2002.

Signature of candidate ..

. Date ..12.11.02

(iii) I hereby certify that the candidate has fulfilled the conditions of the Resolution and Regulations appropriate for the degree of Doctor of Philosophy in the University of St Andrews and that the candidate is qualified to submit this thesis in application for that degree.

Signature of supervisor

.Date ..12 NOV 2002

In submitting this thesis to the University of St Andrews I understand that I am giving permission for it to be made available for use in accordance with the regulations of the University Library for the time being in force, subject to any copyright vested in the work not being affected thereby. I also understand that the title and abstract will be published, and that a copy of the work may be made and supplied to any *bona fide* library or research worker.

Signature of candidate ..

Date ..12.11.02

Synopsis

This thesis presents a detailed account of the design, synthesis and kinetic analysis of minimal self-replicating systems.

Chapter 1 – This chapter provides an introduction to the origins of self-replicating systems, and looks at their related effects of catalysis, intramolecularity and stereoselectivity. Self-replicating systems and their associated AB-complex systems are introduced. Literature examples of biomimetic and synthetic self-replicating systems are presented along with the associated recognition-mediated systems. The problems encountered in the literature of the design of self-replicating systems are reported and discussed.

Chapter 2 – This chapter describes the design and synthesis of a structurally simple self-replicating system. The design utilises the interaction between an amidopyridine unit and a carboxylic acid with a view to creating a system which autocatalyses the 1,3-dipolar cycloaddition reaction between an azide and a maleimide. The synthetic strategies and procedures that were employed are reported. The kinetic analysis of this system is reported and data interpretation discussed. Further study upon this system investigates the effect of temperature upon the self-replicating ability of the system.

Chapter 3 – This chapter provides an extensive investigation into a successful autocatalytic self-replicating system, which exploits the 1,3-dipolar cycloaddition between a nitron and a maleimide; with a view to providing a rationale of the necessary requirements for a successful self-replicating system. The investigation reveals the effects, upon the successful system, of the addition of substituents to affect the electronic and steric properties, as well as the effects of regiochemistry upon the efficiency and stereoselectivity of the system. Further studies are presented which investigate the effects of altering the design of some of the systems, which disrupt the self-replicating nature in favour of an AB-complex pathway. This work highlights the importance of molecular shape and template flexibility upon the efficiency of an autocatalytic self-replicating system. The effect of temperature upon some of the systems is also investigated and the change in efficiency and stereoselectivity reported.

Chapter 4 – This chapter also reports the design and synthesis of a structurally simple self-replicating system, utilising the experience gained from the previous two chapters. The aim of the investigation is to accelerate a 1,3-dipolar cycloaddition reaction between a nitron and

maleimide. The subsequent synthetic difficulties encountered have been reported and discussed, along with the full analysis and characterisation of the products obtained.

Chapter 5 – This chapter gives a summary of the general conclusions that can be drawn from the research presented within this thesis and highlights some of the possible future directions.

Chapter 6 – This chapter describes, in detail, the methodology employed to perform the all the kinetic studies upon the systems studied. Synthetic procedures for all the compounds presented within this thesis are given, along with full characterisation. This chapter also presents all the crystal data for the crystal structures presented.

References and Appendices are presented at the end of this thesis.

Acknowledgements

Firstly, I would like to thank my supervisor Dr Douglas Philp for all his help, support and guidance over the last three years. I wish you all the very best for your future career in St. Andrews and wherever else you may go.

I would also like to thank all the members of the Philp group, both past and present; Dr Vikki Allen, Dr Raphael Benes, Dr Patrizia Calcagno, Dr Paul Comina, (Dr) Rosalyne Cowie, Dr Lyndsey Grieg, Dr Rachel Hopper, Dr Sarah Howell, (Dr) Eleftherios Kassianidis, (Dr) Mairead Minto, Dr Russell Pearson, Dr PC Samantha Rigby, Dr Heidi Rowe and Dr Andrew Sinclair.

The work presented in this thesis relies heavily upon ^1H NMR spectroscopy. I would like to thank for their expertise, help and guidance Neil Spencer and Malcolm Tolley at the University of Birmingham for running my kinetic experiments and for their continued help and support when I moved to St. Andrews. I would also like to thank Melanja Smith at the University of St. Andrews for all her help, cheery disposition and teaching me to lock and shim Oscar and for making sure it was always better than “it’ll do”.

I would like to thank Peter Ashton, Nick May and Lianne Hill at the University of Birmingham and Caroline Horsburgh at the University of St. Andrews for running my mass spectra. I would also like to thank Sylvia Williamson at the University of St. Andrews for running my elemental analysis.

A huge thank you must go to Dr Alex Slawin at the university of St. Andrews for solving all the crystal structures presented in this thesis.

There are many people whom I want to mention who have helped me, in many ways, get through the last three years and more.

I want to give a MASSIVE thank you to Simon. Ever since I became a member of the failure club (and yes I do still have my membership card) eight years ago, we became good friends. You, however, have never failed to make me laugh and have always been there for me whenever I needed a friend, a chat, a place to stay or just an honest opinion. I really want you to know I’m grateful for all the help and support you’ve given me over the last eight years. I hope you enjoy your time in Japan and I’ll be over to see you when you get out there yessir.

I want to say a huge thank you to Jo, ever since Boddington you’ve always been there for me when I needed a chat, a laugh or a shoulder to cry on. I appreciate all your help and honest advice, and for making the intrepid journey all the way up here. I’d also like to thank you for letting me stay with you whenever I visit London. I’ll be back down soon for more eye spy

and charades on the tube, to take my mind off more persistent situations; I think I'm still in the lead with Dido though, and Jo, you are not Sparticus.

Thanks to Rob for coming all the way up here to see me in St. Andrews, it was good to see you again, and Rob... I feel your pain...

I'd like to thank Catherine Reinhold, my undergrad mukka who made the move with me from Leeds to Birmingham and who helped me get settled in Brum, I hope all is going well and you'll be finished soon.

From my first year at Birmingham University, I'd like to thank the people that made me feel welcome. I would like to thank Catherine (the greatest dancer) Skinner, Rich (fire starter) Ward (ever been picked up by the fuzz?) Dr P.C. Sam (Batty) Rigby, Sarah (Skoog) Howell, Suzi (Floozy) White, Mikee (very tidy) Edmondson, Paul (beer and curry monster) Shrimpton and Taryn (Beatch) Kinnhan.

I'd like to give a huge thank you to Sarah again, for keeping me sane and laughing during my second year in St. Andrews, I think we must have kept the restaurants and pubs in business. Cheers Big Ears!!!

I think that the people you work with, can and do make a huge difference to your day, and this is one thing my PhD has proved to me. I would like to thank (Dr) Mairead "beautiful" Minto, (Dr) Rosalyne "pool shark" Cowie, (Dr) Elef "houmous" Kassiandis and Dr Russell "orange scooter" Pearson, for all their lab banter and support this year. To Mairead and Rosalyne, I think we got through our list of "things to do" in St. Andrews, and I even surprised myself by discovering that putting is not that bad, but it is as close to golf as I think I ever want to get. I want to take this opportunity to wish you all the very best in the future.

I would like to thank Gareth, my lab-demonstrating partner, for always being so happy and ready with an endless supply of hugs. I would like to also thank you for being toight like a toiger, your support helped me a lot when I needed it, and thanks for letting me use your room whilst finishing my thesis. MOLE!

I'd like to thank Brian for being "naturally funny" and Cobby for making me realise that toilet ducks should be set free. I'd like to thank Amy for making sure the place is always lively and keeping Russell under control. Also, thanks are due to Mairead and Amy for letting me stay at the Hotel Clark-Minto.

I would like to thank my housemates from this year for providing laughs and amusement. MONKEY! Thanks to Claire for organising a trip to new newly named Avivimore. We didn't manage to find Nessie, even though we tried to entice her with an orange, or perhaps it was our renditions of "she'll be coming" and "blow my whistle" which scared her away!

Finally, I would like to thank all my family. Thanks to Alan and Linda for being there and providing a place to stay in the US. Thanks to Stephen and Mandi and my nieces Rosie-Jane, Yasmine and Coral for always being pleased to see me.

And finally thanks to the two most important people, my mum and dad, they have always been there for me to provide financial and more importantly emotional support. Without their endless love, support and encouragement, I would not have got this far and so it is to my parents, Barry and Sandra, I dedicate this thesis.

Abbreviations and Acronyms

Ac	acetyl
Ar	aryl
Bu	butyl
<i>ca.</i>	approximately
Calc.	calculated
CI	chemical ionisation
d	day
decomp.	decomposes
DCM	dichloromethane
de	diastereomeric excess
DMF	dimethylformamide
DMSO	dimethylsulfoxide
DNA	deoxyribonucleic acid
DTT	dithiothreitol
ee	enantiomeric excess
EI	electron ionisation
Et	ethyl
EtOAc	ethyl acetate
EtOH	ethanol
eq.	molar equivalents
ESI	electrospray ionisation
h	hour
HPLC	high performance liquid chromatography
HRMS	high resolution mass spectroscopy
HTMA	hexamethylene tetraamine
IR	infrared (spectroscopy)
LSI	liquid secondary ion
M.p.	melting point
Me	methyl
MeOH	methanol
MS	mass spectrometry
min	minute
NMR	nuclear magnetic resonance

<i>p</i> -TSA	<i>para</i> -toluenesulfonic acid
PCC	pyridinium chlorochromate
PDC	pyridinium dichromate
PMA	phosphomolybdic acid
Pr	propyl
recryst.	recrystallised
RNA	ribonucleic acid
r.t.	room temperature
TBAF	tetrabutylammonium fluoride
TBDPSCI	<i>tert</i> -butylchlorodiphenylsilane
THF	tetrahydrofuran
tlc	thin layer chromatography

Contents

Synopsis	i
Acknowledgements	iii
Abbreviations and Acronyms	vi
1 Introduction	1
1.1 In search of the origins of life	1
1.2 Prebiotic chemistry	1
1.3 How did the first bioinformational molecules arise?	5
1.4 What can be learnt from nature?	7
1.4.1 Requirements for catalysis	8
1.4.2 Intramolecularity	8
1.4.3 Effective molarity	8
1.4.4 Proximity effects	9
1.4.5 Near attack conformations	15
1.5 What are self-replicating systems?	16
1.5.1 The minimal model for self-replication	16
1.5.2 Complex stability	18
1.5.3 Autocatalysis vs. general catalysis	19
1.6 [A•B] complexes	19
1.6.1 What are AB complexes?	19
1.6.2 Stereochemical control by transition state stabilisation	22
1.6.3 Stereochemical control by ground state stabilisation	24
1.7 Template-directed control and acceleration of chemical reactions	27
1.8 The evolution of self-replicating systems	30
1.8.1 Natural product based self-replicating systems	30
1.8.2 Synthetic approach to self-replicating systems	38
1.9 The origins of chirality	47
1.9.1 Asymmetric autocatalysis	47
1.10 Aims and objectives	51
2 The design and synthesis of a minimal self-replicating system	53
2.1 The design of a self-replicating system	53
2.1.1 The recognition motif	54

2.1.2	The covalent bond forming reaction	56
2.1.3	The spacer unit	59
2.2	The potential self-replicating system	59
2.2.1	The bimolecular reaction	62
2.3	Synthesis	62
2.3.1	Synthesis of the recognition dipole 5	62
2.3.2	Synthesis of the recognition dipolarophile 77	63
2.3.3	Synthesis of the control dipolarophile 79	63
2.3.4	Synthesis of the recognition-mediated cycloadduct 78 and control cycloadduct 80	63
2.4	¹ H NMR spectroscopic assignment of the cycloadduct 78	64
2.5	Kinetic analysis	67
2.5.1	Optimisation of the reaction conditions to promote the autocatalytic cycle	67
2.6	The kinetic experiment	67
2.7	The results of the recognition-mediated kinetic experiments	68
2.8	Demonstrating the operation of a self-replicating system	70
2.8.1	The uncatalysed bimolecular reaction	70
2.8.2	Competition experiment	71
2.8.3	Doping experiment	73
2.9	Single crystal X-ray analysis of template 78	74
2.10	Summary of evidence for a self-replicating pathway	75
2.11	Fitting the experimental data to the kinetic model	76
2.12	Measuring the association constant of the product duplex [78•78]	79
2.13	What happens to the reaction pathway at an elevated temperature?	79
2.14	Fitting the experimental data to the kinetic model	82
2.15	Conclusion	85
3	What makes a system a successful autocatalytic self-replicator?	86
3.1	The search for a self-replicating system	86
3.2	Examples of recognition-mediated systems which react <i>via</i> an AB- complex pathway	86
3.2.1	An AB-complex system which utilises a 1,3 dipolar cycloaddition	86
3.2.2	An AB-complex system which utilises a 1,4 cycloaddition	87

3.2.3	An AB-complex reaction between a 2 substituted furan and a maleimide	89
3.2.4	An AB-complex reaction between a 3 substituted furan and a maleimide	90
3.3	An example of recognition mediated systems, which react <i>via</i> a self-replicating pathway	92
3.4	The design of a recognition-mediated system	97
3.4.1	Isloxazolidines	98
3.4.2	The new recognition-mediated system	98
3.5	Kinetic analysis	100
3.5.1	Optimisation of the reaction conditions to promote the autocatalytic cycle	100
3.5.2	The kinetic experiment	101
3.5.3	Demonstrating the operation of a self-replicating system	103
3.5.4	The uncatalysed bimolecular reaction	103
3.5.5	Competition experiment	104
3.5.6	Doping experiment	106
3.5.7	Kinetic fitting of the experimental data	107
3.6	AB systems vs. self-replicating systems	108
3.7	Testing the isloxazolidine system	109
3.8	Synthesis	111
3.8.1	Synthesis of maleimide building block 77	111
3.8.2	Synthesis of the control dipolarophile 79	111
3.8.3	Synthesis of aldehydes 123	111
3.8.4	Synthesis of 4-nitro-tert-butyl-benzene 125	112
3.8.5	Synthesis of nitrones 104, 109, 110, 111 and 112	112
3.8.6	Synthesis of cycloadducts 105, 136, 137, 138 and 139	113
3.8.7	Synthesis of cycloadducts 108, 140, 141, 142 and 143	114
3.8.8	Synthesis of aldehydes 146	114
3.8.9	Synthesis of nitrones 113, 114, 115, 116 and 117	115
3.8.10	Synthesis of cycloadducts 147, 148, 149, 150 and 151	116
3.8.11	Synthesis of cycloadducts 152, 153, 154, 155 and 156	116
3.8.12	Synthesis of nitrones 118 and 119	117
3.8.13	Synthesis of cycloadducts 159 and 160	117
3.9	Structural assignment of the 4 nitrones	118

3.10	Kinetic analysis	118
	3.10.1 The reaction conditions	118
	3.10.2 The kinetic experiments	119
3.11	The experimental data for the 3 nitrones	119
	3.11.1 Nitrone 109	119
	3.11.2 Nitrone 110	121
	3.11.3 Nitrone 111	123
	3.11.4 Nitrone 112	125
3.12	Conclusion for the series of 3-nitrones	127
3.13	The experimental data for the 4 nitrones	128
	3.13.1 Nitrone 113	128
	3.13.2 Nitrone 114	130
	3.13.3 Nitrone 115	132
	3.13.4 Nitrone 116	134
	3.13.5 Nitrone 117	136
3.14	What conclusions can be drawn from the experimental data?	138
3.15	Percentage completion and diastereoisomer ratios	138
3.16	Hammett plot	140
3.17	Fitting the data to the kinetic model	141
3.18	Comparison of the diastereoisomeric excesses	142
3.19	X-ray crystal structure of the cycloadduct 148	145
3.20	Conclusion	147
3.21	Can the pathway of a recognition-mediated system be changed?	151
	3.21.1 The effect of oligomethylene chain length on a self-replicating system	151
3.22	The kinetic experiments	151
3.23	The effect of oligomethylene chain length on the nitrone systems 109 and 113	155
3.24	Synthesis	155
	3.24.1 Synthesis of maleimide 6 and 161	155
	3.24.2 Synthesis of control dipolarophiles 12 and 164	156
	3.24.3 Synthesis of nitrones 104 , 109 and 113	156
	3.24.4 Synthesis of cycloadducts 162 and 163	156
	3.24.5 Synthesis of cycloadducts 165 and 166	156
	3.24.6 Synthesis of cycloadducts 169 , 170 , 171 , 172 , 173 , 174 ,	

	175 and 176	157
3.25	The effect of oligomethylene chain length on system 113	158
	3.25.1 The kinetic experiments	158
3.26	The effect of oligomethylene chain length on system 109	160
	3.26.1 The kinetic experiments	160
3.27	Conclusion	163
3.28	Temperature effects upon the efficiency of a self-replicating system	163
3.29	Synthesis of nitrones 110 and 117	164
3.30	The kinetic experiments	164
3.31	The effect of varying the temperature upon system 110	164
3.32	The effect of varying the temperature upon system 117	165
3.33	Percentage completion and diastereoisomer ratios	167
3.34	Conclusions	170
4	The design and synthesis of a new self-replicating system	171
4.1	Aspects of autocatalytic self-replicator design	171
4.2	An example of a self-replicating system	171
	4.2.1 Comparison to compound 5	172
4.3	The design of a new system	172
4.4	Synthesis	173
	4.4.1 Synthesis of maleimide building blocks 77 and 6	173
	4.4.2 Synthesis of the recognition dipoles	173
	4.4.2.1 Retro synthesis of compounds 179 and 182	174
	4.4.3 Synthesis of chlorides 188 and 189	174
	4.4.4 Attempted synthesis of aldehydes 186 and 187	175
4.5	An alternative retro synthetic analysis of compounds 179 and 182	176
	4.5.1 Synthesis of the protected diols 203 and 204	177
	4.5.2 Synthesis of the carboxylic acids 201 and 202	178
	4.5.3 Synthesis of the acid chlorides 199 and 200	178
	4.5.4 Synthesis of the amides 197 and 198	179
	4.5.5 Synthesis of alcohol 196	179
	4.5.6 Attempted synthesis of aldehydes 187	179
4.6	Structural assignment of compound 208	180
	4.6.1 Accurate and low resolution mass analysis	180

4.6.2	¹ H and ¹³ C NMR of compound 208	180
4.6.3	COSY NMR experiment performed upon compound 208	183
4.6.4	HSQC NMR experiment performed upon compound 208	184
4.6.5	HMBC NMR experiment performed upon compound 208	185
4.7	Attempted synthesis of aldehydes 187	186
4.8	Alternative nitrene building blocks	186
4.8.1	Retro synthesis of compounds 209 and 210	187
4.9	Synthesis	187
4.9.1	Synthesis of ketone 211	187
4.9.2	Synthesis of ketone 212	187
4.9.3	Synthesis of nitrenes 209 and 210	189
4.10	Conclusion	189
5	General conclusions and future directions	190
6	Experimental	192
6.1	General procedures	192
6.2	Mass spectrometry	192
6.3	NMR spectroscopy	192
6.4	Kinetic measurements	193
6.5	Molecular mechanics calculations	193
6.6	Crystal structure determination	194
6.7	Synthetic procedures	194
6.8	Data parameters for X-ray crystallography determination	246
6.8.1	Crystal data and structure refinement for compound 78	246
6.8.2	Crystal data and structure refinement for compound 7	247
6.8.3	Crystal data and structure refinement for compound 104	248
6.8.4	Crystal data and structure refinement for compound 148	249
6.8.5	Crystal data and structure refinement for compound 113	250
6.8.6	Crystal data and structure refinement for compound 105	251
7	References	252
8	Appendices	260

1. Introduction

1.1 In search of the origins of life

The question of how and when life began¹⁻⁵ has undergone many transformations over the last century. It is a question that has inspired the imagination of scientists and non-scientists alike. About a thousand years ago it was assumed that life formed spontaneously from non-life, for example maggots seemed to appear from nothing. It was not until 1862 that Louis Pasteur performed a very simple experiment to show that bacteria do not simply appear in a sterile broth, it needs to be open to the air in order for bacteria to grow. Hence, he demonstrated that air was the source of bacteria and so proved that life generated life, but from where did life originate?

1.2 Prebiotic chemistry

In the mid-nineteenth century a scientist called Friedrich Wöhler synthesised urea, an organic compound, from ammonium cyanate, an inorganic compound. Wöhler's experiment was very important because it is part of a chain of evidence that demonstrates that the gap between the chemistry of living and lifeless chemistry is bridgeable. There have since been many other experiments⁶, which qualify as "prebiotic chemistry". For example glycine, an important amino acid, was synthesised from hydrogen cyanide and formaldehyde, also sugars have been synthesised from formaldehyde. Since both hydrogen cyanide and formaldehyde had been synthesised from inorganic sources these reactions are considered prebiotic. Prebiotic chemistry in the sense of the deliberate simulation of reactions that occurred on primitive earth is of much more recent origin. Oparin² and Haldane⁷ emphasized that in the period before the first living organisms evolved, the Earth's atmosphere must have been reducing. It was suggested that a mixture of organic compounds was formed in such an atmosphere and that the first living organisms were assembled from a selection of these compounds.

Using this assumption, Miller⁸ performed an experiment, which is still considered one of the most important experiments in prebiotic chemistry. Working with Urey in Chicago, Miller demonstrated that important biochemicals are indeed formed in surprisingly large amounts when an electric discharge is passed through a reducing atmosphere of the kind proposed by Oparin and Haldane. The experiment was performed by using a mixture of methane, ammonia, hydrogen and water to mimic a prebiotic soup, which was then subjected to a continuous electric discharge (**Figure 1.1**).

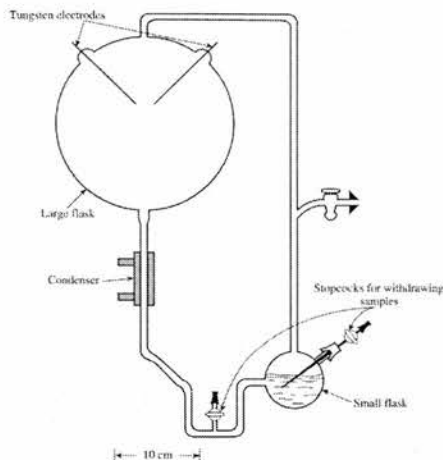


Figure 1.1 The apparatus used in Miller's prebiotic experiment. Diagram taken from ref. 9.

The experiment was designed to recreate the conditions assumed on primitive earth. The starting mixture of gaseous compounds was intended to simulate the reducing atmosphere that was assumed to exist on the prebiotic earth and the electric discharge intended to simulate lightning. The electric discharge was operated for one week after which the gases were pumped out and the products analysed by paper chromatography. The products contained a variety of α -hydroxyacids, urea and α -amino acids, which included glycine, alanine, aspartic acid and glutamic acid (**Figure 1.2**).

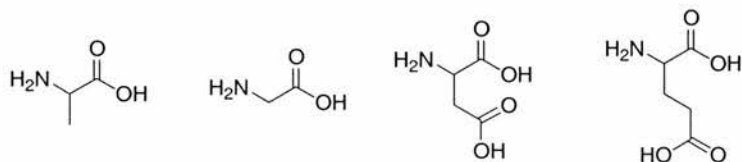
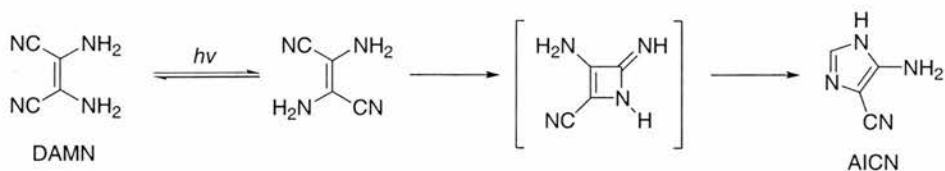
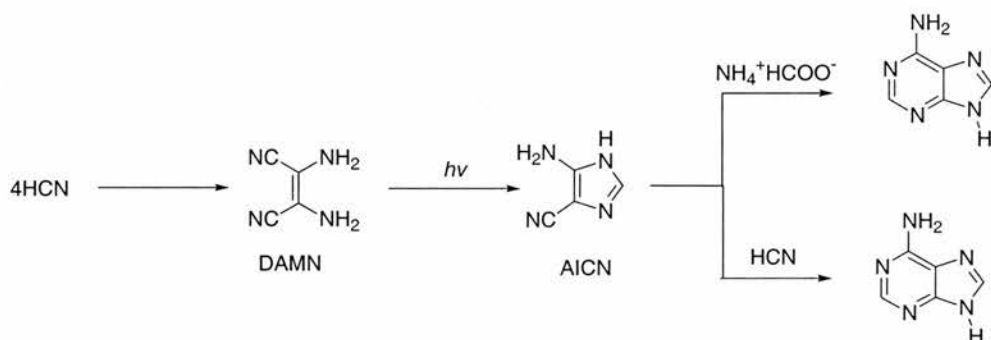


Figure 1.2 Four of the amino acids formed in Miller's experiment, alanine, glycine, aspartic acid and glutamic acid.

Miller had proved that Oparin and Haldane's predictions were correct. This result is quite surprising because many millions of organic compounds are known and many thousands have structures, which are no more complex than amino acids. Before this experiment was reported, it would have been anticipated that that an electric discharge acting on a mixture of methane, hydrogen, ammonia and water would result in a mixture containing small quantities of many different substances. It surely cannot be a coincidence that relatively few substances were formed and that many of them are biologically important. Since Miller's original experiment, nearly all of the natural occurring amino acids have been identified from prebiotic experiments. It is interesting to note that none of the experiments involve free oxygen and no amino acids are formed from a mixture of carbon dioxide, nitrogen and water; this is an important negative result and again supports the Oparin-Haldane theory of a



Scheme 1.2 Proposed formation of aminoimidazolecarbonitrile (AICN) from diaminomaleonitrile (DAMN). Mechanism taken from ref. 9.



Scheme 1.3 The proposed formation of adenine from hydrogen cyanide. Mechanism taken from ref. 9.

It has been demonstrated that most of the essential building blocks of life can be formed under assumed prebiotic conditions. Even sugars have been synthesised under prebiotic conditions by a Russian scientist, Butlerov in the 1860s. His discovery involved warming an aqueous solution of formaldehyde in the presence of a calcium hydroxide suspension from which a mixture of sugars was formed. The process is referred to as the *formose* reaction.

Thus, it has been demonstrated that most of the important precursors to our very own building blocks can be synthesised under assumed prebiotic conditions, but how do these simple compounds become such complex arrays of molecules, which eventually reach the stage where they become sentient?

There have been many theories postulated as to how these building blocks assemble to form organised arrays of molecules, but overall the origin of life can be thought of as occurring in three overlapping phases (**Figure 1.4**).

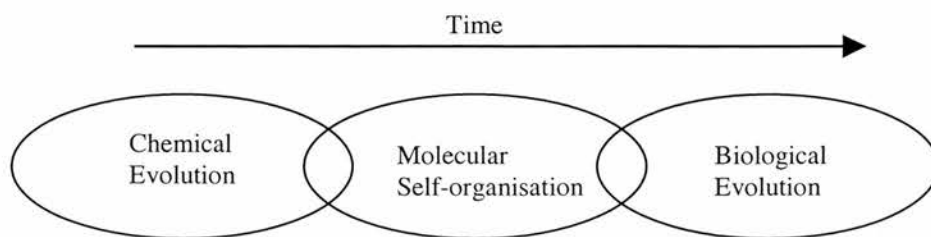


Figure 1.4 The origin of life can be considered in three overlapping phases

Initially, there was a phase during which the chemicals needed for synthesis of instructional polymers were assembled. Modifications of these polymers would take place to enhance replication and catalysis. At this stage the polymers must display two key features of living systems: the ability to replicate and the ability to evolve. At an advanced stage in their evolution, the polymers would develop the capacity to direct the synthesis and organisation of other types of polymers and of membrane phospholipids: only then would the first living cells emerge. In the third phase, the divergent process of biological evolution would commence, leading to further development of single celled organisms, including the differentiation of some of them into multicellular organisms.

1.3 How did the first informational biomolecules arise?

At some point in evolution, the prebiotic building blocks must have begun to assemble into instructional polymers. However, it is unknown what these first polymers were based upon? The possibilities have been summarised by Orgel¹¹:

1. Early nucleic acid or related molecules replicated directly. They ‘invented’ protein synthesis. Uncoded polypeptides may or may not have been involved in the earliest precoding replication mechanism.
2. Early functional proteins replicated directly. They ‘invented’ nucleic acids and were ultimately enslaved by them.
3. Nucleic acid replication and genetic coding of proteins coevolved.
4. The first form of life on the earth was based on some inorganic or organic system unrelated to proteins or nucleic acids.

A major problem in the origin of life is determining the evolutionary events, which lead up to the first instructional polymers. Since Watson and Crick solved the structure of DNA in 1953¹², it has been understood that DNA is comprised of nucleotides, which stores our very own unique genetic code, in essence our blueprint. However, DNA cannot replicate itself, replication involves enzymes, which are polypeptides, however these polypeptides cannot be formed without the blueprint from DNA. This then leads to a chicken and egg situation, which came first the polypeptide or the polynucleotide?

Since the early 1970s, there has been an accumulation of evidence, which supports the “RNA world” view¹³⁻¹⁷, this supports the first possibility as summarised by Orgel. Fundamentally this viewpoint replaces the central dogma of molecular biology which states that “DNA makes RNA makes proteins” with the view that in the beginning, both genetic material and the enzymatic catalysts were comprised of RNA. In 1989 Altman and Cech^{18,19} won the Nobel Prize in chemistry for demonstrating that RNA does indeed possess catalytic powers and

that there are naturally occurring enzymes made of RNA, now known as ribozymes. As a result of this catalytic ability, it has been thought that RNA could have been the original machinery of life. Although, it has also been suggested that a non-enzymatic reaction related to nucleic acid replication played an essential role in the origins of life^{20,21}. According to Benner *et al.*^{22,23} the presence of translation and proteins occurred at a relatively late evolutionary stage. Some of RNA's functions were in time replaced by the better suited DNA and enzymes. However, this theory does have its flaws. It seems from Miller's experiment that amino acids can be synthesised under prebiotic conditions and so perhaps proteins were the first bio-molecules. The second possibility has led to a school of thought that does consider peptides²⁴⁻²⁶ to be the original precursors to life. In particular, research performed by Fox²⁷ demonstrated that it was possible to synthesise polypeptides by heating without degradation to a carbonised tar. In the experiment, Fox created an amino acid melt by using one or two low melting point amino acids (aspartic and glutamic acids) as a solvent, mixed with other amino acids. Upon heating to 150°C the water was distilled from the melt, shifting the equilibrium in favour of the peptide bond formation. After a certain length of time the reaction mixture was plunged into water, which gave rise to an aggregated structure that formed spherules called proteinoids. The proteinoids were found to exhibit catalytic, enzyme like properties, they also demonstrate a selective recognition of nucleotides. The facile nature of the proteinoids formation and their catalytic behaviour lends itself to the possibility of being the first instructional polymers.

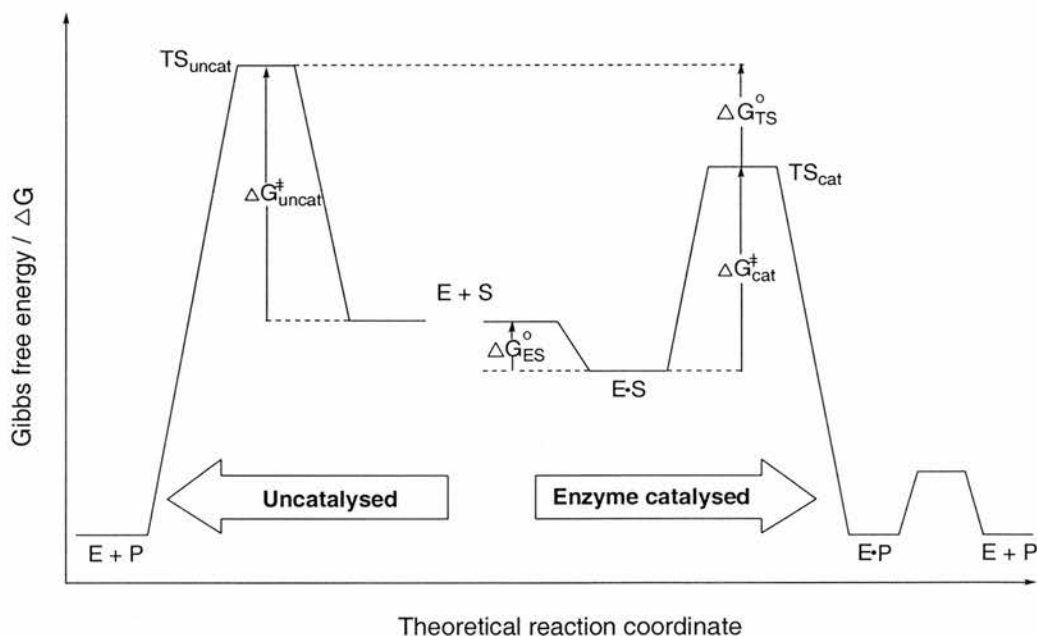
The third possibility, which considers the co-existence of polypeptides and polynucleotides, has also been addressed^{28,29}. Eigen³⁰ used a model of *hypercycles*, a mathematical network that introduces higher-order catalytic action in the form of positive feedback loops among members of different classes of self-replicating macromolecules.

The final possibility has been examined by Cairns-Smith³¹, who proposed that certain structures of the clay mineral surface could act as mineral 'genes' by assembling organic compounds into specific configurations and aiding their self-assembly. The resulting macromolecules would later be able to code for their own self-assembly in a more efficient process and thus take over the genetic function. It is known that clay surfaces have catalytic properties, as demonstrated by Ferris *et al.*³² on montmorillonite clay. However there is no convincing evidence that supports the view that mineral surfaces are required to provide a transition between inorganic and organic structures.

It is hoped that by studying self-replicating systems it will be possible to shed some light on the origins of life as well as providing a useful tool for the synthetic chemist due to the fact that self-replicating systems have the potential to act as the ultimate synthetic machines.³³⁻³⁷

1.4 What can be learnt from nature?

The chemical processes that occur within biological systems, proceed at extremely high rates compared to the analogous reactions which could be performed under laboratory conditions. The ability to accelerate these chemical processes within biological systems is provided by enzymes. Enzymes are biological catalysts, although this statement does underestimate the ability of enzymes. They have the ability to recognise and respond to specific substrates, which can then accelerate a particular chemical transformation (often in the order of 10^8 to 10^{10}), which may or may not occur stereospecifically. The function of enzymes³⁸⁻⁴⁰ is very complex. For the last 50 years, organic chemists have tried to understand how and why enzymes are so good at accelerating chemical reactions, in order to exploit enzymatic behaviour to meet their own needs⁴¹. There have been as many as 21 different hypotheses⁴² to try to explain enzyme function. The general consensus of opinion is that enzymes function by lowering the energy of the transition-state or of high-energy intermediates or by raising the energy of the ground state thereby favouring the forward reaction (**Scheme 1.4**).



Scheme 1.4 Schematic representation of energy profiles for both enzyme-catalysed and uncatalysed reactions of a substrate S.

Thus, it is from these biological catalysts that we hope to understand how to control and accelerate reactions.

1.4.1 Requirements for catalysis

As mentioned previously, there is much to be learnt from nature and hence there are a number of areas identified where the chemist can begin to develop their understanding of catalysis in order to begin to develop systems that can function as catalysis with a view to ultimately self-replicating.

1.4.2 Intramolecularity

It is thought that one of the major factors involved in the massive rate accelerations within enzymes is the fact that the reaction occurs within a [enzyme•substrate] complex. Within the complex the reactive sites are brought into close proximity compared to the corresponding mixture of reactants present in free solution. The complex then renders the reaction *pseudo* intramolecular as opposed to intermolecular. A comparison can be drawn between this [enzyme•substrate] complex and the behaviour of a synthetic intramolecular reaction. The close proximity of the reactive sites leads to an increase in the rate of reaction and it is this behaviour that is described as intramolecularity.

1.4.3 Effective molarity⁴³

In order to quantify the rate enhancement observed for intramolecular reactions, 'effective molarity' EM is used, which is also sometimes referred to as an effective concentration. The effective molarity is a hypothetical concentration of one of the reactants required to make the intermolecular reaction proceed at the same rate as that observed for the intramolecular process. The ratio (**Equation 1.1**) should ideally be calculated from accurately determined experimental measurements using reactions in which the intermolecular and intramolecular processes occur with as similar a mechanism as possible. Rates of reaction should ideally be determined from reactions that are observed under identical experimental conditions.

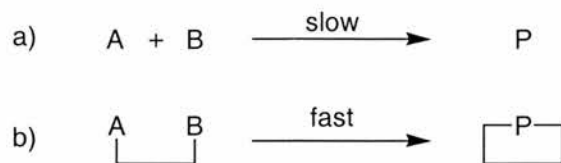
$$EM (M) = \frac{k_{cat}}{k_{uncat}} = \frac{k_{intramolecular}}{k_{intermolecular}}$$

Equation 1.1 Calculation required to determine effective molarity (EM).

Effective molarities ranging from 10^{-3} to 10^{16} M have been recorded⁴³.

1.4.4 Proximity effects

There have been many studies⁴⁴ undertaken to try to reveal why there is such a huge variation in effective molarities. **Scheme 1.5** shows the schematic view of the difference between intramolecular and intermolecular reactions.

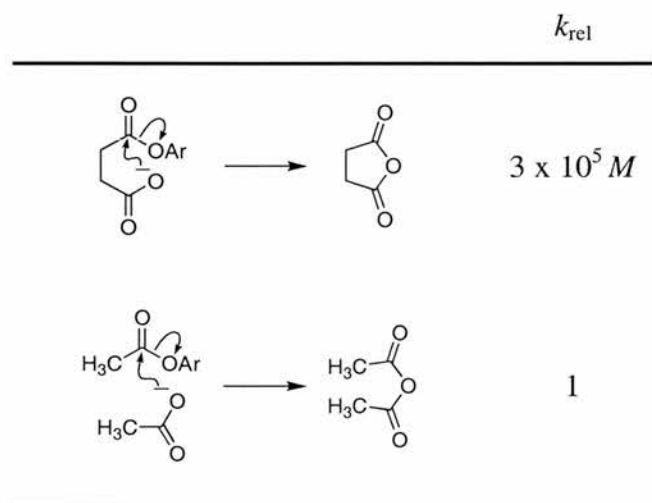


Scheme 1.5 General schematic representation for a) an intermolecular reaction and b) intramolecular reaction.

In the vast majority of examples, the intramolecular reaction exhibits an increased rate of reaction over that of its counterpart intermolecular reaction.

A very simple demonstration of the effect of intramolecularity⁴⁵ is through the formation of succinic anhydride and acetic anhydride. A comparison of the relative rates of formation is drawn between the cyclisation of an aromatic succinic monoester and the reaction of an acetate anion and an aryl acetic monoester (**Table 1.1**).

Table 1.1 The relative rates of formation of succinic anhydride and acetic anhydride

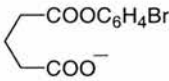
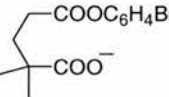
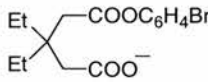
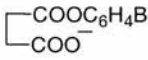
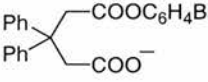
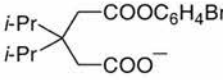
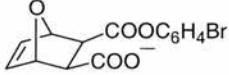


The formation of acetic anhydride is *via* a simple bimolecular reaction and the analogous intramolecular reaction gave a relative rate constant that was 3×10^5 times more favourable (an EM of $3 \times 10^5 M$), which illustrates the rate enhancement induced through proximity of the reactive sites. This demonstrates that bringing the reactive sites together in the same

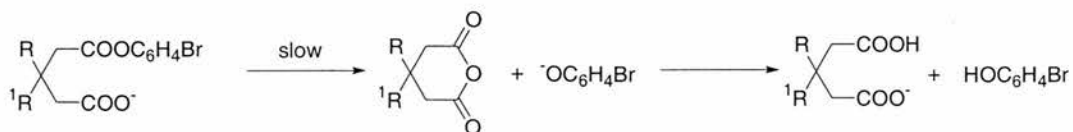
molecule enhances the rate, the efficiency of the reaction then comes from eliminating conformational flexibility of the molecule and enforcing a transition-state like geometry.

Bruice *et al.* performed a comprehensive and detailed study⁴⁶⁻⁴⁸ of proximity effects and intramolecularity. In this study, the maximum rate enhancements observed in intramolecular reactions with varying degrees of induced proximity and enforced geometry between reactive sites, was detailed. The study details the efficiencies of intramolecular carboxyl group nucleophilic catalysis of the hydrolysis of certain esters (**Table 1.2**)

Table 1.2 The relative rates of reaction, b) to h), for the interaction of a carboxylate anion with a monophenyl ester to form the corresponding cyclic anhydride, compared to, a), a standard intermolecular reaction

		k_{rel}
a)	$\text{CH}_3\text{COO}^- + \text{CH}_3\text{COOC}_6\text{H}_4\text{Br}$	1.0
b)		$\sim 1 \times 10^3 M$
c)		$\sim 3.6 \times 10^3 M$
d)		$\sim 1.8 \times 10^5 M$
e)		$\sim 2.3 \times 10^5 M$
f)		$\sim 2.7 \times 10^5 M$
g)		$\sim 1.3 \times 10^6 M$
h)		$\sim 8 \times 10^7 M$

The reactions (b to h) all involve an initial ring closure followed by hydrolytic scission (**Scheme 1.6**).



Scheme 1.6 Mechanism of intermolecular carboxyl group nucleophilic catalysis of the hydrolysis of esters.

It was therefore expected that the overall process would be very sensitive to factors such as proximity and geometry of the reactive functionalities and so in each case varying degrees of proximity and fixed geometry were studied. The rates are all compared to a corresponding bimolecular reaction (reaction **(a)**). From the study it was proposed that, in the absence of strain the rates for formation of cyclic anhydrides could be increased by a factor of $10^8 M$. From the results shown and from subsequent work performed by Bruice and Pandit^{45,49,50} they concluded that rate enhancement could be achieved by fixing the reacting species in a steric conformation that closely resembles the transition state for the reaction. Also they stated that in the enzymatic and intramolecular reactions considerable loss of translational entropy must accompany the bringing together of reactants, if the bond undergoing scission is held in the proper orientation to the catalytic groups, then an additional advantage is gained over the bimolecular reaction. This explanation of rate enhancement in terms of proximity effects was widely accepted and is used in many texts⁵¹⁻⁵³. However around the same time Koshland⁵⁴ and Jencks⁵² proposed that by holding two reactants in close proximity would only result in a rate enhancement of $55 M$. This figure was derived from the assumption that if **A** and **B** are the size of water molecules, and substrate **A** is dissolved in neat **B** then the observed *psuedo*-first order rate constant (k_{obs}) could only be 55.5 times greater than k_{obs} when **B** is at $1.0 M$. Koshland attributed⁵⁵⁻⁵⁷ the large rate enhancements observed in some intramolecular reactions, and by analogy enzymes, to the severe angular dependence of some organic reactions, such as nucleophilic substitutions. It was argued that although the reactive sites may be placed in close proximity within an intramolecular reaction, large rate accelerations would only result if an optimal orbital alignment between the reactive functionalities was achieved, thereby explaining the hugely variant efficiencies of intramolecular reactions. It was determined that a deviation of only 10° away from an optimal orientation would be sufficient to result in a 10^4 fold decrease in the rate of the intramolecular reaction (**Figure 1.5**).

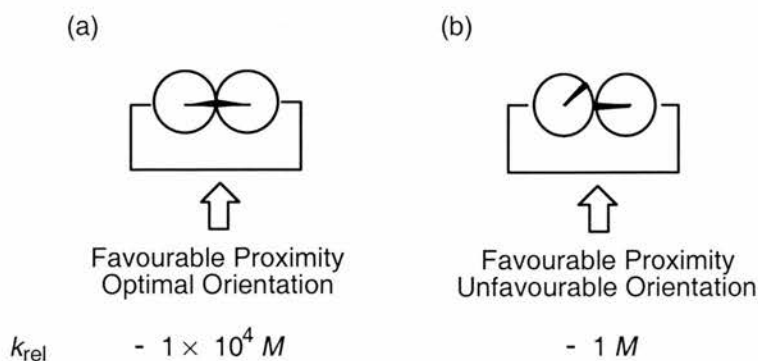


Figure 1.5 Koshland proposed that fast intramolecular rates of reaction were attributable to precise alignment of orbitals between the reactive sites: (a) describes an intramolecular reaction that achieves proximity and an optimal alignment of orbitals (b) describes an intramolecular reaction that achieves proximity, but the reactive sites are orientated more than 10° away from the optimal alignment.

The authors concluded that enzymes not only enforced proximity on the reactive partners but were also able to precisely orientate the reacting orbitals in an optimal position at the reactive site, this was referred to as '*orbital steering*'. He also stated that as intermolecular reactions in the solution phase were highly unlikely to attain an optimal orientation *via* random collisions this provided an acceptable explanation for the lower rates of reaction observed for bimolecular reactions.

Bruice attacked⁵⁸ the theory of orbital steering on the grounds that it requires an unreasonably large force constant; the theory was however upheld^{59,60} by two theoretical studies. Also a study performed by Menger⁶¹ inferred that the influence of orbital steering on the rates of intramolecular reactions was not as great as first thought.

At this stage, Page and Jencks looked at a new approach to explaining the efficiency of intramolecular reactions. They proposed that intramolecular reactions gained their acceleration from the entropic differences^{44,52,62} between unimolecular and bimolecular reactions. They believed that enzymes carry out a large fraction of their rate acceleration by virtue of their ability to utilise substrate-binding forces, to act as an 'entropy-trap'. Therefore it will be useful to examine the differences of the entropic contributions between intra and intermolecular forces.

For a non-linear molecule containing n atoms there are three degrees of translational freedom, three degrees of rotational freedom, which leaves $3n-6$ degrees of freedom, associated with internal molecular vibrations. During the course of a bimolecular reaction, three degrees of translational freedom and three degrees of rotational freedom will be lost upon formation of the product. This loss will be compensated to a lesser extent by the formation of six new modes of internal vibration in the product (**Table 1.3**).

Table 1.3 The change in molecular degrees of freedom during a bimolecular reaction. Data taken from ref. 39.

	A	+	B	\rightleftharpoons	P
Translation	3		3		3
Rotation	3		3		3
Vibration	$3n-6$		$3n'-6$		$3n+3n'-6$

If an analogous intramolecular reaction is now considered there should be no overall change in the molecular degrees of freedom over the course of a reaction (**Table 1.4**). In the intramolecular reaction the reactants are already bound to one another and so there is very little loss in entropy in going from the ground state to the transition state.

Table 1.4 The changes in molecular degrees of freedom during the course of a unimolecular reaction. Data taken from ref. 39.

	A		B	\rightleftharpoons	P
Translation	3				3
Rotation	3				3
Vibration	$3n-6$				$3n-6$

The change in the number of degrees of freedom on passing from reactants to product during a bimolecular reaction can be quantified in terms of a change in entropy (**Table 1.5**)

Table 1.5 Typical values for the entropy associated with translational, rotational and vibrational degrees of freedom at 298 K.

Motion	Entropy ($\text{JK}^{-1}\text{mol}^{-1}$)
3 degrees of translation freedom for molecular weights 20 to 200 (standard state = 1 M)	120-150
3 degrees of rotational freedom	
water	44
<i>n</i> -propane	90
<i>endo</i> -dicyclopentadiene $\text{C}_{10}\text{H}_{12}$	114
Internal rotation	13-21
Vibrations (cm^{-1})	
1000	0.4
800	0.8
400	4.2
200	9.2
100	14.2

It is evident from the data shown in **Table 1.5** that the translational and rotational motions contribute significantly to the entropy of molecules, whereas the internal rotations and vibrations are relatively entropy deficient and contribute minimally. It is therefore expected that during the course of a bimolecular reaction there will be a significant loss of entropy, making the process unfavourable. Page and Jencks estimated that the total translational and rotational entropy change during a solution phase bimolecular reaction is approximately $-200 \text{ JK}^{-1}\text{mol}^{-1}$ (at 298K and at a standard state of 1 M), but expected that this would be balanced by a gain of up to $+50 \text{ JK}^{-1}\text{mol}^{-1}$ associated with the formation of new, low frequency vibrations in the product. Typical entropy change associated with a bimolecular reaction was estimated to be $-150 \text{ JK}^{-1}\text{mol}^{-1}$. By comparison of an analogous intramolecular reaction, it would be expected that it would possess a considerable entropic advantage because it does not have to overcome the high free energy of activation ($-150 \text{ JK}^{-1}\text{mol}^{-1}$). Page and Jencks proposed that the entropic advantage would accelerate an intramolecular reaction 10^8 -fold over an analogous intermolecular reaction. It should be noted that in the rare cases where a bimolecular reaction has a 'loose' transition state or product, then association will be less entropically unfavourable, since the entropy of the low-frequency vibrations in the 'loose' complex will counterbalance the large loss of translational and rotational entropy. Typically for these systems rate enhancements are in the order of $10^2 M$.

This entropy theory was not without its critics, Menger⁶³ introduced what can be considered a refinement of the proximity theory proposed by Bruice⁴⁵. He stated that “the rate of reaction between functionalities **A** and **B** is proportional to the time that **A** and **B** reside within a critical distance”. It was proposed that intramolecular reactions occur at enzyme like rates when van der Waals contact distances (less than solvent distance) are imposed for a finite time upon the reactive groups, i.e. intramolecular reactivity is a function of both time and distance. This he then termed his ‘*spatiotemporal theory*’. Menger stated that the critical distance between reacting groups should be no larger than 3\AA , as this would guarantee the exclusion of solvent molecules.

1.4.5 Near attack conformations

Thirty years after the original study into the rates of intramolecular reactions Bruice and Lightstone^{64,65} put forward a theory for the efficiency of intramolecular reactions based on what they called the Near Attack Conformation (NAC). They undertook a complex theoretical computational study to establish the relationship between the importance of the ground state conformation of a reactant and the rate at which the reaction proceeds. They define the NAC as being the ground state conformation in which the reactants are correctly aligned and at a 3\AA separation, in order to enter the transition state. This is the situation just before bond making and breaking has been initiated. The study focuses on the results of a previous study; the carboxyl group nucleophilic catalysis of the hydrolysis of esters (**Table 1.2**) (**Figure 1.6**).

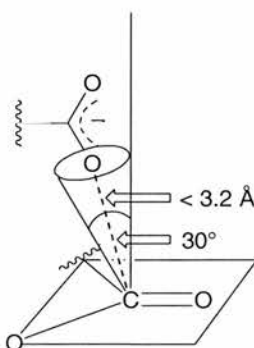


Figure 1.6 The geometry of a NAC^{64,65} for intramolecular carboxylate anion interaction with a carbonyl ester.

In the NAC the carbon on the carbonyl is still sp^2 hybridised. The carboxylate anion is positioned above the carbonyl carbon of the ester at no more than a 30° angle from the perpendicular trajectory. This allowed calculations to be undertaken associated with an approach angle of 109° of the carboxylate anion, with respect to the carboxyl group, into the antibonding orbital of the C=O bond. The calculations involved taking between 10,000 and

40,000 unique conformations of each monoester and minimising each structure before determining the mole fraction of the NAC's present using a Boltzmann distribution profile. A plot of the log of the probability for the formation of a NAC (P) vs. the log of the experimental relative rate constants (k_{rel}) for anhydride formation revealed a linear free energy relationship between the \log_{10} of the fraction of conformations present as NACs and ΔG (Figure 1.7)

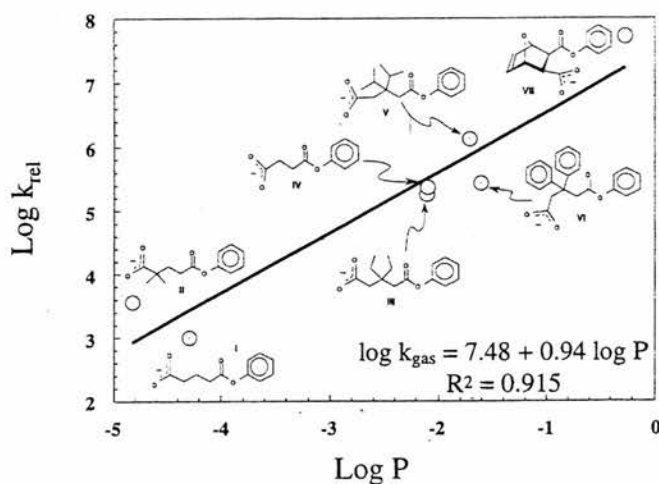


Figure 1.7 Log of the relative rate constants vs. the log of the probability for the formation of a NAC, for the formation of cyclic anhydrides. Diagram taken from ref. 47.

It was also noted that there is a linear correlation of $\log_{10}(k_{rel})$ to ΔH and ΔS , from which is concluded that the observed rate differences for these reactions were as a result of enthalpic and not entropic contributions. In conclusion it was stated that the rate of reaction was directly proportional to the mole fraction of the reactants in a ground state NAC. In summary the NAC conformer must be reasonably stable in order for the transition state to be entered into, and if this is not the case then energy is required to form such a NAC *i.e.* a decrease in enthalpy.

1.5 What are self-replicating systems?

1.5.1 The minimal model for self-replication^{66,67}

The simplest model devised to represent self-replication is that of the minimal self-replicating cycle (Figure 1.8).

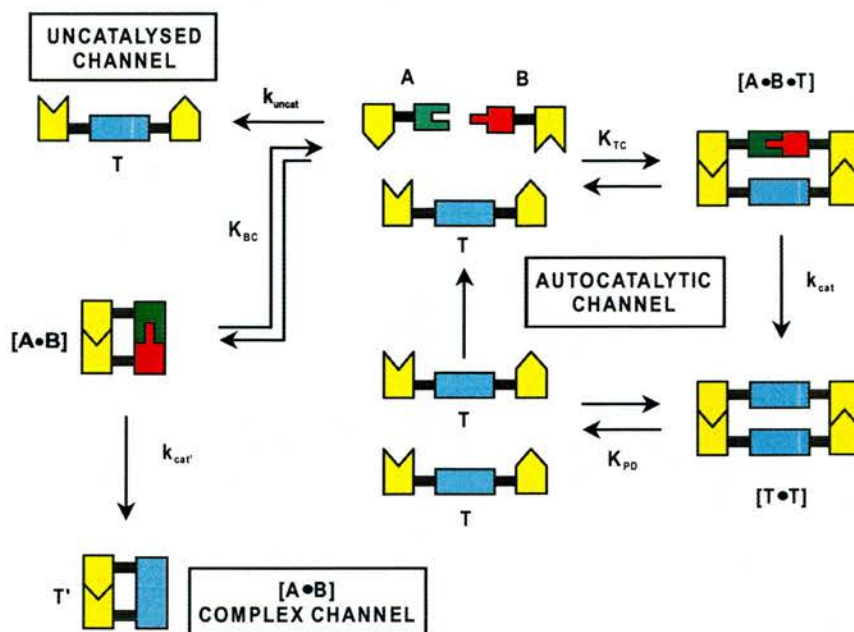


Figure 1.8 Schematic representation of the minimal model for self-replication.

The minimal self-replicating model is based upon template⁶⁸⁻⁷⁰ directed synthesis. Within this system there are three reaction channels available to the starting materials **A** and **B**. The first channel available to the starting materials is that *via* the uncatalysed bimolecular reaction, this occurs when **A** and **B** reactively collide in solution to form the product **T**. This bimolecular reaction pathway is characterised by the rate constant k_{uncat} . The second possible channel is recognition mediated. The starting materials **A** and **B** are designed so that they each bear one of two complementary recognition sites and so may bind reversible together to form a binary complex **[A•B]**. This binding equilibrium is characterised by the equilibrium constant K_{BC} . If the starting materials are designed in such a way that allows the reactive sites to come close enough to react then this complex may facilitate the covalent bond forming reaction to yield the product **T'**, which has the rate constant $k_{\text{cat}'}$. It should be noted that the reaction between the two starting materials has now become *pseudo*-unimolecular due to the complementary binding sites. Also, by binding the starting materials together in such a way it is possible to control the approach of the reactive sites and hence regio- and stereochemical control of the product is achievable. Although facilitation and acceleration of the reaction may occur, this reaction channel does not exhibit autocatalysis as any template formed by this route usually retains the complementary binding of the recognition sites in the product and turnover cannot be achieved. This product is termed the closed template **T'**.

The third reaction channel possible is that of an autocatalytic cycle. In this cycle, **A** and **B** bind reversibly to template **T** *via* the complementary recognition sites, forming the catalytic ternary complex **[A•B•T]**. This binding event is governed by the equilibrium K_{TC} . This termolecular complex can bring the reactive sites on **A** and **B** into close proximity to facilitate

the covalent bond forming reaction to yield the product duplex $[T \cdot T]$. Again, as observed in the **AB** complex channel, by binding the starting materials to a template the reaction is rendered *pseudo*-unimolecular, and by controlling the approach of the reactive sites regio- and stereochemical control of the product is obtained. The product duplex formation is characterised by the rate constant k_{cat} . Once the product duplex $[T \cdot T]$ has been formed the system can be considered self-replicating. If the duplex $[T \cdot T]$ subsequently dissociates to return two free molecules of template to the start of the cycle, the reaction is then considered autocatalytic. It is this autocatalytic behaviour, which ideally leads to exponential growth (**Figure 1.9**) of the template concentration as two templates make four, four make eight and so on.

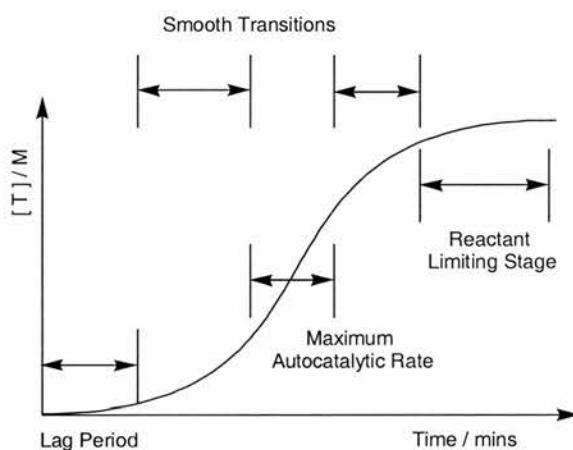


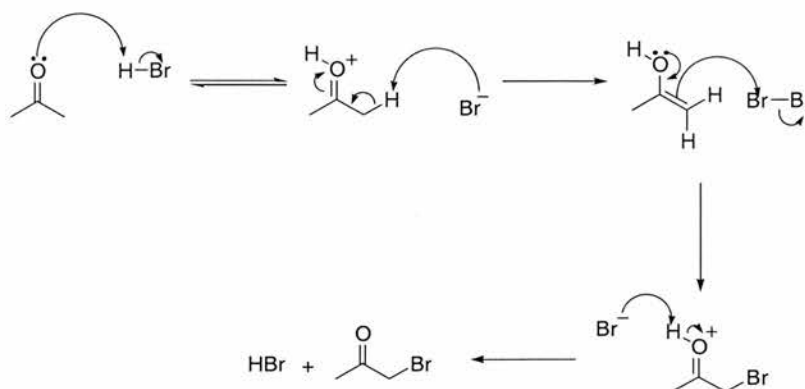
Figure 1.9 Rate curve expected for an ideal autocatalytic self-replicating system.

1.5.2 Complex stability

A major problem, which may be encountered with autocatalytic self-replicating systems, is that of complex stability. As mentioned previously in order for a self-replicating system to be considered autocatalytic, the product duplex needs to be unstable enough to dissociate and release the template molecules back into the autocatalytic cycle. However, the product duplex formed should be more strongly bound than the termolecular complex. This is because in the termolecular complex, three molecules are bound together *via* two complementary sites whereas in the product duplex only two molecules are bound *via* two complementary sites. This could potentially lead to the problem of a stable product duplex, which would hinder or prevent the release of the template molecules and so not complete the autocatalytic cycle. However, this system would still be considered self-replicating, as a parent molecule has constructed an exact copy of itself. This type of behaviour will be discussed further in **Chapter 2**.

1.5.3 Autocatalysis vs. general catalysis

At this point an important distinction should be made between an autocatalytic self-replicating system and a general autocatalytic system. An example of general catalysis is the bromination of acetone (**Scheme 1.7**).



Scheme 1.7 An example of an autocatalytic system showing the bromination of acetone.

The mechanism proceeds *via* attack of a bromide ion on one of the acidic α-protons on the protonated carbonyl to generate an enol and HBr. Nucleophilic attack of the double bond upon bromine generates an intermediate. Electrophilic attack of the bromonium ion on the intermediate yields the product 1-bromopropan-2-one. The by-product from this reaction, HBr, can catalyse the reaction by stabilising the intermediate as well as providing a conjugate base for the α-proton abstraction. However, in this type of catalysis there is no type of specificity within the system and any Bronsted acid would catalyse the reaction.

Self-replicating systems unlike general autocatalytic systems show a degree of specificity, and it is this, which forms the distinction between the two types of catalysis. In an ideal autocatalytic self-replicating system the product should only replicate itself possibly with complete regio- and stereoselectivity, whereas in general autocatalysis this selfish behaviour would not be seen.

1.6 [A•B] complexes

1.6.1 What are AB complexes?

It was from the study of self-replicating systems (**Section 1.7**) that an alternative competing pathway was identified, which can prevent a self-replicating pathway from occurring.

This alternative pathway involves [A•B] complexes, which also possess the ability to accelerate the rate and control the stereochemistry of a reaction. The self-complementary nature of the recognition motifs employed in template directed systems allows the two reactive partners to associate with each other within a bimolecular complex. This complex

may then hold the reactive sites in close proximity and actively accelerate the bond forming reaction.

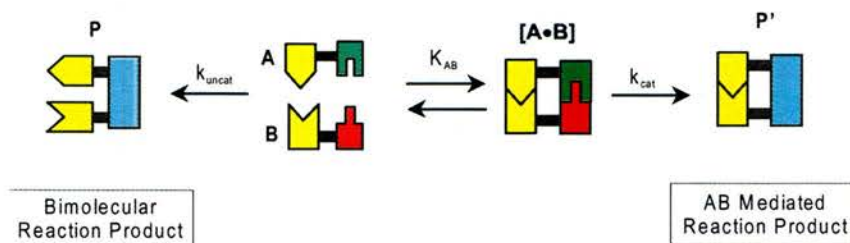
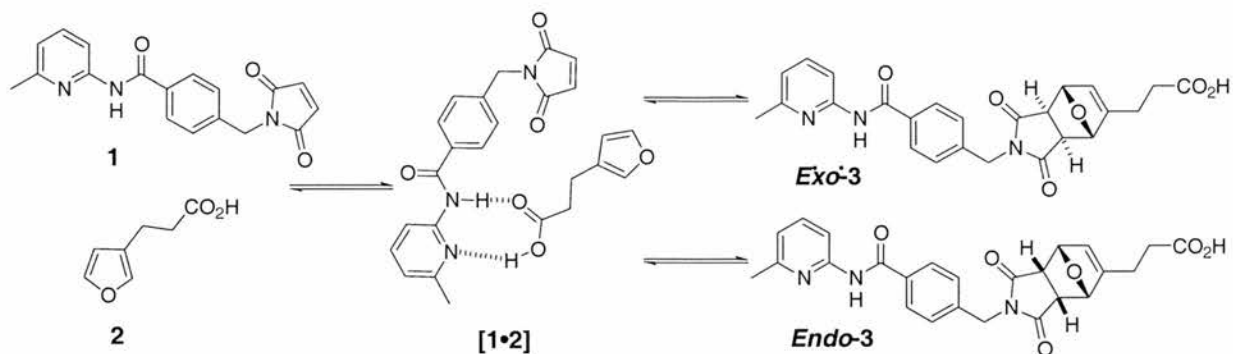


Figure 1.10 Schematic representation of an AB-mediated reaction pathway.

If there are complementary recognition sites located on the reactive partners **A** and **B** of a bimolecular reaction this allows **A** and **B** to associate with each other *via* a non-covalent interaction forming an **[A•B]** complex (**Figure 1.10**). If the reactive sites are held in a suitable geometry then reaction between **A** and **B** is now rendered *pseudo*-unimolecular, as opposed to bimolecular. By forming the binary complex the potentially unfavourable entropic cost of organising the reagents at the transition state is moved to a favourable binding event early in the reaction sequence, and so it could be expected^{43,44,62,71-74} to see significant rate acceleration. Also, by pre-organising⁷⁵ the reactive partners, the approach of the reactive sites is controlled and so stereo- and or regiochemical control of the reaction is achievable. This means that it could be possible to engineer such a reaction that proceeds through an **[A•B]** complex channel which affords a structurally different product **P'** from that obtained when the reaction between **A** and **B** proceeds *via* a simple bimolecular pathway to form product **P**. However, the product **P'** from an **[A•B]** complex generally retains the non-covalent intramolecular interactions, unlike the product from the bimolecular reaction.

In this type of system, the sigmoidal shape of the rate curve for a system which proceeds *via* the termolecular complex channel, is not present for an **[A•B]** complex route. This is because, the pre-formation of template is not required for catalysis, so there is no 'lag period' also an **[A•B]** complex is incapable of autocatalytic turnover and therefore there is no exponential growth.

Several examples of this type of rate enhancement have been published⁷⁶⁻⁸¹. Using this methodology Philp and Robertson^{76,78} designed a potential AB-system, utilising the Diels Alder reaction between a maleimide **1** and a furan **2** (**Scheme 1.8**).



Scheme 1.8 The use of an AB-complex to control and accelerate a Diels-Alder reaction between diene **2** and dienophile **1**.

The use of a Diels-Alder reaction allowed the stereoselectivity of the reaction to be investigated. The building blocks can associate through the recognition between an amidopyridine unit and a carboxylic acid. Association of the building blocks **1** and **2** affords the **[1·2]** complex. Upon analysis of this system by ^1H NMR, it was found that the *endo* isomer was favoured in a ratio of 600:1 (**Figure 1.11a**).

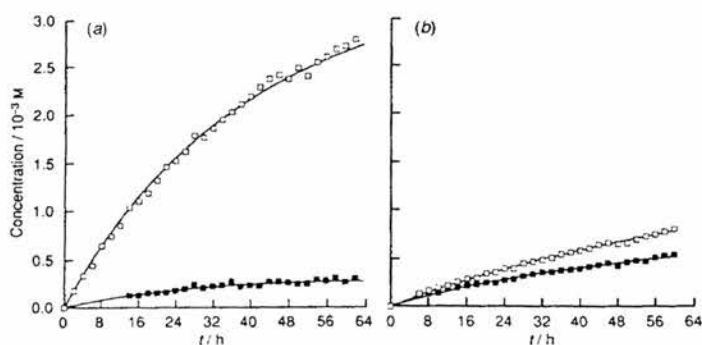


Figure 1.11 Rate profiles for a) the recognition mediated reaction between **1** and **2**, and b) bimolecular control reaction between **2** and **4**. The open squares represent the *endo* product and the closed squares represent the *exo* product. Figures taken from ref. 78.

A control reaction was performed where benzyl maleimide **4** was used to replace **1** (**Figure 1.12**), this does not contain a complementary binding site and so renders the **[A·B]** complex inactive. In the control reaction the high degree of selectivity was not observed (**Figure 1.11b**)

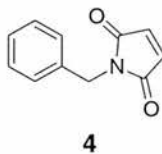


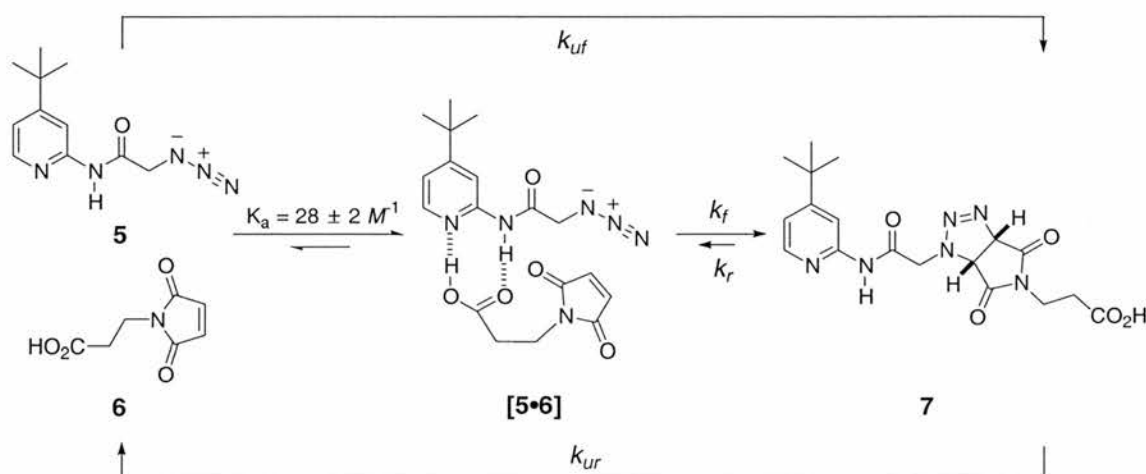
Figure 1.12 Control compound **4** used in the Diels-Alder reaction.

The high stereoselectivity was attributed to being a result of extra thermodynamic stabilisation present in the *endo*-product, arising from the intramolecular hydrogen bonding

available which was absent in the *exo* isomer as a result of the differences in molecular shape. A thermodynamic effective molarity of 11 M for this system was calculated, however the efficiency of the [A•B] complex gave only a kinetic effective molarity of 65 mM, which indicates that the [A•B] complex is inefficient at accelerating the cycloaddition reaction. Although this reaction does demonstrate the success in controlling and improving the stereochemical outcome of a reaction

1.6.2 Stereochemical control by transition state stabilisation

This system was based upon work previously carried out with the group⁸² Booth *et al.* used AB-methodology to accelerate the 1,3-dipolar cycloaddition reaction between azide **5** and maleimide **6** (Scheme 1.9).



Scheme 1.9 AB-mediated 1,3 dipolar cycloaddition between azide **5** and maleimide **6** to afford cycloadduct **7**.

In this system, hydrogen bonding between an amidopyridine and a carboxylic acid were employed to form the intramolecular complex [5•6]. Molecular mechanics calculations had indicated that the two hydrogen bonding interactions within the recognition motif would serve to pre-associate the reactive groups in a favourable orientation [5•6] for the subsequent cycloaddition to occur. In order to assess the extent of the effect that the recognition process has upon the rate of reaction for this system, it was necessary to measure the extent of the bimolecular reaction and for this the control compound **8** was employed (Figure 1.13).

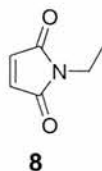


Figure 1.13 The control compound **8** used to demonstrate the bimolecular reaction with **5** in comparison to the recognition-mediated reaction between **6** and **5**.

In the control compound, the hydrogen-bonding site has been removed and hence **8** is unable to associate with **5** to form the reactive binary $[A \cdot B]$ complex that is required for the reaction to proceed *via* a *pseudo*-unimolecular pathway.

Optimum conditions were found to be at a concentration of 50 mM with respect to all reagents in $CDCl_3$ and the reaction was performed at 50°C. When the bimolecular and recognition reactions were studied under these conditions it was found that the rate of product formation for the AB-mediated reaction between **5** and **6** (**Figure 1.14**) was considerably faster than that of the bimolecular reaction between **5** and **8**.

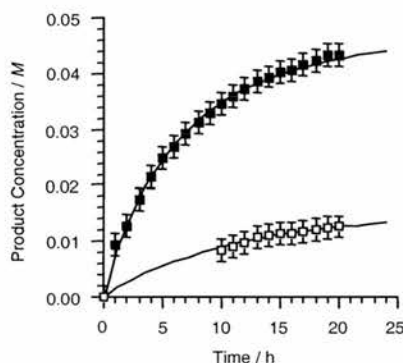


Figure 1.14 Concentration-time profile for the recognition-mediated reaction between **5** and **6** (solid squares) and the bimolecular control reaction between **5** and **8** (open squares) performed in $CDCl_3$ at 50°C at a concentration of 50 mM with respect to all reagents. Solid lines represent the best fit of the appropriate kinetic model to the experimental data. Figure taken from ref. 83.

Determination of the kinetic and thermodynamic effective molarities (kEM and tEM) will reveal whether the observed rate enhancement is due to either a transition state stabilisation or product stabilisation.

The kEM is a direct comparison of the forward rate of the recognition-mediated reaction (k_f) and the forward rate of the corresponding uncatalysed bimolecular reaction (k_{uf}) (**Equation 1.2**).

$$\text{kEM} = \frac{k_f}{k_{uf}} = \frac{\text{s}^{-1}}{\text{M}^1\text{s}^{-1}} = M$$

Equation 1.2 Kinetic effective molarity (kEM) expressed in M and where k_f and k_{uf} represent the forward rate of the AB-mediated and bimolecular reaction respectively.

The kEM represents transition state stabilisation, and if this is the dominating effect with an AB-mediated system then **A** and **B** are said to be *pre-organised* to react with each other.

The tEM is a direct comparison of the equilibrium constants of the recognition-mediated reaction (K_{AB}) and the corresponding uncatalysed bimolecular reaction (K_{BI}) (**Equation 1.3**).

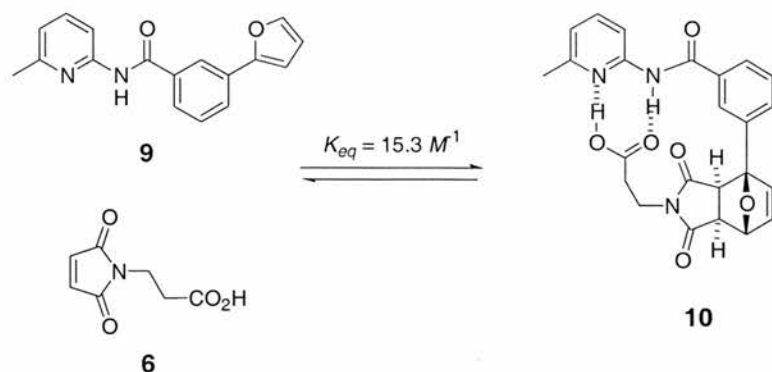
$$\text{tEM} = \frac{K_{AB}}{K_{BI}} = \frac{k_f}{k_r} \times \frac{k_{ur}}{k_{uf}} = \frac{\text{s}^{-1} \times \text{s}^{-1}}{\text{s}^{-1} \times \text{M}^1\text{s}^{-1}} = M$$

Equation 1.3 Calculation of the thermodynamic effective molarity (tEM), where K_{AB} and K_{BI} represent the equilibrium constant of the AB-mediated and bimolecular reactions respectively. k_f , k_r , k_{uf} and k_{ur} represent the forward and backward rate constants associated with the recognition-mediated and bimolecular reactions, respectively.

If the tEM is the dominating effect within an AB-mediated reaction then **A** and **B** are said to be *predisposed* to react with each other. In a reversible reaction the tEM gives an indication of the stabilisation of the product ground state that is due to the recognition-mediated process. The thermodynamic and kinetic EM for the recognition-mediated process shown in **Scheme 1.9** were calculated to be 1.07 M and 2.16 M respectively. Therefore, consideration of the system shown in **Scheme 1.9**, it is clear that the dominating effect is the kEM and hence, the majority of the observed rate acceleration is due to the *pre-organisation* of the reactants in the transition state.

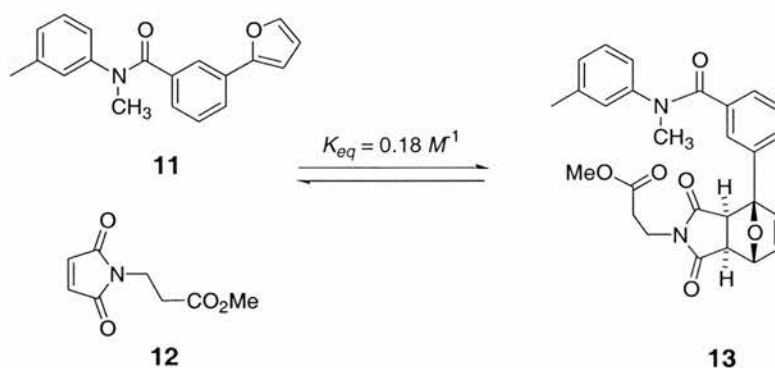
1.6.3 Stereochemical control by ground state stabilisation

The retained binding of the recognition sites of an **[A•B]** product is often seen as a disadvantage, however, it is this binding which can play a crucial role in the stabilisation of the ground state, which was utilised⁷⁹ by Philp and Bennes. In this system a Diels–Alder cycloaddition between a 2-aryl furan **9** and a maleimide **6** was investigated (**Scheme 1.10**).



Scheme 1.10 Recognition-mediated Diels-Alder reaction between furan **9** and maleimide **6**. K_{eq} represents the equilibrium constant for the reaction

In the absence of any recognition (**Scheme 1.11**) the reaction between furan **11** and maleimide **12** in CDCl_3 at 50°C resulted in less than 1% of the desired product **13** after 15 hours (**Figure 1.16**).



Scheme 1.11 Bimolecular Diels-Alder reaction between furan **11** and maleimide **12**. K_{eq} represents the equilibrium constant for the reaction.

Only the *exo* cycloadduct was observed, as would be expected, as it is the thermodynamically favoured product. The equilibrium constant was determined for the reaction at 100 mM in CDCl_3 at 50°C to be 0.18 M^{-1} . This result reflects the notoriously low reactivity of 2-arylfurans in Diels-Alder cycloaddition reactions due to the high levels of π -conjugation on the furan needed to be disrupted in order to undergo cycloaddition. As a consequence the equilibrium lies to the left, favouring the starting materials. It should be noted that only the *exo* cycloadduct was formed. In the presence of recognition, a very different result was obtained. In this case the reactants incorporate two hydrogen-bonding sites, a carboxylic acid and an amidopyridine, which can associate to form a binary complex between **6** and **9**. Within this complex the reactive sites are brought into close proximity and in the correct orientation to allow the [4+2] cycloaddition to proceed. In this system the equilibrium is shifted in favour of the product **10** with $K_{eq} = 15.3\text{ M}^{-1}$, hence the tEM is 85 M. The rate profile is shown in **Figure 1.15**.

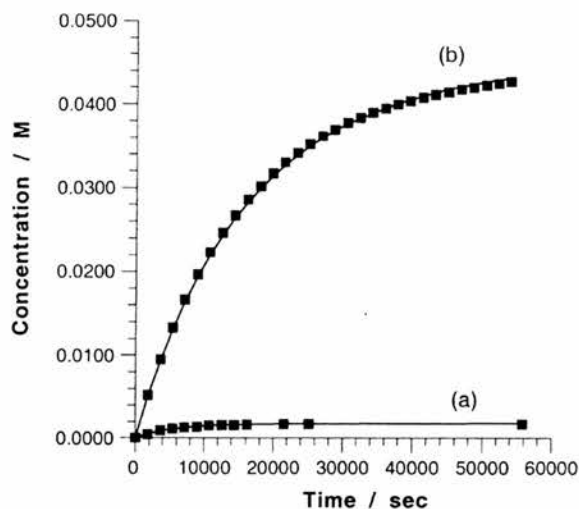
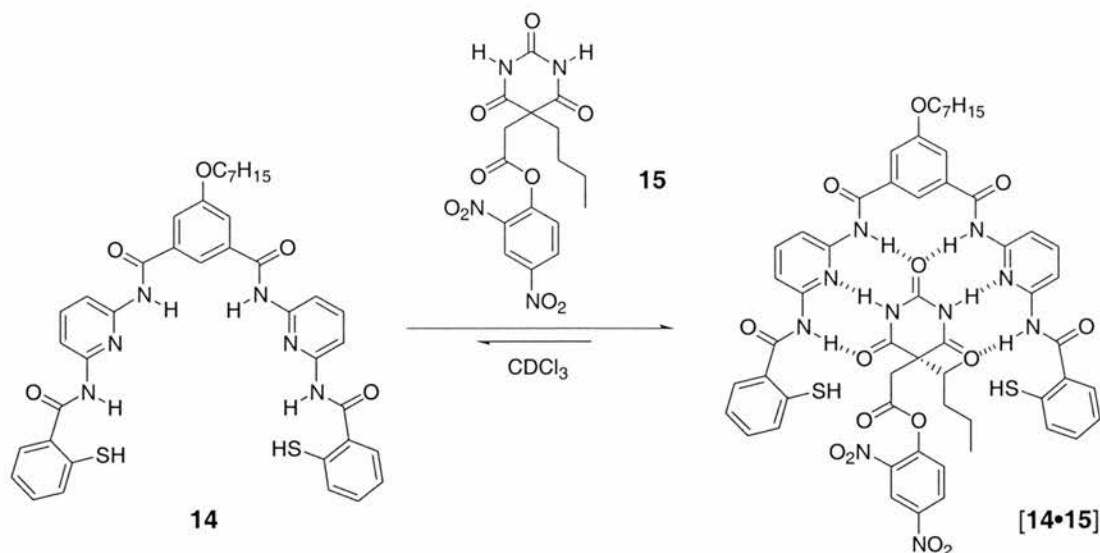


Figure 1.15 Rate profiles for the Diels-Alder reactions between (a) **11** and **12** and (b) **6** and **9**. Reactions undertaken at 100 mM in CDCl₃ at 50 °C. Figure taken from ref. 79.

The recognition mediated system shows that a normally disfavoured reaction can be altered to become a favoured reaction by employing a simple hydrogen-bonding motif. Again only one product is observed, the *exo* cycloadduct. Analysis of the cycloadduct **10** by using ¹H NMR and crystallographic data showed that the molecular recognition persisted within the reaction product. They concluded by stating that the **AB** complex reactivity not only facilitated the extent to which the reaction proceeded, but also accelerated the rate at which the position of equilibrium was achieved.

Another successful approach to **AB** methodology was designed by Hamilton *et al.*⁸⁰. This system involves a barbiturate receptor **14** (**Scheme 1.12**) with an appended thiol that was capable of binding activated ester **15**. The recognition motif utilised in this system is a hexahydrogen bonding motif between two 2,6-diaminopyridine units linked *via* an isophthalate spacer⁸⁴ and the pyrimidine trione.

It was suggested through molecular mechanics calculations on the binary complex [**14**•**15**], that upon binding of **14** and **15** a significant rate acceleration of the subsequent thiolysis reaction due to the enforced proximity of the ester and catalytic thiol functionality would be observed. Experimentally it was observed that a rate enhancement of 10⁴-fold was obtained through the recognition-mediated reaction compared to the analogous bimolecular reaction between **15** and **16** (**Figure 1.16**).



Scheme 1.12 Hamilton's barbiturate receptor **14**, which is capable of accelerating an acyl transfer reaction in the presence of activated ester **15**.

This is an excellent rate enhancement which shows that the rate achieved by nature are attainable by the synthetic chemist. Hamilton has continued his work⁸⁵⁻⁸⁸ in this area and designed and synthesised a series of receptors.

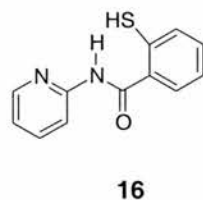


Figure 1.16 Control compound **16** used in Hamilton's system to represent the bimolecular reaction by replacing **14**.

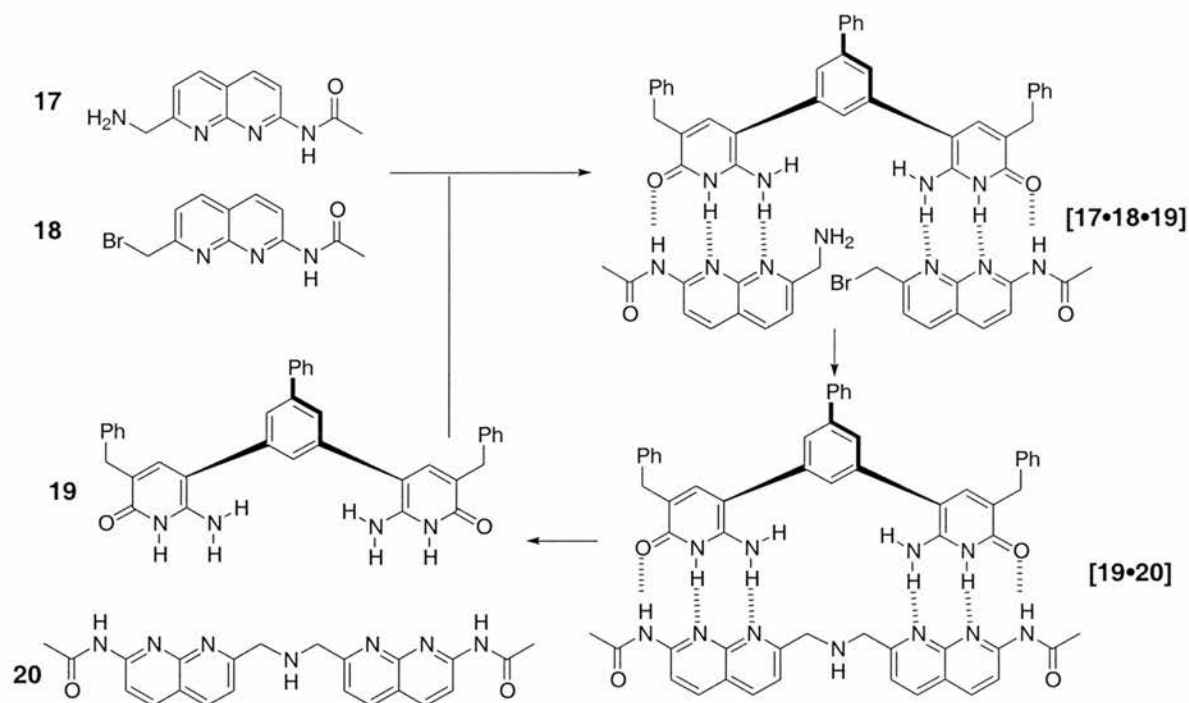
1.7 Template-directed control and acceleration of chemical reactions

In **Section 1.8** the use of templates will be described in the formation of self-replicating systems, however there are a few examples of synthetic systems, which utilise a template to enhance product formation.

An example of a template-directed synthesis was reported^{89,90} by Kelly *et al.* The system designed involved a completely synthetic template **19** that could accelerate a simple $\text{S}_{\text{N}}2$ alkylation of a primary amine **17** by an alkyl halide **18** (**Scheme 1.13**).

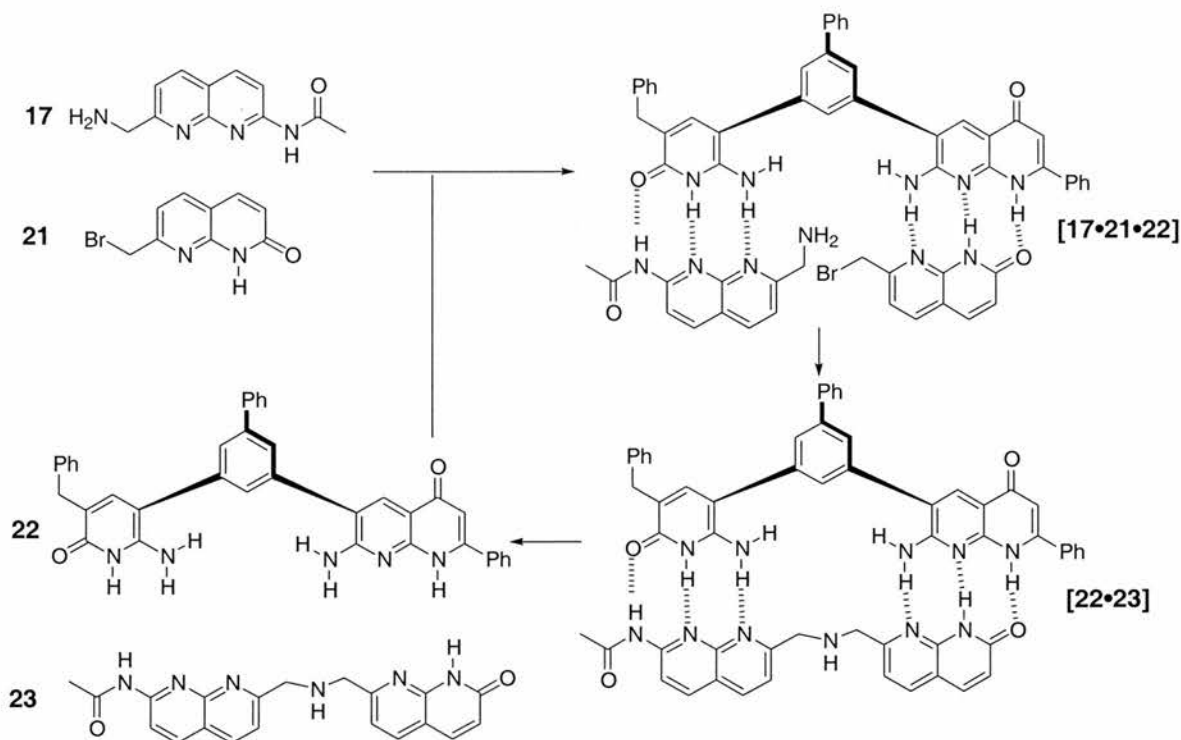
The template contains two naphthyridine recognition sites that can associate with the reactive components **17** and **18** through complementary recognition sites, which in this case involves a triple hydrogen bonded motif. The highly directional nature of the recognition motif allows the template to efficiently pre-organise the substrates within the ternary complex **[17•18•19]**. This allows the reactive sites to come into close proximity, in order to react. It was found that

at 298K in CDCl_3 the rate of the $\text{S}_{\text{N}}2$ reaction was enhanced 6-fold in the presence of an equimolar quantity of the template **19**, compared to the uncatalysed reaction between the amine **17** and the alkyl bromide **18**.



Scheme 1.13 The recognition-mediated reaction of **17** and **18**, forming the fused product **20**. The formation of the catalytic ternary complex is directed by the host template **19**. Reagents and conditions: the initial concentration of reactive components was 4 mM, *d*-chloroform, 25°C.

It was unclear from this system however as to whether turnover of the catalyst is achieved, but it is observed that the product **20** is precipitated from the reaction mixture as its hydrobromide salt, and so not inhibiting the catalyst. Therefore the template must be returned unbound to the reaction mixture. Kelly *et al.* then improved the efficiency of the system through a simple synthetic modification. It was thought that due to the identical nature of the recognition sites on the substrates that the template could not distinguish between them and so catalysis could be hindered due to the formation of unproductive ternary complexes **[17•17•19]** or **[18•18•19]**. In order to overcome this problem the design of the template **19** and substrate **18** as modified to alter the recognition motifs so that they were specific to each substrate. This led to the synthesis of template **22** and substrate **21** (**Scheme 1.14**). The preassociation of template **22** with substrates **17** and **21** can now only form one ternary complex **[17•21•22]**. The reaction was again performed at 298K in CDCl_3 in the presence of **22** and it resulted in a 12-fold increase in the rate of reaction compared to the bimolecular reaction between **17** and **21**.



Scheme 1.14 The recognition-mediated reaction of **17** and **21**, forming the fused product **23**. The formation of the catalytic ternary complex is directed by the host template **22**. Reagents and conditions: the initial concentration of reactive components was 4 mM, *d*-chloroform, 25°C.

In order to make a fair comparison between the two systems to assess the relative efficiencies the association of the recognition motifs must be considered. The binding between the alkyl bromide **21** and template **22** ($K_{\text{assoc}} = 4.4 \times 10^2 M^{-1}$) is weaker than that between alkyl bromide **18** and template **19** ($K_{\text{assoc}} = 1.7 \times 10^4 M^{-1}$). This means that the relative population of the respective ternary complexes will differ between the two systems. It was calculated that the percentage of the ternary complex [17•18•19] present in the first system was 84%, whereas the percentage of the ternary complex [17•22•23] was 41% in the second system. This suggests that the ternary complex [17•22•23] is actually four times more efficient than [17•18•19] in catalysing the S_N2 alkylation.

However, the rate enhancement is quite disappointing especially if compared to that achieved by enzymes, a reason proposed for the poor acceleration in both systems is the inability of the template to hold the substrates in an effective transition state.

1.8 The evolution of self-replicating systems

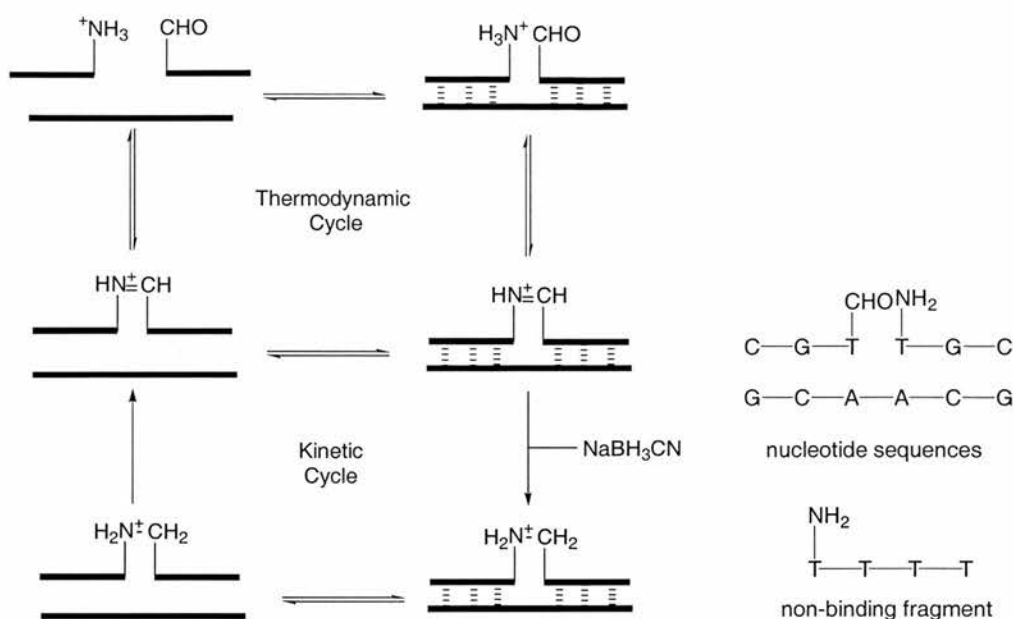
1.8.1 Natural product based self-replicating systems

The field of self-replication owes its existence to natural biological systems and so it was from these systems where the first natural analogues of replicators began, in particular RNA. The first reported non-enzymatic catalytic system was reported by Schramm *et al.*⁹¹ in 1962. This system involved the synthesis of polynucleotides *in vitro*. The polymerization of uridylic acid, activated by polyphosphate ester, in the presence and absence of its complementary species polyadenylic acid was studied. It was found that in the presence of polyadenylic acid the polymerization of uridylic acid was accelerated more than 10-fold whereas in the presence of polyuridylic acid has no such effect. This led Schramm *et al.* to the conclusion that that this kind of non-enzymatic formation of oligonucleotides could be involved in the self-replicating cycles in the prebiotic earth, in which the formation of nucleotide strands carried certain selective advantages, they favoured the formation of the complementary strand by a templating effect, and the complementary strand in turn enhanced the formation of the original strand.

Gilham *et al.* reported a more convincing experiment in 1966, by looking at the interactions and reaction of oligonucleotides in aqueous solution⁹². The experiment involved using a mixture of thymidine hexanucleotide and polyadenylic acid with an activating diimide in aqueous solution. The synthesis of thymidine dodecanucleotide was achieved in a 5% yield, however when the polyadenylic acid was omitted from the reaction no dodecanucleotide was produced. This result demonstrated that the hexanucleotides bound to polyadenylic acid gave a head to tail 'Watson – Crick' arrangement which results in close proximity between 5'-phosphate and the 3'-hydroxyl groups of adjacent residues.

Extensive research into nonenzymatic synthesis of oligonucleotides by using templates was performed by Orgel *et al.*⁹³⁻⁹⁸ during the 1970's and 1980's. Orgel⁹⁹ was able to demonstrate information transfer by starting with a mixture of two activated mononucleotides, guanosine 5'-phospho-2-methylimidazolide and cytidine 5'-phospho-2-methylimidazolide, and the pentanucleotide C-C-G-C-C as a template. The major product formed in a 17% yield and had the sequence pG-G-C-G-G. This demonstrates that a template with a definite sequence can catalyse the synthesis of its complementary strand under non-enzymatic conditions.

An elegant example of thermodynamic templating was reported by Goodwin and Lynn¹⁰⁰. The system reported involves a hexanucleotide template, which directs the synthesis of a non-identical hexanucleotide. The system utilises a reversible imine bond formation to perform the covalent linkage of the substrates. After ligation, the new covalent bond is fixed by reduction with NaBH₃CN to the secondary amine (**Scheme 1.15**).



Scheme 1.15 The recognition-mediated reaction between the trinucleotides shown above to form the fused product.

The reversible bond-forming step allows the products to reach a thermodynamic equilibrium before fixing, and removal from the thermodynamic cycle. When the reaction was performed in the presence of template and a competitive non-complementary oligomer the reaction performed at 0°C was more selective and produced a greater yield than when the reaction was performed at room temperature. It was concluded that the reaction proceeds under template-mediated thermodynamic control (**Figure 1.17**).

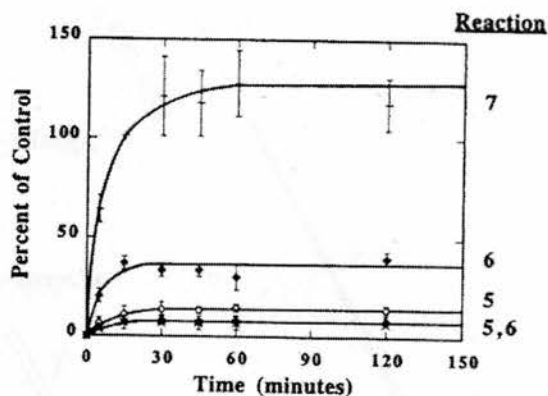
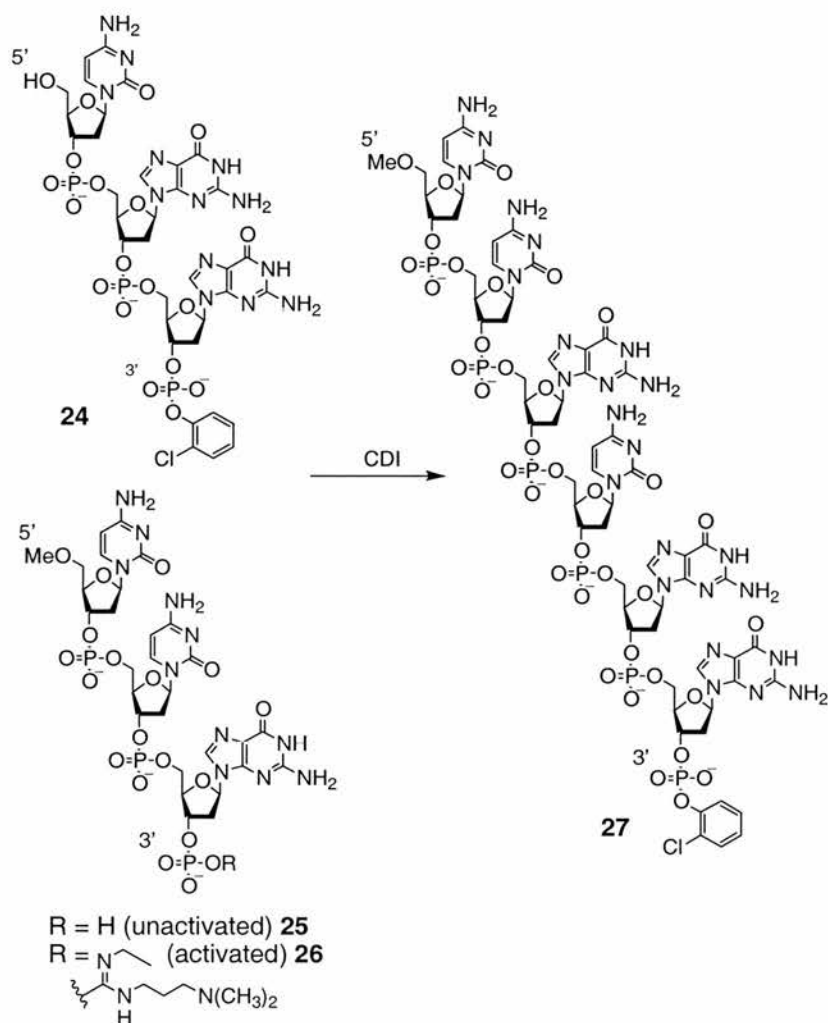


Figure 1.17 Template reactions 5 and 6 (as labelled) performed at room temperature and template reaction 7 performed at 0°C. Values are concentration as a percentage of the corresponding control reaction performed. Figure taken from ref. 99.

The work reported so far only investigated reciprocal systems where complementary strands were produced; von Kiedrowski *et al.* reported¹⁰¹ the first example of a true self-replicating system in 1986.

The minimal self-replicating system was based on deoxyribonucleotides oligomers (**Scheme 1.16**). The template is the hexadeoxynucleotide **27** with a 5'-CCGCGG-3' base sequence, protected at its 5' terminus by a methyl ether and at the 3' terminus with an *o*-chlorophenyl group to prevent ligation at the template termini. The starting materials are two trideoxynucleotides of sequences 5'-CCG-3' **25** and 5'-CGG-3' **24**. Recognition between the template and the building blocks occurred *via* strong cytosine-guanine base pairing.



Scheme 1.16 Kiedrowski's minimal self-replicating system based upon a hexadeoxynucleotide.

Activation of the hydroxy group at the 3'-phosphate position of **25** was undertaken using 1-(3-dimethylaminopropyl)-3-ethylcarbodiimide (CDI) affording the carbodiimide adduct. Once the hydroxy group was activated as the carbodiimide adduct, the condensation reaction with phosphate **24** could then take place. This reaction was aided by the fact that the two starting

materials would be bound on to the template to form a ternary complex, and that it resulted in the formation of a palindromic product duplex. The newly formed hexamer was not only a complementary strand of template, but also a template itself. Therefore, dissociation of this product duplex would then result in turnover within the reaction mixture. However upon kinetic analysis of this reaction by HPLC it was noted that a sigmoidal rate profile for the reaction was not observed (**Figure 1.18**) and the rate of formation was extremely slow, with only a 12% yield of product **27** formed after 4 days.

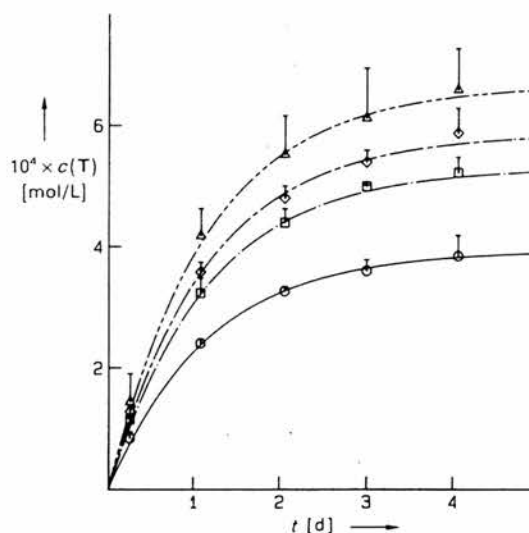


Figure 1.18 Time course of template **27** production in reaction mixtures containing different initial concentrations of template. Circles = 0 mM, squares = 0.2 mM (1 eq.), diamonds = 0.4 mM (2 eq.) and triangles = 0.8 mM (4 eq.). Figure taken from ref. 101.

The lack of a sigmoidal rate profile and poor yield was attributed to a number of factors. Firstly, von Kiedrowski proposed that the CDI activated phosphate functionality on **26** is rapidly hydrolysed under the conditions employed, even though a 17-fold excess of CDI was used to try to avoid this problem. Secondly, there is the possibility of a number of unreactive binding events, which may occur within this system. For example, **26** could bind to **25** through their complementary base pairs to form the unproductive dimer [**24•25**], which would inhibit the formation of the template **27** and so hinder autocatalysis. Also, within this system there is no preference for the ternary complex to bind with the activated **26** or unactivated **25** building blocks, and so this may lead to an unproductive [**25•26•27**] ternary complex. Furthermore the reaction mixture gave rise to an unwanted side product of a 5'-CCGGCC-5' sequence which resulted from the self-condensation of **26**. This compound is also capable of non-productive binding between itself and the building blocks.

However, even though a sigmoidal rate profile was not obtained von Kiedrowski demonstrated the importance of the template directed pathway by the external addition of various amounts of pre-formed template at the start of the reaction (**Figure 1.19**). This

addition gave rise to an increase in the initial rate of formation of template, but did not dramatically improve the overall percentage conversion of the starting materials to template. It was concluded that the high stability of the product duplex [27•27] was responsible for the lack of turnover within this system. Hence, this system could be described as self-replicating but with an extremely inefficient autocatalytic behaviour.

Von Kiedrowski demonstrated that the kinetics of his system could be described by the **Equation 1.4**.

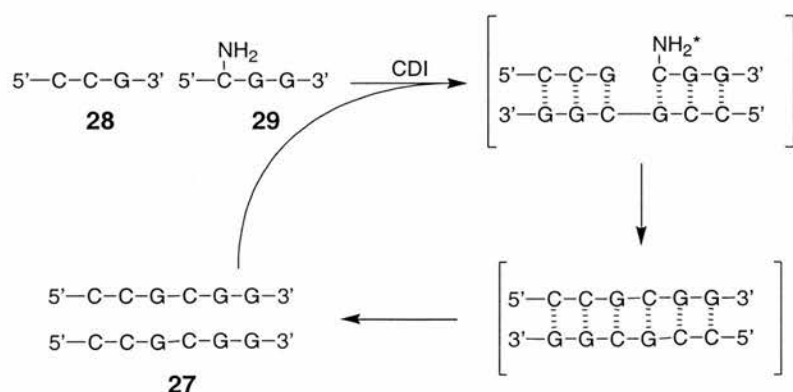
$$\{d[T]/dt\}_{\text{initial}} = k_a [T]_0^p + k_b$$

Equation 1.4 Equation used by von Kiedrowski to describe the kinetics of self-replicating system.

Where $[T]_0$ represents the concentration of the added template and k_a is the rate constant of the catalytic process, p is the reaction order with respect to T and k_b is the *pseudo* zero order rate constant for the non-catalysed reaction.

Using least-squares curve fitting, von Kiedrowski obtained a best-fit value for p of 0.48 and used this value to assume a reaction order of $1/2$ with respect to the initial stages of the reaction.

In an attempt to try and create a more efficient system, von Kiedrowski *et al.* made a slight alteration¹⁰² to the original system. The original base sequence was kept the same but the hydroxyl functionality on **24** was replaced by an amine group **29** (**Scheme 1.17**), and the 5' terminus of **26** was protected with a methylthiomethyl group to give **28**.



Scheme 1.17 Schematic representation of a self-replicating system⁸⁸ developed by von Kiedrowski.

Again the coupling is catalysed by CDI, however this time the system exhibits a sigmoidal rate profile for the formation of template **27** (**Figure 1.20**). In addition the hexameric template **27** was reported to be the only product of the reaction. The rate of reaction for this new

modified reaction was much faster than the original, in this case the reaction reached approximately 50% conversion to template **27** in just 2 hours. The behavioural change was attributed to the change in the rate of ligation between the two building blocks when changing the 5' group of **26** from a hydroxyl to an amine **29**. Von Kiedrowski also states that the shape of the curve is not a result of the sequential activation, as this process would only take a couple of minutes to reach equilibrium, whereas the inflection does not occur until about 15 minutes into the reaction.

The templating effects on the system were investigated by performing the reaction in the presence of preformed template. However, the preformed template was modified to include the 5' terminus being protected as the methyl ether and the ligation between the central base units being a simple phosphoester. The justification for these alterations are unclear, however its use does lead to an enhancement in the rate of formation of template **27** and the disappearance of the sigmoidal curve (**Figure 1.19**).

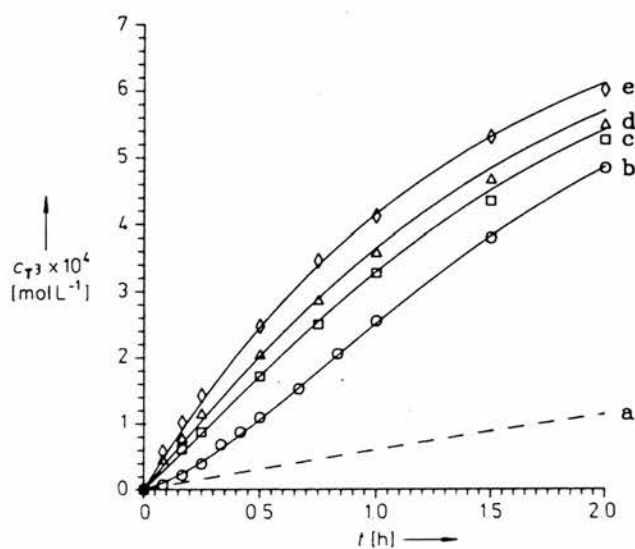
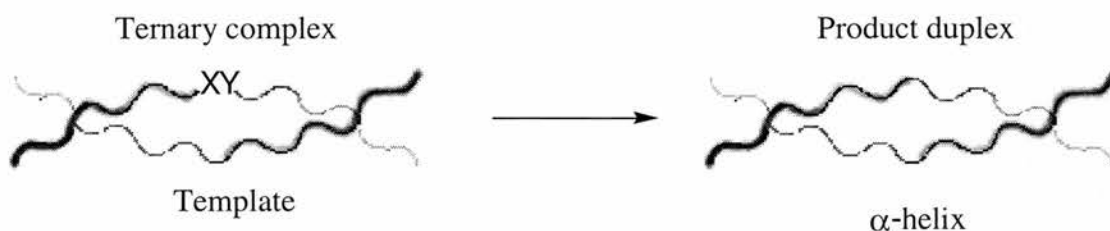


Figure 1.19 Rate profiles obtained for the formation of phosphoramidate template **27**. b = rate of formation of **27** in the absence of added template, c-e = rate of formation of template **27** with increasing amounts of pre-formed modified template and a = theoretical calculation for the rate of the uncatyalsed bimolecular reaction. Figure taken from ref. 100.

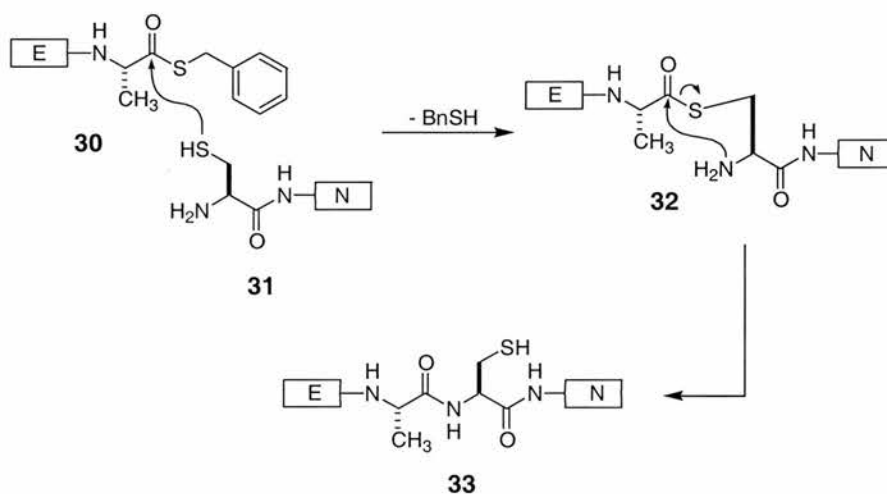
This system was the first reported self-replicating system to exhibit a sigmoidal curve. Von Kiedrowski describes the growth of the template in the system as parabolic due to the production of template with a reaction order of $\frac{1}{2}$ in its rate expression and so can be described as a second order with respect to the early reaction times. Parabolic growth infers that a significant amount of product inhibition is still present within the system, and so even though a sigmoidal curve is still obtained this indicates that the system exhibits an unusually strong template directed catalysis¹⁰³.

The use of natural product based systems as self-replicating systems has been the focus of other groups¹⁰⁴⁻¹⁰⁶ in particular Ghadiri and co-workers^{107, 108} devised a system which is based on a polypeptide framework that relied on both the peptide sequence and structure for molecular recognition. A 32-residue 'leucine zipper' peptide sequence was employed to induce molecular recognition by acting as the template. The leucine zipper can form an α -helical coiled coil consisting of two identical α -helical peptides that wrap around each other. The template strand assembles a 15 and 17 residue strand orientation that brings the reactive sites, an amine and an activated benzylthio ester, together for ligation *via* condensation thus creating a template duplex (**Scheme 1.18**).



Scheme 1.18 Use of an α -helix as a self-replicating template. X and Y represent the two reactive sites.

The bond-forming step is based on the condensation strategy developed by Kent¹⁰⁹, which requires a cysteine residue at the ligation site. The thioester of the cysteine attacks the thiobenzyl ester of the complementary building block before being displaced by the amine to form the amide link (**Scheme 1.19**).



Scheme 1.19 Mechanism of the condensation reaction. E represents the electrophilic peptide sequence and N represents the nucleophilic peptide sequence.

Analysis of the reaction profile for the formation of template showed no sigmoidal character however upon addition of preformed template to the reaction mixture, an increase in the rate

of formation of template was evident, demonstrating that the reaction proceeds *via* a template directed mechanism (**Figure 1.20**).

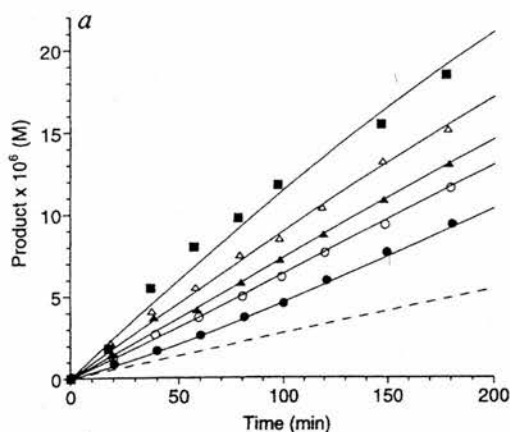


Figure 1.20 Rate of formation of template **32** vs. time, filled circles = 0 μM , open circles = 5 μM , filled triangles = 10 μM , open triangles = 20 μM , filled squares = 40 μM added template **33**. Figure taken from ref. 109.

The data shown gives a reasonable fit to the square root law, which demonstrated a degree of turnover within the reaction, but also reflected some product inhibition, presumably as a result of template aggregation.

The lack of sigmoidal character could be attributed to processing errors of the HPLC chromatograph, especially at low concentrations. On inspection of the chromatograph at $t=14$ minutes, two small peaks flank the product peak (**Figure 1.21**) one of which is attributed to the hydrolysis product and the other is unidentified.

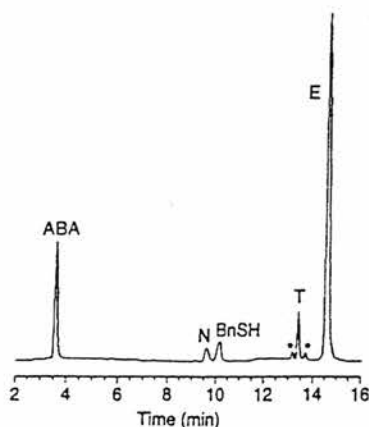


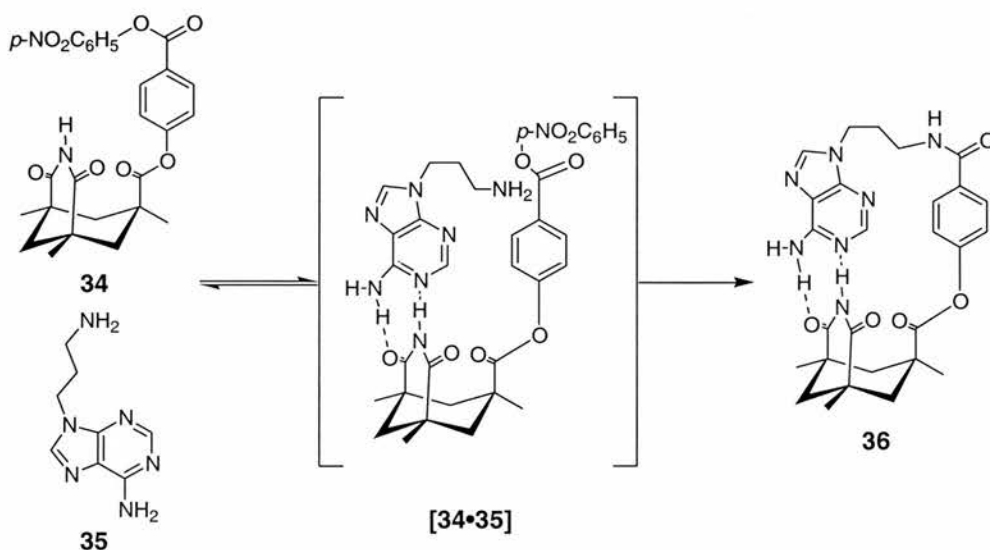
Figure 1.21 HPLC chromatogram obtained for the reaction, E represents the electrophilic peptide fragment **31**, N represents the nucleophilic peptide fragment **30**, BnSH is benzyl mercaptan, T represents the template **33** and * represents the two impurities within the reaction mixture. Figure taken from ref. 109.

To confirm that the reaction was template directed Ghadiri *et al.* went on to perform a number of control experiments. The first was to use ‘crippled’ templates that contained sequence

mutations that would disrupt the binding of either one of the building blocks. The second was to use guanidinium hydrochloride in a buffered solution to disrupt the formation of the α -helix. In both cases the rate of formation of template was not catalysed which led to the conclusion that template formation proceeded *via* a recognition-mediated pathway and *via* a catalytic ternary complex.

1.8.2 Synthetic approach to self-replicating systems^{67, 110-114}

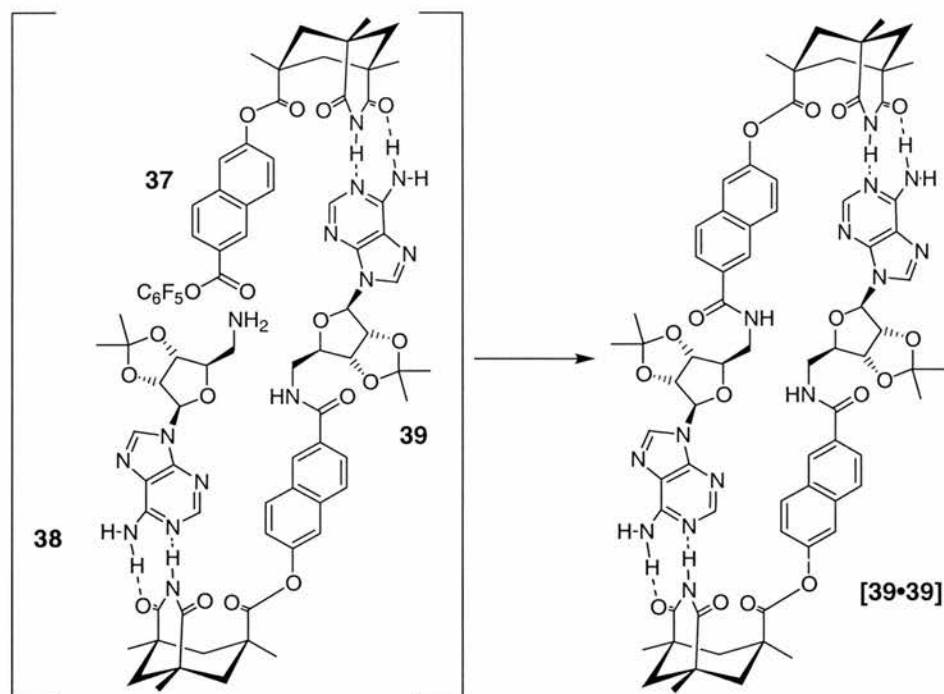
As an alternative route to self-replicating systems, purely synthetic systems were employed. The first of which were devised by Rebek *et al.*¹¹⁵⁻¹¹⁷ Rebek developed¹¹⁸ the first fully synthetic system which contained all the requirements for a template of a minimal self-replicating system. The first attempt was based around molecular recognition between an imide of Kemp's triacid¹¹⁹ **34** bearing an acyl functionality, protected as the *p*-nitrophenyl ester, and an adenine unit **35** bearing an amino alkyl group. The reaction between the two building blocks results in the formation of amide **36** (Scheme 1.20). It was hoped that **36** would then go on to template its own formation. However upon analysis of the system, it was noted that the short phenyl spacer unit, along with the formation of the favoured *trans* amide, resulted in a reactive AB-complex pathway and the template **36** instead retained the intramolecular non-covalent interactions.



Scheme 1.20 The reactive AB-complex system designed by Rebek, incorporating a phenyl spacer.

Rebek then modified¹¹⁵ this system by replacing the phenyl spacer with a naphthalene **39** in an attempt to separate the two reactive groups and so prevent the reaction from occurring *via* the AB-pathway. The system was also modified by introducing a ribosyl adenine in compound **38** whose role was to provide a bulky substituents and thus aid the dissociation of

the product duplex [39•39] (Scheme 1.21). The product duplex observed a dimerisation constant of 630 M^{-1} which was expected for the base pairing and aryl stacking with steric interactions, this then enabled the duplex to dissociate to release free template into solution (Scheme 1.21).



Scheme 1.21 Reбек's synthetic self-replicating system incorporating a template with a naphthalene spacer **39** showing the two building blocks **37** and **38** assembled on the template to give the catalytic ternary complex and the resulting product **39**.

To prove that the system is self-replicating, Reбек performed a number of control experiments, which involved; the addition of a competitive binding compound, which led to a decrease in the rate of formation of template; the use of a non-binding control compound (methylation of the imide) which was used to mimic the bimolecular reaction; and addition of 0.2 and 0.5 equivalents of preformed template which enhances the initial rate of reaction (Figure 1.22).

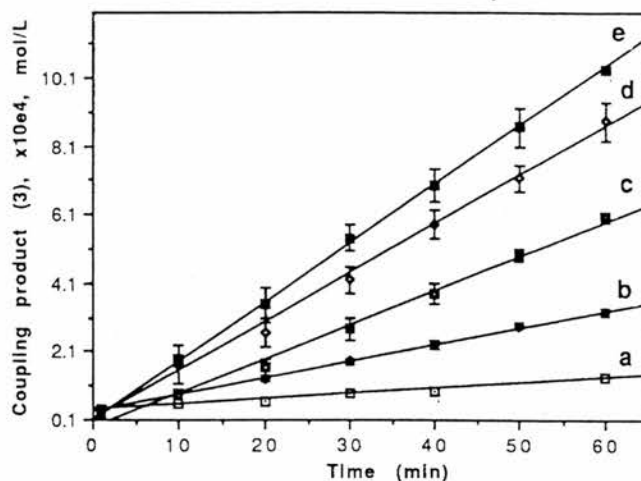


Figure 1.22 Rate of production of template **39** (a) using a non-binding control compound, (b) using a competitive binding compound, (c) with only the building blocks, (d) with 0.2 eq. of added template **39**, (e) with 0.5 eq. of added template **39**. Figure taken from ref. 119.

Rebek went on to conclude¹¹⁶ that the reason for the lack of sigmoidal character was due to the action of an AB-complex and contributions from “systematic” errors. He reasoned that the AB-complex pathway would form the *cis* amide product, which upon isomerisation to the *trans* conformation would then yield free template, which would be capable of catalysing the reaction *via* a ternary complex. Rebek and co-workers estimated an association constant of $3600 M^{-2}$ for the termolecular complex and so calculated that only 2% of the building blocks were assembled in the termolecular complex. This suggested that the template must be an effective catalyst to catalyse its own formation from such a small quantity of catalytic complex.

Rebek’s next modification¹¹⁷ of this system was to replace the naphthyl spacer with a biphenyl spacer. This increase in length was an attempt to separate the reactive centres and so eliminate the AB-complex pathway (**Figure 1.23**).

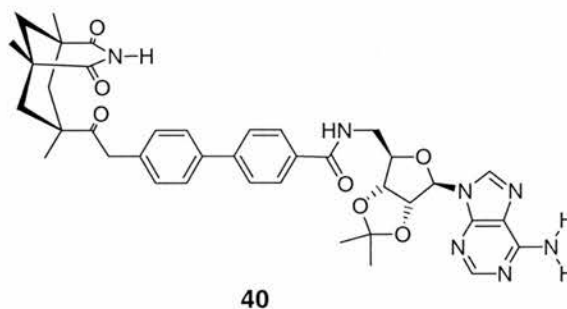


Figure 1.23 Template **40** incorporating a biphenyl spacer.

Upon analysis, the rate of formation of **40**, gave rise to a sigmoidal curve (**Figure 1.24**), which suggests an efficient autocatalytic self-replicating system.

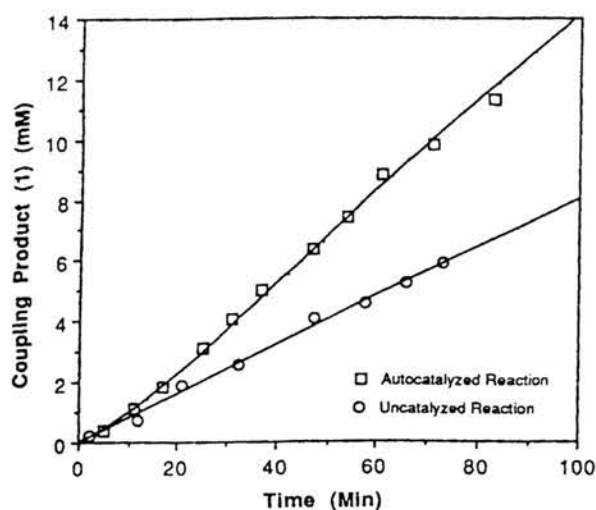
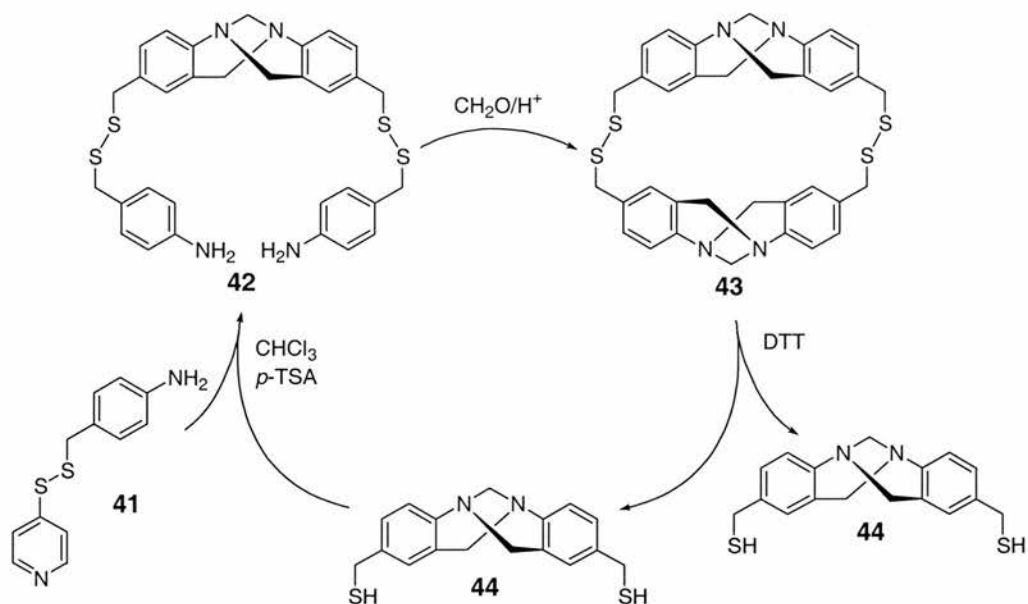


Figure 1.24 Rate of formation of template **40**. Open squares represent the recognition-mediated reaction and the open circles represent the control reaction. Figure taken from ref. 117.

Rebek's work on self-replicating systems has resulted in much controversy¹²⁰⁻¹²⁴. Having reported a new self-replicating template Rebek *et al.* attempted to demonstrate some simple principles of evolution using their system¹²⁵. By addition of a bulky group to the adenosine amine function of the 'amine' building block, they apparently reduced the binding constant between the partially blocked adenosine and the imide, although no actual binding studies have been reported. It was shown that the Watson-Crick binding mode was interrupted and not the Hoogsteen mode, but why both were not interrupted is unclear from the diagrams and data. Rebek¹²⁶ continues the comparison of these self-replicating systems and extrabiological chemistry.

Rebek continued with his work on template effects, self-replication¹²⁷⁻¹²⁹ and moved into the area of reciprocal template¹³⁰ effects.

Another example of a synthetic self-replicating system was published by von Kiedrowski¹³¹ and Bag. In this system the self-replication was undertaken in a stepwise manner to form a Tröger's base analogue **44** (Scheme 1.22).



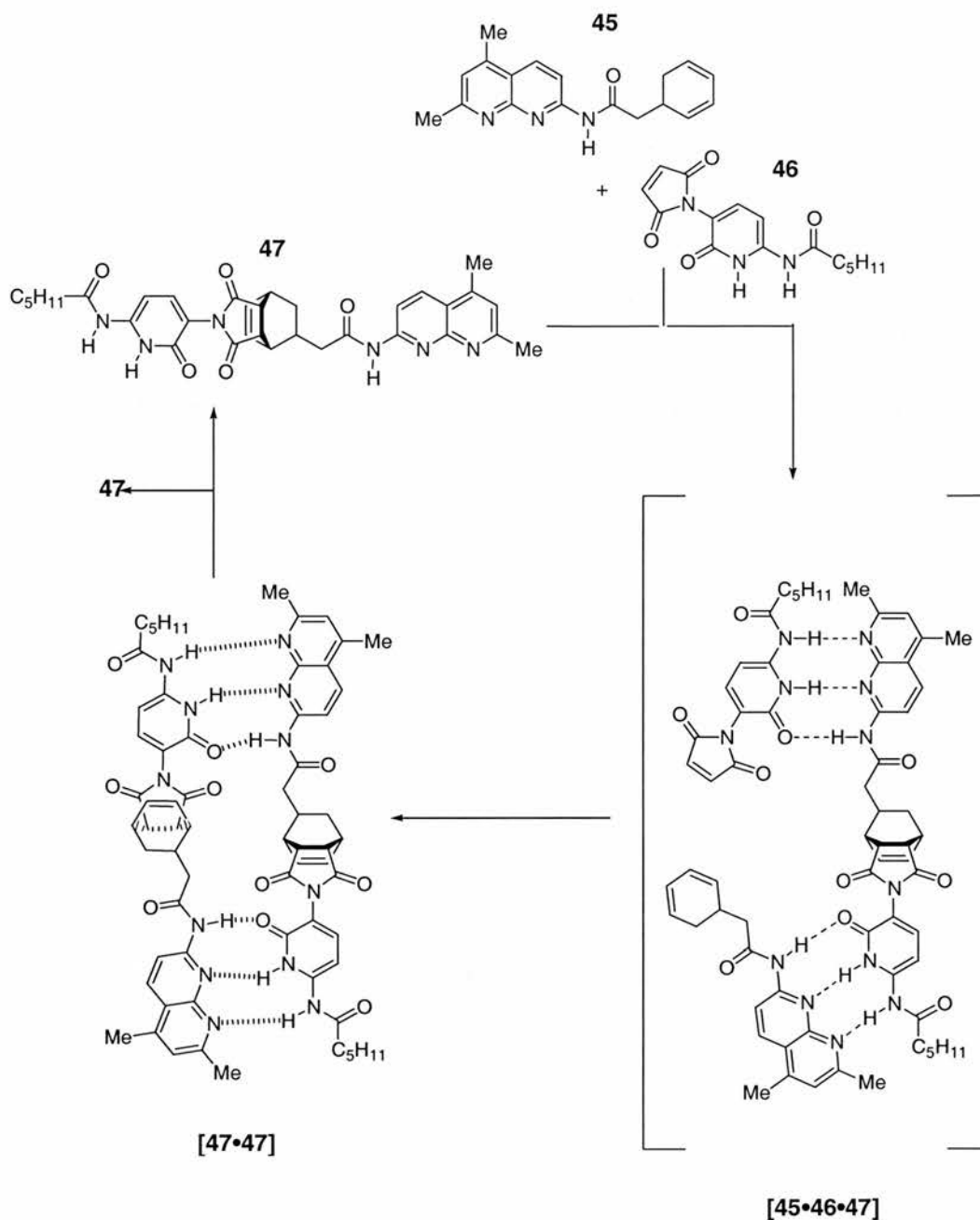
Scheme 1.22 The stepwise replicating cycle for the formation of a Tröger's base analogue **44** by macrocyclisation and covalent templating. *p*-TSA represents *p*-toluene sulfonic acid and DTT represents dithiothreitol.

Unlike previously published self-replicating systems, the building blocks **41** and **41**, were to be covalently linked to form the active macrocyclisation precursor **42**. This different approach meant that the reaction would now be intramolecular as opposed to intra-complex. Once the building blocks were successfully linked to the template, the macrocyclisation step could then be initiated resulting in the formation of a Tröger's base "dimeric" species **43**. Facile cleavage of the covalent bonds required for templating would then result in the formation of two molecules of free template **44** and the catalytic cycle would be complete. Condensation of **42** resulted in the formation of **43** as the major product of the reaction, proving that dimeric **44** should be the product of the reaction within a self-replicating system. Within the system, treatment of **44** with two equivalents of **41** in chloroform in the presence of *p*-toluene sulphonic acid effected the thiol-disulphide exchange reaction to afford the precursor **42** in quantitative yield. Filtration of the insoluble by-product 4-thiopyridone from the bis-amine **42** followed by treatment with formalin in a chloroform/ethanol solvent with an acid catalyst gave the macrocycle **43** as a 1:1:8 mixture of diastereoisomers. Subsequent neutralisation followed by reductive cleavage using dithiothreitol (DTT) of the disulphide linkage afforded free template **44**. After one complete replication cycle the amount of compound **44** had increased by 40%. This stepwise procedure was then repeated several times, each time using the product of the previous cycle. Satisfactory results for the replication cycle were obtained for up to three generations with each cycle increasing the overall product yield by 30-40%. A control experiment was performed to demonstrate the importance of the template-mediated pathway. This was done by performing the reaction as

previously, but in the absence of any preformed template **44**, this resulted in only trace amounts of the desired Tröger's base derivative **44** being formed. It is unclear as to why the reaction does not produce higher amounts of the desired compound **44** in each consecutive autocatalytic step. The formation of the macrocyclisation precursor **42** reportedly proceeds in a quantitative yield. Thus, it follows that the problem with this system must then occur either during cyclisation where, upon reduction the initial template **44** will be returned to the cycle, or, during the reduction itself where incomplete reduction of the disulphide linkages would result in the carry through of template as the macrocyclic species **43**. If the concentration of the template within the system also includes the concentration of template existing as macrocycle **43**, this would account for the reaction's low yield as only free template **44** can go on to form precursor **42** in the following cycle.

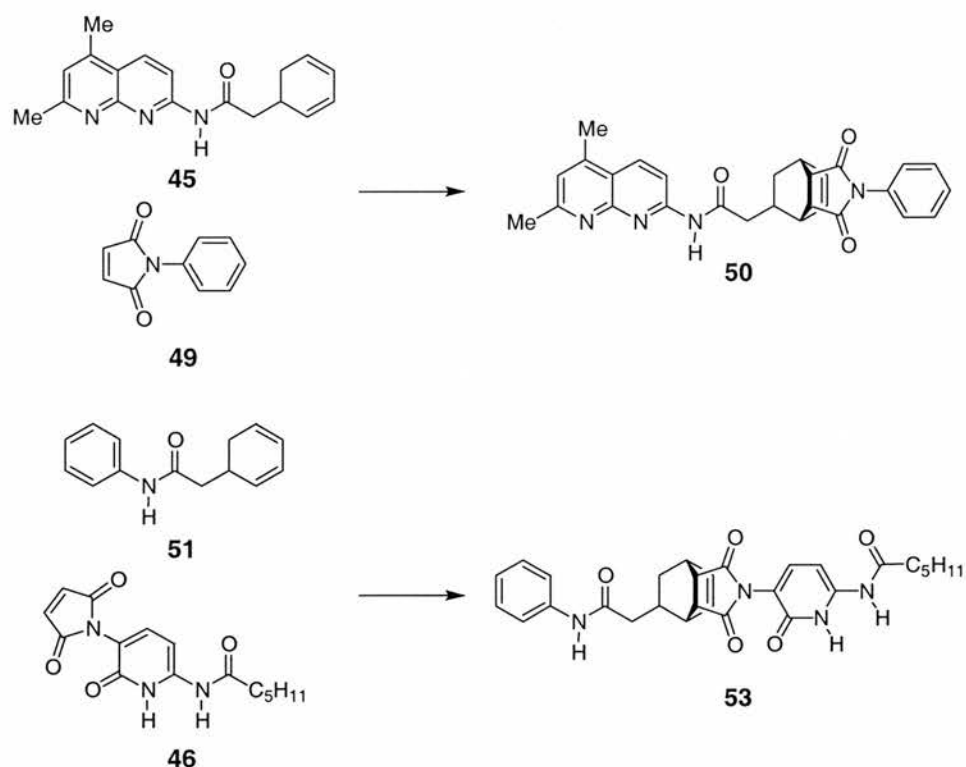
This system clearly shows the importance of templating effects in the formation of compound **44** and overall may be said to be self-replicating *via* the operation of templating effects of the Tröger's base derivative. However this system may not be described as being autocatalytic as the product formation is through a sequence of oxidation and reduction reactions.

A further self-replicating example has been published by Wang and Sutherland¹³². This system is based around the [4+2] Diels-Alder cycloaddition reaction between a 2-acylaminonaphthyridine **45** and a 6-acylamino-2-pyridine **46** (Scheme 1.23).



Scheme 1.23 The self-replicating system proposed by Wang and Sutherland.

The recognition between the 2-pyridine and the naphthyridine results in three hydrogen bonds and careful choice of the substitution pattern about the aromatic backbone meant that the binding of the two building blocks within a binary complex was unproductive rendering the AB-complex route inactive. To determine the bimolecular reaction control compounds were chosen carefully to resemble the recognition-capable system whilst removing any possibility of association between the two reactive partners (**Scheme 1.24**).



Scheme 1.24 Control compounds chosen for the Diels-Alder reaction.

The rate profile obtained for the reaction between **45** and **46** to afford **47** displayed a sigmoidal character (**Figure 1.25**).

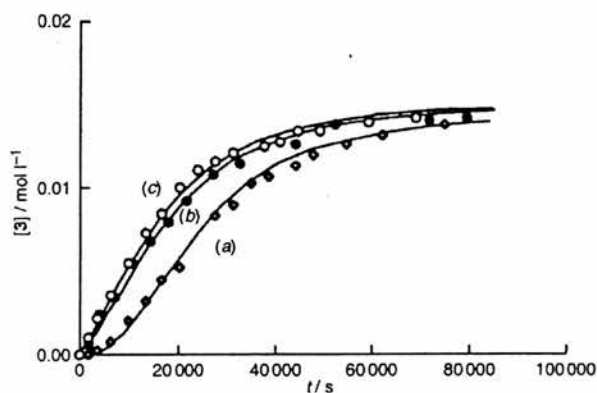


Figure 1.25 Rate profiles obtained for the reaction of **45** and **46** at 40°C in CD_2Cl_2 with a) 0% added template **47** at $t = 0$, b) 5% added template and c) 10% added template. Figure taken from ref. 132 [3] on y axis = [47].

When the reaction was treated with 5 and 10 mol% of preformed template **47** at the start of the reaction. The initial lag period disappeared which indicates that the reaction is autocatalytic (**Figure 1.25**).

The kinetic modelling for this system gave a rate of $2.8 \times 10^{-4} \text{ mol}^{-1}\text{s}^{-1}$ for the uncatalysed reaction and a rate of $2.0 \times 10^{-3} \text{ mol}^{-1}\text{s}^{-1}$ for the recognition-mediated reaction. This gave an estimated effective molarity of 7 M indicating efficient catalysis of the reaction *via* the recognition-mediated reaction.

This study however poses many unanswered questions. The communication reports that the cycloadduct formed **47** is presumably of *endo* stereochemistry but there is no characterisation to support this evidence. It states that the template may be a mixture of diastereoisomers but again there is no characterisation to support this, as ^1H NMR should easily distinguish diastereoisomers. Also there is no mention of whether any of the *exo* cycloadduct is formed in this reaction. Self-replication of this system is further complicated by the presence of stereogenic centres in both the building blocks and the template itself. Consider a template directed reaction forming a template with a single chiral centre with *R* stereochemistry (**Figure 1.26 (a)**).

The template can associate with the achiral building blocks to form the corresponding ternary complex. The complex can then react through two diastereomeric transition states. The energies of these transition states may differ, leading to preferential selection of one pathway. The relative transition state energies will determine whether a racemic mixture of *R* and *S* templates is produced or a stereoselective turnover of *R* template (amplification) occurs. If one of the building blocks contains a chiral centre (**Figure 1.26 (b)**), and is added to the reaction as a racemate, the *R* template can assemble the building blocks to form two diastereomeric complexes.

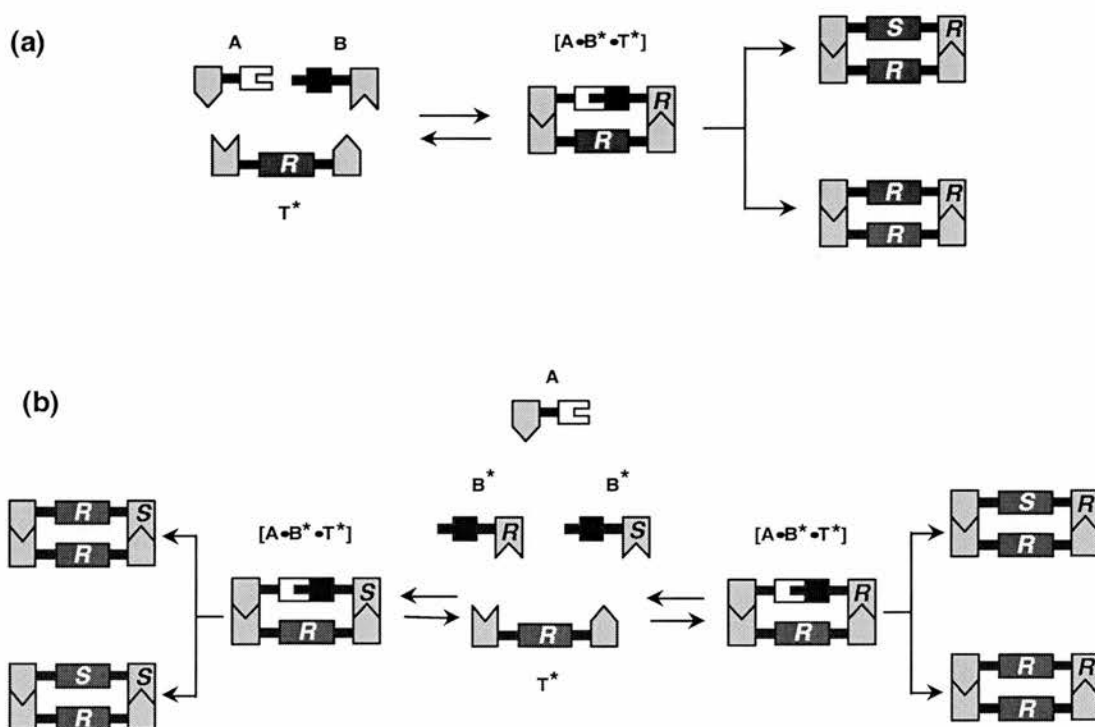


Figure 1.26 (a) Template-directed synthesis forming a template T^* with a single chiral centre *R*, resulting in either amplification of the *R* template or a racemic mixture of *R* and *S* templates. (b) Reaction of a chiral template T^* (*R*) with a racemic mixture of chiral building block B^* and achiral building block *A*.

Each of these complexes can proceed through two diastereoisomeric transition states leading to four possible product duplexes.

The diene building block in Wang and Sutherland's system contains a chiral centre and is used as a racemate. Also the cycloadduct formed contains a further four chiral centres which means a much more complex version of the reaction scheme described above, is in operation. However, the communication makes no effort to assign the stereochemistry of the template, or quantify the stereochemical effects that the recognition pathway may induce over the independent bimolecular reaction pathway.

1.9 The origins of chirality

Consideration of **Section 1.8.2** leads to the discussion of chirality within natural systems. The question of the origin of life is invariably linked to the origin of enantiomerically pure compounds¹³³. It is believed that homochirality was a pre-condition for life because racemic molecules would have been too inefficient for achieving biological processes such as self-replication, protein synthesis and gene expression. Polymerisation reactions affording long-chain stereo-regular polymers will not proceed in racemic solution since addition of a wrong monomer will stop the process. In principle, a biochemistry made up of *D*-amino acids and *L*-sugars should be just as efficient as the *L*-amino acids and *D*-sugars that are found in our terrestrial life. Nature has perfected the ability to replicate in a homochiral manner and it is precisely this behaviour that is the motivation for the development of stereospecific reactions, whether they are *via* catalysts or templates.

There are many cases where the stereochemistry of a reaction can be controlled by addition of a catalyst, for example the Sharpless epoxidation, however these types of reactions are not autocatalytic and require the use of a chiral auxiliaries. Often synthetic steps are required in the preparation of the auxiliary and then subsequent separation from the product can be quite tedious.

1.9.1 Asymmetric autocatalysis

Asymmetric autocatalysis (or automultiplication)¹³⁴ reactions are potentially more advantageous compared to conventional asymmetric autoinduction reactions¹³⁵ because the chiral product acts as the chiral catalyst and so there is less need for subsequent separation/purification (**Figure 1.27**).

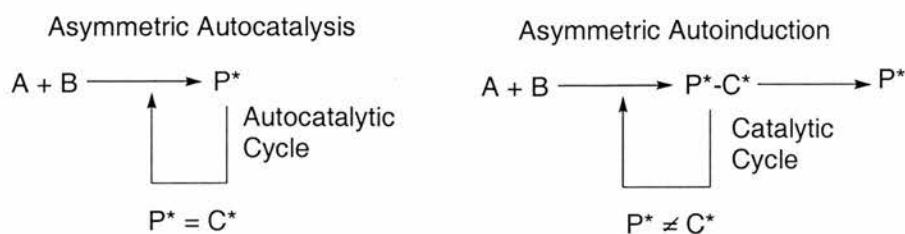
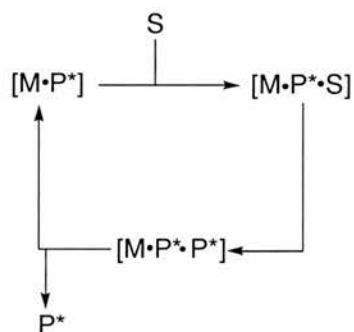


Figure 1.27 In asymmetric autocatalysis the product acts as the catalyst of its own synthesis whereas asymmetric autoinduction requires the use of a chiral auxiliary.

In addition, catalytic automultiplication is considered to be the asymmetric version of molecular replication.

An extension of chiral catalysis and the use of chiral auxiliaries is the area of chiral amplification¹³⁶⁻¹⁴³. Chiral amplification is said to occur when the chiral product of a reaction influences the outcome of further reactions to yield a stereo-controlled product. Chiral amplification can occur when either the product is acting as its own catalyst, or when a co-factor has been added to the reaction.

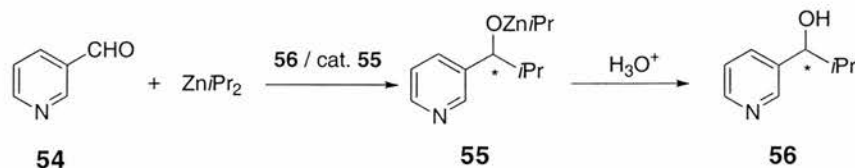
Soai *et al.* have undertaken a considerable amount of work in the area of catalytic asymmetric automultiplication reactions. Their work was based upon the use of a chiral product, which could act as a ligand to a Lewis acidic metal ion, which would then act as a catalyst (**Scheme 1.25**).



Scheme 1.25 Schematic view for chiral amplification where the product of a reaction acts as a ligand to the metal auxiliary. **M** indicates the Lewis acidic metal ion, **P*** the chiral product and **S** represents the starting materials.

Chiral amplification occurs when the chiral product **P***, in this case, ligated to the Lewis acid metal ion, can produce an exact copy of itself. Therefore after one cycle of the reaction, there will be two molecules with the same configuration, which can then continue to be turned over within the reaction mixture.

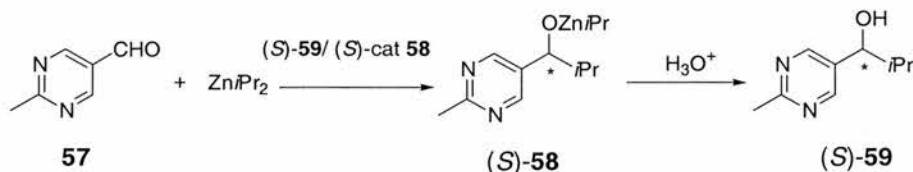
The first successful reactions using chiral catalysts were reported by Soai and co-workers¹⁴⁴ in 1990. It was found that pyridinyl alcohol **56** catalysed its own formation from pyridine-3-carbaldehyde **54** and diisopropylzinc *via* the isopropylzinc alcoholate **55** (**Scheme 1.26**).



Scheme 1.26 Soai's first system to demonstrate asymmetric autocatalysis.

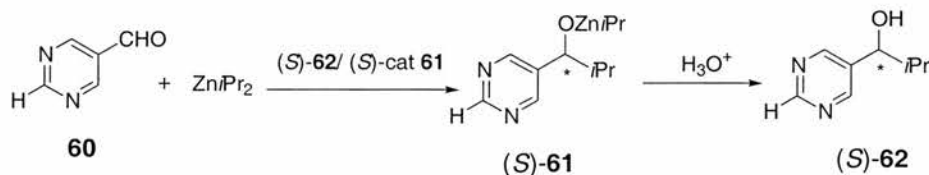
The reaction was performed with 20 mol % of **55** (86% ee), workup afforded **56** in 67% yield with an ee of 35%. The predominant enantiomer of newly formed **56** possessed the same structure and same configuration as the catalyst.

Asymmetric autocatalysis utilising the enantioselective additions of organozinc compounds has also been demonstrated by the groups of Soai¹⁴⁵, Bolm¹⁴⁶ and Li¹⁴⁷. However they always gave a product with a much lower ee value than that of the catalyst used. Then at the end of 1995 Soai and coworkers made an important breakthrough. It was shown that in the presence of 20 mol % of the pyrimidyl alcohol **59** (94.8% ee) in the reaction between the corresponding aldehyde **57** and diisopropylzinc led to the formation of (*S*)-**59** in a 48% yield with an ee of 95.7% (**Scheme 1.27**). The product had undergone automultiplication without a significant change in the enantiomeric excess; even though the starting material is highly enantiomerically enriched.



Scheme 1.27 Soai's asymmetric autocatalytic system demonstrating automultiplication without a change in ee of the product.

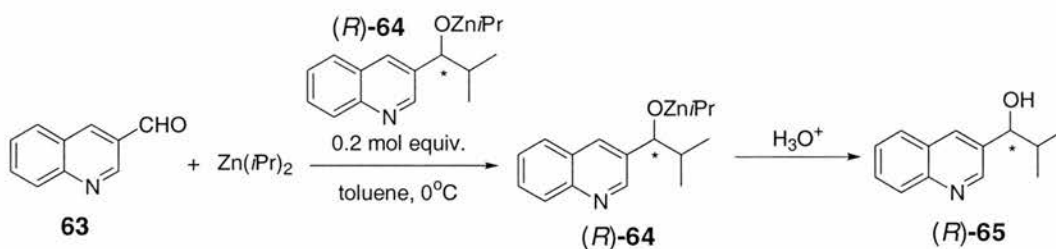
Soai continued to demonstrate that with a slight modification to the previous system **Scheme 1.27**, it was possible to perform asymmetric amplification for the first time (**Scheme 1.28**).



Scheme 1.28 Soai's asymmetric autocatalytic system demonstrating automultiplication with an increase in ee of the product.

Addition of 20 mol% (*S*)-**61** (2% ee) gave, with autocatalysis, (*S*)-**62** with an ee of 10%. In further reaction cycles the enantiomeric excess rose from 10 through 57 to 81 and finally to

88%. There was a 942-fold increase in the amount of product after four cycles. Soai then applied the same procedure to the system outlined in **Scheme 1.29**¹⁴⁹.



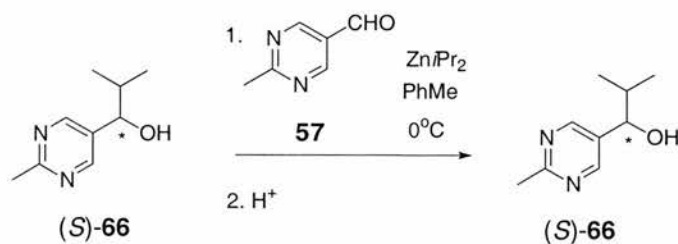
Scheme 1.29 Reaction of 2-methyl-1-(3-quinolyl)propan-1-ol **R-65** acting as catalytic ligand for its own formation from quinoline-3-carbaldehyde.

In this study 2-methyl-1-(3-quinolyl)propan-1-ol was used to prepare the catalyst **65**. When 20 mol% of (*R*)-**64** (9% ee) was used as catalyst, (*R*)-**65** was obtained in a 76% yield and with an improved enantiomeric excess of 43.3%. This yield represented the recovery of (*R*)-**65** as used in the catalyst as well as newly formed (*R*)-**65**. It was shown that the newly formed (*R*)-**65** had been generated with an enantiomeric excess of 55.8%. Recovered (*R*)-**65** was used in subsequent asymmetric alkylation reactions acting as the catalyst. After several cycles the enantiomeric excess of (*R*)-**65** had improved from 9% to 88%.

It was also shown that (*S*)-**65** could automultiply but not with the same efficiency as that observed for (*R*)-**65**. After several cycles the enantiomeric enhancement of (*S*)-**65** had improved from 37% to 70%.

Although successful, Soai's systems described so far had one major disadvantage, the reaction had to be quenched and purified so that the catalyst could be used in the subsequent cycle. The stepwise manner in which the catalyst was generated meant that there was loss of product and the separation procedure was time consuming. These problems lead to the development of a one-pot synthesis, which did not require work-up procedures or purification.

The new system¹⁴⁹ (**Scheme 1.30**) involved treatment of (*S*)-**65** (0.28% ee) portion wise, three times with a mixture of aldehydes **57** and diisopropyl zinc. The reaction yielded (*S*)-**66** in an enriched enantiomeric excess of 87%.



Scheme 1.30 The one-pot procedure utilised by Soai to achieve a dramatic enhancement of the enantiomeric excess from 0.28% to 87% for (*S*)-**66**.

It was also found that by using (*R*)-**66** with an ee of 0.18% as the initial autocatalyst, in the same manner as described previously, the ee was enhanced to 84% after the three portion wise additions of aldehydes **57** and diisopropyl zinc.

These reactions demonstrate that even a very small imbalance of enantiomeric excess at the beginning of a reaction may be dramatically enhanced.

1.10 Aims and objectives

The aim of the research presented in this thesis, is to investigate minimal autocatalytic self-replicating systems with a view to establishing a paradigm which will delineate the necessary requirements for the construction of this type of system. This research will involve the design, synthesis and kinetic analysis of systems, which have the ability to react *via* a recognition-mediated pathway. It will be hoped that the systems designed will either have the ability to autocatalytically self-replicate or be modified so that this pathway can be followed.

The initial investigation will involve the examination of a structurally-simple system, in the hope of producing an autocatalytic self-replicating system.

The investigation will then follow a successful self-replicating system which will be performed by designing, synthesising and kinetically analysing various analogues, to enable a full investigation of the stereochemical, regiochemical, electronic and steric requirements for a successful self-replicating system.

The efficiency of the autocatalytic self-replicating systems developed, will be determined through various control experiments. In particular, comparison with the corresponding bimolecular reactions, the use of a competitive inhibitor to affect the recognition within the systems and also self-doping reactions. Kinetic fitting of the experimental data will be performed to enable extraction of various physical quantities such as rates of reaction, autocatalytic behaviour and the efficiency of the autocatalytic pathway. These values can then be used to compare and contrast the various systems developed.

By developing a range of systems that can autocatalytically self-replicate, they can be compared to systems that do not self-replicate (*i.e.* systems that react *via* an AB-mediated pathway) to try to construct a rationale for the differing behaviour between the systems.

The results and discussion will be presented in three separate sections.

Initially a structurally simple system will be investigated with the view to explaining the recognition-mediated behaviour, compared to a structurally similar system, which reacts *via* an AB-mediated pathway.

The effect of modifications upon a successful autocatalytic self-replicating system will then be presented. Finally, using the experience gained from the previous systems it will be attempted to develop a new autocatalytic system.

2. The Design and Synthesis of a Minimal Self-Replicating System

2.1 The design of a self-replicating system

In Section 1.5 the minimal model for self-replication was introduced (Figure 2.1).

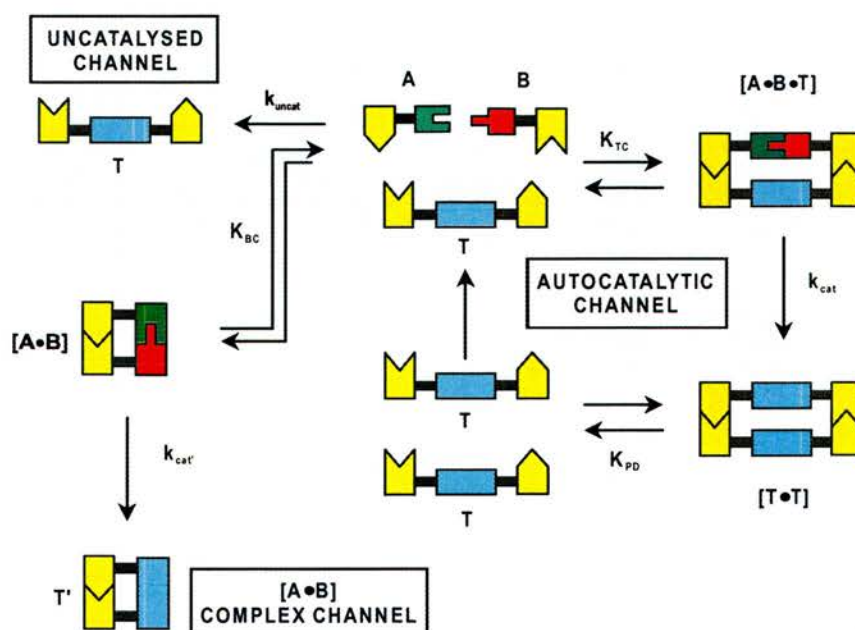


Figure 2.1 Schematic representation of the minimal model for self-replication.

When considering the design of a minimal self-replicating system there are three important design parameters, which need to be considered carefully.

- (i) The covalent bond-forming reaction.
- (ii) The recognition motif.
- (iii) The spacer unit.

Firstly, the bond-forming reaction must be considered. Ideally in a minimal self-replicating system, the bond-forming reaction employed should be kinetically straightforward due to the complex nature of a self-replicating system. The reaction should proceed without the need for added catalysts or cofactors. Simple reactions, which could be utilised, are condensation, substitution or cycloaddition reactions. Cycloaddition reactions have the advantage that they are kinetically straightforward although, if designed to, they can give rise to a number of isomeric products. As a result of this design the template can be used to generate non-linear catalysis with stereo- and / or regiocontrol.

Secondly, the recognition motif employed in the self-replicating system must be chosen carefully, as it will determine physical parameters of the system such as solvent used and working temperature. Some solvents may compete for the binding sites, or may not dissolve the building blocks or template to a suitable concentration. The binding of a recognition motif

within a self-replicating system is a very fine balance between being strong enough at a suitable working temperature to assemble the ternary complex and also being weak enough to render the product duplex relatively unstable to allow dissociation.

Finally, consideration must be given to the spacer units to be used within the self-replicating system. A self-replicating template will benefit from a rigid backbone to enable the assembling of the building blocks on to the template. However, the design of the structure is very delicate, as the fit of the ternary complex must be good enough to assemble the building blocks but must not be too stable upon product formation so the duplex may dissociate. It must also be remembered that the length of the spacer will play an important role in determining the pathway a system will follow. If a system can react *via* the AB-pathway, then it will preferentially over a self-replicating pathway due to the fact that only two molecules associate as opposed to three.

2.1.1 The recognition motif

Previous work performed¹⁵⁰ within our research group has concentrated on the incorporation of the recognition between crown ethers and an ammonium ion¹⁵¹. However, these systems have proved synthetically cumbersome and salt effects confused the observation of recognition-mediated acceleration. Hence, attention has turned to the hydrogen bond association between an amidopicoline unit and a carboxylic acid, which has been studied¹⁵²⁻¹⁵⁶ in particular by Hamilton *et al.*¹⁵⁷⁻¹⁵⁹ (**Figure 2.2**).

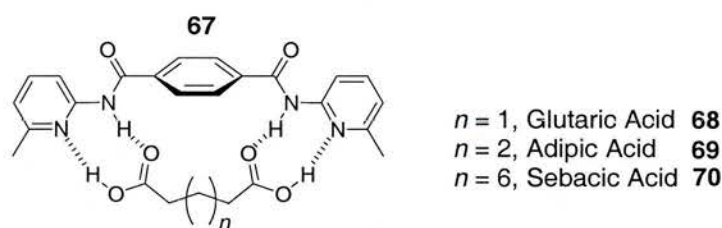


Figure 2.2 A diamide receptor **67** capable of binding with dicarboxylic acids **68**, **69** and **70** *via* hydrogen bond association.

Hamilton¹⁶⁰ studied the binding between various dicarboxylic acid substrates **68**, **69** and **70** and a rigid receptor with two convergent amidopicoline units **67**. It was found that the strongest complexes were formed between glutaric acid **68** and adipic acid **69** with the receptor **67**. This was attributed to their length and complementarity. ¹H NMR spectroscopic studies revealed that complexes of 1:1 were formed, however, the binding constants were too high to be measured by ¹H NMR titration, therefore it was considered to be greater than $10^5 M^{-1}$ in CDCl₃ at 298K. The longer chain sebacic acid **70** was also found to form a 1:1 complex with the receptor, however its affinity was reduced and so a measured association

constant of $10^3 M^{-1}$ was obtained. Association of this magnitude is thought to be due to strong co-operative binding effects, however Hamilton did not report a binding constant for the interaction between molecules containing one binding site each. Although it has been observed¹⁵⁰ that a typical value for a single association between an amidopicoline unit and a carboxylic acid is in the order of $100 M^{-1}$ in $CDCl_3$.

More recently, Goswami *et al.*¹⁶¹ designed and synthesised a molecular cleft **71** based on a derivative of a Tröger's base, that utilised the binding between an amidopicoline and a carboxylic acid (**Figure 2.3**).

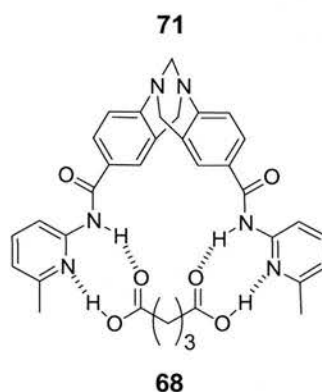


Figure 2.3 Molecular cleft **71** capable of binding to dicarboxylic acid **68**.

It was found that the host **71** was capable of binding glutaric acid **68** with an association constant of $10^3 M^{-1}$ in $CDCl_3$ (2% d_6 -DMSO).

The use of complementary binding sites removes or limits unproductive binding between either the reagents or the template itself (**Figure 2.4**). For example, compare a template, which contains complementary recognition units (**Figure 2.4 (a)**), with a template that contains identical recognition sites (**Figures 2.4 (b), (c) and (d)**). In **Figure 2.4 (a)** there is only one way in which the building blocks can associate, whereas the building blocks in **Figure 2.4 (b)** could then associate unproductively by binding identical building blocks (**Figures 2.4 (c) and (d)**). This situation could exist if the template contains two carboxylic acids as its recognition sites.

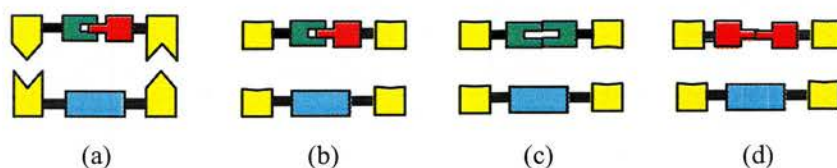
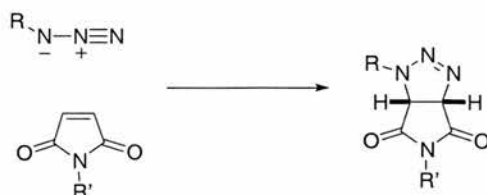


Figure 2.4 Schematic demonstration to show the advantage of using (a) complementary recognition units to promote productive binding compared to (b), (c) and (d) which have identical recognition units, which can promote unproductive binding.

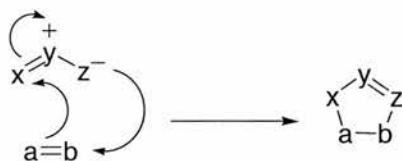
2.1.2 The covalent bond forming reaction

Having identified a suitable complementary recognition motif, attention was then turned to a suitable bond forming reaction. Previous work¹⁶² within our research group, has focused on a [3+2] dipolar cycloaddition between^{163,164} an azide acting as a 1,3-dipole and an activated maleimide alkene, acting as a symmetric dipolarophile (**Scheme 2.1**).



Scheme 2.1 The [3+2] dipolar cycloaddition between an azide 1,3 dipole and a symmetric maleimide dipolarophile to form a 5,5 bicyclic triazoline cycloadduct.

In the 1960's, research was carried out on [3+2] dipolar cycloaddition to construct five membered heterocyclic systems¹⁶⁵. The term "1,3-dipole" refers to a three atom system that can be represented as a zwitterionic octet Lewis structure. The zwitterionic structure may then undergo 1,3 addition across a π bond dipolarophile, such as an alkene or alkyne (**Scheme 2.2**).



Scheme 2.2 General mechanism for a 1,3-dipolar cycloaddition with an alkene as the dipolarophile.

Extensive work performed by Huisgen and co-workers^{165,166} led to the elucidation of the mechanisms, patterns of reactivities and selectivities in 1,3-dipolar cycloaddition reactions. Huisgen proposed that the mechanism for the addition of a 1,3-dipole to a dipolarophile was a concerted process, which involved the 4π electron system on the dipole with the 2π electron system on the dipolarophile without the formation of any intermediates¹⁶⁷. This theory meant that the termini could not be assigned as either nucleophilic or electrophilic and so the resulting electron shift could proceed in either a clockwise or anticlockwise manner.

It is now accepted that regioselectivities observed in 1,3-dipolar cycloaddition reactions are controlled, primarily, by the magnitude of the atomic orbital coefficients and the symmetry of the orbitals concerned. In order to be able to predict the regiochemistry resulting from the addition of a 1,3-dipole to a dipolarophile, the frontier molecular orbitals on both reactive partners must be considered. The magnitude of the frontiers orbital coefficients can be altered significantly by the substituents on the reactive partners. All 1,3-dipoles react with

dipolarophiles containing electron-donating groups according to LUMO-dipole and HOMO-dipolarophile control. However, the effect of conjugated or electron-deficient substituents on the dipolarophile is less easy to predict and is dependent on the specific frontier orbital interaction of the 1,3-dipole in question. Houk¹⁶⁸ estimated the frontier molecular orbital energies for the 1,3-dipolar cycloadditions between phenyl azide and dipolarophiles with electron rich (X), conjugated (C) or electron deficient (Z) substituents (**Figure 2.5**)¹⁶⁹.

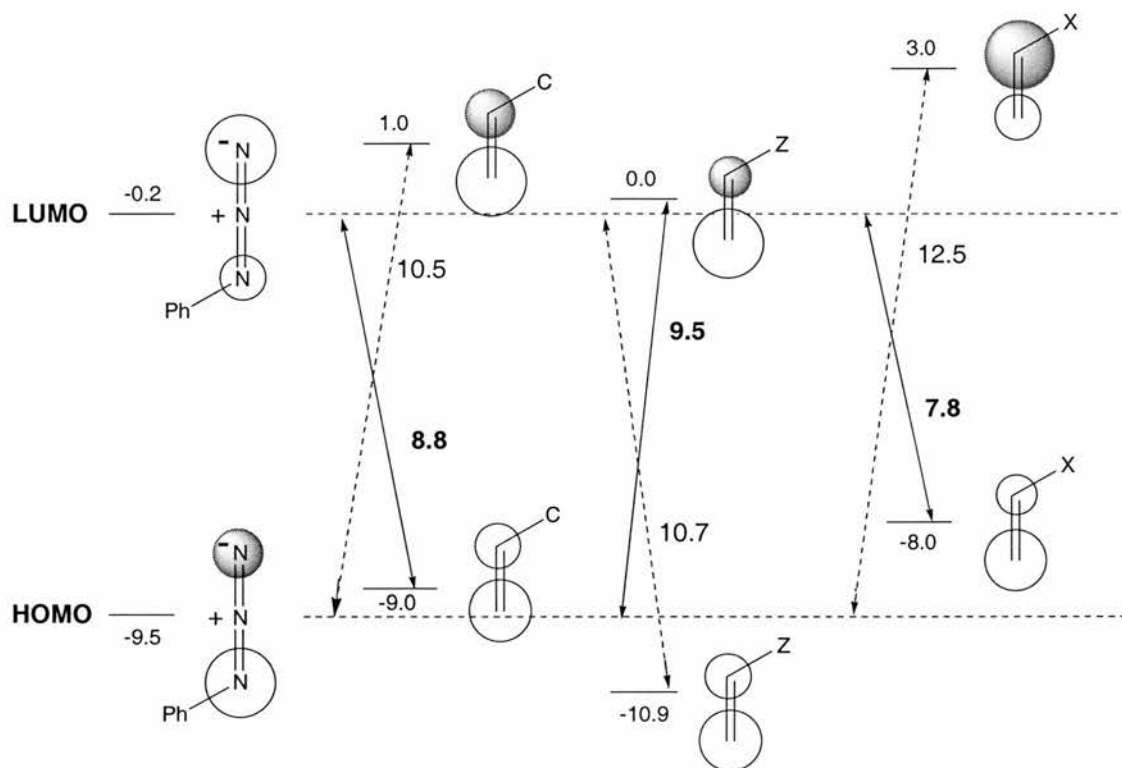


Figure 2.5 Frontier molecular orbital energies for the 1,3 dipolar cycloaddition reaction between phenyl azide **72** and various substituted styrenes. Diagram taken from ref. 169.

The smallest energy gap observed is between phenyl azide and styrene bearing an electron rich substituent (7.8 eV, **Figure 2.5**). This results in the reaction being controlled by the interaction between the dipole-LUMO and dipolarophile-HOMO, resulting in the product regiochemistry as shown in **Figure 2.6**.



Figure 2.6 The observed regiochemical outcome from the reaction between phenyl azide with electron rich and conjugated dipolarophiles.

Using this model the differing regiochemistries observed for the reaction between the addition of phenyl azide **72** to methyl acrylate **75** and 1-hexene **73** can be rationalised (**Figure 2.7**).

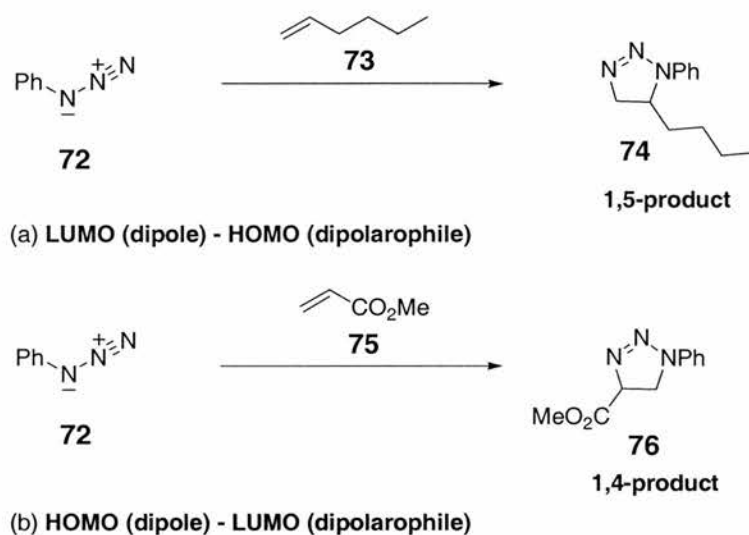


Figure 2.7 The regiochemical outcomes of the addition of phenyl azide **72** to methyl acrylate and 1-hexene. The outcomes can be rationalised by determining the dominant frontier orbital interaction in each case.

In the addition of phenyl azide **72** to methyl acrylate **75** the dominant HOMO-dipole, LUMO-dipolarophile frontier orbital interaction places the substituents remote from the anionic terminus to the azide to give 1,4-regioisomer **76**. However, the addition of phenyl azide **72** to dipolarophile **73** now has a dominant LUMO-dipole, HOMO-dipolarophile frontier orbital interaction that places the substituents adjacent to the anionic terminus of the azide to give the 1,5-regioisomer **74**.

However, by designing a system that utilises a symmetrical maleimide dipolarophile the issue of regiochemistry will be avoided, although frontier molecular orbital interactions may still play a crucial role in determining the reactivity of the 1,3-dipolar cycloaddition. For example, if an electron-donating substituents is added to the azide dipole of a HOMO-dipole, LUMO-dipolarophile controlled cycloaddition, this would raise the HOMO energy and increase the reactivity of the system.

2.1.3 The spacer unit

The spacer unit within a self-replicating system is also a very important design feature. It is essential that the spacer unit be of a sufficient length to ensure that reacting atomic orbitals of the building blocks are too far apart for reaction to occur if the building blocks adopt an AB-type coconformation. This will prevent the system reacting *via* the entropically more favourable AB-mediated pathway (**Section 1.6**). It was therefore decided that rigid spacers, with tautology should be employed (**Figure 2.8**).



Figure 2.8 Potential spacer units with varying flexibility.

2.2 The potential self-replicating system¹⁷⁰

Having identified a potentially useful recognition motif, a suitable covalent bond forming reaction and spacer unit, a target system was designed in the hope of generating a system, which could assemble and react *via* a ternary complex. Azide **5** and maleimide **77** were identified as suitable target compounds for this study (**Figure 2.9**).

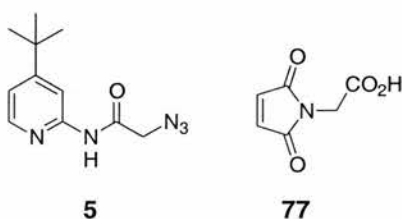
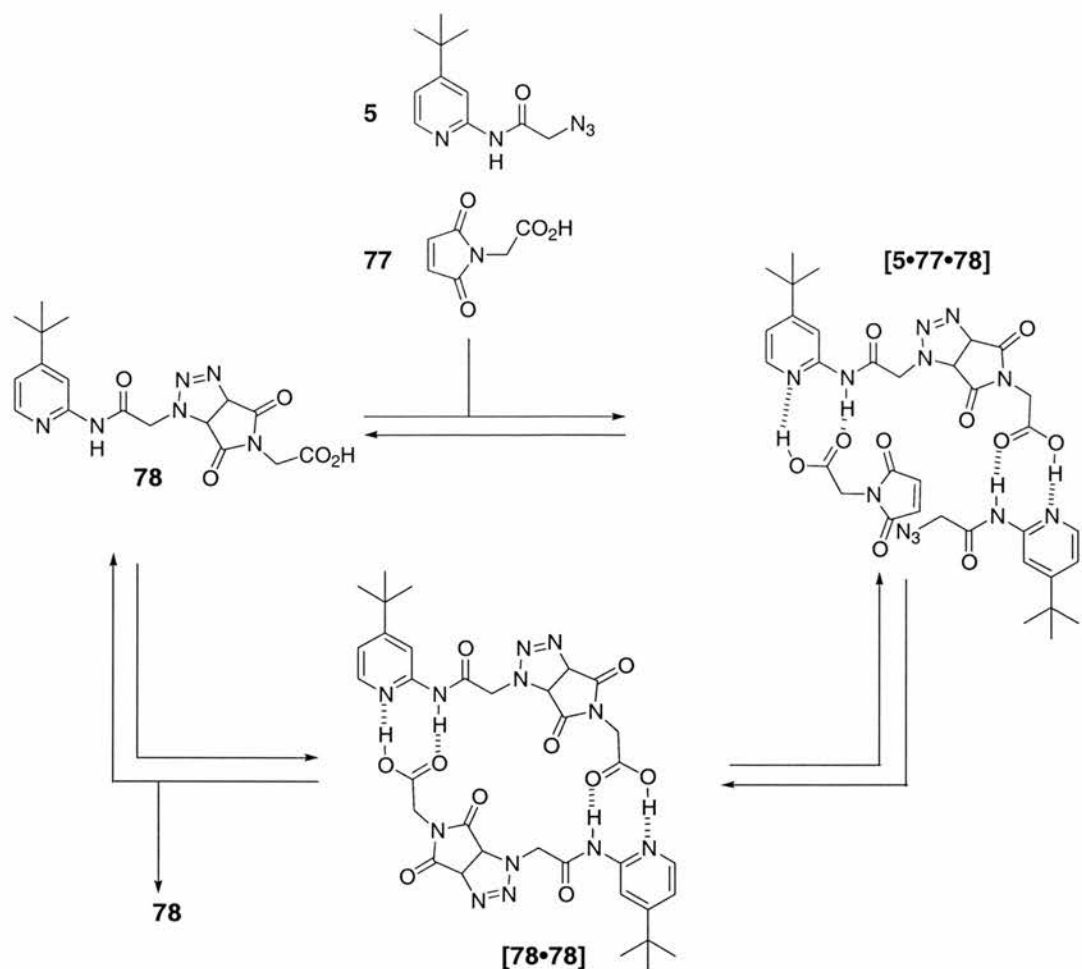


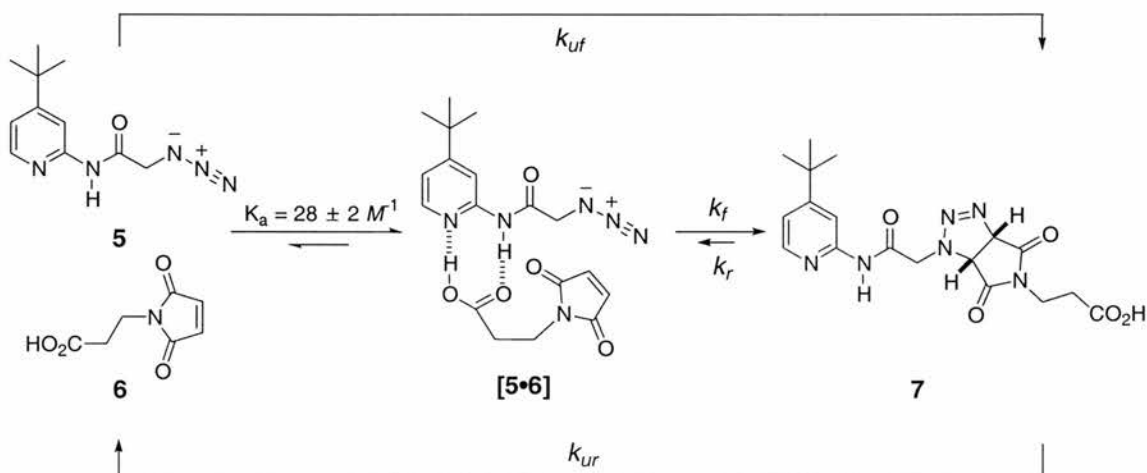
Figure 2.9 Target compounds, azide **5** and maleimide **77** identified for the self-replicating system.

It was hoped that the azide **5** and maleimide **77** will initially react *via* a simple bimolecular reaction to produce the template **78**. Once the template has been formed the building blocks **5** and **77** can then assemble *via* the complementary amidopyridine and carboxylic acid recognition sites to form the ternary complex [**5**•**77**•**78**]. The highly directional nature of the hydrogen bond motif should place the reactive sites in close proximity to each other. The azide dipole and the maleimide dipolarophile would then be non-covalently tethered to each other and so render the reaction *pseudo*-unimolecular (**Scheme 2.3**).



Scheme 2.3 Proposed autocatalytic cycle for the formation of cycloadduct **78** from the 1,3 dipolar cycloaddition between dipole **5** and dipolarophile **77**.

This system was based upon work previously carried out within the group⁸². Booth *et al.* used AB-methodology to accelerate¹⁷¹ the 1,3-dipolar cycloaddition reaction between azide **5** and maleimide **77** (Scheme 2.4) (Section 1.6.2).



Scheme 2.4 AB-mediated 1,3 dipolar cycloaddition between azide **5** and maleimide **6** to afford the cycloadduct **7**. Scheme depicted is the same as that shown in Scheme 1.9.

It was thought that by modifying the system presented above, the reaction pathway could be altered from that of an AB-mediated system to a self-replicating system. The modification involved reducing the spacer unit within the maleimide building block, in the hope that upon formation of an AB-type co-conformation the reactive centres would be too far apart and so render the pathway inactive.

Molecular modelling was performed upon the two templates **7** and **78** (**Figure 2.10**) it was suggested from the global minimum energy structures that template **7** forms a closed template as would be expected whereas template **78** forms both an open and a closed structure and hence could be capable of reacting *via* either a self-replicating or AB-complex pathway.

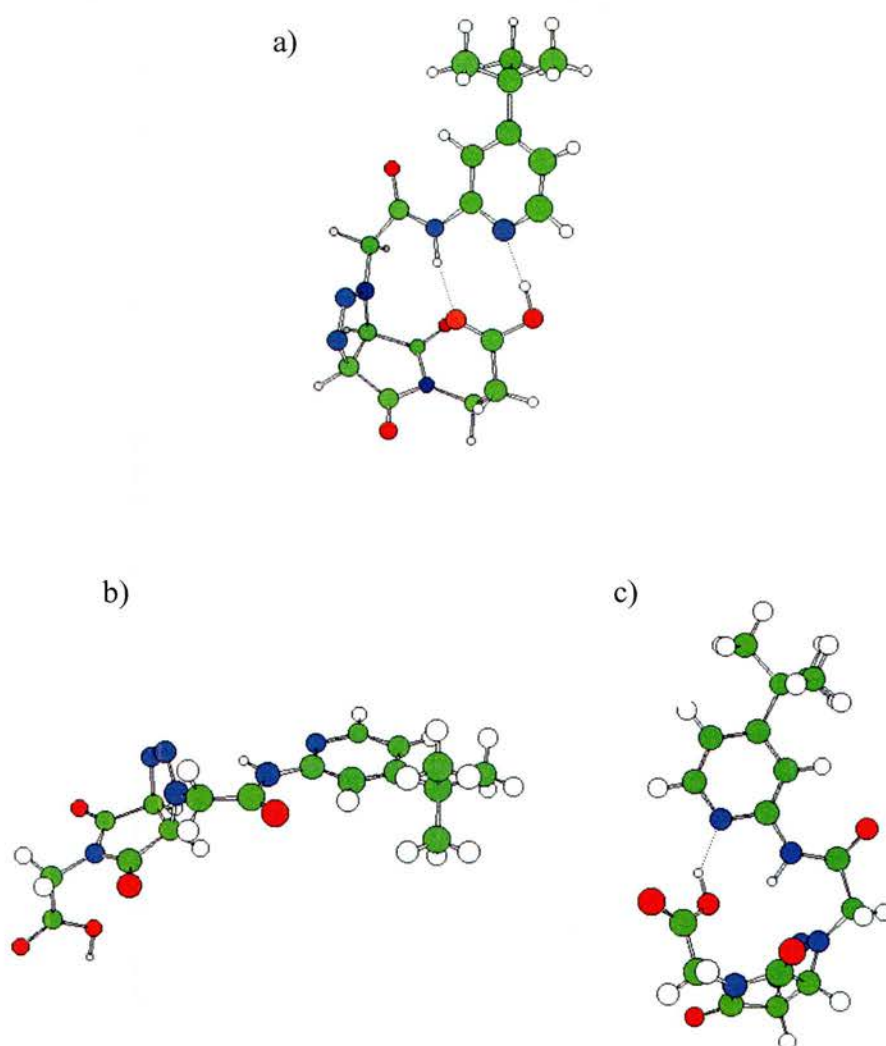
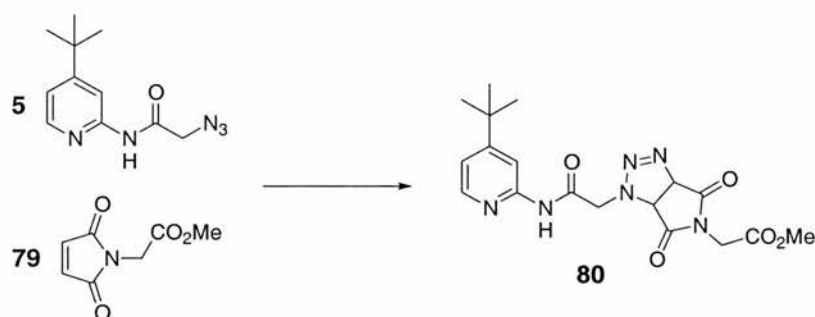


Figure 2.10 Representation of the two lowest energy conformations of the templates (a) **7** and (b) **78**. Template **78** (a) adopts a closed conformation, the possibility of two-hydrogen bonding interactions (dashed lines) is shown. Template **7** adopts (b) an open conformation and (c) a closed conformation, the possibility of a hydrogen bond (dashed line) is shown.

2.2.1 The bimolecular control reaction

In order to make an effective comparison between the recognition-mediated and bimolecular channels, it was necessary to identify a suitable control system. The control system must be as structurally and electronically as similar as possible to the potential self-replicating system (**Scheme 2.3**), but without the ability to form the reactive ternary complex. The system depicted in **Scheme 2.5** was chosen to act a suitable control. The carboxylic acid functionality on **77** has been replaced with an ester functionality **79**, so to remove the possibility of binding occurring between the building blocks and template.

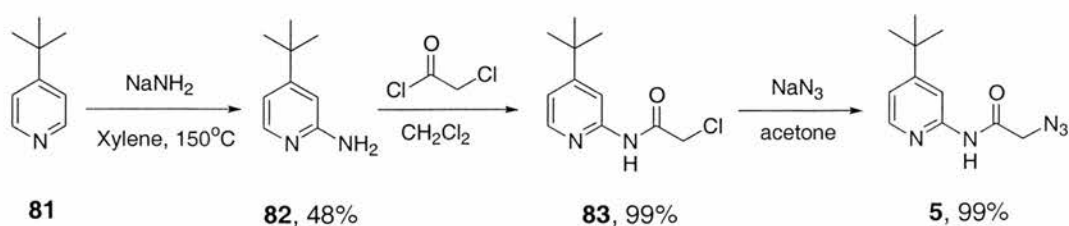


Scheme 2.5 Control system to measure the bimolecular 1,3 dipolar cycloaddition reaction between dipole **5** and dipolarophile **79**.

2.3 Synthesis

2.3.1 Synthesis of recognition dipole **5**

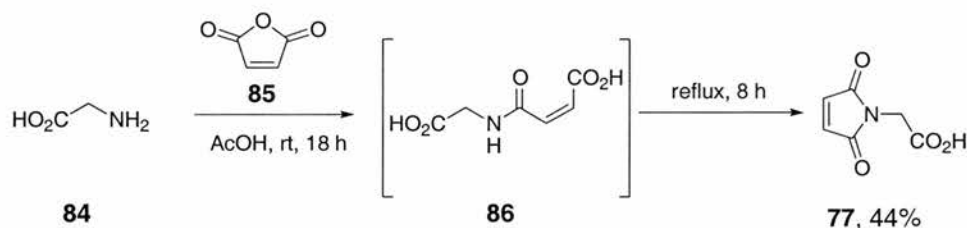
The synthesis of the target azide **5** was achieved in three steps (**Scheme 2.6**). 4-*tert*-butylpyridine **81** was converted to the corresponding aminopyridine **82** by treatment with sodium amide in refluxing xylene, affording **82** in a 48% yield. 4-*tert*-butyl-2-pyridyl-chloroacetamide **83** was prepared by coupling 4-*tert*-butyl-amidopyridine **82** with chloroacetyl chloride in dry dichloromethane. This afforded 4-*tert*-butyl-2-pyridyl-chloroacetamide **83** in an excellent yield of 99%. The synthesis of 4-*tert*-butyl-pyridyl-azidoacetamide **5** was achieved by the nucleophilic displacement of a chloride anion for an azide anion; this displacement was performed by refluxing **83** with sodium azide in acetone, to afford **5** in 99% yield.



Scheme 2.6 The synthetic route for the preparation of the azide recognition building block **5**.

2.3.2 Synthesis of the recognition dipolarophile 77

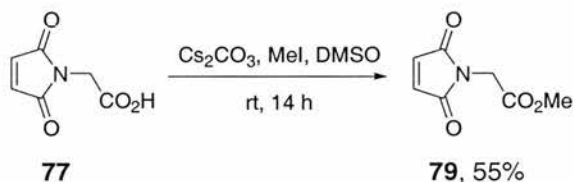
The recognition dipolarophile, maleimide **77** was synthesised in one step from glycine **84** (Scheme 2.7). Glycine **84** was added to one equivalent of maleic anhydride **85** in analytical grade (AR) acetic acid and the resulting reaction mixture stirred at room temperature under nitrogen overnight. This resulted in the formation of the intermediate maleamic acid **86**. The reaction mixture was heated to reflux to promote cyclisation to maleimide **77**. The crude residue was purified by flash chromatography on a short pad of silica gel to afford **77** in 44% yield.



Scheme 2.7 The synthetic route for the preparation of the maleimide dipole recognition building block **77**.

2.3.3 Synthesis of the control dipolarophile 79

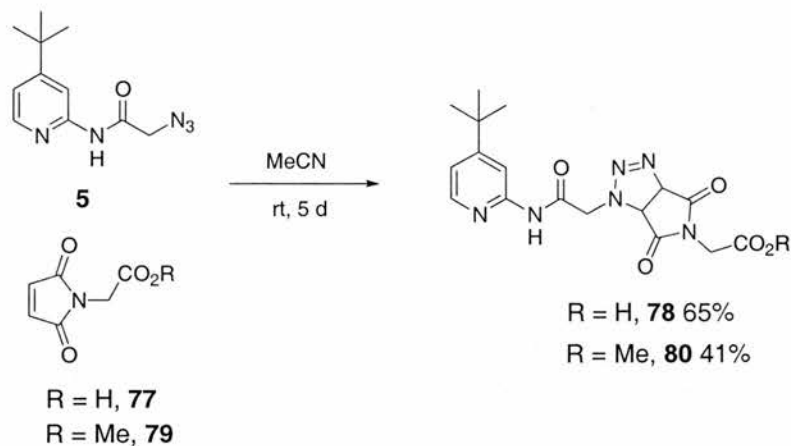
The control dipole **79** was prepared in one step from acid **77** (Scheme 2.8). Maleimide **77** was reacted with Cs₂CO₃ and methyl iodide in dimethyl sulfoxide at room temperature. After stirring for 16 hours the crude residue was partitioned between ethyl acetate and water. The organic layer was dried and removed under reduced pressure. The crude residue was then purified by flash chromatography on silica gel to afford the desired maleimide ester **79** in a yield of 55%.



Scheme 2.8 The synthetic route for the preparation of the maleimide ester dipole control **79**.

2.3.4 Synthesis of the recognition-mediated cycloadduct 78 and control cycloadduct 80

For the accurate assignment of the proton resonances that will arise from the product protons of the cycloadducts in subsequent kinetic analysis, it was necessary to isolate and fully characterise the cycloadducts. A series of small-scale reactions were performed to achieve this (Scheme 2.9).



Scheme 2.9 The synthetic route for the preparation of the cycloadducts **78** and **80**.

One equivalent of the appropriate maleimide, **77** or **79** (R = H or Me) was added to one equivalent of the azide **5** and dissolved in the minimum volume of acetonitrile. The reaction was left to stir in the dark at room temperature for five days. After this time, the cycloadduct **78** had precipitated and was filtered and washed with cold acetonitrile to afford **78** in a 65% yield. The reaction mixture containing cycloadduct **80** had the solvent removed under reduced pressure and the crude residue was purified by flash chromatography on silica gel to afford cycloadduct **80** in a 41% yield.

2.4 ^1H NMR spectroscopic assignment of the cycloadduct **78**

The fused ring system formed from the reaction between the azide and the maleimide results in the formation of a triazolone ring system and the arbitrary proton numbering system that will be used through out this chapter is shown in **Figure 2.11**.

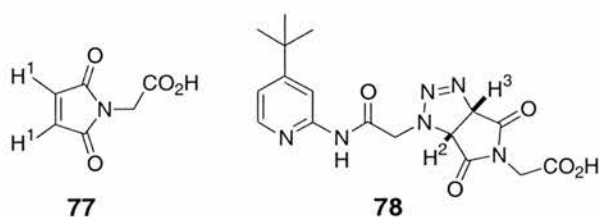
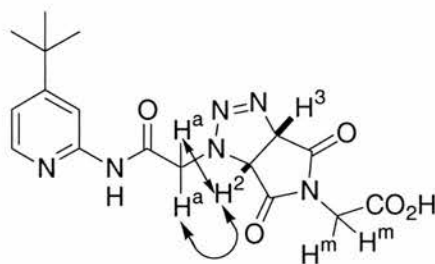


Figure 2.11 The numbering system used for the cycloadduct ring protons and corresponding maleimide precursor protons.

It was hoped that by performing an nOe experiment using 500 MHz ^1H NMR it would be possible to assign the relevant proton resonances H^2 and H^3 present in the ^1H NMR spectrum of the cycloadduct **78**. It was expected that irradiation of either the CH_2 unit (H^a) connecting the triazolone unit and the amide unit or the ring protons H^2 and H^3 would give rise to a corresponding nOe, demonstrating that that these units are spatially close (**Figure 2.12**).



78

Figure 2.12 The expected nOe interactions are shown by the double-headed arrows.

However, upon irradiation of H^2 and H^3 no corresponding signal was observed in the signal for the protons adjacent to the amide unit as had been hoped (**Figure 2.13**).

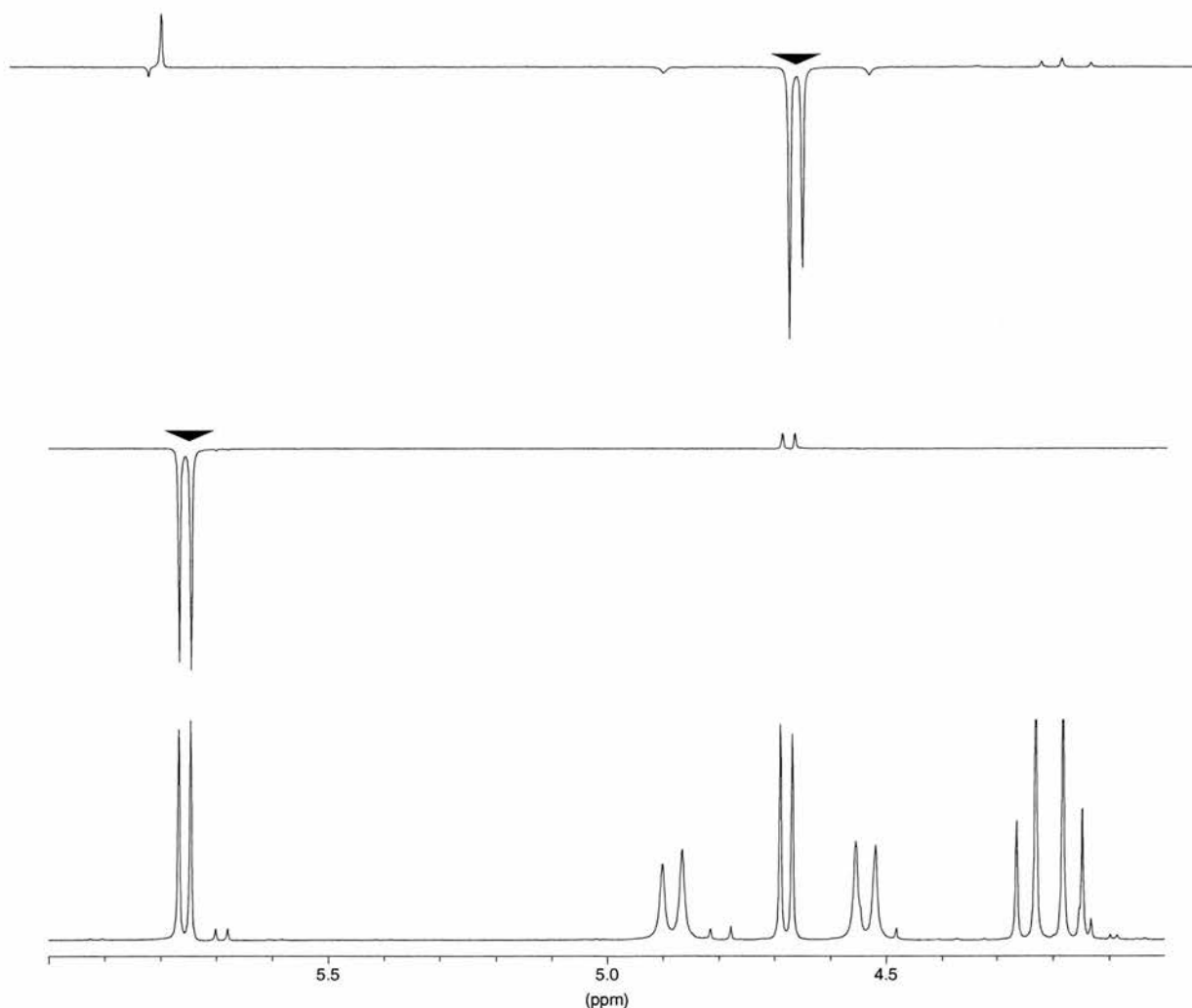


Figure 2.13 NOe study performed on template **78**. Irradiation of protons H^2 and H^3 reveals only the corresponding signals in the adjacent proton, either H^2 or H^3 . The symbol ▼ represents the irradiation point.

Irradiation of the CH_2 units (H^a) within the template gave rise to a corresponding signal in the other CH_2 unit (H^m) (**Figure 2.14**). This indicates that the two methyl spacer units are

spatially close to each other, which infers that the template is held in a closed conformation within the solution phase.

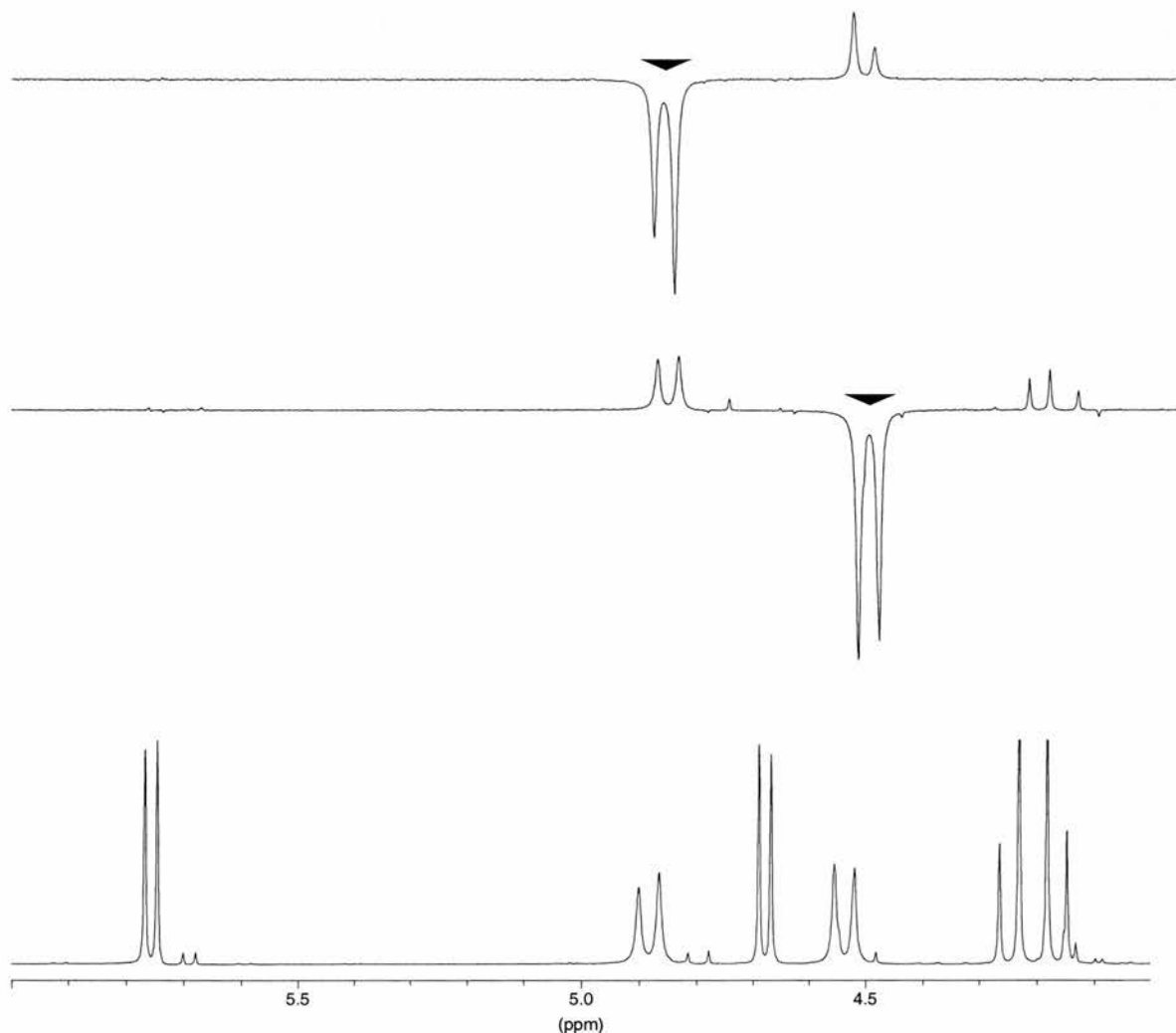


Figure 2.14 NOe study performed on template **78**. Irradiation of the protons next to the amide unit (H^3) reveals only the corresponding signals into the adjacent methyl proton, and the methyl group next to the acid group upon the maleimide unit (H^m). The symbol \blacktriangledown represents the irradiation point.

Hence, from the nOe study it was not possible to assign the protons H^2 and H^3 .

It should be noted that over time, the appearance of small peaks, just offset from the H^1 , H^2 and H^3 proton resonances. Previous studies¹⁷⁷ of these azide cycloaddition systems have shown that these peaks correspond to the decomposition products of the triazoline, which are either the aziridine or enamine compounds.

2.5 Kinetic analysis

2.5.1 Optimisation of the reaction conditions to promote the autocatalytic cycle

For a self-replicating system to operate efficiently it is important that the extent of the template formation *via* the bimolecular reaction is kept to a minimum, while the rate of formation of template *via* the catalysed route be as efficient as possible. The two main variables, which can be altered to optimise the reaction conditions, are concentration and temperature. The concentration at which the reaction is performed is quite important, as it follows that the higher the concentration the faster the bimolecular reaction will proceed. However, it was found that the solubility of **77** in CDCl₃ was limited to a maximum concentration of 50mM. It was found that at concentrations lower than this, problems occurred in the analysis due to large errors in determining the product concentration. The temperature at which the reaction is performed allows a certain degree of control over the rate of reaction. A higher temperature may increase the overall rate of the bimolecular reaction, but at the same time may hinder the rate of formation of the product *via* the recognition-mediated pathway due to the decrease in strength of binding and hence the association of the ternary complex. Due to this uncertainty of the effect of temperature it was decided to look at the system over a range of temperatures from 30-50°C, this allowed the study of the extent of reaction in both the recognition-mediated and bimolecular control reactions.

2.6 The kinetic experiment

The kinetic experiment to analyse the solution phase behaviour of the two building blocks **5** and **77** was then performed. Stock solutions of **5** and **77** were prepared at a concentration of 50 mM in CDCl₃ and were equilibrated to the appropriate temperature for at least one hour before use. Equal volumes of the stock solutions of the building blocks were then mixed together in an NMR tube and a 500 MHz ¹H NMR spectrum was recorded immediately. The progress of the cycloaddition was monitored by recording the 500 MHz ¹H NMR spectrum of the reaction every 30 minutes. All spectra were transformed and phased under identical conditions and the spectral data treated identically in all cases. The course of the reaction was followed by examining the disappearance of the maleimide protons (H¹) and the appearance of the triazoline protons (H², H³) (**Figure 2.15**). The percentage completion of the reaction was quantified by comparison of the disappearance of the starting materials protons and the appearance of the product protons. Quantification of the reactant:product ratio was achieved by deconvolution techniques of the appropriate proton resonances. The results obtained were converted to a concentration, which gave a rate profile for the formation of the product.

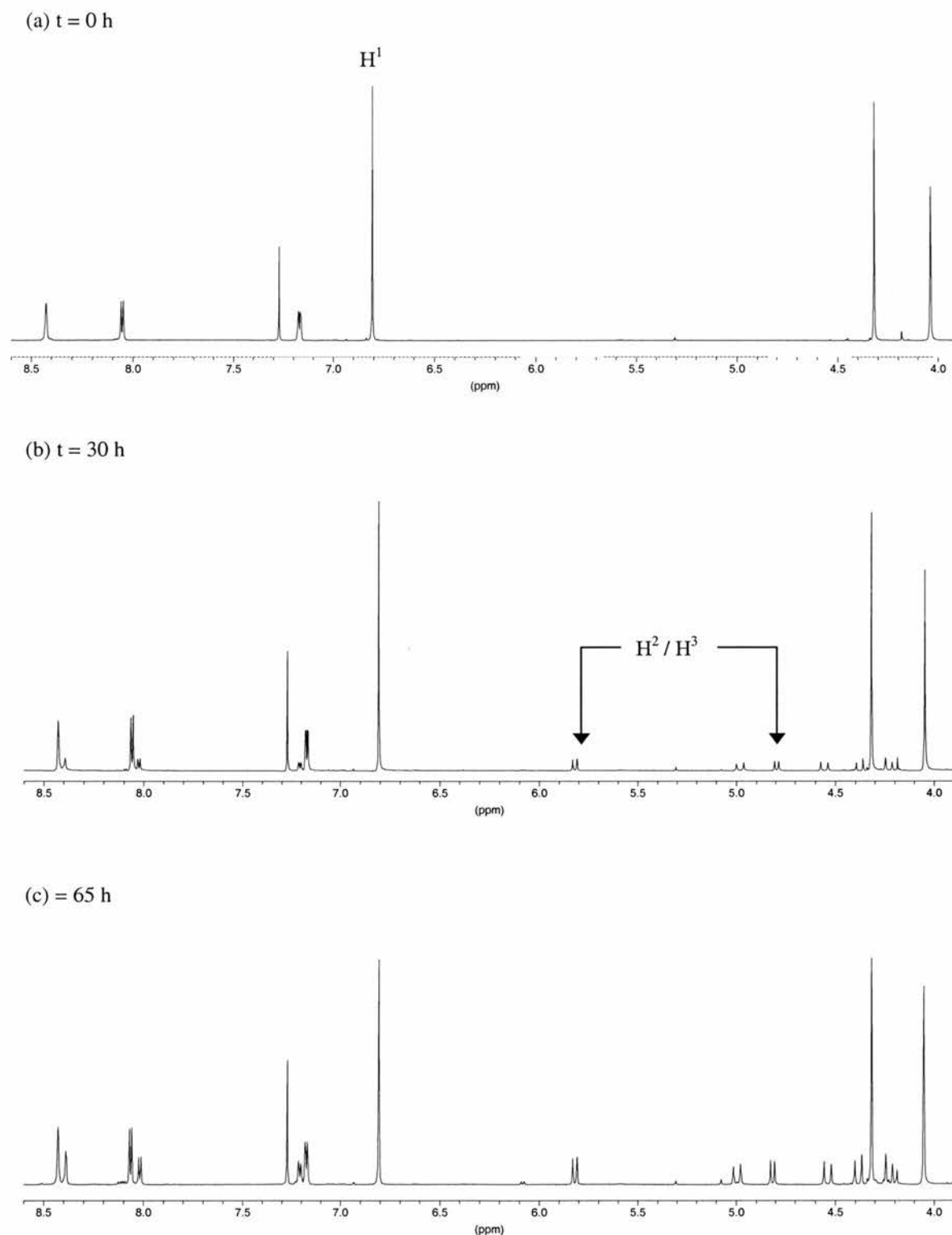


Figure 2.15 500 MHz ^1H NMR spectra of the reaction between **5** and **77** to yield **78** recorded in CDCl_3 at 30°C at (a) $t = 0$ hours, (b) $t = 30$ hours and (c) $t = 65$ hours.

2.7 The results of the recognition-mediated kinetic experiments

Having identified the working solvent and concentration the recognition-mediated reaction between dipole **5** and dipolarophile **77** was performed at 30°C , 35°C , 40°C , 45°C , and 50°C , as described. The results of the recognition-mediated reactions are presented in **Figure 2.16**.

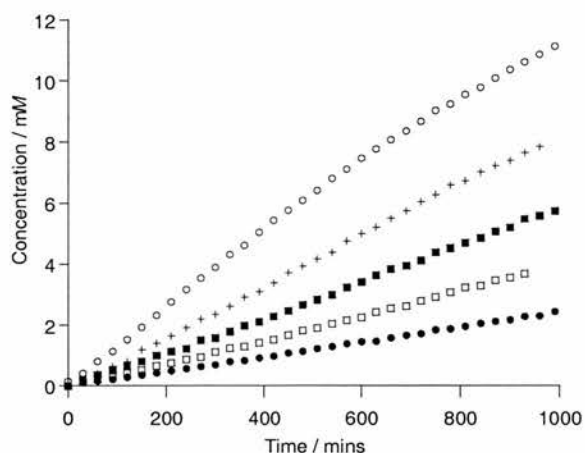


Figure 2.16 The rate profiles for the formation of the triazoline product **78** at various temperatures. 30°C (solid circles), 35°C (open squares), 40°C (solid squares), 45°C (cross), 50°C (open circles).

Initial inspection of the data for the reaction between **5** and **77** at the varying temperatures does not reveal the sigmoidal shape curve that would be hoped to observe for in an autocatalytic self-replicating system. However on closer inspection of the data obtained at the two extremes of the temperature scale, 30°C and 50°C a significant difference is observed in the rate profiles (**Figure 2.17**).

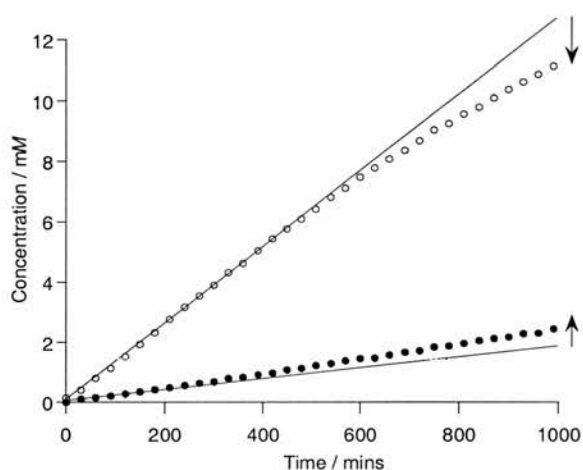


Figure 2.17 The rate profile for the formation of the triazoline product **78** at 30°C (solid circles) and 50°C (open circles). The solid lines act as a guide through the first few data points.

In the data shown in **Figure 2.17** straight line guides have been inserted through the first few data points to extrapolate the initial rate of reaction. It is evident from the data that the rate of reaction at 50°C is decreasing with increasing time whereas the rate of reaction at 30°C is increasing with increasing time. The data at 30°C would be the expected result for a system that has the ability to self-replicating and hence template its own formation, so an increase in the rate of reaction would be observed. To ensure the observed effect is real the reaction between **5** and **77** was performed over a 67-hour period (**Figure 2.18**).

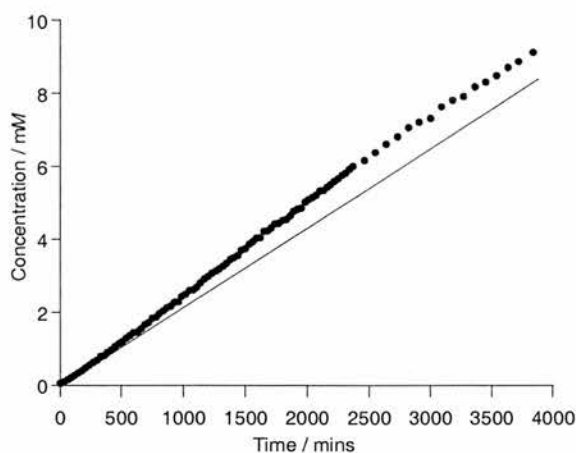


Figure 2.18 The rate profile for the reaction between azide **5** and maleimide **77** over an extended time period showing the increase in the rate of reaction.

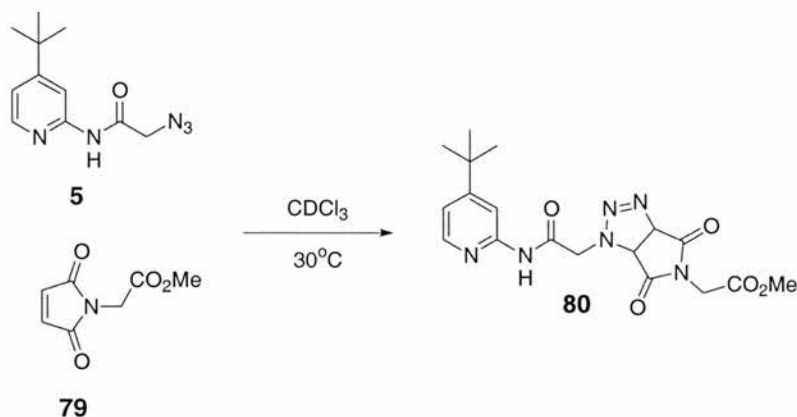
Again, a straight-line guide has been placed through the first few data points and it is quite evident that the rate of reaction is increasing with increasing time. This indicates that the reaction between dipole **5** and dipolarophile **77** may be self-replicating at 30°C at a concentration of 25 mM in CDCl₃.

2.8 Demonstrating the operation of a self-replicating system

In an ideal autocatalytic self-replicating system the shape of the rate profile would be sigmoidal. In the reaction observed between maleimide **77** and azide **5**, a sigmoidal curve is not obtained, however an increase in the rate of reaction is observed for this system, which is indicative of a self-replicating mechanism. This means that the system concerned should involve a recognition-mediated process and the template should have an effect on its own formation and hence there are control reactions, which can be performed to determine whether the system is proceeding *via* a self-replicating pathway.

2.8.1 The uncatalysed bimolecular reaction

To be able to determine the rate of formation of template *via* the uncatalysed bimolecular channel it was necessary to perform a bimolecular control reaction. This kinetic experiment was performed at a concentration of 25 mM in CDCl₃ at 30°C.



Scheme 2.10 Control reaction performed to estimate the bimolecular reaction rate between azide **5** and maleimide ester **79**. The reaction was performed at a concentration of 25 mM in CDCl_3 at 30°C .

In the control reaction outlined in **Scheme 2.10**, the maleimide ester **79** reacts with the azide **5** to afford the template **80**. Esterification of the acid functionality prevents association of the two building blocks. The results of the bimolecular control are presented in **Figure 2.19** with the recognition-mediated rate for comparison.

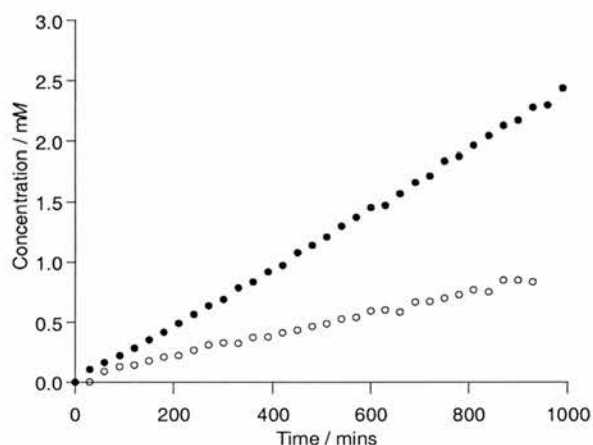
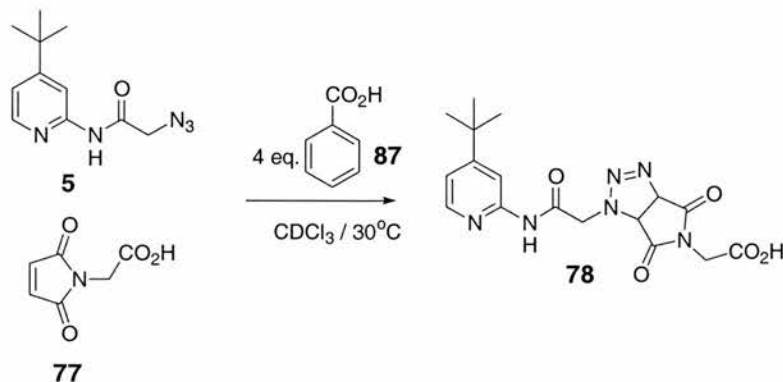


Figure 2.19 The rate profiles to compare the recognition-mediated reaction between azide **5** and maleimide **77** (solid circles) and the bimolecular control reaction between azide **5** and maleimide ester **79** (open circles).

2.8.2 Competition experiment

The ability of a self-replicating system to replicate relies on the binding event, which forms the ternary complex [**5**•**77**•**78**]. This is achieved through formation of hydrogen bonds between the amidopyridine and carboxylic acid recognition motifs. Without this binding event the recognition process would be rendered inactive, as demonstrated in the control reaction between maleimide ester **79** and azide **5**. If the recognition event could be interfered with then the autocatalytic cycle could not operate or would only do so with minimal

efficiency. Hence, by using this feature of a self-replicating system the recognition-mediated pathway can also be demonstrated, along with the evidence from the bimolecular control. This control reaction was performed by the addition of an excess (4 equivalents) of benzoic acid to the reaction between maleimide **77** and azide **5** (Scheme 2.11) (Figure 2.20).



Scheme 2.11 Competition experiment between **5** and **77** with four equivalent of benzoic acid to act as a competitive binder. The reaction was performed at a concentration of 25 mM with respect to the building blocks **5** and **77** at 30°C .

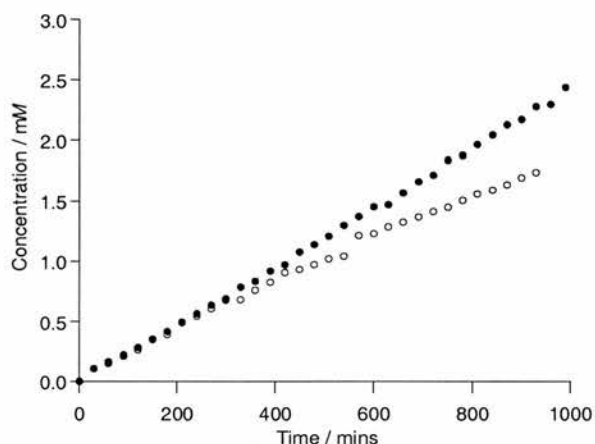


Figure 2.20 The rate profiles to compare the recognition-mediated reaction between azide **5** and maleimide **77** (solid circles) and the control reaction between azide **5** and maleimide **77** and 4 equivalents of benzoic acid (open circles).

When comparing the data obtained in the presence and absence of added benzoic acid it is clear that after 400 minutes the rate of reaction begins to decrease. Up to this time, the reaction is probably only occurring *via* the uncatalysed bimolecular reaction. Then after 400 minutes it is clear that a reduction in the efficiency of the self-replicating system is occurring due to the presence of the benzoic acid. The benzoic acid can form the inactive complex as shown in **Figure 2.21** that will hinder the recognition-mediated reaction.

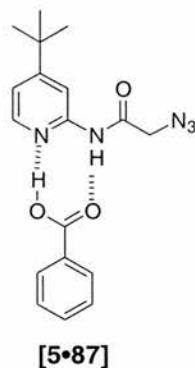
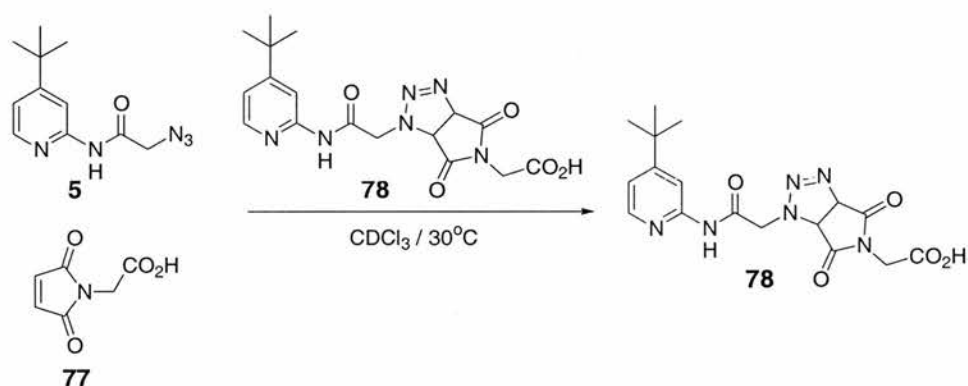


Figure 2.21 Inactive complex potentially formed between benzoic acid **87** and the amidopyridine unit on azide **5**.

2.8.3 Doping experiment

As mentioned previously, the system under investigation does not observe the characteristic sigmoidal shape curve that would be expected for an autocatalytic self-replicating system, however it does observe an increase in the rate of reaction over time, indicating that a self-replicating mechanism may be occurring. This behaviour can also be exploited to determine whether the system is capable of self-replication. By doping the reaction with preformed template, it should be observed that an increase the rate of reaction would occur. The control experiment was then performed by doping the reaction between maleimide **77** and azide **5** with 10 and 50 mol% preformed template (**Scheme 2.12**).



Scheme 2.12 Doping experiment between **5** and **77** with 10 and 50 mol% added preformed template **78**.

The results of the doping control reaction and the recognition-mediated reaction for comparison are shown in **Figure 2.22**.

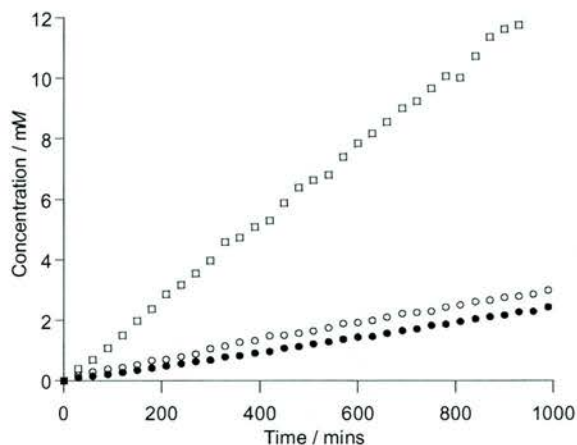


Figure 2.22 The rate profiles to compare the recognition-mediated reaction between azide **5** and maleimide **77** (solid circles) and the control reaction between azide **5** and maleimide **77** and 10 mol% added preformed template **78** (open circles), and 50 mol% added preformed template **78** (open squares).

It is clear from the rate profiles shown in **Figure 2.22** that at both 10 and 50 mol% added template **78** there is an increase in the rate of reaction. At an added concentration of 10 mol% (open circles) there is a very modest increase in the rate of reaction, however at an added concentration of 50 mol% (open squares) there is a significant increase in the rate of reaction. Which indicates that the template can template its own formation.

2.9 Single crystal X-ray analysis of template **78**

Single crystals of template **78**, suitable for analysis by X-ray diffraction were grown by vapour diffusion of hexane into a solution of **78** in chloroform at ambient temperature. The structure determination revealed that **78** exists as a dimer in the solid state (**Figure 2.23**). Template **78** crystallises in the $P2_1/c$ space group and exhibits a monoclinic crystal system (**Figure 2.24**), (**Table 6.1**).

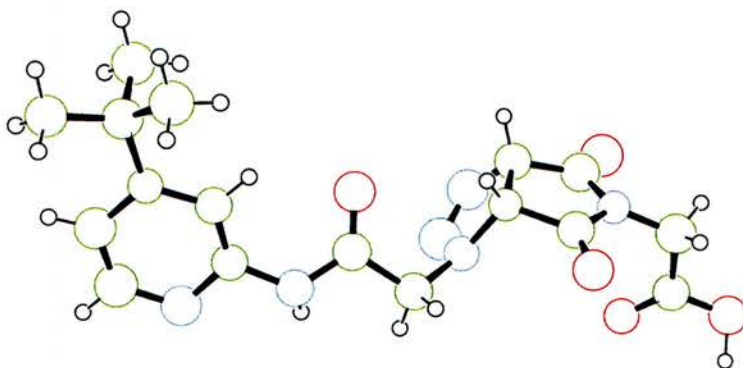


Figure 2.23 Single crystal X-ray structure obtained for template **78**.

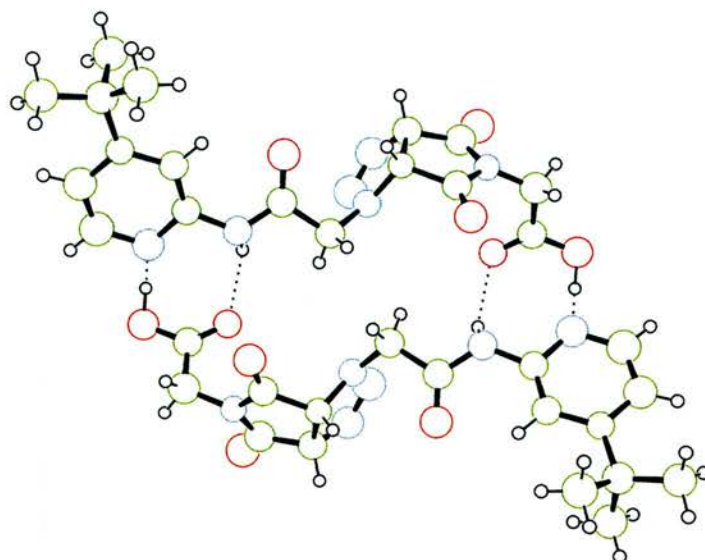


Figure 2.24 Single crystal X-ray structure showing the product duplex obtained for template **78** in the solid state. Hydrogen bonding interactions are shown by dotted lines.

2.10 Summary of evidence for a self-replicating pathway

It has been demonstrated that the recognition-mediated reaction demonstrates an enhanced rate over the bimolecular reaction and that the control reactions performed (doping and competition) suggest that the system operates under a self-replicating pathway. However the sigmoidal curve is not observed for the recognition-mediated reaction as would be expected and so this indicates that the system is not autocatalytic and product inhibition is being observed, *i.e.* the product duplex has been formed however the binding between the templates is quite strong and so it is inefficiently or not dissociating and releasing the template molecules back into the catalytic channel (**Figure 2.25**). The X-ray crystallographic data supports this finding due to the observation of a product duplex.

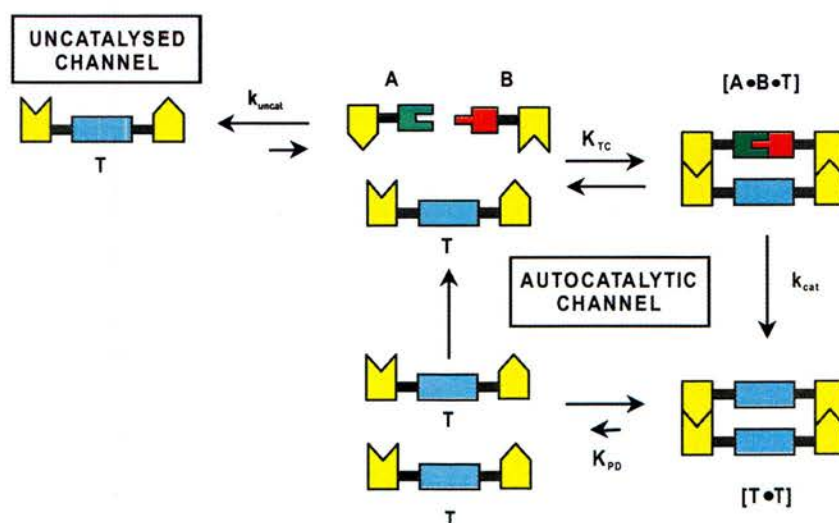


Figure 2.25 Proposed self-replicating pathway observed for the reaction between **5** and **77**.

Previous literature examples^{101,102} of self-replicating systems have also observed this product inhibition due to the strong association within the product duplex [T.T]. This hinders the release of the template back into the autocatalytic cycle, consequently efficient turnover is not achieved. This led to the development of the square root law, an empirical relationship established by von Kiedrowski^{172,173} and Orgel^{174,175} to describe self-replicating behaviour in minimal systems. This relationship is described in **Equation 2.1**.

$$\frac{dT}{dt} = k_1 [A].[B] + k_2 [A].[B].[T]^p$$

Equation 2.1 The rate equation used by von Kiedrowski to describe the behaviour within a minimal self-replicating system. k_1 = rate constant of the uncatalysed bimolecular reaction. k_2 = rate constant associated with the autocatalytic cycle. T = replicator concentration and p = order of rate of autocatalysis with respect to the replicator concentration.

The experimentally determined reaction order (p) was found to be 0.48, which was approximated to 0.5 as shown in **Equation 2.1** and the relationship named the Square Root Law. This relationship when $[T]^{0.5}$ implies that product inhibition exists within the system.

A minimal autocatalytic self-replicating system displays ideal behaviour when the rate of the uncatalysed bimolecular reaction is at a minimum, ideally this would be equal to 0, however in reality this would never occur because the bimolecular reaction is necessary for the formation of template in the initial stages of the self-replicating system. Ideal behaviour is also maximised when k_2 is large (*i.e.* the rate of the catalysed reaction is a maximum).

Von Kiedrowski also defined the value ϵ (**Equation 2.2**), which is a measure of the relative importance of the two pathways to the overall rate.

$$\epsilon = k_2/k_1$$

Equation 2.2 Equation used to measure the relative importance of the two pathways to the overall rate. k_2 = rate of the recognition-mediated reaction, k_1 = rate of uncatalysed bimolecular reaction.

If ϵ is large then this infers that there is a greater contribution from the autocatalytic system than the bimolecular pathway, and so efficient autocatalysis in the self-replicating system is occurring. If ϵ is small then the contribution to the system from the bimolecular reaction is greater and so the autocatalytic self-replicating pathway is inefficient. ϵ also gives the number of autocatalytic cycles that are generated by the template.

2.11 Fitting the experimental data to the kinetic model.

By using the square root approximation it is possible to fit the experimental data to this simple model (**Figure 2.26**) to obtain the rate values.

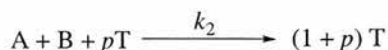
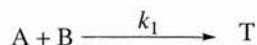


Figure 2.26 Square root approximation used to fit the experimentally determined rate data for minimal self-replicating systems. A and B correspond to the building blocks, T to the template. The values p , k_1 and k_2 correspond to the autocatalytic order, bimolecular rate and the recognition-mediated rate constants respectively.

In the rate equations shown above, the value p represents the autocatalytic rate constant and is a direct measure of the efficiency of the autocatalytic cycle. If a system is operating at its maximum capacity then $p = 1$. However if a system were suffering from product inhibition then a value close to 0.5 would be expected. Using this relationship the experimental data was fitted to the kinetic model shown in **Figure 2.27**.

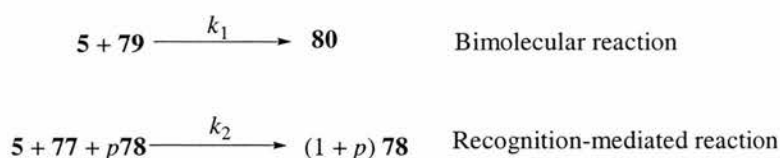


Figure 2.27 Kinetic model used to describe the bimolecular and recognition-mediated reactions between **5** and **79** and **5** and **77** respectively. k_1 represents the rate constant for the bimolecular reaction and k_2 represents the rate constant for the recognition-mediated reaction.

Using this model the experimental data was entered into the simulation and fitting package SIMFIT¹⁷⁶. The program provided a good fit (solid lines, **Figure 2.28**) of the kinetic model to the experimentally determined rate profiles. The rate values are presented in **Table 2.1**.

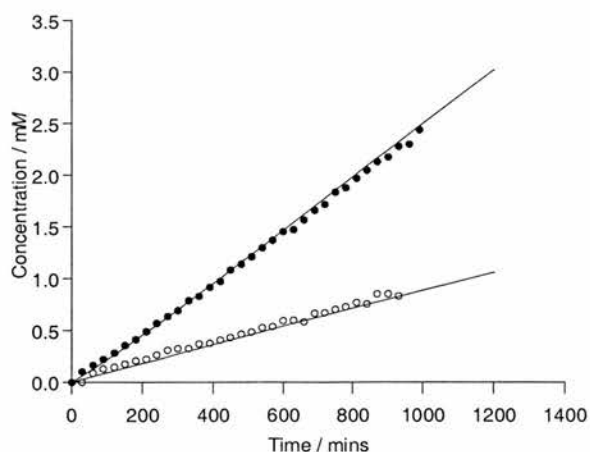


Figure 2.28 Rate profiles for the recognition-mediated reaction between **5** and **77** (closed circles) and the control reaction between **5** and **79** (open circles). The solid lines represent the best fit of the experimental data to the kinetic model.

Table 2.1 Kinetic rate values generated from the simulation and fitting of the bimolecular and recognition-mediated models to the rate profiles.

k_1 ($M^{-1}s^{-1}$)	k_2 ($s^{-1/2}$)
2.45×10^{-5}	4.14×10^{-4}

Upon fitting the experimental to the kinetic model it was found that the best fit occurred when $p = 0.4$. This value is below the value expected for product inhibition within an autocatalytic system of 0.5, as observed by von Kiedrowski, and hence suggests that this system is extremely inefficient at turning over the template within the autocatalytic system. Using the rate constants presented in **Table 2.1** a value of 17 is obtained for ϵ , this again indicates that the autocatalytic pathway is extremely inefficient.

Although the system is inefficient as an autocatalytic system, it is efficient at accelerating the reaction. This conclusion can be realised by looking at the transition state energy profiles for the bimolecular and recognition-mediated reactions (**Figure 2.29**).

In order to do so the Eyring equation (**Equation 2.3**) must be employed to determine the transition state free energy differences of the reaction pathways.

$$\Delta G^\ddagger = -RT \ln(kh/k_b T)$$

Equation 2.3 The Eyring equation, used to calculate transition state free energies, ΔG^\ddagger . R represents the gas constant ($8.341 \text{ Jmol}^{-1}\text{K}^{-1}$), T represents the temperature in Kelvin (K), k , h and k_b represent the forward rate constant of the reaction in question, the Planck constant ($6.62608 \times 10^{-34} \text{ Js}$) and the Boltzmann constant ($1.38066 \times 10^{-23} \text{ JK}^{-1}$), respectively.

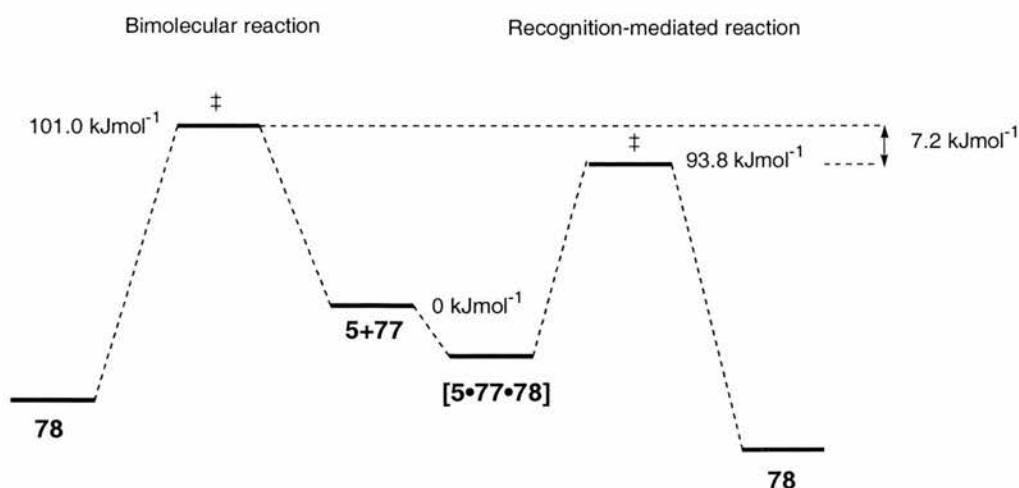


Figure 2.29 Thermodynamic profile for the bimolecular reaction between 5 and 77 and the recognition-mediated reaction between 5 and 77 at 30°C. The energy of the uncomplexed reactants is set as the zero point energy.

The thermodynamic profile shows that the transition state for the recognition-mediated pathway is stabilised by 7.2 kJmol^{-1} compared to the bimolecular reaction.

2.12 Measuring the association constant of the product duplex [78•78]

The efficiency of an autocatalytic cycle hinges on the effective dissociation of the product duplex [78•78] in the autocatalytic cycle. If the duplex is too stable then dissociation of the duplex is either very inefficient or does not occur at all, and so no template is returned to solution and hence autocatalysis fails. To try to test this it was necessary to measure the dimerisation constant for the [78•78] duplex. This would have been performed by measuring the dimerisation constant for the [78•78] duplex directly using ^1H 500 MHz NMR spectroscopy, unfortunately the template **78** was not soluble enough in CDCl_3 and the ^1H NMR chemical shift changes observed too small to allow accurate determination of the association constant.

2.13 What happens to the reaction pathway at an elevated temperature?

As shown in **Figure 2.17** the rate for the reaction between **5** and **77** shows differing behaviours at 30°C and 50°C . The self-replicating pathway indicated at 30°C disappears at 50°C . However, the system contains recognition sites so it is possible that the system is proceeding *via* an alternative route, either through the AB-mediated pathway or purely *via* the bimolecular reaction or it could be a combination of both, so it would be instructive to perform and examine the control reactions described for the system as described previously. Firstly, the bimolecular control reaction must be examined to evaluate whether any catalysis of the reaction is occurring within the system at 50°C . This was performed in an identical manner as before by using the methyl ester of the maleimide (**Figure 2.30**).

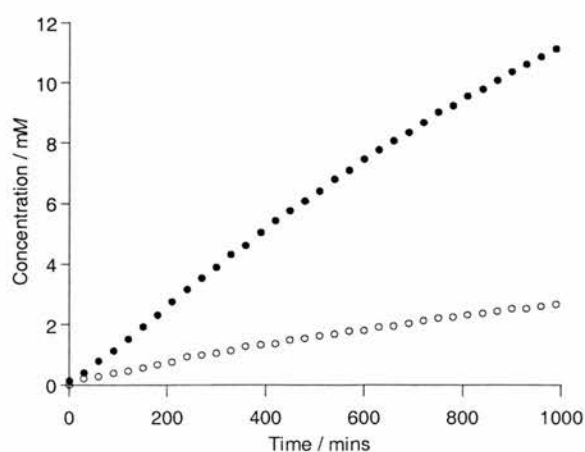


Figure 2.30 Rate profiles for the reaction between azide **5** and maleimide **77** (closed circles) and azide **5** and maleimide ester **79** (open circles) at a concentration of 25 mM in CDCl_3 at 50°C .

It is evident from the bimolecular control reaction that removal of the recognition has significantly decreased the rate of reaction between **5** and **79** at 50°C. To provide further evidence of the recognition-mediated nature of the reaction the doping experiment was performed by the addition of 4 equivalents of benzoic acid to the reaction between **5** and **77** (**Figure 2.31**).

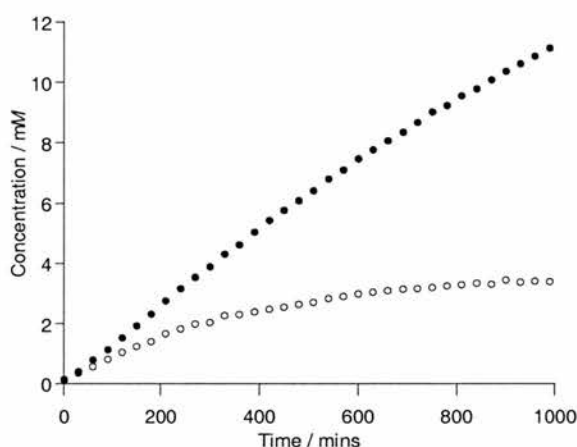


Figure 2.31 The rate profiles to compare the recognition-mediated reaction between azide **5** and maleimide **77** (solid circles) and the control reaction between azide **5** and maleimide **77** and 4 equivalents of benzoic acid (open circles) in CDCl_3 at 50°C.

It is evident from both the bimolecular control reaction and the doping study that the reaction between **5** and **77** at a concentration of 25 mM in CDCl_3 at 50°C occurs *via* a recognition-mediated process. Although on the evidence presented in **Figure 2.32** it is apparent that the rate of reaction is observed to decrease with increasing time. This evidence suggests an alternative pathway is occurring to the self-replicating mechanism at 30°C, as the reaction appears to be recognition-mediated the alternative pathway must be that of an AB-mediated route.

To ensure that self-replication is not occurring a third control experiment was performed which involved doping the reaction with preformed template. Addition of preformed template to the reaction should result in an increase in the rate of reaction if the system can act as its own template.

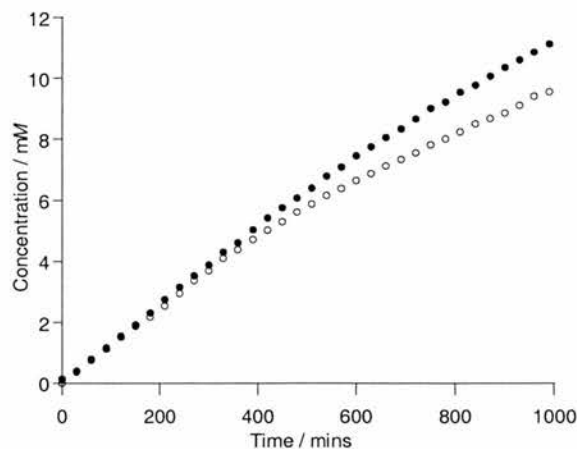


Figure 2.32 The rate profiles to compare the recognition-mediated reaction between azide **5** and maleimide **77** (solid circles) and the control reaction between azide **5** and maleimide **77** and 10 mol% of added preformed template **77** (open circles) at a concentration of 25 mM in CDCl_3 with respect to **5** and **77** at 50°C.

It can be observed from the doping experiment that initially addition of preformed template has no effect upon the rate of formation of template **78**, then after approximately 400 minutes the rate of reaction begins to slow compared to the original recognition-mediated reaction, this indicates that the template must be having an inhibitory effect upon the system. If the system is reacting *via* an AB-type mechanism, the presence of open template (through external addition and bimolecular formation) may be binding the building blocks but reaction is not facilitated due to the alternative pathway required.

This inhibitory effect was also observed when the system depicted in **Scheme 2.4**, which shows the AB-mediated reaction between azide **5**, and maleimide **6** was doped with 10 mol% template **7** (**Figure 2.33**).

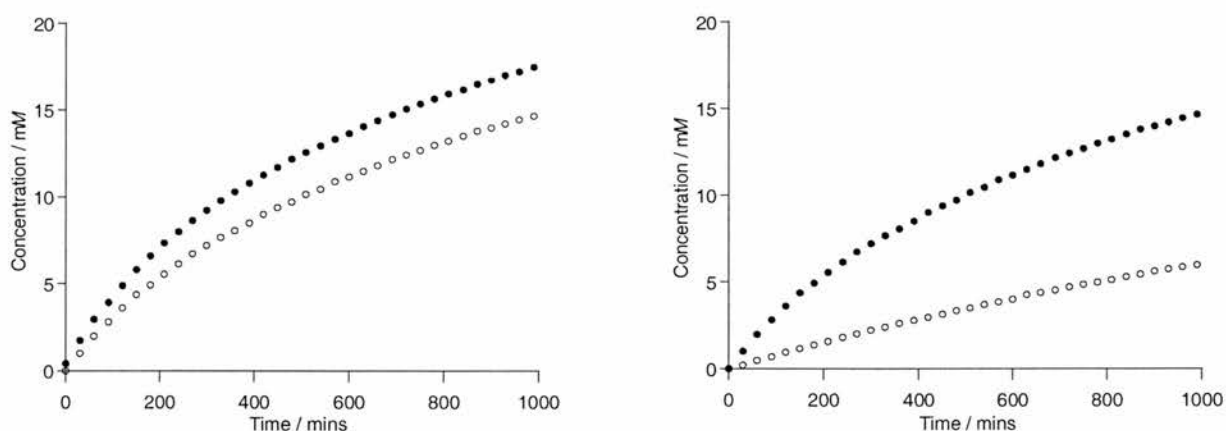


Figure 2.33 The rate profiles to compare (a) the recognition-mediated reaction between azide **5** and maleimide **6** (solid circles) and the control reaction between azide **5** and maleimide **6** and 10 mol% of added preformed template **7** (open circles) at a concentration of 25 mM in CDCl_3 with respect to **5** and **6** at 50°C. (b) the recognition-mediated reaction between azide **5** and maleimide **6** (solid circles) and the control reaction between azide **5** and maleimide **6** and 10 mol% of added preformed template **7** (open circles) at a concentration of 25 mM in CDCl_3 with respect to **5** and **6** at 30°C.

The data in **Figure 2.33** clearly shows that addition of 10 mol% template to the AB-mediated reaction causes a reduction in the rate of reaction. The effect of added template is much more pronounced at (b) 30°C than (a) 50°C. This indicates that the template has an inhibitory effect upon the rate of reaction between azide **5** and maleimide **6**, its function is comparable to that of benzoic acid, by blocking the recognition sites. This also indicates that the template **7** does not retain its closed conformation upon formation, inspection of the single crystal X-ray structure obtained, reveals that the conformation is closed *via* the recognition between the amide proton and maleimide oxygen which leaves the carboxylic acid free to bind (**Figure 2.34**) (**Table 6.2**).

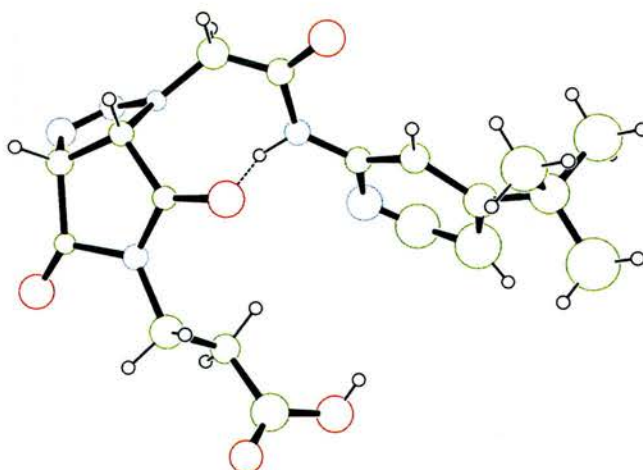


Figure 2.34 Single crystal X-ray structure obtained for compound **7**. A hydrogen bonding interaction is shown by a dashed line.

2.14 Fitting the experimental data to the kinetic model

The experimental data obtained for the bimolecular and recognition-mediated reactions in CDCl_3 at 50°C was fitted to kinetic model described (**Figure 2.35**) using the SIMFIT program as previously.

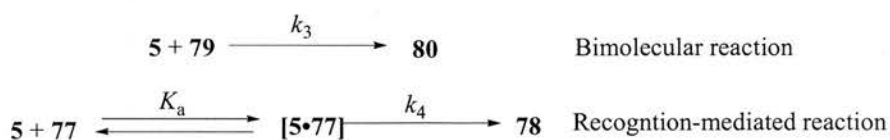


Figure 2.35 Kinetic model used to describe the bimolecular and recognition-mediated reactions in CDCl_3 at 50°C. k_3 and k_4 represent the rate constants *via* the bimolecular and recognition-mediated reactions respectively.

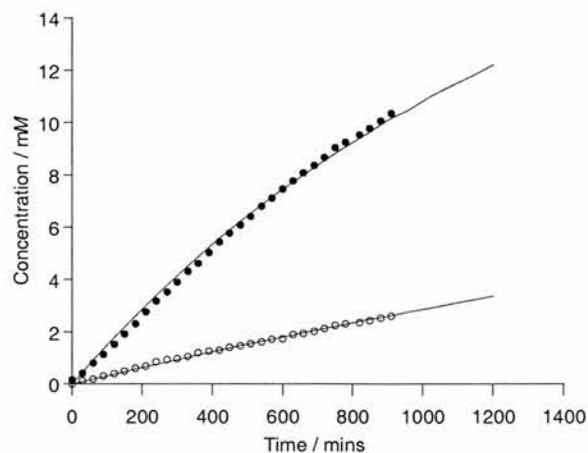


Figure 2.36 Rate profiles for the recognition-mediated reaction between **5** and **77** (closed circles) and the control reaction between **5** and **79** (closed squares). The solid lines represent the best fit of the experimental data to the kinetic model.

The rate values for the respective reactions could then be extracted from the fitted data (**Table 2.2**).

Table 2.2 Kinetic rate values generated from the simulation and fitting of the bimolecular and recognition-mediated models to the rate profiles.

$k_3 (M^{-1}s^{-1})$	$k_4 (s^{-1})$
8.63×10^{-5}	1.86×10^{-5}

From the rate constants obtained it is possible to determine the kinetic effective molarity (kEM). As discussed in **Section 1.6.2**, the kEM (**Equation 2.4**) is a direct comparison of the forward rates of the recognition-mediated reaction (k_f) and the uncatalysed bimolecular reaction (k_{uf}).

$$\text{kEM} = \frac{k_f}{k_{uf}} = \frac{s^{-1}}{M^{-1}s^{-1}} = M$$

Equation 2.4 Kinetic effective molarity (kEM) expressed in M and where k_f and k_{uf} represent the forward rate of the AB-mediated and bimolecular reaction, respectively.

Using this equation a value of 216 mM was obtained for the kEM for the formation of cycloadduct **78** at 50°C. As discussed in **Section 1.6.2** the kEM is a measure of the relative efficiency of a system. If the kEM is greater than 1M then the system is said to be operating efficiently, conversely if the kEM is less than 1M the system is said to be operating inefficiently. Therefore in this system it can be said that the system is not operating efficiently as a value less than one is obtained. To elucidate why this system is kinetically inefficient yet still seems to be accelerating the reaction, the rate constants for the bimolecular and recognition-mediated reactions can be converted into energy profiles. In this case the

association constant K_a for the duplex [5•77] is known so the Gibbs equation (Equation 2.5) can be used to calculate the ground state energy for the duplex.

$$\Delta G = -RT \ln K_{eq}$$

Equation 2.5 The Gibbs equation used to calculate the ground state energy in Figure 2.38 relative to the ground state of the reactants (zero energy point). ΔG represents the free energy of the cycloadduct ground states, T the reaction temperature in Kelvin (K) and R the gas constant in $\text{Jmol}^{-1}\text{K}^{-1}$; K_{eq} represents the equilibrium constant.

Using the Gibbs equation (Equation 2.5) and the Eyring equation (Equation 2.3) the relative free energies of the ground and transition states respectively can be determined.

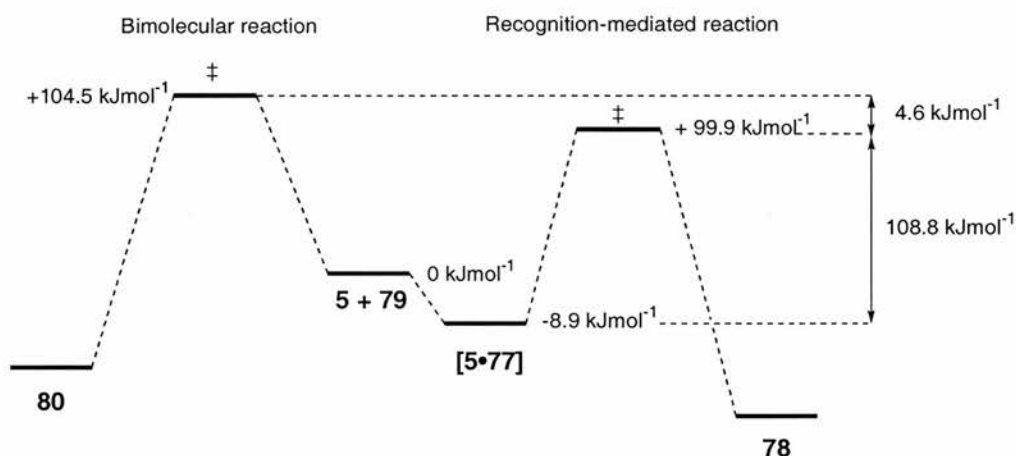


Figure 2.37 Thermodynamic profile for the bimolecular reaction between 5 and 79 and the recognition-mediated reaction between 5 and 77 at 50°C. The energy of the uncomplexed reactants is set as the zero point energy.

Examination of the energy profile shows that the transition state leading to the recognition-mediated reaction product 78 is stabilised by 4.6 kJmol^{-1} compared to the bimolecular reaction product 80. However this stabilisation is not enough to offset the increase in the activation barrier of 8.9 kJmol^{-1} required by the formation of the [A•B] complex [5•77]. As a result of the energy required to associate the building blocks, the activation energy for the recognition-mediated pathway is actually 4.3 kJmol^{-1} higher than that required for the bimolecular reaction. Hence, the k_{EM} (216 mM) is less than one and indicates that the system is operating inefficiently. The observation of an increase in the rate of reaction (Figure 2.36) can be explained by looking at the value of the k_{EM} . The effective molarity can also be described as the concentration required for the bimolecular reaction to proceed at the same rate as the *pseudo*-unimolecular recognition-mediated reaction. Hence, as a value of 216 mM was obtained for this system and the reactions were performed at a concentration of 25 mM, it is not surprising that acceleration was observed for this system at 25 mM.

2.15 Conclusion

In conclusion, it has been demonstrated that the reaction between azide **5** and maleimide **77** at a concentration of 25 mM in CDCl₃ at 30°C is capable of forming a template **78** which can undergo self-replication, although not autocatalytically. It has been demonstrated by X-ray crystallography that the template **78** forms a strong product duplex [**78**•**78**] in the solid state. It has also been suggested indirectly through kinetic simulation that the template duplex is stable in solution. The stability of the product duplex prevents the release of the template and so autocatalysis is extremely inefficient. This inefficiency has been noted in previous literature examples and is an important factor to overcome when designing minimal self-replicating systems. It would be instructive to be able to determine why these systems differ from minimal replicators, which do show efficient autocatalysis. An understanding of this is necessary for the successful application of self-replication in synthetic chemistry. However, conflicting evidence has also been demonstrated through the nOe study, which demonstrates that the template seems to be held in a closed type conformation, which indicates that the system can also proceed through the AB-pathway at 30°C. This means that all three pathways (**Figure 2.1**) are open to this system, which leads to a very complicated analysis, and so it can be concluded that self-replication is evident but it is not the sole pathway for this system.

It has also been demonstrated that by increasing the temperature at which the reaction is performed, the dominant pathway that the system reacts *via* can be changed. This was observed by increasing the temperature from 30°C where the system reacted predominantly *via* a self-replicating pathway, to 50°C where the reaction pathway followed the AB-mediated route. This demonstrates the delicate nature of a self-replicating system.

3. What Makes a System a Successful Autocatalytic Self-Replicator?

3.1 The search for a self-replicating system

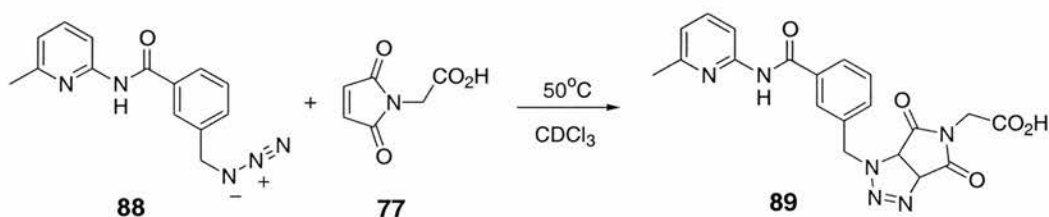
Within the Philp group, many systems have been developed in the hope that they may have the ability to self-replicate autocatalytically. However, in the search for self-replicators it has been discovered that AB-systems are more easily produced. This observation is not wholly surprising, as the two systems are closely related and as a result of entropy, the AB-complex pathway is the favoured channel for a system to react through.

3.2 Examples of recognition-mediated systems which react *via* an AB-complex pathway

As mentioned previously, there have been many systems developed with the intention of producing a self-replicating system, however, it has been revealed upon kinetic analysis that the systems react *via* an AB-complex pathway instead. Four of these systems will be briefly discussed below.

3.2.1 An AB-complex system which utilises a 1,3-dipolar cycloaddition

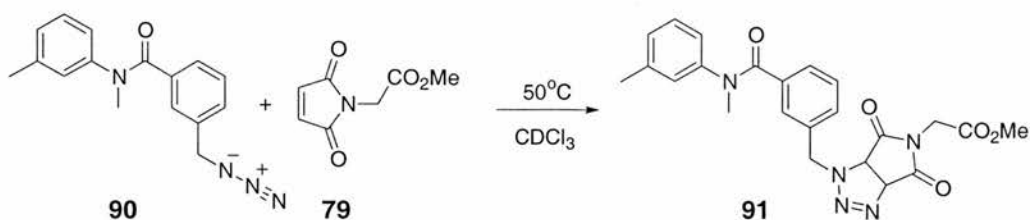
One of the first systems investigated^{83,177} involves the 1,3-dipolar cycloaddition reaction between azide **88** and maleimide **77** (Scheme 3.1).



Scheme 3.1 The design of a potential self-replicating system using the 1,3 dipolar cycloaddition reaction between azide **88** and maleimide **77** to afford the template **89**. The reaction was performed at a concentration of 25 mM in CDCl₃ with respect to the building blocks **77** and **88** at 50°C.

This system is similar to that presented in **Chapter 2** except the CH₂ spacer unit within the azide building block **5** has been replaced with a benzyl group in **88**. The kinetic analysis was performed upon this system at 50°C with starting concentrations of 25 mM in CDCl₃ with respect to the building blocks **77** and **88** (Scheme 3.1).

In order to demonstrate the recognition-mediated ability of this system, a bimolecular control reaction was performed, which involved the use of azide **90** and maleimide ester **79** (Scheme 3.2). The control compounds have the recognition sites blocked so cannot associate through complementary recognition to form a reactive complex. The control reaction was performed under the same conditions as the recognition-mediated reaction.



Scheme 3.2 The control reaction performed between azide **90** and maleimide ester **79** to afford cycloadduct **91**. The reaction was performed at a concentration of 25 mM in CDCl_3 with respect to the starting materials **90** and **79** at 50°C .

The results of the recognition-mediated reaction and the bimolecular control reaction are presented in **Figure 3.1**.

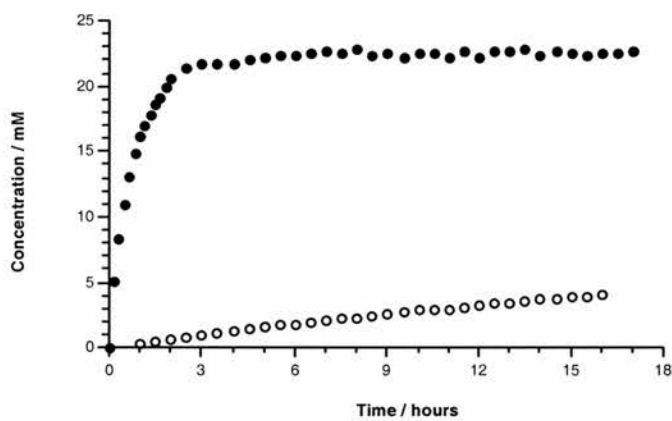
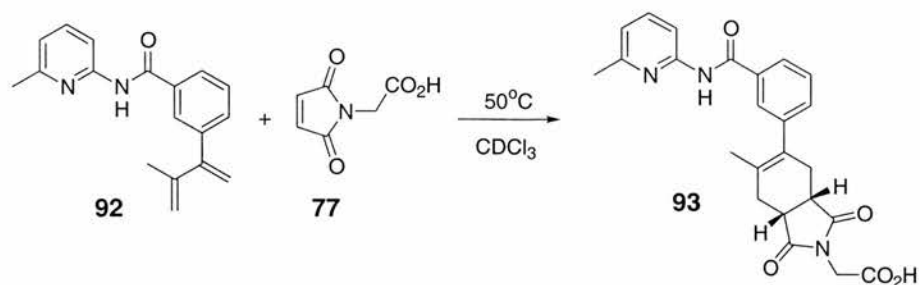


Figure 3.1 The rate profiles obtained for the recognition-mediated reaction between azide **88** and maleimide **79** (closed circles) compared to the bimolecular control reaction between azide **90** and maleimide ester **79** (open circles). Figure taken from ref. 177.

It is evident from the data that the recognition-mediated reaction achieves almost complete consumption of the starting materials after only three hours, whereas the bimolecular control reaction is much slower. It was postulated that the reactants could form the recognition-mediated complex [**88**•**77**], which would facilitate the reaction and so account for the increased reactivity in the recognition-mediated reaction. Hence, it was concluded that this system operated under an AB-complex pathway. A criticism of this system would be that the recognition-mediated reaction should have been repeated at lower temperatures to slow down the initial stage of the reaction. The rate at which this reaction occurs means that if there was a lag period (which would be expected for an autocatalytic self-replicating system), it would not be observed at this temperature.

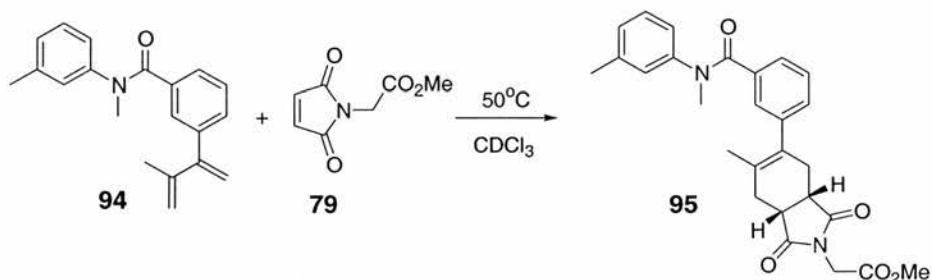
3.2.2 An AB-complex system which utilises a 1,4 cycloaddition

The second system¹⁷⁸ involves a cycloaddition between diene **92** and maleimide **77** to form the cycloadduct **93** (**Scheme 3.3**).



Scheme 3.3 The recognition-mediated reaction between diene **92** and maleimide **77** to afford cycloadduct **93**. The reaction was performed at a concentration of 10 mM in CDCl₃ with respect to both building blocks **77** and **92** at 50°C.

This system is structurally similar to that shown in **Scheme 3.1**, the recognition occurs between an amidopyridine unit and a carboxylic acid. The spacer units are similar, and the reaction observed is another cycloaddition, between a diene **93** and dienophile **77**. In order to determine the extent of the rate enhancement that the recognition has upon the system, a control reaction was performed (**Scheme 3.4**). Again, the control compounds have the recognition sites blocked to prevent association of the reactants; hence, the system should operate as the purely bimolecular reaction.



Scheme 3.4 The bimolecular control reaction performed between diene **94** and maleimide ester **79** to afford cycloadduct **95**. The reaction was performed at a concentration of 10 mM in CDCl₃ with respect to both starting materials **79** and **94** at 50°C.

The results of the recognition-mediated reaction and the control reaction are presented in **Figure 3.2**.

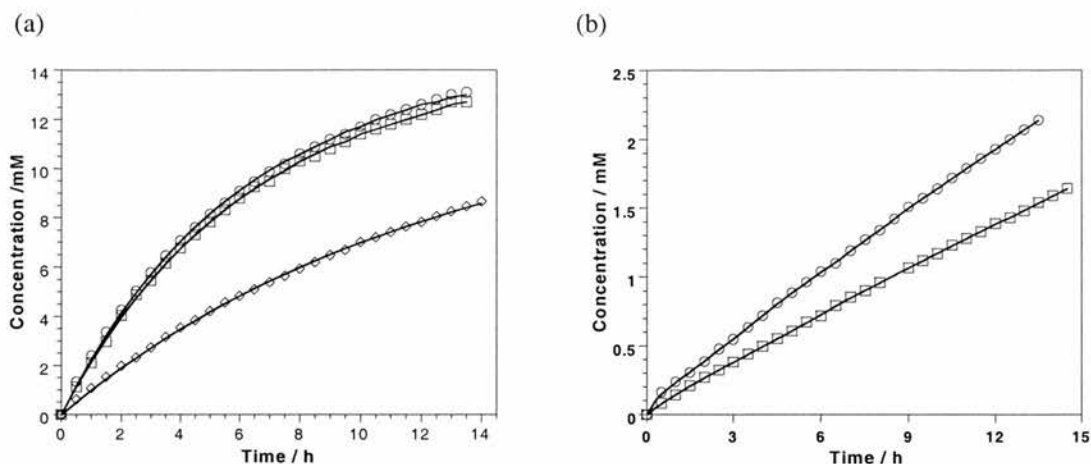
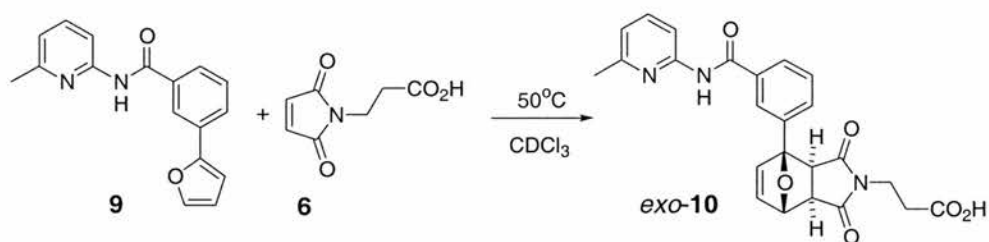


Figure 3.2 The rate profiles obtained for (a) the recognition-mediated reaction between azide **92** and maleimide **77** (open circles) compared to (b) the bimolecular control reaction between azide **94** and maleimide ester **79** (open circles). Figures taken from ref 178.

Comparison of the data for the recognition-mediated reaction (**Figure 3.2 (a)** open circles) with the bimolecular control (**Figure 3.2 (b)** open circles) reveals that there is a significant rate enhancement. No sigmoidal rate profile is obtained for the recognition-mediated reaction so it was concluded that the system followed an AB-complex pathway through the formation of the complex [**77**•**92**] to afford the cycloadduct **93**.

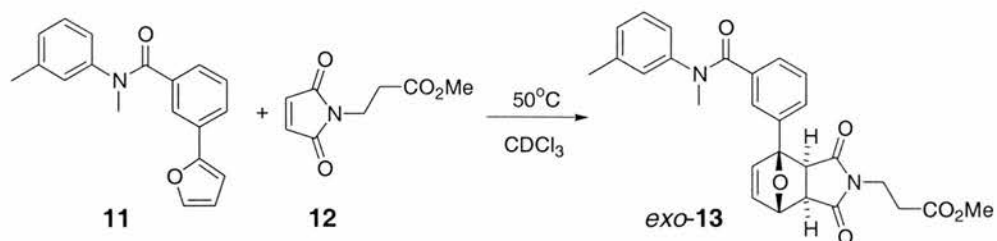
3.2.3 An AB-complex reaction between a 2 substituted furan and a maleimide

The third system utilises the same recognition as the previous two systems between an amidopyridine unit and a carboxylic acid. The spacer units are similar, and the reaction performed was a cycloaddition between a furan **9** and maleimide **6** (**Scheme 3.5**).



Scheme 3.5 The recognition-mediated reaction between furan **9** and maleimide **6** to afford **10**. The reaction was performed at a concentration of 12.5 mM in CDCl₃ with respect to the building blocks **6** and **9** at 50°C.

In order to determine the extent of the rate enhancement that the recognition has upon the system, a control reaction was performed using furan **11** and maleimide **12** (**Scheme 3.6**).



Scheme 3.6 The bimolecular control reaction performed between diene **11** and maleimide **12** to afford cycloadduct **13**. The reaction was performed at a concentration of 12.5 mM in CDCl₃ with respect to the building blocks **11** and **12** at 50°C.

The results of the recognition-mediated and bimolecular control reactions are presented in **Figure 3.3**.

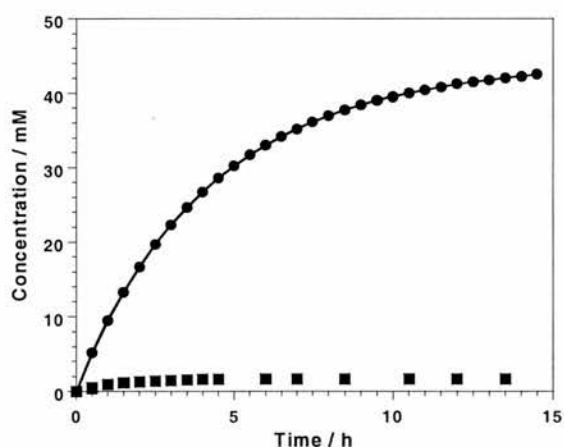
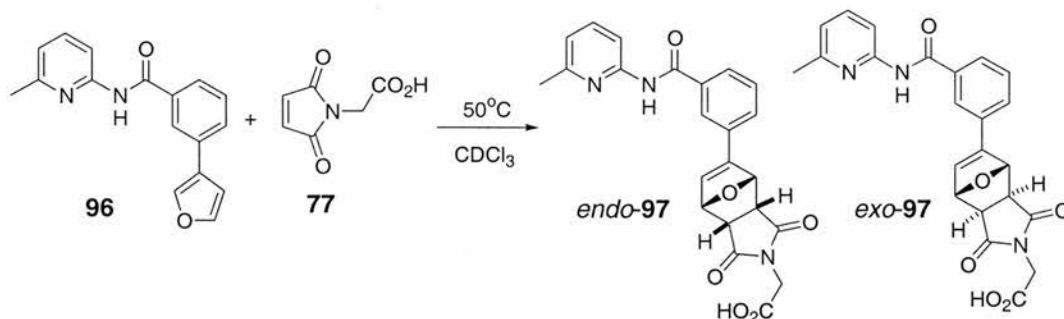


Figure 3.3 The rate profiles for the recognition-mediated reaction between furan **5** and maleimide **6** to afford the cycloadduct **10** (closed circles) and the bimolecular control reaction between furan **11** and maleimide **12** (closed squares). Figure taken from ref. 178.

The formation of cycloadduct *exo*-**10** (closed circles) *via* the recognition-mediated channel shows a significant rate enhancement compared to the bimolecular control reaction (closed squares). It is evident that no sigmoidal rate profile was obtained for the formation of *exo*-**13** and so the rate enhancement was attributed¹⁷⁸ to an AB-complex pathway.

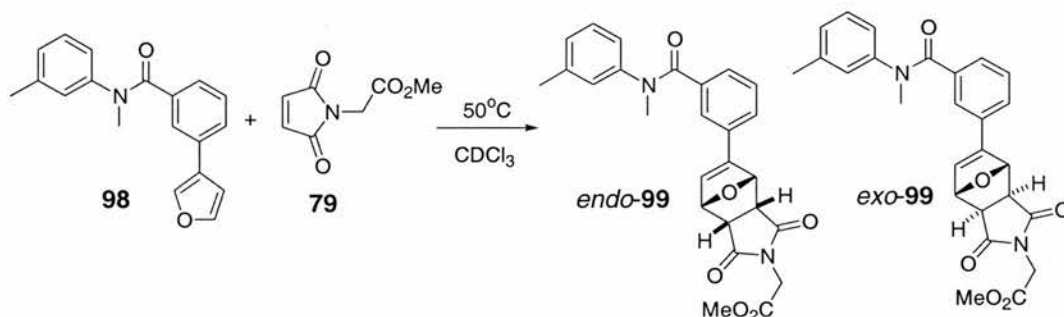
3.2.4 An AB-complex reaction between a 3 substituted furan and a maleimide

The fourth system, is similar to the previous system except the furan is attached to the phenyl ring at its 3- rather than the 2-position (**Scheme 3.7**).



Scheme 3.7 The recognition-mediated reaction between furan **96** and maleimide **77** to afford the *endo-97* and *exo-97* cycloadducts. The reaction was performed at a concentration of 10 mM in CDCl₃ with respect to the building blocks **96** and **77** at 50°C.

In order to determine whether the reaction was enhanced as a result of the recognition a control reaction was performed between furan **98** and maleimide ester **79** (Scheme 3.8).



Scheme 3.8 The bimolecular control reaction between furan **98** and maleimide **79** to afford the *endo-99* and *exo-99* cycloadducts. The reaction was performed at a concentration of 20 mM in CDCl₃ with respect to the starting materials **98** and **79** at 50°C.

The results of the recognition-mediated reaction and the bimolecular control reaction are presented in Figure 3.4.

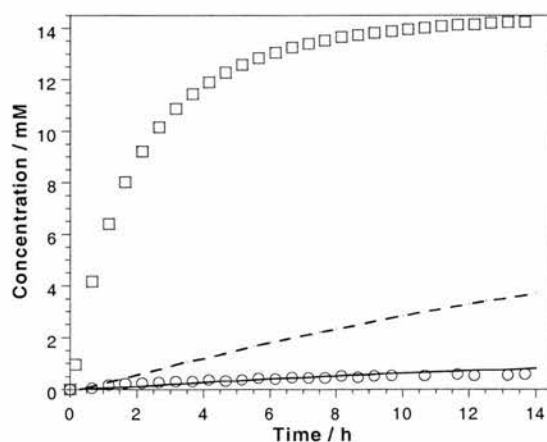


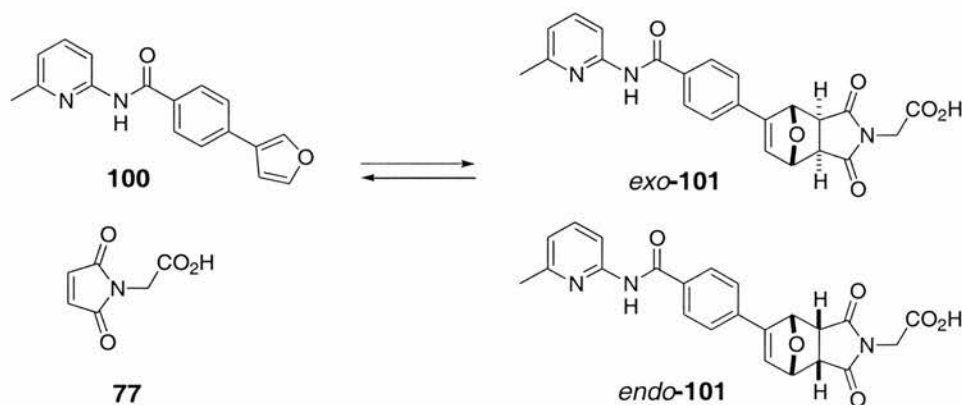
Figure 3.4 The rate profiles for the recognition-mediated reaction between furan **96** and maleimide **77**. Formation of the *endo-97* isomer is represented by the open squares and the *exo-97* isomer is represented by the open circles. Compared with the reaction between furan **98** and maleimide **79**, the dashed line represents the formation of the *exo-99* isomer and the solid line represents the formation of the *endo-99* isomer. The reaction was performed at a concentration of 20 mM with respect to all reagents in CDCl₃ at 50°C. Figure taken from ref. 178.

The data in **Figure 3.4** shows an excellent example of an AB-complex pathway reaction. It is clear that the formation of the *endo*-**97** isomer (open squares) is significantly enhanced compared to the corresponding bimolecular control reaction (solid line). After 14 hours the extent of the bimolecular reaction was approximately 23% complete compared to the recognition-mediated reaction which reached 75% completion over the same time period. It is also evident that the stereochemical outcome of the reaction has been reversed; in the bimolecular control reaction the *exo* diastereoisomer was favoured whereas in the recognition-mediated reaction the *endo* diastereoisomer was predominant. From the fitting of the kinetic data, it was discovered that the *exo* and *endo* adducts were the thermodynamically most stable products of the bimolecular and recognition-mediated pathways, respectively. The degree of selectivity at equilibrium is dramatically altered for the two pathways – an *exo:endo* ratio of 67:1 for the control reaction becomes 189:1 in favour of the *endo* cycloadduct for the AB-mediated reaction. This result implied that the formation of the pre-reactive complex [**96**•**77**] had a profound effect upon the stereochemical outcome of the reaction.

3.3 An example of recognition mediated systems which react *via* a self-replicating pathway

The necessary components required for a self-replicating system were discussed in **Section 1.5**, along with those required for an AB system. The differences between the two sets of requirements are very small. Within the Philp group there have been successful examples¹⁷⁸⁻¹⁸¹ of self-replicating systems.

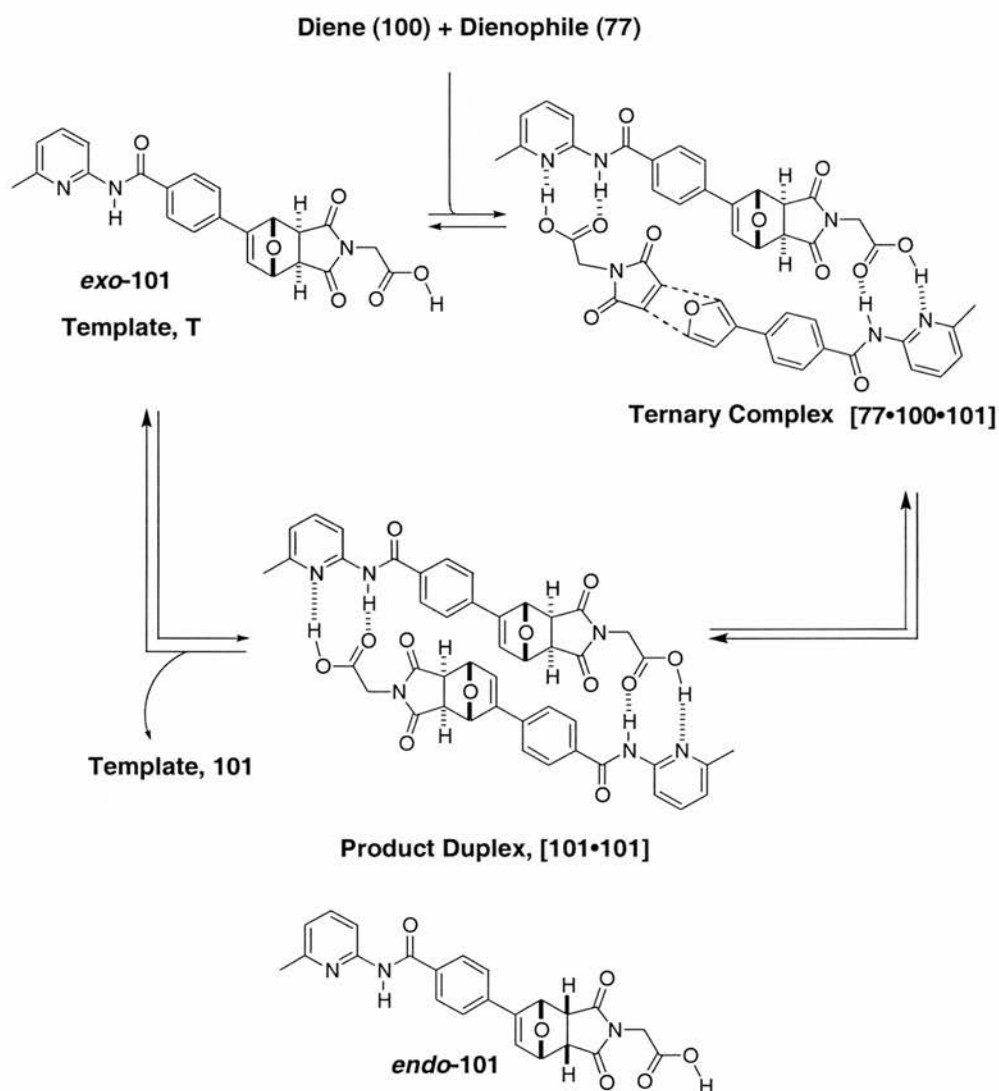
One such system was designed and synthesised, based upon the Diels-Alder reaction between a furan **100** (diene) and maleimide **77** (dienophile) (**Scheme 3.9**).



Scheme 3.9 Diels-Alder reaction between diene **100** and dienophile **77** to afford two possible stereoisomers, *exo*-**101** and *endo*-**101**.

It should be noted that this system is similar to the system shown in **Section 3.2.4**. The furan attached at its 3-position is joined to the phenyl ring at its *para* rather than *meta* position. The reaction between diene **100** and dienophile **77** can lead to the formation of two possible

isomeric templates *exo*-**101** and *endo*-**101**. Molecular mechanics calculations performed upon the system outlined in **Scheme 3.9** suggested that only the *exo*-**101** template was of the correct geometry to replicate itself. This difference was due to the relatively linear nature of the ternary complex $[77\cdot100\cdot101]$ (*exo*) which brought the reacting centres into close proximity, whereas in the ternary complex $[77\cdot100\cdot101]$ (*endo*), the co-conformation became quite angular and held the reacting centres at a distance of greater than 5 Å, hence the reaction would not be favourable within this complex, suggesting that the *endo*-**101** isomer is incapable of templating its own formation or that of the *exo*-**101** template through formation of the $[77\cdot100\cdot101]$ (*endo*) complex.

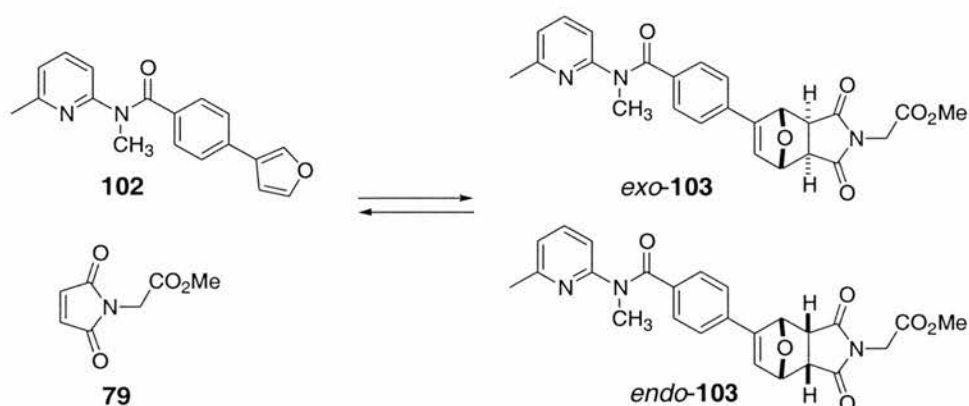


Scheme 3.10 Proposed autocatalytic cycle for the formation of the *exo*-**101** and *endo*-**101** cycloadducts produced from the Diels-Alder reaction between **77** and **100**.

From the molecular mechanics study it was proposed that the formation of the *exo*-**101** stereoisomer would proceed *via* a self-replicating mechanism (**Scheme 3.10**) through the ternary complex $[77\cdot100\cdot101]$ (*exo*) and its autocatalytic nature would have to be determined

experimentally. It was expected that the formation of *endo*-**101** would proceed only *via* the bimolecular reaction. Due to the reversible nature of the Diels-Alder reaction it was thought that over time, the *endo*-**101** template would be converted to the *exo*-**101** template.

The effect that the recognition motif has upon the outcome of the reaction needed to be determined and for this the model compounds **79** and **102** were used to measure the uncatalysed bimolecular reaction (**Scheme 3.11**). By using compound **102**, the amidopyridine NH recognition site on **100** has been methylated, hence blocking this hydrogen-bonding site. The second hydrogen bonding interaction between the aromatic nitrogen of **100** and the hydroxyl of acid **77** was also blocked by the conversion of the acid to the methyl ester and the carboxylic acid. This prevents the formation of the ternary complex [**79**•**102**•**103**] and hence self-replication was not achievable.



Scheme 3.11 Control system designed to measure the outcome of the bimolecular Diels-Alder reaction between diene **102** and dienophile **79** to afford *exo*-**103** and *endo*-**103**.

It was found that at a concentration of 5 mM with respect to **79** and **102** in CDCl₃ at a temperature of 50°C, the bimolecular control reaction was found to be 31% complete after a period of 50 hours with a product ratio of 3.6:1 in favour of the *exo*-**103** stereoisomer (**Figure 3.5 (b)**). The recognition-mediated reaction performed under the same conditions resulted in a 48% completion with a product ratio of 6.8:1 in favour of the *exo*-**101** stereoisomer (**Figure 3.5 (a)**).

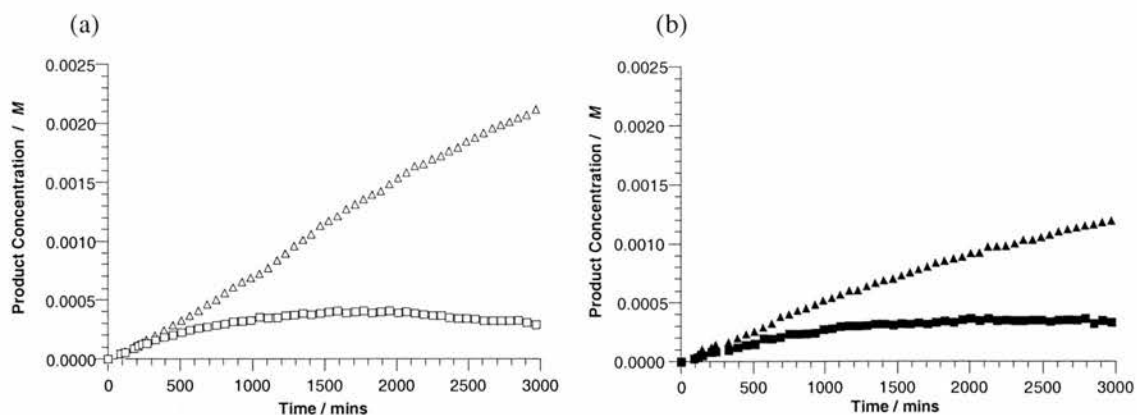


Figure 3.5 Rate profiles demonstrating the ratio of the *exo:endo* cycloadducts formed (represented by triangles and squares respectively) for (a) the recognition-mediated Diels-Alder reaction between **77** and **100** and (b) the bimolecular Diels-Alder reaction between **79** and **102**. Both reactions were performed at a starting concentration of 5 mM with respect to all reagents in CDCl_3 at 50°C . NB. 0.005 M corresponds to a 100% conversion. Figures taken from ref. 180.

By comparison of the data it is clear that the recognition-mediated system is having an effect upon the rate of formation of the *exo*-isomer and the overall stereoselectivity of the reaction. It was also evident from inspection of the experimental data for the recognition-mediated reaction that a lag period was observed for the formation of the *exo-101* isomer as predicted. This indicates that a self-replicating mechanism may be in operation for the *exo-101* template, whereas the *endo-101* isomer is formed only through the uncatalysed bimolecular reaction channel. What is particularly interesting about this reaction, is that over time the concentration of the *endo-101* isomer begins to decrease, and so it would be expected that eventually, only the *exo-101* isomer would be present in solution.

The observation of a lag period alone is insufficient evidence to prove that a self-replicating mechanism is occurring. A number of control experiments must also be performed to prove that the system can self-replicate. The two experiments performed to demonstrate this are (i) a doping study and (ii) a competition experiment. The doping experiment was performed by addition of 20 mol% preformed template to the recognition-mediated reaction between **77** and **100** (Figure 3.6).

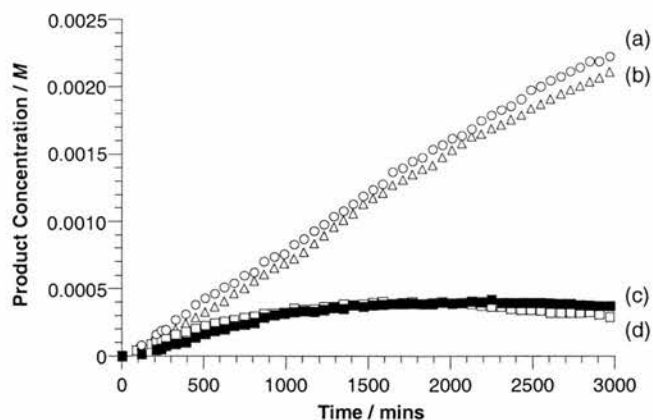


Figure 3.6 Rate profiles for the recognition mediated Diels-Alder reaction between **77** and **100**, performed at a starting concentration of 5 mM with respect to **77** and **100** at 50°C in CDCl₃. The data show the formation of (a) *exo*-**101** in the presence of 20 mol% pre-formed template **101**, (b) *exo*-**101**, (c) *endo*-**101** in the presence of 20 mol% pre-formed template **101** and (d) *endo*-**101**. Figure taken from ref. 180.

A system that operates *via* a self-replicating mechanism will display a lag period, this is due to the uncatalysed bimolecular reaction occurring to form template **T**, once the concentration of the template has reached a critical value it is then possible for the template to begin to catalyse its own formation. Addition of pre-formed template will eradicate the need for the bimolecular reaction to occur before autocatalysis can begin and, hence, the lag period is removed. From inspection of the experimental data it was shown that, although the effect is small the apparent lag period observed in the recognition-mediated reaction does disappear upon addition of preformed template and so substantiates the claim that this system can operate *via* a self-replicating pathway.

The second control experiment involved the addition of three equivalents of benzoic acid. The operation of a self-replicating system relies on the formation of the [**77**•**100**•**101**] ternary complex. If this binding event can be disrupted then the self-replicating cycle should be rendered inefficient, or obsolete. In this case the benzoic acid can competitively bind to the amidopyridine unit within **100**. The results of this control experiment are presented in **Figure 3.7**.

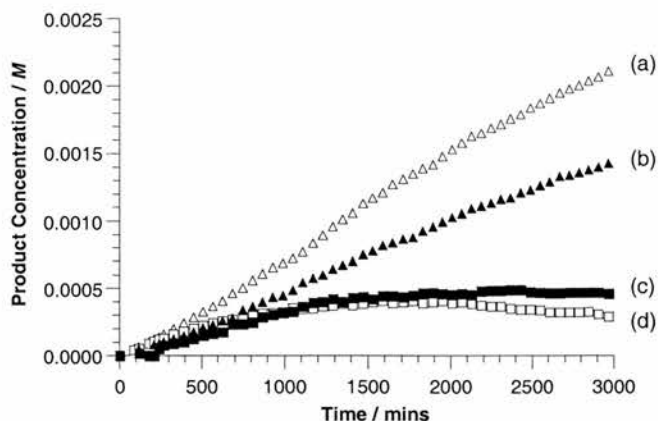


Figure 3.7 Rate profile for the recognition-mediated Diels-Alder reaction between **77** and **100**, performed at a starting concentration of 5 mM with respect to **77** and **100**, at 50°C in CDCl₃. The data shows the formation of (a) *exo*-**101**, (b) *exo*-**101** in the presence of three equivalents of benzoic acid, (c) *endo*-**101** in the presence of three equivalents of benzoic acid and (d) *endo*-**101**. Figure taken from ref. 180.

The results show that the addition of benzoic acid has very little effect upon the formation of the *endo*-**101** isomer, which again supports the theory that its formation is *via* a bimolecular pathway. However the addition of benzoic acid has decreased the rate of formation of the *exo*-**101** isomer, which indicates that it has had an effect upon the formation of the ternary complex [**77**•**100**•**101**] inferring that it is important for the formation of *exo*-**101**. This result again provides supporting evidence for the self-replicating nature of the *exo*-isomer. It was concluded that the *exo*-**101** isomer is formed *via* an autocatalytic self-replicating pathway. Kinetic studies on this system revealed (Section 2.11) that it has an ϵ value of 290 and a p value of 0.74, which indicates that this is a reasonably efficient self-replicating system. By contrast, the formation of *endo*-**101** is purely *via* a bimolecular pathway.

3.4 The design of a recognition-mediated system

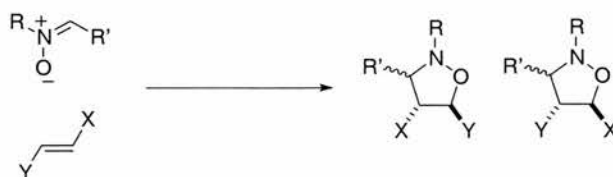
As discussed in Section 1.6, there are three important considerations to be made when designing a recognition-mediated system.

- (i) The recognition motif.
- (ii) The spacer unit.
- (iii) The covalent bond forming reaction.

The next system to be investigated utilises the successful hydrogen-bonding motif between an amido pyridine and a carboxylic acid (Section 2.1.1). The spacer unit used was a phenyl group, the reason for this was to try to provide a certain amount of rigidity to the template in the hope that it will facilitate the assembly of the building blocks. Finally, the covalent bond forming reaction investigated was a 1,3-dipolar cycloaddition this time between a nitron and a maleimide to form an isoxazolidine.

3.4.1 Isoxazolidines

Isoxazolidines are five-membered heterocyclic rings, which contain nitrogen and oxygen. They are the product of the 1,3-dipolar cycloaddition reactions between a nitron^{181,182} and an unsaturated unit, for example an alkene (**Scheme 3.12**).



Scheme 3.12 The 1,3 dipolar cycloaddition reaction between a simple nitron and an alkene to yield two regioisomeric isoxazolidine products.

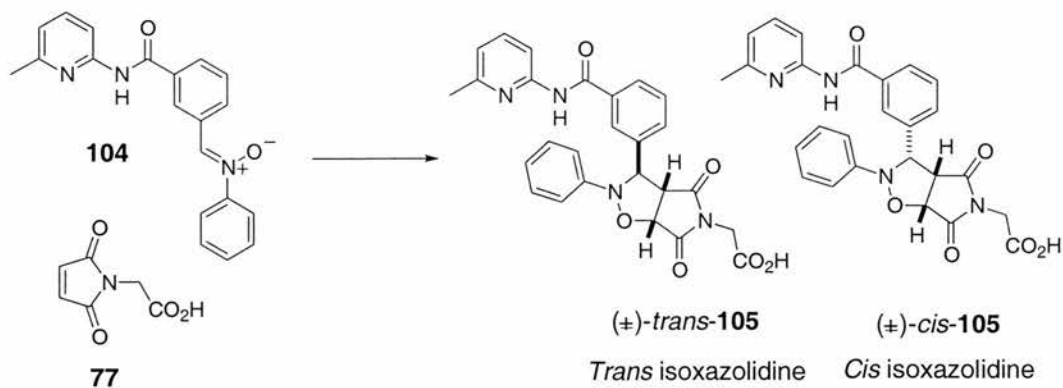
Isoxazolidines can play a key role as an intermediate¹⁸³ in synthetic chemistry. They can be used as 1,3-aminoalcohol equivalents that may be further transformed or as target structures themselves. The lability of the N-O bond mean that they are important in the synthesis of many alkaloids^{184,185} amino acids¹⁸⁷ and amino sugars¹⁸⁷.

The cycloaddition reaction between nitrones and alkenes has been studied by several groups¹⁸⁷⁻¹⁹⁰. In particular, Huisgen and co-workers¹⁹²⁻¹⁹⁴ made major advances in the area of 1,3-dipolar cycloaddition concerning the addition of nitrones to alkenes, which lead to the elucidation of the mechanisms, patterns of reactivities and selectivities in 1,3-dipolar cycloaddition reactions (**Section 2.1.2**).

3.4.2 The new recognition-mediated system

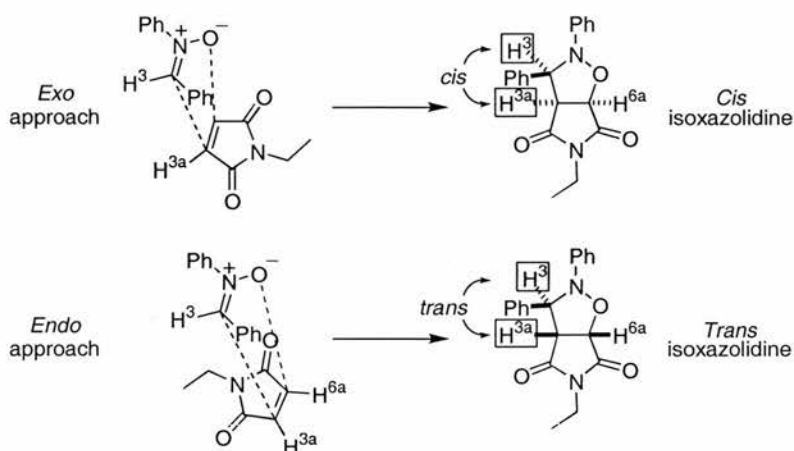
The target building blocks for the new system **77** and **104** were identified (**Scheme 3.13**), the reaction from which can lead to two possible diastereoisomeric products *trans*-**105** and *cis*-**105** (this nomenclature will be explained subsequently).

The covalent bond forming step, is the 1,3-dipolar cycloaddition reaction between a nitron **104** and a maleimide **77**. The maleimide **77** is activated towards dipolar cycloaddition reactions as a result of the two C=O groups conjugated to the double bond. Use of the maleimide **77** also simplifies the system due to its symmetrical nature there is only one possible regioisomeric outcome. The use of an alkyl chain also allows for tuning of the system by altering the length of the spacer unit.



Scheme 3.13 Building blocks **77** and **104** for the potential self-replicating system, affording products *trans*-**105** isoxazolidine and *cis*-**105** isoxazolidine.

Molecular modelling of this system showed that these building blocks would provide a good fit for the catalytic ternary complex and may prevent reactivity *via* the AB complex. The reaction between the nitron **104** and maleimide **77** produces two diastereoisomeric products (along with corresponding enantiomers). This is due to the two possible modes of attack of the nitron upon the maleimide (**Scheme 3.14**).



Scheme 3.14 Transition state orientation of the nitron and maleimide to give the *trans*- and *cis*-isoxazolidine products.

It should be noted that during the course of the reaction three chiral centres are generated. The type of approach, governs the stereochemistry of the chiral centre at the 3 position of the heterocycle. The *exo* attack ('extended' transition state)^{195,196} leads to the *cis*-isoxazolidine and the *endo* attack ('compressed' transition state)^{195,196} leads to the *trans*-isoxazolidine. In this system, the labels *cis* and *trans* are used to describe the relationship between the protons labelled 3 and 3a, and will be the identification labels used through this chapter for these products.

Structure elucidation for these products was determined¹⁹⁷ through 300 MHz ¹H NMR spectroscopy and gradient nOe spectroscopy, which indicated that the nitronne possessed the *Z* conformation about the C=N double bond (**Figure 3.8**).

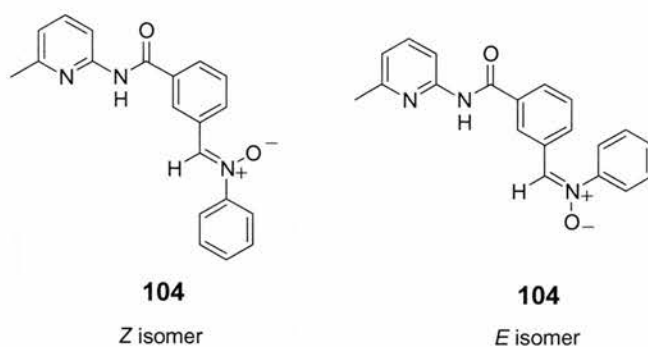


Figure 3.8 The possible *E* and *Z* configurations for nitronne **104**.

However, the structural assignment was substantiated using single crystal X-ray diffraction techniques. Vapour diffusion of hexane into a solution of nitronne **104** in chloroform afforded single crystals of **104** suitable for X-ray diffraction. The solid-state structure (**Figure 3.9**) (**Table 6.3**) clearly shows that the C=N double bond is in a *Z* configuration.

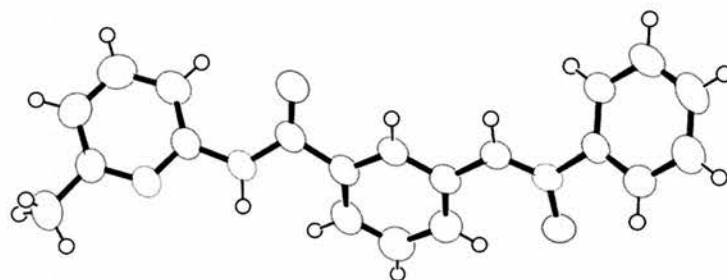


Figure 3.9 Single crystal X-ray structure for Nitronne **104**.

3.5 Kinetic analysis

3.5.1 Optimisation of the reaction conditions to promote the autocatalytic cycle

The operation of a self-replicating system will be most efficient when the formation of the template through the bimolecular channel (bimolecular leakage) is kept to a minimum whilst keeping the formation of template through the autocatalytic channel at a maximum.

When determining the optimum reaction conditions to run a self-replicating system under, there are two variables, which should be considered, concentration and temperature.

As discussed in **Section 2.5** the concentration will have an effect upon the system because the higher the concentration the faster the bimolecular reaction will proceed. However, due to the limited solubility of the maleimide **77** in CDCl₃, the concentration at which this reaction could be studied was limited to a maximum of 25 mM. Concentrations lower than this

resulted in large errors in determining low product concentrations. Varying the temperature at which a reaction is performed also has an effect on the reaction channel the system may proceed by. Higher temperatures may increase the rate of template production as well as hindering the recognition-mediated reaction from occurring due to disturbing the association between the hydrogen bonding sites. The reaction was performed over a range of temperatures from 0 to 30°C and it was decided that 10°C gave the best working temperature.

3.5.2 The kinetic experiment

The kinetic experiment to analyse the solution phase behaviour of the two building blocks was then performed. Stock solutions of **77** and **104** were prepared to a concentration of 50 mM in CDCl₃ and were equilibrated to 10°C for at least one hour before use. Equal volumes of the stock solutions of the building blocks were mixed together in an NMR tube and a 500 MHz ¹H NMR spectrum was recorded immediately. The progress of the cycloaddition was monitored by recording the 500 MHz ¹H NMR spectrum every 30 minutes. All spectra were transformed and phased under identical conditions and the spectral data treated identically in all cases. The reaction course was followed by examining the disappearance of either the resonance arising from the proton attached to the C=N double bond, or if this was obscured, the resonance arising from the aromatic protons adjacent to the C=N double bond, or by following the disappearance of the maleimide singlet corresponding to the protons attached to the double bond. The percentage completion was quantified by comparison of these proton signals to those arising from the equivalent protons in the isoxazolidine product (**Figure 3.10**).

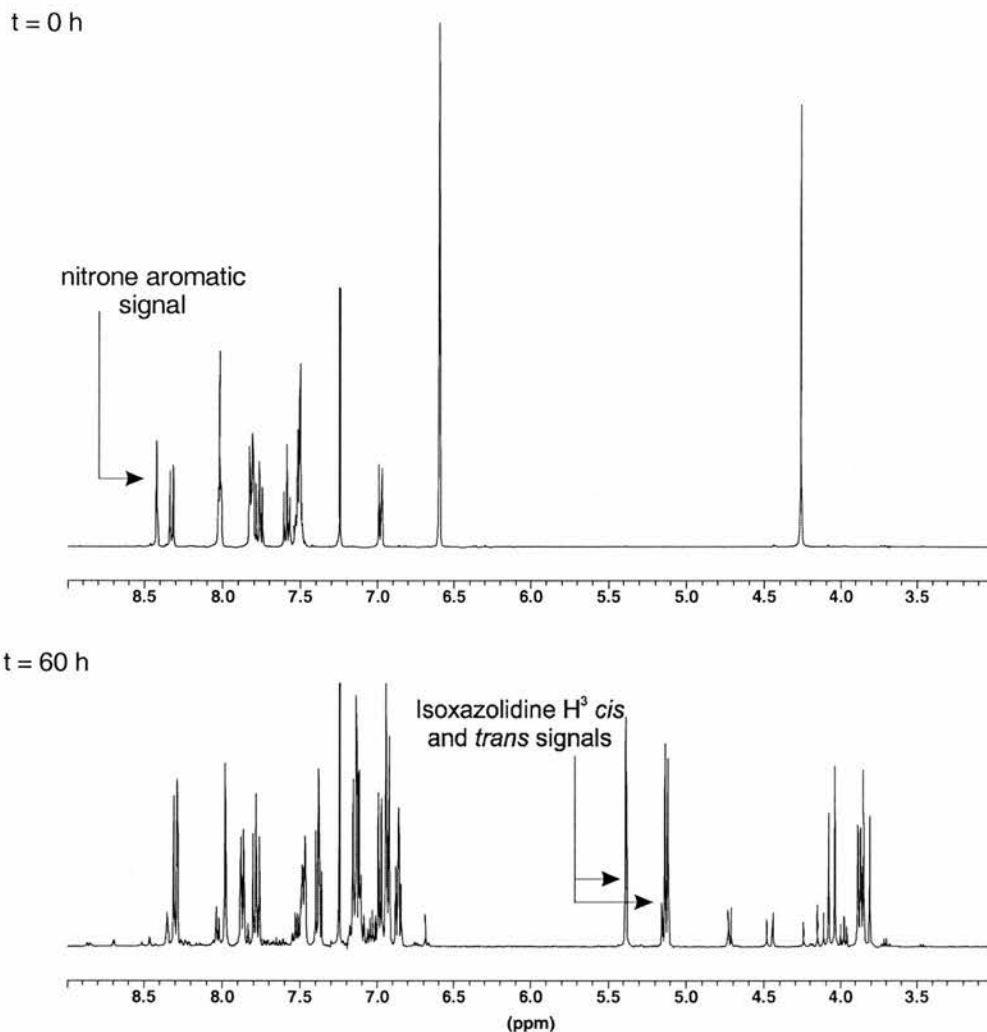


Figure 3.10 Partial 500 MHz ^1H NMR spectra recorded after time (a) $t=0$ and after (b) $t=60$ hours showing the disappearance of proton resonances corresponding to the starting material and the formation of signals arising from the formation of isoxazolidine product **105**.

Quantification of the reactant:product ratio was obtained by deconvolution techniques, which were converted to concentrations, which could then be used to build a rate profile for the formation of the template (**Figure 3.11**).

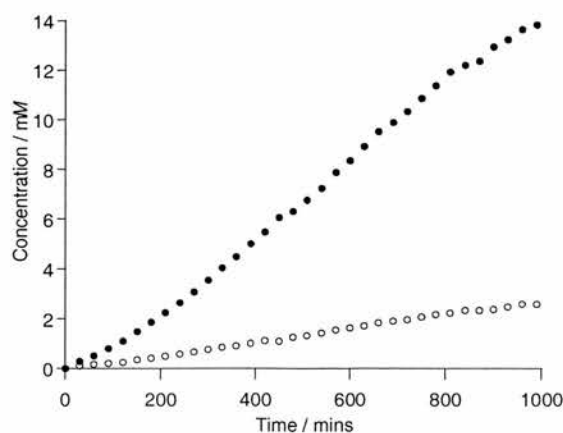


Figure 3.11 The rate profile for the formation of template product **105** in the reaction between nitron **104** and maleimide **77** performed at 10°C and at a concentration of 25 mM with respect to both building blocks. The *trans*-isoxazolidine is represented by the filled circles and the *cis*-isomer is represented by the open circles. Data taken from ref. 150.

On inspection of the kinetic data (**Figure 3.11**) it is apparent that a sigmoidal shape curve is obtained for the major isomer (*trans*-isomer), which is indicative of an autocatalytic self-replicating system. Upon closer inspection of the data it is also evident that the minor isomer (*cis*-isomer) also displays some sigmoidal character, although much less pronounced than the major isomer.

3.5.3 Demonstrating the operation of a self-replicating system

There are a number of control reactions, which may be performed, to prove that the system is operating *via* a self-replicating pathway.

3.5.4 The uncatalysed bimolecular reaction

To determine the rate of formation of template *via* the uncatalysed bimolecular channel it was necessary to perform a bimolecular control reaction. For this study, the control compounds shown in **Figure 3.12** were identified.

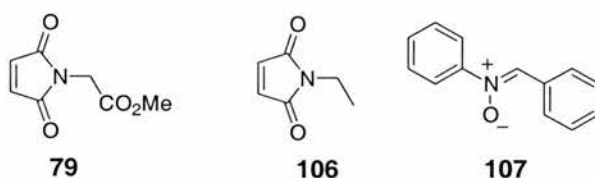
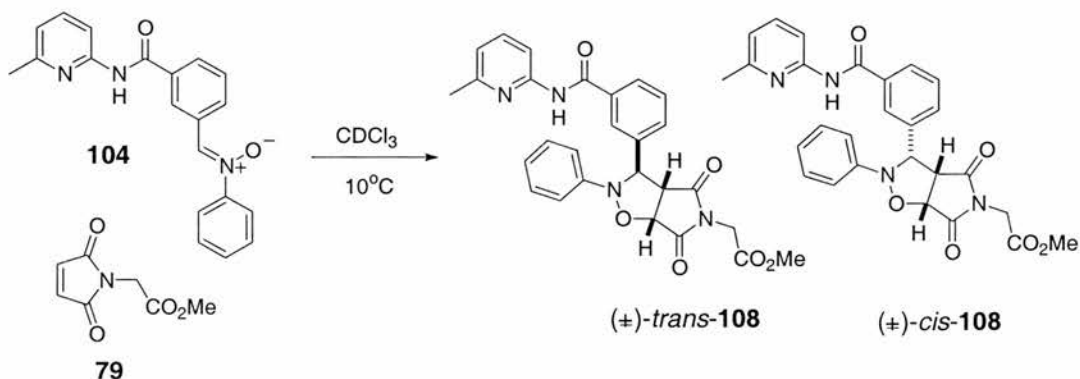


Figure 3.12 Control compounds used to simulate the uncatalysed bimolecular reaction.

It was found that they all gave similar rates of reaction with removal of the sigmoidal shape of the curve. The data for the reaction between control compound **79** and nitron **104** (**Scheme 3.15**) is presented (**Figure 3.13**). The reaction was carried out at a concentration of 25 mM in CDCl_3 at 10°C .



Scheme 3.15 The control reaction used to estimate the bimolecular reaction rate.

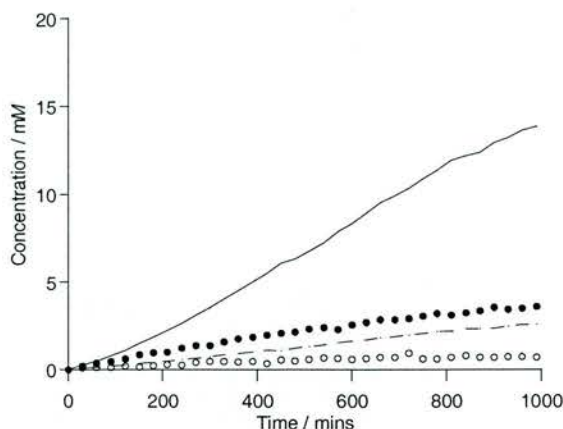
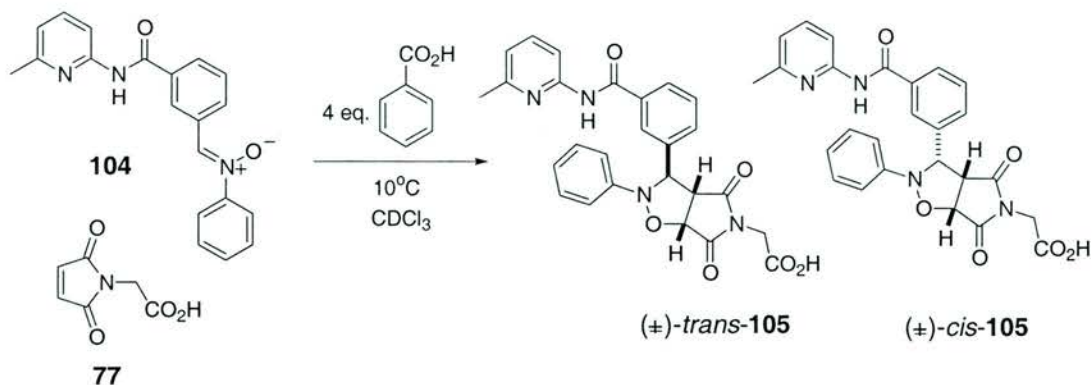


Figure 3.13 Comparison of the rate profiles for the bimolecular control reaction between nitrone **104** and maleimide ester **79** (*trans*-isomer represented as filled circles and the *cis*-isomer as by open circles) and the recognition-mediated reaction between nitrone **104** and maleimide **77** (*trans*-isomer represented as a solid line and *cis*-isomer as a dashed line). Data taken from ref. 150.

Immediately, it can be observed that there is a large difference in the rate of reaction between the recognition-mediated reaction and the bimolecular control reaction. This indicates that there is a significant degree of rate enhancement through the recognition-mediated pathway.

3.5.5 Competition experiment

As discussed in **Section 2.8.2** the ability of a self-replicating system to replicate relies upon the binding event, which forms the ternary complex [**77**·**104**·**105**]. In this system, the binding is achieved through the formation of hydrogen bonds between the amidopyridine and the carboxylic acid recognition motifs. Without the binding, the recognition process would be rendered inactive, as was demonstrated in the bimolecular control reaction. If the recognition could be interfered with, then the autocatalytic cycle could not operate efficiently or would do so with only minimal efficiency. Hence, an experiment was performed where an excess of benzoic acid was added to the reaction between nitrone **104** and maleimide **77** to act as a competitive inhibitor for the amidopyridine site (**Scheme 3.16**), the results of the control experiment are presented in **Figure 3.14**.



Scheme 3.16 Competition experiment between nitron **104** and maleimide **77** performed at a concentration of 25 mM in CDCl₃ at 10°C with 4 equivalents of benzoic acid (100 mM) to act as a competitive inhibitor.

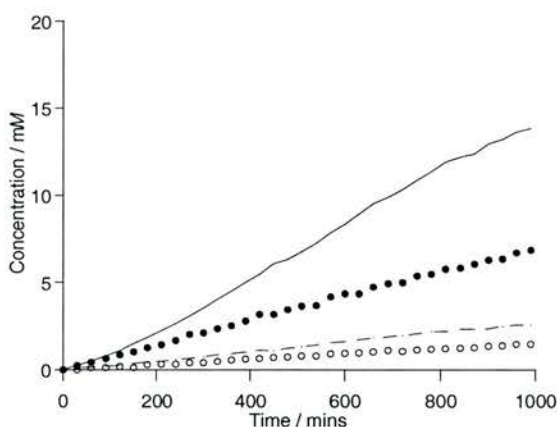
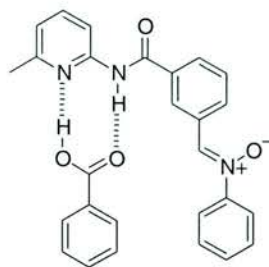


Figure 3.14 Comparison of the rate profiles obtained for the reaction between nitron **104** and maleimide **77** with 4 equivalent of benzoic acid (*trans*-isomer represented by solid circles and the *cis*-isomer by open circles) and the reaction between nitron **104** and maleimide **77** (*trans*-isomer represented by a solid line and the *cis*-isomer represented by a dashed line). Data taken from ref. 150.

On comparison of the recognition-mediated (solid and dashed lines) and the control (solid and open circles) data it is clear that there is a significant decrease in the rate of reaction for both isomers. Presumably this is as a result of the reduced efficiency of the autocatalytic cycle due to the presence of benzoic acid forming the inactive complex **[87•104]** (Figure 3.15). It is also evident that the sigmoidal shape of the curve has disappeared again indicating that the efficiency of the system has been reduced.

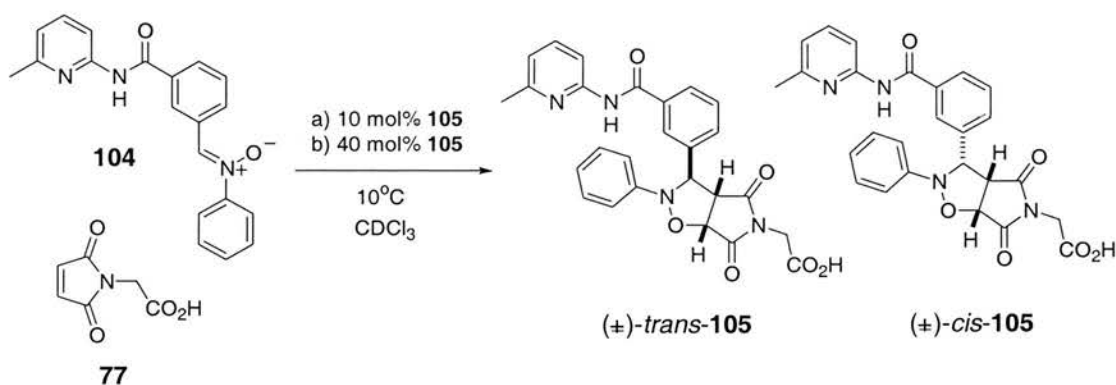


[87•104]

Figure 3.15 The inactive complex potentially formed between benzoic acid and the amidopyridine unit upon the nitron.

3.5.6 Doping experiment

During the initial stages of its formation, a self-replicating template, must rely upon the bimolecular reaction for its production; this is shown by the lag period that is observed in an autocatalytic self-replicating system. Once the template in solution has reached a critical concentration then the autocatalytic cycle may then begin to operate and exponential growth of the template is observed. If, however, there is template present at the beginning of the reaction, then the autocatalytic cycle can begin to operate without the need for the bimolecular reaction and so the initial lag period should be lost. In order to demonstrate this effect two control experiments were performed. Preformed template was added to the reaction between nitron **104** and maleimide **77** at concentrations of 10 and 40 mol% (**Scheme 3.17**). The results of this control reaction are presented in **Figure 3.16 (a)** and **Figure 3.16 (b)**.



Scheme 3.17 The doping experiment performed between nitron **104** and maleimide **77** at a concentration of 25 mM in CDCl_3 at 10°C with (a) 10 mol% added preformed template **105** and (b) 40 mol% added preformed template **105**.

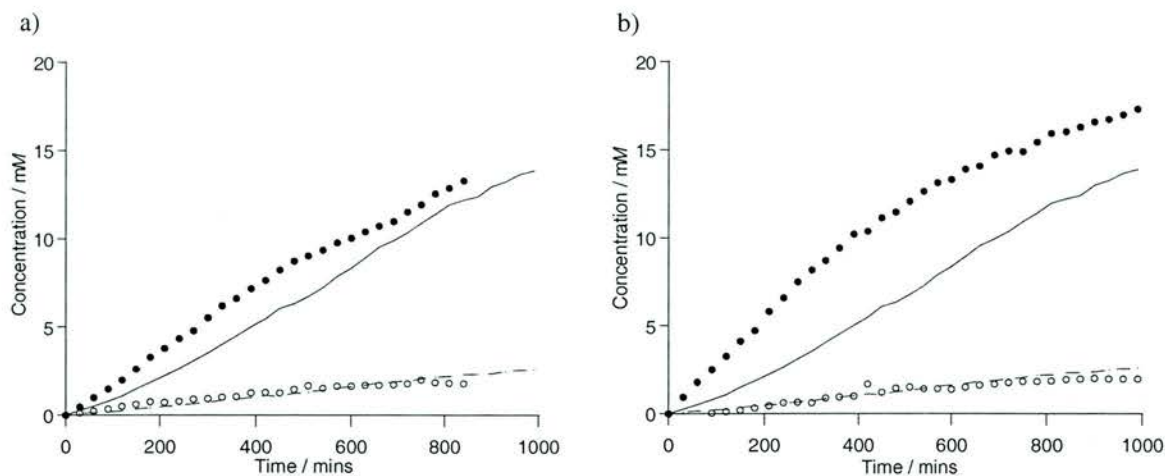


Figure 3.16 Data for the reaction between nitrene **104** and maleimide **77** at 25 mM in CDCl_3 at 10°C (a) in the presence of 10 mol% added template **105** and (b) in the presence of 40 mol% added preformed template **105**. The undoped data is represented by solid lines for the *trans*-isomer and dashed lines for the *cis*-isomer and the doped reactions are represented by solid circles for the *trans*-isomer and open circles for the *cis*-isomer. Data taken from ref. 150.

It is immediately obvious from both sets of data that the lag period is removed from the rate profile, indicating that the autocatalytic cycle can begin immediately, which adds further evidence that this is an autocatalytic self-replicating system. Rate enhancement is only observed for the major (*trans*) isomer, which indicates that the minor (*cis*) isomer is not capable of self-replication or amplification.

This result also implies that there is a level of specificity for the catalysis within the system, as the major isomer does not appear to catalyse the formation of the minor isomer as no enhancement of the minor isomer concentration was observed. Hence on the basis of the control experiments performed it was concluded that the major (*trans*) isomer can act an autocatalytic self-replicator whereas the minor (*cis*) does not.


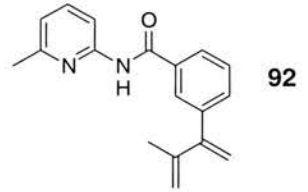
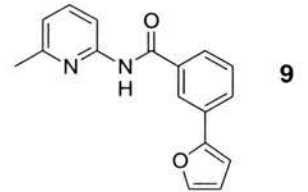
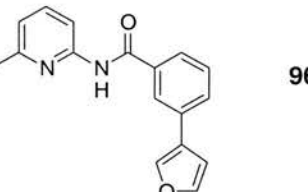

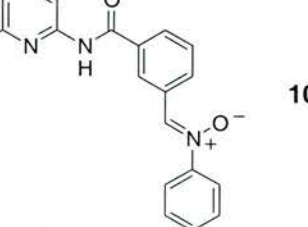
3.5.7 Kinetic fitting of the experimental data

As mentioned in the previous chapter the efficiency of a self-replicating system relies upon the dissociation of the product duplex $[\mathbf{T}\cdot\mathbf{T}]$ in the autocatalytic cycle. If the duplex is too stable then no dissociation can occur, hence no new template is returned to the autocatalytic cycle and so autocatalysis fails. The experimental data was fitted to the kinetic model (Section 2.11) and it was found that best fit values of p and ϵ of 0.9 and 700 were obtained respectively. These results indicate that the product duplex $[\mathbf{105}\cdot\mathbf{105}]$ is unstable and leads to efficient turnover in the autocatalytic cycle.

3.6 AB systems vs. self-replicating systems

There have been six examples of recognition-mediated systems discussed so far; four of which followed an AB-mediated pathway and two, which acted as self-replicating systems. The building blocks and their mode of reaction have been summarised in **Table 3.1**. In all cases the second building block is the respective maleimide.

Table 3.1 List of building blocks developed within the Philp group and their mode of recognition mediated reaction when reacted with their respective maleimide.

	Building block	Mode of recognition-mediated reaction when reacted appropriate maleimide.
(a)	 88	AB-System
(b)	 92	AB-System
(c)	 9	AB-System
(d)	 96	AB-System
(e)	 100	Self-Replicating System
(f)	 104	Self-Replicating System

By comparing the systems shown in **Table 3.1** it can be seen that all except (e) have the basic structure as shown in **Figure 3.17**.

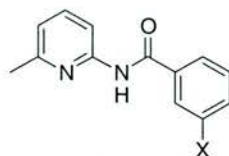


Figure 3.17 Shows the basic structure of the systems outlined in **Table 3.1**. Where X = the reactive functionality.

However, 4 out of the 5, which possess this basic structure react with the appropriate maleimide *via* an AB-pathway whereas, **104** reacts with **77** *via* a self-replicating pathway. The other self-replicating system **100**, involves placing the reactive site in the *para* position on the phenyl group rather than *meta*, however the analogous *meta* **96** building block reacts *via* an AB-complex system.

This observation then poses the question, can the mode of operation be predicted; can we set out to intentionally design a system that self-replicates?

3.7 Testing the isoxazolidine system

It was decided to investigate the system outlined in **Scheme 3.13** further. The robustness of the system was to be tested; alterations were made to the regiochemistry, steric and/or electronic properties to observe the effects they had on the system's replicating ability. It was decided to look at a series of analogues based upon the system outlined in **Scheme 3.13**. The analogues devised are shown in **Figure 3.18**.

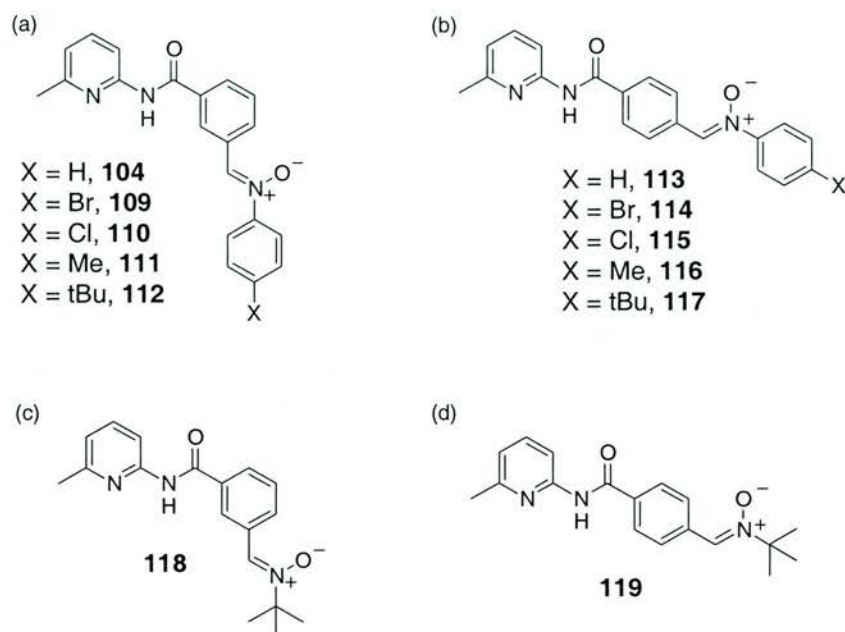


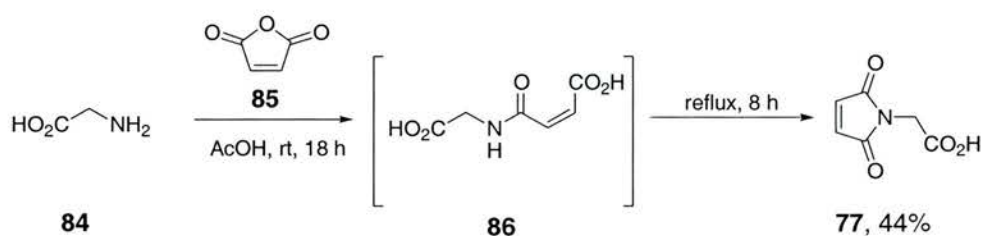
Figure 3.18 The analogues devised to test the original system shown in **Scheme 3.13**.

Inspection of the analogues shows that in the first case (a) these compounds are the same as the original nitron **104** but different functionalities have been placed in the *para* position to the nitron group. The hydrogen functionality **104** is being replaced with a bromine **109**, chlorine **110**, methyl **111**, and *tert*-butyl **112** groups. This group of nitrones will be referred to as the 3-nitrones, due to the nitron functionality being placed *meta* with respect to the middle phenyl ring. This set of nitrones will test if electronic effects have any role in the operation of a self-replicating system, also they will be used to observe whether steric effects disrupt this system. The second set of nitrones (b) will be referred to as the 4-nitrones due to the nitron functionality being placed *para* with respect to the middle phenyl ring. This set of nitrones will be used to observe the effect that altering the regiochemistry has upon the system. These also have the varying functionality as shown in the 3-nitrones, to further test the electronic and steric effects upon the system. The final two analogues prepared are shown in (c) and (d), these contain the *meta* and *para* regiochemistry as before but in these compounds, the terminal phenyl group attached to the nitron has been removed and replaced with a *tert*-butyl group. In order to test the new systems, they will be subjected to the same recognition-mediated reaction conditions as performed in the original system, if a sigmoidal rate profile is obtained then the system will be subjected to the same control reactions as before. This required the synthesis and full analysis of all the new nitrones and all the corresponding cycloadducts.

3.8 Synthesis

3.8.1 Synthesis of maleimide building block 77

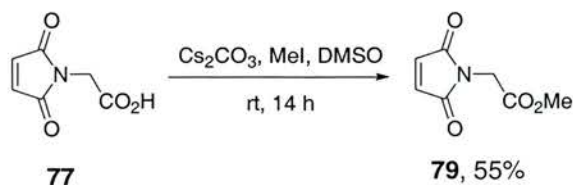
The recognition dipolarophile, maleimide **77** was synthesised in one step from glycine **84** (Scheme 3.18). Glycine **84** was added to one equivalent of maleic anhydride **83** in analytical grade (AR) acetic acid and the resulting reaction mixture stirred at room temperature under nitrogen overnight. This resulted in the formation of the intermediate maleamic acid **86**. The reacting reaction mixture was heated to reflux to promote cyclisation to maleimide **77**. The crude residue was purified by flash chromatography on a short pad of silica gel to afford **77** in a yield of 44% (Scheme 3.18).



Scheme 3.18 The synthetic route for the preparation of the maleimide dipolarophile recognition building block **77**.

3.8.2 Synthesis of the control dipolarophile 79

The control dipole **79** was subsequently prepared in one step from the maleimide acid **77** (Scheme 3.19). Maleimide **77** was reacted with Cs₂CO₃ and methyl iodide in dimethyl sulfoxide at room temperature. After stirring for 16 hours the solvent was removed under reduced pressure and the crude residue was portioned between ethyl acetate and water. The crude residue was then purified by flash chromatography on silica gel to afford the desired maleimide ester **79** in a yield of 55%.

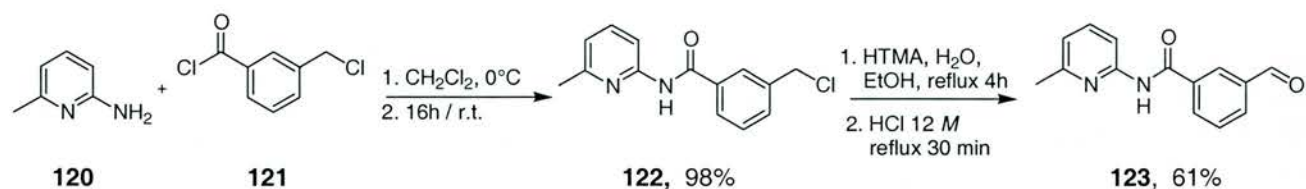


Scheme 3.19 The synthetic route for the preparation of the maleimide ester dipole control **79**.

3.8.3 Synthesis of aldehyde 123

3-(chloromethyl)benzoyl chloride **121** was reacted with three equivalents of 2-amino-6-picoline **120** in dichloromethane at 0°C. After stirring at room temperature for 16 hours the solvent was removed *in vacuo* and the residue purified using flash chromatography on silica gel to give the required chloride **122** in 98% yield. Chloride **122** was then heated to reflux in

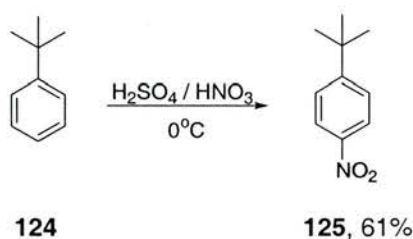
ethanol/water 50:50 with hexamethylene tetraamine (HTMA). After 16 hours at reflux, 12 M hydrochloric acid was added and the crude product was extracted using dichloromethane and the solvent removed *in vacuo*. The crude product was then purified using flash chromatography on silica gel to afford aldehyde **123** in 61% yield (**Scheme 3.20**).



Scheme 3.20 Synthesis of aldehyde **123**

3.8.4 Synthesis of 4-nitro-*tert*-butyl-benzene **125**

4-nitro-*tert*-butyl-benzene **125** was prepared by the careful addition of concentrated H₂SO₄ and HNO₃ to *tert*-butylbenzene **124** at 0°C. The mixture was stirred for one hour then extracted with ether and purified on silica gel to afford **125** in a yield of 61% (**Scheme 3.21**).

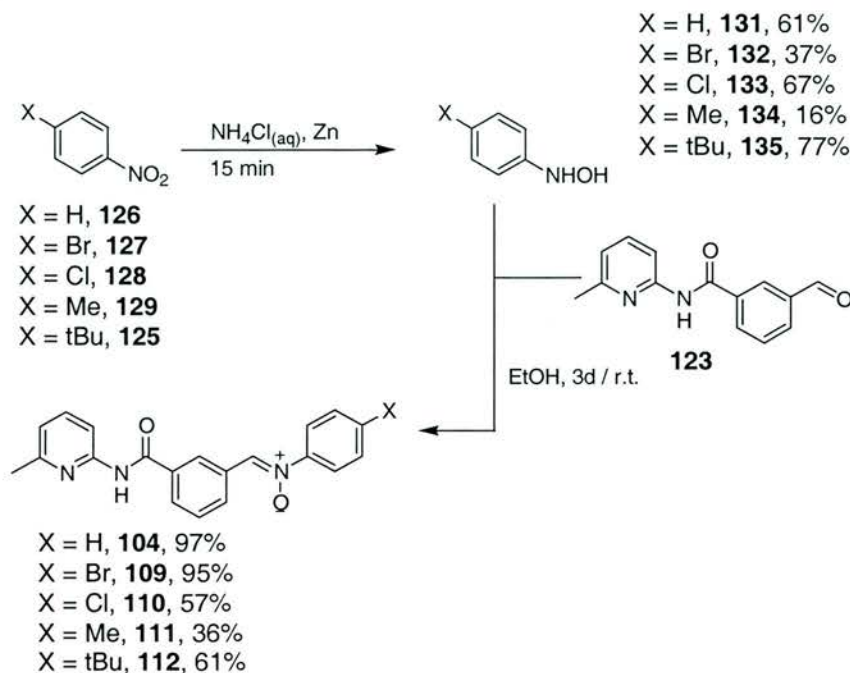


Scheme 3.21 Synthesis of 4-nitro-*tert*-butyl-benzene **125**.

3.8.5 Synthesis of nitrones **104, 109, 110, 111 and 112**

Zinc dust was added portion-wise to a stirred solution of ammonium chloride and the appropriate nitro compound **126, 127, 128, 129** or **130** in water/ethanol at room temperature. After addition of the zinc dust was complete, the reaction mixture was stirred for a further 15 minutes. The resulting slurry was filtered through Celite® and the residue washed with hot water. The filtrate was extracted using dichloromethane. The combined organic extracts were washed once with water then dried over MgSO₄ and concentrated *in vacuo*. For the purification method of the individual hydroxylamines see **Chapter 6**. Aldehyde **123** was then reacted with the appropriate phenylhydroxylamine **131, 132, 133, 134** and **135** in ethanol. The reaction flask was stoppered and left to stand in the dark for 3 days at room temperature. The resulting precipitate formed was filtered and recrystallised from diethyl

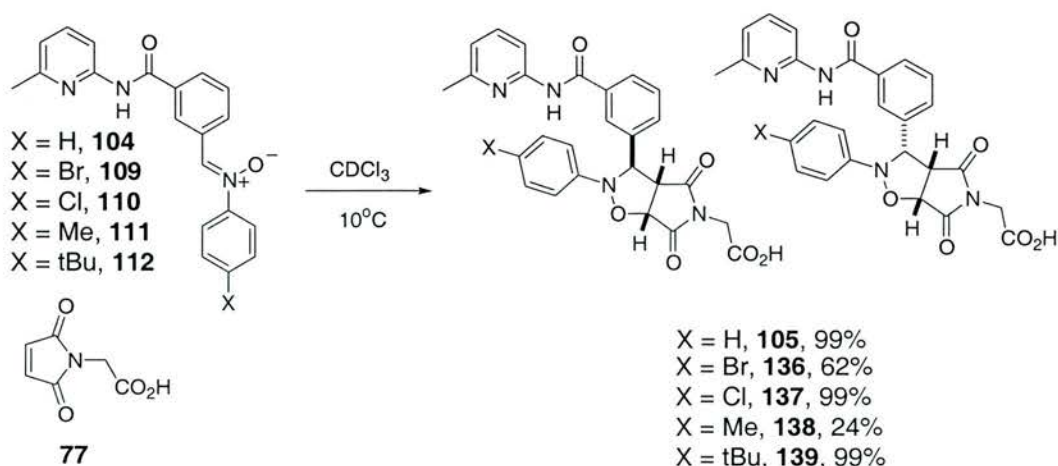
ether and dichloromethane, to afford the required nitrones **104**, **109**, **110**, **111** and **112** (Scheme 3.22).



Scheme 3.22 Synthetic route used to prepare nitrones **104**, **109**, **110**, **111** and **112**.

3.8.6 Synthesis of cycloadducts **105**, **136**, **137**, **138** and **139**

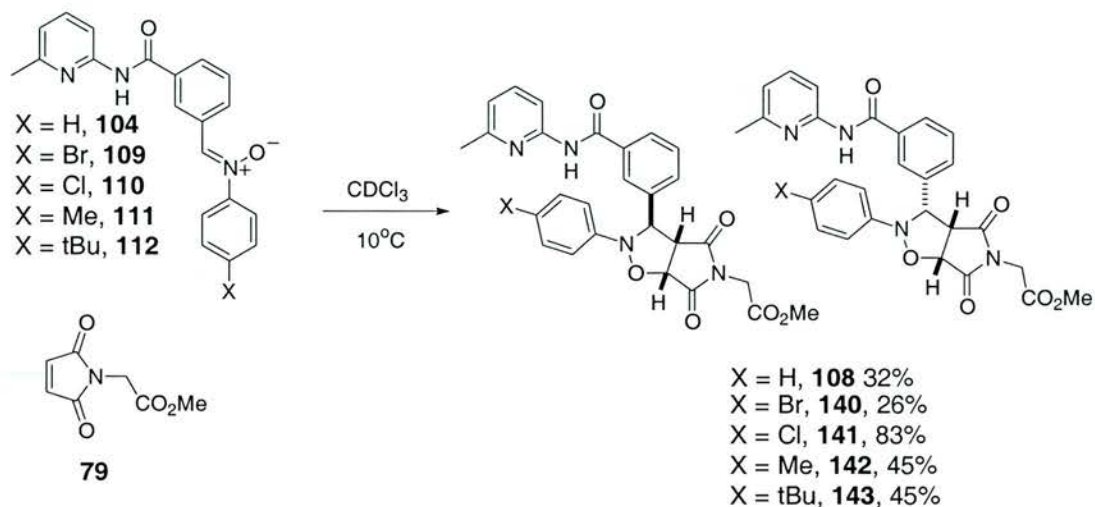
In order to obtain an accurate assignment of the proton resonances that will arise from the product protons of the cycloadducts in the kinetic analysis, it was necessary to isolate and fully characterise the cycloadducts. The cycloadducts **105**, **136**, **137**, **138** and **139** were prepared by the addition of maleimide **77** into a solution of the appropriate nitronone **104**, **109**, **110**, **111** and **112** in chloroform. The reaction was allowed to stand for 3 days in the dark, after which time the precipitate was filtered and washed with hexane to afford **105**, **136**, **137**, **138** and **139** (Scheme 2.23).



Scheme 2.23 The synthetic route used to prepare cycloadducts **105**, **136**, **137**, **138** and **139**.

3.8.7 Synthesis of cycloadducts 108, 140, 141, 142 and 143

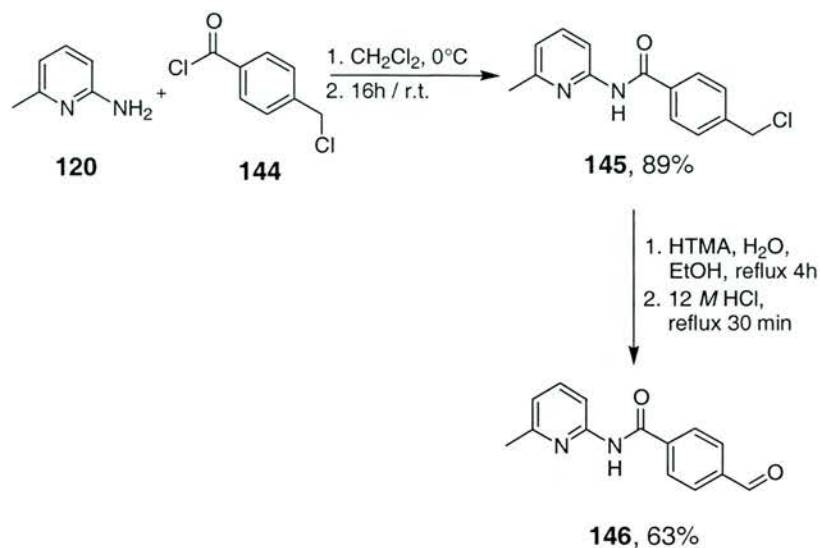
It was also necessary to isolate and fully characterise the cycloadducts from the bimolecular control reactions. These cycloadducts **108**, **140**, **141**, **142** and **143** were prepared (Scheme 3.24) in an analogous manner to the cycloadducts in Section 3.8.5.



Scheme 3.24 Synthetic routes used to prepare cycloadducts **108**, **140**, **141**, **142** and **143**.

3.8.8 Synthesis of aldehyde 146

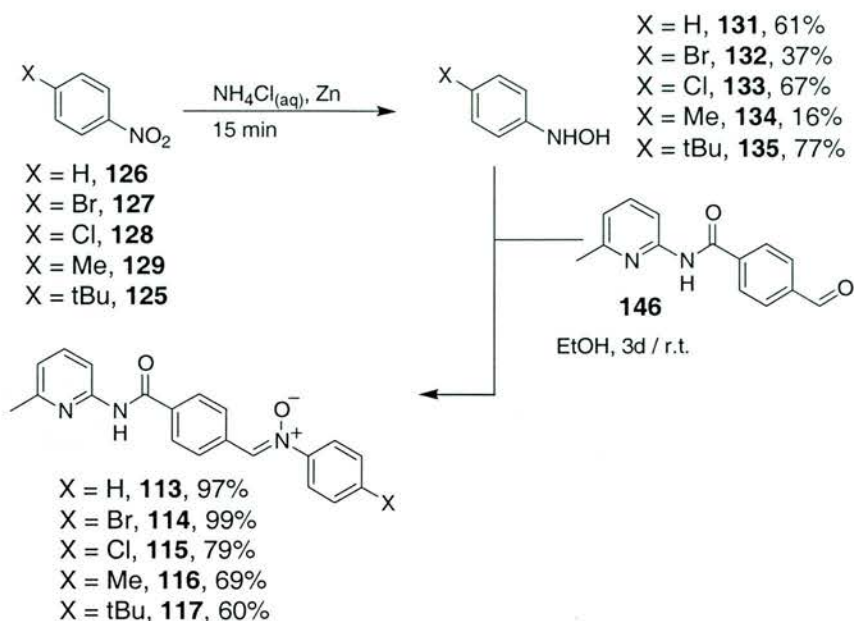
4-(chloromethyl)benzoyl chloride **144** was reacted with three equivalents of 2-amino-6-picoline **120** in dichloromethane at 0°C. After stirring at room temperature for 16 hours the solvent was removed *in vacuo* and the residue purified using flash chromatography on silica gel to give the required chloride **145** in 89% yield. Chloride **145** was then heated to reflux in ethanol/water 50:50 with hexamethylene tetraamine (HTMA). After 16 hours at reflux, 12 M hydrochloric acid was added and the crude product was extracted using dichloromethane and the solvent removed *in vacuo*. The crude product was then purified using flash chromatography on silica gel to give the aldehyde **146** in 63% yield (Scheme 3.25).



Scheme 3.25 Synthetic route used for the preparation of aldehyde **146**.

3.8.9 Synthesis of nitrones **113**, **114**, **115**, **116** and **117**

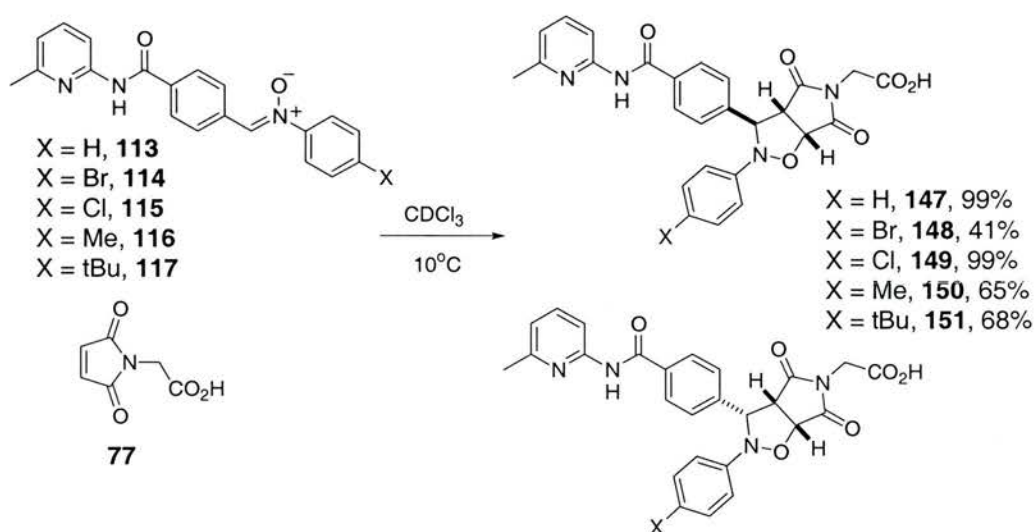
Zinc dust was added portion-wise to a stirred solution of ammonium chloride and the appropriate nitro compound **126**, **127**, **128**, **129** or **130** in water/ethanol at room temperature. After addition of the zinc dust was complete the reaction mixture was stirred for a further 15 minutes. The resulting slurry was filtered through Celite® and the residue washed with hot water. The filtrate was extracted using dichloromethane. The combined organic extracts were washed once with water then dried over $MgSO_4$ and concentrated *in vacuo*. For the purification of the individual hydroxylamines see **Chapter 6**. Aldehyde **146** was then reacted with the appropriate phenylhydroxylamine **131**, **132**, **133**, **134** and **135** in ethanol. The reaction flask was stoppered and left to stand in the dark for 3 days at room temperature. The resulting precipitate formed was filtered and recrystallised from diethyl ether and dichloromethane, to afford the required nitrones **113**, **114**, **115**, **116** and **117** (**Scheme 3.26**).



Scheme 3.26 Synthetic route used to prepare nitrones **113**, **114**, **115**, **116** and **117**.

3.8.10 Synthesis of cycloadducts **147**, **148**, **149**, **150** and **151**

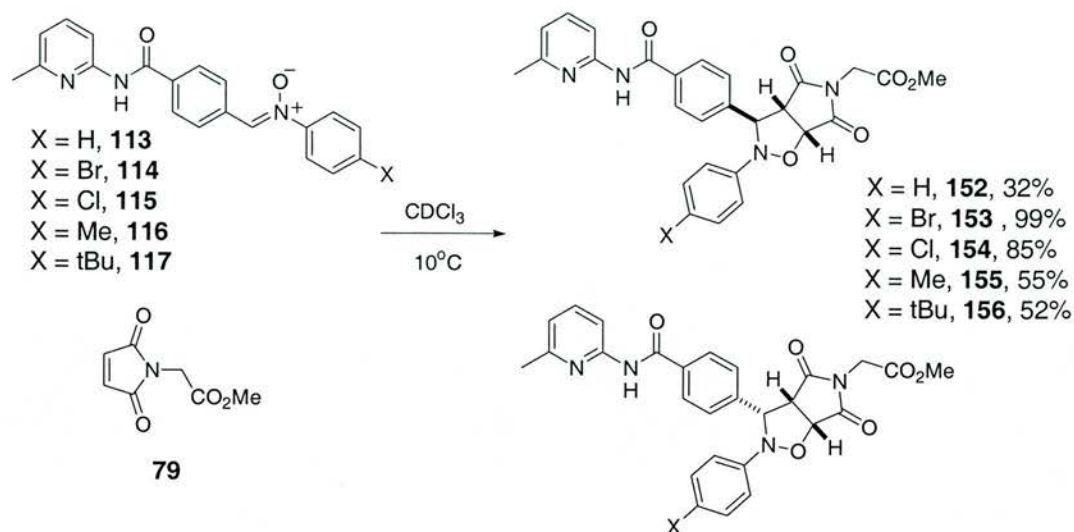
Cycloadducts **147**, **148**, **149**, **150** and **151** were prepared (**Scheme 3.27**) in an analogous manner to the cycloadducts in **Section 3.8.5**.



Scheme 3.27 The synthetic route used to prepare cycloadducts **147**, **148**, **149**, **150** and **151**.

3.8.11 Synthesis of cycloadducts **152**, **153**, **154**, **155** and **156**

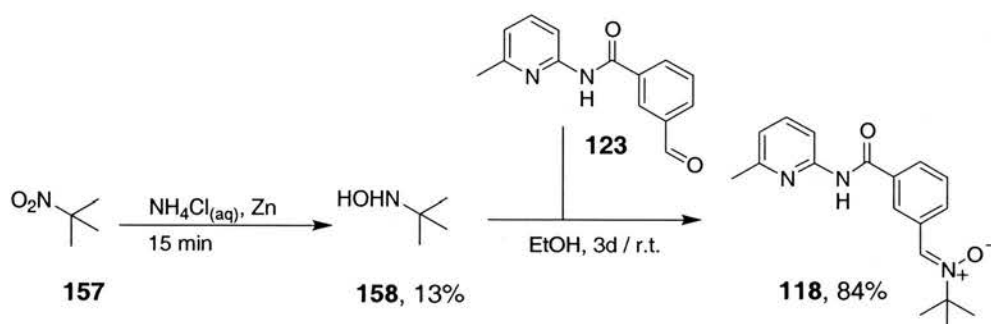
The cycloadducts **152**, **153**, **154**, **155** and **156** were prepared (**Scheme 3.28**) in an analogous manner to the cycloadducts in **Section 3.8.5**.



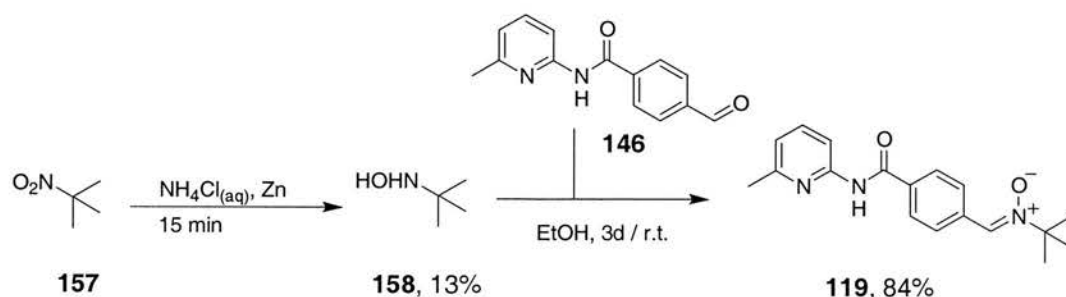
Scheme 3.28 Synthetic routes used to prepare cycloadducts **152**, **153**, **154**, **155** and **156**.

3.8.12 Synthesis of nitrones **118** and **119**

The syntheses of nitrones **118** and **119**, **Schemes 3.29** and **3.30** respectively, were performed as described in **Section 3.8.8**.



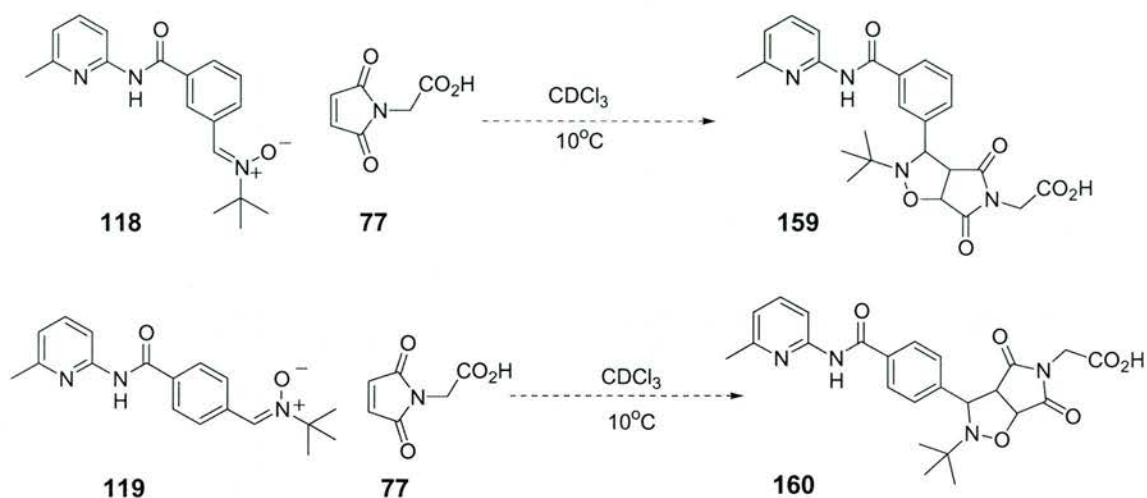
Scheme 3.29 Synthetic routes used to prepare the nitrone **118**.



Scheme 3.30 Synthetic routes used to prepare the nitrone **119**.

3.8.13 Synthesis of the cycloadducts **159** and **160**

Upon addition of nitrones **118** and **119** to maleimide **77** it was found that no reaction occurred for either isomer (**Scheme 3.31**), and hence it was decided not to pursue these compounds further.



Scheme 3.31 The failed synthesis of cycloadducts **159** and **160**.

3.9 Structural assignment of the 4 nitrones

The configuration of the 3-nitronone **104** was proved to be of *Z* stereochemistry about the C=N double bond, this was determined by the single crystal X-ray structure (Section 3.4.2). Hence, it was necessary to determine the configuration the 4-nitronone. Vapour diffusion of hexane into a solution of nitronone **113** in chloroform afforded single crystals of **113** suitable for X-ray diffraction. The solid-state structure (Figure 3.19) (Table 6.4) clearly shows that the C=N double bond possesses a *Z* configuration.

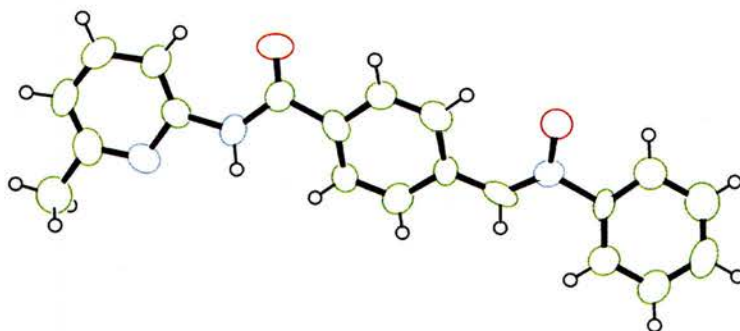


Figure 3.19 Single crystal X-ray structure for nitronone **113**.

3.10 Kinetic analysis

3.10.1 The reaction conditions

In order to maintain consistency and a fair comparison between systems the reaction conditions under which the kinetic analysis was performed was 25 mM in CDCl_3 with respect to all building blocks at 10°C in all cases.

3.10.2 The kinetic experiments

The kinetic experiments were prepared and analysed in the same manner as before. Stock solutions of the building blocks were prepared to a concentration of 50 mM in CDCl₃ and were equilibrated to 10°C for at least one hour before use. Equal volumes of the stock solutions were combined and a 500 MHz ¹H NMR spectrum recorded immediately. The progress of the cycloaddition was monitored by recording the 500 MHz ¹H NMR spectrum every 30 minutes. The proton resonances followed for deconvolution purposes depended on which could be easily identified throughout the reaction course.

As a result of the number of experiments performed each analogue will be shown along with its control data. Then the data will be compared to the original experiment.

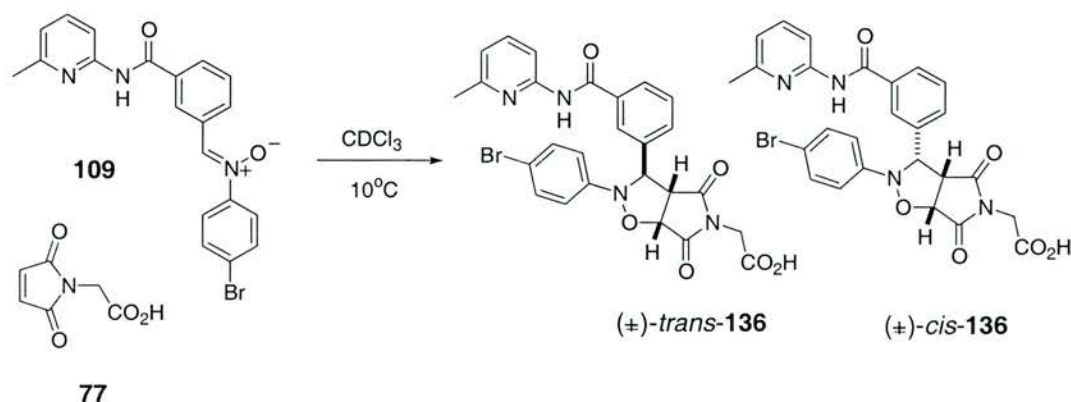
Firstly, the recognition-mediated experiment will be shown to demonstrate whether a sigmoidal rate profile is obtained. If it is obtained then the control experiments will be performed to prove that an autocatalytic pathway is in operation. The control experiments to be performed are:

- i) The bimolecular mimic, using the methyl ester.
- ii) The competition experiment using 4 equivalents of benzoic acid.
- iii) The doping experiment using 10 mol% added preformed template.

3.11 The experimental data for the 3 nitrones

3.11.1 *N*-[3-(*N*'-6-Methyl-2-pyridyl)-amidobenzylidene]-4-bromophenylamine *N*-oxide **109**

The first analogue to be examined involved replacing the *para* hydrogen with a bromine (Scheme 3.32).



Scheme 3.32 Proposed autocatalytic self-replicating system utilising the 1,3 dipolar cycloaddition reaction between building blocks **77** and **109** to form the cycloadduct **136** performed at a concentration of 25 mM in CDCl₃ at 10°C.

The results of this recognition-mediated reaction are presented in **Figure 3.20 (a)** along with the corresponding results from the control experiments **Figure 3.20 (b), (c) and (d)**.

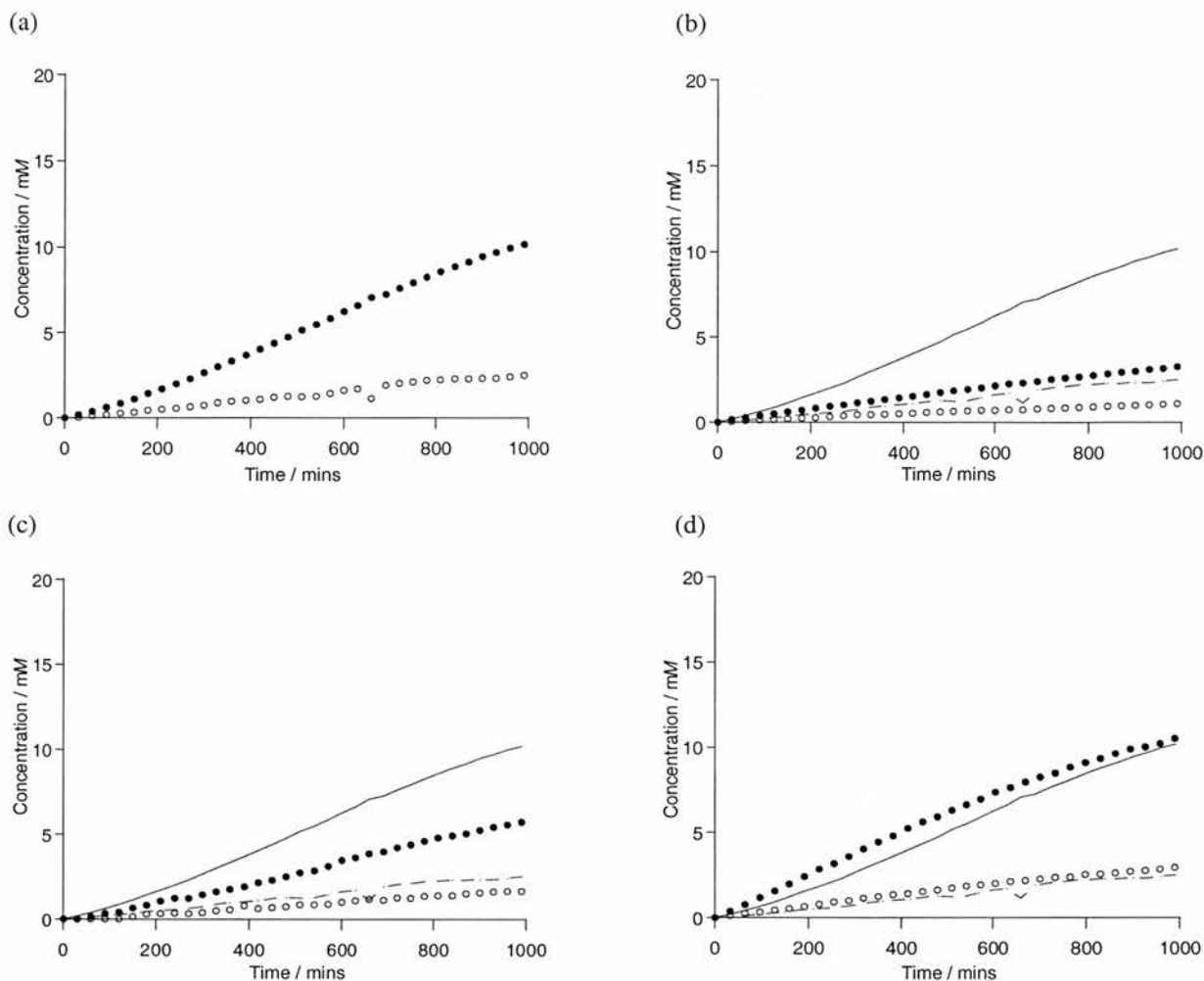


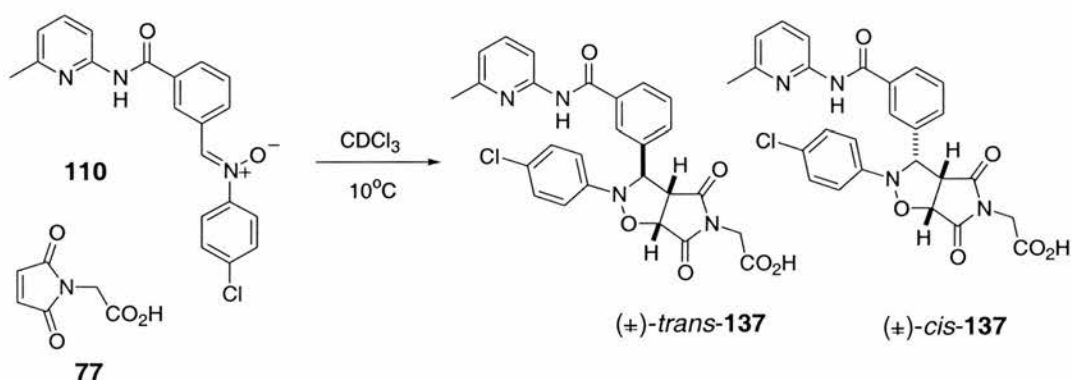
Figure 3.20 The rate profiles showing (a) the formation of the template **136** in the reaction between nitron **109** and maleimide **77** to afford the products *trans*-**136** and *cis*-**136**, performed at 10°C and at a concentration of 25 mM in CDCl₃ with respect to both building blocks **77** and **109**. The *trans*-isoxazolidine is represented by the filled circles and the *cis*-isoxazolidine is represented by the open circles. Graphs (b), (c) and (d) show the control reactions performed upon nitron **109** and maleimide **77**, all reactions were performed at concentrations of 25 mM in CDCl₃ with respect to the building blocks **77** and **109** at 10°C. Control reaction (b) demonstrates the bimolecular mimic where the control ester **79** was used to replace maleimide **77**, (c) involves the addition of 4 equivalents of benzoic acid to the reaction between nitron **109** and maleimide **77** and (d) shows the effect of the addition of 10 mol% preformed template **136**. In the control reactions the original recognition-mediated reaction results are shown as solid lines for the *trans* isoxazolidine and dashed lines for the *cis*-isoxazolidine, and the control reaction results are shown as a solid circles for the *trans*-isoxazolidine and a open circles for the *cis*-isoxazolidine.

On inspection of the recognition-mediated data it is evident that the reaction between nitron **109** and maleimide **77** to form cycloadduct **136** displays a sigmoidal rate profile for the major (*trans*) isomer, which is indicative of a self-replicating system and hence the system was tested further by performing the control reactions.

In the first control reaction (b) the methyl ester of the acid is used as a bimolecular mimic, the experimental data reveals that the rates of both the major and minor isomers have significantly been decreased indicating that recognition is important within this reaction. The second control reaction (c) also demonstrates the importance of the recognition within the reaction through the addition of four equivalents of benzoic acid. It is evident that the rates of formation of **136** have been decreased for both the major and minor isomers. Finally, the third control reaction (d) demonstrates the addition of 10 mol% preformed template removes the lag period and so demonstrates the importance of the cycloadduct **136** as a template for its own formation. Hence, on the basis of the evidence, it can be stated that this system also exhibits autocatalytic self-replication.

3.11.2 *N*-[3-(*N'*-6-Methyl-2-pyridyl)-amidobenzylidene]-4-chlorophenylamine *N*-oxide **110**

This experiment involves using chlorine to replace the *para* hydrogen (**Scheme 3.33**)



Scheme 3.33 Proposed autocatalytic self-replicating system utilising the 1,3 dipolar cycloaddition reaction between building blocks **77** and **110** to form the cycloadduct **137** performed at a concentration of 25 mM in CDCl_3 at 10°C .

The results of the kinetic experiment shown in **Scheme 3.33** are presented in **Figure 3.21 (a)** along with the corresponding control reaction results **Figure 3.21 (b), (c)** and **(d)**.

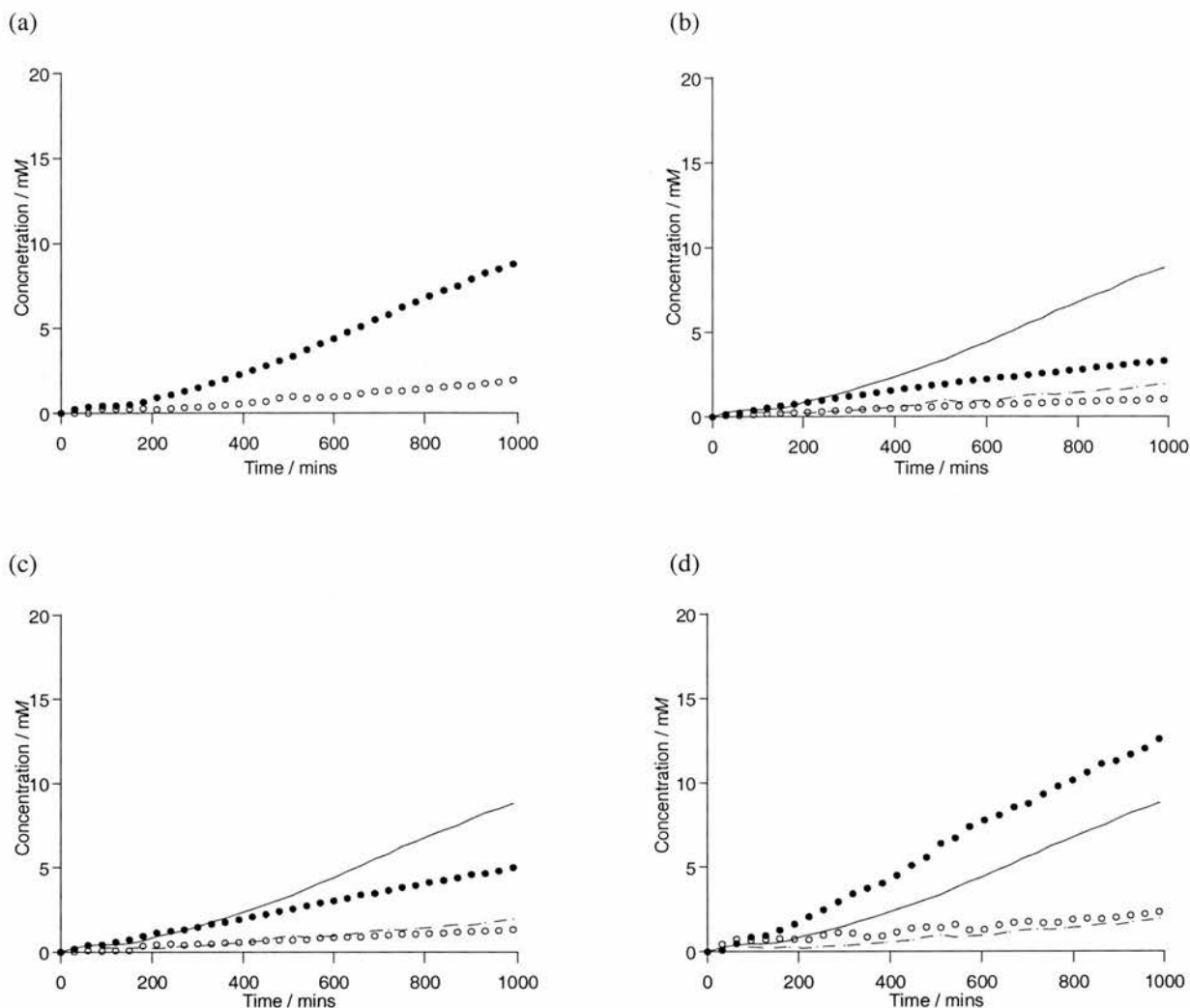


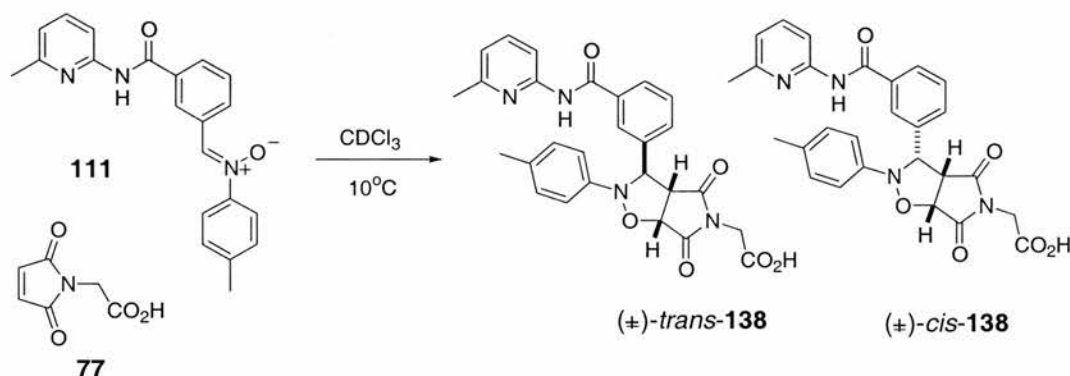
Figure 3.21 The rate profiles showing (a) the formation of the template **137** in the reaction between nitron **110** and maleimide **77** to afford the products *trans*-**137** and *cis*-**137**, performed at 10°C and at a concentration of 25 mM in CDCl₃ with respect to both building blocks **77** and **110**. The *trans*-isoxazolidine is represented by the filled circles and the *cis*-isoxazolidine is represented by the open circles. Graphs (b), (c) and (d) show the control reactions performed upon nitron **110** and maleimide **77**, all reactions were performed at concentrations of 25 mM in CDCl₃ with respect to the building blocks **77** and **110** at 10°C. Control reaction (b) demonstrates the bimolecular mimic where the control ester **79** was used to replace maleimide **77**, (c) involves the addition of 4 equivalents of benzoic acid to the reaction between nitron **110** and maleimide **77** and (d) shows the effect of the addition of 10-mol% preformed template **137**. In the control reactions the original recognition-mediated reaction results are shown as solid lines for the *trans*-isoxazolidine and dashed lines for the *cis*-isoxazolidine, and the control reaction results are shown as a solid circles for the *trans*-isoxazolidine and a open circles for the *cis*-isoxazolidine.

Again, a sigmoidal rate profile was obtained for the recognition-mediated reaction and so the control experiments were performed (**Figure 3.21**). Inspection of the experimental data for the control experiments (graphs (b), (c) and (d)) reveals that the major isomer for this system can also react *via* an autocatalytic self-replicating system. The bimolecular control reaction (b) shows loss of the sigmoidal rate profile for the major isomer as well as a significant decrease in the rate of reaction, hence, demonstrating that recognition is important in the original experiment (a). The addition of a competitive inhibitor (c) also shows a significant

decrease in the rate of reaction for the major isomer, which helps to confirm that the reaction follows a recognition-mediated pathway. The third control reaction (d) involved the addition of 10 mol% added preformed template. Inspection of graph (d) shows that the control experiment increased the rate of reaction, however the data still revealed a slight lag period. This could be due to the fact that the addition of 10 mol% preformed template **137** might be slightly below the critical concentration for autocatalysis to occur. The rate of reaction observed appears to be slower than the previous systems, hence, the production of template is slower and so reaching the critical concentration will take longer, therefore the lag period is still observed. Attempts to repeat this control reaction with increased dopant were hampered due to solubility problems. However, the increased rate of formation by addition of preformed template still confirms that the major isomer can catalyse its own formation. The control reactions confirm that this system reacts *via* an autocatalytic self-replicating pathway.

3.11.3 *N*-[3-(*N'*-6-Methyl-2-pyridyl)-amidobenzylidene]-4-methylphenylamine *N*-oxide **111**

This kinetic experiment involves a nitron, which has a methyl group in the *para* position instead of hydrogen (**Scheme 3.34**).



Scheme 3.34 Proposed autocatalytic self-replicating system utilising the 1,3 dipolar cycloaddition reaction between building blocks **77** and **111** to form the cycloadduct **138** performed at a concentration of 25 mM in CDCl₃ at 10°C.

The results of the recognition-mediated experiment outlined in **Scheme 3.34** are presented in **Figure 3.22 (a)** along with the corresponding control reactions **Figure 3.22 (b)**, **(c)** and **(d)**.

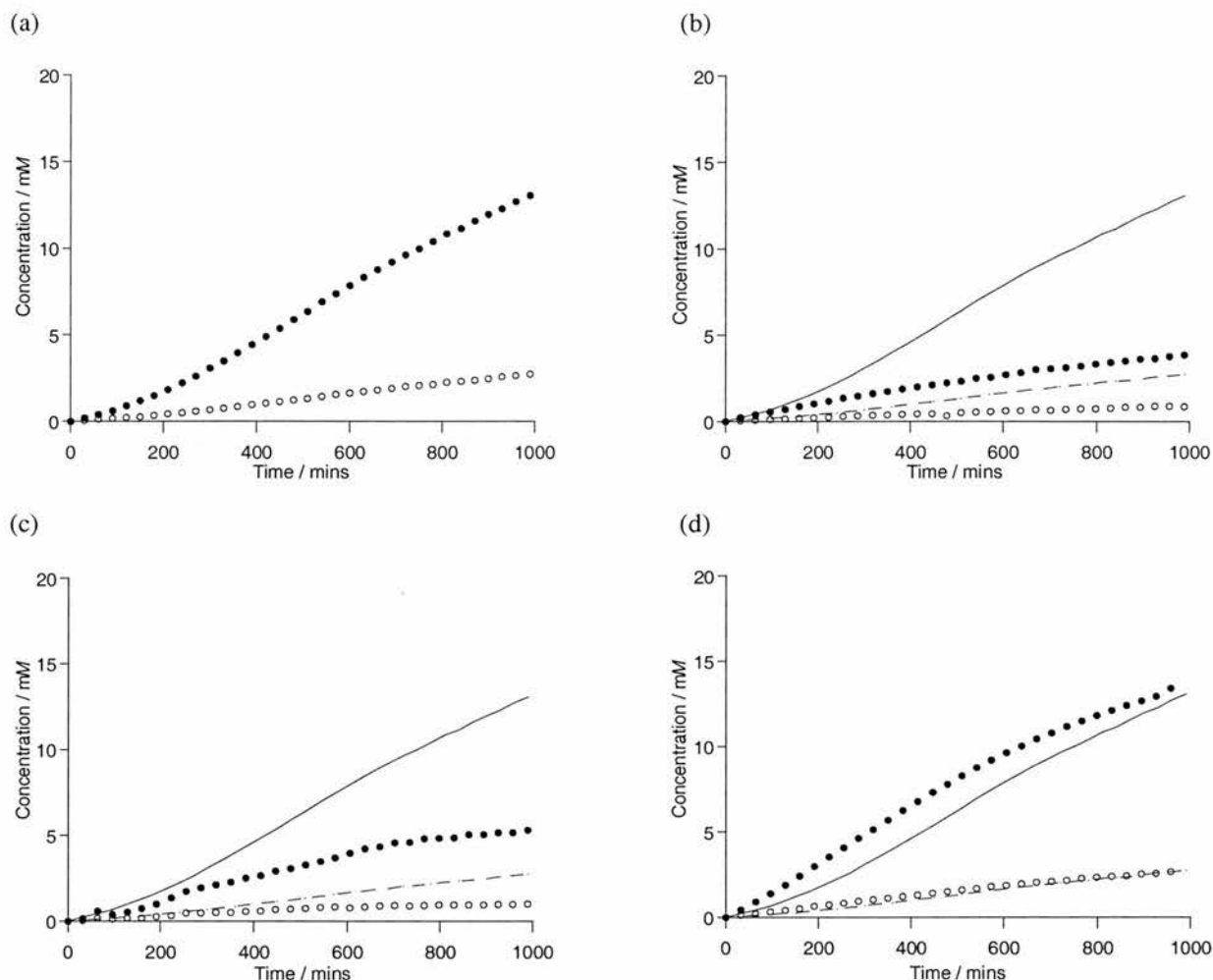


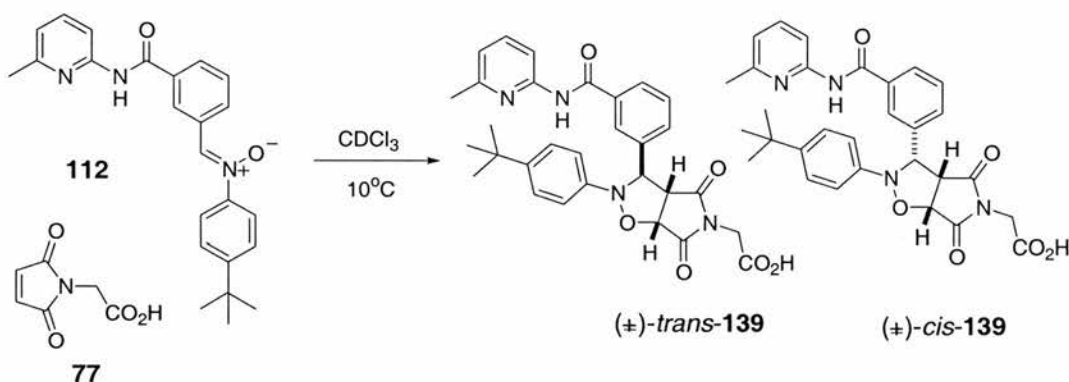
Figure 3.22 The rate profiles showing (a) the formation of the template **138** in the reaction between nitrone **111** and maleimide **77** to afford the products *trans*-**138** and *cis*-**138**, performed at 10°C and at a concentration of 25 mM in CDCl₃ with respect to both building blocks **77** and **111**. The *trans*-isoxazolidine is represented by the filled circles and the *cis*-isoxazolidine is represented by the open circles. Graphs (b), (c) and (d) show the control reactions performed upon nitrone **111** and maleimide **77**, all reactions were performed at concentrations of 25 mM in CDCl₃ with respect to the building blocks **77** and **111** at 10°C. Control reaction (b) demonstrates the bimolecular mimic where the control ester **79** was used to replace maleimide **77**, (c) involves the addition of 4 equivalents of benzoic acid to the reaction between nitrone **111** and maleimide **77** and (d) shows the effect of the addition of 10 mol% preformed template **138**. In the control reactions the original recognition-mediated reaction results are shown as solid lines for the *trans*-isoxazolidine and dashed lines for the *cis*-isoxazolidine, and the control reaction results are shown as a solid circles for the *trans*-isoxazolidine and a open circles for the *cis*-isoxazolidine.

This system shows evidence of a sigmoidal rate profile for the major isomer and so the control reactions were performed upon this system (**Figure 3.22**). As before, the control reactions (b), (c) and (d) indicate that this systems reaction *via* an autocatalytic self-replicating system. The bimolecular control reaction (b) demonstrates that by using the methyl ester maleimide **79** instead of the acid maleimide **77** to block the recognition significantly decreases the rate of reaction for both the major and minor isomers. This demonstrates that the original experiment (a) is recognition-mediated. The second control

experiment involving the addition of 4 equivalent of benzoic acid also reveals loss of the sigmoidal rate profile for the major isomer and a significant decrease in the rate of formation for both isomers. Again, this confirms the recognition is important in the original experiment. Finally the addition of 10-mol% preformed template **138** clearly removes the lag period from the rate profile of the major isomer and so demonstrates that **138** can catalyse its own formation. However, the experimental data shows that the minor isomer seems to be unaffected by the addition of template. These control reactions confirm that the major isomer can act as an autocatalytic self-replicator, whereas the minor isomer does not.

3.11.4 *N*-[3-(*N'*-6-Methyl-2-pyridyl)-amidobenzylidene]-4-*tert*-butylphenylamine *N*-oxide **112**

The final nitron in this series involves the use of a *tert*-butyl group in the *para* position; this will act as quite a bulky substituent and, hence, may have a significant effect on the system.



Scheme 3.35 Proposed autocatalytic self-replicating system utilising the 1,3 dipolar cycloaddition reaction between building blocks **77** and **112** to form the cycloadduct **139** performed at a concentration of 25 mM in CDCl_3 at 10°C .

The results of the kinetic experiment outlined in **Scheme 3.35** are presented in **Figure 3.23 (a)** along with the corresponding control reactions **Figure 3.23 (b)**, **(c)** and **(d)**.

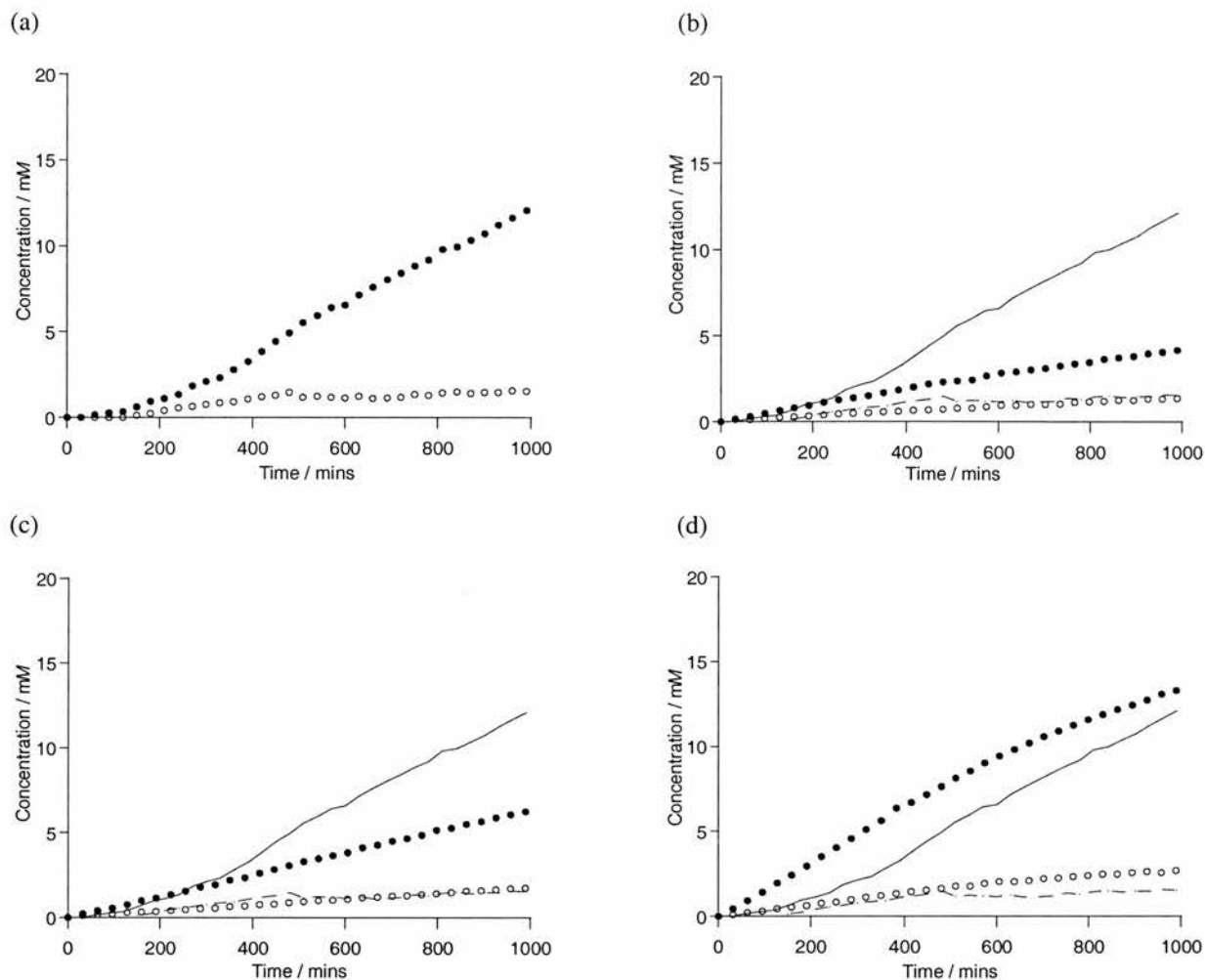


Figure 3.23 The rate profiles showing (a) the formation of the template **139** in the reaction between nitrone **112** and maleimide **77** to afford the products *trans*-**139** and *cis*-**139**, performed at 10°C and at a concentration of 25 mM in CDCl₃ with respect to both building blocks **77** and **112**. The *trans*-isoxazolidine is represented by the filled circles and the *cis*-isoxazolidine is represented by the open circles. Graphs (b), (c) and (d) show the control reactions performed upon nitrone **112** and maleimide **77**, all reactions were performed at concentrations of 25 mM in CDCl₃ with respect to the building blocks **77** and **112** at 10°C. Control reaction (b) demonstrates the bimolecular mimic where the control ester **79** was used to replace maleimide **77**, (c) involves the addition of 4 equivalents of benzoic acid to the reaction between nitrone **112** and maleimide **77** and (d) shows the effect of the addition of 10-mol% preformed template **139**. In the control reactions the original recognition-mediated reaction results are shown as solid lines for the *trans*-isoxazolidine and dashed lines for the *cis*-isoxazolidine, and the control reaction results are shown as a solid circles for the *trans*-isoxazolidine and a open circles for the *cis*-isoxazolidine.

The addition of a bulky substituent has slowed the rate of reaction compared to other systems, however, the sigmoidal rate profile is quite evident for the major isomer in this system and so the control experiments were performed as before.

The bimolecular control reaction (b) reveals that by blocking the recognition, the sigmoidal rate profile of the major isomer is removed and its rate of formation is also reduced significantly. However, unlike the other systems tested the rate of formation for the minor

isomer appear unaltered which indicates that its formation is purely *via* the uncatalysed bimolecular pathway. Addition of four equivalents of benzoic acid (c), to act as a competitive inhibitor, also removes the sigmoidal rate profile for the major isomer and reduces its rate of formation. It is also evident from this control data (c) that the rate of formation for the minor isomer is again unaltered as observed in the bimolecular control reaction. This suggests that the formation of the minor isomer occurs only through the bimolecular pathway. The final control experiment (d), involved addition of 10 mol% preformed template **139** to the recognition-mediated reaction. The addition of template at the beginning of the reaction has removed the lag period from the rate profile of the major isomer, which shows that the major isomer can catalyses its own formation. Hence, it can be concluded from the evidence obtained from the control reactions that the major isomer (*trans*) of this system can autocatalytically self-replicate whereas the minor isomer (*cis*) does not, its formation is *via* the uncatalysed bimolecular pathway.

3.12 Conclusion for the series of 3-nitrones

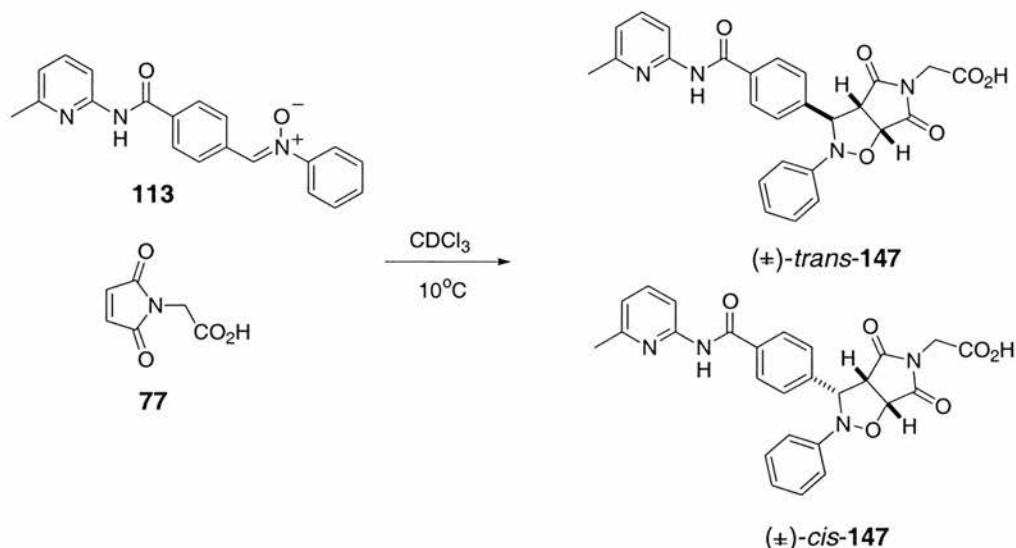
It appears on the basis of the results presented in **Section 3.11** that the addition of various substituents has not had a significant effect upon the operation of the self-replicating system. The only noticeable differences are the rates at which the reaction occurs; however the rate of reaction is not a measure of the efficiency of a self-replicating system as will be explained later. In order to rationalise these results, kinetic simulation and other physical quantities will be extracted and discussed along with the results of the 4-nitrone series in **Section 3.14**.

3.13 The experimental data for the 4-nitrones

This series of nitrones involves the functionality changes as used in the 3-nitrone family plus they also involve a regiochemical change as well. The nitrone group has been moved from the *meta* to the *para* position on the middle ring.

3.13.1 *N*-[4-(*N'*-6-Methyl-2-pyridyl)-amidobenzylidene]-phenylamine *N*-oxide **113**

This kinetic experiment is regioisomeric to the original experiment (**Scheme 3.36**), this system involves no additional functionality.



Scheme 3.36 Proposed autocatalytic self-replicating system utilising the 1,3 dipolar cycloaddition reaction between building blocks **77** and **113** to form the cycloadduct **147**, performed at a concentration of 25 mM in CDCl_3 at 10°C .

The results of the kinetic experiment outlined in **Scheme 3.36** are presented in **Figure 3.24 (a)** along with the corresponding control reaction results **Figure 3.24 (b)**, **(c)** and **(d)**.

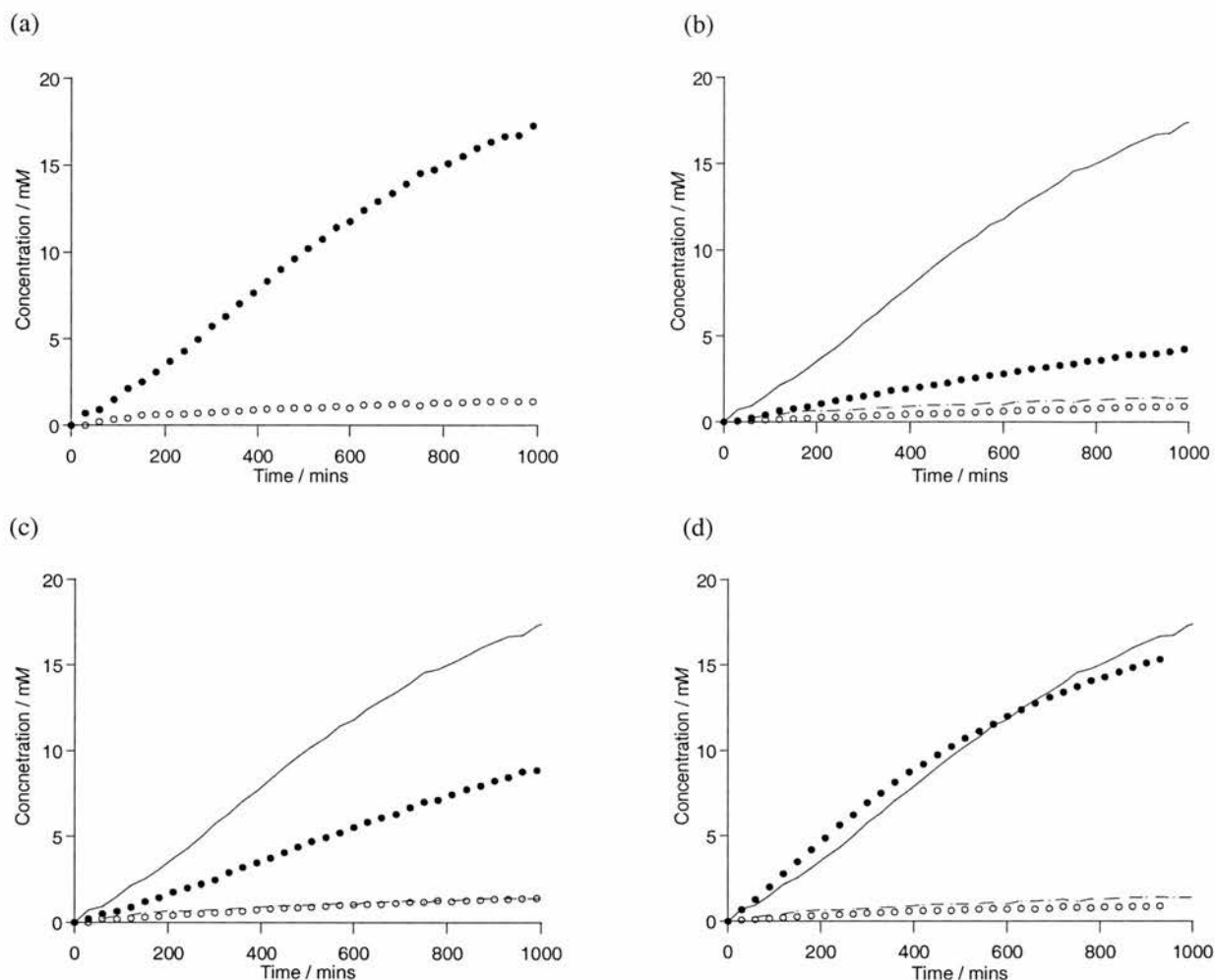


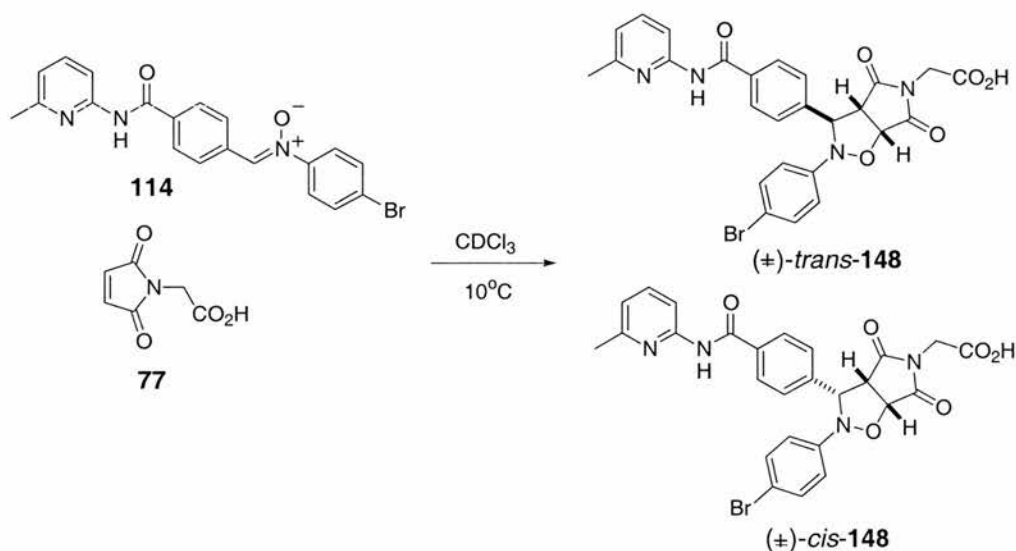
Figure 3.24 The rate profiles showing (a) the formation of the template **147** in the reaction between nitrone **113** and maleimide **77** to afford the products *trans*-**147** and *cis*-**147**, performed at 10°C and at a concentration of 25 mM in CDCl₃ with respect to both building blocks **77** and **113**. The *trans*-isoxazolidine is represented by the filled circles and the *cis*-isoxazolidine is represented by the open circles. Graphs (b), (c) and (d) show the control reactions performed upon nitrone **113** and maleimide **77**, all reactions were performed at concentrations of 25 mM in CDCl₃ with respect to the building blocks **77** and **113** at 10°C. Control reaction (b) demonstrates the bimolecular mimic where the control ester **79** was used to replace maleimide **77**, (c) involves the addition of 4 equivalents of benzoic acid to the reaction between nitrone **113** and maleimide **77** and (d) shows the effect of the addition of 10 mol% preformed template **147**. In the control reactions the original recognition-mediated reaction results are shown as solid lines for the *trans*-isoxazolidine and dashed lines for the *cis*-isoxazolidine, and the control reaction results are shown as a solid circles for the *trans*-isoxazolidine and a open circles for the *cis*-isoxazolidine.

The experimental data for the recognition-mediated reaction (a) displays a sigmoidal rate profile for the major (*trans*) isomer, although the sigmoidal shape is less pronounced than that observed for the analogous 3-nitron system. The rate of reaction between the 4-nitron **113** and maleimide **77** is faster and more stereoselective than the reaction between the 3-nitron **104** and maleimide **77**, a further detailed comparison between these systems will be given in **Section 3.14**. Having observed a sigmoidal rate profile, the control reactions were then

performed upon the system. The first control reaction performed (b), involved using the maleimide methyl ester **79** to mimic the bimolecular reaction. The experimental data (b) reveals the loss of the sigmoidal rate profile for the major (*trans*) isomer as well as a significant decrease in the rate of formation of the major isomer. A slight decrease in the rate of formation was also observed for the minor (*cis*) isomer. The second control reaction involved the addition of 4 equivalents of benzoic acid to the recognition-mediated reaction. The addition of this competitive inhibitor (c) lead to the loss of the sigmoidal rate profile for the major isomer with a decreased rate of formation, whereas the rate profile for the minor isomer is unaltered. The third control reaction, addition of 10 mol% preformed template **147** to the recognition-mediated reaction, shows that the lag period in the rate profile of the major isomer is removed accompanied with an increases rate of formation of template **147**. This result indicates that the major isomer can act as an autocatalyst. Addition of preformed template appears to have no effect upon the rate of formation of the minor isomer. It is interesting to note is that with the addition of 10 mol% preformed cycloadduct **147**, after 600 minutes the rate of reaction appears to decreases for the major isomer compared to the undoped reaction **Figure 3.24 (d)**.

3.13.2 *N*-[4-(*N'*-6-Methyl-2-pyridyl)-amidobenzylidene]-4-bromophenylamine *N*-oxide **114**

The next nitron to be investigated in the 4-nitron series involves the addition of bromine at the *para* position (**Scheme 3.37**).



Scheme 3.37 Proposed autocatalytic self-replicating system utilising the 1,3 dipolar cycloaddition reaction between building blocks **77** and **114** to form the cycloadduct **148** performed at a concentration of 25 mM in CDCl_3 at 10°C .

The results of the kinetic experiment shown in **Scheme 3.37** are presented in **Figure 3.25 (a)** along with the corresponding control experiment results **Figure 3.25 (b), (c)** and **(d)**.

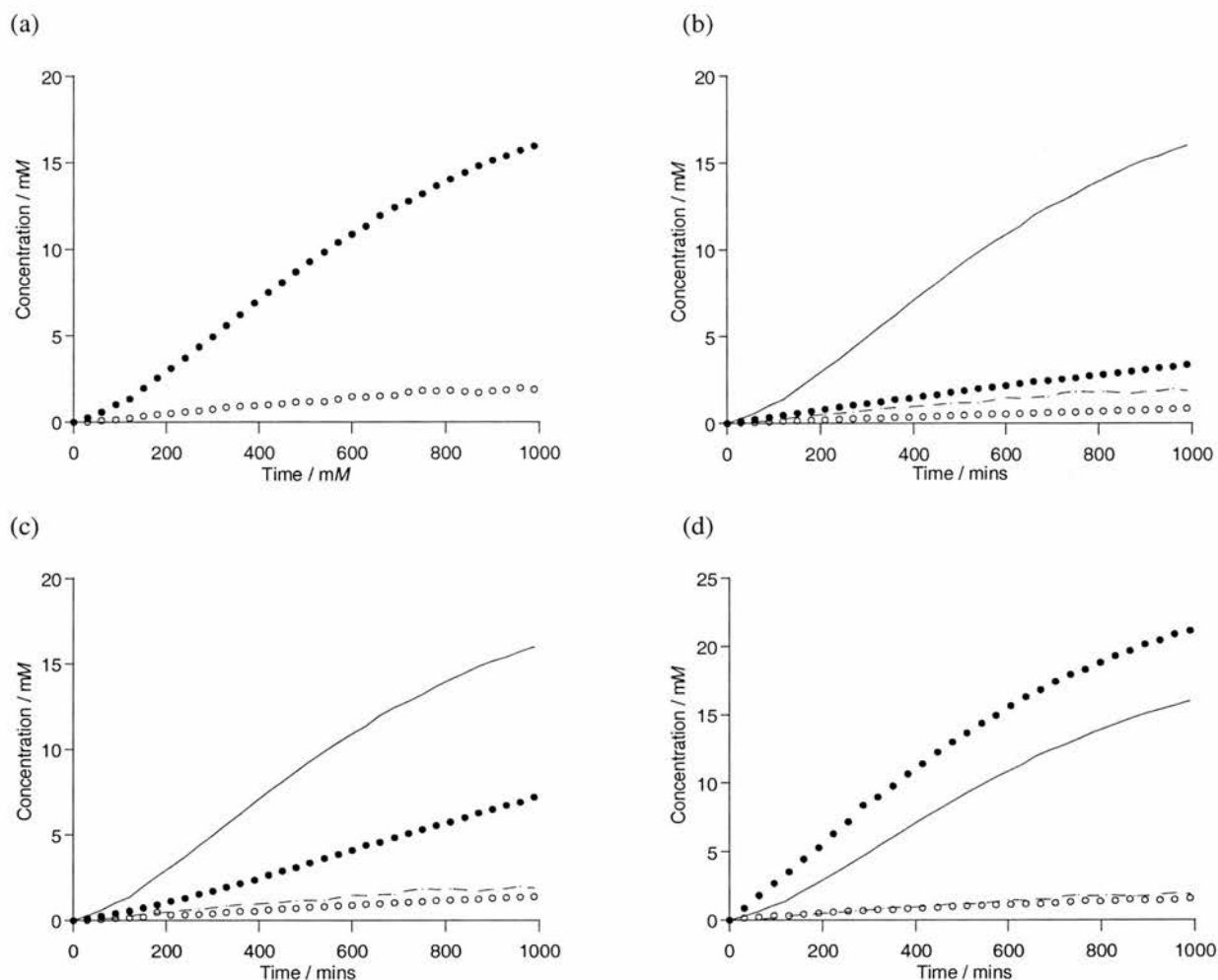


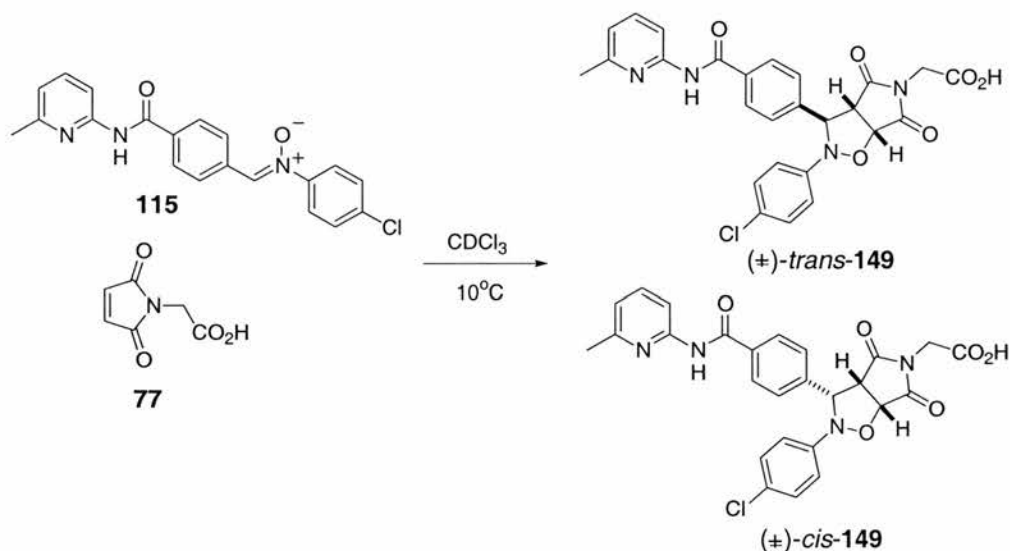
Figure 3.25 The rate profiles showing (a) the formation of the template **148** in the reaction between nitron **114** and maleimide **77** to afford the products *trans*-**148** and *cis*-**148**, performed at 10°C and at a concentration of 25 mM in CDCl₃ with respect to both building blocks **77** and **114**. The *trans*-isoxazolidine is represented by the filled circles and the *cis*-isoxazolidine is represented by the open circles. Graphs (b), (c) and (d) show the control reactions performed upon nitron **114** and maleimide **77**, all reactions were performed at concentrations of 25 mM in CDCl₃ with respect to the building blocks **77** and **114** at 10°C. Control reaction (b) demonstrates the bimolecular mimic where the control ester **79** was used to replace maleimide **77**, (c) involves the addition of 4 equivalents of benzoic acid to the reaction between nitron **114** and maleimide **77** and (d) shows the effect of the addition of 10-mol% preformed template. In the control reactions the original recognition-mediated reaction results are shown as solid lines for the *trans*-isoxazolidine and dashed lines for the *cis*-isoxazolidine, and the control reaction results are shown as a solid circles for the *trans*-isoxazolidine and a open circles for the *cis*-isoxazolidine.

The experimental data of the recognition-mediated reaction (a) displays a sigmoidal rate profile for the major isomer, and so the system was subjected to the control experiments. The bimolecular control reaction (b) demonstrates that by blocking the recognition sites, the rate of formation is significantly reduced for the major and minor isomers, which shows that the recognition is important in the original experiment (a). The second control (b) experiment involved the addition of 4 equivalents of benzoic acid to the recognition-mediated reaction; the experimental data shows that there is a decrease in the rate of formation of both isomers, and the loss of the sigmoidal profile of the major isomer. The final control experiment

involved the addition of 10 mol% preformed template **148** to the recognition-mediated reaction. The experimental data (d) shows that the lag period is removed from the rate profile for the major isomer with an increased rate of formation and so demonstrates that it can template its own formation whereas the rate of formation of the minor isomer is unaffected. This reveals that the minor isomer does not catalyse its own formation, and also the major isomer does not aid the formation of the minor isomer. The control experiments confirm that this system proceeds *via* an autocatalytic self-replicating pathway.

3.13.3 *N*-[4-(*N'*-6-Methyl-2-pyridyl)-amidobenzylidene]-4-chlorophenylamine *N*-oxide **115**

This system uses chlorine instead of bromine, it is hoped to observe whether the use of a smaller halogen has a different effect upon the self-replicating ability of the system.



Scheme 3.38 Proposed autocatalytic self-replicating system utilising the 1,3 dipolar cycloaddition reaction between building blocks **77** and **115** to form the cycloadduct **149** performed at a concentration of 25 mM in CDCl₃ at 10°C.

The results of the proposed self-replicating system outlined in **Scheme 3.38**, are presented in **Figure 3.26 (a)** along with the corresponding control reaction results **Figure 3.26 (b), (c)** and **(d)**.

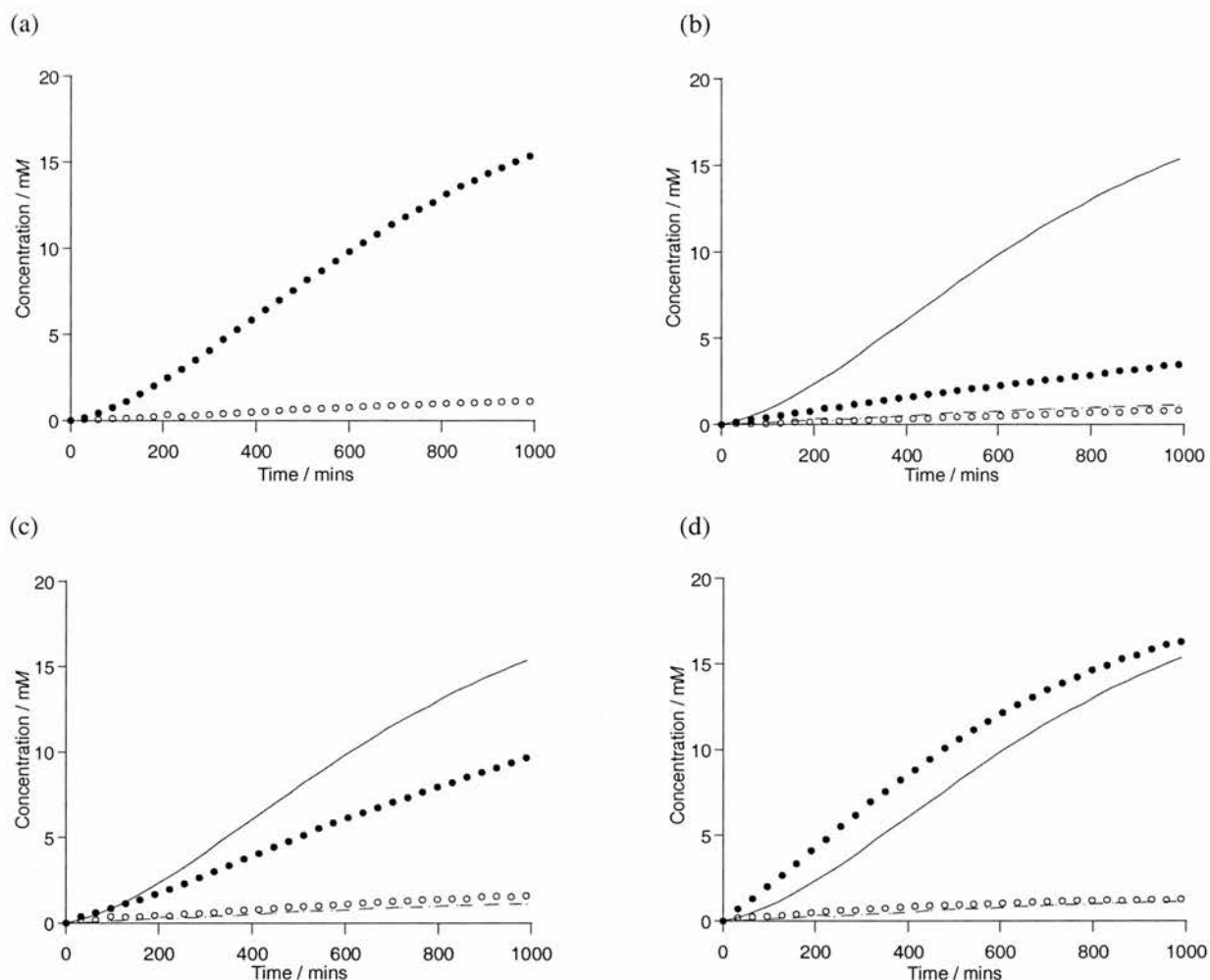


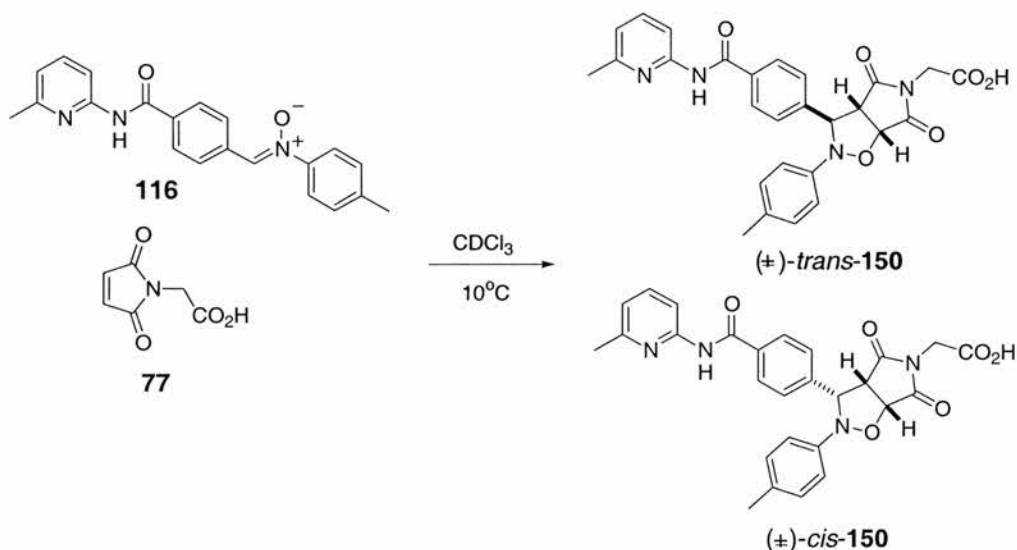
Figure 3.26 The rate profiles showing (a) the formation of the template **149** in the reaction between nitrone **115** and maleimide **77** to afford the products *trans*-**149** and *cis*-**149**, performed at 10°C and at a concentration of 25 mM in CDCl₃ with respect to both building blocks **115** and **149**. The *trans*-isoxazolidine is represented by the filled circles and the *cis*-isoxazolidine is represented by the open circles. Graphs (b), (c) and (d) show the control reactions performed upon nitrone **115** and maleimide **77**, all reactions were performed at concentrations of 25 mM in CDCl₃ with respect to the building blocks **77** and **115** at 10°C. Control reaction (b) demonstrates the bimolecular mimic where the control ester **79** was used to replace maleimide **77**, (c) involves the addition of 4 equivalents of benzoic acid to the reaction between nitrone **115** and maleimide **77** and (d) shows the effect of the addition of 10 mol% preformed template **149**. In the control reactions the original recognition-mediated reaction results are shown as solid lines for the *trans*-isoxazolidine and dashed lines for the *cis*-isoxazolidine, and the control reaction results are shown as a solid circles for the *trans*-isoxazolidine and a open circles for the *cis*-isoxazolidine.

The experimental data for the recognition-mediated reaction (a) clearly displays a sigmoidal rate profile for the major *trans* isomer and so the control reactions were performed upon the system. The first control reaction involved the use of the methyl ester instead of the acid to act as a bimolecular mimic, the results (b) clearly show that the sigmoidal rate profile of the major isomer has been destroyed along with a significant decrease in the rate of formation whereas the rate of formation of the minor isomer is relatively unaltered, indicating that its formation is *via* the uncatalysed bimolecular pathway. The second control reaction involved the addition of 4 equivalents of benzoic acid to the recognition-mediated reaction; the

experimental data (c) reveals a significant decrease in the rate of formation of the major isomer accompanied by a loss of the sigmoidal rate profile. The addition of a competitive inhibitor does not appear to have any effect upon the rate of formation of the minor isomer. These control reactions confirm that the reaction is recognition-mediated for the major isomer and not for the minor isomer. The final control reaction involved the addition of 10 mol% template **149** to the recognition-mediated control reaction, the experimental data (d) reveals that the lag period is lost and the rate of formation of the major isomer is enhanced, indicating that the major isomer can catalyses its own formation. The rate of formation of the minor isomer is unaffected by the addition of preformed template. The control reactions confirm that the major isomer reacts *via* an autocatalytic self-replicating pathway whereas the minor isomer reacts *via* the uncatalysed bimolecular pathway.

3.13.4 *N*-[4-(*N*'-6-Methyl-2-pyridyl)-amidobenzylidene]-4-methylphenylamine *N*-oxide **116**

This system involves the use of a methyl group in the *para* position (**Scheme 3.39**).



Scheme 3.39 Proposed autocatalytic self-replicating system utilising the 1,3 dipolar cycloaddition reaction between building blocks **77** and **116** to form the cycloadduct **150** performed at a concentration of 25 mM in CDCl_3 at 10°C .

The results of the kinetic experiment (**Scheme 3.39**) are presented in **Figure 3.27 (a)** along with the corresponding control reaction results **Figure 3.27 (b)**, (c) and (d).

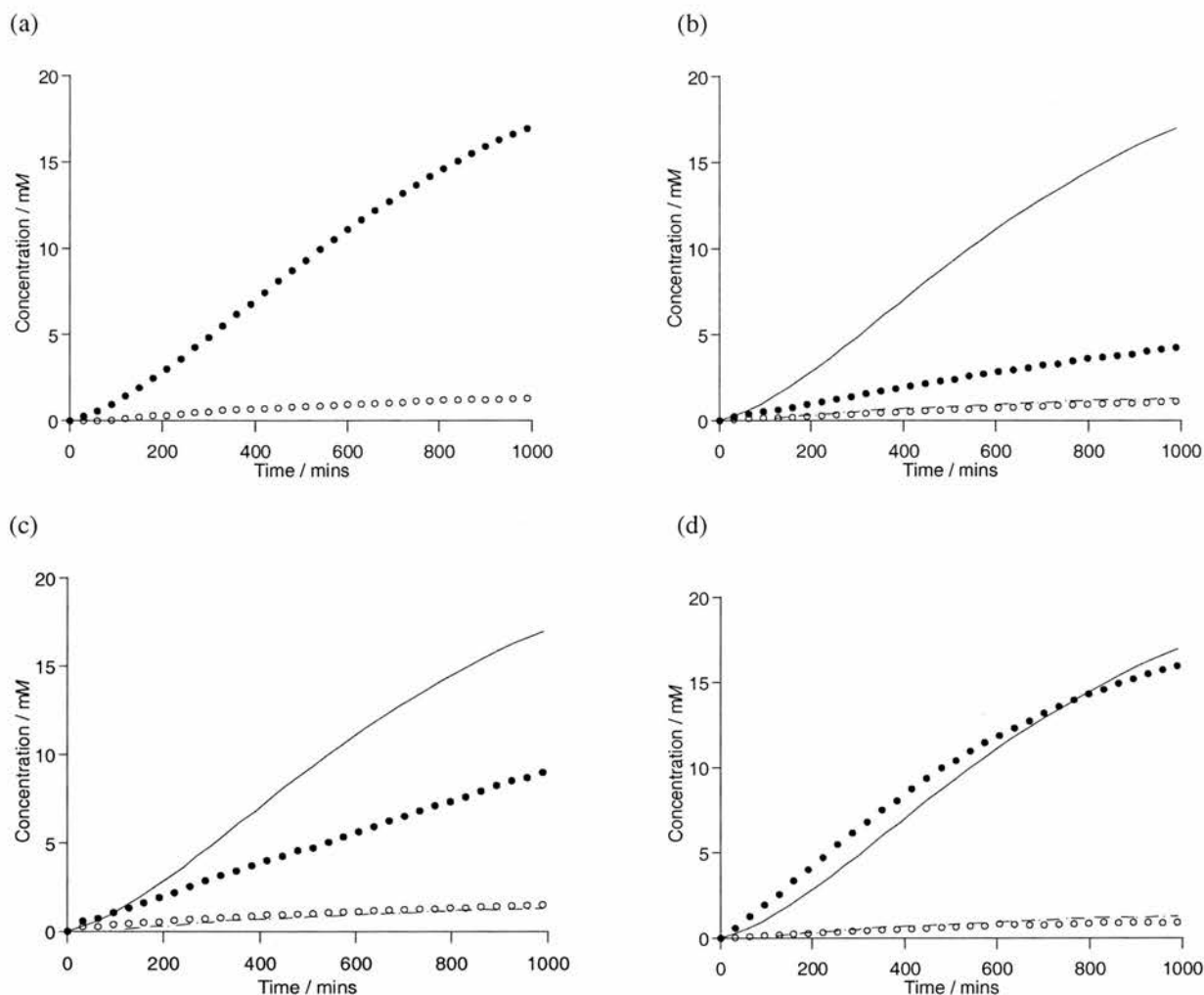


Figure 3.27 The rate profiles showing (a) the formation of the template **150** in the reaction between nitrone **116** and maleimide **77** to afford the products *trans*-**150** and *cis*-**150**, performed at 10°C and at a concentration of 25 mM in CDCl₃ with respect to both building blocks **77** and **116**. The *trans*-isoxazolidine is represented by the filled circles and the *cis*-isoxazolidine is represented by the open circles. Graphs (b), (c) and (d) show the control reactions performed upon nitrone **116** and maleimide **77**, all reactions were performed at concentrations of 25 mM in CDCl₃ with respect to the building blocks **77** and **116** at 10°C. Control reaction (b) demonstrates the bimolecular mimic where the control ester **79** was used to replace maleimide **77**, (c) involves the addition of 4 equivalents of benzoic acid to the reaction between nitrone **116** and maleimide **77** and (d) shows the effect of the addition of 10 mol% preformed template **150**. In the control reactions the original recognition-mediated reaction results are shown as solid lines for the *trans*-isoxazolidine and dashed lines for the *cis*-isoxazolidine, and the control reaction results are shown as a solid circles for the *trans*-isoxazolidine and a open circles for the *cis*-isoxazolidine.

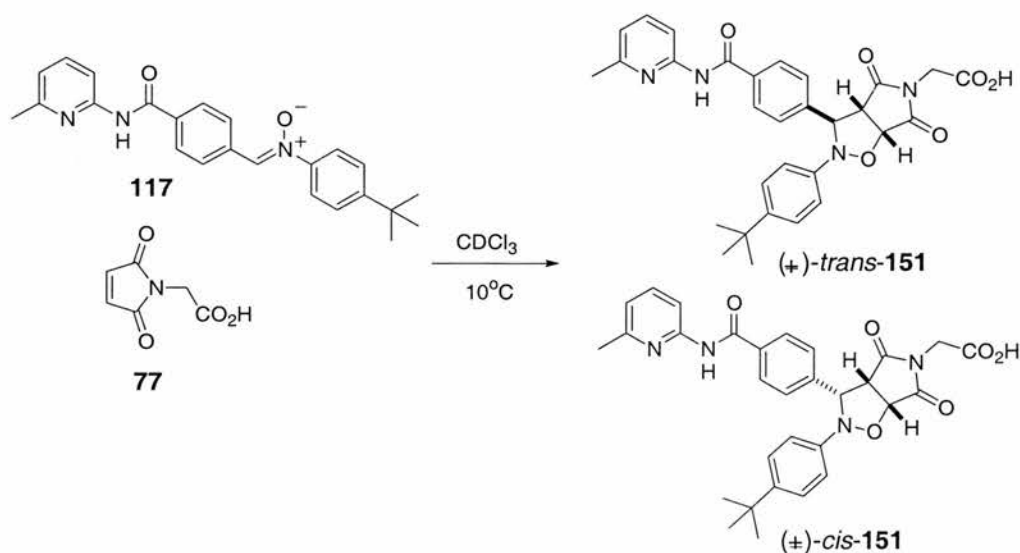
The rate profile for the reaction outlined in **Scheme 3.39** clearly displays a sigmoidal rate profile for the major isomer, hence the control reactions were performed to investigate whether this system can operate as an autocatalytic self-replicator.

The first control reaction involved the use of the methyl ester instead of the acid to act as a bimolecular mimic, the results (b) clearly show that the sigmoidal rate profile of the major isomer has been destroyed along with a significant decrease in the rate of formation whereas the rate of formation of the minor isomer is relatively unaltered, indicating that its formation

is *via* the uncatalysed bimolecular pathway. The second control reaction involved the addition of 4 equivalents of benzoic acid to the recognition-mediated reaction; the experimental data (c) reveals a significant decrease in the rate of formation of the major isomer accompanied by a loss of the sigmoidal rate profile. The addition of a competitive inhibitor does not appear to have any effect upon the rate of formation of the minor isomer. These control reactions confirm that the reaction is recognition-mediated only for the major. The final control reaction involved the addition of 10 mol% template **150** to the recognition-mediated control reaction, the experimental data (d) reveals that the lag period is lost and the rate of formation of the major isomer is initially enhanced, indicating that the major isomer can catalyses its own formation. However, after about 800 minutes the rate of formation of the major isomer appears to decrease, this effect was also observed in the 4-nitrone **113** system. The rate of formation of the minor isomer is unaffected by the addition of preformed template. The control reactions confirm that the major isomer reacts *via* an autocatalytic self-replicating pathway whereas the minor isomer reacts *via* the uncatalysed bimolecular pathway.

3.13.5 *N*-[4-(*N'*-6-Methyl-2-pyridyl)-amidobenzylidene]-4-*tert*butylphenylamine *N*-oxide **117**

This system uses a bulky *tert*-butyl substituent in the *para* position, again it is hoped to see an effect on the self-replicating system due to steric hindrance (**Scheme 3.40**).



Scheme 3.40 Proposed autocatalytic self-replicating system utilising the 1,3 dipolar cycloaddition reaction between building blocks **77** and **117** to form the cycloadduct **151** performed at a concentration of 25 mM in CDCl_3 at 10°C .

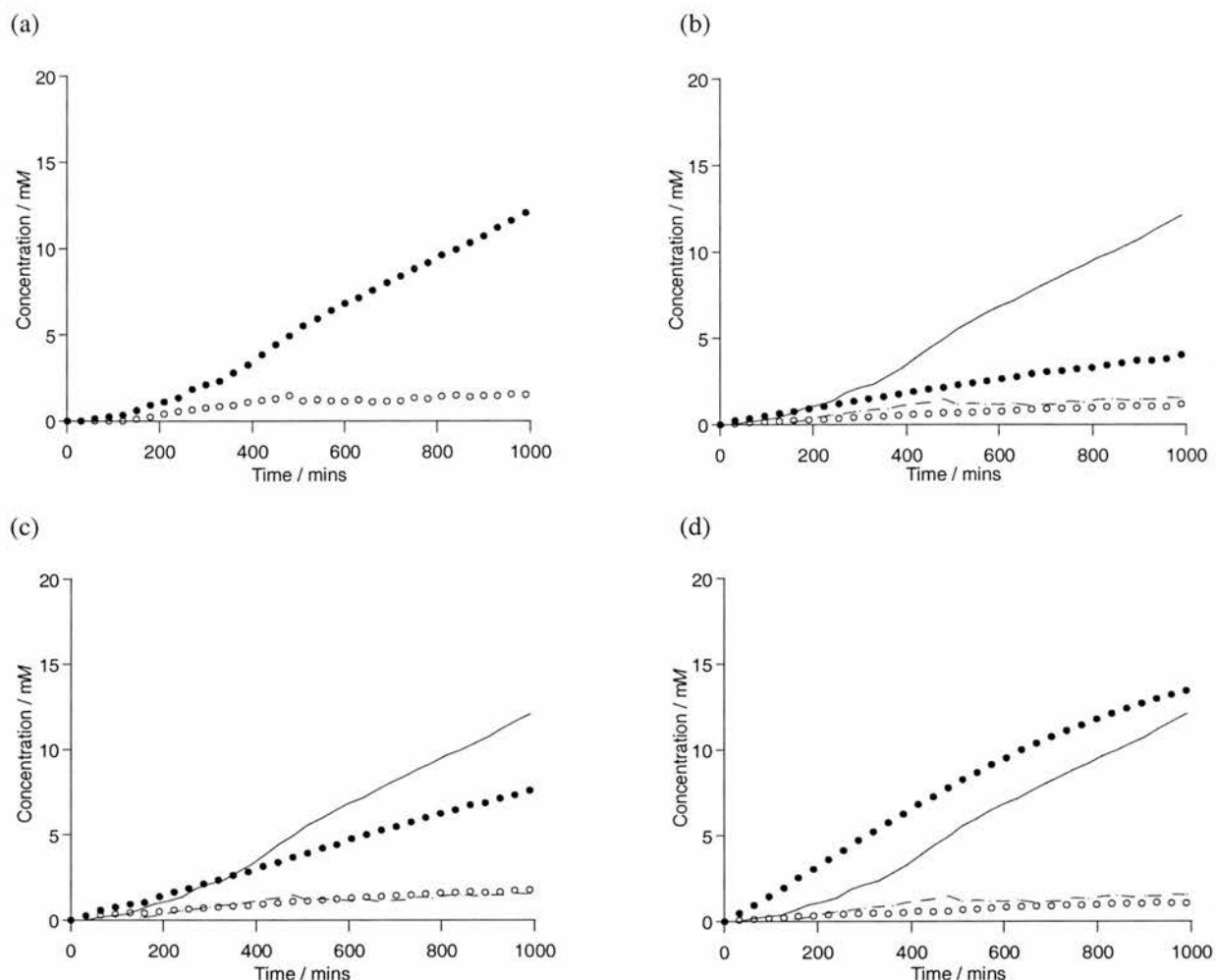


Figure 3.28 The rate profiles showing (a) the formation of the template **151** in the reaction between nitron **117** and maleimide **77** to afford the products *trans*-**151** and *cis*-**151**, performed at 10°C and at a concentration of 25 mM in CDCl₃ with respect to both building blocks **77** and **117**. The *trans*-isoxazolidine is represented by the filled circles and the *cis*-isoxazolidine is represented by the open circles. Graphs (b), (c) and (d) show the control reactions performed upon nitron **117** and maleimide **77**, all reactions were performed at concentrations of 25 mM in CDCl₃ with respect to the building blocks **77** and **117** at 10°C. Control reaction (b) demonstrates the bimolecular mimic where the control ester **79** was used to replace maleimide **77**, (c) involves the addition of 4 equivalents of benzoic acid to the reaction between nitron **117** and maleimide **77** and (d) shows the effect of the addition of 10 mol% preformed template **151**. In the control reactions the original recognition-mediated reaction results are shown as solid lines for the *trans*-isoxazolidine and dashed lines for the *cis*-isoxazolidine, and the control reaction results are shown as a solid circles for the *trans*-isoxazolidine and a open circles for the *cis*-isoxazolidine.

The rate profile for the reaction outlined in **Scheme 3.40** reveals a significant sigmoidal appearance for the major isomer and so the control reactions were performed upon the system. The first control reaction involved the use of the methyl ester instead of the acid to act as a bimolecular mimic, the experimental data (b) clearly shows that the sigmoidal rate profile of the major isomer has been destroyed along with a significant decrease in the rate of formation whereas the rate of formation of the minor isomer is relatively unaltered, indicating that its formation is *via* the uncatalysed bimolecular pathway. The second control reaction involved the addition of 4 equivalents of benzoic acid to the recognition-mediated reaction; the

experimental data (c) reveals a modest decrease in the rate of formation of the major isomer after approximately 400 minutes. This is not surprising however, because up to 400 minutes the system is still in its 'lag period' where predominately the bimolecular reaction is occurring to form enough template for autocatalysis to begin. The addition of an inhibitor should not have an effect on the rate of the bimolecular reaction and so the rates are comparable. This control reaction also displays the loss of the sigmoidal rate profile for the major isomer. The addition of a competitive inhibitor does not appear to have any effect upon the rate of formation of the minor isomer. These control reactions confirm that the reaction is recognition-mediated for the major isomer and not for the minor isomer. The final control reaction involved the addition of 10 mol% template **151** to the recognition-mediated control reaction, the experimental data (d) reveals that the lag period is lost and the rate of formation of the major isomer is significantly enhanced, indicating that the major isomer can catalyse its own formation. The rate of formation of the minor isomer is unsurprisingly unaffected by the addition of preformed template. The control reactions confirm that the major isomer reacts *via* an autocatalytic self-replicating pathway whereas the minor isomer reacts *via* the uncatalysed bimolecular pathway.

3.14 What conclusions can be drawn from the experimental data

It has been demonstrated that all except two of the systems investigated have the ability to self-replicate (**Figure 3.18 (c) and (d)**). The effect of adding substituents has meant the systems still operate as self-replicators; it is only the rates of reaction, which are affected by the altering the functionality at the *para* position. Altering the regiochemistry of the system, by moving the nitron group from the *meta* to *para* position, also meant that the system remained self-replicating, and again substituent effects only lead to changes in the rate of reaction within the systems. However in order to compare the systems, various physical values must be extracted from the experimental data to determine whether any patterns emerge.

3.15 Percentage completion and diastereoisomer ratio

In an attempt to assess the relative efficiencies of the data obtained from all the nitron series, certain physical quantities were extracted from the experimental data. Initially, the relative percentage completions of the recognition-mediated reactions (graph **(a)** in all cases) will be calculated; the values determined were the relative amounts at 1000 minutes reaction time. The percentage completions at 1000 minutes were tabulated (**Appendix 8.2**) and presented in **Figure 3.29**.

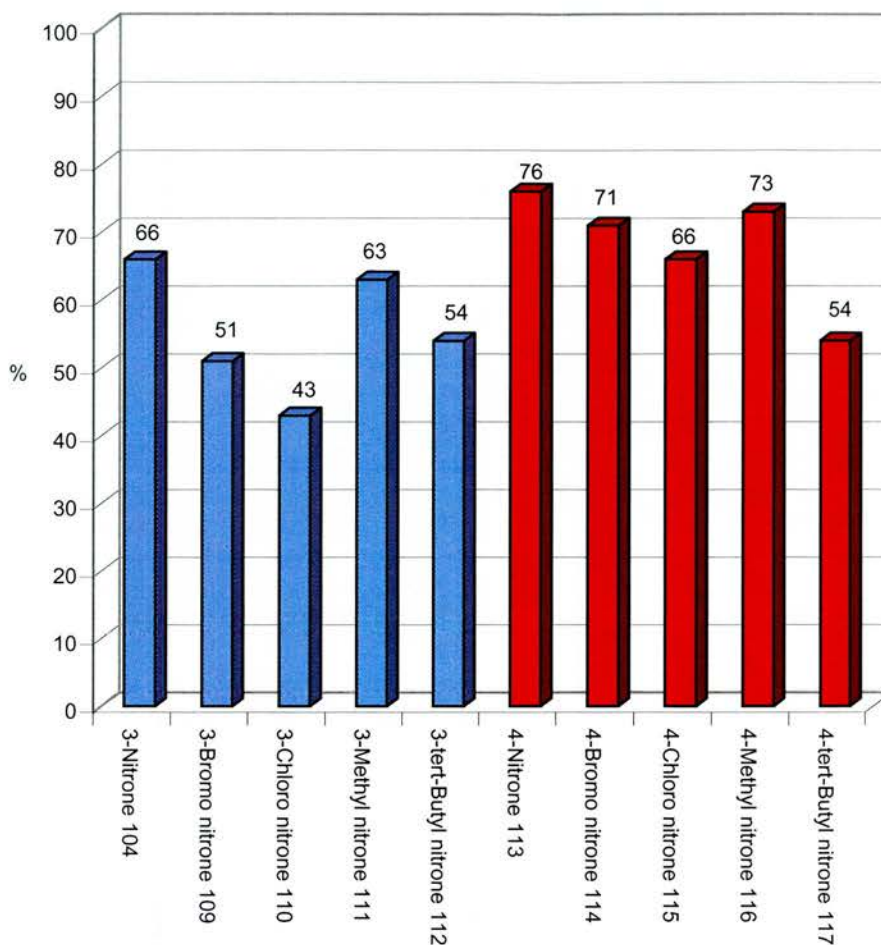


Figure 3.29 A bar chart to show the percentage completion values for the recognition-mediated reactions between all the nitrones and maleimide **77** to afford the corresponding cycloadduct. The values presented are the relative percentages at 1000 minutes.

It is evident from the data, that at 1000 minutes the percentage completion of reaction between 4-nitron **113** and maleimide **77** is the greatest. Its overall percentage completion at 1000 minutes is approximately 10% greater than its 3-nitron counterpart. This is a general trend where the 4-nitrones have achieved a greater percentage completion at 1000 minutes than their 3- counterparts.

It is interesting to note that as the series of nitrones is descended the trend between the 3- and 4-nitrones substituents is not identical. This indicates that the electronic effects do not play such a dominant role within these systems and to try to confirm this, a Hammett plot was constructed.

3.16 Hammett plot

In order to determine the electronic effects a substituent has upon a system, Hammett described the following equation (**Equation 3.1**).

$$\log k_X / k_H = \sigma\rho$$

Equation 3.1 The Hammett equation where k_X is the rate constant for the reaction with substituent X, k_H is the rate constant for the reaction where X=H, σ is the constant characteristic of the group and ρ is a constant for a given reaction under a given set of conditions.

The σ value within this equation sums up the total electrical effects (resonance plus field) of a group X when attached to a benzene ring. The σ values for many substituents have been measured and tabulated¹⁹⁸.

If this equation holds true for the self-replicating systems then a plot of $\log k_X/k_H$ against the corresponding σ value should reveal a straight line. These graphs were plotted for the 3- and 4-nitro series **Figure 3.30**.

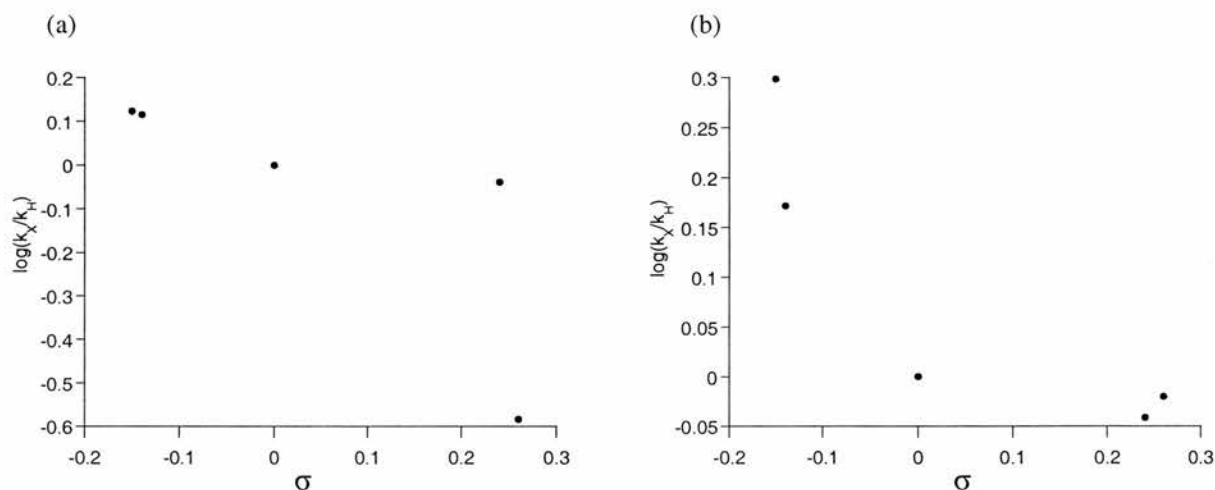
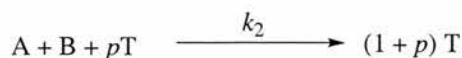
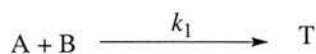


Figure 3.30 The Hammett plots for the (a) 3- and (b) 4-nitro series. The graphs demonstrate the non-linear relationship for a plot of $\log(k_X/k_H)$ against σ for both the 3- and 4-nitro series, which indicates that electronic effects are not having a significant effect within these series.

The graphs shown in **Figure 3.30 (a)** and **(b)** reveal that neither the 3- or 4-nitro series produces a straight line graph for their corresponding Hammett plots, this indicates that the electronic effects are not playing a dominant role in the operation of the self-replicating systems. If it is not an electronic effect, which is causing the difference in reactivity, then this leads to the conclusion that it must be a steric effect.

3.17 Fitting the data to the kinetic model

As discussed in **Section 2.11** the square root law approximation can be used to fit the experimental data to obtain the rate values (**Equation 3.2**).



Equation 3.2 Square root approximation used to fit the experimentally determined rate data for minimal self-replicating systems. **A** and **B** correspond to the building blocks, **T** to the template. The values p , k_1 and k_2 correspond to the autocatalytic order, bimolecular rate and the recognition mediated rate constants respectively.

Using this model the experimental data was entered into the simulation and fitting package SIMFIT¹⁷⁶. The value of p was varied until the best fit of the kinetic model was obtained for the experimentally determined data. In the interest of brevity only the fitting for the 4-bromo nitrone system will be presented. The command and data files for this system obtained from the Simfit program are presented in **Appendix 1**.

Initially the fitting of the bimolecular control data was performed (**Figure 3.31 (a)**) followed by the fitting of the recognition-mediated data (**Figure 3.31 (b)**).

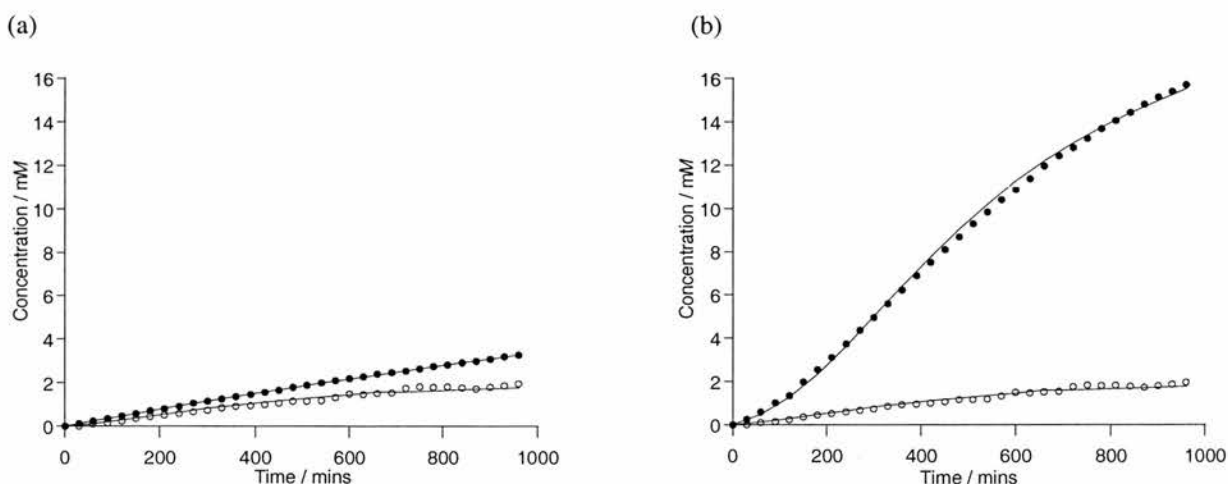


Figure 3.31 Experimental rate profiles (circles) and best fit to the kinetic model (solid lines) for (a) the bimolecular control reaction between nitrone **114** and maleimide ester **79** and (b) the recognition-mediated reaction between nitrone **114** and maleimides **77**.

Rate values were obtained for the major and minor isomers for all the systems investigated however, as the experimental data revealed that only the major isomers seemed capable of autocatalytic self-replication, only the rate values for the major isomers have been presented

Table 3.2. From the kinetic fitting the value of p was obtained and from the rate constants a value of ϵ was calculated (**Table 3.21**).

Table 3.2 The rate values obtained for the recognition-mediated reactions between the nitrones and maleimide **77** (k_2) and rate values obtained for the bimolecular control reactions between the nitrones and maleimide ester **79** (k_1). The rate values presented are for the major isomers only. The table also presents the calculated values of p and ϵ .

	k_1 + maleimide ester 79 $10^{-4} M^{-1} s^{-1}$	k_2 + maleimide 77 $10^{-2} s^{-1}$	p	ϵ
3-Nitron 104	1.28	8.43	0.9	659
3-Bromo nitron 109	1.13	2.20	0.73	195
3-Chloro nitron 110	1.10	7.71	1	701
3-Methyl nitron 111	1.45	11.00	0.98	759
3- <i>tert</i> -Butyl nitron 112	1.36	11.20	1	783
4-Nitron 113	1.45	5.82	0.77	401
4-Bromo nitron 114	1.09	5.04	0.74	462
4-Chloro nitron 115	1.14	4.80	0.78	421
4-Methyl nitron 116	1.33	7.84	0.84	590
4- <i>tert</i> -Butyl nitron 117	1.36	1.05	1	772

From the p and ϵ values obtained the most efficient systems appear to be the 3- and 4-*tert*-butyl nitron systems and the 3-chloro nitron system.

It should be noted from the table above that for the 3-nitrons the p value tends to fall between 0.9 and 1 with the exception of the 3-bromo system, and the ϵ values are between 650 and 800, again with the exception of the 3-bromo nitron system. Whereas the 4-nitrons tend to have lower p values between 0.77 and 0.84 with the exception of the 4-*tert*-butyl nitron system and the ϵ values are also lower, between 400 and 600.

This reveals that although the 4-nitron systems appear to have faster rates of reaction and better percentage completions at 1000 minutes they are generally more inefficient at turnover of template in the autocatalytic cycle than their 3-counterparts.

3.18 Comparison of the diastereoisomeric excesses (d.e.)

It was noted that in all the systems examined, the recognition-mediated reaction improved the stereoselective outcome of the reaction relative to the bimolecular control. The diastereoisomeric excess (d.e.) values were calculated for the bimolecular control reactions and

the recognition-mediated reactions (**Appendix 2**) and the difference presented in **Figure 3.32**, all the values obtained were the relative diastereoisomeric excess values calculated at 1000 minutes.

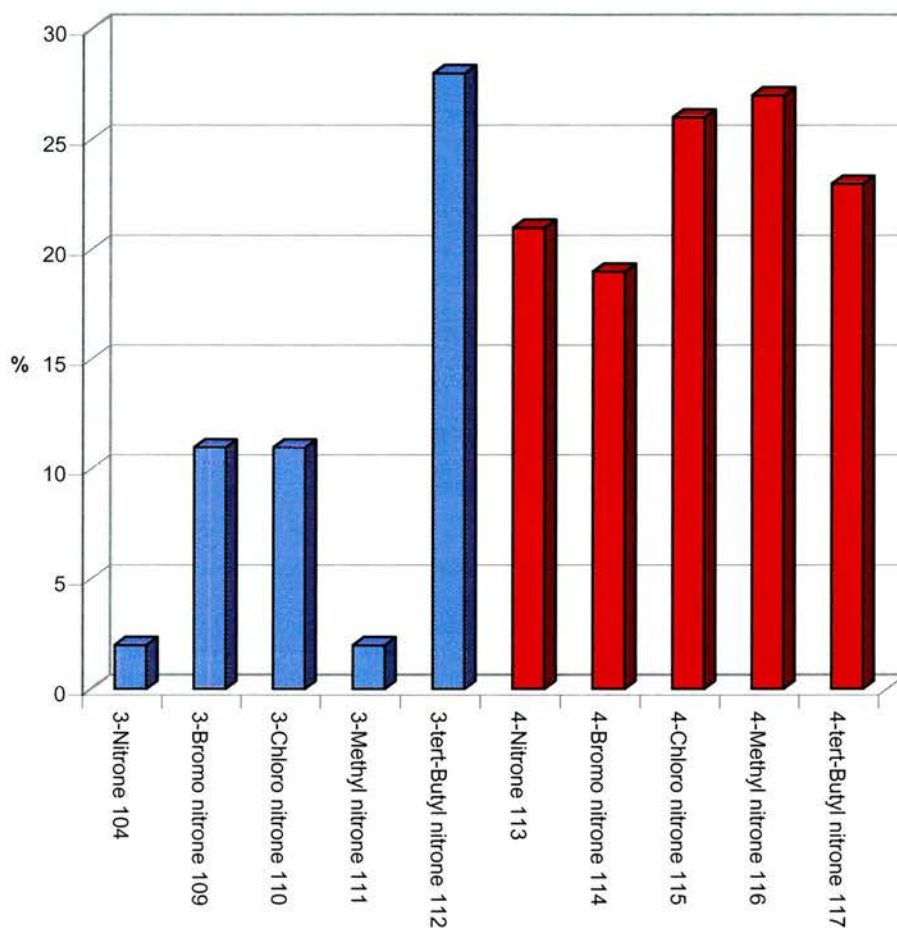


Figure 3.32 A bar chart to show the difference in the d.e values between the recognition-mediated reaction between the nitrones and maleimide **77**, and the bimolecular control reaction between the nitrones and maleimide ester **78**. All the d.e data presented are the relative values calculated at 1000 minutes.

The general trend for the nitrones shown in **Figure 3.32** shows that there is an increase in the diastereoisomeric excess (d.e.) from bimolecular control reaction to the recognition-mediated reaction for all the systems. However, the difference is generally greater for the 4-nitrones than the 3-nitron. The most notable system is the 3-*tert*-butyl system, the difference between the bimolecular control reaction and the undoped recognition-mediated reaction for this system is 28% which is the largest of all the systems.

It was also noted that upon addition of 10 mol% preformed template the stereoselectivity of some of the reactions improved further. This demonstrated that not only were the systems acting as autocatalysts but they also had the ability to act as asymmetric autocatalysts. The d.e. values were calculated for the doped reactions (graph (d) in all cases) and the difference

calculated relative to the bimolecular control reaction (**Appendix 2**). The differences between the diastereoisomeric excess values are presented in **Figure 3.33**, all the values obtained were the relative diastereoisomeric excesses calculated at 1000 minutes.

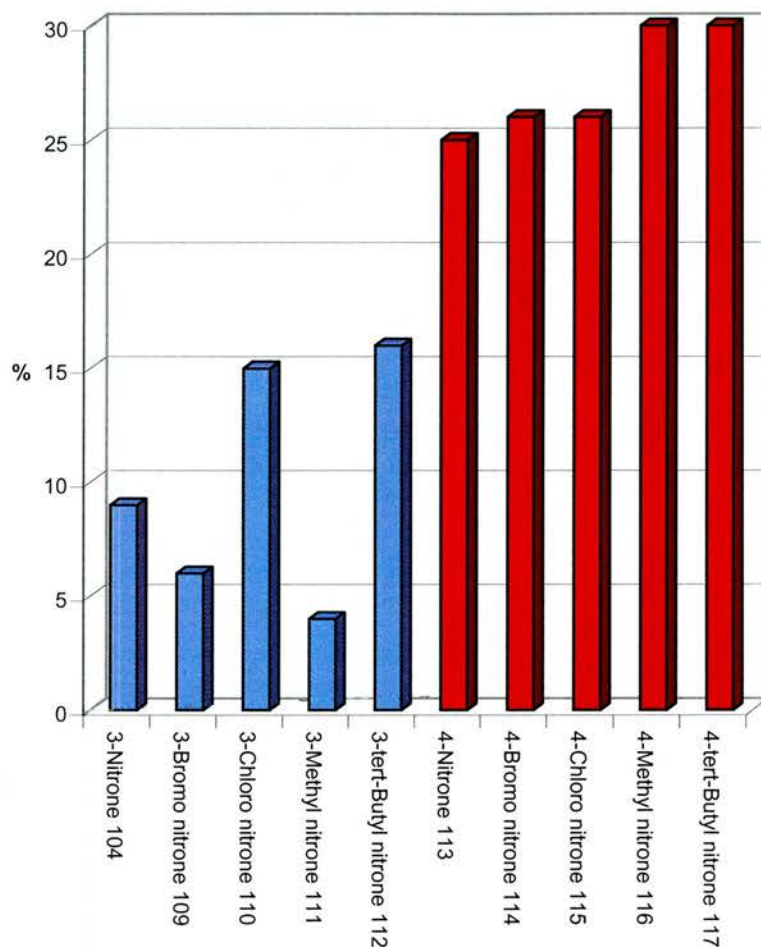


Figure 3.33 A bar chart to show the difference in the d.e. values between the recognition-mediated reactions involving the nitrones, maleimide **77** and 10 mol% added preformed template, and the bimolecular control reaction between the nitrones and maleimide ester **79**. All the d.e. data presented are the relative values calculated at 1000 minutes.

Again, it is apparent from the data presented in **Figure 3.33** that the 4-nitron series display a greater increase in the d.e. value than the 3 series. It should be noted that the system which observed the largest increase in d.e. in **Figure 3.33** (3-*tert*-butyl nitron), upon addition of template, decreases its d.e. value by 12%, which infers that the template from this reaction could be capable of crosscatalysis and so is a poor autocatalyst. The 4-*tert*-butyl-nitron counterpart, however, increases its d.e. by 7% to give the largest increase of all the systems between the bimolecular reaction and the doped reaction of 30%. This indicates that the system is acting as a very good asymmetric autocatalyst (**Section 1.9.1**). The basis for its

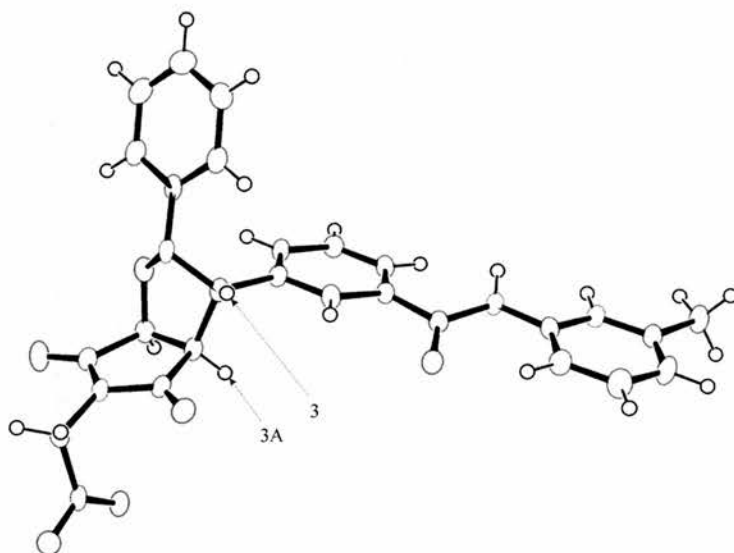
improvement could be down to steric factors. The addition of the bulky *tert*-butyl group slightly hinders the bimolecular reaction (*c.f.* $1.45 \times 10^{-4} \text{ M}^{-1}\text{s}^{-1}$ for the 4-nitrone **113** bimolecular control reaction with maleimide ester **79** and $1.36 \times 10^{-4} \text{ M}^{-1}\text{s}^{-1}$ for the 4-*tert*-butyl nitrone **117** bimolecular control reaction with maleimide ester **79**). The formation of the [77•117•151] complex may reduce the effect of the steric hindrance by moving the bulky substituents away from the reacting centres and so again leading to preference for the autocatalytic pathway.

The other two systems, which show a large increase between the bimolecular control reaction and the doped recognition-mediated reaction, are the 4-bromo nitrone and 4-nitrone systems which showed 26% and 25% increase respectively in their diastereoisomeric excess. Again, it is shown that these systems can act as asymmetric autocatalysts. This is not necessarily what would have been expected as the data obtained from the 3-nitrone systems infers that they act as better autocatalytic self-replicators, however if the experimental data is re-examined it is apparent that the data for the minor isomers for the 3-nitrone and 3-bromo nitrone series, appears to be slightly affected by the recognition control reactions, but not significantly by the doping reaction. This suggests that the minor isomer could be formed *via* an alternative recognition-mediated pathway, which means its formation could occur (although very inefficiently), through the AB-mediated pathway, or possibly through cross catalysis. Whereas the minor isomer in the 4-nitrone series is only formed through the uncatalysed bimolecular control reaction, and hence the production of major isomer through a catalysed channel leads to a greater d.e.

3.19 X-ray crystal structures of the cycloadducts **105** and **148**

Single crystals of templates *trans*-**105** and *trans*-**148**, suitable for analysis by X-ray diffraction were grown by vapour diffusion of hexane into solutions of *trans*-**105** and *trans*-**148** in chloroform at ambient temperature. Both templates *trans*-**105** (Figure 3.34 (a)) (Table 6.5) and *trans*-**148** (Figure 3.34 (b)) (Table 6.6) crystallise in the $P_2(1)/c$ space group and exhibit a monoclinic crystal systems.

a)



b)

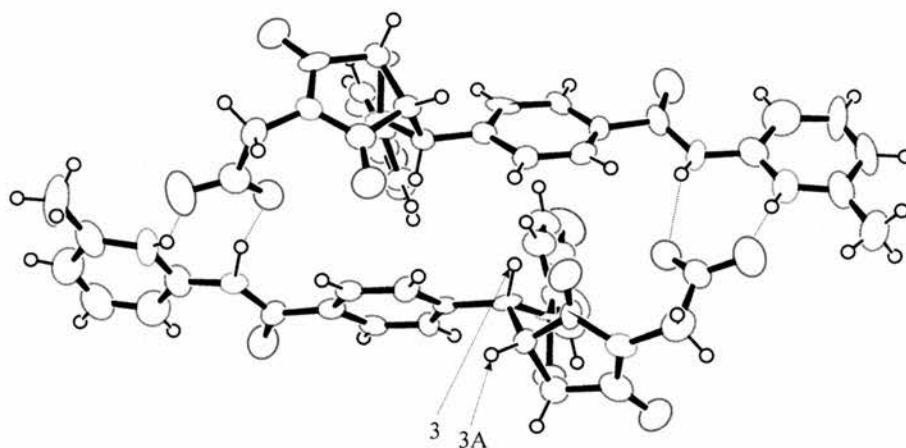


Figure 3.34 Single crystal X-ray structure obtained for templates (a) *trans*-105 and (b) *trans*-148.

The solid-state structures serve to confirm the relative stereochemistry of the major *trans*-isoxazolidine products. In the isolated molecule the protons on the heterocyclic ring in positions 3 and 3a are located on opposite faces of the heterocyclic ring system, confirming the major isomer to be the *trans* product. Examination of the packing of the templates is instructive with regard to the stability of the product duplex. *Trans*-148 crystallises as a dimer and *trans*-105 crystallises (Figure 3.34 (c)) in a layered structure with the cycloadducts forming infinite hydrogen bonded tapes. This infers that the product duplex for the *trans*-148 (and the 4-nitrone series) is quite stable and hence autocatalysis is not as efficient as it could be, whereas the monomeric state of *trans*-105 suggest that the product duplex is unstable and does not retain its binding, hence autocatalysis is efficient. This observation is an excellent result and helps to confirm the difference in the ρ and ϵ values for the 3- and 4-nitrone series.

3.20 Conclusion

It can be concluded from the evidence obtained that the prediction of an autocatalytic self-replicating system is not particularly straightforward or easy.

To try to summarise this chapter so far, the operation of an autocatalytic self-replicating system will be broken down into its components parts:

- a) The recognition unit.
- b) The reactive sites.
- c) The spacer units.

Firstly, the only recognition unit used within this thesis has been between an amidopyridine and carboxylic acid. This recognition motif has worked well in providing a suitable binding site. Much research has gone into suitable recognition sites and this unit appears to be the most successful to date. It must be remembered that the binding within the recognition unit must be strong enough to hold the ternary complex together to enable the reactive sites to come into close proximity in order to react, whilst being weak enough to dissociate and release the product duplex. The strength of the binding site is not however a single factor which can determine the success or failure of a self-replicating system. Its overall effect upon a system is one of many contributing factors, which will be explained subsequently.

The reactive sites are also very important in the operation of an autocatalytic self-replicating system however, like the recognition units they are not a single determining factor in the success or failure of a self-replicating system, but do contribute significantly to the overall success. This statement can be rationalised by examining the systems presented in **Table 3.1**. The reactions of the systems shown in **(c)**, **(d)** and **(e)** are all between furans and a maleimide **77**, however two of the systems proceed through an AB-mediated pathway and the other one is formed *via* a self-replicating pathway. Hence the same reaction is occurring but the pathways are different. Another example is system **(a)** in **Table 3.1**, if this is compared to the system presented in **Chapter 2, Scheme 2.3**, both utilise the reaction between an azide and a maleimide however one self-replicates and the other follows an AB-mediated pathway. Although this infers that the reactive sites in a system are unimportant in determining the pathway a system takes, this is not true. The effect the reactive sites have is subtler and is concerned with the co-conformation formed by the building blocks in order for the reaction to occur (**Figure 3.35**).

The third part of a self-replicating system, the spacer unit, appears to play quite a dominant but not individual role in the success of a self-replicating system. This is because it appears that the most important factor in determining whether a system can self-replicate is the co-

conformation of the building blocks, and hence, the spacer unit plays an important role in determining this shape. This is why the reactive sites also play a role in the effectiveness of the system due to the orientation and flexibility of the reactive sites. The key feature of a self-replicating system is ensuring that the system cannot proceed through the AB-mediated reaction channel.

To explain what is meant by the effect of the spacer unit and the orientational effects of the reactive sites it is most instructive to examine the situation pictorially.

Initially the effect of the spacer unit will be examined, as mentioned previously, the two systems **(a)** and **(b)** shown in **Figure 3.35** are the same except for their spacer units of the dipoles, one is benzyl while the other is alkyl. The recognition sites are shown in green, the spacer units in blue and the reactive sites are shown in red. The diagrams below the systems are used to try to demonstrate how the co-conformation bring the reactive sites together (although this is only a very crude representation) with the same colour coding as before.

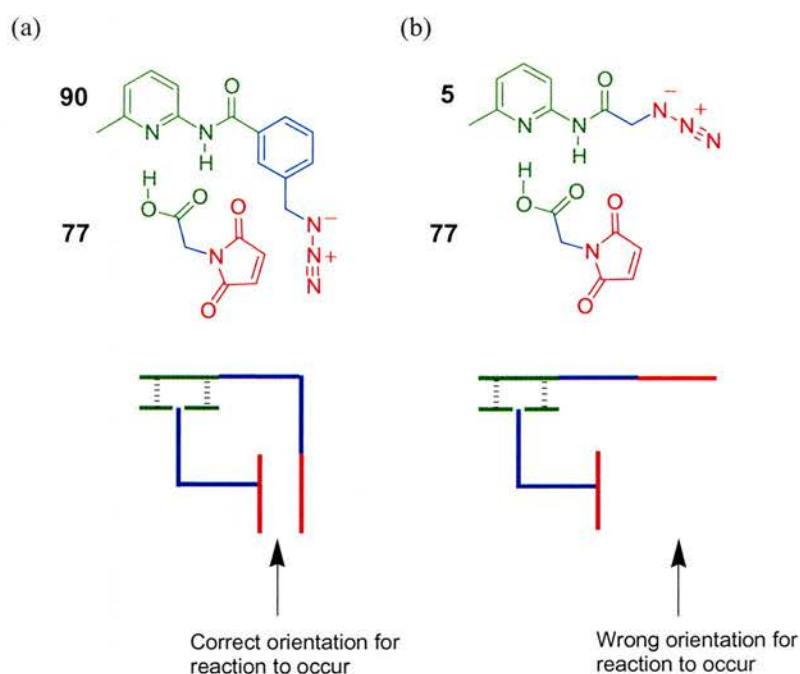


Figure 3.35 Diagram to show the difference in coconformation between (a) an AB-complex pathway and (b) a self-replicating pathway. The recognition sites are shown in green, the spacer units are in blue and the reactive sites are in red.

By examining the co-conformation of the two systems, it is apparent that the system in **(a)** places the reactive sites in the correct orientation for the reaction to occur, whereas the co-conformation in **(b)** places the reactive sites in the wrong orientation for the reaction to occur. This means that system **(a)** can react *via* an AB-complex pathway, which is the observed pathway for this system, and system **(b)** cannot react *via* the AB-complex pathway. This then prevents system **(b)** from reacting *via* the AB-complex pathway and so the building blocks

may then assemble with template to form a ternary complex, which is the observed pathway for this system (**Chapter 2**).

As mentioned previously the spacer unit is a major factor in the success of a self-replicating system but not the only factor, the orientation of the reactive site, also determines the success of the system, **Figure 3.36** demonstrates this effect. The spacer units within these systems **(a)** and **(b)** are identical whereas the reacting centres are not. Examination of the schematic coconformations reveals that the reactive sites in **(a)** are correctly aligned for the reaction to occur and so this system may proceed through an AB-complex pathway, which is the experimentally determined pathway for this system. However, the reactive sites in **(b)** are not correctly aligned for reaction to occur and hence prevent this system from reacting *via* the AB-complex pathway, which again is the experimentally determined result for the system.

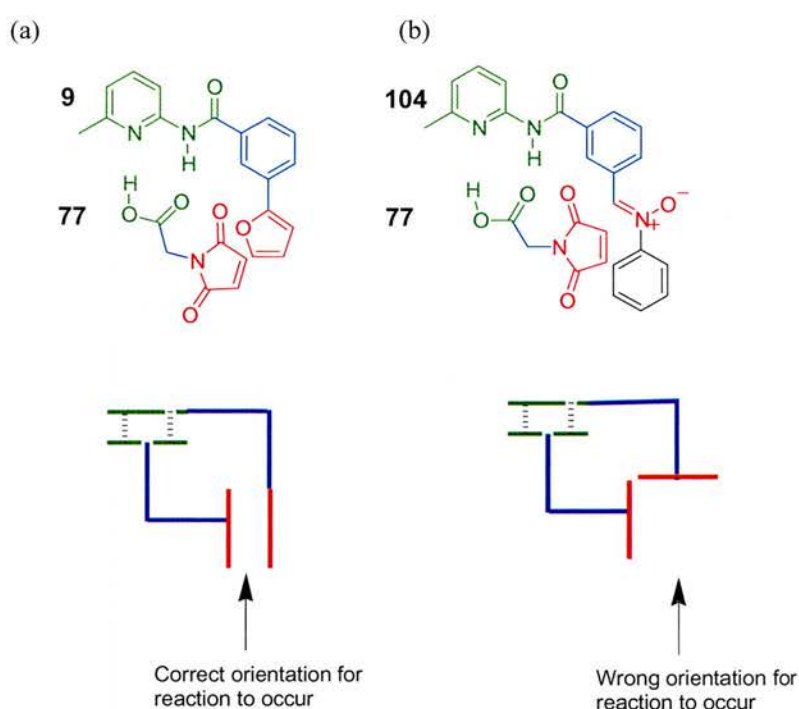


Figure 3.36 Diagram to show the difference in coconformation between (a) an AB-complex pathway and (b) a self-replicating pathway. The recognition sites are shown in green, the spacer units are in blue and the reactive sites are in red.

It has been demonstrated that the analogues based upon the system outlined in **Scheme 3.13** presented in this chapter all possessed the ability to autocatalytically self-replicate. However, the evidence collated for the 3- and 4-nitrone series seemed to be conflicting. The 3-nitrone systems had better p and ϵ values, but their percentage completion and the stereoselectivity of the systems were worse than the percentage completion and stereoselectivity of the 4-nitrone systems. Although the 4-nitrone systems generally had lower p and ϵ values, which implies that, these systems are less efficient self-replicators than their 3 counterparts.

These findings can be rationalised by looking at the minimal model for self-replication (**Figure 3.37**)

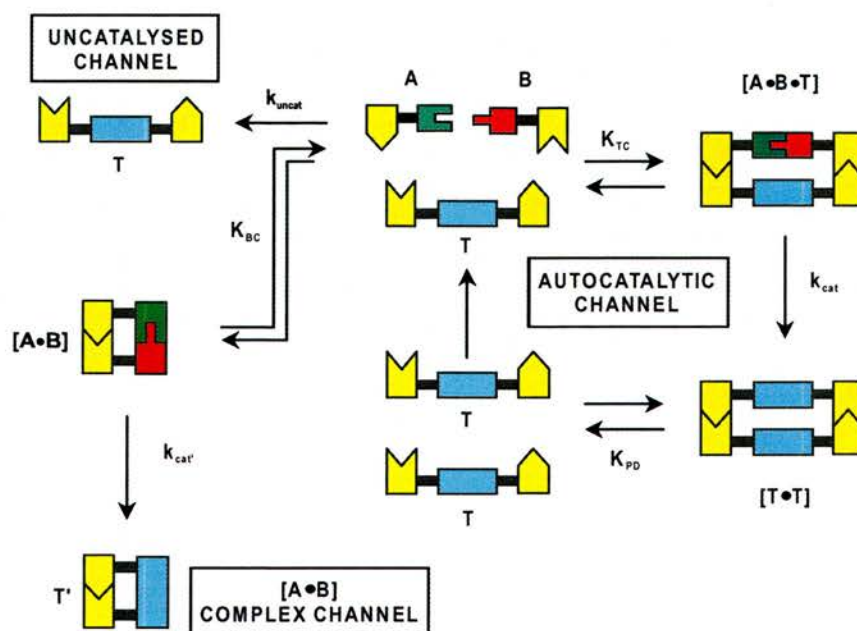


Figure 3.37 Schematic representation of the minimal model for self-replication.

It has been demonstrated that both the 3- and 4-nitron systems can react *via* the autocatalytic channel as shown in **Figure 3.37**. The 4-nitron systems are generally faster and more stereospecific than their 3-nitron counterparts, this indicates that the formation of the ternary complex, **[A.B.T]** then reaction to form the product duplex **[T.T]** is faster and more efficient for the 4-nitrones than the 3-nitrones. This infers that the 4-nitrones are better self-replicators than the 3-nitrones. The enhanced rate of formation of the ternary complex for the 4-nitrones could be due to a “better fit” for the building blocks within ternary complex. However, this “better fit” then becomes the downfall of the 4-nitrones, because the shape complementarity means that the product duplex is more stable for the 4-nitron systems than the 3-nitrones. Hence the product duplex of the 3-nitron systems, due to their poorer fit, dissociate much more rapidly than the 4-nitrones and, hence, achieve better turnover of the autocatalytic cycle. This explains why the p and ϵ values are generally higher for the 3-nitron systems. In summary the 4-nitrones are better replicators whereas the 3-nitrones are more efficient autocatalysts. The design of a self-replicating system would ideally have a system, which maximises both the self-replicating and autocatalytic nature of a system however the two properties must be traded off against each other in order to obtain the most efficient system.

3.21 Can the pathway of a recognition-mediated system be changed?

It has been observed that slight modifications to the regiochemistry and steric constraints of the self-replicating system under investigation has not significantly affected the self-replicating ability of the system, so this poses the question can the self-replication be disrupted or destroyed? For this it was decided to look at the spacer units within the system.

3.21.1 The effect of oligomethylene chain length on a self-replicating system

In the original study¹⁹⁷ the effect of chain length within the maleimide building block was investigated. The maleimides used are shown in **Figure 3.38**.

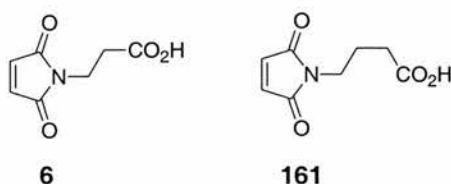
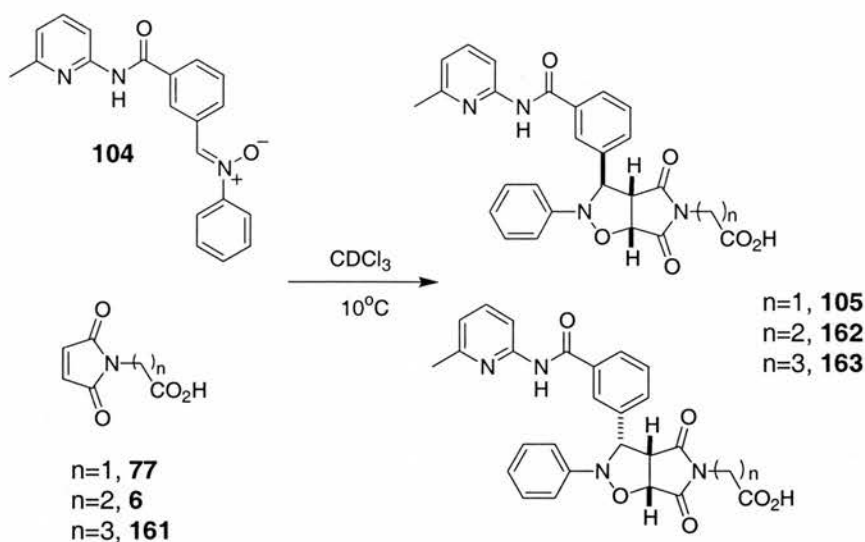


Figure 3.38 The proposed new maleimide building blocks **6** and **161**.

The addition of extra rotors into the system meant that in order for the ternary complex to assemble there must be a further degree of pre-organisation. This extra pre-organisation comes in the form of an entropic cost, which is approximately 15 entropy units for each additional rotor. It would be reasonable to assume that unless the reactivity of the autocatalytic cycle is significantly improved through a better fit for the ternary complex then addition of rotors should decrease the efficiency of the system. To test the theory the maleimide **6** and **161** were synthesised.

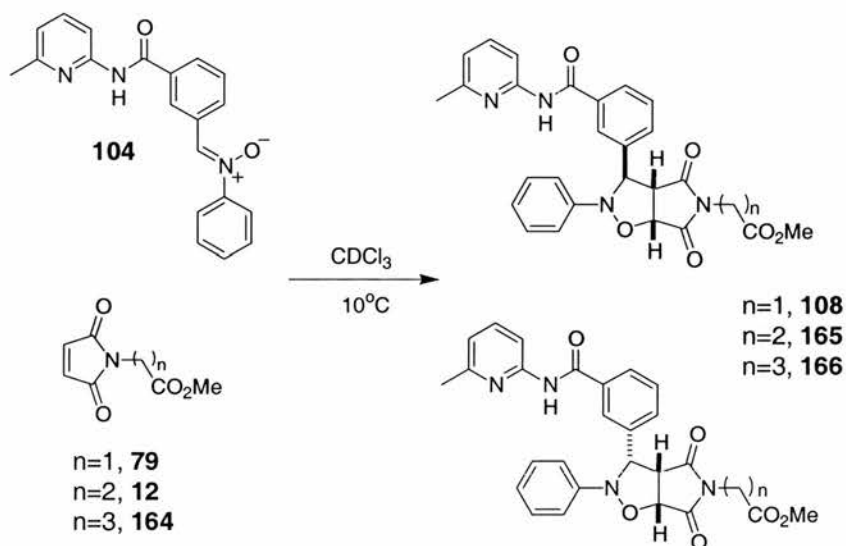
3.22 The kinetic experiments

The kinetic analysis was performed in the same manner as previously at concentrations of 25 mM in CDCl₃ with respect to all starting materials and a temperature of 10°C (**Scheme 3.41**).



Scheme 3.41 The recognition-mediated reactions between nitroene **104** and maleimides **77**, **6** and **161**.

The control reactions for the recognition-mediated reactions were also performed under identical conditions (**Scheme 3.42**).



Scheme 3.42 The control reactions between nitroene **104** and maleimide esters **79**, **12** and **164**.

The results of the recognition-mediated reactions and the corresponding control reactions are presented in **Figure 3.39**.

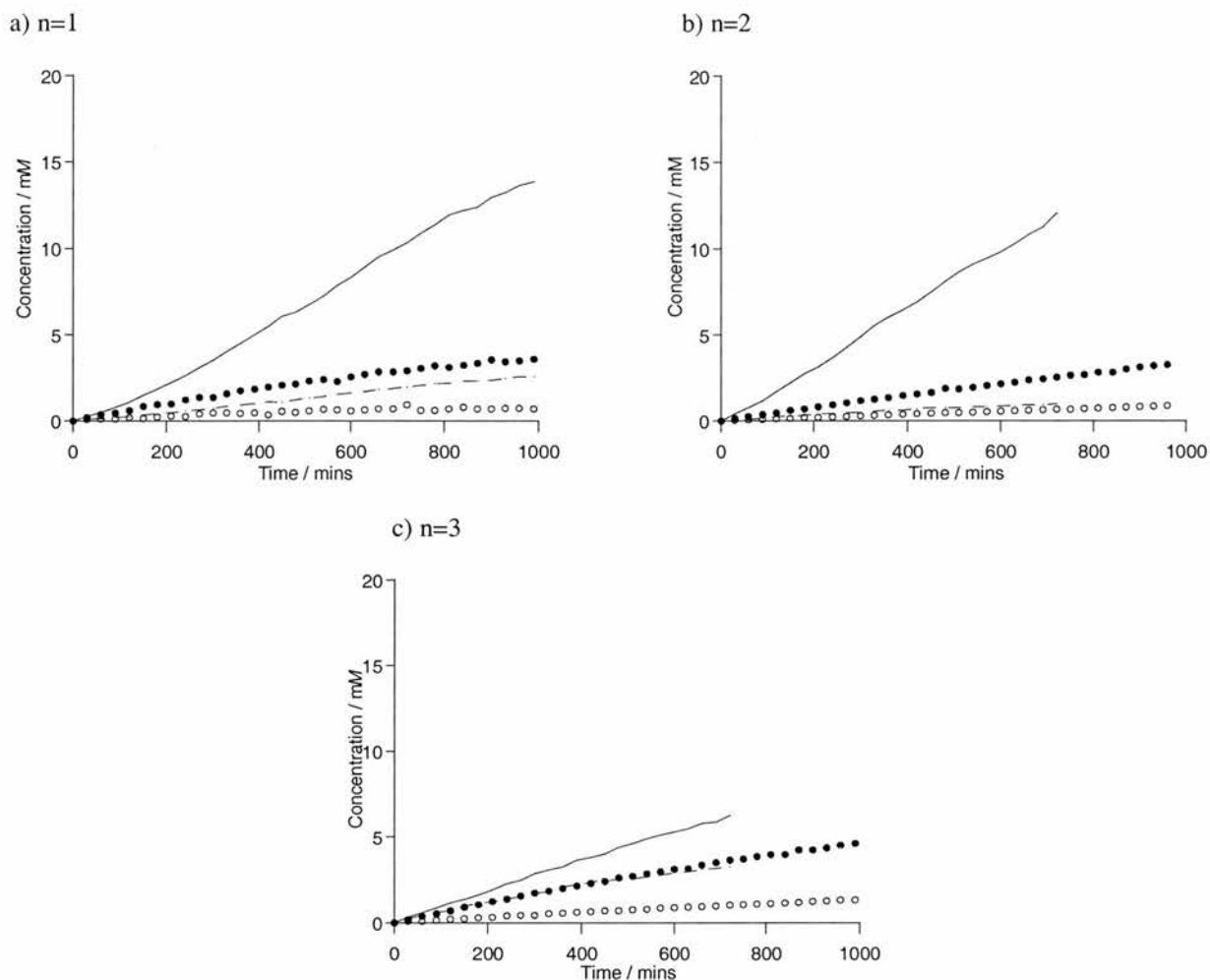


Figure 3.39 The rate profiles for the reactions performed between nitrone **104** and the maleimides with increasing chain length, all reactions were performed at concentrations of 25 mM in CDCl_3 with respect to the building blocks at 10°C . a) Shows the original recognition-mediated reaction between nitrone **104** and maleimide **77** and the bimolecular control reaction between nitrone **104** and maleimide ester **79** b) shows the reaction between nitrone **104** and maleimide **6** and the bimolecular control reaction between nitrone **104** and maleimide ester **12** and c) shows the reaction between nitrone **104** and maleimide **161** and the bimolecular control reaction between nitrone **104** and maleimide ester **164**. In all cases the recognition-mediated reaction results are shown as straight lines for the *trans*-isoxazolidine and as dashed lines for the *cis*-isoxazolidine, and the bimolecular control reaction results are shown as solid circles for the *trans*-isoxazolidine and as open circles for the *cis*-isoxazolidine.

Figure 3.39 compares the experimental data for all three maleimides used ($n = 1, 2$ and 3). Graph (a) shows the data for the reaction between nitrone **104** and the shortest chain maleimide ($n = 1$) **77** and maleimide ester ($n = 1$) **79**. The rate profile displays a sigmoidal shape, it has been demonstrated that this system reacts *via* an autocatalytic self-replicating pathway (**Section 3.5.2**). Graph (b) shows the data for the reaction between nitrone **104** and maleimides **6** and **12** where $n = 2$. On inspection of this data, it can be observed that a sigmoidal rate profile is obtained for the major *trans*-isoxazolidine. The minor *cis*-isoxazolidine does not appear to display any sigmoidal character. In this reaction the rate of formation of the cycloadduct **162** is slightly faster than in the original experiment between

nitron **104** and maleimide **77**. At 700 minutes the reaction between nitron **104** and maleimide **6** is 54% complete compared to 50% for the original reaction between nitron **104** and maleimide **77**. The control reaction (circles) shows a reduced rate for both isomers and the profiles indicate that the reaction is purely bimolecular. The data reveals that the major *trans*-isoxazolidine is clearly enhanced *via* the recognition-mediated reaction compared to the control reaction. The sigmoidal shape of the curve is indicative of an autocatalytic self-replicating pathway. The rate of formation of the *cis*-isoxazolidine does not differ significantly from the control reaction, indicating that its formation is *via* the bimolecular reaction. It was concluded that the formation of the major *trans*-isomer was through a self-replicating pathway whereas the formation of the *cis*-isomer was *via* the uncatalysed bimolecular pathway. Also, it was noted that cross catalysis did not occur, as this behaviour would have led to an increase in the formation of the *cis*-isomer in the recognition-mediated reaction. The *trans*-isomer acted as a faithful replicator.

Graph (c) shows completely different behaviour to that observed for the other two systems. In this reaction, maleimide **161** and maleimide ester **164** are used where $n = 3$. The reactions were performed under identical conditions as before. The experimental data for the recognition-mediated reaction (straight lines) shows that no sigmoidal character is observed. In this reaction the rate of formation is much slower than in the other two systems, at 700 minutes the reaction is 36% complete. The control reaction (circles) shows a rate profile indicative of a bimolecular reaction. It is clear from the data that the reaction between nitron **104** and maleimide **161** is recognition-mediated when compared to its control reaction. Although no sigmoidal character is observed there is still a rate enhancement observed for this reaction, which occurs at the beginning of the reaction. It was assumed that the rate of reaction was enhanced *via* the formation of an AB-type complex. Molecular modelling of the system revealed that nitron **104** and maleimide **161** could associate *via* the complementary hydrogen bonding, and due to the increase in spacer length upon complex formation the reactive sites could be held in a suitable orientation to facilitate the reaction. Enhancement for both isomers is observed, which suggests that the bimolecular complex is reasonably flexible and so allows the maleimide **161** to orient itself both *exo* and *endo* with respect to the nitron **104** when approaching the transition state. It was also noted that the recognition-mediated reaction gave a product ratio of 3:2, however over the same time period the control reaction gave a product ratio of 4:1. This result shows that the formation of the *cis*-isoxazolidine is being enhanced more than the formation of the *trans*-isoxazolidine. This was reasoned to be an effect of strain within the binary complex.

3.23 The effect of oligomethylene chain length on nitrone systems 109 and 113

In order to assess if this effect of increasing the oligomethylene chain length was common among the other self-replicating systems it was decided to look at the effect increasing the spacer unit would have upon the other nitrone systems and for this the nitrones shown in **Figure 3.40** were chosen.

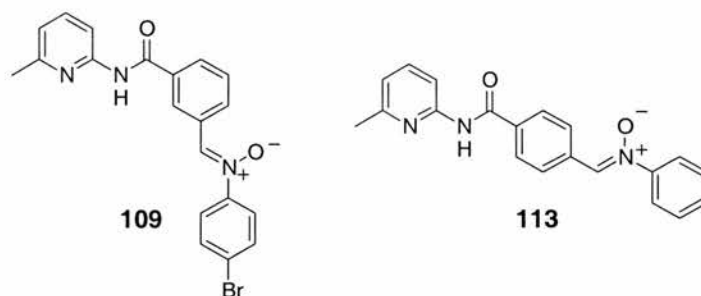


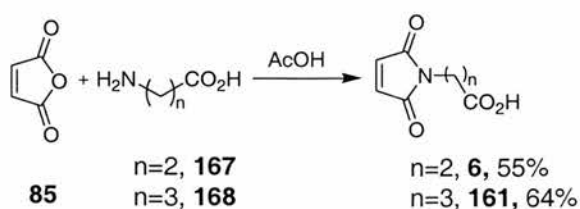
Figure 3.40 Nitrones used to examine the effect of increasing oligomethylene chain length.

It was decided to look at the 3-bromo nitrone **109** and 4-nitro nitrone **113** systems to observe whether the same trend would be observed for these systems as was observed for the original system. These two were chosen as the 3-bromo is part of the same series so will provide a close comparison of the same family and the 4-nitro was chosen to assess the effects upon the regioisomer.

3.24 Synthesis

3.24.1 Synthesis of maleimides **6** and **161**

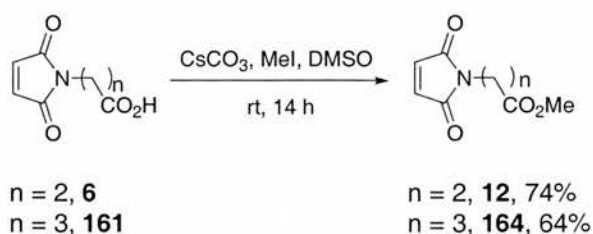
Maleimides **6** and **161** were synthesised in an analogous manner to maleimide **77**, which is described in **Section 3.8.1 (Scheme 3.43)**.



Scheme 3.43 Reaction to form maleimide building blocks, **6** and **161**.

3.24.2 Synthesis of control dipolarophiles **12** and **164**

The control dipolarophiles **12** and **164** were prepared in an analogous manner to control dipolarophile **79** (Section 3.8.2) (Scheme 3.44).



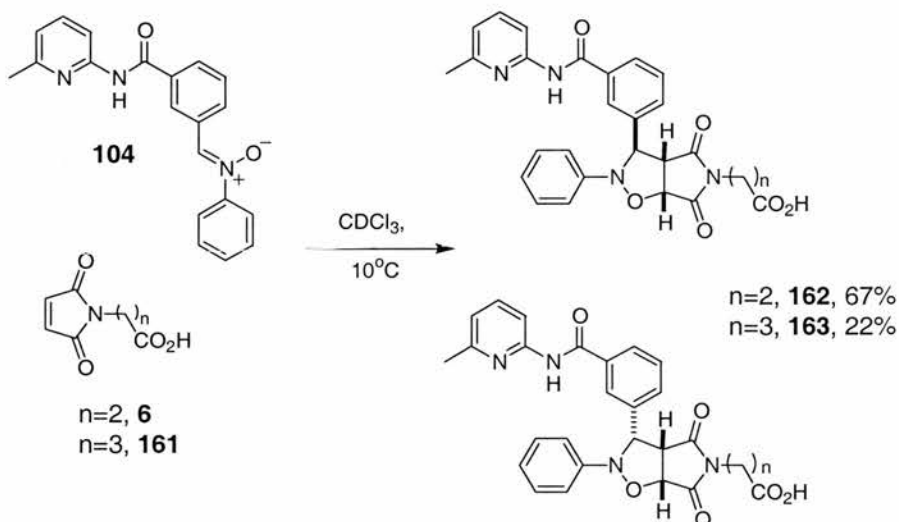
Scheme 3.44 The synthetic route used to prepare the control compounds **12** and **164**.

3.24.3 Synthesis of the nitrones **104**, **109** and **113**

For the synthetic preparation of the nitrones **104**, **109** and **113** see Section 3.8.4 see Section 3.8.8.

3.24.4 Synthesis of cycloadducts **162** and **163**.

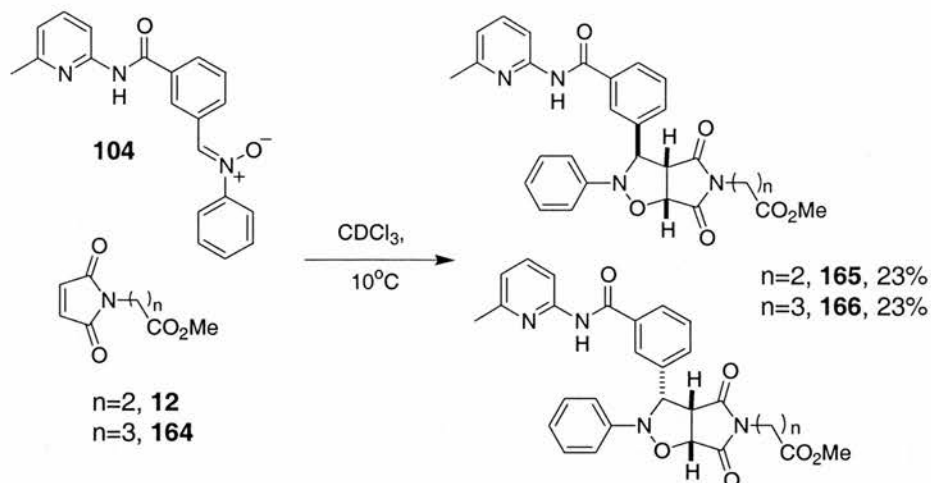
The cycloadducts **162** and **163** were prepared in an analogous manner to the cycloadduct **105** (Section 3.8.5) (Scheme 3.45).



Scheme 3.45 The synthetic route used to prepare cycloadducts **162** and **163**.

3.24.5 Synthesis of cycloadducts **165** and **166**.

The cycloadducts **165** and **166** were prepared in an analogous manner to the cycloadduct **105** (Section 3.8.5) (Scheme 3.46).



Scheme 3.46 The synthetic route used to prepare cycloadducts **165** and **166**.

3.24.6 Synthesis of cycloadducts **169**, **170**, **171**, **172**, **173**, **174**, **175** and **176**

The synthesis of these cycloadducts (**Figure 3.41**) was performed as described in **Section 3.8.5**.

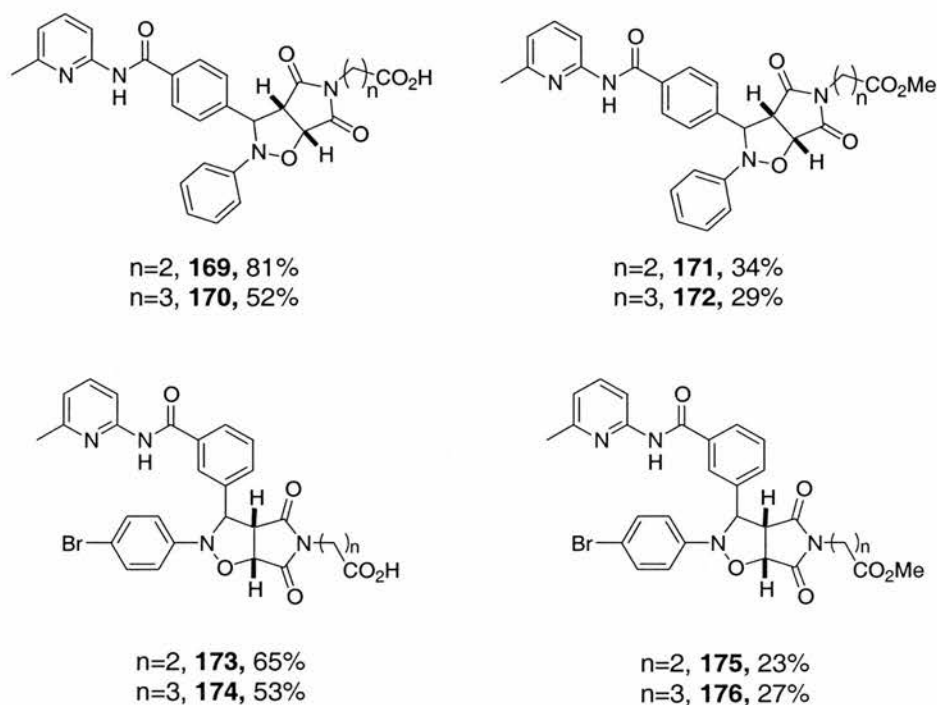
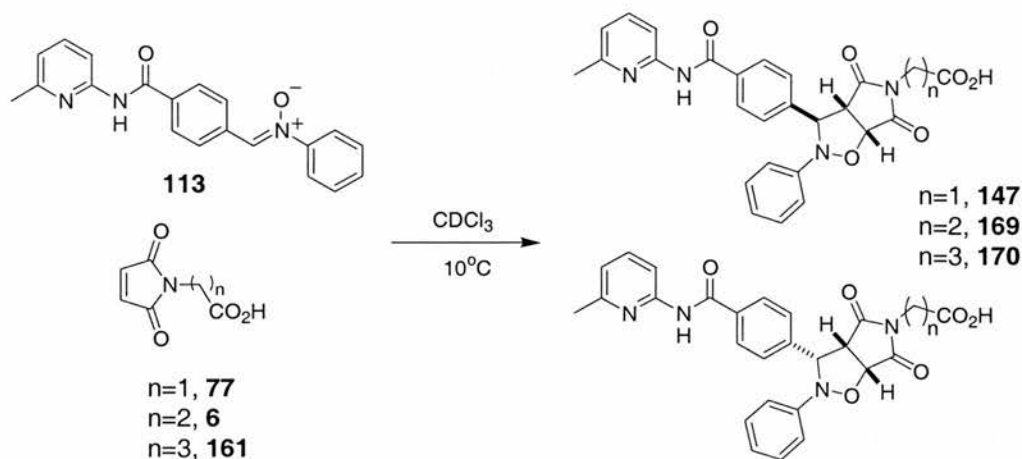


Figure 3.41 The cycloadducts prepared.

3.25 The effect of oligomethylene chain length upon the rate of the 4-nitrone system

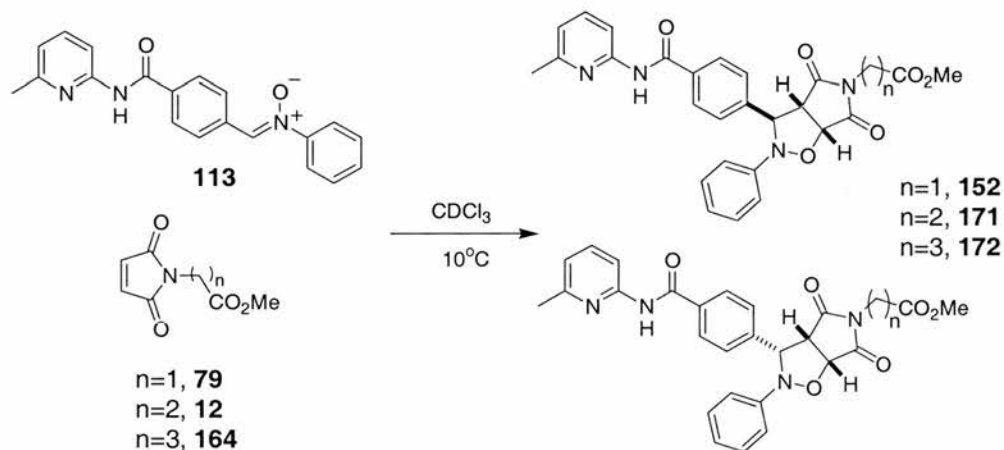
3.25.1 The kinetic experiments

The kinetic analysis was performed in the same manner as before at a concentration of 25 mM in CDCl₃ with respect to all building blocks at 10°C (Scheme 3.47).



Scheme 3.47 The recognition-mediated reaction between nitrone **113** and maleimides **77**, **6** and **161**. The reactions were performed at concentrations of 25 mM in CDCl₃ with respect to all building blocks at 10°C.

The control reactions were also performed under identical conditions (Scheme 3.48).



Scheme 3.48 The control reaction between nitrone **113** and maleimides **79**, **12** and **164**. The reactions were performed at concentrations of 25 mM in CDCl₃ with respect to all building blocks at 10°C.

The results are presented in Figure 3.42.

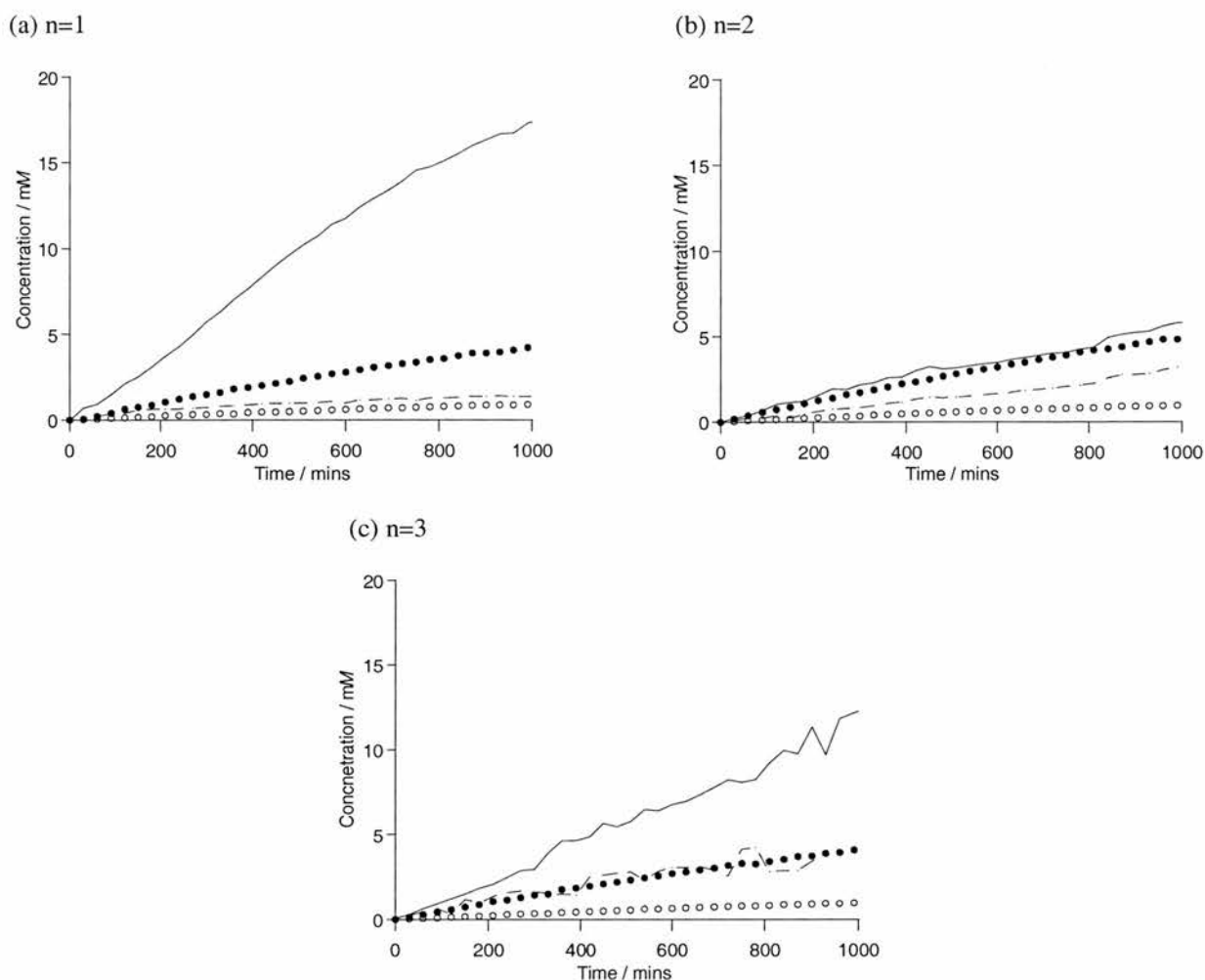


Figure 3.42 The rate profiles for the reactions performed between nitrone **113** and the maleimides with increasing chain length, all reactions were performed at concentrations of 25 mM in CDCl_3 with respect to the building blocks at 10°C . (a) Shows the original recognition-mediated reaction between nitrone **113** and maleimide **77** and the bimolecular control reaction between nitrone **113** and maleimide ester **79** (b) shows the reaction between nitrone **113** and maleimide **6** and the bimolecular control reaction between nitrone **113** and maleimide ester **12** and (c) shows the reaction between nitrone **113** and maleimide **161** and the bimolecular control reaction between nitrone **113** and maleimide ester **164**. In all cases the recognition-mediated reaction results are shown as straight lines for the *trans*-isoxazolidine and as dashed lines for the *cis*-isoxazolidine, and the bimolecular control reaction results are shown as closed circles for the *trans*-isoxazolidine and as open circles for the *cis*-isoxazolidine.

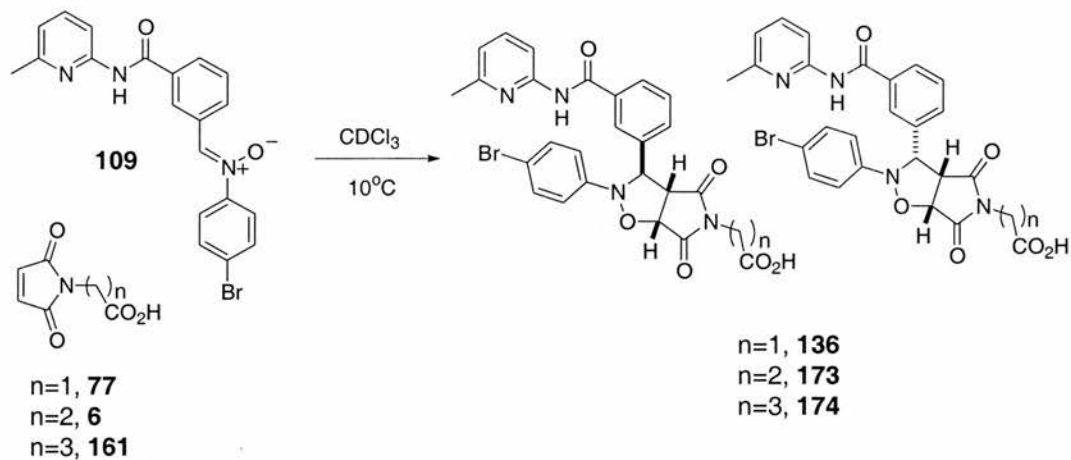
Examination of the data in **Figure 3.42** shows some interesting results and a different trend to that observed for the 3-nitron system. Graph (a) shows the original data for the reaction between nitrone **113** and maleimide **77** ($n = 1$) see **Section 3.13.1** for the full analysis. Graph (b) shows the reaction between nitrone **113** and maleimide **6** ($n = 2$), immediately it is obvious that the self-replicating behaviour has been removed and the rate of reaction has been significantly reduced compared to the original system where $n = 1$. When compared to the bimolecular control reaction (circles) it is evident that the formation of the major *trans*-isoxazolidine occurs at the same rate as the bimolecular reaction and hence no recognition-mediated pathway is being followed. However the formation of the *cis*-isoxazolidine does

show a rate enhancement compared to the bimolecular control reaction. Hence, its formation is *via* a recognition-mediated process. The rate profile does not show evidence of a sigmoidal shape, however this does not necessarily imply that the system is not capable of self-replication (**Chapter 2**), although it could also be following an AB-type pathway. Unfortunately due to insolubility problems, the template could not be used to perform a doping study on this system, which would reveal the mode of formation, the lack of solubility also prevented a suitable crystal being grown, which could have revealed the mode of formation. It is an interesting result however that the formation of the minor isoxazolidine is the only isomer enhanced within this system, which is the opposite effect of all the system examined so far. Examination of graph (c) reveals a similar trend to that observed for the 3-nitrone **113** system with maleimide **161**. It is evident that on comparison of the recognition-mediated reaction with the control reaction that the recognition is playing an important role within the system as the formation of both isomers is enhanced. Again no sigmoidal character is obtained within this system, but rate acceleration is observed from the beginning of the reaction. This situation implies that the system is reacting *via* an AB-complex. Hydrogen bonding between the two recognition sites could hold the reactive sites in a suitable orientation to facilitate the reaction. Again, as was observed in the 3-nitrone system both isomers are enhanced suggesting that the flexible maleimide can orient itself both *exo* and *endo* relative to the nitrone **113** when approaching the transition state. The recognition-mediated reaction gave a product ratio of approximately 7:3, and the control reaction ratio gave a product ratio of 8:2, which shows that the formation of the *cis*-isoxazolidine is being enhanced more than the formation of the *trans*-isoxazolidine.

3.26 The effect of oligomethylene chain length upon the rate of the 3-bromo nitrone systems

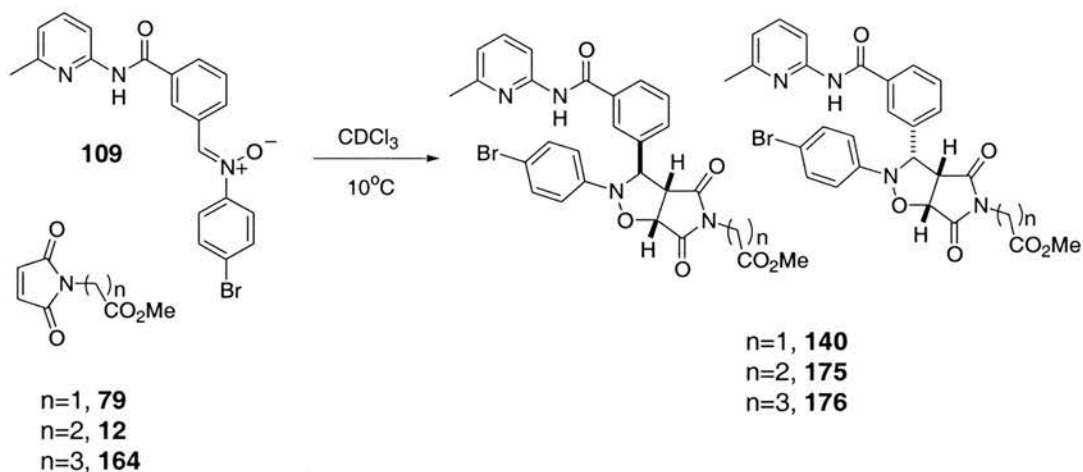
3.26.1 The kinetic experiments

The kinetic analysis was performed in the same manner as before at a concentration of 25 mM in CDCl₃ with respect to all building blocks at 10°C (**Scheme 3.49**).



Scheme 3.49 The recognition mediated reaction between nitron **109** and maleimides **77**, **6** and **161**. The reactions were performed at concentrations of 25 mM in CDCl_3 with respect to all building blocks at 10°C .

The control reactions were also performed under identical conditions (**Scheme 3.50**).



Scheme 3.50 The control reaction between nitron **109** and maleimides **79**, **12** and **164**. The reactions were performed at concentrations of 25 mM in CDCl_3 with respect to all building blocks at 10°C .

The results of the recognition-mediated reactions and the control reactions are presented in **Figure 3.43**.

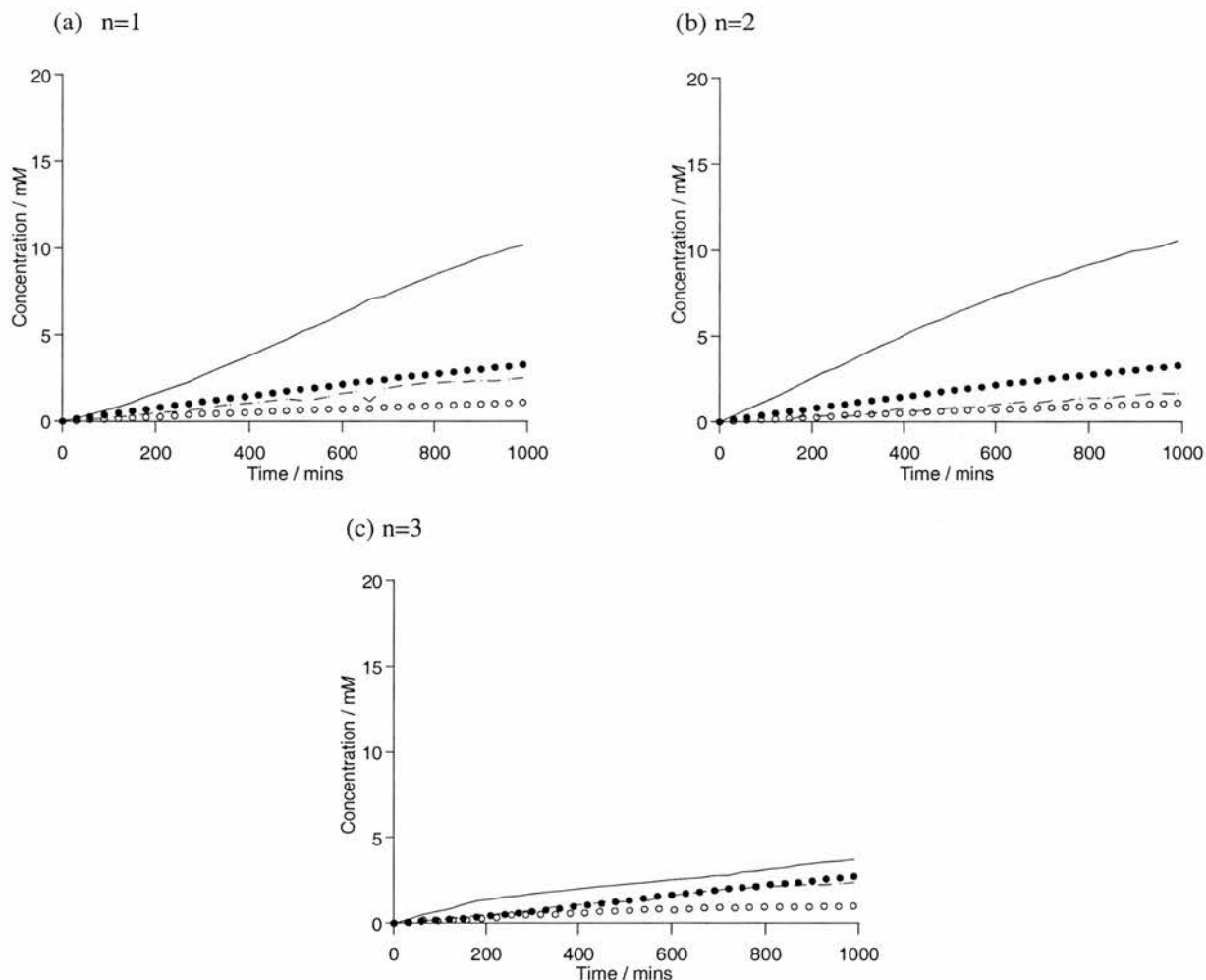


Figure 3.43 The rate profiles for the reactions performed between nitrone **109** and the maleimides with increasing chain length, all reactions were performed at concentrations of 25mM in CDCl_3 with respect to the building blocks at 10°C . (a) Shows the original recognition-mediated reaction between nitrone **109** and maleimide **77** and the bimolecular control reaction between nitrone **109** and maleimide ester **79** (b) shows the reaction between nitrone **109** and maleimide **6** and the bimolecular control reaction between nitrone **109** and maleimide ester **12** and (c) shows the reaction between nitrone **109** and maleimide **161** and the bimolecular control reaction between nitrone **109** and maleimide ester **164**. In all cases the recognition-mediated reaction results are shown as straight lines for the *trans*-isoxazolidine and dashed lines for the *cis*-isoxazolidine, and the bimolecular control reaction results are shown as a solid circles for the *trans*-isoxazolidine and a open circles for the *cis*-isoxazolidine.

Initial inspection of the data reveals that the 3-bromo nitrone **109** system and the varying length maleimides follow a similar trend to that observed by the 3-nitron **104** system. Graph (a) shows the original experiment between nitrone **109** and maleimide **77** where $n=1$. Graph (b) shows the data for the reactions between nitrone **109** and maleimides **6** and **12** ($n=2$). The data for the recognition-mediated reaction does not show a sigmoidal shape curve for the major *trans*-isomer, although a significant rate enhancement is observed its formation, which indicates that it is reacting *via* an AB-complex pathway.

Graph (c) shows that there is not a significant difference between the recognition-mediated and bimolecular control system. The slight increase in the rate of reaction for the recognition-

mediated reaction does not show a sigmoidal rate profile, which indicates that the reaction may proceed through the AB-complex pathway, but not very efficiently.

3.27 Conclusion

The results of this experiment reveal that the spacer unit with the self-replicating system is again very important, and that its effects between the 3- and 4-nitron systems are similar although not identical. Addition of one rotor in all the systems examined destroyed their self-replicating ability. In the 3-nitron systems, the reaction pathway changed to that of an AB-complex pathway, whereas in the 4-nitron system, recognition seemed to play no role in the reaction for the major *trans*-isomer and only a small amount for the *cis*-isomer.

Addition of two rotors converted all the reactions to AB-mediated reactions with varying degrees of enhancement. The most successful enhancement was that observed for the 4-nitron system, which could be attributed to the coconformation becoming favourable for reaction to occur. In the 3-nitron systems the recognition did not have such a large effect, which again could be attributed to the coconformation becoming more unfavourable than that observed in the system with one less rotor.

3.28 Temperature effects upon the efficiency of a self-replicating system

When the conditions for these nitron systems were first devised it was based upon the most suitable conditions for the 3-nitron **104** system, all analysis of subsequent systems have been performed at the same temperature to maintain consistency. It was then decided to investigate how temperature affected the ability of a self-replicating system to replicate; would an increase or decrease in temperature improve or destroy the self-replicating ability of the systems. The use of 10°C may not be the ideal temperature for all system. Due to the sheer number of systems possible it was decided to concentrate on the nitrones presented in **Figure 3.44**.

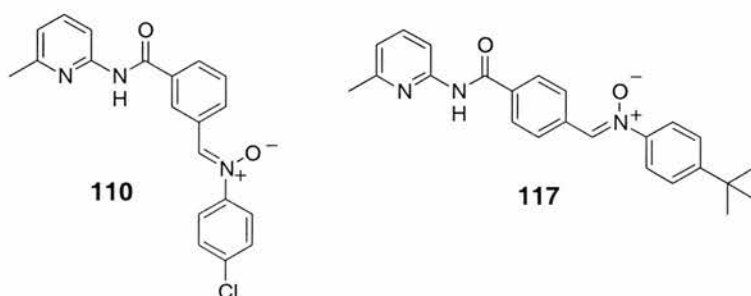


Figure 3.44 Nitrones used to observe the effect that varying the temperature of the reaction has upon the rate and efficiency of the self-replicating systems.

3.29 Synthesis of nitrones **110** and **117**

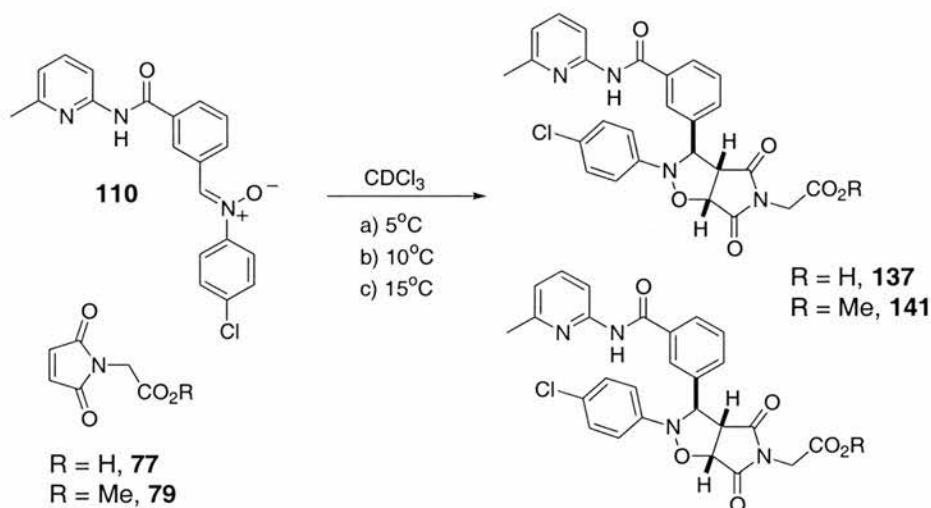
For the synthetic procedures used to prepare the nitrones **110** and **117** and all the corresponding cycloadducts see **Section 3.8.4** and **Section 3.8.8**.

3.30 The kinetic experiments

The kinetic experiments were performed in exactly the same manner as previously at a concentration of 25 mM with respect to both building blocks. The experiments were performed at temperatures of 5 and 15°C. The ester control reactions were also performed at these temperatures to demonstrate the bimolecular mimic, and so enable the rate constants to be determined.

3.31 The effect of varying the temperature upon the 3-chloro nitrone system.

The kinetic experiments performed are shown in **Scheme 3.51**



Scheme 3.51 Kinetic experiments performed to demonstrate temperature effects upon the recognition mediated reaction between nitrone **110** and maleimide **77** (R = H) and the corresponding control reactions between nitrone **110** and maleimide ester **79** (R = Me).

The results of the recognition-mediated and bimolecular control kinetic experiments are shown below in **Figure 3.45**.

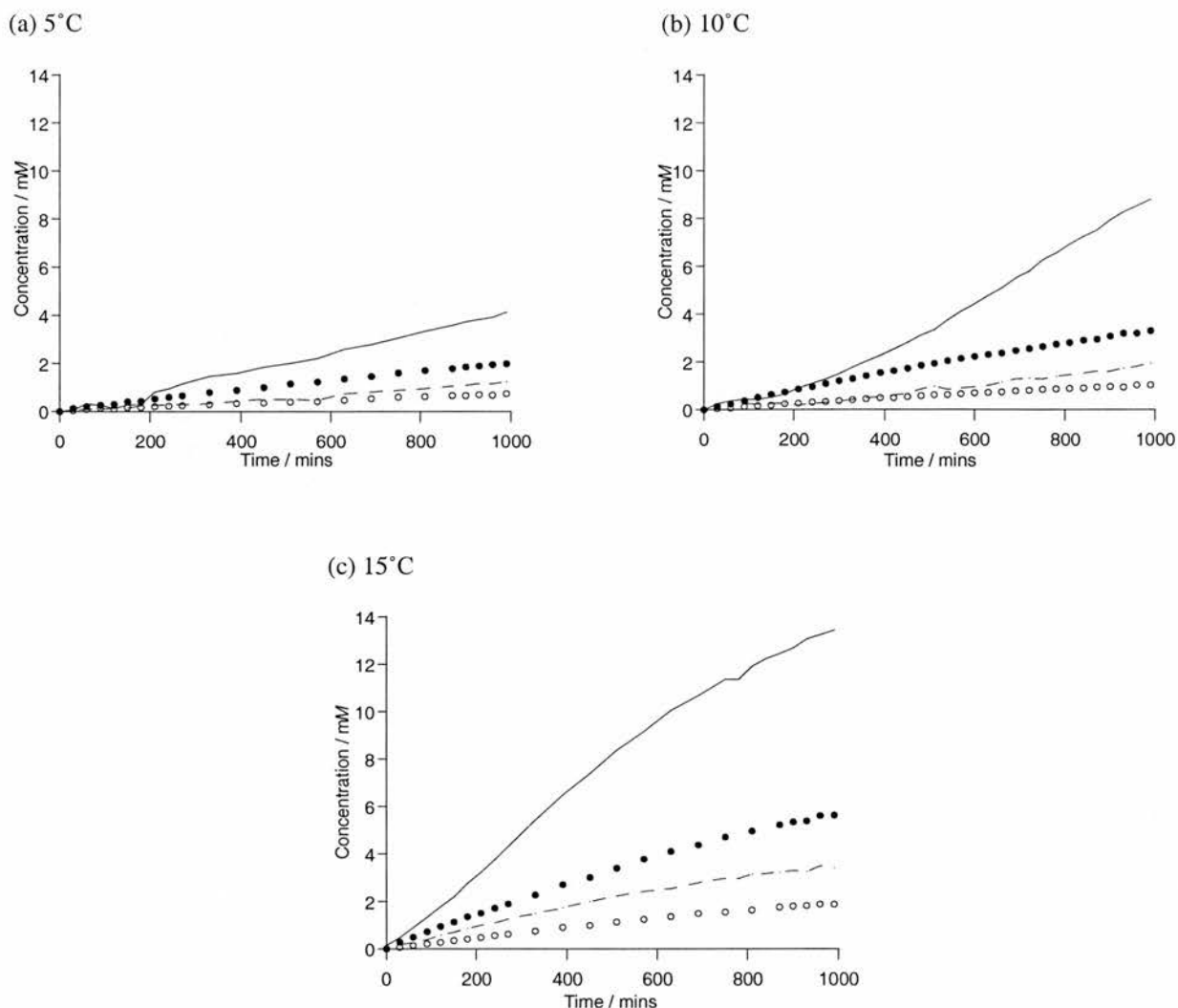
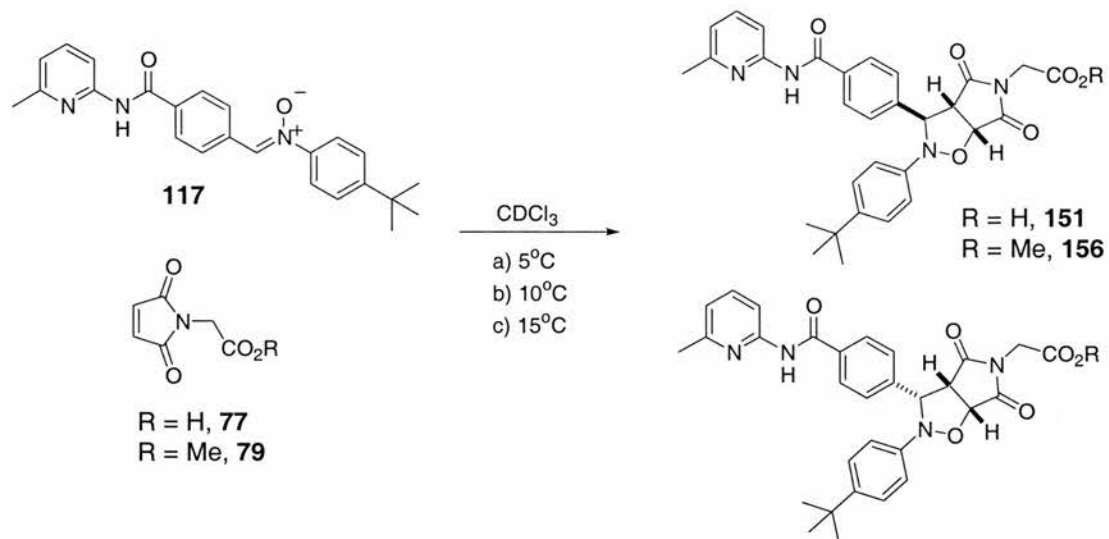


Figure 3.45 Rate profiles for the reaction between nitrone **110** and maleimide **77** (straight lines represent the *trans*-isoxazolidine and dashed lines represent the *cis*-isoxazolidine), and the control reaction between nitrone **110** and maleimide ester **79** (closed circles represent the *trans*-isoxazolidine and open circles represent the *cis*-isoxazolidine). The rate profiles shown are performed at (a) 5°C, (b) 10°C and (c) 15°C.

Inspection of the data shows that the rate of reaction increases upon increasing temperature as would be expected and the sigmoidal rate profile is retained by increasing and decreasing the temperature by 5°C.

3.32 The effect of varying the temperature upon the 4-*tert*-butyl nitrone

The same treatment was applied to the 4-*tert*-butyl nitrone system. The kinetic experiments performed are shown in **Scheme 3.52**, and the results of the recognition-mediated and bimolecular control reactions are shown in **Figure 3.46**



Scheme 3.52 Kinetic experiments performed to demonstrate temperature effects upon the recognition-mediated reaction between nitron **117** and maleimide **77** (R = H) and the corresponding control reactions between nitron **117** and maleimide ester **79** (R = Me).

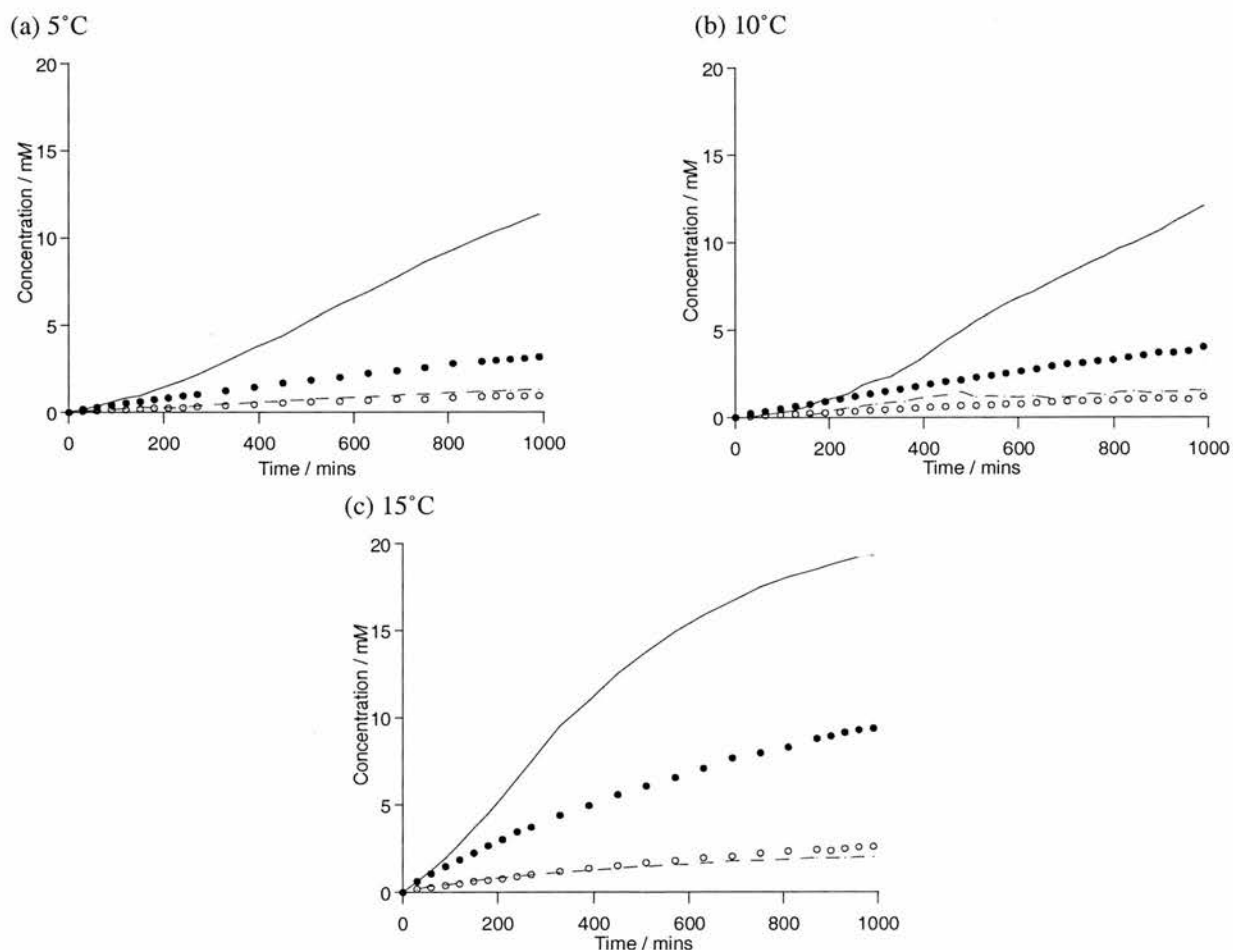


Figure 3.46 Rate profiles for the reaction between nitron **117** and maleimide **77** straight lines represent the *trans*-isoxazolidine and dashed lines represent the *cis*-isoxazolidine), and the control reaction between nitron **117** and maleimide ester **79** (closed circles represent the *trans*-isoxazolidine and open circles represent the *cis*-isoxazolidine). The rate profiles shown are performed at (a) 5°C, (b) 10°C and (c) 15°C.

Again it is, observed that increasing and decreasing the reaction temperature increases and decreases the overall rate of reaction respectively and the sigmoidal rate profiles are still

retained. However to make a fair comparison of this data the physical parameters must be extracted and it must be fitted to the kinetic model as before.

3.33 Percentage completion and diastereoisomer ratios

All the values determined will be calculated as the relative amounts at 1000 minutes reaction time.

3.33.1 3-Chloro nitrone

Initially the percentage completion and the d.e. values at 1000 minutes were calculated and tabulated (**Table 3.3**).

Table 3.3 The percentage completion values and d.e values for the nitrone **110** and maleimide **77** at 1000 minutes.

	Percentage completion at 1000 minutes	d.e. of bimolecular control reaction (+79)	d.e. of recognition-mediated reaction (+77)	Δ d.e.
5°C	22 %	46 %	54 %	8
10°C	43 %	53 %	64 %	11
15°C	67 %	50 %	59 %	9

The data reveals that the rate of reaction increases with increasing temperature, however the diastereoisomeric excess has its maximum at 10°C. These values were plotted on a double Y axis graph (**Figure 3.47**) to demonstrate the effect of temperature upon this system.

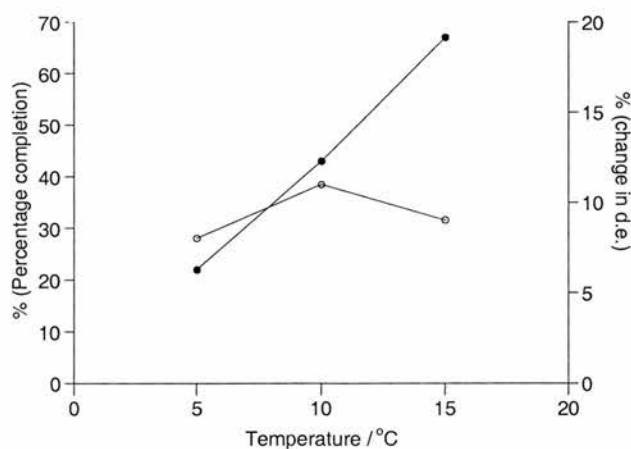


Figure 3.47 A plot to show the relative percentage completion values (closed circles) for the various temperatures for the reaction between nitrone **110** and maleimide **77** and change in d.e values (open circles) between the recognition-mediated reaction between nitrone **110** and maleimide **77** and the bimolecular control reaction between nitrone **110** and maleimide ester **79**.

3.33.2 Fitting the data to the kinetic model

See **Section 2.11** for the kinetic fitting equation. From the fitting the value of p is obtained and from the rate constants the values ϵ can be calculated (**Table 3.4**).

Table 3.4 The rate values obtained for the recognition-mediated reactions of the nitron **110** and maleimide **77** and the bimolecular control reactions between nitron **110** and maleimide **79**.

	k_1 110 + 79 $10^{-5} M^{-1} s^{-1}$	k_2 110 + 77 $10^{-2} s^{-1}$	p	ϵ
5°C	6.22	1.34	1	215
10°C	11.0	7.71	1	701
15°C	22.0	1.98	0.6	90

The values of p and ϵ confirm the statement above that the 3-chloro nitron self-replicating system is indeed operating most efficiently at 10°C. The data in **Table 3.3** is presented in **Figure 3.48**. It is immediately obvious from the graph that the efficiency of the 3-chloro system is at a maximum at 10°C.

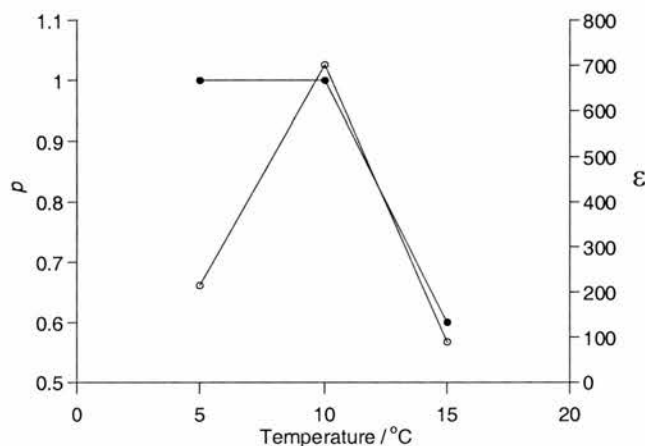


Figure 3.48 A plot to show the p (closed circles) and ϵ (open circles) values for the 3-chloro nitron system at the various temperatures.

3.33.3 4-*tert*-butyl nitron

The same extraction of data was performed for the 4-*tert*-butyl system and tabulated (**Table 3.5**).

Table 3.5 The percentage completion values and d.e values for the nitron **117** and maleimide **77** at 1000 minutes.

	Percentage completion at 1000 minutes.	d.e. of bimolecular control reaction (+79)	d.e. of recognition-mediated reaction (+77)	Δ d.e.
5°C	50 %	54 %	79 %	25
10°C	54 %	55 %	78 %	23
15°C	85 %	56 %	81 %	25

This data set shows that as the temperature is increased, the percentage completion increases as would be expected but this time the diastereoisomeric excess has a minimum at 10°C and maxima at 5 and 15°C.

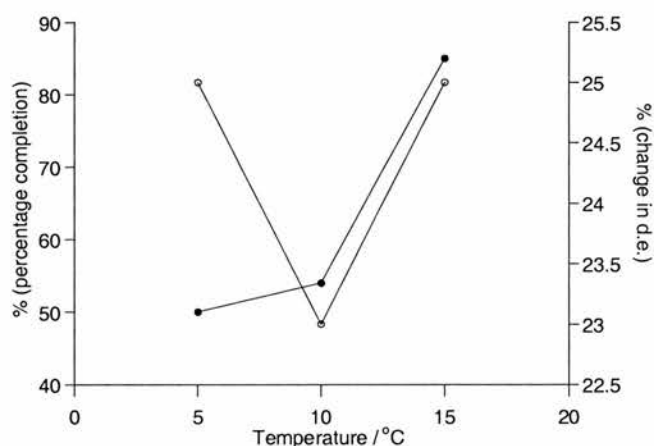


Figure 3.49 A plot to show the relative percentage completion values (closed circles) for the various temperatures for the reaction between nitron **117** and maleimide **77** and change in d.e values (open circles) between the recognition-mediated reaction between nitron **117** and maleimide **77** and the bimolecular control reaction between nitron **117** and maleimide ester **79**.

3.33.4 Fitting the data to the kinetic model

See **Section 2.11** for the kinetic fitting equation. From the fitting the value of p is obtained and from the rate constants the values ϵ can be calculated (**Table 3.6**).

Table 3.6 The rate values obtained for the recognition-mediated reactions of the nitrone **117** and maleimide **77** and the bimolecular control reactions between nitrone **117** and maleimide **79**. The calculated values of p and ϵ are also presented.

	k_1 117 + 79 $10^{-4} M^{-1}s^{-1}$	k_2 117 + 77 $10^{-2} s^{-1}$	p	ϵ
5°C	1.06	5.59	0.9	527
10°C	1.36	10.5	1	772
15°C	4.78	11.1	0.8	232

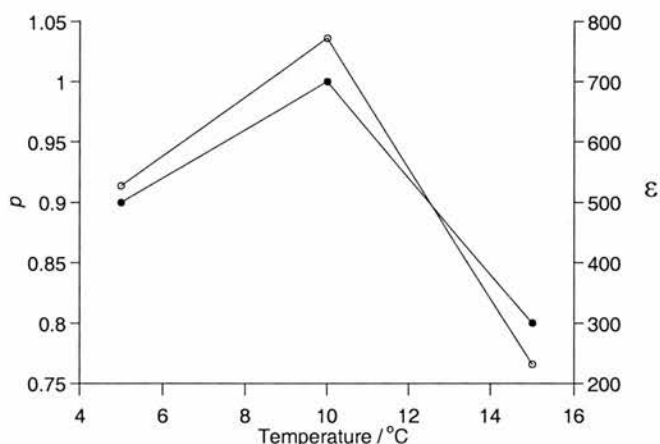


Figure 3.50 A plot to show the p (closed circles) and ϵ (open circles) values for the 3-chloro nitrone system at the various temperatures.

This data reveals that although at 10°C this system has its lowest d.e. values, it operates most efficiently at this temperature, with the highest p and ϵ values occurring at this temperature.

3.34 Conclusions

It can be concluded that the temperature a self-replicating system is performed at will have a significant effect on the performance and efficiency of the system. It has been shown from this work that the percentage completion of a reaction and the d.e. value of a system is not a measure of the efficiency or autocatalytic nature of the self-replicating system, as demonstrated by the 4-tert butyl nitrone system. The variable temperature experiments confirm however, that the optimum temperature for these systems is 10°C.

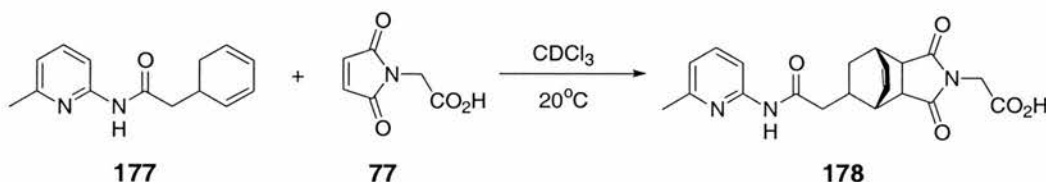
4. The Design and Synthesis of a New Self-Replicating System

4.1 Aspects of autocatalytic self-replicator design

The design of an autocatalytic self-replicating system was discussed in **Section 2.1, Chapter 2**. In **Chapter 3** it was attempted to provide a rationale for the type of system, which would self-replicate. The general conclusion from this work, was that the co-conformation of the ternary complex, essentially the “goodness of fit”, and inability to form a successful AB complex were important requirements for a system to act as a self-replicating system.

4.2 An example of a self-replicating system

In **Chapter 1, Section 1.8** a selection of self-replicating systems were discussed. However during the course of this project it came to our attention that work within the von Kiedrowski group¹⁹⁹ had produced a self-replicating system (**Scheme 4.1**) similar to the types of systems that were under investigation within the Philp group.



Scheme 4.1 The self-replicating system devised by von Kiedrowski *et al.*¹⁹⁹ between diene **177** and maleimide **77** to afford cycloadduct **178**. The reaction was performed at a concentration of 15 mM in CDCl_3 with respect to the building blocks at 20°C .

The kinetic data for the reaction shown in **Scheme 4.1** is presented in **Figure 4.1**, along with the results for the reaction that has been doped with 10 mol% template **178**.

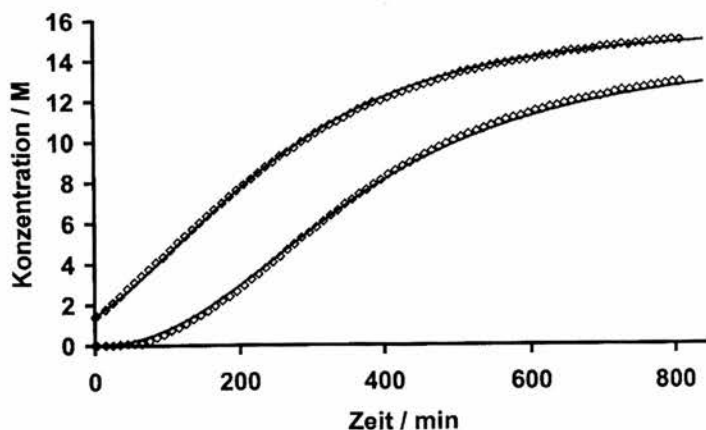
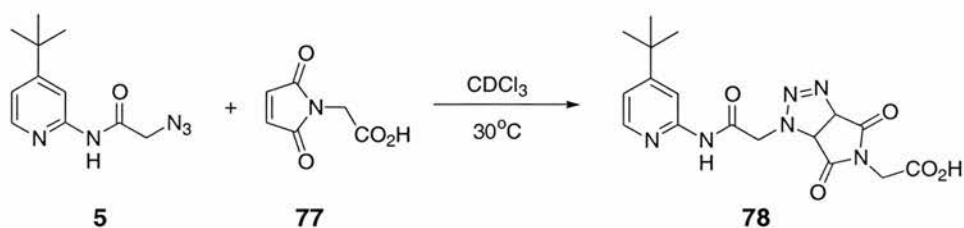


Figure 4.1 The kinetic data from the self-replicating system devised by von Kiedrowski *et al.* The bottom line represents the result from the undoped reaction between diene **177** and maleimide **77** and the top line represents the result from the doped reaction between diene **177**, maleimide **77** and 10 mol% **178**. Taken from ref. 199.

Inspection of the experimental data shown in **Figure 4.1** clearly shows a lag period (lower line), which indicates that an autocatalytic recognition-mediated reaction is in operation. The operation of an autocatalytic pathway is confirmed by the addition of 10 mol% preformed template, which removes the lag period from the graph (top line).

4.2.1 Comparison to compound 5

Chapter 2 discussed the self-replicating ability of the system outlined in **Scheme 4.2**, between azide **5** and maleimide **77**.

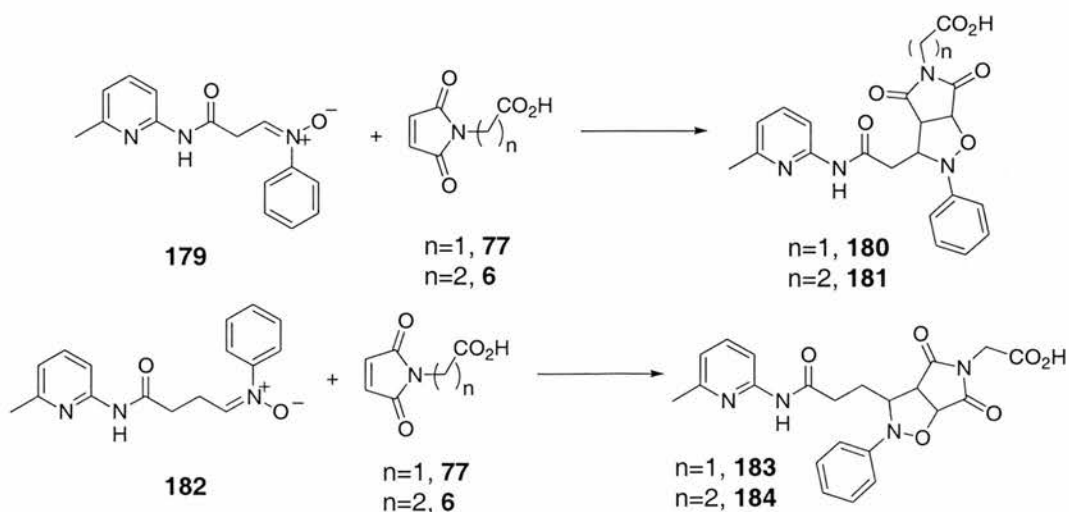


Scheme 4.2 The self-replicating system discussed in **Chapter 2** devised by Philp *et al.*¹⁷⁰.

Inspection of compound **5** reveals a similar type of structure to compound **177** used within the von Kiedrowski system. However one self-replicates very well and the other does so inefficiently, it would be useful to understand what differences make one system self-replicate and the other one not (see **Chapter 3**).

4.3 The design of a new system

Using the experience gained from the self-replicating systems developed within our group and the system presented by Kiedrowski, it was decided to investigate a new system shown in **Scheme 4.3**.



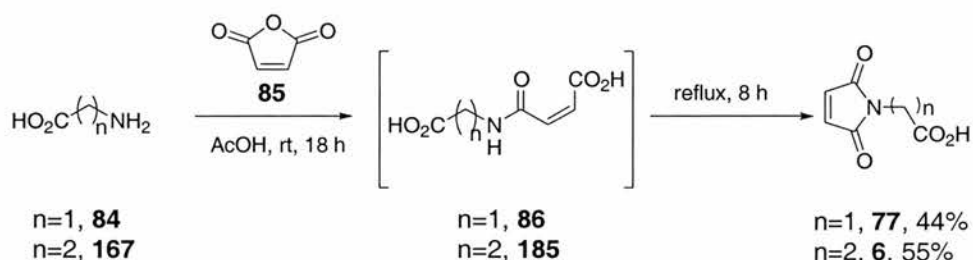
Scheme 4.3 The proposed new self-replicating systems

The system shown above, involves the use of the amidopyridine and carboxylic acid recognition as used before and also the reaction between a nitron and a maleimide (**Chapter 3**). However this time it was decided to incorporate an alkyl instead of a phenyl spacer unit into the system.

4.4 Synthesis

4.4.1 Synthesis of maleimide building block 77 and 6

Initially, the recognition dipolarophiles, maleimides **77** and **6** (**Scheme 4.4**), were synthesised as previously described in **Section 2.3.2**.



Scheme 4.4 The synthetic route for the preparation of the maleimide dipolarophile recognition building blocks **77** and **6**.

4.4.2 Synthesis of the recognition 1,3 dipoles

The dipoles to be synthesised are shown in **Figure 4.2**.

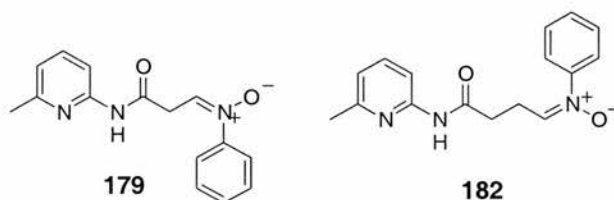
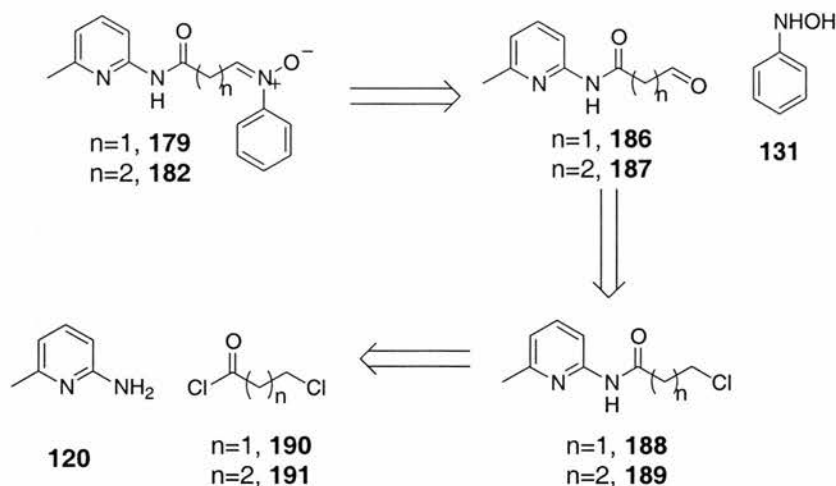


Figure 4.2 The recognition dipoles to be synthesised.

Unfortunately, the syntheses of these compounds proved to be somewhat problematic. The retro-synthetic analysis will be discussed followed by the synthetic routes followed to try to synthesise these compounds.

4.4.2.1 Retro-synthesis of compounds 179 and 182

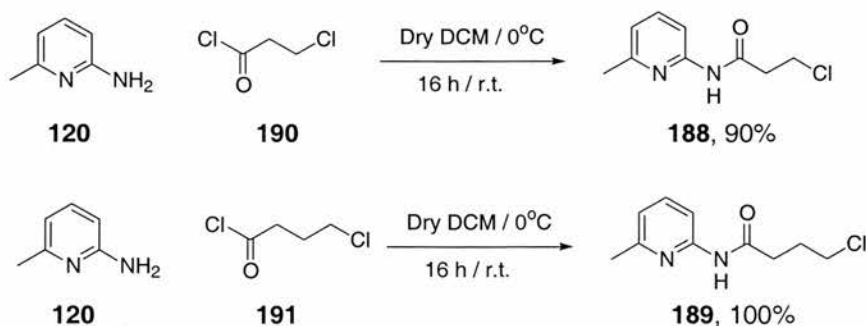


Scheme 4.5 Retro-synthetic analysis of compounds **179** and **182**.

It was decided to follow a synthetic route similar to that used to prepare the nitrones in **Chapter 3**. This meant the coupling of acyl chlorides **190** and **191** with aminopicoline **120**, which would then be converted to the corresponding aldehydes **186** and **187**, which in turn would be reacted with phenyl hydroxylamine **131** to form the nitrones **179** and **182**.

4.4.3 Synthesis of chlorides **188** and **189**

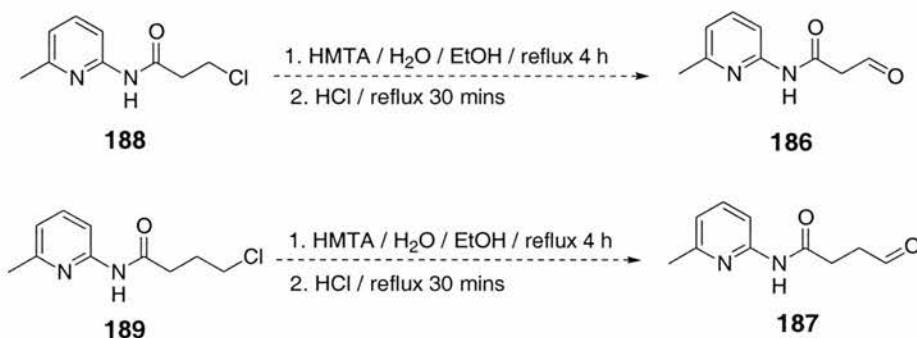
A solution of 2-amino-6-picoline **120** in dry dichloromethane was added neat, dropwise to the appropriate chloropropionyl chloride **190** or **191** at 0°C . The reaction mixture was warmed to room temperature and left to stir for 16 hours. The solvent was removed *in vacuo* and the crude products purified by column chromatography, to afford **188** in a 90% yield and **189** in a 100% yield (**Scheme 4.6**).



Scheme 4.6 The synthetic routes for the preparation of chlorides **188** and **189**.

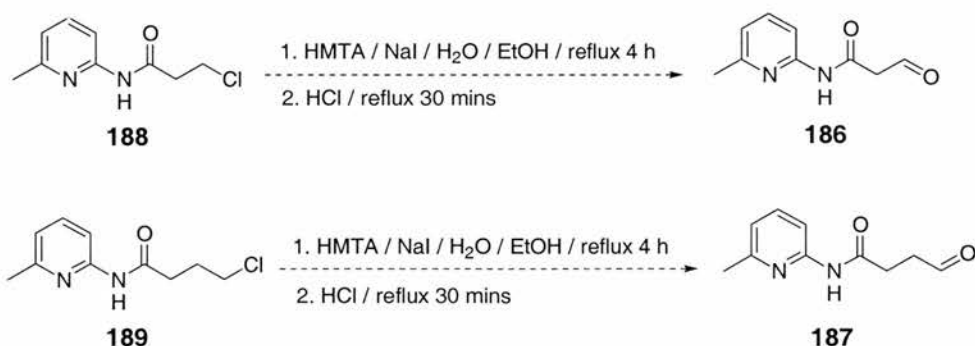
4.4.4 Attempted synthesis of aldehydes **186** and **187**

A mixture of the appropriate chloride **188** or **189** and hexamethylene tetraamine in ethanol/water (50:50; v/v) was heated to reflux for 16 hours. After this time, 12 M HCl was added and the reaction mixture and refluxed for a further 30 minutes. After cooling to room temperature the mixture was diluted with water and extracted using dichloromethane. The combined organic extracts were washed with water, dried over MgSO₄ and removed *in vacuo*. Unfortunately, only starting materials were recovered from this reaction (**Scheme 4.7**).



Scheme 4.7 Attempted synthesis of aldehydes **186** and **187**.

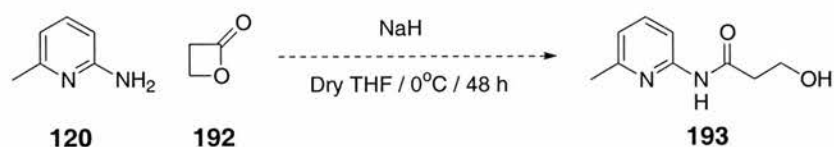
It was thought that perhaps the leaving group ability could be enhanced by performing an *in situ* Finkelstein reaction by replacing the chloride with an iodide using NaI. The reaction was performed as before but with the addition of NaI at the beginning of the reaction (**Scheme 4.8**). However, again after work-up only starting material and some of the iodide was recovered.



Scheme 4.8 Attempted synthesis of aldehydes **186** and **187**.

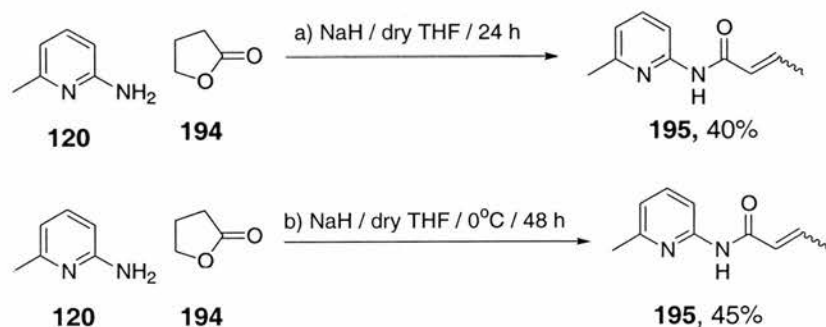
It was decided to try an alternative approach to the formation of aldehydes **186** and **187** by using the ring opening of lactones to form alcohols, which could be oxidised to the aldehydes. Sodium hydride was added cautiously to a stirred solution of 2-amino-6-picoline **120** in dry THF at 0°C. The β -lactone **192** was added dropwise and the reaction was left to stir for 48

hours (**Scheme 4.9**). After which time no reaction appeared to have occurred by tlc. The reaction was left for a further 5 days but still no reaction had occurred. A small amount of reaction mixture was worked up and a crude NMR performed which revealed that there was only 2-amino-6-picoline and some degradation products present.



Scheme 4.9 Attempted synthesis of alcohol **193**

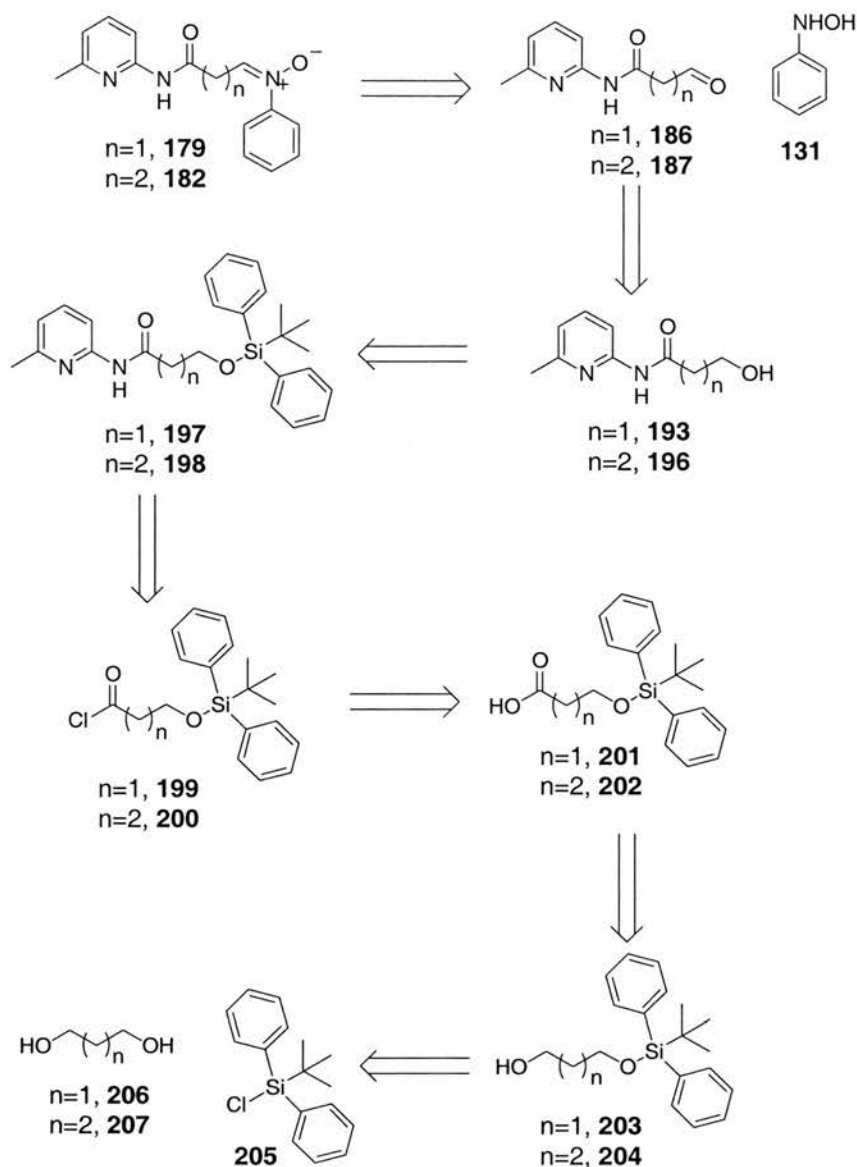
Sodium hydride was added cautiously to a stirred solution of 2-amino-6-picoline **120** in dry THF. The γ -lactone **194** was added slowly and the reaction was left to stir for 24 hours. The reaction mixture was quenched by pouring on to ethanol. The solvent was removed *in vacuo* and the crude product purified by column chromatography, to afford alkene **195** rather than the desired alcohol in a 40% yield. The reaction was repeated at 0°C and stirred for 48 hours but again the reaction afforded alkene **195** instead of the desired alcohol in a 45% yield (**Scheme 4.10**).



Scheme 4.10 Attempted synthesis of an alcohol

4.5 An alternative retro-synthetic analysis of compounds **179** and **182**

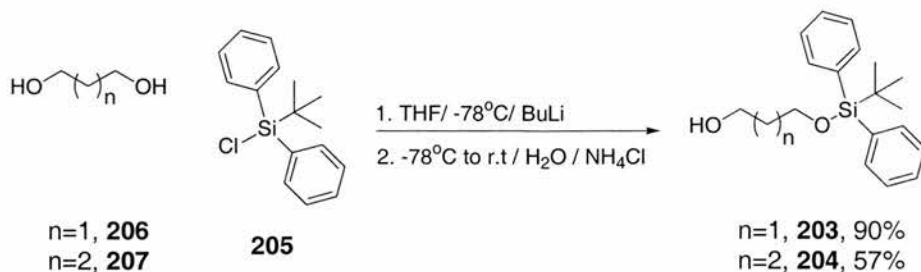
Due to the problems encountered in the synthesis of the nitrones **179** and **182** *via* the previous route it was decided to pursue an alternative method. The retro-synthesis of nitrones **179** and **182** was re-examined and a new scheme devised (**Scheme 4.11**)



Scheme 4.11 Retro-synthetic analysis of compounds **179** and **182**.

4.5.1 Synthesis of the protected diols **203** and **204**

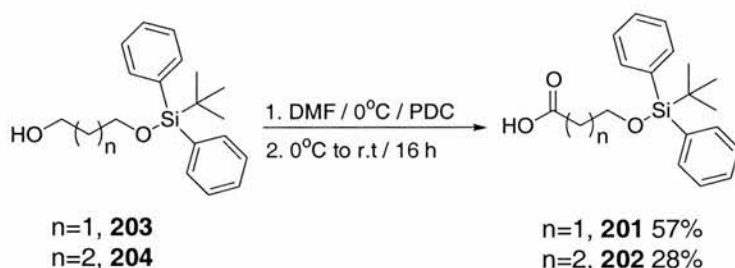
A solution of the appropriate diol **206** or **207** in dry THF was cooled to -78°C under nitrogen. *n*-Butyl lithium was added dropwise with vigorous stirring. After an additional stir for 5 minutes, *tert*-butylchlorodiphenylsilane (TBDPSCl) was added dropwise. The resulting mixture was then allowed to warm to room temperature, and stirred for 40 minutes. The reaction mixture was treated with water and sat. NH_4Cl (aq.). The aqueous layer was extracted with diethyl ether. The combined organic extracts were, dried, reduced *in vacuo* and purified by column chromatography to afford **203** in a 90% yield and **204** in a 57% yield (**Scheme 4.12**).



Scheme 4.12 The synthetic route for the preparation of the protected diols **203** and **204**.

4.5.2 Synthesis of the carboxylic acids **201** and **202**

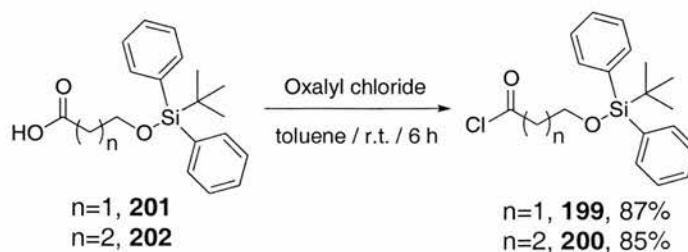
A solution of the appropriate protected diol **203** or **204** in DMF was cooled to 0°C under nitrogen and then treated portionwise with pyridinium dichromate. The resulting mixture was warmed to room temperature and stirred for 16 hours. The reaction mixture was then poured onto water and extracted with diethyl ether. The combined organic layers were dried MgSO_4 , reduced *in vacuo* and purified by gradient elution column chromatography to afford **201** in a 57% yield and **202** in a 28% yield (**Scheme 4.13**).



Scheme 4.13 The synthetic route for the preparation of the carboxylic acids **201** and **202**.

4.5.3 Synthesis of the acid chlorides **199** and **200**

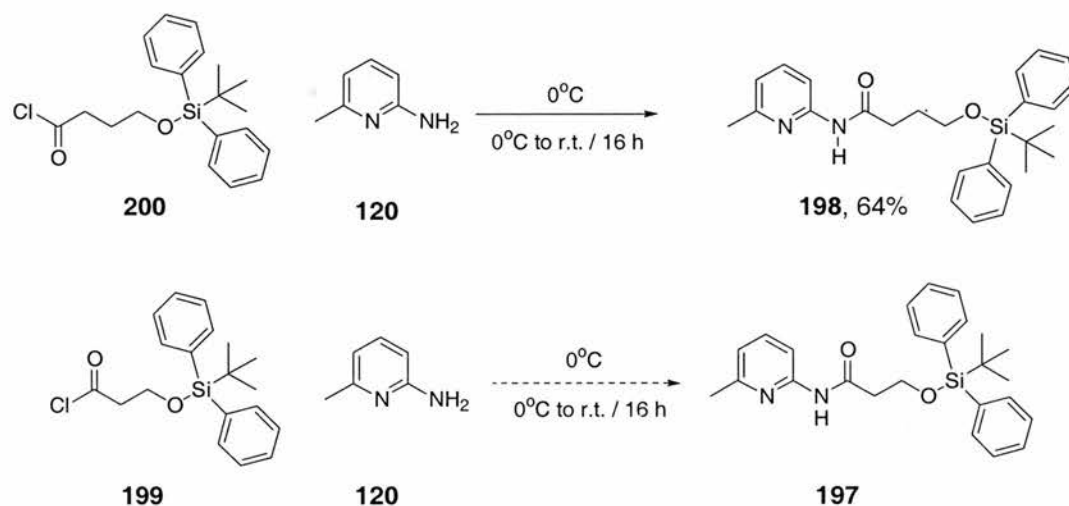
Oxalyl chloride was carefully added to a stirred solution of the appropriate carboxylic acid **201** or **202** in toluene, at room temperature. After 6 hours the solvent and excess oxalyl chloride was removed under reduced pressure to give **199** in an 87% yield and **200** in an 85% yield (**Scheme 4.14**).



Scheme 4.14 The synthetic route for the preparation of the acid chloride **199** and **200**.

4.5.4 Synthesis of the amides **197** and **198**

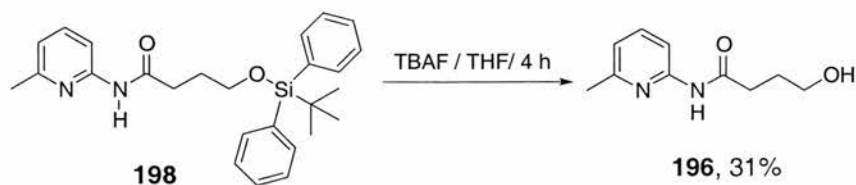
A solution of 2-amino-6-picoline **120** in dry dichloromethane was added dropwise to the appropriate neat acid chloride **199** or **200** at 0°C. After addition the reaction was allowed to warm to room temperature and stirred for 16 hours. The solvent was removed *in vacuo* and the crude product purified by column chromatography to afford **198** in a 64% yield. However upon purification of the reaction to form **197**, only 2-amino-6-picoline and degradation products were recovered (**Scheme 4.15**).



Scheme 4.15 The synthetic route for the preparation of amide **198** and the attempted synthesis of amide **197**.

4.5.5 Synthesis of the alcohol **196**

4-(*tert*-Butyl-diphenyl-silanyloxy)-*N*-(6-methyl-pyridin-2-yl)-butyramide **198** was added to a stirred solution of tetrabutylammonium fluoride in THF. After 4 hours the reaction mixture was poured onto ethyl acetate and washed with water. The solvent was removed *in vacuo* and the crude product purified by column chromatography to afford **196** in a 31% yield (**Scheme 4.16**).

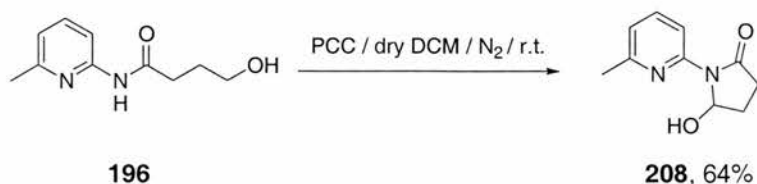


Scheme 4.16 The synthetic route for the preparation of alcohol **196**.

4.5.6 Attempted synthesis of aldehyde **187**

4-Hydroxy-*N*-(6-methyl-pyridin-2-yl)-butyramide **196** was added to a stirred solution of pyridinium chlorochromate in dry dichloromethane. The reaction was stirred under nitrogen for 2 hours. The crude product was filtered through Celite®, then reduced *in vacuo* and

purified by column chromatography, to afford **208** instead of the desired **187** in a yield of 64% (**Scheme 4.17**).



Scheme 4.17 Attempted synthesis of aldehyde **187**.

It was evident immediately, from the ^1H NMR spectrum **Figure 4.4** that the desired aldehyde was not the product formed from the reaction presented in **Scheme 4.17**. Examination of the spectrum in the region 1-3 ppm revealed four proton resonances with identical integrals. If the aldehyde had been produced, it would not have been expected to observe four inequivalent proton resonances and so the actual structure of the product formed was unclear. It was proposed that the product had the structure **208** but in order to unequivocally prove this assignment; accurate mass and further NMR experiments were performed upon the product of the reaction shown in **Scheme 4.17**.

4.6 Structural assignment of compound **208**

4.6.1 Accurate and low resolution mass analysis

The accurate mass of compound **208**, determined by CI mass spectroscopy, was found to be 193.0982. This corresponds to the molecular formula $\text{C}_{10}\text{H}_{13}\text{N}_2\text{O}_2$, which is the $(\text{M}+\text{H})^+$ ion, therefore the actual molecular formula is $\text{C}_{10}\text{H}_{12}\text{N}_2\text{O}_2$. It should be noted that this is the same molecular formula that would have been expected for the aldehyde **187**.

The low-resolution mass spectrum gave rise to the peaks $193 (\text{M}+\text{H})^+$, $175 (\text{M}-\text{OH})^+$ and $58 (\text{C}_3\text{H}_6\text{O})^+$. On the basis of this spectrum it appears that the compounds contains an alcohol functionality due to the loss of H_2O from the molecular ion peak, and also an alkyl chain containing $\text{C}_3\text{H}_6\text{O}$.

4.6.2 ^1H and ^{13}C NMR of compound **208**

In order to aid the elucidation of the structure of compound **208**, fragments from the ^1H and ^{13}C NMR were identified.

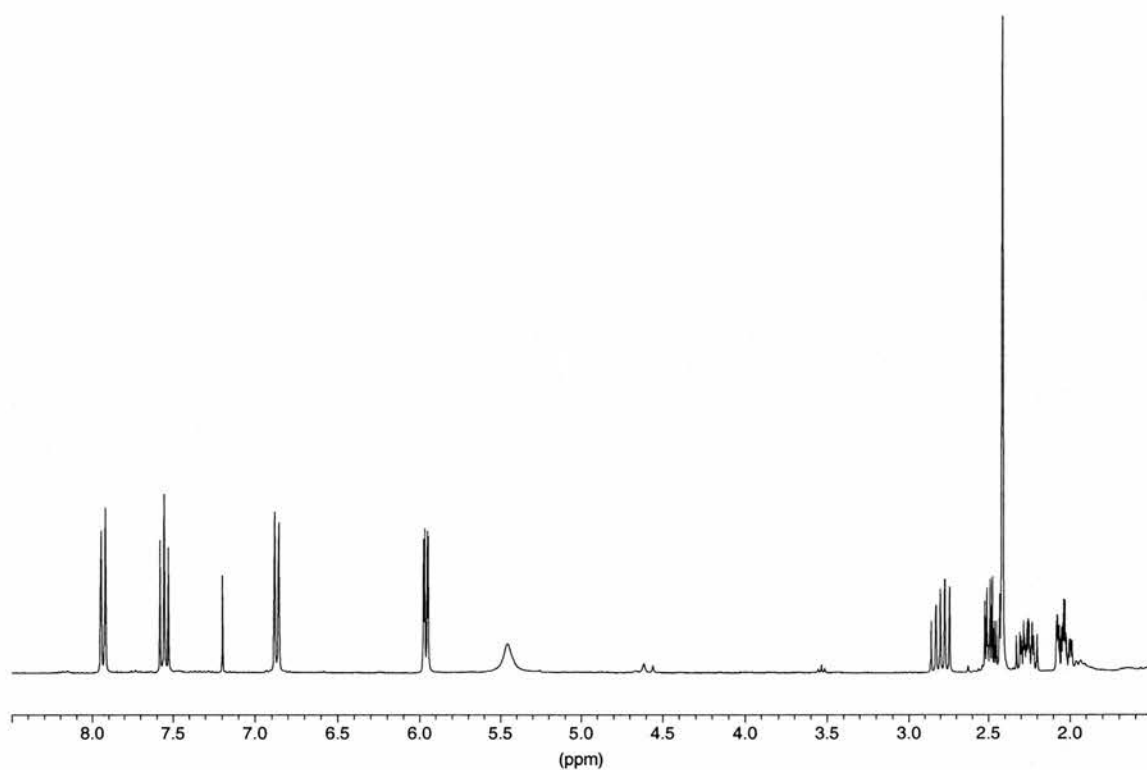


Figure 4.3 Partial 300 MHz ¹H NMR spectrum of compound **208** recorded in CDCl₃.

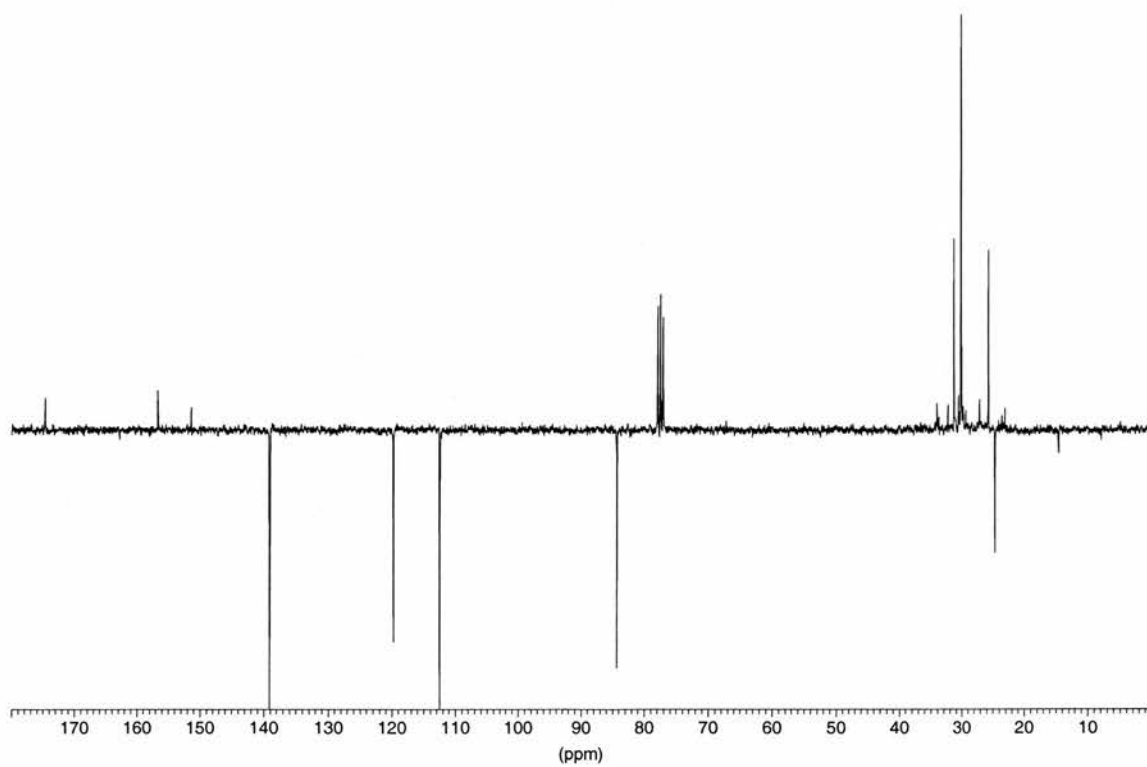
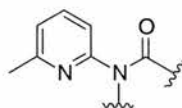


Figure 4.4 75 MHz ¹³C NMR spectrum, acquired using a PENDANT experiment, of compound **208** recorded in CDCl₃.

Examination of the ^1H NMR (**Figure 4.3**) in the aromatic region and the singlet at 2.4 ppm showed the characteristic proton resonances obtained for the amidopicoline unit, however there was no amide proton resonance observed, although the ^{13}C NMR (**Figure 4.4**) reveals three quaternary resonances, one of which occurs in the carbonyl region. These findings led to the conclusion that the fragment **209** is contained within the unknown product (**Figure 4.5**).

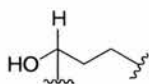


209

Figure 4.5 Fragment **209** identified from the ^1H and ^{13}C NMR spectra of the unknown compound.

The fragment **209** has the formula $\text{C}_7\text{H}_6\text{N}_2\text{O}$, which leaves a total of $\text{C}_3\text{H}_6\text{O}$ to be accounted for.

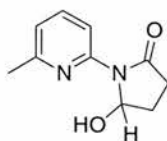
If this amidopicoline unit is present, then there are 6 separate ^1H resonances to account for in the spectrum presented, one of which is very broad and in conjunction with the evidence from the mass spectrum led to the conclusion that this is a proton resonance of an alcohol. The ^{13}C spectrum reveals that there are 2 x CH_2 and 1 x CH (quite low field) resonances. This led to the fragment **210** (**Figure 4.6**).



210

Figure 4.6 Fragment **210** identified from the ^1H and ^{13}C NMR spectra of the unknown compound.

If the two fragments identified **209** and **210**, are assembled in the most sensible fashion, the structure outlined in **Figure 4.7** is obtained.



208

Figure 4.7 Proposed structure of the product obtained from the reaction presented in **Scheme 4.17**.

To confirm this structure is correct further NMR experiments were performed.

4.6.3 COSY NMR experiment performed upon compound 208

To aid the identification of the relevant proton and carbon resonances the following labelling systems will be used for the protons and carbons (**Figure 4.8**).

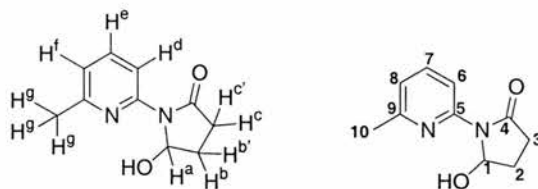


Figure 4.8 The proton and carbon labels used for compound 208.

A 2D COSY (CORrelation Spectroscopy) experiment was performed upon sample 208, the results of which are presented in **Figure 4.9**. This experiment creates a 2D homonuclear chemical shift correlation map between directly coupled ¹H and ¹H nuclei.

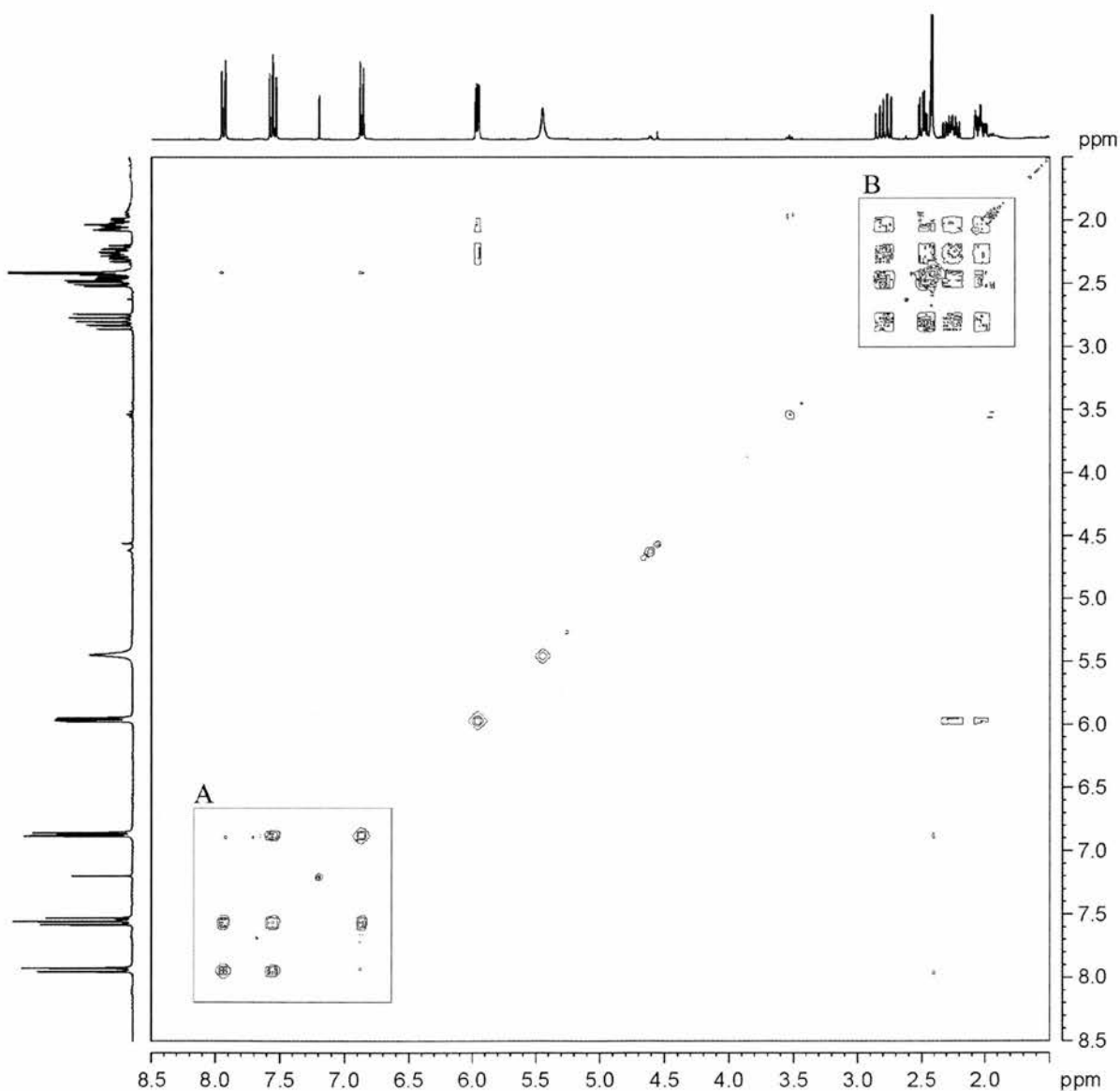


Figure 4.9 300 MHz ¹H-¹H 2D COSY correlation map of compound 208.

Examination of the 2D COSY spectrum confirms the assignment of the three aromatic protons (H^d , H^e and H^f) and their adjacent nature (box A). The four-multiplet protons resonances in the alkyl region all show coupling to each other (box B), the two higher field protons of which display a coupling to the proton resonance at 6 ppm. This infers that a fragment consisting of CH_2-CH_2-CH is contained within this structure. The low field nature of the resonance at 6ppm implies that the proton is attached to the same carbon as a deshielding group, which in this case could be an alcohol unit. This leads to the assignment $X-CH_2^{c/c'}-CH_2^{b/b'}-CH^aOHX$.

4.6.4 HSQC NMR experiment performed upon compound 208

A 2D HSQC (Heteronuclear Single-Quantum Correlation) experiment was performed upon compound **208**. This experiment creates a 2D heteronuclear chemical shift correlation map between directly bonded 1H and ^{13}C nuclei ($^1J_{CH}$). The correlation map obtained for compound **208** is presented in **Figure 4.10**. This experiment was performed to ensure that the assignment of the number of protons attached to each carbon was correct.

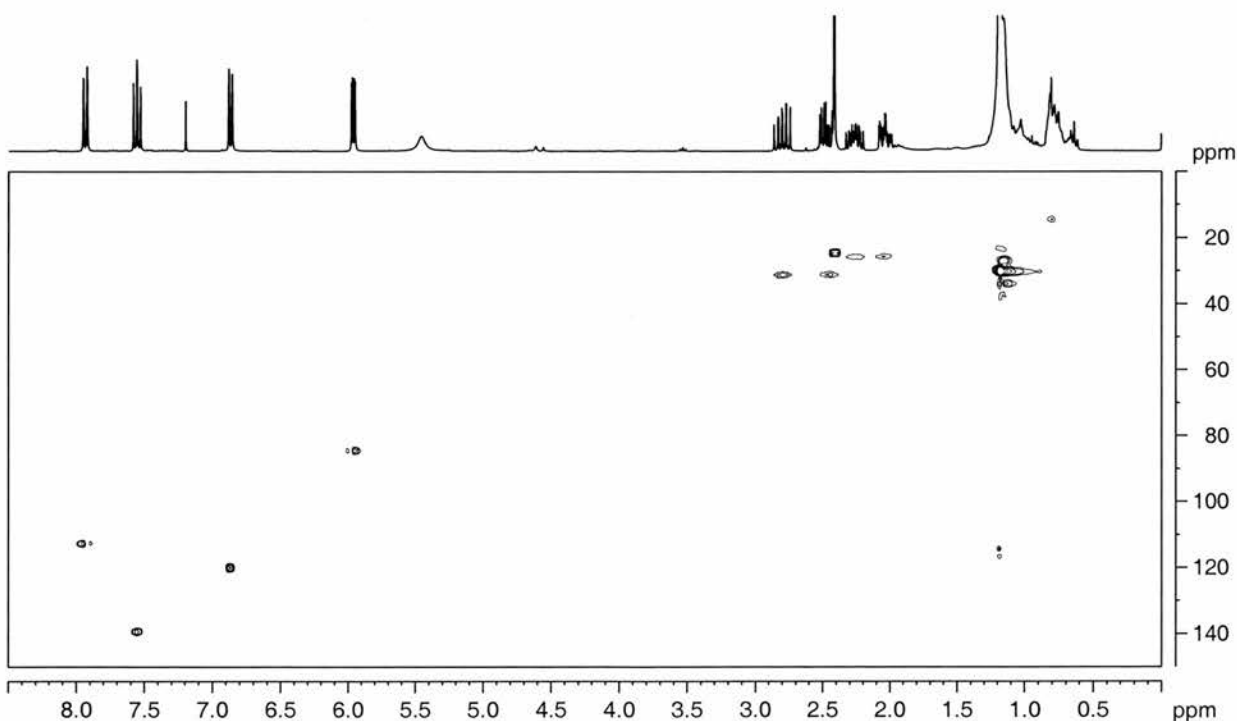


Figure 4.10 $^1H-^{13}C$ 2D HSQC map for compound **208** showing the relationship between directly bonded 1H and ^{13}C nuclei.

Examination of the 2D HSQC map confirms the aromatic proton (CH) assignments, and that the doublet at 6 ppm is a CH unit. The map also reveals that the alkyl protons in the region 1.5-3 ppm are all inequivalent CH_2 resonances.

So far the two fragments and the relative proton and carbon relationships have been assigned and confirmed, however, it would be useful to have evidence that connects the two fragments together. This would provide definitive proof of the structure of **208** and for this a 2D HMBC NMR experiment was performed.

4.6.5 HMBC NMR experiment performed upon compound **208**

A 2D HMBC (Heteronuclear Multiple-Bond Correlation) experiment was performed upon compound **208**. This experiment creates a 2D heteronuclear chemical shift correlation map between long range bonded ^1H and ^{13}C nuclei ($^2J_{\text{CH}}$ and $^3J_{\text{CH}}$). The correlation map obtained for compound **208** is presented in **Figure 4.11**.

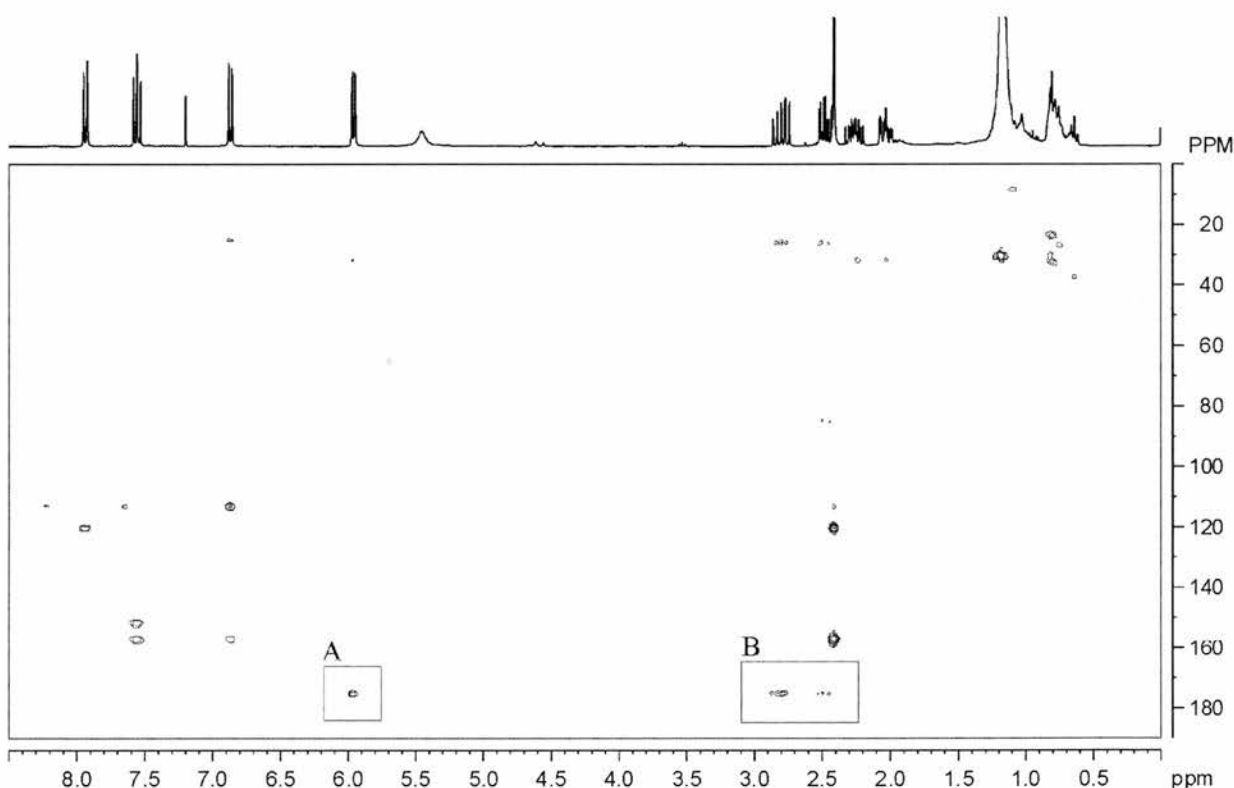


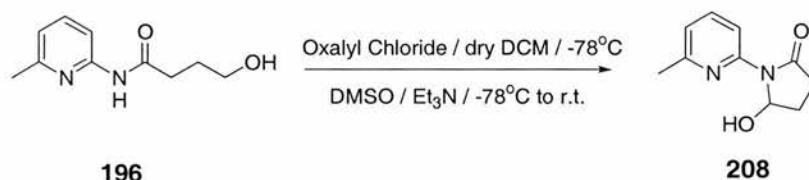
Figure 4.11 A 2D HMBC map for compound **208** showing the relationship between long range bonded ^1H and ^{13}C nuclei.

The 2D HMBC correlation map (**Figure 4.11**) provided the final evidence required to prove the structure of **208**. Inspection of the map reveals a long range coupling between H^{a} on C^1 and the carbonyl carbon C^4 (box A), it also shows a long range coupling between H^{c} and $\text{H}^{\text{c}'}$ and the carbonyl carbon C^4 (box B). The 2D COSY NMR showed that H^{a} and $\text{H}^{\text{c}}/\text{H}^{\text{c}'}$ were joined through $\text{H}^{\text{b}}/\text{H}^{\text{b}'}$ and so this implies a ring system has been formed through the carbonyl unit which must be part of the amide group which joins the amidopyridine unit. Hence by walking through structure using the 2D map it has been shown that the structure of **208** is correct.

Unfortunately, due to the number of synthetic steps required to prepare **196** only a small amount was recovered upon purification. The entire synthesis was repeated in the hope improve the overall yields however the second attempt afforded a comparative yield to the first attempt and so the synthesis of **187** was only performed one more time.

4.7 Second attempt at the synthesis of aldehyde **187**

The final attempt to produce **187** involved the dropwise addition of dimethyl sulphoxide to a stirred solution of oxalyl chloride in dry dichloromethane at -78°C . 4-Hydroxy-N-(6-methylpyridin-2-yl)-butyramide **196** in dry dichloromethane was then added dropwise followed by slow addition of triethylamine. This was then left to stir for a further 45 mins after which time the reaction mixture was allowed to warm to room temperature. The solvent was removed *in vacuo* and the crude product purified by column chromatography to again afford **208** instead of the desired **187** in a 55% yield (**Scheme 4.18**).



Scheme 4.18 Attempted synthesis of aldehyde **187**

4.8 Alternative nitron building blocks

It was decided as a result of the unsuccessful syntheses of **179** and **182** that alternative building blocks should be pursued. The targets identified are shown in **Figure 4.12**.

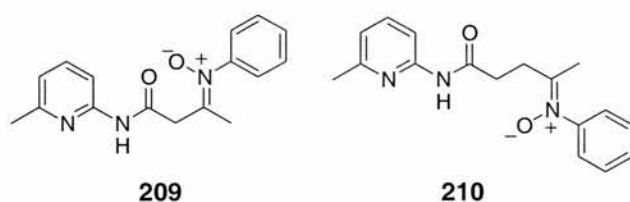
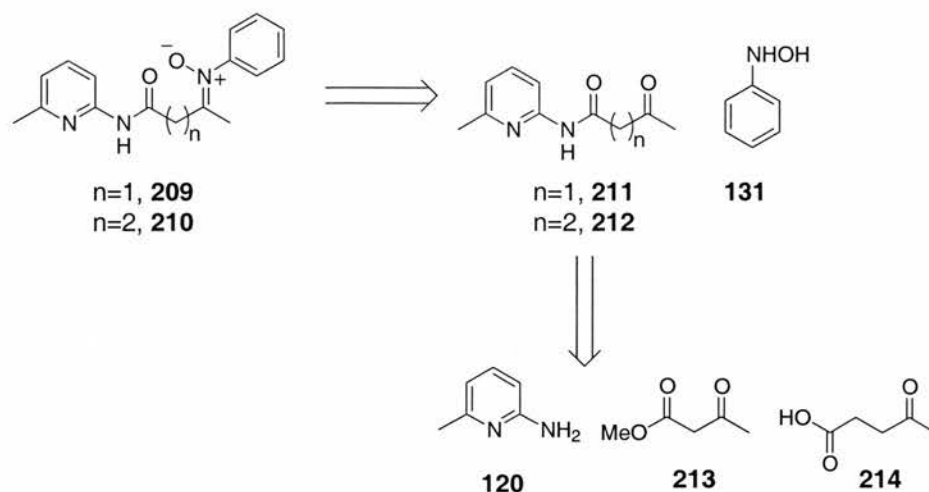


Figure 4.12 The new target building blocks **209** and **210**

4.8.1 Retro-synthesis of compounds 209 and 210.



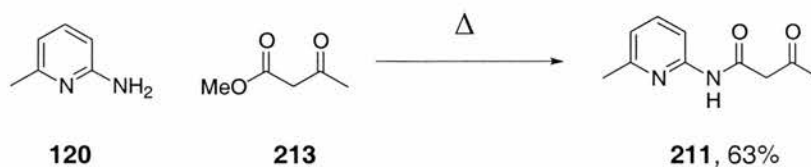
Scheme 4.19 Retro-synthetic analysis of building blocks **209** and **210**.

The new targets are similar in structure to compounds **179** and **182**; however, these compounds **209** and **210** contain an extra CH_3 group. Upon the retro-synthetic analysis it was determined that the ketones rather than the aldehydes were to be prepared. It was hoped that the ketones would be more stable than their aldehyde counterparts.

4.9 Synthesis

4.9.1 Synthesis of ketone 211

2-amino-6-picoline **120** was dissolved in methyl acetoacetate **213**, the stirred reaction mixture was heated to reflux. After 24 hours a colourless precipitate had formed which was isolated by filtration and washed with hexane to afford **211** in a 63% yield (**Scheme 4.20**).

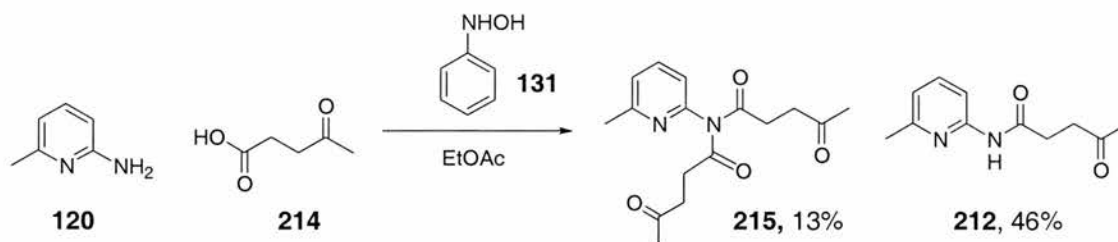


Scheme 4.20 The synthetic route for the preparation of **211**.

4.9.2 Synthesis of ketone 212

β -Phenylhydroxylamine **131** and 4-oxo-pentanoic acid **214** were dissolved in ethyl acetate. 2-Amino-6-picoline **120** was added and the reaction mixture stirred for 4 days. A precipitate formed which was filtered and washed with cold ethyl acetate and hexane to afford **215** in a 13% yield. Hexane was added to the filtrate to effect the precipitation of **212**, which was re-

filtered and washed with cold ethyl acetate and hexane to afford **212** in a 46% yield (**Scheme 4.21**).



Scheme 4.21 The synthetic route for the preparation of **212**.

The reaction presented in **Scheme 4.21** appears quite unusual and its success was discovered accidentally. Whilst designing and synthesising a recognition-mediated system attention is also focused on to the design of possible control compounds for this system. It was hoped that coupling of **214** and **131** to form the respective nitron **216** (**Figure 4.13**) would provide a suitable bimolecular control compound for the recognition-mediated reaction, due to the lack of an amidopyridine recognition site

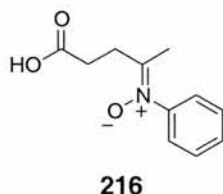
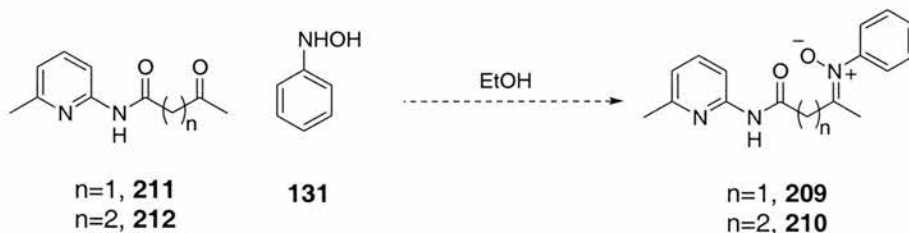


Figure 4.13 Possible bimolecular control compound identified

The synthesis of **216** proved problematic, addition of **214** to a solution of **131** in ethyl acetate lead to the formation of nitron **216** however due to the highly soluble nature of **216** it could not be precipitated out of solution. Efforts were made to perform a column upon the crude reaction mixture however each time this lead to degradation of the nitron upon the column. It was then decided to see if the recognition building block **212** could be prepared in a one-pot synthesis from this nitron. Aminopyridine was added to the reaction mixture and immediately a precipitate formed, which was filtered and washed with cold ethyl acetate, this afforded the ketone **215**, further precipitation of the reaction mixture was performed by the addition of hexane yielded the ketone **212**. The reaction was performed a further three times to ensure its repeatability and each time the same products were obtained in comparable yields.

4.9.3 Synthesis of nitrones 209 and 210

The appropriate ketone was added to a solution of β -phenylhydroxylamine **131** dissolved in ethanol. The reaction was left in the dark for three days whilst being monitored by tlc, unfortunately no reaction appeared to occur. The reaction was repeated with gentle warming however, warming the reaction mixture lead to the degradation of the β -phenylhydroxylamine (**Scheme 4.22**). Finally the reaction was repeated with the addition of a couple of drops of dilute HCl, which again lead to the degradation of the β -phenylhydroxylamine.



Scheme 4.22 Attempted synthesis of nitrones **209** and **210**.

Due to the problematic synthesis of forming these alkyl nitrones it was decided not to pursue the formation of these building blocks any further.

4.10 Conclusion

It was somewhat disappointing that the synthesis of the recognition building blocks outlined in this chapter was unachievable. However, this does demonstrate that the design of self-replicating systems and, in fact, the design of any recognition-mediated system is not without its pit falls. The aim of the work presented in this chapter was to develop a system that was as structurally simple as possible so that a better understanding of its behaviour and comparison to previous systems may be achieved. It has been shown that the synthesis of these structurally small systems does rely significantly upon the effect that different functionalities closely linked have upon each other, which will inevitably have some effect upon the reactivity and ability to synthesise certain compounds. In conclusion it has been shown that although the synthesis did not produce the desired products, it has shown that there are limitations to the types of systems that can be investigated.

5. General Conclusions and Future Directions

The research presented in this thesis has tried to provide a rationale for the design of minimal self-replicating systems. The research has shown that self-replication is an effective tool in obtaining stereochemical and rate enhancements in 1,3-dipolar cycloaddition reactions, however it highlighted that this is not the only reaction which may be enhanced by this pathway.

Initially, this research concentrated on structurally simple systems to enable a better understanding of how systems self-replicate. It was determined from the first system investigated, which involved the reaction between an azide and a maleimide that self-replication is achievable from these small units. However, the design of this system led to a product duplex which was very stable and hence autocatalysis was not achieved. This is as a result of the ternary complex having a late “product-like” transition state and hence upon formation the product duplex does not dissociate with ease, if at all. This demonstrates a system, which is an excellent self-replicator however it is not autocatalytic. Modifications to this system reveal that the pathway, which the reaction proceeds through, can be altered from self-replicating to an AB complex. Hence, revealing that by lengthening the spacer units, the reactive sites can come into close contact *via* the entropically more favourable AB-complex.

The third chapter investigated the effects of various modifications made upon an autocatalytic self-replicating system. It was concluded that only one out of the three modifications investigated had significant effects upon the self-replicating and autocatalytic nature of the system. It was demonstrated that the electronic and steric effects of the substituents placed upon the system did not significantly affect the self-replicating or autocatalytic ability of the systems. The only significant difference noted was the rates that the reactions proceeded at, however it should also be noted that the rate of reaction is not a measure of the efficiency of a self-replicating system. Altering the regiochemistry of the systems caused the most significant affect upon the efficiency of the autocatalysis and self-replication. It was concluded that the co-conformations adopted by the ternary complex and its subsequent early or late transition state determines the efficiency of the self-replication and the autocatalysis. This co-conformation adopted is a direct result of the conformation of the individual building blocks. This balance between the co-conformations ability to determine the self-replication and autocatalysis was elegantly demonstrated between the 3- and 4-nitrone systems. In this case of the 4-nitrone series, they are better self-replicators and possess a higher stereoselectivity, however they are more inefficient autocatalysts. The “better fit” of the product duplex, due to a late product-like transition state, means that the product duplex does not dissociate as well (relative to the 3-nitrone series) and hence cannot turnover the

autocatalytic cycle as well, again relative to the 3-nitrone counterparts. This was demonstrated by a lower average ϵ values for the 4-nitrones than the 3-nitrone series. However, the 3-nitrone series has demonstrated they are more efficient autocatalyst but their self-replicating ability is not as good as the 4-nitrone series. This is due to an early reactant-like transition state which leads to an unstable product duplex which can dissociate easily and hence turnover of the autocatalytic cycle is better than in the 4-nitrones. Again the basis for the differences is due to the co-conformations adopted by the ternary complex and the product duplex, demonstrating that shape is a major factor in determining whether a system may proceed *via* a self-replicating mechanism and if so how efficiently it does so. Finally, it was demonstrated that although all the necessary requirements for a self-replicating system have been identified, in making these systems structurally small, the effects of differing functionalities within such small systems, could determine what is possible to synthesise, showing that it is not a universal route to any compound.

Although there are synthetic limitations to this area, the future directions of this work could investigate the general application of the self-replication methodology by the use of removable binding sites and/or solid supports. This would aid the formation of synthetic intermediates, possibly stereospecifically without the need for costly or toxic metal-based catalysts. This area could also be expanded, now that there is a small database of self-replicators, to looking at the possibility to create synthetic reciprocal replicating system, through cross catalysis, initial studies into this area show that cross catalysis between the systems appears to be possible, however further investigations into this area will be required.

6. Experimental

6.1 General procedures

Chemicals and solvents were purchased from Acros, Aldrich, Avocado, BDH or Fluka and used as received unless otherwise stated. Dichloromethane and hexane were distilled from calcium hydride under an N₂ atmosphere. Tetrahydrofuran and diethyl ether were dried by refluxing with sodium-benzophenone under an N₂ atmosphere. DMF was distilled from calcium hydride under reduced pressure and stored over 4Å molecular sieves. Pyridine and triethylamine were both dried by distillation from potassium hydroxide pellets. Thin layer chromatography (TLC) was carried out on aluminium sheets coated with Merck 5554 Kieselgel 60 F₂₅₄. Developed plates were air-dried and scrutinised under a UV lamp (366nm) and further developed in KMnO₄, phosphomolybdic acid (PMA) solutions or iodine vapour where appropriate. Column chromatography was performed using Merck Kieselgel 60 (230-400 nm mesh) or ICN EcoChrom Silica 32-63 µm, 60Å. Melting points were determined using an Electrothermal 9200 melting point apparatus and are uncorrected. Infra-red (IR) spectra were recorded as KBr discs or thin films using a Perkin-Elmer Paragon spectrometer. Microanalyses (CHN) were carried out at the University of Birmingham and the University of St. Andrews. Chemicals and samples used prior to kinetic experiments were weighed using a Sartorius balance (MC1 Analytical AC 120S) with an accuracy of ±0.1mg.

6.2 Mass spectrometry

Electron impact mass spectrometry (EI) and high-resolution mass spectrometry (HRMS) were carried out on either a VG PROSPEC or a VG AUTOSPEC mass spectrometer. Liquid Secondary Ion Mass Spectrometry (LSI) was carried out on a VG ZABSPEC instrument equipped with a cesium ion gun, using *m*-nitrobenzyl alcohol matrix. Electrospray mass spectrometry (ESI) was recorded on a VG PLATFORM mass spectrometer. Chemical ionisation mass spectrometry (CI) was carried out on a VG PROSPEC instrument.

6.3 NMR spectroscopy

¹H Nuclear Magnetic Resonance (NMR) spectra were recorded using a Bruker AC300 (300 MHz), Bruker AMX400 (400 MHz), Bruker DRX500 (500 MHz), Varian UNITYplus (500 MHz), Bruker Avance 300 (300 MHz) or a Varian Gemini 2000 (300 MHz) spectrometers. ¹³C NMR spectra were recorded using Bruker AC300 (75.5 MHz) or Bruker Avance 300 (75.5 MHz) spectrometers using a PENDANT pulse sequence. The deuterated solvent was used as the lock and the residual solvent as an internal reference for all ¹H and ¹³C spectra.

All ^1H -coupling constants are quoted in Hz and all spectra were recorded at 298K unless otherwise stated. The symbols s, d, t, q used in the assignment of ^1H NMR spectra denote singlet, doublet, triplet and quartet respectively. The abbreviations quat. and Ar in the assignment of both ^1H and ^{13}C spectra are used to denote quaternary and aromatic respectively.

6.4 Kinetic measurements

All stock solutions of the appropriate compounds were prepared by dissolving the relevant sample in 2 ml of CDCl_3 . Volumetric flasks ($2\text{ ml} \pm 0.02\text{ ml}$) were used for accuracy. The stock solutions were equilibrated at the appropriate temperature where necessary, for at least one hour prior to use. Experimental samples were prepared by mixing equal volumes of the appropriate stock solutions together using a Hamilton 1 ml gas tight syringe in a Wilmad 528PP NMR tube, which was then fitted with a polyethylene pressure cap when appropriate to minimise solvent evaporation. Once mixed, the samples were analysed immediately by 400 or 500 MHz ^1H NMR spectroscopy over a fixed period of time. In each case the probe had been pre-equilibrated at the appropriate temperature for at least one hour prior to use. The rate of reaction was monitored using the deconvolution tool available in 1D WIN-NMR²⁰⁰. Kinetic simulation and fitting of the resultant data to the appropriate kinetic models was accomplished using the SIMFIT¹⁷⁶ program, then presented using the KaleidaGraph 3.51 program²⁰¹.

6.5 Molecular mechanics calculations

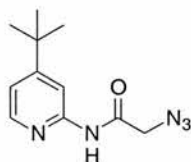
All molecular mechanics calculations were performed on a Silicon Graphics O2 workstation using the AMBER* forcefield as implemented in the Maestro program together with the GB/SA solvation model²⁰² for chloroform. Initially, each molecule was energy-minimised using a conjugate gradient (PRCG). Initially minimised complexes were further analysed using a Monte-Carlo conformational search technique minimising up to 2000 structures using a maximum of 5000 iterations, all conformations generated within 50 kJmol^{-1} of the global minimum were minimised. Global minima structures were exported and visualised using Chem3D or Ortep3. Data collected during the Monte-Carlo conformational search was exported into KaleidaGraph 3.51.

6.6 Crystal structure determination

Single crystals were formed by slow vapour diffusion of hexane into a solution of the relevant compound. X-ray diffraction data was recorded on a Bruker SMART CCd or MSC Mercury CCD X-ray diffractometer. The data tables are presented at the end of the experimental section. It should be noted that for the compounds **78** and especially **7** the crystals were small and diffracted poorly. This is reflected in the R-values of 0.1166 and 0.3009 respectively. Therefore, the crystal structures obtained for these compounds should only be used as a guide to the actual conformation of the templates.

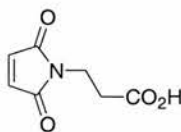
6.7 Synthetic procedures

N-(4-*tert*-Butyl-2-pyridyl)-azidoacetamide **5**



Sodium azide (2.67 g, 41 mmol) was added to a solution of N-(4-*tert*-butyl-2-pyridyl)-chloroacetamide **83** (3.12 g, 14 mmol) in acetone and heated to reflux for 16 hours. The sodium chloride by-product was removed by vacuum filtration and the residue washed thoroughly with acetone. The filtrates were combined and the solvent removed *in vacuo*, affording **5** as a colourless powder (3.19 g, 99%): M.p. 116-118°C; $\nu_{\max}(\text{KBr})/\text{cm}^{-1}$ 2965, 2113, 1614, 1578; δ_{H} (300 MHz, CDCl_3) 8.72 (br s, NH) 8.17-8.12 (2H, m, Ar CH), 7.02 (1H, d, $^3J_{\text{H,H}}$ 5.5, Ar CH), 4.06 (2H, s, CH_2), 1.26 (9H, s, $(\text{CH}_3)_3$); δ_{C} (75.5 MHz, CDCl_3) 165.2 (quat. C), 163.2 (quat. C), 150.9 (quat. C), 147.4 (Ar CH), 117.5 (Ar CH), 111.2 (Ar CH), 53.0 (CH_2), 35.5 (quat. C), 35.1 (3 x CH_3); m/z (ESI) 234 ($\text{M}+\text{H}^+$, 30%); Found 234.1366 [$\text{M}+\text{H}^+$], $\text{C}_{11}\text{H}_{16}\text{N}_5\text{O}$ requires 234.1277.

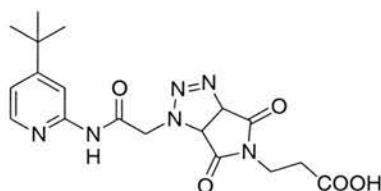
3-Maleimidopropanoic acid²⁰³ **6**



β -Alanine **167** (5.00 g, 56 mmol) and maleic anhydride **85** (5.50 g, 56 mmol) were stirred in acetic acid (AR) (100 ml) at room temperature for 16 hours under nitrogen. The reaction mixture was then heated to reflux for 8 hours before being cooled to room temperature. The solvent was removed *in vacuo* and the crude residue was purified using flash column chromatography (SiO_2 , 10:1 chloroform:methanol) affording 3-maleimidopropanoic acid **6** as

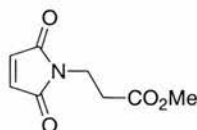
a colourless solid (5.17 g, 55%): M.p. 102-103°C (lit.²⁰³ 105-105.5°C); $\nu_{\max}(\text{KBr})/\text{cm}^{-1}$ 3093, 2949, 2646, 1704, 1694, 1446, 1414, 959, 835; δ_{H} (300 MHz, CDCl_3) 10.26 (1H, br s, CO_2H), 6.71 (2H, s, maleimide H), 3.83 (2H, t, $^3J_{\text{H,H}}$ 7, CH_2), 2.68 (2H, t, $^3J_{\text{H,H}}$ 7, CH_2); δ_{C} (75.5 MHz, CDCl_3) 176.6 (quat. C), 170.4 (2 x quat. C), 134.3 (2 x CH), 33.3 (CH_2), 32.5 (CH_2); m/z (EI) 169 (M^+ , 40%), 151 (45), 123 (100), 110 (95), 96 (19), 82 (65); Found 169.0378 [M^+], $\text{C}_7\text{H}_7\text{NO}_4$ requires 169.0375.

3-[1-{2-[*N*-(4-*tert*-butyl-2-pyridyl)-acetamidyl]-2-oxoethan-1-yl}-3a,6a-dihydromaleimido[3,4-d]-1,2,3-triazol-5-yl]propanoic acid **7**



N-(4-*tert*-Butyl-2-pyridyl)-azidoacetamide **5** (51 mg, 0.22 mmol) and 3-maleimidopropanoic acid **6** (37 mg, 0.22 mmol) were dissolved in acetonitrile (2 ml) and left to stir for 5 days. After this time the precipitate was filtered and washed with hexane. **7** was isolated as a colourless solid (118 mg, 75%): M.p. 220-221°C; Found: C, 52.5; H, 5.2; N, 20.7. Calc. for $\text{C}_{18}\text{H}_{22}\text{N}_6\text{O}_5$: C, 53.7; H, 5.5; N, 20.9. $\nu_{\max}(\text{KBr})/\text{cm}^{-1}$ 3273, 2962, 1714, 1562, 1417, 1211, 824; δ_{H} (300 MHz, CDCl_3) 8.52 (1H, s, Ar CH), 8.16 (1H, d, $^3J_{\text{H,H}}$ 5.7, Ar CH), 7.30 (1H, d, $^3J_{\text{H,H}}$ 5.7, Ar CH), 5.88 (1H, d, $^3J_{\text{H,H}}$ 10.6 CH), 5.04 (1H, d, $^2J_{\text{H,H}}$ 17.7 CH_2), 4.60 (1H, d, $^2J_{\text{H,H}}$ 17.7 CH_2), 4.47 (1H, d, $^3J_{\text{H,H}}$ 10.6 CH), 4.19-4.10 (1H, m, CH_2), 3.96-3.88 (1H, m, CH_2), 2.91-2.81 (1H, m, CH_2), 2.75-2.67 (1H, m, CH_2), 1.48 (9H, s, $(\text{CH}_3)_3$); δ_{C} (75.5 MHz, CDCl_3) 172.5 (quat. C), 171.4 (quat. C), 170.3 (2 x quat. C), 167.5 (quat. C), 167.2 (quat. C), 150.7 (quat. C), 144.2 (Ar CH), 118.2 (Ar CH), 113.7 (Ar CH), 83.6 (CH), 60.5 (CH), 54.2 (CH_2), 36.0 (CH_2), 31.5 (CH_2), 30.7 (3x CH_3); m/z (CI) 403 ($\text{M}+\text{H}^+$, 20%), 375 ($\text{M}-\text{N}_2^+$); Found 375.1659 [$\text{M}-\text{N}_2^+$], $\text{C}_{18}\text{H}_{22}\text{N}_4\text{O}_5$ requires 375.1668.

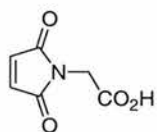
3-Maleimidopropanoic acid, methyl ester^{204,205} **12**



Methyl iodide (1.49 ml, 24.0 mmol) was added dropwise to a stirred solution of 3-maleimidopropanoic acid **6** (2.00 g, 12.0 mmol) and Cs_2CO_3 (1.93 g, 6.0 mmol) in pre-dried DMSO (over 4Å molecular sieves) (30 ml). After stirring at room temperature for 16 hours in the dark, the reaction mixture was diluted with water (*ca.* 50 ml) and extracted using

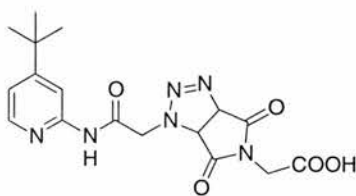
dichloromethane (200 ml). The combined organic extracts were washed once with water (50 ml) and dried over MgSO₄. Solvent was removed *in vacuo* and the residue purified by flash column chromatography (SiO₂, 7:3 hexane:ethyl acetate) to afford **12** as an orange oil (1.50 g, 74%): Found: C, 52.5; H, 5.1; N, 7.8. Calc. for C₈H₉NO₄: C, 52.5; H, 5.0; N, 7.7. $\nu_{\max}(\text{neat})/\text{cm}^{-1}$ 3462, 3098, 2998, 2846, 1713, 1584, 1447, 958; δ_{H} (300 MHz, CDCl₃) 6.70 (2H, s, maleimide CH), 3.82 (2H, t, ³J_{H,H} 7, CH₂), 3.66 (3H, s, CO₂CH₃), 2.63 (2H, t, ³J_{H,H} 7, CH₂); δ_{C} (75.5 MHz, CDCl₃) 171.2 (quat. C), 170.4 (2 x quat. C), 134.3 (2 x CH), 52.0 (CH₃), 33.6 (CH₂), 32.7 (CH₂); *m/z* (EI) 183 (M⁺, 5%), 151 (29), 123 (70), 110 (100), 102 (17), 82 (46), 54 (38); Found 183.0529 [M⁺], C₈H₉NO₄ requires 183.0532.

2-Maleimidoethanoic acid²⁰³ **77**



Glycine **84** (5.00 g, 67 mmol) and maleic anhydride **85** (6.53 g, 67 mmol) were stirred in acetic acid (AR) (150 ml) for 16 hours at room temperature under nitrogen. The reaction mixture was then heated to reflux for 8 hours before being cooled to room temperature. The solvent was removed *in vacuo* and the residue was purified by column chromatography (SiO₂, 20:1 dichloromethane:acetic acid) to give a pale yellow solid, which was recrystallised from dichloromethane and hexane to give 2-maleimidoacetic acid **77** as a colourless solid (4.50 g, 44%): M.p. 113-114°C (lit.²⁰³ 113-133.5°C); Found: C, 46.6; H, 3.3; N, 9.0. Calc. for C₆H₅NO₄: C, 46.5; H, 3.3; N, 9.0. $\nu_{\max}(\text{KBr})/\text{cm}^{-1}$ 3101, 2726, 1755, 1446, 1397, 1193, 699, 675, 632; δ_{H} (300 MHz, d₆-DMSO) 13.12 (1H, br s, CO₂H), 7.15 (2H, s, maleimide H), 4.16 (2H, s, CH₂); δ_{C} (75.5 MHz, d₆-DMSO) 172.6 (quat. CO₂H), 169.7 (2 x quat. C), 134.6 (2 x CH), 38.3 (CH₂); *m/z* (EI) 155 (M⁺, 9%) 138 (3), 110 (100), 82 (92), 54 (85), 45 (61); Found 155.0218 [M⁺], C₆H₅NO₄ requires 155.0218.

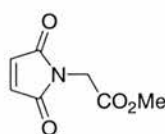
3-[1-{2-[N-(4-*tert*-butyl-2-pyridyl)-acetamidyl]-2-oxoethan-1-yl}-3a,6a-dihydromaleimido[3,4-d]-1,2,3-triazol-5-yl]ethanoic acid **78**



N-(4-*tert*-Butyl-2-pyridyl)-azidoacetamide **5** (51 mg, 0.22 mmol) and 2-maleimidoethanoic acid **77** (34 mg, 0.22 mmol) were dissolved in acetonitrile (2 ml) and left to stir for 5 days

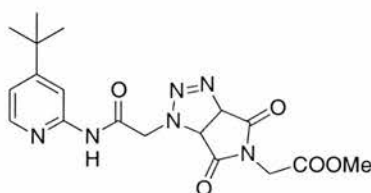
after this time the precipitate was filtered and washed with hexane. **78** was isolated as a colourless solid (55 mg, 65%): M.p. >180°C (decomp.); Found: C, 52.3; H, 5.3; N, 21.5. Calc. for C₁₇H₂₀N₆O₅: C, 52.6; H, 5.2; N, 21.6; $\nu_{\max}(\text{KBr})/\text{cm}^{-1}$ 3234, 2968, 1719, 1577, 1418, 1168, 946; δ_{H} (300 MHz, CDCl₃) 8.25 (1H, s, Ar CH) 8.01 (1H, d, $^3J_{\text{H,H}}$ 5.8, Ar CH), 7.12 (1H, d, $^3J_{\text{H,H}}$ 5.8, Ar CH), 5.75 (1H, d, $^3J_{\text{H,H}}$ 10.7 CH), 4.89 (1H, d, $^2J_{\text{H,H}}$ 17.8 CH₂), 4.68 (1H, d, $^3J_{\text{H,H}}$ 10.7 CH), 4.51 (1H, d, $^2J_{\text{H,H}}$ 17.8 CH₂), 4.21 (2H, m, CH₂), 1.27 (9H, s, (CH₃)₃); δ_{C} (75.5 MHz, CDCl₃) 172.2 (quat. C), 171.1 (quat. C), 170.2 (2 x quat. C), 167.4 (quat. C), 167.1 (quat. C), 150.4 (quat. C), 144.1 (Ar CH), 118.2 (Ar CH), 112.9 (Ar CH), 83.4 (CH), 58.7 (CH), 50.1 (CH₂), 40.5 (CH₂), 30.6 (3 x CH₃); m/z (EI) 390 (M⁺, 25%).

2-Maleimidoethanoic acid, methyl ester^{204,205} **79**



Methyl iodide (0.40 ml, 6.4 mmol) was added dropwise to a stirred solution of 2-maleimidoacetic acid **77** (500 mg, 3.2 mmol) and Cs₂CO₃ (530 mg, 1.6 mmol) in pre-dried DMSO (over 4Å molecular sieves) (15 ml). After stirring at room temperature for 16 hours in the dark, the reaction mixture was diluted with water (*ca.* 25 ml) and extracted using dichloromethane (100 ml). The combined organic extracts were washed once with water (25 ml) and dried over MgSO₄. Solvent was removed *in vacuo* and the residue purified by flash column chromatography (SiO₂, 7:3 hexane:ethyl acetate) affording **79** as a pale yellow oil (300 mg, 55%): Found: C, 49.8; H, 4.2; N, 8.4. Calc. for C₇H₇NO₄: C, 49.7; H, 4.2; N, 8.3. $\nu_{\max}(\text{neat})/\text{cm}^{-1}$ 3100, 2954, 1715, 907, 830, 697; δ_{H} (300 MHz, CDCl₃) 6.78 (2H, s, maleimide CH), 4.28 (2H, s, CH₂), 3.75 (3H, s, CO₂CH₃); δ_{C} (75.5 MHz, CDCl₃) 169.7 (quat. CO₂H), 167.6 (2 x quat. C=O), 134.5 (2 x CH), 52.7 (CH₃), 38.4 (CH₂); m/z (EI) 169 (M⁺, 72%) 110 (100), 82 (80), 54 (60), Found 169.0382 [M⁺], C₇H₇NO₄ requires 169.0375.

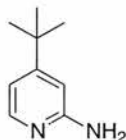
3-[1-{2-[N-(4-*tert*-butyl-2-pyridyl)-acetamidyl]-2-oxoethan-1-yl}-3a,6a-dihydromaleimido[3,4-d]-1,2,3-triazol-5-yl]ethanoic acid, methyl ester **80**



N-(4-*tert*-Butyl-2-pyridyl)-azidoacetamide **5** (51 mg, 0.22 mmol) and 2-maleimidoethanoic acid, methyl ester **79** (37 mg, 0.22 mmol) were dissolved in acetonitrile (2 ml) and left to stir

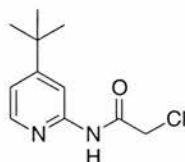
for 5 days. The crude product was then reduced *in vacuo* and purified by column chromatography (SiO₂, 1:1 hexane:ethyl acetate). **80** was isolated as a colourless solid (36 mg, 41%): M.p. 79-80°C; Found: C, 53.5; H, 5.4; N, 20.6. Calc. for C₁₈H₂₂N₆O₅: C, 53.7; H, 5.5; N, 20.9. $\nu_{\max}(\text{KBr})/\text{cm}^{-1}$ 3330, 2964, 1722, 1559, 1414, 1177, 945; δ_{H} (300 MHz, CDCl₃) 9.59 (br s, NH) 8.14-8.12 (2H, m, Ar CH), 7.05 (1H, d, $^3J_{\text{H,H}}$ 5.4, Ar CH), 5.73 (1H, d, $^3J_{\text{H,H}}$ 10.7, CH), 4.89 (1H, d, $^2J_{\text{H,H}}$ 10.1, CH₂), 4.63 (1H, d, $^3J_{\text{H,H}}$ 10.7, CH), 4.56 (1H, d, $^2J_{\text{H,H}}$ 10.1, CH₂), 4.18 (2H, d, $^2J_{\text{H,H}}$ 3, CH₂), 3.68 (3H, s, CH₃), 1.26 (9H, s, (CH₃)₃); δ_{C} (75.5 MHz, CDCl₃) 171.7 (quat. C), 169.6 (quat. C), 166.7 (quat. C), 166.3 (quat. C), 164.3 (quat. C), 151.4 (2 x quat. C), 147.2 (Ar CH), 118.3 (Ar CH), 112.2 (Ar CH), 83.5 (CH), 58.2 (CH), 53.4 (CH₃), 51.5 (CH₂), 40.2 (CH₂) 30.9 (3xCH₃); m/z (CI) 375 (M-N₂⁺, 70%); Found 375.1657 C₁₈H₂₂N₄O₅ [M-N₂⁺], requires 375.1655.

2-Amino-4-*tert*-butylpyridine²⁰⁶ **82**



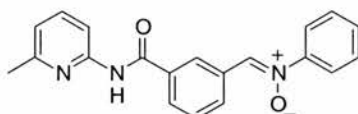
4-*tert*-Butylpyridine **81** (20.8 g, 154 mmol) was added to a suspension of sodium amide (12.0 g, 308 mmol) in xylene (40 ml) under N₂. The temperature was increased at a steady rate until a maximum of 140°C was reached. The reaction was kept at 140°C for a further 5 hours, or until the reaction was black and viscous in appearance. The cooled mixture was neutralised with 10% HCl solution, then extracted into dichloromethane. The combined aqueous layers were basified with 10% NaOH solution and re-extracted with dichloromethane. The organic layers were collected and dried with MgSO₄. The solvent was removed *in vacuo*, affording **82** as a yellow solid (11.1 g, 48%): M.p. 81-82°C; $\nu_{\max}(\text{KBr})/\text{cm}^{-1}$ 3441, 3283, 3156, 2958, 1627, 1551, 1429, 807; δ_{H} (300 MHz, CDCl₃) 7.96 (1H, d, $^3J_{\text{H,H}}$ 5.5, Ar CH), 6.65 (1H, d, $^3J_{\text{H,H}}$ 5.5, Ar CH), 6.47 (1H, s, Ar CH), 4.43 (br s, NH₂), 1.25 (9H, s, (CH₃)₃); δ_{C} (75.5 MHz, CDCl₃) 161.9 (quat. C), 158.7 (quat. C), 147.7 (Ar CH), 111.9 (Ar CH), 105.3 (Ar CH), 34.6 (quat. C), 30.4 (3 x CH₃); m/z (CI) 150 (M⁺, 15%).

N-(4-*tert*-Butyl-2-pyridyl)-chloroacetamide **83**



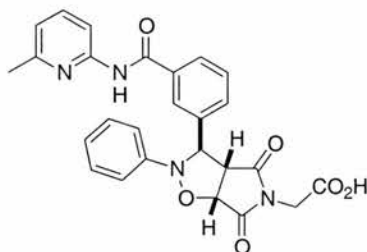
A solution of 4-*tert*-butyl-aminopyridine **82** (5.9 g, 40 mmol) in dry dichloromethane, was added dropwise to chloroacetyl chloride (1.5 g, 14 mmol) at 0°C under N₂. The reaction mixture was gradually warmed to room temperature once the addition was complete, then stirred overnight. Purification of the crude product was achieved by vacuum filtration through a short pad of silica using dichloromethane as the eluent. The solvent was removed *in vacuo*, affording **83** as a colourless powder (3.12 g, 99%): M.p. 105-107°C; $\nu_{\max}(\text{KBr})/\text{cm}^{-1}$ 2970, 1660, 1581, 791; δ_{H} (300 MHz, CDCl₃) 9.10 (br s, NH), 8.24-8.21 (2H, m, Ar CH), 7.09 (1H, d, $^3J_{\text{H,H}}$ 5.5, Ar CH), 4.18 (2H, s, CH₂), 1.32 (9H, s, (CH₃)₃); δ_{C} (75.5 MHz, CDCl₃) 172.3 (quat. C), 163.5 (quat. C), 151.1 (quat. C), 147.9 (Ar CH), 118.4 (Ar CH), 111.5 (Ar CH), 43.3 (CH₂), 35.5 (quat. C), 30.4 (3 x CH₃); m/z (ESI) 229 (M+H⁺, 25%), 227 (M+H⁺, 75).

N-[3-(*N'*-6-Methyl-2-pyridyl)-amidobenzylidene]-phenylamine *N*-oxide **104**



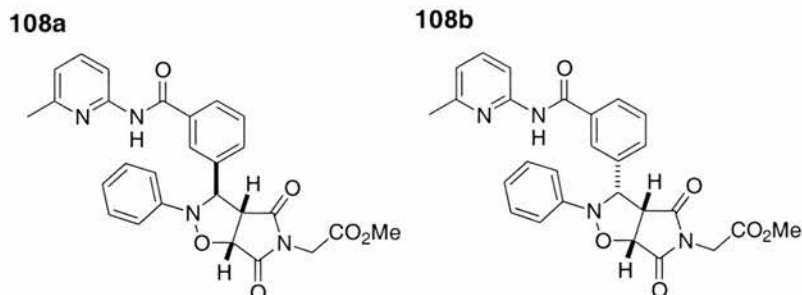
β -Phenylhydroxylamine **131** (460 mg, 4.2 mmol) and *N*-(6-Methyl-2-pyridyl)-3-formylbenzamide **123** (1.00 g, 4.2 mmol) were dissolved in ethanol (25 ml). The solution was left to stand in the dark at room temperature for 4 days. The resulting precipitate was filtered then recrystallised from ether/dichloromethane. Additionally the original filtrate was reduced *in vacuo* and the resulting solid recrystallised from ether/dichloromethane. Nitron **104** was isolated as a colourless solid (850 mg, 62%): M.p. 170-172°C; $\nu_{\max}(\text{KBr})/\text{cm}^{-1}$ 3184, 3066, 1675, 1600, 1452, 1069, 785, 731, 684; δ_{H} (300 MHz, CDCl₃) 8.92 (1H, s, NH), 8.83 (1H, s, Ar CH), 8.71 (1H, d, $^3J_{\text{H,H}}$ 8, Ar CH), 8.17 (1H, d, $^3J_{\text{H,H}}$ 8, Ar CH), 8.02 (1H, d, $^3J_{\text{H,H}}$ 8, Ar CH), 7.98 (1H, s, N=CH), 7.79-7.76 (2H, m, Ar CH), 7.64-7.58 (2H, m, Ar CH), 7.50-7.47 (3H, m, Ar CH), 6.90 (1H, d, $^3J_{\text{H,H}}$ 7, Ar CH), 2.43 (3H, s, CH₃); δ_{C} (75.5 MHz, CDCl₃) 165.5 (quat. C), 157.4 (quat. C), 151.1 (quat. C), 149.2 (quat. C), 139.1 (Ar CH), 135.2 (quat. C), 133.8 (Ar CH), 132.3 (Ar CH), 131.6 (quat. C), 130.6 (N=CH), 129.9 (Ar CH), 129.7 (3 x Ar CH), 127.9 (Ar CH), 122.1 (2 x Ar CH), 119.9 (Ar CH), 111.4 (Ar CH), 24.3 (CH₃); m/z (LSI) 332 (M+H⁺, 100%), 316 (9); Found 332.1397 [M+H⁺], C₂₀H₁₈N₃O₂ requires 332.1399.

2-{3c-[N-(6-Methyl-2-pyridyl)-3-benzamidyl]-4,6-dioxo-2-phenyl-(3ar,6ac)-hexahydropyrrolo[3,4-d]isoxazol-5-yl}-ethanoic acid **105**



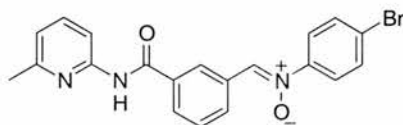
N-[3-(*N'*-6-Methyl-2-pyridyl)-amidobenzylidene]-phenylamine *N*-oxide **104** (270 mg, 0.83 mmol), was added to a solution of the 2-maleimidoethanoic acid **77** (130 mg, 0.83 mmol), in chloroform (20 ml). The reaction was then allowed to stand at 10°C in the absence of light for 3 days. An excess of ethyl acetate was then added to the reaction mixture to effect the precipitation of the cycloadduct. The precipitate was filtered, washed with ethyl acetate and dried under vacuum. Cycloadduct **105** was obtained as a colourless solid as a single diastereoisomer (400 mg, 99%): M.p. >165°C (decomp.); Found: C, 64.2; H, 4.6; N, 11.8. Calc for C₂₆H₂₂N₄O₆: C, 64.2; H, 4.6; N, 11.5. ν_{\max} (KBr)/cm⁻¹ 3396, 3254, 3062, 1719, 1452, 1418, 1166, 794, 753, 695; δ_{H} (300 MHz, CDCl₃) 11.57 (1H, br s, CO₂H), 10.93 (1H, s, NH), 8.13 (1H, d, ³J_{H,H} 8, Ar CH), 7.98 (1H, s, Ar CH), 7.88 (1H, d, ³J_{H,H} 8, Ar CH), 7.82-7.76 (1H, m, Ar CH), 7.49-7.46 (1H, m, Ar CH), 7.41-7.35 (1H, m, Ar CH), 7.17-7.11 (2H, m, Ar CH), 6.99 (1H, d, ³J_{H,H} 7, Ar CH), 6.93 (2H, d, ³J_{H,H} 8, Ar CH), 6.89-6.84 (1H, m, Ar CH), 5.37 (1H, s, cyclic CH), 5.14 (1H, d, ³J_{H,H} 7, cyclic CH), 4.05 (1H, d, ²J_{H,H} 12, CH₂), 3.88 (1H, d, ³J_{H,H} 7, cyclic CH), 3.83 (1H, d, ²J_{H,H} 12, CH₂), 2.49 (3H, s, CH₃); δ_{C} (75.5 MHz, CDCl₃) 174.9 (quat. CO₂H), 173.1 (quat. C), 171.3 (quat. C), 166.6 (quat. C), 154.8 (quat. C), 150.7 (quat. C), 147.4 (quat. C), 141.5 (Ar CH), 138.2 (quat. C), 134.4 (quat. C), 131.1 (Ar CH), 129.2 (2 x Ar CH), 128.9 (Ar CH), 128.7 (Ar CH), 126.2 (Ar CH), 122.9 (Ar CH), 120.0 (Ar CH), 115.3 (2 x Ar CH), 113.5 (Ar CH), 76.7 (CH), 69.4 (CH), 57.0 (CH), 40.8 (CH₂), 21.0 (CH₃); *m/z* (LSI) 487 (M+H⁺, 75%), 457 (15), 366 (39), 332 (100); Found 487.1625 [M+H⁺], C₂₆H₂₃N₄O₆ requires 487.1617.

2-[3*c*-[*N*-(6-Methyl-2-pyridyl)-4-benzamidyl]-4,6-dioxo-2-phenyl-(3*ar*,6*ac*)-hexahydropyrrolo[3,4-*d*]isoxazol-5-yl]-ethanoic acid, methyl ester **108**



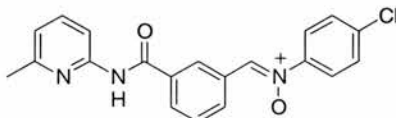
N-[4-(*N'*-6-Methyl-2-pyridyl)-amidobenzylidene]-phenylamine *N*-oxide **104** (150 mg, 0.45 mmol), was added to a solution of 2-maleimidoethanoic acid, methyl ester **79** (77 mg, 0.45 mmol) in chloroform (18 ml). The reaction was then allowed to stand at 10°C in the absence of light for 3 days. An excess of hexane was then added to the reaction mixtures to effect the precipitation of the cycloadduct. The precipitate was filtered, washed with hexane then recrystallised from chloroform/hexane and dried under vacuum to afford **108** a beige solid as a 7:3 ratio of diastereoisomers (70 mg, 32%): M.p. >80°C (decomp.); $\nu_{\max}(\text{KBr})/\text{cm}^{-1}$ 3351, 1792, 1753, 1676, 1271, 845, 792, 760, 695; δ_{H} (300 MHz, CDCl_3 , major isomer **108a**) 8.63 (br s, NH), 8.21-8.14 (1H, m, Ar CH), 7.92-7.87 (2H, m, Ar CH), 7.67-7.61 (1H, m, Ar CH), 7.57-7.52 (2H, m, Ar CH), 7.21-7.15 (2H, m, Ar CH), 7.10-7.05 (1H, m, Ar CH), 6.99-6.93 (3H, m, Ar CH), 5.49 (1H, s, CH), 5.13 (1H, d, $^3J_{\text{H,H}}$ 7, CH), 3.97-3.95 (3H, m, CH and CH_2), 3.70 (3H, s, OCH_3), 2.46 (3H, s, CH_3); δ_{H} (300 MHz, CDCl_3 , minor isomer **108b**) 8.63 (br s, NH), 8.50 (1H, d, $^3J_{\text{H,H}}$ 8, Ar CH), 8.21-8.14 (1H, m, Ar CH), 8.05-8.01 (1H, m, Ar CH), 7.92-7.87 (1H, m, Ar CH), 7.67-7.61 (1H, m, Ar CH), 7.57-7.52 (1H, m, Ar CH), 7.21-7.15 (2H, m, Ar CH), 7.10-7.05 (1H, m, Ar CH), 6.99-6.93 (3H, m, Ar CH), 5.18 (1H, d, $^3J_{\text{H,H}}$ 7, CH), 4.77 (1H, d, $^3J_{\text{H,H}}$ 9, CH), 4.21 (2H, dd, $^2J_{\text{H,H}}$ 17, CH_2), 4.03 (1H, dd, $^3J_{\text{H,H}}$ 7, $^3J_{\text{H,H}}$ 9, CH), 3.76 (3H, s, OCH_3), 2.45 (3H, s, CH_3); δ_{C} (75.5 MHz, CDCl_3 , major isomer **108a**) 173.7 (quat. C), 172.4 (quat. C), 166.4 (quat. C), 165.0 (quat. C), 156.9 (quat. C), 150.6 (quat. C), 147.2 (quat. C), 141.9 (quat. C), 138.8 (Ar CH), 134.7 (quat. C), 128.3 (2 x Ar CH), 127.5 (2 x Ar CH), 125.6 (2 x Ar CH), 123.2 (Ar CH), 119.5 (Ar CH), 115.3 (2 x Ar CH), 111.0 (Ar CH), 76.6 (CH), 69.4 (CH), 57.0 (CH), 52.7 (CH_3), 39.5 (CH_2), 23.9 (CH_3); m/z (FAB) 523 ($\text{M}+\text{Na}^+$, 38%), 501 ($\text{M}+\text{H}^+$, 100), 413 (10); Found 501.1760 [$\text{M}+\text{H}^+$], $\text{C}_{27}\text{H}_{25}\text{N}_4\text{O}_6$ requires 501.1774.

N-[3-(*N'*-6-Methyl-2-pyridyl)-amidobenzylidene]-4-bromophenylamine *N*-oxide **109**



p-Bromophenylhydroxylamine **132** (200 mg, 1.1 mmol) was dissolved in ethanol (4 ml) and *N*-(6-Methyl-2-pyridyl)-3-chloromethylbenzamide **123** (260 mg, 1.1 mmol) was added. The reaction was left to stand in the absence of light for 16 hours. The resulting precipitate was filtered then recrystallised from ethanol. Nitron **109** was isolated as a colourless solid (430 mg, 95%): M.p. 188-189°C; $\nu_{\max}(\text{KBr})/\text{cm}^{-1}$ 3423, 3046, 1682, 1600, 798, 685; δ_{H} (300 MHz, CDCl_3) 8.88 (1H, br s, NH), 8.83 (1H, s, Ar CH), 8.70 (1H, d, $^3J_{\text{H,H}}$ 8, Ar CH), 8.18 (1H, d, $^3J_{\text{H,H}}$ 8, Ar CH), 8.04 (1H, d, $^3J_{\text{H,H}}$ 8, Ar CH), 7.98 (1H, s, N=CH), 7.57-7.69 (6H, m, Ar CH), 6.93 (1H, d, $^3J_{\text{H,H}}$ 7, Ar CH), 2.44 (3H, s, CH_3); δ_{C} (75.5 MHz, CDCl_3) 165.0 (quat. C), 156.8 (quat. C), 150.6 (quat. C), 147.7 (quat. C), 139.0 (Ar CH), 134.8 (quat. C), 133.4 (Ar CH), 132.5 (Ar CH), 132.1 (N=CH), 131.0 (quat. C), 129.8 (Ar CH), 129.4 (2 x Ar CH), 127.7 (Ar CH), 124.3 (quat. C), 123.3 (2 x Ar CH), 119.7 (Ar CH), 111.2 (Ar CH), 23.9 (CH_3); m/z (ESI) 450 ($\text{M}+\text{K}^+$ (^{81}Br), 7%), 448 ($\text{M}+\text{K}^+$ (^{79}Br), 7%), 434 ($\text{M}+\text{Na}^+$ (^{81}Br), 92%), 432 ($\text{M}+\text{Na}^+$ (^{79}Br), 100%), 412 (M^+ (^{81}Br), 5%), 410 (M^+ (^{79}Br), 5%); Found 410.0504 [M^+], $\text{C}_{20}\text{H}_{16}\text{N}_3\text{O}_2\text{Br}$ requires 410.0495.

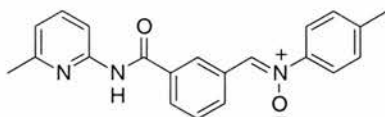
N-[3-(*N'*-6-Methyl-2-pyridyl)-amidobenzylidene]-4-chlorophenylamine *N*-oxide **110**



p-Chlorophenylhydroxylamine **133** (250 mg, 1.74 mmol) and *N*-(6-Methyl-2-pyridyl)-3-formylbenzamide **123** (420 mg, 1.74 mmol) were dissolved in ethanol (10 ml). The solution was left to stand in the dark at room temperature for 4 days. The resulting precipitate was filtered and recrystallised from ethanol. Nitron **110** was isolated as a colourless solid (360 mg, 57%): M.p. 150-151°C; Found: C, 65.9; H, 4.1; N, 11.6. Calc. for $\text{C}_{20}\text{H}_{16}\text{N}_3\text{O}_2\text{Cl}$: C, 65.7; H, 4.4; N, 11.5. $\nu_{\max}(\text{KBr})/\text{cm}^{-1}$ 3379, 3095, 1680, 1579, 1456, 1185, 1080, 840, 792, 684; δ_{H} (300 MHz, CDCl_3) 8.90-8.80 (2H, m, NH, ArCH), 8.69 (1H, d, $^3J_{\text{H,H}}$ 8, Ar CH), 8.18 (1H, d, $^3J_{\text{H,H}}$ 8, Ar CH), 8.05 (1H, d, Ar CH), 7.98 (1H, s, N=CH), 7.74 (2H, d, $^3J_{\text{H,H}}$ 8, Ar CH), 7.69-7.56 (2H, m, Ar CH), 7.47 (2H, d, $^3J_{\text{H,H}}$ 8, Ar CH), 6.92 (1H, d, $^3J_{\text{H,H}}$ 8, Ar CH), 2.45 (3H, s, CH_3); δ_{C} (75.5 MHz, CDCl_3) 165.0 (quat. C), 157.0 (quat. C), 150.7 (quat. C), 147.2 (quat. C), 138.8 (Ar CH), 136.2 (quat. C), 134.9 (quat. C), 133.5 (Ar CH), 132.0 (Ar CH), 131.0 (quat. C), 129.8 (N=CH), 129.5 (2 x Ar CH), 127.7 (Ar CH), 123.0 (3 x Ar CH),

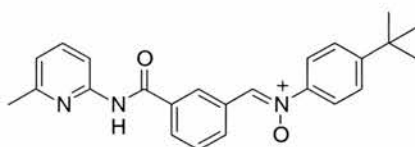
119.6 (Ar CH), 111.1 (Ar CH), 24.0 (CH₃); *m/z* (EI) 365 (³⁵M⁺, 4%), 349 (100), 320 (62); Found 388.0824 [M+Na⁺], C₂₀H₁₆N₃O₂³⁵ClNa requires 388.0829.

N-[3-(*N'*-6-Methyl-2-pyridyl)-amidobenzylidene]-4-methylphenylamine *N*-oxide **111**



p-Methyl-phenylhydroxylamine **134** (300 mg, 2.4 mmol) was dissolved in ethanol (10 ml) and *N*-(6-methyl-2-pyridyl)-3-chloromethylbenzamide **123** (585 mg, 2.4 mmol) was added. The reaction was left to stand in the absence of light for 16 hours. The resulting precipitate was filtered then recrystallised from ethanol. Nitron **111** was isolated as a colourless solid (300 mg, 36%): M.p. 198-200°C; Found: C, 72.8; H, 5.3; N, 12.3. Calc. for C₂₁H₁₉N₃O₂: C, 73.0; H, 5.5; N, 12.2. ν_{\max} (KBr)/cm⁻¹ 3224, 3043, 2918, 1660, 1596, 1535, 1453, 1063, 791, 682; δ_{H} (300 MHz, CDCl₃) 8.82 (1H, br s, NH), 8.83 (2H, m, Ar CH), 8.70 (1H, d, ³J_{H,H} 8, Ar CH), 8.16 (1H, d, ³J_{H,H} 8, Ar CH), 8.01 (1H, d, ³J_{H,H} 8, Ar CH), 7.96 (1H, s, N=CH), 7.67-7.55 (4H, m, Ar CH), 7.27 (1H, d, ³J_{H,H} 9 Ar CH), 6.91 (1H, d, ³J_{H,H} 8, Ar CH), 2.42 (6H, s, 2xCH₃); δ_{C} (75.5 MHz, CDCl₃) 164.6 (quat. C), 156.8 (quat. C), 150.6 (quat. C), 146.7 (quat. C), 140.6 (Ar CH), 138.6 (quat. C), 135.7 (quat. C), 134.0 (Ar CH), 132.8 (Ar CH), 129.7 (quat. C), 129.8 (N=CH), 129.5 (2 x Ar CH), 127.7 (Ar CH), 123.0 (3 x Ar CH), 119.6 (Ar CH), 111.1 (Ar CH), 23.9 (CH₃) 21.1 (CH₃); *m/z* (ESI) 346 (M+H⁺, 100%); Found 368.1365 [M+Na⁺], C₂₁H₁₉N₃O₂Na requires 368.1365.

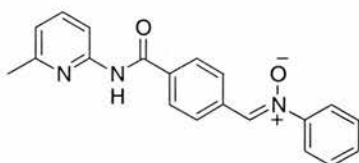
N-[3-(*N'*-6-Methyl-2-pyridyl)-amidobenzylidene]-4-*tert*-butylphenylamine *N*-oxide **112**



p-tert-Butyl-phenylhydroxylamine **135** (315 mg, 1.67 mmol) was dissolved in ethanol (5 ml) and *N*-(6-methyl-2-pyridyl)-3-formylbenzamide **123** (400 mg, 1.67 mmol) was added. The reaction was left to stand in the absence of light for 16 hours. The resulting precipitate was filtered then recrystallised from ethanol. Nitron **112** was isolated as a colourless solid (420 mg, 61%): M.p. 133-135°C; Found: C, 69.8; H, 6.7; N, 13.7. Calc. for C₂₄H₂₅N₃O₂: C, 69.4; H, 6.8; N, 13.5. ν_{\max} (KBr)/cm⁻¹ 3429, 3064, 2962, 1681, 1450, 786; δ_{H} (300 MHz, CDCl₃) 10.05 (br s, NH) 8.92-8.81 (1H, br m, Ar CH), 8.71 (1H, d, ³J_{H,H} 8, Ar CH), 8.17 (2H, d, ³J_{H,H} 8, Ar CH), 7.98 (1H, s, N=CH), 7.72-7.61 (5H, m, Ar CH), 7.49 (1H, d, ³J_{H,H} 8 Ar CH), 6.92 (1H, d, ³J_{H,H} 8 Ar CH), 2.44 (3H, s, CH₃), 1.35 (9H, s, (CH₃)₃); δ_{C} (75.5 MHz,

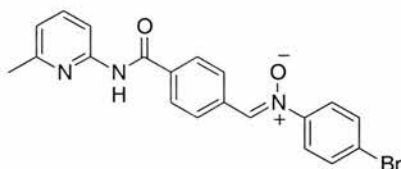
CDCl₃) 165.1 (quat. C), 157.0 (quat. C), 153.8 (quat. C), 150.7 (quat. C), 146.5 (quat. C), 138.8 (Ar CH), 134.8 (quat. C), 133.0 (Ar CH), 132.0 (Ar CH), 131.4 (quat. C), 129.4 (N=CH), 129.3 (Ar CH), 127.4 (Ar CH), 126.2 (2 x Ar CH), 121.2 (2 x Ar CH), 119.6 (Ar CH), 111.0 (Ar CH), 34.9 (quat. C), 31.3 (3 x CH₃), 24.0 (CH₃); *m/z* (ESI) 410 (M+Na⁺, 18%), 388 (100); Found 410.1844 [M+Na⁺], C₂₄H₂₅N₃O₂Na requires 410.1844.

N-[4-(*N'*-6-Methyl-2-pyridyl)-amidobenzylidene]-phenylamine *N*-oxide **113**



β -Phenylhydroxylamine **131** (460 mg, 4.2 mmol) and *N*-(6-Methyl-2-pyridyl)-4-formylbenzamide **146** (1.0 g, 4.2 mmol) were dissolved in ethanol (25 ml). The solution was left to stand in the dark at room temperature for 4 days. The precipitate formed was filtered and recrystallised from ethanol. Nitron **113** was isolated as a beige solid (1.42 g, 97%): M.p. 154-156°C; ν_{\max} (KBr)/cm⁻¹ 3343, 3120, 1666, 1607, 1576, 1070, 794, 772, 684; δ_{H} (300 MHz, CDCl₃) 8.72 (1H, s, NH), 8.48 (2H, d, ³J_{H,H} 8, Ar CH), 8.19-8.15 (1H, m, Ar CH), 8.03-7.81 (3H, m, 2 x Ar CH and 1 x N=CH), 7.80-7.77 (2H, m, Ar CH), 7.67-7.61 (1H, m, Ar CH), 7.49-7.47 (3H, m, Ar CH), 6.93 (1H, d, ³J_{H,H} 8, Ar CH), 2.45 (3H, s, CH₃); δ_{C} (75.5 MHz, CDCl₃) 165.5 (quat. C), 157.3 (quat. C), 151.0 (quat. C), 149.4 (quat. C), 139.2 (Ar CH), 136.0 (quat. C), 134.3 (quat. C), 133.8 (N=CH), 130.7 (Ar CH), 129.7 (2 x Ar CH), 129.4 (2 x Ar CH), 127.9 (2 x Ar CH), 122.1 (2 x Ar CH), 120.0 (Ar CH), 111.5 (Ar CH), 24.4 (CH₃); *m/z* (FAB) 332 (M+H⁺, 100%), 316 (11), 224 (9), 208 (7); Found 332.1389 [M+H⁺], C₂₀H₁₈N₃O₂ requires 332.1399.

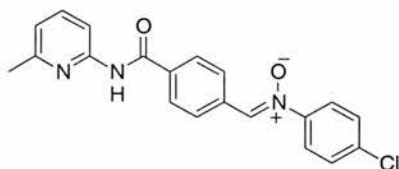
N-[4-(*N'*-6-Methyl-2-pyridyl)-amidobenzylidene]-4-bromophenylamine *N*-oxide **114**



p-Bromophenylhydroxylamine **132** (250 mg, 1.3 mmol) was dissolved in ethanol (5 ml) and *N*-(6-methyl-2-pyridyl)-4-chloromethylbenzamide **146** (320 mg, 1.3 mmol) was added. The reaction was left to stand in the absence of light for 16 hours. The resulting precipitate was filtered then recrystallised from ethanol. Nitron **114** was isolated as a colourless solid (530 mg, 99%): M.p. 210-212°C; Found: C, 58.5; H, 3.6; N, 10.7. Calc. for C₂₀H₁₆N₃O₂Br: C, 58.6; H, 3.8; N, 10.6; ν_{\max} (KBr)/cm⁻¹ 3339, 3046, 1647, 1597, 1416, 787; δ_{H} (300 MHz,

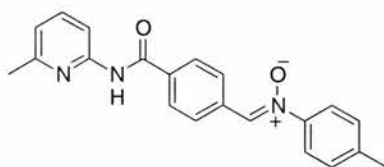
CDCl₃) 8.63 (br s, NH), 8.48 (2H, d, ³J_{H,H} 8, Ar CH), 8.19 (1H, d, ³J_{H,H} 8, Ar CH), 8.03 (2H, d, ³J_{H,H} 8, Ar CH), 7.99 (1H, s, N=CH), 7.71-7.62 (5H, m, Ar CH), 6.97-6.94 (1H, d, Ar CH), 2.49 (3H, s, CH₃); δ_C (75.5 MHz, CDCl₃) 164.5 (quat. C), 156.8 (quat. C), 150.5 (quat. C), 148.8 (quat. C), 138.7 (Ar CH), 135.4 (quat. C), 133.4 (quat. C), 133.2 (Ar CH), 132.2 (2 x Ar CH), 129.0 (2 x Ar CH), 127.4 (2 x Ar CH), 124.2 (quat. C), 123.11 (2 x Ar CH), 119.5 (Ar CH), 110.9 (Ar CH), 23.8 (CH₃); *m/z* (EI+) 410 (M⁺, 5%); Found 434.0298 [M+Na⁺ (⁸¹Br)], C₂₀H₁₆N₃O₂⁸¹BrNa requires 434.0303; Found 432.0326, [M+Na⁺ (⁷⁹Br)], C₂₀H₁₆N₃O₂⁷⁹BrNa requires 432.0324.

N-[4-(*N'*-6-Methyl-2-pyridyl)-amidobenzylidene]-4-chlorophenylamine *N*-oxide **115**



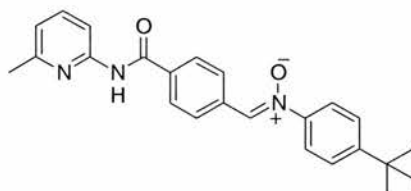
p-Chlorophenylhydroxylamine **133** (250 mg, 1.72 mmol) was dissolved in ethanol (10 ml) and *N*-(6-methyl-2-pyridyl)-4-chloromethylbenzamide **146** (420 mg, 1.72 mmol) was added. The reaction was left to stand in the absence of light for 16 hours. The resulting precipitate was filtered then recrystallised from ethanol. Nitron **115** was isolated as a colourless solid (490 mg, 79%); M.p. 218-220°C; Found: C, 65.7; H, 4.3; N, 11.3. Calc. for C₂₀H₁₆N₃O₂Cl: C, 65.7; H, 4.4; N, 11.5. ν_{max}(KBr)/cm⁻¹ 3410, 3046, 1670, 1597, 1453, 1073, 831, 789; δ_H (300 MHz, CDCl₃) 9.00 (br s, NH), 8.80 (1H, s, Ar CH), 8.79 (1H, d, ³J_{H,H} 8, Ar CH), 8.16 (1H, d, ³J_{H,H} 8, Ar CH), 7.95 (1H, s, N=CH), 7.73 (2H, d, ³J_{H,H} 8, Ar CH), 7.65-7.55 (2H, m, Ar CH), 7.44 (2H, d, ³J_{H,H} 8, Ar CH), 6.91 (2H, d, ³J_{H,H} 8, Ar CH), 2.42 (3H, s, CH₃); δ_C (75.5 MHz, CDCl₃) 165.0 (quat. C), 157.0 (quat. C), 150.7 (quat. C), 147.2 (quat. C), 138.8 (Ar CH), 136.2 (quat. C), 134.8 (quat. C), 133.5 (Ar CH), 132.0 (Ar CH), 131.0 (quat. C), 129.8 (N=CH), 129.4 (2 x Ar CH), 127.8 (Ar CH), 123.0 (3 x Ar CH), 119.6 (Ar CH), 111.1 (Ar CH), 24.0 (CH₃); *m/z* (ESI) 388 (³⁵M+Na⁺, 100%), 366 (³⁵M⁺, 80%); Found 388.0840 [³⁵M⁺+Na], C₂₀H₁₆N₃O₂³⁵ClNa requires 388.0829.

N-[4-(*N'*-6-Methyl-2-pyridyl)-amidobenzylidene]-4-methylphenylamine *N*-oxide **116**



p-Methyl-phenylhydroxylamine **134** (300 mg, 2.4 mmol) was dissolved in ethanol (10 ml) and *N*-(6-methyl-2-pyridyl)-4-chloromethylbenzamide **123** (585 mg, 2.4 mmol) was added. The reaction was left to stand in the absence of light for 16 hours. The resulting precipitate was filtered then recrystallised from ethanol. Nitrone **116** was isolated as a colourless solid (570 mg, 69%): M.p. 147-149°C; Found: C, 72.9; H, 5.3; N, 12.1. Calc. for C₂₁H₁₉N₃O₂: C, 73.0; H, 5.5; N, 12.2. $\nu_{\max}(\text{KBr})/\text{cm}^{-1}$ 3339, 1669, 1598, 1524, 1453, 1073, 784; δ_{H} (300 MHz, CDCl₃) 8.67 (br s, NH), 8.48 (2H, d, $^3J_{\text{H,H}}$ 8, Ar CH), 8.19 (1H, d, $^3J_{\text{H,H}}$ 8, Ar CH), 8.04-7.99 (3H, m, N=CH, Ar CH), 7.69-7.63 (3H, m, Ar CH), 7.28 (2H, d, $^3J_{\text{H,H}}$ 8, Ar CH), 6.94 (1H, d, $^3J_{\text{H,H}}$ 8, Ar CH), 2.45 (3H, s, CH₃) 2.42 (3H, s, CH₃); δ_{C} (75.5 MHz, CDCl₃) 165.0 (quat. C), 156.8 (quat. C), 150.6 (quat. C), 147.7 (quat. C), 140 (quat. C), 139.0 (Ar CH), 134.8 (quat. C), 134.1 (quat. C), 133.3 (Ar CH), 130.0 (N=CH), 129.8 (2 x Ar CH), 129.0 (Ar CH), 127.6 (Ar CH), 121.5 (3 x Ar CH), 119.7 (Ar CH), 111.1 (Ar CH), 24.0 (CH₃) 21.3 (CH₃); *m/z* (ESI) 368 (M+Na⁺, 10%), 346 (M+H⁺, 100%); Found 368.1368 [M+Na⁺], C₂₁H₁₉N₃O₂Na requires 368.1375.

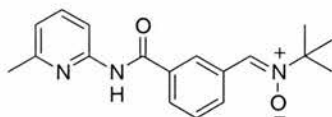
N-[4-(*N'*-6-Methyl-2-pyridyl)-amidobenzylidene]-4-*tert*butylphenylamine *N*-oxide **117**



p-tert-Butyl-phenylhydroxylamine **135** (315 mg, 1.67 mmol) was dissolved in ethanol (5 ml) and *N*-(6-methyl-2-pyridyl)-4-formylbenzamide **146** (260 mg, 1.60 mmol) was added. The reaction was left to stand in the absence of light for 16 hours. The resulting precipitate was filtered then recrystallised from ethanol. Nitrone **117** was isolated as a colourless solid (410 mg, 60%); M.p. 160-162°C; $\nu_{\max}(\text{KBr})/\text{cm}^{-1}$ 3303, 2956, 1672, 1531, 1454, 1271, 794; δ_{H} (500 MHz, CDCl₃) 8.72 (br s, NH), 8.49 (1H, d, $^3J_{\text{H,H}}$ 8, Ar CH), 8.20 (2H, d, $^3J_{\text{H,H}}$ 8, Ar CH), 8.02 (2H, d, $^3J_{\text{H,H}}$ 8, Ar CH), 7.99 (1H, s, N=CH), 7.71-7.69 (2H, m, Ar CH), 7.66 (1H, t, $^3J_{\text{H,H}}$ 8, Ar CH), 7.50-7.48 (2H, m, Ar CH), 6.94 (1H, d, $^3J_{\text{H,H}}$ 8, Ar CH), 2.48 (3H, s, CH₃) 1.38 (9H, s, CH₃); δ_{C} (75.5 MHz, CDCl₃) 164.7 (quat. C), 156.8 (quat. C), 153.8 (quat. C), 150.6 (quat. C), 146.5 (quat. C), 138.9 (Ar CH), 135.3 (quat. C), 134.0 (quat. C), 133.0 (Ar

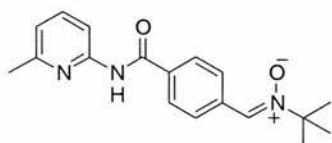
CH), 128.9 (N=CH), 127.5 (2 x Ar CH), 126.1 (2 x Ar CH), 121.3 (2 x Ar CH), 119.6 (Ar CH), 111.1 (2 x Ar CH), 34.9 (quat. C), 31.2 (3 x CH₃), 23.9 (CH₃); *m/z* (ESI) 388 (M+H⁺, 100%); Found 410.1838 [M+Na⁺], C₂₄H₂₅N₃O₂Na requires 410.1838.

N-[3-(*N*'-6-Methyl-2-pyridyl)-amidobenzylidene]-4-*tert*butylamine *N*-oxide **118**



tert-Butylhydroxylamine **158** (120 mg, 1.30 mmol) was dissolved in ethanol (5 ml) and *N*-(6-methyl-2-pyridyl)-3-chloromethylbenzamide **123** (300 mg, 1.24 mmol) was added. The reaction was left to stand in the absence of light for 16 hours. The resulting precipitate was filtered then recrystallised from ethanol. Nitron **118** was isolated as a colourless solid (340 mg, 84%); M.p. 157-159°C; Found: C, 68.9; H, 7.0; N, 13.6. Calc. for C₁₈H₂₁N₃O₂: C, 69.4; H, 6.8; N, 13.5. ν_{\max} (KBr)/cm⁻¹ 3165, 3039, 2972, 1661, 1539, 793; δ_{H} (300 MHz, CDCl₃) 8.84 (br s, NH), 8.75 (1H, s, Ar CH), 8.53 (1H, d, ³*J*_{H,H} 8, Ar CH), 8.14 (1H, d, ³*J*_{H,H} 8, Ar CH), 7.97 (1H, d, ³*J*_{H,H} 8, Ar CH), 7.63-7.58 (2H, m, N=CH, Ar CH), 7.51 (1H, t, ³*J*_{H,H} 8 Ar CH), 6.88 (1H, d, ³*J*_{H,H} 8 Ar CH), 2.39 (3H, s, CH₃), 1.60 (9H, s, 3 x CH₃); δ_{C} (75.5 MHz, CDCl₃) 165.3 (quat. C), 157.0 (quat. C), 150.7 (quat. C), 138.7 (Ar CH), 134.6 (quat. C), 131.9 (Ar CH), 131.6 (quat. C), 129.0 (N=CH, Ar CH), 127.1 (2 x Ar CH), 119.5 (Ar CH), 111.1 (Ar CH), 71.3 (quat. C), 28.3 (3 x CH₃), 23.9 (CH₃); *m/z* (ESI) 334 (M+Na⁺, 100%), 312 (M+H⁺, 70); Found 334.1524 [M+Na⁺], C₁₈H₂₁N₃O₂Na requires 334.1531.

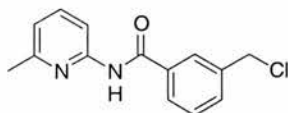
N-[4-(*N*'-6-Methyl-2-pyridyl)-amidobenzylidene]-4-*tert*-butylamine *N*-oxide **119**



tert-Butylhydroxylamine **188** (120 mg, 1.30 mmol) was dissolved in ethanol (5 ml) and *N*-(6-Methyl-2-pyridyl)-4-chloromethylbenzamide **146** (300 mg, 1.24 mmol) was added. The reaction was left to stand in the absence of light for 16 hours. The resulting precipitate was filtered then recrystallised from ethanol. Nitron **119** was isolated as a colourless solid (340 mg, 84%); M.p. 201-203°C; Found: C, 69.1; H, 7.0; N, 13.4. Calc. for C₁₈H₂₁N₃O₂: C, 69.4; H, 6.8; N, 13.5. ν_{\max} (KBr)/cm⁻¹ 3223, 3058, 2979, 1658, 1538, 1454, 1296, 1129, 871, 781, 670; δ_{H} (300 MHz, CDCl₃) 8.60 (br s, NH), 8.38 (2H, d, ³*J*_{H,H} 9, Ar CH), 8.17 (1H, d, ³*J*_{H,H} 8, Ar CH), 7.96 (2H, d, ³*J*_{H,H} 9, Ar CH), 7.66-7.61 (2H, m, N=CH, Ar CH), 6.92 (1H, d, ³*J*_{H,H} 8 Ar CH), 2.46 (3H, s, CH₃) 1.62 (9H, s, 3xCH₃); δ_{C} (75.5 MHz, CDCl₃) 165.0 (quat.

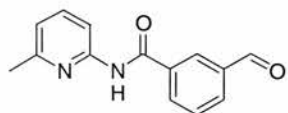
C), 157.1 (quat. C), 150.9 (quat. C), 139.0 (Ar CH), 135.1 (quat. C), 134.6 (quat. C), 129.1 (N=CH), 129.0 (2 x Ar CH), 127.5 (2 x Ar CH), 119.8 (Ar CH), 111.2 (Ar CH), 71.8 (quat. C), 28.6 (3 x CH₃), 24.2 (CH₃); *m/z* (ESI) 334 (M+Na⁺, 100%), 278 (75); Found 334.1541 [M⁺], C₁₈H₂₁N₃O₂Na requires 334.1531.

***N*-(6-Methyl-2-pyridyl)-3-chloromethylbenzamide 122**



2-Amino-6-picoline **120** (5.15 g, 48 mmol) as a solution in dry dichloromethane (50 ml) was added dropwise to neat 3-(chloromethyl)benzoyl chloride **121** (3.00 g, 16 mmol) at 0°C. The solution was then allowed to warm to room temperature and stirred for 16 hours. The solvent was removed *in vacuo* and the crude residue was purified using flash column chromatography (SiO₂, 3:2 hexane:ethyl acetate) to give **122** as a colourless solid (4.05 g, 98%): M.p. 66-67°C; $\nu_{\max}(\text{KBr})/\text{cm}^{-1}$ 3264, 3060, 1676, 1605, 1455, 788, 709, 685, 661; δ_{H} (300 MHz, CDCl₃) 8.53 (br s, NH), 8.17 (1H, d, ³*J*_{H,H} 8, Ar CH), 7.94 (1H, s, Ar CH), 7.86 (1H, d, ³*J*_{H,H} 8, Ar CH), 7.64 (1H, dd, ³*J*_{H,H} 8, ³*J*_{H,H} 7, Ar CH), 7.54 (1H, d, ³*J*_{H,H} 8, Ar CH), 7.51 (1H, dd, ³*J*_{H,H} 8, ³*J*_{H,H} 8, Ar CH), 6.93 (1H, d, ³*J*_{H,H} 7, Ar CH), 4.63 (2H, s, CH₂Cl), 2.47 (3H, s, CH₃); δ_{C} (75.5 MHz, CDCl₃) 165.2 (quat. C), 156.9 (quat. C), 150.8 (quat. C), 138.9 (Ar CH), 138.3 (quat. C), 134.9 (quat. C), 132.2 (Ar CH), 129.3 (Ar CH), 127.5 (Ar CH), 127.2 (Ar CH), 119.6 (Ar CH), 111.2 (Ar CH), 45.5 (CH₂Cl), 23.9 (CH₃); *m/z* (EI) 262 (M⁺ (³⁷Cl), 15%), 260 (M⁺ (³⁵Cl), 32), 232 (39), 231 (100), 197 (9), 153 (97), 125 (57), 89 (62); Found 260.0719 [M⁺], C₁₄H₁₃N₂OCl requires 260.0716.

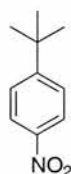
***N*-(6-Methyl-2-pyridyl)-3-formylbenzamide²⁰⁷ 123**



A mixture of *N*-(6-Methyl-2-pyridyl)-3-chloromethylbenzamide **122** (3.90 g, 15 mmol) and hexamethylene tetraamine (6.45 g, 45 mmol) in ethanol/water 18 ml (50:50; V:V) was heated to reflux for 16 hours. After this time 12M HCl (*ca.* 3 ml) was added and the reaction mixture was refluxed for a further 30 mins. After cooling to room temperature the mixture was diluted with water (100 ml) and extracted using dichloromethane (300 ml). The combined organic extracts were washed with water and dried over MgSO₄ and removed *in vacuo*. The residue was purified using flash column chromatography on silica gel (6:4 hexane:ethyl acetate) affording **123** as a colourless solid (2.20 g, 61%): M.p. 126-128°C; $\nu_{\max}(\text{KBr})/\text{cm}^{-1}$

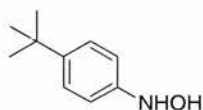
3263 (N-H), 1678, 1601, 1534, 1577, 1455; δ_{H} (300 MHz, CDCl_3) 10.10 (1H, s, CHO), 8.70 (1H, br s, NH), 8.43 (1H, s, Ar CH), 8.24-8.17 (2H, m, Ar CH), 8.10-8.07 (1H, m, Ar CH), 7.73-7.65 (2H, m, Ar CH), 6.97 (1H, d, $^3J_{\text{H,H}}$ 8, Ar CH), 2.49 (3H, s, CH_3); δ_{C} (75.5 MHz, CDCl_3) 191.5 (CHO), 164.3 (quat. C), 156.8 (quat. C), 150.4 (quat. C), 139.0 (Ar CH), 136.5 (quat. C), 135.2 (quat. C), 133.0 (Ar CH), 132.6 (Ar CH), 130.6 (Ar CH), 128.3 (Ar CH), 119.7 (Ar CH), 111.1 (Ar CH), 23.7 (CH_3); m/z (CI) 241 ($\text{M}+\text{H}^+$, 100%), 211 (5). Found 240.0888 [M^+], $\text{C}_{14}\text{H}_{12}\text{N}_2\text{O}_2$ requires 240.0899.

4 Nitro-*tert*-butyl-benzene²⁰⁸ **124**



A mixture of conc. H_2SO_4 (54 ml) and HNO_3 (36 ml) was added to *tert*-butylbenzene (56 g, 420 mmol) in an ice bath at such a rate that the temperature was kept below 5°C . After stirring for 1 hour the mixture was poured onto an ice-water bath. The crude mixture was extracted with ether, dried (MgSO_4) and removed *in vacuo*. The crude product was purified by flash column chromatography (SiO_2 , 1:20 hexane:ethyl acetate) affording **124** as a yellow oil (52 g, 61%): δ_{H} (300 MHz, CDCl_3) 8.09 (2H, d, $^3J_{\text{H,H}}$ 7, Ar H), 7.45 (2H, d, $^3J_{\text{H,H}}$ 7, Ar H), 1.31 (9H, s, $(\text{CH}_3)_3$); m/z (EI) 179 (M^+ , 15%), 164 (100), 136 (14).

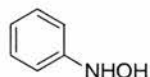
p-*tert*-Butylphenylhydroxylamine **125**



Zinc dust (9.22 g, 141 mmol) was added portion-wise to a stirred solution of NH_4Cl (1.84 g, 34 mmol) and 4-nitro-*tert*-butyl-benzene **124** (5.00 g, 30 mmol) in water (30 ml) at room temperature. After addition of the zinc dust was complete the reaction mixture was stirred for a further 15 minutes. The resulting slurry was filtered, and the filtrate saturated with NaCl (60 g) and cooled to 0°C . The resulting precipitate was collected and dissolved in diethyl ether (80 ml). The organic solution was then dried (MgSO_4), and the solvent removed *in vacuo*. The resulting residue, containing *p*-*tert*-butylphenylhydroxylamine **125** was used immediately without further purification (4.40 g, 77%): M.p $74\text{--}76^\circ\text{C}$; $\nu_{\text{max}}(\text{KBr})/\text{cm}^{-1}$ 3267, 2956, 1512, 1462, 1363, 1020, 899, 780; δ_{H} (300 MHz, CDCl_3) 7.33 (2H, d, $^3J_{\text{H,H}}$ 7, Ar H), 6.95 (2H, d, $^3J_{\text{H,H}}$ 7, Ar H), 5.45 (br s, NH or OH), 1.31 (9H, s, $(\text{CH}_3)_3$); δ_{C} (75.5 MHz,

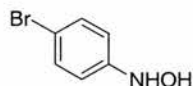
CDCl₃) 147.0 (quat. C), 145.5 (quat. C), 125.8 (2 x Ar CH), 155.0 (2 x Ar CH), 58.5 (quat. C), 31.5 (3 x CH₃); *m/z* (EI) 165 (M⁺, 35%), 150 (100), 134 (74), 118 (17), 105 (15).

***β*-Phenylhydroxylamine^{209,210} 131**



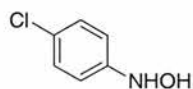
Zinc dust (24.8 g, 380 mmol) was added portion-wise to a stirred solution of ammonium chloride (5.0 g, 90 mmol) and nitrobenzene (10.0 g, 80 mmol) in water (160 ml) at room temperature. After addition of the zinc dust was complete the reaction mixture was stirred for a further 15 minutes. The resulting slurry was filtered, and the filtrate saturated with sodium chloride (60.0 g) and cooled to 0°C. The resulting precipitate was collected and dissolved in diethyl ether (100 ml). The organic solution was then dried (MgSO₄), and the solvent removed *in vacuo*. The resulting residue, containing *β*-phenylhydroxylamine **131** was used immediately without further purification (5.40 g, 61%).

***p*-Bromophenylhydroxylamine²¹⁰ 132**



Zinc dust (12.3 g, 190 mmol) was added portion-wise to a stirred solution of ammonium chloride (15.4 g, 290 mmol) and *p*-bromonitrobenzene **127** (10.0 g, 80 mmol) in water/ethanol 210 ml (2:5; V:V) at room temperature. After addition of the zinc dust was complete the reaction mixture was stirred for a further 15 minutes. The resulting slurry was filtered through Celite® and the residue washed with hot water (100 ml). The filtrate was extracted using dichloromethane (400 ml). The combined organic extracts were washed once with water then dried over MgSO₄ and concentrated *in vacuo*. The resulting solid was recrystallised from hexane and diethyl ether to afford **132** as colourless rhombs that were used immediately. (1.73 g, 37%): M.p. >83°C (decomp.); $\nu_{\max}(\text{KBr})/\text{cm}^{-1}$ 3275, 2800 (br), 1487, 835, 788, 623; δ_{H} (300 MHz, CDCl₃) 7.38-7.36 (2H, m, Ar H), 6.88-6.86 (2H, m, Ar H), 4.52 (1H, br s, NH or OH); *m/z* (CI) 189 (M⁺, 4%), 187 (M⁺, 5%), 174 (42), 108 (100), 52 (15).

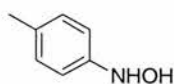
***p*-Chlorophenylhydroxylamine 133**



Zinc dust (6.23 g, 95.3 mmol) was added portion-wise to a stirred solution of NH₄Cl (6.79 g, 127.0 mmol) and *p*-chloronitrobenzene **128** (2.00 g, 12.7 mmol) in water/ethanol 100 ml (2:5;

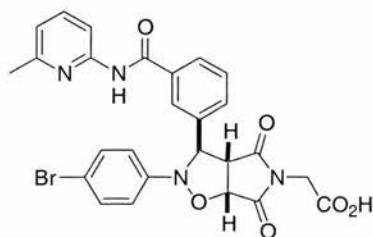
V:V) at room temperature. After addition of the zinc dust was complete the reaction mixture was stirred for a further 15 minutes. The resulting slurry was filtered through Celite® and the residue washed with hot water (100 ml). The filtrate was extracted using dichloromethane (400 ml). The combined organic extracts were washed once with water then dried over MgSO₄ and concentrated *in vacuo*. The resulting solid was then recrystallised from hexane/diethyl ether to afford **133** as a colourless solid that was used immediately. (1.22g, 67%): M.p. 81-83°C; $\nu_{\max}(\text{KBr})/\text{cm}^{-1}$ 3276, 2918, 1492, 1464, 1435, 1218, 1094, 836, 793; δ_{H} (300 MHz, CDCl₃) 7.22 (2H, d, $^3J_{\text{H,H}}$ 7, Ar H), 6.91 (2H, d, $^3J_{\text{H,H}}$ 7, Ar H), 5.56 (br s, NHOH); m/z (EI) 143 (M⁺, 35%), 126 (100), 111 (42), 99 (29), 92 (15); Found 143.0138 [M⁺], C₆H₆NOCl requires 143.0136.

p-Methylphenylhydroxylamine **134**



Zinc dust (33.60 g, 512 mmol) was added portion-wise to a stirred solution of NH₄Cl (6.73 g, 126 mmol) and 4-methylnitrobenzene **129** (15.00 g, 109 mmol) in water/ethanol 210 ml (2:5; V:V) at room temperature. After addition of the zinc dust was complete the reaction mixture was stirred for a further 15 minutes. The resulting slurry was filtered through Celite® and the residue washed with hot water (100 ml). The filtrate was extracted using dichloromethane (400 ml). The combined organic extracts were washed once with water then dried over MgSO₄ and concentrated *in vacuo*. The resulting solid was then recrystallised from hexane/diethyl ether to afford **134** as colourless platelets that were used immediately. (2.10 g, 16%): M.p. 81-83°C; $\nu_{\max}(\text{KBr})/\text{cm}^{-1}$ 3277, 2913, 1512, 1464, 1389, 824, 736; δ_{H} (300 MHz, CDCl₃) 7.12 (2H, d, $^3J_{\text{H,H}}$ 7, Ar H), 6.89 (2H, d, $^3J_{\text{H,H}}$ 7, Ar H), 6.23 (br s, NHOH), 2.26 (3H, s, CH₃) m/z (EI) 123 (M⁺, 56%), 106 (100), 91 (27), 91 (25), 79 (33).

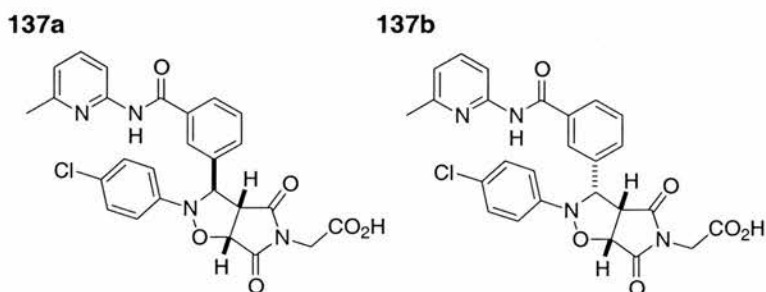
2-{3*c*-[N-(6-Methyl-2-pyridyl)-3-benzamidyl]-2-(4-bromophenyl)-4,6-dioxo-(3*ar*,6*ac*)-hexahydropyrrolo[3,4-*d*]isoxazol-5-yl}-ethanoic acid **136**



N-[3-(*N'*-6-Methyl-2-pyridyl)-amidobenzylidene]-4-bromophenylamine *N*-oxide **109** (200 mg, 0.49 mmol), was added to a solution of the 2-maleimidoethanoic acid **77** (76 mg, 0.49

mmol) and chloroform (5 ml). The reaction was then allowed to stand at 10°C in the absence of light for 3 days. An excess of ethyl acetate was then added to the reaction mixtures to effect the precipitation of the cycloadduct. The precipitate was filtered, washed with hexane to afford **136** as a colourless solid as a single diastereoisomer (171 mg, 62%): M.p. >185°C (decomp.); $\nu_{\max}(\text{KBr})/\text{cm}^{-1}$ 3254, 2992, 1792, 1723, 1618, 1579, 1415, 1279, 790, 728; δ_{H} (300 MHz, CDCl_3) 8.08 (1H, d, $^3J_{\text{H,H}}$ 8, Ar CH), 7.92 (1H, s, Ar CH), 7.80 (1H, d, $^3J_{\text{H,H}}$ 8, Ar CH), 7.62 (1H, dd, $^3J_{\text{H,H}}$ 8, $^3J_{\text{H,H}}$ 8 Ar CH), 7.48 (1H, d, $^3J_{\text{H,H}}$ 8, Ar CH), 7.40-7.35 (1H, m, Ar CH), 7.16 (2H, d, $^3J_{\text{H,H}}$ 9, Ar CH), 6.89 (1H, d, $^3J_{\text{H,H}}$ 8, Ar CH), 6.77 (2H, d, $^3J_{\text{H,H}}$ 9, Ar CH), 5.32 (1H, s, cyclic CH), 5.17 (1H, d, $^3J_{\text{H,H}}$ 7, cyclic CH), 4.23-3.87 (3H, m, cyclic CH and CH_2), 2.55 (3H, s, CH_3); δ_{C} (75.5 MHz, CDCl_3) 174.1 (quat. C), 172.9 (quat. C), 168.1 (quat. C), 165.4 (quat. C), 156.0 (quat. C), 150.3 (quat. C), 146.1 (quat. C), 139.6 (Ar CH), 138.0 (quat. C), 134.3 (quat. C), 131.5 (2 x Ar CH), 131.0 (Ar CH), 129.2 (Ar CH), 127.2 (Ar CH), 126.0 (Ar CH), 119.6 (Ar CH), 117.1 (2 x Ar CH), 115.4 (quat. C), 111.6 (Ar CH), 76.7 (CH), 69.3 (CH), 56.7 (CH), 39.5 (CH_2), 23.2 (CH_3); m/z (LSI) 567 (M^+ 97%), 565 (M^+ 100), 460 (8), 412 (17), 410 (17), 391 (37); Found 567.0679 [M^+ (^{81}Br)], $\text{C}_{26}\text{H}_{21}\text{N}_4\text{O}_6$ ^{81}Br requires 567.0702; Found 565.0710 [M^+ (^{79}Br)], $\text{C}_{26}\text{H}_{21}\text{N}_4\text{O}_6$ ^{79}Br requires 565.0723.

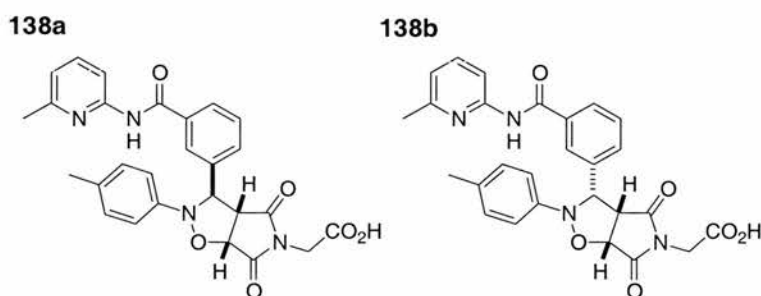
2-{3c-[N-(6-Methyl-2-pyridyl)-3-benzamidyl]-2-(4-chlorophenyl)-4,6-dioxo-(3ar,6ac)-hexahydropyrrolo[3,4-d]isoxazol-5-yl}-ethanoic acid **137**



N-[3-(*N'*-6-Methyl-2-pyridyl)-amidobenzylidene]-4-chlorophenylamine *N*-oxide **110** (100 mg, 0.27 mmol), was added to a solution of the 2-maleimidoethanoic acid **77** (42 mg, 0.27 mmol), in chloroform (10 ml). The reaction was then allowed to stand at 10°C in the absence of light for 3 days. An excess of hexane was then added to the reaction mixtures to effect the precipitation of the cycloadduct. The precipitate was filtered, washed with hexane and dried under vacuum. Cycloadduct **137** was obtained as a colourless solid as a 7:3 mixture of diastereoisomer (140 mg, 99%): M.p. >160°C (decomp.); Found: C, 59.6; H, 3.9; N, 10.4. Calc. for $\text{C}_{26}\text{H}_{21}\text{N}_4\text{O}_6\text{Cl}$: C, 60.0; H, 4.1; N, 10.7. $\nu_{\max}(\text{KBr})/\text{cm}^{-1}$ 3399, 3252, 3062, 2993, 1719, 1488, 1452, 1419, 1328, 1274, 1168, 793, 756, δ_{H} (300 MHz, CDCl_3 , major isomer **137a**) 11.76 (br s, CO_2H), 8.98 (br s, NH), 8.39-8.33 (1H, m, Ar CH), 7.98 (1H, s, ArCH),

7.94-7.82 (2H, m, Ar CH), 7.54-7.52 (1H, m, Ar CH), 7.15-7.02 (4H, m, Ar CH), 6.86 (2H, d, $^3J_{\text{H,H}}$ 8, Ar CH), 5.31 (1H, s, cyclic CH), 5.22 (1H, d, $^3J_{\text{H,H}}$ 10, cyclic CH), 4.26-4.03 (1H, m, cyclic CH) 4.00-3.95 (2H, m, CH₂), 2.55 (3H, s, CH₃); δ_{H} (300 MHz, CDCl₃, minor isomer **137b**) 11.76 (br s, CO₂H), 8.98 (br s, NH), 8.39-8.33 (2H, m, Ar CH), 8.08-8.04 (1H, m, Ar CH), 7.98 7.94-7.82 (1H, m, Ar CH), 7.45-7.37 (2H, m, Ar CH), 7.15-7.02 (4H, m, Ar CH), 6.74 (1H, s, Ar CH), 5.17 (1H, d, $^3J_{\text{H,H}}$ 10, cyclic CH), 4.67 (1H, d, $^3J_{\text{H,H}}$ 11, cyclic CH), 4.75 (1H, d, $^3J_{\text{H,H}}$ 22, cyclic CH), 4.26-4.03 (2H, m, CH₂), 2.6 (3H, s, CH₃); δ_{C} (75.5 MHz, CDCl₃, major isomer **137a**) 174.8 (quat. C), 173.0 (quat. C), 171.2 (quat. C), 166.5 (quat. C), 154.4 (quat. C), 150.4 (quat. C), 145.5 (quat. C), 142.0 (Ar CH), 137.6 (quat. C), 134.4 (quat. C), 131.4 (Ar CH), 128.7 (3 x Ar CH), 126.4 (Ar CH), 122.6 (Ar CH), 120.1 (Ar CH), 120.0 (Ar CH), 117.0 (Ar CH), 114.8 (quat. C), 113.7 (Ar CH), 69.4 (CH), 56.9 (CH), 54.6 (CH), 40.8 (CH₂), 21.2 (CH₃); δ_{C} (75.5 MHz, CDCl₃, minor isomer **137b**) 174.1 (quat. C), 173.7 (quat. C), 172.7 (quat. C), 171.1 (quat. C), 165.5 (quat. C), 153.8 (quat. C), 149.8 (quat. C), 144.8 (quat. C), 142.7 (Ar CH), 133.4 (quat. C), 132.6 (Ar CH), 128.9 (Ar CH), 128.8 (Ar CH), 126.6 (Ar CH), 122.6 (Ar CH), 120.1 (Ar CH), 120.0 (Ar CH), 117.0 (2 x Ar CH), 114.8 (quat. C), 113.7 (Ar CH), 69.4 (CH), 56.9 (CH), 54.6 (CH), 41.4 (CH₂), 22.6 (CH₃); m/z (ESI) 543 ($^{35}\text{M}+\text{Na}^+$, 15%), 523 (40) 521 (100); Found 565.0862 [$^{35}\text{M}+2\text{Na}^+$], C₂₆H₂₀N₄O₆³⁵ClNa₂ requires 565.0867.

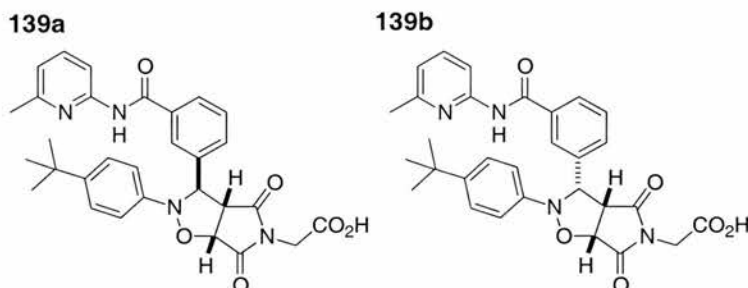
2-{3c-[N-(6-Methyl-2-pyridyl)-3-benzamidyl]-2-(4-methylphenyl)-4,6-dioxo-(3ar,6ac)-hexahydropyrrolo[3,4-d]isoxazol-5-yl}-ethanoic acid **138**



N-[3-(*N'*-6-Methyl-2-pyridyl)-amidobenzylidene]-4-methylphenylamine *N*-oxide **111** (290 mg, 0.84 mmol), was added to a solution of the 2-maleimidoethanoic acid **77** (130 mg, 0.84 mmol), in chloroform (10 ml). The reaction was then allowed to stand at 10°C in the absence of light for 3 days. An excess of ethyl acetate was then added to the reaction mixtures to effect the precipitation of the cycloadduct. The precipitate was filtered, washed with ethyl acetate and dried under vacuum. Cycloadduct **138** was obtained as a colourless solid as a 9:1 ratio of diastereoisomers (100 mg, 24%): M.p. >190°C (decomp.); Found: C, 64.5; H, 4.6; N, 10.9. Calc. for C₂₇H₂₄N₄O₆: C, 64.8; H, 4.8; N, 11.2. ν_{max} (KBr)/cm⁻¹ 2951, 1719, 1678, 1453,

1283, 1166, 794; δ_{H} (300 MHz, CDCl_3 , major isomer **138a**) 10.77 (br s, NH), 8.21 (1H, s, Ar CH), 8.14-8.11 (1H, m, Ar CH), 8.02 (1H, d, $^3J_{\text{H,H}}$ 8, Ar CH), 7.85 (1H, t, $^3J_{\text{H,H}}$ 8, 8, Ar CH), 7.75-7.70 (1H, m, Ar CH), 7.57 (1H, t, $^3J_{\text{H,H}}$ 8, 8, Ar CH), 7.17-7.05 (5H, m, Ar CH), 5.66 (1H, s, cyclic CH), 5.59 (1H, d, $^3J_{\text{H,H}}$ 7, cyclic CH), 4.42 (1H, dd, $^3J_{\text{H,H}}$ 1, 6, cyclic CH), 4.09-3.98 (2H, m, CH_2), 2.59 (3H, s, CH_3) 2.28 (3H, s, CH_3); δ_{H} (300 MHz, CDCl_3 , minor isomer **138b**) 10.74 (br s, NH), 8.16-8.09 (2H, m, Ar CH), 8.02 (1H, d, $^3J_{\text{H,H}}$ 8, Ar CH), 7.85 (1H, t, $^3J_{\text{H,H}}$ 8, 8, Ar CH), 7.75-7.70 (1H, m, Ar CH), 7.47 (1H, t, $^3J_{\text{H,H}}$ 8, 8, Ar CH), 7.17-7.05 (5H, m, Ar CH), 5.46 (1H, d, $^3J_{\text{H,H}}$ 8, cyclic CH), 4.96 (1H, d, $^3J_{\text{H,H}}$ 9, cyclic CH), 4.34-4.30 (1H, m, cyclic CH), 4.30-4.12 (2H, m, CH_2), 2.61 (3H, s, CH_3) 2.32 (3H, s, CH_3); δ_{C} (75.5 MHz, CDCl_3 , major isomer **138a**) 174.3 (quat. C), 173.3 (quat. C), 167.3 (quat. C), 165.5 (quat. C), 156.4 (quat. C), 151.3 (quat. C), 145.0 (quat. C), 138.4 (Ar CH), 138.2 (quat. C), 134.2 (quat. C), 131.4 (Ar CH), 130.9 (Ar CH), 129.0 (2 x Ar CH), 128.5 (Ar CH), 127.5 (Ar CH), 127.2 (Ar CH), 121.0 (quat. C), 119.0 (Ar CH), 115.3 (Ar CH), 111.6 (Ar CH), 76.5 (CH), 68.6 (CH), 56.0 (CH), 38.8 (CH_3), 23.4 (CH_2), 20.0 (CH_3); δ_{C} (75.5 MHz, CDCl_3 , minor isomer **138b**) 174.3 (quat. C), 173.3 (quat. C), 167.3 (quat. C), 165.5 (quat. C), 156.4 (quat. C), 151.3 (quat. C), 145.0 (quat. C), 138.4 (Ar CH), 138.2 (quat. C), 134.2 (quat. C), 131.4 (Ar CH), 130.9 (Ar CH), 129.0 (2 x Ar CH), 128.5 (Ar CH), 127.5 (Ar CH), 127.2 (Ar CH), 121.0 (quat. C), 119.0 (Ar CH), 115.3 (Ar CH), 111.6 (Ar CH), 76.5 (CH), 68.6 (CH), 56.0 (CH), 38.8 (CH_3), 23.4 (CH_2), 20.0 (CH_3); m/z (ESI) 501 ($\text{M}+\text{H}^+$, 15%), 346 (100), 307 (20), 275 (26); Found 545.1422 [$\text{M}+2\text{Na}^+$], $\text{C}_{27}\text{H}_{24}\text{N}_4\text{O}_6\text{Na}_2$ requires 545.1422.

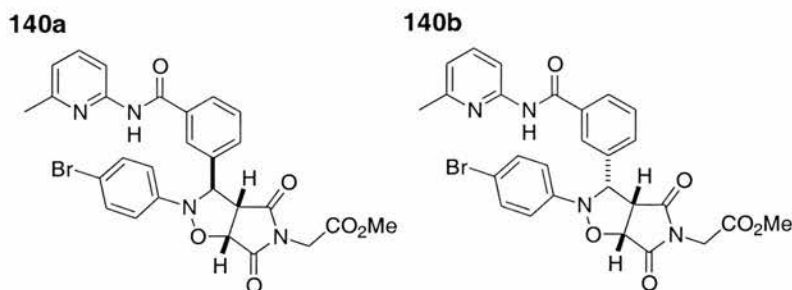
2-{3c-[N-(6-Methyl-2-pyridyl)-3-benzamidyl]-2-(4-*tert*-butylphenyl)-4,6-dioxo-(3ar,6ac)-hexahydropyrrolo[3,4-*d*]isoxazol-5-yl}-ethanoic acid **139**



N-[3-(*N'*-6-Methyl-2-pyridyl)-amidobenzylidene]-4-*tert*-butylphenylamine *N*-oxide **112** (106 mg, 0.26 mmol), was added to a solution of the 2-maleimidoethanoic acid **77** (40 mg, 0.26 mmol), in chloroform (5 ml). The reaction was then allowed to stand at 10°C in the absence of light for 3 days. An excess of ethyl acetate was then added to the reaction mixtures to effect the precipitation of the cycloadduct. The precipitate was filtered, washed with ethyl acetate and dried under vacuum. Cycloadduct **139** was obtained as a colourless solid as a 1:9

ratio of diastereoisomers (160 mg, 99%): M.p. >170°C (decomp.); Found: C, 66.8; H, 5.5; N, 9.9. Calc for C₃₀H₃₀N₄O₆: C, 66.4; H, 5.6; N, 10.3. $\nu_{\max}(\text{KBr})/\text{cm}^{-1}$ 2960, 1719, 1604, 1454, 1274, 1176, 794; δ_{H} (300 MHz, CDCl₃, major isomer **139a**) 11.67 (br s, CO₂H), 10.23 (br s, NH), 8.50-8.44 (1H, m, Ar CH), 8.16 (1H, s, Ar CH), 8.05 (1H, d, ³J_{H,H} 8, Ar CH), 7.97 (1H, t, ³J_{H,H} 8, 8, Ar CH), 7.64 (1H, d, ³J_{H,H} 9, Ar CH), 7.55 (1H, t, ³J_{H,H} 8, 8, Ar CH), 7.35-7.32 (2H, m, Ar CH), 7.16 (1H, d, ³J_{H,H} 7, Ar CH), 7.05-7.02 (2H, m, Ar CH), 5.52 (1H, s, cyclic CH), 5.29 (1H, d, ³J_{H,H} 7, cyclic CH), 4.19-3.91 (2H, AB system, CH₂), 4.06 (1H, d, ³J_{H,H} 7, cyclic CH), 2.68 (3H, s, CH₃) 1.38 (9H, s, CH₃); δ_{C} (75.5 MHz, CDCl₃, major isomer **139a**) 174.8 (quat. C), 173.1 (quat. C), 171.2 (quat. C), 170.0 (quat. C), 166.7 (quat. C), 150.5 (quat. C), 145.8 (quat. C), 144.7 (quat. C), 141.7 (Ar CH), 138.4 (2 x quat. C), 134.4 (Ar CH), 134.2 (quat. C), 131.2 (Ar CH), 129.9 (Ar CH), 128.5 (Ar CH), 126.6 (Ar CH), 125.5 (2 x Ar CH), 121.1 (Ar CH), 115.2 (Ar CH), 113.5 (Ar CH), 77.4 (CH), 69.2 (CH), 56.9 (CH), 40.5 (CH₂), 31.6 (3 x CH₃), 21.3 (CH₃); *m/z* (ESI) 603 (M+2K⁺, 15%), 587 (100), 581 (6), 565 (10), 543 (15); Found 587.1873 [M+2Na⁺], C₃₀H₂₉N₄O₆Na₂ requires 587.1882.

2-{3c-[N-(6-Methyl-2-pyridyl)-3-benzamidyl]-2-(4-bromophenyl)-4,6-dioxo-(3ar,6ac)-hexahydropyrrolo[3,4-d]isoxazol-5-yl}-ethanoic acid, methyl ester **140**

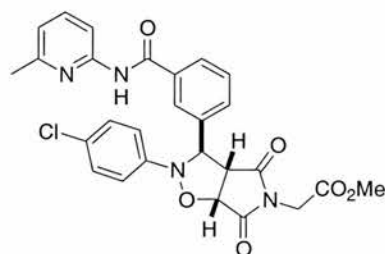


N-[3-(*N'*-6-Methyl-2-pyridyl)-amidobenzylidene]-4-bromophenylamine *N*-oxide **109** (200 mg, 0.49 mmol) was added to a solution of 2-maleimidoethanoic acid methyl ester **79** (83 mg, 0.49 mmol) in chloroform (19.5 ml). The reaction was then allowed to stand at 10°C in the absence of light for 3 days. An excess of hexane was then added to the reaction mixtures to effect the precipitation of the cycloadduct. The precipitate was filtered, washed with hexane then recrystallised from chloroform/hexane and dried under vacuum to afford **140** a colourless

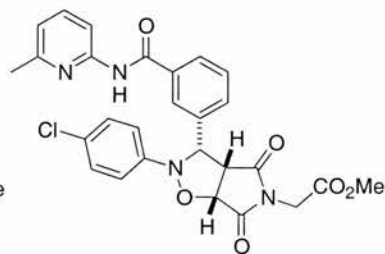
solid as a 7:3 ratio of diastereoisomers (73 mg, 26%): M.p. 102-104°C; Found: C, 56.2; H, 4.0; N, 9.5. Calc. for C₂₇H₂₃N₄O₆Br: C, 56.0; H, 4.0; N, 9.7. $\nu_{\max}(\text{KBr})/\text{cm}^{-1}$ 3339, 2953, 1753, 1721, 1675, 1453, 1271, 824, 791; δ_{H} (300 MHz, CDCl₃, major isomer **140a**) 8.87 (br s, NH), 8.22 (1H, d, $^3J_{\text{H,H}}$ 8, Ar CH), 8.02 (1H, s, Ar CH), 7.86 (1H, d, $^3J_{\text{H,H}}$ 8, Ar CH), 7.71 (1H, t, $^3J_{\text{H,H}}$ 8, 8, Ar CH), 7.60-7.56 (1H, m, Ar CH), 7.49 (1H, d, $^3J_{\text{H,H}}$ 8, Ar CH), 7.32-7.27 (2H, m, Ar CH), 6.99-6.91 (1H, m, Ar CH), 6.87 (2H, d, $^3J_{\text{H,H}}$ 8, Ar CH), 5.41 (1H, s, CH), 5.23 (1H, d, $^3J_{\text{H,H}}$ 7, CH), 4.28-4.27 (1H, m, CH), 4.08 (2H, s, CH₂), 3.73 (3H, s, CH₃), 2.50 (3H, s, CH₃); δ_{H} (300 MHz, CDCl₃, minor isomer **140b**) 9.00 (br s, NH), 8.15 (1H, d, $^3J_{\text{H,H}}$ 8, Ar CH), 7.96-7.93 (2H, m, Ar CH), 7.64 (1H, t, $^3J_{\text{H,H}}$ 8, 8, Ar CH), 7.60-7.56 (1H, m, Ar CH), 7.50 (1H, d, $^3J_{\text{H,H}}$ 8, Ar CH), 7.32-7.27 (2H, m, Ar CH), 6.99-6.91 (3H, m, Ar CH), 5.17 (1H, d, $^3J_{\text{H,H}}$ 7, CH), 4.71 (1H, d, $^3J_{\text{H,H}}$ 7, CH), 4.05-4.00 (3H, m, CH, CH₂), 3.76 (3H, s, CH₃), 2.5 (3H, s, CH₃); δ_{C} (75.5 MHz, CDCl₃, major isomer **140a**) 173.6 (quat. C), 172.3 (quat. C), 166.3 (quat. C), 165.0 (quat. C), 156.3 (quat. C), 150.4 (quat. C), 146.2 (quat. C), 139.6 (Ar CH), 138.3 (quat. C), 134.9 (quat. C), 131.8 (quat. C), 130.9 (quat. C), 129.5 (Ar CH), 127.2 (Ar CH), 126.4 (Ar CH), 122.2 (Ar CH), 119.7 (Ar CH), 117.2 (2 x Ar CH), 115.8 (quat. C), 111.3 (Ar CH), 76.2 (CH), 69.6 (CH), 57.0 (CH), 52.9 (CH₃), 39.6 (CH₂), 23.6 (CH₃); δ_{C} (75.5 MHz, CDCl₃, minor isomer **140b**) 173.6 (quat. C), 172.3 (quat. C), 166.8 (quat. C), 165.0 (quat. C), 156.6 (quat. C), 150.8 (quat. C), 145.3 (quat. C), 138.9 (Ar CH), 138.3 (quat. C), 135.2 (quat. C), 131.8 (quat. C), 131.5 (quat. C), 129.4 (Ar CH), 128.5 (Ar CH), 126.1 (Ar CH), 122.2 (Ar CH), 119.4 (Ar CH), 118.9 (quat. C), 117.2 (2 x Ar CH), 111.3 (Ar CH), 77.2 (CH), 71.2 (CH), 54.6 (CH), 53.2 (CH₃), 39.6 (CH₂), 23.8 (CH₃); m/z (ESI) 603 (M+Na⁺ (⁸¹Br), 36%), 601 (M+Na⁺ (⁷⁹Br), 33), 434 (92), 432 (100); Found 603.0697 [M+Na⁺ (⁸¹Br)], C₂₇H₂₃N₄O₆⁸¹BrNa requires 603.0678; Found 601.0703 [M+Na⁺ (⁷⁹Br)], C₂₇H₂₃N₄O₆⁷⁹BrNa requires 601.0699.

2-{3c-[N-(6-Methyl-2-pyridyl)-3-benzamidyl]-2-(4-chlorophenyl)-4,6-dioxo-(3ar,6ac)-hexahydropyrrolo[3,4-d]isoxazol-5-yl}-ethanoic acid, methyl ester **141**

141a



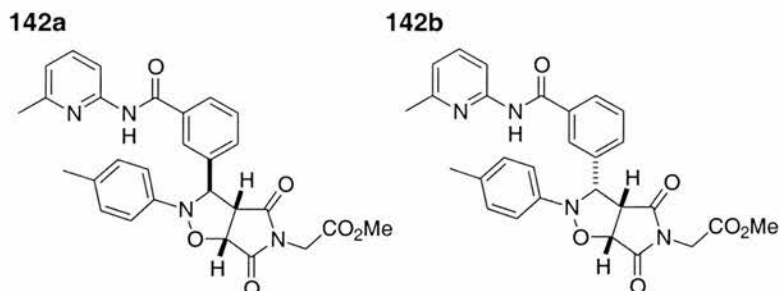
141b



N-[3-(*N'*-6-Methyl-2-pyridyl)-amidobenzylidene]-4-chlorophenylamine *N*-oxide **110** (100 mg, 0.27 mmol), was added to a solution of the 2-maleimidoethanoic acid, methyl ester **79** (42

mg, 0.27 mmol), in chloroform (10 ml). The reaction was then allowed to stand at 10°C in the absence of light for 3 days. An excess of ethyl acetate was then added to the reaction mixtures to effect the precipitation of the cycloadduct. The precipitate was filtered, washed with ethyl acetate and dried under vacuum. Cycloadduct **141** was obtained as a colourless solid as a 7:3 mixture of diastereoisomer (120 mg, 83%): M.p. 93-95°C; Found: C, 60.3; H, 4.1; N, 10.2. Calc. for C₂₇H₂₃N₄O₆Cl: C, 60.6; H, 4.3; N, 10.5. $\nu_{\max}(\text{KBr})/\text{cm}^{-1}$ 3345, 2954, 1721, 1675, 1453, 1224, 1178, 792, 697; δ_{H} (500 MHz, CDCl₃, major isomer **141a**) 8.97 (br s, NH), 8.20 (1H, d, $^3J_{\text{H,H}}$ 8.5, Ar CH), 8.02 (1H, s, Ar CH), 7.86 (1H, d, $^3J_{\text{H,H}}$ 7.5, Ar CH), 7.70 (1H, t, $^3J_{\text{H,H}}$ 8, 8, Ar CH) 7.59-7.55 (1H, m, Ar CH), 4.50-7.46 (1H, m, Ar CH), 7.17-7.13 (2H, m, Ar CH), 7.02-7.00 (1H, m, Ar CH), 6.97 (1H, d, $^3J_{\text{H,H}}$ 7.5, Ar CH) 6.94-6.91 (1H, m, Ar CH), 5.40 (1H, s, cyclic CH), 5.22 (1H, d, $^3J_{\text{H,H}}$ 7, cyclic CH), 4.32-4.24 (1H, d, $^3J_{\text{H,H}}$ 7, cyclic CH), 4.08 (2H, s, CH₂), 3.72 (3H, s, CH₃), 2.50 (3H, s, CH₃); δ_{H} (500 MHz, CDCl₃, minor isomer **141b**) 8.97 (br s, NH), 8.15 (1H, d, $^3J_{\text{H,H}}$ 8.5, Ar CH), 7.96 (1H, s, Ar CH), 7.93 (1H, d, $^3J_{\text{H,H}}$ 8.5, Ar CH), 7.63 (1H, t, $^3J_{\text{H,H}}$ 8, Ar CH), 7.59-7.55 (1H, m, Ar CH), 4.50-7.46 (1H, m, Ar CH), 7.17-7.13 (2H, m, Ar CH), (3H, m, Ar CH), 5.16 (1H, d, $^3J_{\text{H,H}}$ 8, cyclic CH), 4.71 (1H, d, $^3J_{\text{H,H}}$ 9, cyclic CH), 4.04 (1H, dd, $^3J_{\text{H,H}}$ 7.5, 9, cyclic CH), 4.01 (2H, dd, $^2J_{\text{H,H}}$ 7.5, 1.5, CH₂), 3.75 (3H, s, CH₃), 2.45 (3H, s, CH₃); δ_{C} (75.5 MHz, CDCl₃, major isomer **141a**) 174.0 (quat. C), 172.3 (quat. C), 166.3 (quat. C), 164.9 (quat. C), 156.4 (quat. C), 150.4 (quat. C), 145.6 (quat. C), 139.4 (Ar CH), 138.2 (quat. C), 134.9 (quat. C), 129.5 (Ar CH), 128.9 (2 x Ar CH), 128.3 (quat. C), 127.2 (Ar CH), 126.1 (Ar CH), 121.9 (Ar CH), 116.9 (3 x Ar CH), 111.2 (Ar CH), 76.2 (CH), 69.7 (CH), 57.0 (CH), 52.9 (CH₃), 39.6 (CH₂), 23.6 (CH₃); δ_{C} (75.5 MHz, CDCl₃, minor isomer **141b**) 174.0 (quat. C), 171.5 (quat. C), 166.8 (quat. C), 156.6 (quat. C), 150.8 (quat. C), 144.7 (quat. C), 138.8 (Ar CH), 138.2 (quat. C), 135.1 (quat. C), 134.0 (quat. C), 131.5 (Ar CH), 131.1 (quat. C), 130.9 (Ar CH), 129.3 (2 x Ar CH), 128.8 (Ar CH), 119.6 (3 x Ar CH), 119.4 (Ar CH), 111.4 (Ar CH), 77.2 (CH), 71.3 (CH), 54.6 (CH), 53.2 (CH₃), 39.6 (CH₂), 23.8 (CH₃); m/z (ESI) 535 ($^{35}\text{M}+\text{H}^+$, 65%), 366 (100); Found 557.1201 [$^{35}\text{M}+\text{Na}^+$], C₂₇H₂₃N₄O₆³⁵ClNa requires 557.12047.

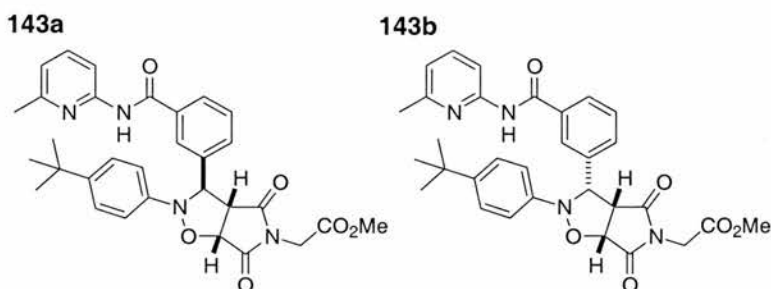
2-{3c-[*N*-(6-Methyl-2-pyridyl)-3-benzamidyl]-2-(4-methylphenyl)-4,6-dioxo-(3ar,6ac)-hexahydropyrrolo[3,4-*d*]isoxazol-5-yl}-ethanoic acid, methyl ester **142**



N-[3-(*N'*-6-Methyl-2-pyridyl)-amidobenzylidene]-4-methylphenylamine *N*-oxide **111** (100 mg, 0.29 mmol), was added to a solution of the 2-maleimidoethanoic acid, methyl ester **79** (45 mg, 0.29 mmol), in chloroform (10 ml). The reaction was then allowed to stand at 10°C in the absence of light for 3 days. An excess of ethyl acetate was then added to the reaction mixtures to effect the precipitation of the cycloadduct. The precipitate was filtered, washed with ethyl acetate and dried under vacuum. Cycloadduct **142** was obtained as a colourless solid as a 7:3 ratio of diastereoisomers (67 mg, 45%): M.p. >73°C (decomp.); Found: C, 65.3; H, 5.0; N, 10.9. Calc. for C₂₈H₂₆N₄O₆: C, 65.4; H, 5.1; N, 10.9. $\nu_{\max}(\text{KBr})/\text{cm}^{-1}$ 3340, 2954, 1722, 1676, 1526, 1453, 1221, 792, 748, 698; δ_{H} (300 MHz, CDCl₃, major isomer **142a**) 8.77 (br s, NH), 8.21 (1H, d, $^3J_{\text{H,H}}$ 8, Ar CH), 7.86 (1H, d, $^3J_{\text{H,H}}$ 8, Ar CH), 7.68 (1H, t, $^3J_{\text{H,H}}$ 8, 8, Ar CH), 7.65-7.62 (2H, m, Ar CH), 7.48 (1H, t, $^3J_{\text{H,H}}$ 7.5, 7.5, Ar CH), 7.00-6.95 (4H, m, Ar CH), 6.89 (1H, d, $^3J_{\text{H,H}}$ 8.5, Ar CH), 5.48 (1H, s, cyclic CH), 5.16 (1H, d, $^3J_{\text{H,H}}$ 7.5, cyclic CH), 4.00 (1H, dd, $^3J_{\text{H,H}}$ 7, 1.5, cyclic CH), 3.99-3.94 (2H, m, CH₂), 3.71 (3H, s, CH₃) 2.50 (3H, s, CH₃) 2.22 (3H, s, CH₃); δ_{H} (500 MHz, CDCl₃, minor isomer **142b**) 8.95 (br s, NH), 8.15 (1H, d, $^3J_{\text{H,H}}$ 8.5, Ar CH), 7.96 (1H, s, Ar CH), 7.91 (1H, d, $^3J_{\text{H,H}}$ 6.5, Ar CH), 7.68 (1H, t, $^3J_{\text{H,H}}$ 8, 8, Ar CH), 7.65-7.62 (2H, m, Ar CH), 7.56 (1H, d, $^3J_{\text{H,H}}$ 8, Ar CH), 7.46 (1H, t, $^3J_{\text{H,H}}$ 8, 8, Ar CH), 7.00-6.95 (2H, m, Ar CH), 6.92-6.89 (1H, m, Ar CH), 5.15 (1H, d, $^3J_{\text{H,H}}$ 7.5, cyclic CH), 4.75 (1H, d, $^3J_{\text{H,H}}$ 8.5, cyclic CH), 4.32-4.24 (2H, m, CH₂), 4.04-4.02 (1H, m, cyclic CH), 3.75 (3H, s, CH₃) 2.46 (3H, s, CH₃) 2.24 (3H, s, CH₃); δ_{C} (75.5 MHz, CDCl₃, major isomer **142a**) 173.9 (quat. C), 172.5 (quat. C), 166.4 (quat. C), 165.1 (quat. C), 156.4 (quat. C), 150.5 (quat. C), 144.9 (quat. C), 139.4 (Ar CH), 138.8 (quat. C), 134.8 (quat. C), 132.9 (quat. C), 130.9 (Ar CH), 129.4 (2 x Ar CH), 127.1 (Ar CH), 126.0 (Ar CH), 121.1 (Ar CH), 119.6 (Ar CH), 115.6 (2 x Ar CH), 111.2 (Ar CH), 76.6 (CH), 69.7 (CH), 57.1 (CH), 52.8 (CH₃), 39.5 (CH₂), 23.7 (CH₃), 20.6 (CH₃); δ_{C} (75.5 MHz, CDCl₃, minor isomer **142b**) 173.9 (quat. C), 171.8 (quat. C), 166.8 (quat. C), 165.5 (quat. C), 156.6 (quat. C), 150.8 (quat. C), 143.4 (quat. C), 138.8 (Ar CH), 135.9 (quat. C), 134.9 (quat. C), 134.3 (quat. C), 131.7 (Ar CH), 129.4 (2 x Ar CH), 129.2 (Ar CH), 128.3 (Ar CH), 126.6 (Ar CH), 119.4 (Ar CH),

115.6 (2 x Ar CH), 111.3 (Ar CH), 76.2 (CH), 71.2 (CH), 54.7 (CH), 53.1 (CH₃), 39.6 (CH₂), 23.8 (CH₃), 20.8 (CH₃); *m/z* (ESI) 515 (M+H⁺, 70%), 346 (100), Found 537.1751 [M+Na⁺], C₂₈H₂₆N₄O₆Na requires 537.1750.

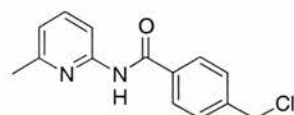
2-{3*c*-[N-(6-Methyl-2-pyridyl)-3-benzamidyl]-2-(4-*tert*-butylphenyl)-4,6-dioxo-(3*a*,6*a*)-hexahydropyrrolo[3,4-*d*]isoxazol-5-yl}-ethanoic acid, methyl ester **143**



N-[3-(*N'*-6-Methyl-2-pyridyl)-amidobenzylidene]-4-*tert*-butylphenylamine *N*-oxide **112** (100 mg, 0.24 mmol), was added to a solution of the 2-maleimidoethanoic acid, methyl ester **79** (40 mg, 0.24 mmol), in chloroform (5 ml). The reaction was then allowed to stand at 10°C in the absence of light for 3 days. An excess of ethyl acetate was then added to the reaction mixtures to effect the precipitation of the cycloadduct. The precipitate was filtered, washed with ethyl acetate and dried under vacuum. Cycloadduct **143** was obtained as a colourless solid as a 9:1 ratio of diastereoisomers (65 mg, 45%): M.p. >120°C (decomp.); Found: C, 66.9; H, 5.8; N, 10.1. Calc. for C₃₁H₃₂N₄O₆: C, 66.8; H, 5.5; N, 10.2. $\nu_{\max}(\text{KBr})/\text{cm}^{-1}$ 3342, 2958, 1755, 1722, 1678, 1524, 1088, 791, 735; δ_{H} (300 MHz, CDCl₃, major isomer **143a**) 8.75 (1H, s, NH), 8.20 (1H, d, ³*J*_{H,H} 8, Ar CH), 8.05 (1H, s, Ar CH), 7.87 (1H, d, ³*J*_{H,H} 8, Ar CH), 7.67 (2H, d, ³*J*_{H,H} 8, Ar CH), 7.49 (1H, t, ³*J*_{H,H} 8, 8, Ar CH), 7.22-7.19 (3H, m, Ar CH), 6.98-6.92 (2H, m, Ar CH), 5.50 (1H, s, cyclic CH), 5.14 (1H, d, ³*J*_{H,H} 7, cyclic CH), 3.99 (1H, dd ³*J*_{H,H} 8, 1.5, cyclic CH), 3.94-3.81 (2H, AB system, CH₂), 3.70 (3H, s, CH₃) 2.49 (3H, s, CH₃), 1.23 (9H, s, CH₃); δ_{H} (300 MHz, CDCl₃, minor isomer **143b**) 8.99 (1H, s, NH), 8.15 (1H, d, ³*J*_{H,H} 8, Ar CH), 7.97 (1H, s, Ar CH), 7.92 (1H, d, ³*J*_{H,H} 8, Ar CH), 7.67 (2H, d, ³*J*_{H,H} 8, Ar CH), 7.62-7.58 (1H, m, Ar CH) 7.47 (1H, t, ³*J*_{H,H} 8, 8, Ar CH), 7.22-7.19 (2H, m, Ar CH), 6.98-6.92 (2H, m, Ar CH), 5.14 (1H, d, ³*J*_{H,H} 7, cyclic CH), 4.78 (1H, d ³*J*_{H,H} 8, cyclic CH), 4.28-4.27 (2H, m, CH₂), 4.06-4.00 (1H, m, cyclic CH), 3.70 (3H, s, CH₃) 2.45 (3H, s, CH₃), 1.23 (9H, s, CH₃); δ_{C} (75.5 MHz, CDCl₃, major isomer **143a**) 173.9 (quat. C), 172.4 (quat. C), 166.4 (quat. C), 165.1 (quat. C), 156.5 (quat. C), 150.5 (quat. C), 146.3 (quat. C), 144.9 (quat. C), 143.4 (quat. C), 139.2 (Ar CH), 138.9 (quat. C), 134.5 (quat. C), 131.6 (Ar CH), 129.4 (2 x Ar CH), 128.3 (Ar CH), 125.7 (3 x Ar CH), 119.6 (Ar CH), 115.1 (Ar CH), 111.3 (Ar CH), 77.2 (CH), 69.4 (CH), 57.1 (CH), 52.8 (CH₃), 39.3 (CH₂), 31.2 (3 x

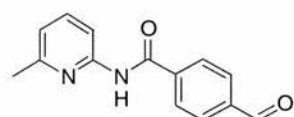
CH₃), 23.7 (CH₃); *m/z* (ESI) 557 (M+H⁺, 100%), 514 (80); Found 579.2207 [M+Na⁺], C₃₁H₃₂N₄O₆Na requires 579.2220.

N-(6-Methyl-2-pyridyl)-4-chloromethylbenzamide **145**



2-Amino-6-picoline **120** (5.15 g, 48 mmol) as a solution in dry dichloromethane (50 ml) was added dropwise to neat 4-(chloromethyl) benzoyl chloride **144** (3.00 g, 16 mmol) at 0°C. The solution was then allowed to warm to room temperature and stirred for 16 hours. The solvent was removed *in vacuo* and the crude residue was purified using flash column chromatography (SiO₂, 3:2 hexane:ethyl acetate) to afford **145** as a colourless solid (3.69 g, 89%): M.p. 80-82°C; $\nu_{\max}(\text{KBr})/\text{cm}^{-1}$ 3440, 2973, 1676, 1598, 1390, 1088, 1048, 766, 740, 701, 671; δ_{H} (300 MHz, CDCl₃) 8.49 (1H, br s, NH), 8.17 (1H, d, ³*J*_{H,H} 8, Ar CH), 7.91 (2H, d, ³*J*_{H,H} 8, Ar CH), 7.65 (1H, dd, ³*J*_{H,H} 8, ³*J*_{H,H} 7, Ar CH), 7.50 (2H, d, ³*J*_{H,H} 8, Ar CH), 6.93 (1H, d, ³*J*_{H,H} 7, Ar CH), 4.62 (2H, s, CH₂Cl), 2.45 (3H, s, CH₃); δ_{C} (75.5 MHz, CDCl₃) 165.0 (quat. C), 156.9 (quat. C), 150.7 (quat. C), 141.5 (quat. C), 138.9 (quat. C), 134.3 (Ar CH), 129.0 (2 x Ar CH), 127.8 (2 x Ar CH), 119.7 (Ar CH), 111.1 (Ar CH), 45.4 (CH₂Cl), 24.2 (CH₃); *m/z* (ESI) 261 (M+H⁺), 283 (M+Na⁺); Found 261.0787 [M+H⁺], C₁₄H₁₄N₂OCl requires 261.0795.

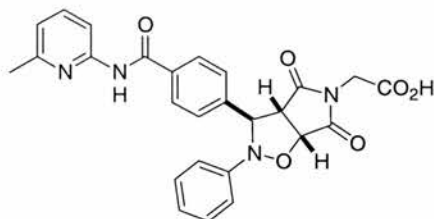
N-(6-Methyl-2-pyridyl)-4-formylbenzamide²⁰⁷ **146**



A mixture of *N*-(6-Methyl-2-pyridyl)-4-chloromethylbenzamide **144** (3.69 g, 14 mmol) and hexamethylenetetraamine (5.95 g, 42 mmol) in ethanol/water 20 ml (50:50; V:V) was heated to reflux for 16 hours. After this time 12 *M* HCl (*ca.* 3 ml) was added and the reaction mixture refluxed for a further 30 minutes. After cooling to room temperature the mixture was diluted with water (100 ml) and extracted using dichloromethane (300 ml). The combined organic extracts were washed with water and dried over MgSO₄ and reduced *in vacuo*. The residue was purified using flash column chromatography (SiO₂, 3:2 hexane:ethyl acetate) resulting **146** as a colourless solid (2.10 g, 63%): M.p. 110-111°C; $\nu_{\max}(\text{KBr})/\text{cm}^{-1}$ 3356, 3265, 1682, 1603, 1576, 1541, 1458, 833, 791, 726; δ_{H} (300 MHz, CDCl₃) 10.10 (1H, s, CHO), 8.65 (1H, br s, NH), 8.17 (1H, d, ³*J*_{H,H} 8, Ar CH), 7.98-8.09 (4H, m, Ar CH), 7.67 (1H, dd, ³*J*_{H,H} 8, ³*J*_{H,H} 7, Ar CH), 6.95 (1H, d, ³*J*_{H,H} 7, Ar CH), 2.45 (3H, s, CH₃); δ_{C} (75.5 MHz, CDCl₃) 191.3 (CHO), 164.4 (quat. C), 156.9 (quat. C), 150.3 (quat. C), 139.6 (quat. C), 138.9

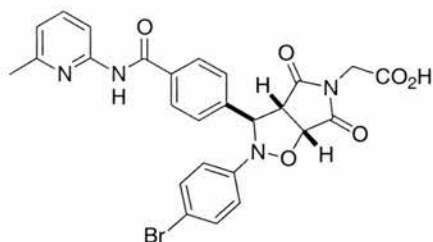
(Ar CH), 138.5 (quat. C), 129.9 (2 x Ar CH), 127.8 (2 x Ar CH), 119.8 (Ar CH), 111.0 (Ar CH), 23.8 (CH₃); *m/z* (EI) 240 (M⁺, 19%), 211 (69), 133 (100), 105 (53), 92 (10), 77 (52); Found 241.0977 [M+H⁺], C₁₄H₁₃N₂O₂ requires 241.0977.

2-{3ξ-[N-(6-Methyl-2-pyridyl)-4-benzamidyl]-4,6-dioxo-2-phenyl-(3ar,6ac)-hexahydropyrrolo[3,4-d]isoxazol-5-yl}-ethanoic acid **147**



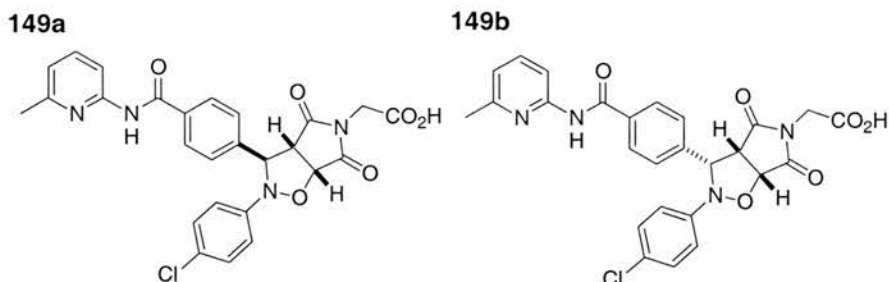
N-[4-(*N'*-6-Methyl-2-pyridyl)-amidobenzylidene]-phenylamine *N*-oxide **113** (150 mg, 0.45 mmol), was added to a solution of the 2-maleimidoethanoic acid **77** (70 mg, 0.45 mmol), in chloroform (10 ml). The reaction was then allowed to stand at 10°C in the absence of light for 3 days. An excess of hexane was then added to the reaction mixture to effect the precipitation of the cycloadduct. The precipitate was filtered, washed with hexane then recrystallised from chloroform/hexane and dried under vacuum to afford **113** a colourless solid as a single diastereoisomer (220 mg, 99%): M.p. >235°C (decomp.); Found: C, 64.2, H, 4.5, N, 11.4. Calc. for C₂₆H₂₂N₄O₆: C, 64.2, H, 4.6, N, 11.5. ν_{\max} (KBr)/cm⁻¹ 3272, 3075, 2995, 2952, 1789, 1713, 1681, 1455, 797, 762, 750; δ_{H} (300 MHz, CDCl₃:CD₃OD, 95:5) 8.19 (1H, d, ³*J*_{H,H} 8, Ar CH), 7.88-7.83 (2H, m, Ar CH), 7.72-7.66 (2H, m, Ar CH), 7.54 (2H, d, ³*J*_{H,H} 8, Ar CH), 7.08-7.14 (2H, m, Ar CH), 6.91-6.95 (2H, m, Ar CH), 6.82-6.87 (1H, m, Ar CH), 5.46 (1H, s, cyclic CH), 5.09 (1H, d, ³*J*_{H,H} 7, cyclic CH), 3.93 (1H, d, ³*J*_{H,H} 7, cyclic CH), 3.90 (2H, s, CH₂), 2.45-2.38 (3H, m, CH₃); δ_{C} (75.5 MHz, CDCl₃:CD₃OD, 95:5) 179.9 (quat. C), 172.9 (quat. C), 167.7 (quat. C), 165.8 (quat. C), 155.6 (quat. C), 149.9 (quat. C), 146.9 (quat. C), 142.0 (quat. C), 139.1 (Ar CH), 132.9 (quat. C), 128.0 (2 x Ar CH), 127.2 (2 x Ar CH), 127.1 (2 x Ar CH), 122.2 (Ar CH), 119.1 (Ar CH), 114.7 (2 x Ar CH), 111.3 (Ar CH), 76.3 (CH), 68.7 (CH), 56.2 (CH), 38.7 (CH₂), 22.1 (CH₃); *m/z* (ESI) 509 (M+Na⁺, 10%), 487 (M+H⁺, 100), 354 (20), 332 (75); Found 487.1615 [M+H⁺], C₂₆H₂₃N₄O₆ requires 487.1618.

2-{3ξ-[N-(6-Methyl-2-pyridyl)-4-benzamidyl]-2-(4-bromophenyl)-4,6-dioxo-(3ar,6ac)-hexahydropyrrolo[3,4-d]isoxazol-5-yl}-ethanoic acid **148**



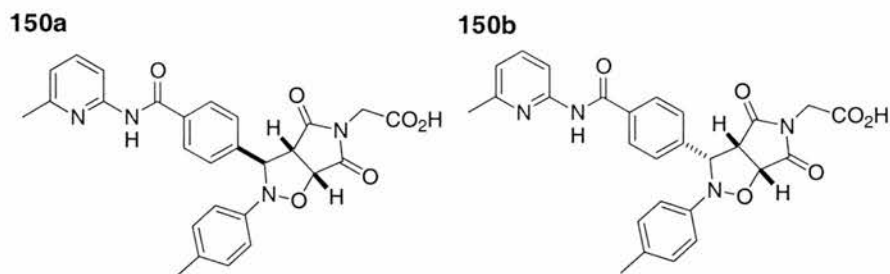
N-[4-(*N'*-6-Methyl-2-pyridyl)-amidobenzylidene]-4-bromophenylamine *N*-oxide **114** (40 mg, 0.97 mmol), was added to a solution of the 2-maleimidoethanoic acid **77** (15 mg, 0.97 mmol), in chloroform (20 ml). The reaction was then allowed to stand at 10°C in the absence of light for 3 days. An excess of hexane was then added to the reaction mixtures to effect the precipitation of the cycloadduct. The precipitate was filtered, washed with hexane then recrystallised from chloroform/hexane and dried under vacuum to afford **148** a colourless solid as a single diastereoisomer (22 mg, 41%); M.p. >180°C (decomp.); Found: C, 55.0; H, 3.7; N, 9.7. Calc. for C₂₆H₂₁N₄O₆Br: C, 55.2; H, 3.7; N, 9.9. ν_{\max} (KBr)/cm⁻¹ 2985, 1716, 1579, 1452, 1174, 796; δ_{H} (300 MHz, CDCl₃) 8.31 (1H, d, ³*J*_{H,H} 8, Ar CH), 7.84 (2H, d, ³*J*_{H,H} 8, Ar CH), 7.77 (1H, t, ³*J*_{H,H} 8, Ar CH), 7.51 (2H, d, ³*J*_{H,H} 8, Ar CH), 7.20 (2H, d, ³*J*_{H,H} 8, Ar CH), 6.98 (1H, d, ³*J*_{H,H} 8, Ar CH), 6.78 (2H, d, ³*J*_{H,H} 8, Ar CH), 5.39 (1H, s, cyclic CH), 5.13 (1H, d, ³*J*_{H,H} 7, cyclic CH), 4.07 (2H, d, ²*J*_{H,H} 3, CH₂), 3.92 (1H, d, ³*J*_{H,H} 8, cyclic CH), 2.49 (3H, s, CH₃); δ_{C} (75.5 MHz, CDCl₃) 174.1 (quat. C), 173.0 (quat. C), 170.0 (quat. C), 165.7 (quat. C), 155.2 (quat. C), 150.1 (quat. C), 146.1 (quat. C), 141.8 (quat. C), 140.8 (Ar CH), 133.7 (quat. C), 131.5 (2 x Ar CH), 128.2 (2 x Ar CH), 127.4 (2 x Ar CH), 119.8 (Ar CH), 116.9 (2 x Ar CH), 115.3 (quat. C), 112.4 (Ar CH), 76.6 (CH), 69.1 (CH), 56.9 (CH), 39.9 (CH₂), 22.1 (CH₃); *m/z* (ESI) 565.08, (M+H⁺ (⁸¹Br), 48%); 566.0, (M+H⁺ (⁷⁹Br), 15) 567.08, (M+2H⁺, 52) 568.08, (M+H⁺, 15); Found 567.0684 [M⁺ (⁸¹Br)], C₂₆H₂₁N₄O₆⁸¹Br requires 567.0702; Found 565.0718 [M⁺ (⁷⁹Br)], C₂₆H₂₁N₄O₆⁷⁹Br requires 565.0723.

2-{3-ξ-[*N*-(6-Methyl-2-pyridyl)-4-benzamidyl]-2-(4-chlorophenyl)-4,6-dioxo-(3*a*,6*a*c)-hexahydropyrrolo[3,4-*d*]isoxazol-5-yl}-ethanoic acid **149**



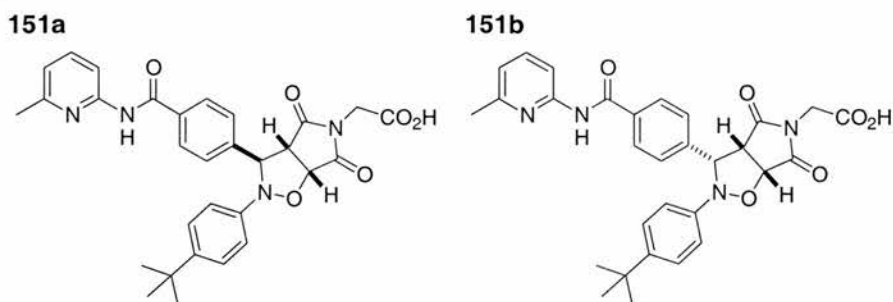
N-[4-(*N'*-6-Methyl-2-pyridyl)-amidobenzylidene]-4-chlorophenylamine *N*-oxide **115** (250 mg, 0.68 mmol), was added to a solution of the 2-maleimidoethanoic acid **77** (110 mg, 0.68 mmol), in chloroform (10 ml). The reaction was then allowed to stand at 10°C in the absence of light for 3 days. An excess of hexane was then added to the reaction mixtures to effect the precipitation of the cycloadduct. The precipitate was filtered, washed with hexane and dried under vacuum. Cycloadduct **149** was obtained as a colourless solid as a 92:8 ratio of diastereoisomers (350 mg, 99%): M.p. >168°C (decomp.); Found: C, 59.9; H, 4.1; N, 10.5. Calc. for C₂₆H₂₁N₄O₆Cl: C, 59.9; H, 4.1; N, 10.7. $\nu_{\max}(\text{KBr})/\text{cm}^{-1}$ 3396, 3062, 2992, 1721, 1578, 1487, 1274, 1166, 794, 753, 695; δ_{H} (300 MHz, CDCl₃, major isomer **149a**) 11.45 (br s, CO₂H), 8.46 (1H, d, ³*J*_{H,H} 8.5, Ar CH), 7.90 (2H, d, ³*J*_{H,H} 8, Ar CH), 7.84 (1H, t, ³*J*_{H,H} 8, 8, Ar CH), 7.58 (2H, d, ³*J*_{H,H} 8, Ar CH), 7.27-7.10 (2H, m, Ar CH), 7.05-7.01 (1H, m, Ar CH), 6.83 (2H, d, ³*J*_{H,H} 9, Ar CH), 5.47 (1H, s, cyclic CH), 5.17 (1H, d, ³*J*_{H,H} 7, cyclic CH), 4.26-4.14 (2H, AB system, CH₂), 3.92 (1H, d, ³*J*_{H,H} 7, cyclic CH), 2.55 (3H, s, CH₃); δ_{H} (300 MHz, CDCl₃, minor isomer **149b**) 11.45 (br s, CO₂H), 8.36 (1H, d, ³*J*_{H,H} 8.5, Ar CH), 8.10 (2H, d, ³*J*_{H,H} 8, Ar CH), 7.99 (1H, t, ³*J*_{H,H} 8, 8, Ar CH), 7.52 (2H, d, ³*J*_{H,H} 8, Ar CH), 7.27-7.10 (2H, m, Ar CH), 7.05-7.01 (1H, m, Ar CH), 6.83 (2H, d, ³*J*_{H,H} 9, Ar CH), 5.47 (1H, s, cyclic CH), 5.17 (1H, d, ³*J*_{H,H} 7, cyclic CH), 4.26-4.14 (2H, AB system, CH₂), 3.92 (1H, d, ³*J*_{H,H} 7, cyclic CH), 2.55 (3H, s, CH₃); δ_{C} (75.5 MHz, CDCl₃, major isomer **149a**) 174.0 (quat. C), 172.7 (quat. C), 172.1 (quat. C), 166.0 (quat. C), 154.3 (quat. C), 150.5 (quat. C), 145.7 (quat. C), 142.0 (2 x quat. C), 133.4 (quat. C), 129.2 (2 x Ar CH), 128.9 (2 x Ar CH), 128.0 (Ar CH), 127.2 (2 x Ar CH), 120.1 (Ar CH), 116.6 (2 x Ar CH), 113.9 (Ar CH), 77.2 (CH), 69.6 (CH), 57.3 (CH), 40.6 (CH₂), 21.1 (CH₃); *m/z* (ESI) 521 (M+H⁺, 100%), 388 (50), 365 (75); Found 565.0873 [M+2Na⁺], C₂₆H₂₀N₄O₆ClNa₂ requires 565.0867.

2-{3ξ-[N-(6-Methyl-2-pyridyl)-4-benzamidyl]-2-(4-methylphenyl)-4,6-dioxo-(3ar,6ac)-hexahydropyrrolo[3,4-d]isoxazol-5-yl}-ethanoic acid **150**



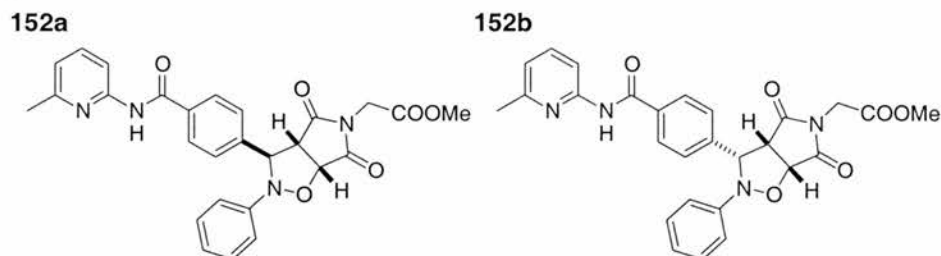
N-[4-(*N'*-6-Methyl-2-pyridyl)-amidobenzylidene]-4-methylphenylamine *N*-oxide **116** (100 mg, 0.29 mmol), was added to a solution of the 2-maleimidoethanoic acid **77** (50 mg, 0.29 mmol), in chloroform (10 ml). The reaction was then allowed to stand at 10°C in the absence of light for 3 days. An excess of ethyl acetate was then added to the reaction mixtures to effect the precipitation of the cycloadduct. The precipitate was filtered, washed with ethyl acetate and dried under vacuum. Cycloadduct **150** was obtained as a colourless solid as a 94:6 ratio of diastereoisomers (90 mg, 65%): M.p. >150°C (decomp.); Found: C, 64.5; H, 4.6; N, 11.6. Calc. for C₂₇H₂₄N₄O₆: C, 64.8; H, 4.8; N, 11.2. $\nu_{\max}(\text{KBr})/\text{cm}^{-1}$ 2924, 1720, 1507, 1453, 1274, 1179, 793; δ_{H} (300 MHz, CDCl₃, major isomer **150a**) 11.45 (br s, CO₂H), 8.45 (1H, d, ³*J*_{H,H} 8.5, Ar CH), 7.98 (2H, d, ³*J*_{H,H} 8, Ar CH), 7.83 (1H, t, ³*J*_{H,H} 8.5, 8.5, Ar CH), 7.59 (2H, d, ³*J*_{H,H} 8, Ar CH), 7.01 (1H, d, ³*J*_{H,H} 8.5, Ar CH), 6.94 (2H, d, ³*J*_{H,H} 8.5, Ar CH), 7.17-7.11 (2H, d, ³*J*_{H,H} 8.5, Ar CH), 5.51 (1H, s, cyclic CH), 5.12 (1H, d, ³*J*_{H,H} 7, cyclic CH), 4.17-4.02 (2H, AB system, CH₂), 3.90 (1H, d, ³*J*_{H,H} 7, cyclic CH), 2.55 (3H, s, CH₃), 2.19 (3H, s, CH₃); δ_{C} (75.5 MHz, CDCl₃, major isomer **150a**) 174.2 (quat. C), 173.0 (quat. C), 172.2 (quat. C), 166.2 (quat. C), 154.3 (quat. C), 150.6 (quat. C), 147.9 (quat. C), 142.6 (quat. C), 142.0 (Ar CH), 133.1 (quat. C), 132.5 (Ar CH), 129.4 (2 x Ar CH), 129.0 (2 x Ar CH), 127.3 (2 x Ar CH), 120.0 (Ar CH), 115.4 (2 x Ar CH), 113.8 (Ar CH), 76.6 (CH), 69.5 (CH), 57.3 (CH), 40.4 (CH₂), 21.1 (CH₃), 20.5 (CH₃); *m/z* (ESI) 501 (M+H⁺, 65%), 346 (100), 274 (25), 257 (18); Found 545.1416 [M+2Na⁺], C₂₇H₂₄N₄O₆Na₂ requires 545.1413.

2-{3ξ-[*N*-(6-Methyl-2-pyridyl)-4-benzamidyl]-2-(4-*tert*-butylphenyl)-4,6-dioxo-(3*ar*,6*ac*)-hexahydropyrrolo[3,4-*d*]isoxazol-5-yl}-ethanoic acid **151**



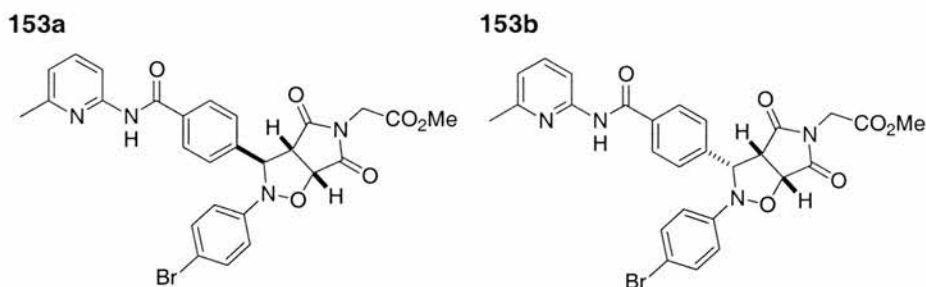
N-[4-(*N'*-6-Methyl-2-pyridyl)-amidobenzylidene]-4-*tert*-butylphenylamine *N*-oxide **117** (106 mg, 0.26 mmol), was added to a solution of the 2-maleimidoethanoic acid **77** (40 mg, 0.26 mmol), in chloroform (5 ml). The reaction was then allowed to stand at 10°C in the absence of light for 3 days. An excess of ethyl acetate was then added to the reaction mixtures to effect the precipitation of the cycloadduct. The precipitate was filtered, washed with ethyl acetate and dried under vacuum. Cycloadduct **151** was obtained as a colourless solid as a 95:5 ratio of diastereoisomers (96 mg, 68%): M.p. >175°C (decomp.); Found: C, 66.1; H, 5.00; N, 9.9. Calc. for C₃₀H₃₀N₄O₆: C, 66.4; H, 5.6; N, 10.3. ν_{\max} (KBr)/cm⁻¹ 2960, 1723, 1609, 1508, 1454, 1273, 1179, 793; δ_{H} (300 MHz, CDCl₃, major isomer **151a**) 8.45 (1H, d, ³*J*_{H,H} 8.5, Ar CH), 7.91 (2H, d, ³*J*_{H,H} 8.5, Ar CH), 7.83 (1H, dd, ³*J*_{H,H} 8, 8, Ar CH), 7.63 (2H, d, ³*J*_{H,H} 8.5, Ar CH), 7.17 (2H, d, ³*J*_{H,H} 8.5, Ar CH), 7.0 (1H, d, ³*J*_{H,H} 8, Ar CH), 6.90 (2H, d, ³*J*_{H,H} 8.5, Ar CH), 5.58 (1H, s, cyclic CH), 5.12 (1H, d, ³*J*_{H,H} 7, cyclic CH), 4.12-3.96 (2H, AB sytem, CH₂), 3.42 (1H, d, ³*J*_{H,H} 7, cyclic CH), 2.55 (3H, s, CH₃), 1.23 (9H, s, CH₃); δ_{C} (75.5 MHz, CDCl₃, major isomer **151a**) 174.3 (quat. C), 173.0 (quat. C), 172.1 (quat. C), 170.2 (quat. C), 166.2 (quat. C), 150.8 (quat. C), 145.9 (quat. C), 144.8 (quat. C), 142.8 (Ar CH), 133.1 (2 x quat. C), 129.1 (2 x Ar CH), 127.3 (2 x Ar CH), 125.7 (2 x Ar CH), 120.1 (Ar CH), 115.0 (2 x Ar CH), 113.9 (Ar CH), 76.6 (CH), 69.1 (CH), 57.4 (CH), 40.3 (CH₂), 34.2 (quat.), 31.3 (3 x CH₃), 21.0 (CH₃); *m/z* (ESI) 543 (M+H⁺, 100%), 388 (60); Found 587.1901 [M+2Na⁺], C₃₀H₃₀N₄O₆Na₂ requires 587.1882.

2-{3 ξ -[*N*-(6-Methyl-2-pyridyl)-4-benzamidyl]-4,6-dioxo-2-phenyl-(3*ar*,6*ac*)-hexahydropyrrolo[3,4-*d*]isoxazol-5-yl)-ethanoic acid, methyl ester **152**



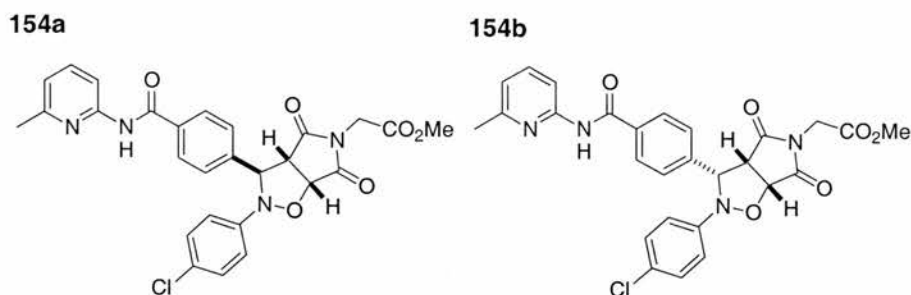
N-[4-(*N'*-6-Methyl-2-pyridyl)-amidobenzylidene]-phenylamine *N*-oxide **113** (150 mg, 0.45 mmol), was added to a solution of the 2-maleimidoethanoic acid, methyl ester **79** (77 mg, 0.45 mmol), in chloroform (20 ml). The reaction was then allowed to stand at 10°C in the absence of light for 3 days. An excess of hexane was then added to the reaction mixtures to effect the precipitation of the cycloadduct. The precipitate was filtered, washed with hexane and dried under vacuum. **152** was obtained as a beige solid as a 7:3 ratio of diastereoisomers (70.0 mg, 32%): M.p. >80°C (decomp.); $\nu_{\max}(\text{KBr})/\text{cm}^{-1}$ 3351, 1792, 1753, 1721, 1676, 1324, 1271, 845, 792, 695; δ_{H} (300 MHz, CDCl_3 , major isomer **152a**) 8.63 (br s, NH), 8.21-8.14 (1H, m, Ar CH), 7.92-7.87 (2H, m, Ar CH), 7.67-7.61 (1H, m, Ar CH), 7.57-7.52 (2H, m, Ar CH), 7.21-7.15 (2H, m, Ar CH), 7.10-7.05 (1H, m, Ar CH), 6.99-6.93 (3H, m, Ar CH), 5.49 (1H, s, CH), 5.13 (1H, d, $^3J_{\text{H,H}}$ 7, CH), 3.97-3.95 (3H, m, CH and CH_2), 3.70 (3H, s, OCH_3), 2.46 (3H, s, CH_3); δ_{H} (300 MHz, CDCl_3 , minor isomer **152b**) 8.63 (br s, NH), 8.50 (1H, d, $^3J_{\text{H,H}}$ 8, Ar CH), 8.21-8.14 (1H, m, Ar CH), 8.05-8.01 (1H, m, Ar CH), 7.92-7.87 (1H, m, Ar CH), 7.67-7.61 (1H, m, Ar CH), 7.57-7.52 (1H, m, Ar CH), 7.21-7.15 (2H, m, Ar CH), 7.10-7.05 (1H, m, Ar CH), 6.99-6.93 (3H, m, Ar CH), 5.18 (1H, d, $^3J_{\text{H,H}}$ 7, CH), 4.77 (1H, d, $^3J_{\text{H,H}}$ 9, CH), 4.21 (2H, dd, $^2J_{\text{H,H}}$ 17, CH_2), 4.03 (1H, dd, $^3J_{\text{H,H}}$ 7, $^3J_{\text{H,H}}$ 9, CH), 3.76 (3H, s, OCH_3), 2.45 (3H, s, CH_3); δ_{C} (75.5 MHz, CDCl_3 , major isomer **152a**) 173.7 (quat. C), 172.4 (quat. C), 166.4 (quat. C), 165.0 (quat. C), 156.9 (quat. C), 150.6 (quat. C), 146.3 (quat. C), 141.9 (quat. C), 138.8 (Ar CH), 134.2 (quat. C), 128.7 (2 x Ar CH), 127.5 (2 x Ar CH), 125.6 (2 x Ar CH), 123.2 (Ar CH), 119.5 (Ar CH), 115.3 (2 x Ar CH), 111.0 (Ar CH), 76.4 (CH), 69.4 (CH), 54.8 (CH), 52.7 (CH_3), 39.5 (CH_2), 23.9 (CH_3); m/z (FAB) 523 ($\text{M}+\text{Na}^+$, 38%), 501 ($\text{M}+\text{H}^+$, 100), 413 (10); Found 501.1760 [$\text{M}+\text{H}^+$], $\text{C}_{27}\text{H}_{25}\text{N}_4\text{O}_6$ requires 501.1774.

2-{3ξ-[*N*-(6-Methyl-2-pyridyl)-3-benzamidyl]-2-(4-bromophenyl)-4,6-dioxo-(3*a*,6*a*)-hexahydropyrrolo[3,4-*d*]isoxazol-5-yl}-ethanoic acid, methyl ester **153**



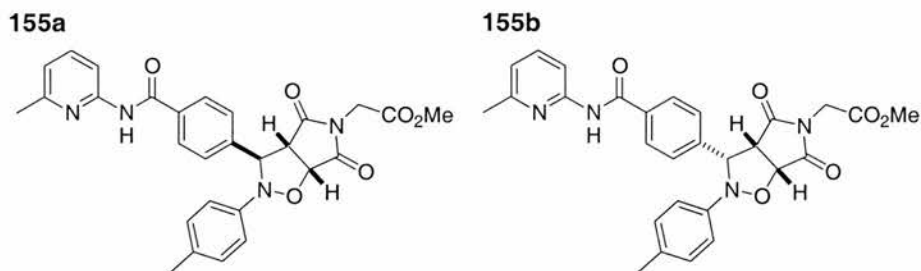
N-[4-(*N'*-6-Methyl-2-pyridyl)-amidobenzylidene]-4-bromophenylamine *N*-oxide **113** (100 mg, 0.24 mmol), was added to a solution of the 2-maleimidoethanoic acid, methyl ester **79** (41 mg, 0.24 mmol), in chloroform (5 ml). The reaction was then allowed to stand at 10°C in the absence of light for 3 days. An excess of hexane was then added to the reaction mixture to effect the precipitation of the cycloadduct. The precipitate was filtered, washed with hexane and dried under vacuum. Cycloadduct **153** was obtained as a colourless solid as a 7:3 ratio of diastereoisomers (140 mg, 99%): M.p 93-94°C; Found: C, 55.8; H, 3.8; N, 9.3. Calc. for C₂₇H₂₃N₄O₆Br: C, 55.9; H, 4.0; N, 9.7. ν_{\max} (KBr)/cm⁻¹ 3396, 2953, 1721, 1674, 1453, 1223, 791, 699; δ_{H} (300 MHz, CDCl₃, major isomer **153a**) 8.65 (br s, NH), 8.20 (1H, d, ³*J*_{H,H} 8, Ar CH), 7.94 (1H, d, ³*J*_{H,H} 8, Ar CH), 7.69 (1H, t, ³*J*_{H,H} 8, 8, Ar CH), 7.54 (2H, d, ³*J*_{H,H} 8, Ar CH), 7.36-7.30 (2H, m, Ar CH), 6.98-6.94 (2H, m, Ar CH), 6.7 (2H, d, ³*J*_{H,H} 8, Ar CH), 5.41 (1H, s, cyclic CH), 5.20 (1H, d, ³*J*_{H,H} 7, cyclic CH), 4.13 (2H, s, CH₂), 3.99 (1H, dd, 7, 1.5, cyclic CH), 3.77 (3H, s, CH₃), 2.50 (3H, s, CH₃); δ_{H} (300 MHz, CDCl₃, minor isomer **152b**) 8.65 (br s, NH), 8.20 (1H, d, ³*J*_{H,H} 8, Ar CH), 8.05 (1H, t, ³*J*_{H,H} 8, 8, Ar CH), 7.92 (1H, d, ³*J*_{H,H} 8, Ar CH), 7.54 (2H, d, ³*J*_{H,H} 8, Ar CH), 7.36-7.30 (2H, m, Ar CH), 6.98-6.94 (2H, m, Ar CH), 6.7 (2H, d, ³*J*_{H,H} 8, Ar CH), 5.21 (1H, d, ³*J*_{H,H} 8, cyclic CH), 4.72 (1H, d, ³*J*_{H,H} 9, cyclic CH), 4.36-4.09 (2H, AB system, CH₂), 4.07-4.04 (1H, m, cyclic CH), 3.80 (3H, s, CH₃), 2.52 (3H, s, CH₃); δ_{C} (75.5 MHz, CDCl₃, major isomer **153a**) 173.8 (quat. C), 173.5 (quat. C), 172.2 (quat. C), 166.3 (quat. C), 164.8 (quat. C), 156.7 (quat. C), 150.7 (quat. C), 147.0 (quat. C), 141.3 (quat. C), 139.0 (Ar CH), 134.3 (quat. C), 131.8 (2 x Ar CH), 127.9 (2 x Ar CH), 127.6 (2 x Ar CH), 119.6 (Ar CH), 117.2 (2 x Ar CH), 111.0 (Ar CH), 76.4 (CH), 69.5 (CH), 57.0 (CH), 52.9 (CH₃), 39.6 (CH₂), 23.8 (CH₃); *m/z* (ESI) 603 (M+Na⁺ (⁸¹Br), 80%), 601 (M+Na⁺ (⁷⁹Br), 80%), 434 (100), 432 (80); Found 603.0674 [M+Na⁺ (⁸¹Br)], C₂₇H₂₃N₄O₆⁸¹BrNa requires 603.0678, Found 601.0692 [M+Na⁺ (⁷⁹Br)], C₂₇H₂₃N₄O₆⁷⁹BrNa requires 601.0699.

2-{3 ξ -[*N*-(6-Methyl-2-pyridyl)-3-benzamidyl]-2-(4-chlorophenyl)-4,6-dioxo-(3*ar*,6*ac*)-hexahydropyrrolo[3,4-*d*]isoxazol-5-yl}-ethanoic acid, methyl ester **154**



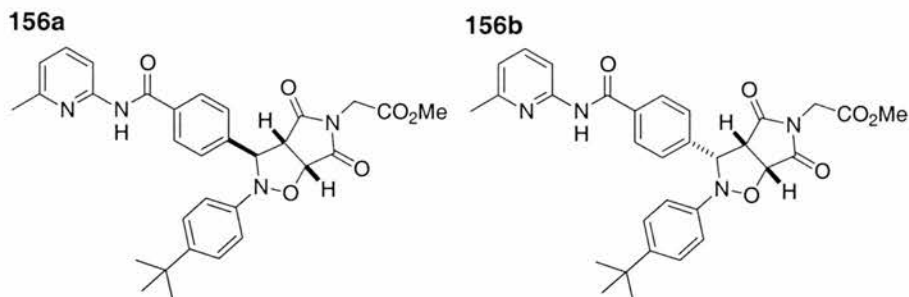
N-[4-(*N'*-6-Methyl-2-pyridyl)-amidobenzylidene]-4-chlorophenylamine *N*-oxide **115** (100 mg, 0.27 mmol), was added to a solution of the 2-maleimidoethanoic acid, methyl ester **79** (42 mg, 0.27 mmol), in chloroform (10 ml). The reaction was then allowed to stand at 10°C in the absence of light for 3 days. An excess of ethyl acetate was then added to the reaction mixtures to effect the precipitation of the cycloadduct. The precipitate was filtered, washed with ethyl acetate and dried under vacuum. Cycloadduct **154** was obtained as a colourless solid as an 8:2 ratio of diastereoisomers (124 mg, 85%): M.p. 95-96°C; Found: C, 60.3; H, 4.3; N, 9.9. Calc. for C₂₇H₂₃N₄O₆Cl: C, 60.6; H, 4.3; N, 10.5. ν_{\max} (KBr)/cm⁻¹ 3337, 2954, 1754, 1722, 1674, 1453, 1224, 1090, 823, 791, 755, 699; δ_{H} (500 MHz, CDCl₃, major isomer **154a**) 8.71 (br s, NH), 8.18 (1H, d, ³*J*_{H,H} 8, Ar CH), 7.92 (2H, d, ³*J*_{H,H} 8, Ar CH), 7.67 (1H, t, ³*J*_{H,H} 7.5, 7.5, Ar CH), 7.51 (2H, d, ³*J*_{H,H} 8, Ar CH), 7.14 (2H, d, ³*J*_{H,H} 9, Ar CH), 6.96-6.94 (1H, m, Ar CH), 6.90 (2H, d, ³*J*_{H,H} 9, Ar CH), 5.38 (1H, s, cyclic CH), 5.16 (1H, d, ³*J*_{H,H} 7, cyclic CH), 4.10 (2H, s, CH₂), 3.96 (1H, dd, ³*J*_{H,H} 1.5, 7, cyclic CH), 3.73 (3H, s, CH₃) 2.48 (3H, s, CH₃); δ_{H} (500 MHz, CDCl₃, minor isomer **154b**) 8.71 (br s, NH), 8.21 (1H, d, ³*J*_{H,H} 8, Ar CH), 7.90 (2H, d, ³*J*_{H,H} 8, Ar CH), 7.67 (1H, t, ³*J*_{H,H} 7.5, 7.5, Ar CH), 7.48 (2H, d, ³*J*_{H,H} 8, Ar CH), 7.17 (2H, d, ³*J*_{H,H} 9, Ar CH), 6.99-6.97 (1H, m, Ar CH), 6.90 (2H, d, ³*J*_{H,H} 9, Ar CH), 5.18 (1H, d, ³*J*_{H,H} 7.5, cyclic CH), 4.69 (1H, d, ³*J*_{H,H} 9, cyclic CH), 4.31-4.13 (2H, AB system, CH₂), 4.05-4.01 (1H, m, cyclic CH), 3.78 (3H, s, CH₃) 2.50 (3H, s, CH₃); δ_{C} (75.5 MHz, CDCl₃, major isomer **154a**) 173.6 (quat. C), 172.2 (quat. C), 166.3 (quat. C), 164.8 (quat. C), 156.5 (quat. C), 150.5 (quat. C), 145.5 (quat. C), 141.4 (quat. C), 139.2 (Ar CH), 139.2 (quat. C), 134.3 (quat. C), 128.9 (2 x Ar CH), 127.9 (2 x Ar CH), 127.6 (2 x Ar CH), 119.6 (Ar CH), 116.9 (2 x Ar CH), 111.2 (Ar CH), 76.5 (CH), 69.6 (CH), 57.0 (CH), 52.8 (CH₃), 39.6 (CH₂), 23.7 (CH₃); *m/z* (ESI) 535 (³⁵M+H⁺, 100%), 366 (83), 241 (92); Found 557.1202 [³⁵M+Na⁺], C₂₇H₂₃N₄O₆³⁵ClNa requires 557.1204.

2-{3 ξ -[*N*-(6-Methyl-2-pyridyl)-3-benzamidyl]-2-(4-methylphenyl)-4,6-dioxo-(3*ar*,6*ac*)-hexahydropyrrolo[3,4-*d*]isoxazol-5-yl}-ethanoic acid, methyl ester **155**



N-[4-(*N'*-6-Methyl-2-pyridyl)-amidobenzylidene]-4-methylphenylamine *N*-oxide **116** (100 mg, 0.29 mmol), was added to a solution of the 2-maleimidoethanoic acid, methyl ester **79** (45 mg, 0.29 mmol), in chloroform (10 ml). The reaction was then allowed to stand at 10°C in the absence of light for 3 days. An excess of ethyl acetate was then added to the reaction mixtures to effect the precipitation of the cycloadduct. The precipitate was filtered, washed with ethyl acetate and dried under vacuum. Cycloadduct **155** was obtained as a colourless solid as a 7:3 ratio of diastereoisomers (82 mg, 55%): M.p. >86°C (decomp.); Found: C, 65.8; H, 5.1; N, 10.5. Calc. for C₂₈H₂₆N₄O₆: C, 65.4; H, 5.1; N, 10.9. ν_{\max} (KBr)/cm⁻¹ 3340, 2953, 2923, 1754, 1721, 1676, 1222, 792, 747, 698; δ_{H} (300 MHz, CDCl₃, major isomer **155a**) 11.45 (br s, CO₂H), 8.45 (1H, d, ³*J*_{H,H} 8.5, Ar CH), 7.98 (2H, d, ³*J*_{H,H} 8, Ar CH), 7.83 (1H, t, ³*J*_{H,H} 8.5, 8.5, Ar CH), 7.59 (2H, d, ³*J*_{H,H} 8, Ar CH), 7.01 (1H, d, ³*J*_{H,H} 8.5, Ar CH), 6.94 (2H, d, ³*J*_{H,H} 8.5, Ar CH), 7.17-7.11 (2H, d, ³*J*_{H,H} 8.5, Ar CH), 5.51 (1H, s, cyclic CH), 5.12 (1H, d, ³*J*_{H,H} 7, cyclic CH), 4.17-4.02 (2H, AB system, CH₂), 3.90 (1H, d, ³*J*_{H,H} 7, cyclic CH), 3.70 (3H, s, CH₃), 2.55 (3H, s, CH₃), 2.19 (3H, s, CH₃); δ_{H} (300 MHz, CDCl₃, minor isomer **155b**) 11.45 (br s, CO₂H), 8.40 (1H, d, ³*J*_{H,H} 8.5, Ar CH), 7.80 (2H, d, ³*J*_{H,H} 8, Ar CH), 7.63 (1H, t, ³*J*_{H,H} 8.5, 8.5, Ar CH), 7.45 (2H, d, ³*J*_{H,H} 8, Ar CH), 7.05 (1H, d, ³*J*_{H,H} 8.5, Ar CH), 6.85 (2H, d, ³*J*_{H,H} 8.5, Ar CH), 7.17-7.11 (2H, d, ³*J*_{H,H} 8.5, Ar CH), 5.45 (1H, d, ³*J*_{H,H} 7, cyclic CH), 5.12 (1H, d, ³*J*_{H,H} 7, cyclic CH), 4.17-4.02 (2H, AB system, CH₂), 3.92 (1H, d, ³*J*_{H,H} 15, cyclic CH), 3.71 (3H, s, CH₃), 2.60 (3H, s, CH₃), 2.21 (3H, s, CH₃); δ_{C} (75.5 MHz, CDCl₃, major isomer **155a**) 174.2 (quat. C), 173.0 (quat. C), 172.2 (quat. C), 166.2 (quat. C), 154.3 (quat. C), 150.6 (quat. C), 147.9 (quat. C), 142.6 (quat. C), 142.0 (Ar CH), 133.1 (quat. C), 132.5 (Ar CH), 129.4 (2 x Ar CH), 129.0 (2 x Ar CH), 127.3 (2 x Ar CH), 120.0 (Ar CH), 115.4 (2 x Ar CH), 113.8 (Ar CH), 76.6 (CH), 69.5 (CH), 57.3 (CH), 52.5 (CH₃), 40.4 (CH₂), 21.1 (CH₃), 20.5 (CH₃); *m/z* (ESI) 515 (M+H⁺, 68%), 346 (100), 275 (22); Found 537.1741 [M+Na⁺], C₂₈H₂₆N₄O₆Na requires 537.1750.

2-{3ξ-[N-(6-Methyl-2-pyridyl)-3-benzamidyl]-2-(4-*tert*-butylphenyl)-4,6-dioxo-(3ar,6ac)-hexahydropyrrolo[3,4-*d*]isoxazol-5-yl}-ethanoic acid, methyl ester **156**



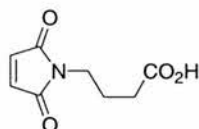
N-[4-(*N'*-6-Methyl-2-pyridyl)-amidobenzylidene]-4-*tert*-butylphenylamine *N*-oxide **117** (100 mg, 0.24 mmol), was added to a solution of the 2-maleimidoethanoic acid, methyl ester **79** (40 mg, 0.24 mmol), in chloroform (5 ml). The reaction was then allowed to stand at 10°C in the absence of light for 3 days. An excess of ethyl acetate was then added to the reaction mixtures to effect the precipitation of the cycloadduct. The precipitate was filtered, washed with ethyl acetate and dried under vacuum. Cycloadduct **156** was obtained as a colourless solid as a 7:3 ratio of diastereoisomers (74 mg, 52%): M.p. 98-100°C; Found: C, 67.2; H, 5.4; N, 9.8. Calc. for C₃₁H₃₂N₄O₆: C, 66.9; H, 5.8; N, 10.1. ν_{\max} (KBr)/cm⁻¹ 2958, 1756, 1722, 1677, 1453, 1220, 1180, 753; δ_{H} (300 MHz, CDCl₃, major isomer **156a**) 8.66 (br s, NH), 8.18 (1H, d, ³*J*_{H,H} 8, Ar CH), 7.92 (2H, d, ³*J*_{H,H} 9, Ar CH), 7.67 (1H, t, ³*J*_{H,H} 8, 8, Ar CH), 7.58 (2H, d, ³*J*_{H,H} 9, Ar CH), 7.20 (2H, d, ³*J*_{H,H} 9, Ar CH), 6.91-6.78 (3H, m, Ar CH), 5.48 (1H, s, cyclic CH), 5.10 (1H, d, ³*J*_{H,H} 7, cyclic CH), 3.94 (1H, dd, ³*J*_{H,H} 7, 1.5, cyclic CH), 3.93-3.70 (2H, AB system, CH₂), 3.70 (3H, s, CH₃), 2.46 (3H, s, CH₃), 1.24 (9H, s, CH₃); δ_{H} (300 MHz, CDCl₃, minor isomer **156b**) 8.66 (br s, NH), 8.16-8.17 (1H, m, Ar CH), 7.88 (2H, d, ³*J*_{H,H} 9, Ar CH), 7.65 (1H, t, ³*J*_{H,H} 8, 8, Ar CH), 7.52 (2H, d, ³*J*_{H,H} 9, Ar CH), 7.23-7.19 (2H, m, Ar CH), 7.01 (1H, d, ³*J*_{H,H} 8, Ar CH), 6.91-6.78 (2H, m, Ar CH), 5.15 (1H, d, ³*J*_{H,H} 7, cyclic CH), 4.76 (1H, d, ³*J*_{H,H} 7, cyclic CH), 4.31-4.14 (2H, AB system, CH₂), 4.01 (1H, dd, ³*J*_{H,H} 7, 1.5, cyclic CH), 3.70 (3H, s, CH₃), 2.45 (3H, s, CH₃), 1.23 (9H, s, CH₃); δ_{C} (75.5 MHz, CDCl₃, major isomer **156a**) 173.8 (quat. C), 172.4 (quat. C), 171.0 (quat. C), 166.4 (quat. C), 156.7 (quat. C), 150.5 (quat. C), 146.2 (quat. C), 144.7 (quat. C), 142.2 (quat. C), 140.0 (Ar CH), 139.0 (quat. C), 127.8 (2 x Ar CH), 127.5 (2 x Ar CH), 125.7 (2 x Ar CH), 120.2 (Ar CH), 115.1 (2 x Ar CH), 111.0 (Ar CH), 76.6 (CH), 69.2 (CH), 57.2 (CH), 52.8 (CH₃), 39.3 (CH₂), 34.1 (quat. C), 31.2 (3 x CH₃), 23.8 (CH₃); *m/z* (ESI) 557 (M+H⁺, 45%), 388 (62), 274 (70), 210 (100); Found 579.2211 [M+Na⁺], C₃₁H₃₂N₄O₆Na requires 579.2220.

tert-Butylhydroxylamine 158



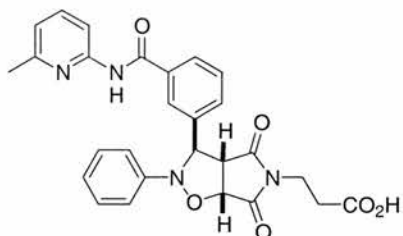
Zinc dust (65.80 g, 364 mmol) was added portion-wise to a stirred solution of NH_4Cl (53.60 g, 485 mmol) and 2-methyl-2-nitrobenzene **157** (5.00 g, 48 mmol) in water/ethanol 200 ml (2:5; V:V) at room temperature. After addition of the zinc dust was complete the reaction mixture was stirred for a further 15 minutes. The resulting slurry was filtered through Celite® and the residue washed with hot water (100 ml). The filtrate was extracted using dichloromethane (400 ml). The combined organic extracts were washed once with water then dried over MgSO_4 and concentrated *in vacuo* to afford **158** as a colourless solid with a distinctive smell that was used immediately. (550 mg, 13%): M.p. 99-101°C; $\nu_{\text{max}}(\text{KBr})/\text{cm}^{-1}$ 3315, 3213, 2799, 1690, 1475, 1363, 1217; δ_{H} (300 MHz, CDCl_3) 7.57 (br s, NHOH), 1.28 (9H, s, $(\text{CH}_3)_3$); δ_{C} (75.5 MHz, CDCl_3) 58.9 (quat. C), 24.2 (3 x CH_3); m/z (EI) 89 (M^+ , 8%), 74 (100) 57 (95), 41 (51).

4-Maleimido-*n*-butanoic acid²⁰³ 161



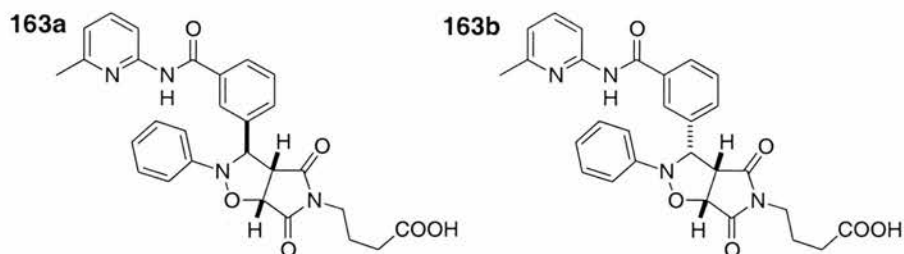
γ -Aminobutyric acid **168** (5.00 g, 49 mmol) and maleic anhydride **86** (4.75 g, 49 mmol) were stirred in acetic acid (AR) (100 ml) for 16 hours at room temperature under nitrogen. The reaction mixture was then heated to reflux for 8 hours before being cooled to room temperature. The solvent was removed *in vacuo* and the crude residue was purified using flash column chromatography (SiO_2 , 20:1 dichloromethane:methanol) affording 4-maleimidobutanoic acid **161** as a colourless solid (5.75 g, 65%): M.p. 87-88°C (lit.²⁰³ 90-92°C); Found: C, 52.6; H, 5.0; N, 7.6. Calc. for $\text{C}_8\text{H}_9\text{NO}_4$: C, 52.5; H, 5.0; N, 7.6. $\nu_{\text{max}}(\text{KBr})/\text{cm}^{-1}$ 3087, 2951, 1732, 1714, 1651, 1415, 965, 922, 881; δ_{H} (300 MHz, CDCl_3) 10.34 (1H, br s, CO_2H), 6.70 (2H, s, maleimide H), 3.57 (2H, t, $^3J_{\text{H,H}}$ 7, CH_2), 2.35 (2H, t, $^3J_{\text{H,H}}$ 7, CH_2), 1.85-1.95 (2H, m, CH_2); δ_{C} (75.5 MHz, CDCl_3) 173.7 (quat. C), 171.0 (2 x quat. C), 134.3 (2 x CH), 36.4 (CH_2), 30.7 (CH_2), 23.3 (CH_2); m/z (EI) 183 (M^+ , 20%), 165 (63), 137 (61), 124 (61), 110 (100), 99 (78), 82 (89); Found 183.3108 [M^+], $\text{C}_8\text{H}_9\text{NO}_4$ requires 183.3114.

3-{3c-[N-(6-Methyl-2-pyridyl)-3-benzamidyl]-4,6-dioxo-2-phenyl-(3ar,6ac)-hexahydropyrrolo[3,4-d]isoxazol-5-yl}-propanoic acid 162



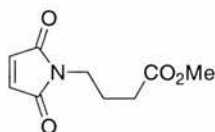
N-[3-(*N'*-6-Methyl-2-pyridyl)-amidobenzylidene]-phenylamine *N*-oxide **104** (250 mg, 0.76 mmol), was added to a solution of 3-maleimidopropanoic acid **6** (130 mg, 0.76 mmol) and chloroform (10 ml). The reaction was then allowed to stand at 10°C in the absence of light for 3 days. An excess of hexane was then added to the reaction mixture to effect the precipitation of the cycloadduct. The precipitate was filtered, washed with hexane, recrystallised from chloroform/hexane and dried under vacuum to afford **102** as a colourless solid as a single diastereoisomer (300 mg, 81%): M.p. >230°C (decomp.); $\nu_{\max}(\text{KBr})/\text{cm}^{-1}$ 3072, 2969, 2476, 1714, 1672, 1613, 1454, 803, 721, 690; δ_{H} (300 MHz, $\text{CDCl}_3:\text{CD}_3\text{OD}$ 95:5) 8.07 (1H, d, $^3J_{\text{H,H}}$ 8, Ar CH), 7.98 (1H, s, Ar CH), 7.81 (1H, d, $^3J_{\text{H,H}}$ 8, Ar CH), 7.62-7.56 (2H, m, Ar CH), 7.44-7.38 (1H, m, Ar CH), 7.13-7.08 (1H, dd, $^3J_{\text{H,H}}$ 8, $^3J_{\text{H,H}}$ 8, Ar CH), 6.96-6.93 (2H, m, Ar CH), 6.88-6.82 (2H, m, Ar CH), 5.54 (1H, s, cyclic CH), 4.98 (1H, d, $^3J_{\text{H,H}}$ 7, cyclic CH), 3.90-3.88 (1H, m, cyclic CH), 3.37 (2H, d, $^3J_{\text{H,H}}$ 7, CH_2), 2.37 (3H, s, CH_3), 1.99-1.91 (2H, m, CH_2); δ_{C} (75.5 MHz, $\text{CDCl}_3:\text{CD}_3\text{OD}$ 95:5) 174.7 (quat. C), 173.5 (quat. C), 172.7 (quat. C), 165.6 (quat. C), 156.4 (quat. C), 150.4 (quat. C), 147.9 (quat. C), 139.0 (quat. C), 138.9 (Ar CH), 134.3 (quat. C), 130.4 (Ar CH), 129.0 (2 x Ar CH), 128.8 (Ar CH), 126.9 (Ar CH), 125.4 (Ar CH), 122.8 (Ar CH), 119.4 (Ar CH), 114.2 (2 x Ar CH), 111.4 (Ar CH), 76.9 (CH), 68.9 (CH), 56.4 (CH), 34.4 (CH_2), 30.2 (CH_2), 23.1 (CH_3); m/z (ESI) 523 ($\text{M}+\text{Na}^+$, 23%), 501 ($\text{M}+\text{H}^+$, 100), 354 (24), 332 (55); Found 501.1761 [$\text{M}+\text{H}^+$], $\text{C}_{27}\text{H}_{25}\text{N}_4\text{O}_6$ requires 501.1774.

4-{3 ξ -[*N*-(6-Methyl-2-pyridyl)-3-benzamidyl]-4,6-dioxo-2-phenyl-(3*ar*,6*ac*)-hexahydropyrrolo[3,4-*d*]isoxazol-5-yl}-*n*-butanoic acid **163**



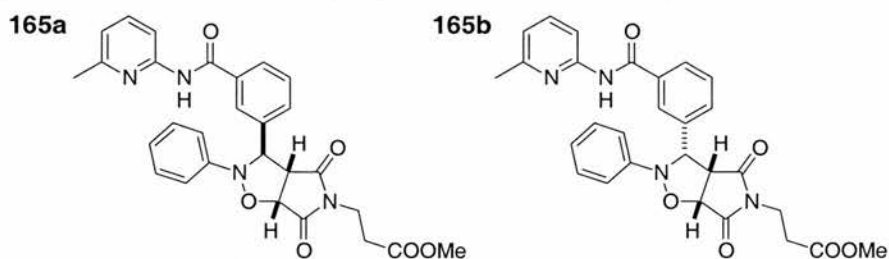
N-[3-(*N'*-6-Methyl-2-pyridyl)-amidobenzylidene]-phenylamine *N*-oxide **104** (150 mg, 0.45 mmol), was added to a solution of the 4-maleimido-*n*-butanoic acid **161** (83 mg, 0.45 mmol), in chloroform (20 ml). The reaction was then allowed to stand at 10°C in the absence of light for 3 days. An excess of hexane was then added to the reaction mixture to effect the precipitation of the cycloadduct. The precipitate was filtered, washed with hexane and dried under vacuum. **163** was obtained as a colourless solid as a 7:3 ratio of diastereoisomers (52 mg, 22%): M.p. >175°C (decomp.); $\nu_{\max}(\text{KBr})/\text{cm}^{-1}$ 3433, 1783, 1711, 1278, 791, 757, 694; δ_{H} (300 MHz, d_6 -DMSO, major isomer **163a**) 10.85 (1H, s, NH), 8.13 (1H, s, Ar CH), 8.04-8.02 (1H, m, Ar CH), 7.98-7.91 (1H, m, Ar CH), 7.77-7.67 (2H, m, Ar CH), 7.50 (1H, t, $^3J_{\text{H,H}}$ 8, Ar CH), 7.29-7.24 (1H, m, Ar CH), 7.22-7.16 (1H, m, Ar CH), 7.11-7.03 (3H, m, Ar CH), 6.87 (1H, dd, $^3J_{\text{H,H}}$ 7, $^3J_{\text{H,H}}$ 8, Ar CH), 5.78 (1H, s, CH), 5.29 (1H, d, $^3J_{\text{H,H}}$ 7, CH), 4.14-4.07 (1H, m, CH), 3.15-3.11 (2H, m, CH₂), 2.50 (3H, m, CH₃), 2.01-1.96 (2H, m, CH₂), 1.37-1.19 (2H, m, CH₂); δ_{H} (300 MHz, d_6 -DMSO, minor isomer **163b**) 10.73 (1H, s, NH), 8.04-8.02 (1H, m, Ar CH), 7.98-7.91 (2H, m, Ar CH), 7.77-7.67 (1H, m, Ar CH), 7.41-7.34 (2H, m, Ar CH), 7.29-7.24 (1H, m, Ar CH), 7.22-7.16 (1H, m, Ar CH), 7.11-7.03 (4H, m, Ar CH), 5.24 (1H, d, $^3J_{\text{H,H}}$ 7, CH), 4.97 (1H, d, $^3J_{\text{H,H}}$ 9, CH), 4.14-4.07 (1H, m, CH), 3.34-3.31 (2H, m, CH₂), 2.50 (3H, m, CH₃), 2.20-2.15 (2H, m, CH₂), 1.60-1.55 (2H, m, CH₂); δ_{C} (75.5 MHz, d_6 -DMSO, major isomer **163a**) 175.3 (quat. C), 173.7 (quat. C), 172.9 (quat. C), 165.7 (quat. C), 156.6 (quat. C), 151.5 (quat. C), 147.0 (quat. C), 138.4 (Ar CH), 135.6 (quat. C), 134.0 (quat. C), 130.5 (Ar CH), 128.8 (2 x Ar CH), 128.4 (Ar CH), 127.6 (Ar CH), 126.8 (Ar CH), 122.3 (Ar CH), 119.8 (Ar CH), 114.2 (2 x Ar CH), 111.5 (Ar CH), 77.3 (CH), 69.9 (CH), 56.8 (CH), 37.5 (CH₂), 30.8 (CH₂), 23.5 (CH₃), 20.9 (CH₂); m/z (ESI) 537 (M+Na⁺, 78%), 514 (M+H⁺, 30), 354 (100), 332 (24); Found 537.1749 [M+Na⁺], C₂₈H₂₆N₄O₆Na requires 537.1750.

4-Maleimido-*n*-butanoic acid, methyl ester **164**



Methyl iodide (1.37 ml, 22.0 mmol) was added dropwise to a stirred solution of 4-maleimidobutanoic acid **161** (2.00 g, 11.0 mmol) and Cs₂CO₃ (1.78 g, 6.5 mmol) in pre-dried DMSO (over 4Å molecular sieves) (30 ml). After stirring at room temperature for 16 hours in the dark, the reaction mixture was diluted with water (*ca.* 50 ml) and extracted using dichloromethane (200 ml). The combined organic extracts were washed once with water (50 ml) and dried over MgSO₄. Solvent was removed *in vacuo* and the residue purified by flash column chromatography (SiO₂, 7:3 hexane:ethyl acetate) affording **164** as a colourless solid, (1.39 g, 64%): M.p. 55-56°C; Found: C, 54.8; H, 5.7; N, 7.0. Calc. for C₉H₁₁NO₄: C, 54.8; H, 5.6; N, 7.1. $\nu_{\max}(\text{KBr})/\text{cm}^{-1}$ 3449, 3166, 2965, 2945, 1707, 1584, 1444, 1410; δ_{H} (300 MHz, CDCl₃) 6.69 (2H, s, maleimide CH), 3.65 (3H, s, CO₂CH₃), 3.56 (2H, t, ³J_{H,H} 7, CH₂), 2.31 (2H, t, ³J_{H,H} 7, CH₂), 1.86-1.96 (2H, m, CH₂); δ_{C} (75.5 MHz, CDCl₃) 172.9 (quat. C), 170.7 (2 x quat. C), 134.1 (2 x CH), 51.7 (CH₃), 37.0 (CH₂), 31.1 (CH₂), 23.7 (CH₂); *m/z* (EI) 197 (M⁺, 42%), 165 (89), 137 (38), 124 (45), 110 (100), 82 (65). Found 197.0684 [M⁺], C₉H₁₁NO₄ requires 197.0688.

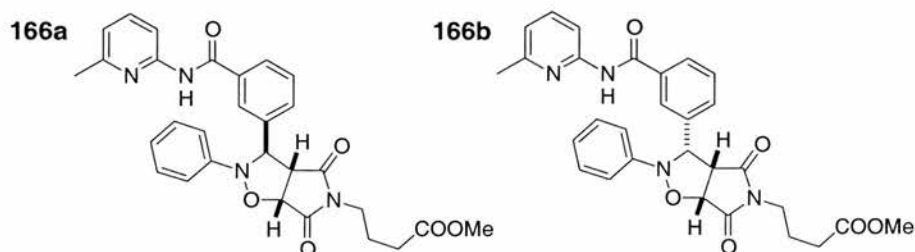
3-{3 ζ -[*N*-(6-Methyl-2-pyridyl)-3-benzamidyl]-4,6-dioxo-2-phenyl-(3*ar*,6*ac*)-hexahydropyrrolo[3,4-*d*]isoxazol-5-yl]-propanoic acid, methyl ester **165**



N-[3-(*N*'-6-Methyl-2-pyridyl)-amidobenzylidene]-phenylamine *N*-oxide **104** (150 mg, 0.45 mmol), was added to a solution of the 3-maleimidopropanoic acid, methyl ester **12** (83 mg, 0.45 mmol), in chloroform (20 ml). The reaction was then allowed to stand at 10°C in the absence of light for 3 days. An excess of hexane was then added to the reaction mixture to effect the precipitation of the cycloadduct. The precipitate was filtered, washed with hexane and dried under vacuum. Cycloadduct **165** was obtained as a colourless solid as a 9:1 ratio of diastereoisomers (55 mg, 23%): M.p. >220°C (decomp.); $\nu_{\max}(\text{KBr})/\text{cm}^{-1}$ 3432, 1744, 1711, 1682, 1241, 795, 772, 759, 743; δ_{H} (300 MHz, CDCl₃:CD₃OD, 95:5, major isomer **165a**) 8.85

(br s, NH), 8.20-8.17 (1H, m, Ar CH), 7.99 (1H, s, Ar CH), 7.92-7.89 (1H, m, Ar CH), 7.69-7.63 (1H, m, Ar CH), 7.53-7.44 (2H, m, Ar CH), 7.25-7.19 (2H, m, Ar CH), 7.09-7.07 (3H, m, Ar CH), 6.96-6.92 (1H, m, Ar CH), 5.11 (1H, d, $^3J_{\text{H,H}}$ 8, CH), 4.83 (1H, d, $^3J_{\text{H,H}}$ 9, CH), 3.96 (1H, dd, $^3J_{\text{H,H}}$ 8, $^3J_{\text{H,H}}$ 9, CH), 3.75 (2H, t, $^3J_{\text{H,H}}$ 7, CH₂), 3.65-3.61 (3H, m, CH₃), 2.69-2.64 (2H, t, $^3J_{\text{H,H}}$ 7, CH₂), 2.15-2.45 (3H, m, CH₃); δ_{H} (300 MHz, CDCl₃:CD₃OD, 95:5, minor isomer 165b) 8.85 (br s, NH), 8.20-8.17 (1H, m, Ar CH), 8.10 (1H, s, Ar CH), 7.92-7.89 (1H, m, Ar CH), 7.69-7.63 (1H, m, Ar CH), 7.53-7.44 (2H, m, Ar CH), 7.25-7.19 (2H, m, Ar CH), 7.09-7.07 (2H, m, Ar CH), 6.96-6.92 (2H, m, Ar CH), 5.64 (1H, s, CH), 5.06 (1H, d, $^3J_{\text{H,H}}$ 7, CH), 3.86 (1H, d, $^3J_{\text{H,H}}$ 7, CH), 3.65-3.61 (5H, m, CH₂ and CH₃), 2.66 (2H, t, $^3J_{\text{H,H}}$ 7, CH₂), 2.15-2.45 (3H, m, CH₃); δ_{C} (75.5 MHz, CDCl₃, major isomer **165a**) 173.9 (quat. C), 172.0 (quat. C), 170.8 (quat. C), 164.8 (quat. C), 156.6 (quat. C), 150.6 (quat. C), 146.5 (quat. C), 139.0 (Ar CH), 135.3 (quat. C), 134.8 (quat. C), 131.0 (Ar CH), 129.3 (2 x Ar CH), 128.8 (Ar CH), 127.5 (Ar CH), 126.9 (Ar CH), 125.4 (Ar CH), 119.8 (Ar CH), 119.5 (2 x Ar CH), 111.2 (Ar CH), 76.4 (CH), 70.9 (CH), 54.5 (CH), 51.9 (CH₃), 34.8 (CH₂), 31.0 (CH₂), 23.7 (CH₃); *m/z* (ESI) 537 (M+Na⁺, 100%), 515 (M+H⁺, 50) 354 (16), 332 (11); Found 515.1938 [M+H⁺], C₂₈H₂₆N₄O₆ requires 515.1931.

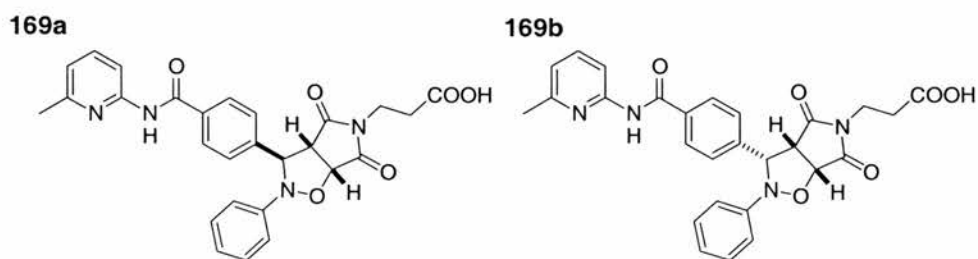
4-{3 ξ -[N-(6-Methyl-2-pyridyl)-3-benzamidyl]-4,6-dioxo-2-phenyl-(3ar,6ac)-hexahydropyrrolo[3,4-d]isoxazol-5-yl]-*n*-butanoic acid, methyl ester **166**



N-[3-(*N'*-6-Methyl-2-pyridyl)-amidobenzylidene]-phenylamine *N*-oxide **104** (150 mg, 0.45 mmol), was added to a solution of the 4-maleimido-*n*-butanoic acid, methyl ester **164** (89 mg, 0.45 mmol), in chloroform (20 ml). The reaction was then allowed to stand at 10°C in the absence of light for 3 days. An excess of hexane was then added to the reaction mixture to effect the precipitation of the cycloadduct. The precipitate was filtered, washed with hexane and dried under vacuum. **166** was obtained as a pale yellow solid as a 7:3 ratio of diastereoisomers (55 mg, 23%): M.p. 73-75°C; Found: C, 65.9; H, 5.4; N, 10.4. Calc. for C₂₉H₂₈N₄O₆: C, 65.9; H, 5.3; N, 10.6. ν_{max} (KBr)/cm⁻¹ 3474, 1784, 1711, 1304, 1272, 793, 759, 695; δ_{H} (300 MHz, CDCl₃, major isomer **166a**) 8.80 (br s, NH), 8.16-8.12 (1H, m, Ar CH), 8.05 (1H, s, Ar CH), 7.84 (1H, d, $^3J_{\text{H,H}}$ 7, Ar CH), 7.67-7.59 (2H, m, Ar CH), 7.49-7.38 (1H, m, Ar CH), 7.20-7.15 (2H, m, Ar CH), 7.08-6.99 (2H, m, Ar CH), 6.93-6.87 (2H, m, Ar

CH), 5.58 (1H, s, CH), 5.00 (1H, d, $^3J_{\text{H,H}}$ 8, CH), 3.85 (1H, d, $^3J_{\text{H,H}}$ 8, CH), 3.62 (3H, m, OCH₃), 3.25 (2H, t, $^3J_{\text{H,H}}$ 7, CH₂), 2.42 (3H, s, CH₃), 2.04 (2H, t, $^3J_{\text{H,H}}$ 7, CH₂), 1.49-1.36 (2H, m, CH₂); δ_{H} (300 MHz, CDCl₃, minor isomer **166b**) 8.80 (br s, NH), 8.16-8.12 (1H, m, Ar CH), 7.99 (1H, s, Ar CH), 7.67-7.59 (1H, m, Ar CH), 7.49-7.38 (2H, m, Ar CH), 7.20-7.15 (3H, m, Ar CH), 7.08-6.99 (3H, m, Ar CH), 6.93-6.87 (1H, m, Ar CH), 5.10 (1H, d, $^3J_{\text{H,H}}$ 8, CH), 4.85 (1H, d, $^3J_{\text{H,H}}$ 9, CH), 3.94 (1H, dd, $^3J_{\text{H,H}}$ 8, $^3J_{\text{H,H}}$ 9, CH), 3.62 (3H, m, OCH₃), 3.49-3.38 (2H, m, CH₂), 2.42 (3H, s, CH₃), 2.23 (2H, t, $^3J_{\text{H,H}}$ 7, CH₂), 1.25-1.23 (2H, m, CH₂); δ_{C} (75.5 MHz, CDCl₃, major isomer **166a**) 174.7 (quat. C), 172.9 (quat. C), 172.3 (quat. C), 165.1 (quat. C), 156.8 (quat. C), 150.7 (quat. C), 148.0 (quat. C), 146.7 (quat. C), 138.8 (Ar CH), 135.4 (quat. C), 130.9 (Ar CH), 129.3 (2 x Ar CH), 128.8 (Ar CH), 127.3 (Ar CH), 126.9 (Ar CH), 123.0 (Ar CH), 119.7 (Ar CH), 114.5 (2 x Ar CH), 111.1 (Ar CH), 77.0 (CH), 70.8 (CH), 56.9 (CH), 51.6 (CH₃), 38.4 (CH₂), 31.2 (CH₂), 23.9 (CH₃), 22.8 (CH₂); m/z (ESI) 551 (M+Na⁺, 100%), 529 (M+H⁺, 16), 354 (99), 332 (15); Found 551.1913 [M+Na⁺], C₂₉H₂₈N₄O₆ requires 551.1907.

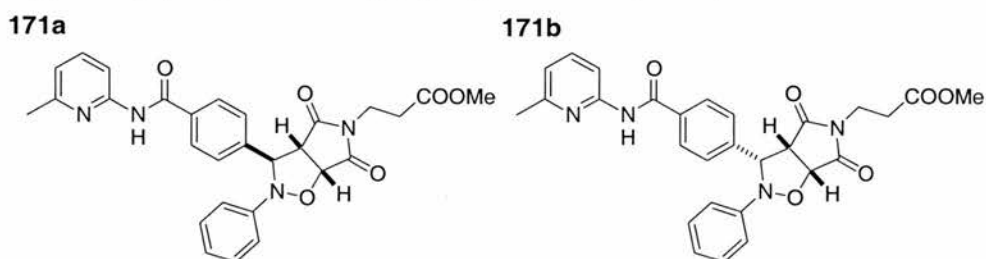
3-{3 ζ -[N-(6-Methyl-2-pyridyl)-4-benzamidyl]-4,6-dioxo-2-phenyl-(3ar,6ac)-hexahydropyrrolo[3,4-d]isoxazol-5-yl]-propanoic acid **169**



N-[4-(*N'*-6-Methyl-2-pyridyl)-amidobenzylidene]-phenylamine *N*-oxide **113** (150 mg, 0.45 mmol), was added to a solution of the 3-maleimidopropanoic acid **6** (77 mg, 0.45 mmol), in chloroform (20 ml). The reaction was then allowed to stand at 10°C in the absence of light for 3 days. An excess of hexane was then added to the reaction mixtures to effect the precipitation of the cycloadduct. The precipitate was filtered, washed with hexane and dried under vacuum. **169** was obtained as a colourless solid as a 1:1 ratio of diastereoisomers (150 mg, 67%): M.p. >145°C (decomp.); ν_{max} (KBr)/cm⁻¹ 3262, 1789, 1715, 1682, 1295, 839, 793, 757, 696; δ_{H} (300 MHz, CDCl₃:CD₃OD, 95:5, major isomer **169a**) 8.11-8.05 (1H, m, Ar CH), 7.91-7.88 (1H, m, Ar CH), 7.87-7.83 (1H, m, Ar CH), 7.63-7.55 (2H, m, Ar CH), 7.42-7.39 (1H, m, Ar CH), 7.18-7.11 (2H, m, Ar CH), 7.01-6.95 (2H, m, Ar CH), 6.90-6.86 (2H, m, Ar CH), 5.06 (1H, d, $^3J_{\text{H,H}}$ 8, CH), 4.81 (1H, d, $^3J_{\text{H,H}}$ 9, CH), 3.91 (1H, dd, $^3J_{\text{H,H}}$ 8, $^3J_{\text{H,H}}$ 9, CH), 3.73-3.60 (1H, m, CH₂), 2.41-2.33 (5H, m, CH₂ and CH₃); δ_{H} (300 MHz, CDCl₃:CD₃OD, 95:5, minor isomer **169b**) 8.11-8.05 (1H, m, Ar CH), 7.91-7.88 (1H, m, Ar CH), 7.87-7.83

(1H, m, Ar CH), 7.63-7.55 (2H, m, Ar CH), 7.42-7.39 (1H, m, Ar CH), 7.18-7.11 (2H, m, Ar CH), 7.01-6.95 (2H, m, Ar CH), 6.90-6.86 (2H, m, Ar CH), 5.55 (1H, s, CH), 4.96 (1H, d, $^3J_{\text{H,H}}$ 8, CH), 3.91 (1H, dd, $^3J_{\text{H,H}}$ 8, $^3J_{\text{H,H}}$ 9, CH), 3.44-3.39 (2H, m, CH₂), 2.41-2.33 (3H, m, CH₃), 1.99-1.95 (2H, m, CH₂); δ_{C} (75.5 MHz, CDCl₃:CD₃OD, 95:5, major isomer **169a**) 174.6 (quat. C), 173.4 (quat. C), 165.5 (quat. C), 165.3 (quat. C), 156.5 (quat. C), 150.7 (quat. C), 147.9 (quat. C), 142.6 (quat. C), 139.1 (Ar CH), 133.5 (quat. C), 128.7 (2 x Ar CH), 127.2 (2 x Ar CH), 125.2 (2 x Ar CH), 123.1 (Ar CH), 119.2 (Ar CH), 114.5 (2 x Ar CH), 111.4 (Ar CH), 76.9 (CH), 70.6 (CH), 56.8 (CH), 31.4 (CH₂), 30.5 (CH₂), 23.4 (CH₃); m/z (FAB) 501 (M+H⁺, 100%), 460 (8), 391 (6); Found 501.1759 [M+H⁺], C₂₇H₂₅N₄O₆ requires 501.1774.

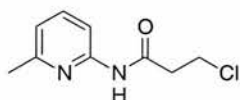
3-{3ξ-[N-(6-Methyl-2-pyridyl)-4-benzamidyl]-4,6-dioxo-2-phenyl-(3ar,6ac)-hexahydropyrrolo[3,4-d]isoxazol-5-yl]-propanoic acid, methyl ester **171**



N-[4-(*N'*-6-Methyl-2-pyridyl)-amidobenzylidene]-phenylamine *N*-oxide **113** (150 mg, 0.45 mmol), was added to a solution of the 3-maleimidopropanoic acid, methyl ester **12** (83 mg, 0.45 mmol), in chloroform (20 ml). The reaction was then allowed to stand at 10°C in the absence of light for 3 days. An excess of hexane was then added to the reaction mixtures to effect the precipitation of the cycloadduct. The precipitate was filtered, washed with hexane and dried under vacuum. **171** was obtained as a cream solid as a 4:1 ratio of diastereoisomers (80 mg, 34%): M.p. >70°C (decomp.); Found: C, 65.4; H, 5.0; N, 10.8. Calc. for C₂₈H₂₆N₄O₆: C, 65.4; H, 5.1; N, 10.9. ν_{max} (KBr)/cm⁻¹ 3342, 1786, 1714, 1675, 1271, 840, 759, 694; δ_{H} (300 MHz, CDCl₃, major isomer **171a**) 8.63 (br s, NH), 8.19-8.13 (1H, m, Ar CH), 7.95-7.88 (2H, m, Ar CH), 7.68-7.60 (3H, m, Ar CH), 7.51-7.45 (1H, m, Ar CH), 7.26-7.19 (1H, m, Ar CH), 7.06-6.93 (4H, m, Ar CH), 5.61 (1H, s, CH), 4.99 (1H, d, $^3J_{\text{H,H}}$ 7, CH), 3.85 (1H, d, $^3J_{\text{H,H}}$ 7, CH), 3.62 (3H, s, OCH₃), 3.51 (2H, t, $^3J_{\text{H,H}}$ 7, CH₂), 2.46-2.35 (3H, m, CH₂ and CH₃), 2.10-2.01 (2H, m, CH₂); δ_{H} (300 MHz, CDCl₃, minor isomer **171b**) 8.68 (br s, NH), 8.50 (1H, d, $^3J_{\text{H,H}}$ 8, Ar CH), 8.19-8.13 (1H, m, Ar CH), 8.05-8.00 (1H, m, Ar CH), 7.95-7.88 (1H, m, Ar CH), 7.80-7.77 (1H, m, Ar CH), 7.68-7.60 (2H, m, Ar CH), 7.26-7.19 (2H, m, Ar CH), 7.06-6.93 (3H, m, Ar CH), 5.12 (1H, d, $^3J_{\text{H,H}}$ 8, CH), 4.84 (1H, d, $^3J_{\text{H,H}}$ 9, CH), 3.96 (1H, dd, $^3J_{\text{H,H}}$ 8, $^3J_{\text{H,H}}$ 9, CH), 3.73-3.70 (2H, m, CH₂), 3.65 (3H, s, OCH₃), 2.46-2.35 (5H, m, CH₂ and CH₃); δ_{C} (75.5 MHz, CDCl₃, major isomer **171a**) 174.2 (quat. C), 172.9

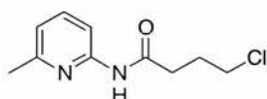
(quat. C), 171.8 (quat. C), 170.7 (quat. C), 164.9 (quat. C), 157.0 (quat. C), 150.7 (quat. C), 146.7 (quat. C), 138.8 (Ar CH), 134.9 (quat. C), 128.0 (2 x Ar CH), 127.2 (2 x Ar CH), 125.3 (2 x Ar CH), 123.2 (Ar CH), 119.6 (Ar CH), 114.6 (2 x Ar CH), 111.0 (Ar CH), 76.6 (CH), 69.2 (CH), 54.5 (CH), 51.8 (CH₃), 34.7 (CH₂), 30.6 (CH₂), 24.0 (CH₃); *m/z* (FAB) 515 (M+H⁺, 100%), 332 (27), 224 (8); Found 515.1925 [M+H⁺], C₂₈H₂₇N₄O₆ requires 515.1931.

3-Chloro-N-(6-methyl-pyridin-2-yl)-propionamide **188**



A solution of 2-amino-6-picoline **120** (12.80 g, 108.1 mmol) in dry dichloromethane (30 ml) was added dropwise to neat 3-chloropropionyl chloride **190** (5.00 g, 39.4 mmol) at 0°C. The reaction mixture was warmed to room temperature and left to stir for 16 hours. The crude product was then reduced *in vacuo* and purified by column chromatography (SiO₂, 7:3 hexane:ethyl acetate), to afford **188** as a yellow solid (7.04 g, 90%): M.p. 29-30°C; ν_{\max} (KBr)/cm⁻¹ 3308, 2962, 1772, 1733, 1691, 1600, 1578, 1454, 1171, 1037, 793, 640; δ_{H} (300 MHz, CDCl₃) 8.31 (br s NH), 7.94 (1H, d, ³J_{H,H} 8, Ar CH), 7.54 (1H, dd, ³J_{H,H} 8, ³J_{H,H} 8, Ar CH), 6.83 (1H, d, ³J_{H,H} 8, Ar CH), 3.72 (2H, t, ³J_{H,H} 7, CH₂), 2.72 (2H, t, ³J_{H,H} 7, CH₂), 2.35 (3H, s, CH₃). δ_{C} (75.5 MHz, CDCl₃) 171.3 (quat. C), 156.7 (quat. C), 150.3 (quat. C), 138.7 (Ar CH), 119.3 (Ar CH), 110.8 (Ar CH), 44.2 (CH₂), 34.1 (CH₂), 23.9 (CH₃); *m/z* (EI) 198 (M⁺, 15%), 108 (100).

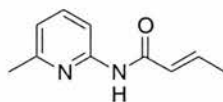
4-Chloro-N-(6-methyl-pyridin-2-yl)-butyramide **189**



A solution of 2-amino-6-picoline **120** (11.5 g, 106.4 mmol) in dry dichloromethane (30 ml) was added dropwise to neat 4-chlorobutyl chloride **191** (5.0 g, 35.5 mmol) at 0°C. The reaction mixture was warmed to room temperature and left to stir for 16 hours. The crude product was then reduced *in vacuo* and purified by column chromatography (SiO₂, 7:3 hexane:ethyl acetate) to afford **189** as a pale yellow solid (7.55 g, 100%): M.p. 31-33°C; ν_{\max} (KBr)/cm⁻¹ 3308, 2961, 1732, 1691, 1538, 1454, 1171, 1036, 792, 639; δ_{H} (300 MHz, CDCl₃) 8.08 (br s NH), 7.96 (1H, d, ³J_{H,H} 8, Ar CH), 7.58 (1H, dd, ³J_{H,H} 8, ³J_{H,H} 8, Ar CH), 6.90 (1H, d, ³J_{H,H} 8, Ar CH), 3.63 (2H, t, ³J_{H,H} 7, CH₂), 2.56 (2H, t, ³J_{H,H} 7, CH₂), 2.44 (3H, s, CH₃), 2.22-2.16 (2H, m, CH₂). δ_{C} (75.5 MHz, CDCl₃) 170.2 (quat. C), 156.0 (quat. C), 150.7 (quat. C), 138.9 (Ar CH), 119.9 (Ar CH), 110.0 (Ar CH), 44.2 (CH₂), 34.1 (CH₂), 27.7 (CH₂),

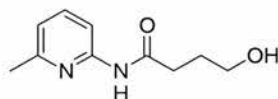
23.5 (CH₃); *m/z* (EI) 212 (M⁺, 13%), 163 (25), 108 (100); Found 212.0705 [M⁺], C₁₀H₁₃N₂OCl requires 212.0716.

But-2-enoic acid (6-methyl-pyridin-2-yl-amide) **195**



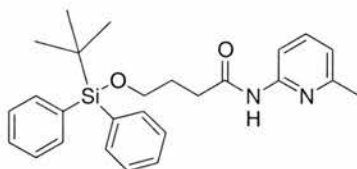
Sodium hydride (2.09 g, 87 mmol) was added cautiously to a stirred solution of 2-amino-6-picoline **120** (6.28 g, 58 mmol) in dry THF (30 ml). The β -lactone **194** (5.00 g, 58 mmol) was added slowly and the reaction was left to stir for 16 hours. The reaction mixture was quenched by pouring on to ethanol (30 ml). The crude product was then reduced *in vacuo* and purified by column chromatography (SiO₂, 3:2 hexane:ethyl acetate), to afford **195** as a colourless solid (4.10 g, 40%): M.p. 101-103°C; ν_{\max} (KBr)/cm⁻¹ 3267, 1671, 1638, 1531, 1451, 1291, 1188, 785; δ_{H} (300 MHz, CDCl₃) 8.08 (1H, d, ³*J*_{H,H} 8, Ar CH), 7.60 (1H, dd, ³*J*_{H,H} 8, ³*J*_{H,H} 8, Ar CH), 7.02 (1H, dq, ³*J*_{H,H} 15, ⁴*J*_{H,H} 7), 6.88 (1H, d, ³*J*_{H,H} 8, Ar CH), 5.89 (1H, dq, ³*J*_{H,H} 2, ⁴*J*_{H,H} 15), 2.43 (3H, s, CH₃), 1.90 (3H, dd, ³*J*_{H,H} 2, ⁴*J*_{H,H} 7). δ_{C} (75.5 MHz, CDCl₃) 163 (quat. C), 156.7 (quat. C), 150.8 (quat. C), 142.3 (Ar CH), 138.7 (Ar CH), 125.3 (Ar CH), 119.1 (N=CH), 111.0 (N=CH), 29.7 (CH₃), 17.9 (CH₃). *m/z* (EI) 176 (M⁺, 55%), 161 (39), 148 (72), 133 (27), 125 (14), 108 (100), 69 (92); Found 176.0955 [M⁺], C₁₀H₁₂N₂O requires 176.0950.

4-Hydroxy-*N*-(6-methyl-pyridin-2-yl)-butyramide **196**



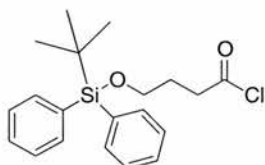
4-(*tert*-Butyl-diphenyl-silanyloxy)-*N*-(6-methyl-pyridin-2-yl)-butyramide **198** (1.75 g, 4 mmol) was added to a stirred solution of tetrabutylammonium fluoride (4.17 ml, 4 mmol) in THF (10 ml). After 4 hours the reaction mixture was poured onto ethyl acetate (20 ml) and washed with water (3 x 30 ml). The crude product was reduced *in vacuo* and purified by column chromatography (10:1 hexane:ethyl acetate) to afford **196** as a pale yellow oil (220 mg, 31%): δ_{H} (300 MHz, CDCl₃) 8.21 (br s, NH), 7.91 (1H, d, ³*J*_{H,H} 8, Ar CH), 7.50 (1H, dd, ³*J*_{H,H} 8, ³*J*_{H,H} 8, Ar CH), 6.79 (1H, d, ³*J*_{H,H} 8, Ar CH), 3.62 (2H, t, ³*J*_{H,H} 6, CH₂), 2.50 (2H, t, ³*J*_{H,H} 8, CH₂), 2.41 (3H, s, CH₃), 1.99-1.81 (2H, m, CH₂); δ_{C} (75.5 MHz, CDCl₃) 171.3 (quat. C), 156.6 (quat. C), 150.6 (quat. C), 138.6 (Ar CH), 118.9 (Ar CH), 110.7 (Ar CH), 62.9 (CH₂), 36.1 (CH₂), 25.9 (CH₂), 29.8 (CH₃); *m/z* (CI) 195 (M+H⁺, 26%), 109 (73), 87 (34), 75 (14), 55 (100); Found 195.113 [M+H⁺], C₁₀H₁₅N₂O₂ requires 195.1133

4-(*tert*-Butyl-diphenyl-silyloxy)-*N*-(6-methyl-pyridin-2-yl)-butyramide **198**



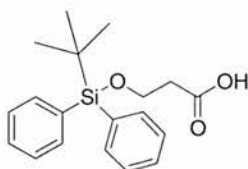
A solution of 2-amino-6-picoline (2.1 g, 19 mmol) **120** in dry dichloromethane was added dropwise to neat 4-(*tert*-Butyl-diphenyl-silyloxy)-butyryl chloride (2.3 g, 6.4 mmol) **200** at 0°C. After addition the reaction was allowed to warm to room temperature and stirred for 16 hours. The crude product was reduced *in vacuo* and purified by column chromatography (SiO₂, 4:1 hexane:ethyl acetate) to afford **198** as a colourless solid (1.75 g, 64%): δ_{H} (300 MHz, CDCl₃) 8.10 (1H, d, $^3J_{\text{H,H}}$ 8, Ar CH), 7.95 (br s, NH), 7.60-7.56 (4H, m, Ar CH), 7.52 (1H, dd, $^3J_{\text{H,H}}$ 8, $^3J_{\text{H,H}}$ 8, Ar CH), 7.35-7.22 (6H, m, Ar CH), 6.81 (1H, d, $^3J_{\text{H,H}}$ 8, Ar CH), 3.66 (2H, t, $^3J_{\text{H,H}}$ 6, CH₂), 2.46 (2H, t, $^3J_{\text{H,H}}$ 8, CH₂), 1.94-1.85 (2H, m, CH₂), 1.42 (3H, s, CH₃), 0.98 (9H, s, CH₃); δ_{C} (75.5 MHz, CDCl₃) 171.3 (quat. C), 157.0 (quat. C), 150.6 (quat. C), 138.6 (Ar CH), 135.5 (4 x Ar.CH), 134.6 (2 x quat. C), 133.6 (Ar CH), 129.6 (2 x Ar CH), 127.6 (4 x Ar CH), 118.9 (Ar CH), 110.7 (Ar CH), 62.9 (CH₂), 34.1 (CH₂), 27.9 (CH₂), 26.8 (CH₃), 19.6 (3 x quat. C); m/z (CI) 433 (M+H⁺, 100%), 375 (14), 75 (14), Found 433.2321 [M+H⁺], C₂₆H₃₃N₂O₂Si requires 433.2311.

4-(*tert*-Butyl-diphenyl-silyloxy)-butyryl chloride²¹¹ **200**



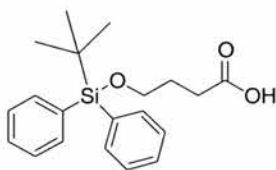
Oxalyl chloride (5.3 g, 42 mmol) was carefully added to a stirred solution of 4-(*tert*-Butyl-diphenyl-silyloxy)-butyric acid **202** (2.5 g, 7 mmol) in toluene (25 ml) at room temperature. After 6 hours the solvent and oxalyl chloride was removed under reduced pressure to give **200** as an unstable colourless oil (2.3 g, 87%): δ_{H} (300 MHz, CDCl₃) 7.80-7.77 (4H, m, Ar CH), 7.56-7.49 (6H, m, Ar CH), 3.83 (2H, t, $^3J_{\text{H,H}}$ 6, CH₂), 2.62 (2H, t, $^3J_{\text{H,H}}$ 8, CH₂), 2.16-1.99 (2H, m, CH₂), 0.95 (9H, s, CH₃); δ_{C} (75.5 MHz, CDCl₃) 135.9 (4 x Ar CH), 133.8 (2 x quat. C), 130.0 (2 x Ar CH), 129.5 (quat. C) 128.1 (4 x Ar CH), 62.3 (CH₂), 44.3 (CH₂), 28.3 (CH₂), 26.9 (3 x CH₃) 19.6 (quat. C).

3-(*tert*-Butyl-diphenyl-silyloxy)-propionic acid²¹¹ **201**



A solution of the protected diol **203** (11.2 g, 36 mmol) in DMF (60 ml) was cooled to 0°C under nitrogen and then treated portion-wise with pyridinium dichromate (46.9 g 125 mmol). The resulting mixture was warmed to room temperature and stirred for 16 hours. The reaction mixture was then poured onto water (350 ml) and extracted with diethyl ether (5 x 200 ml). The combined organic layers were dried MgSO₄, reduced *in vacuo* and purified by gradient elution column chromatography (SiO₂, 20:1 hexane:ethyl acetate followed by 75:25:0.3 hexane:ethyl acetate:acetic acid), to afford **201** as a colourless solid (3.3 g, 28%): M.p. 97-99°C; $\nu_{\max}(\text{KBr})/\text{cm}^{-1}$ 3305 (br.), 3060, 2975, 2918, 1670, 1579, 1452, 1298, 1230, 1152, 1082, 979, 787, 663; δ_{H} (300 MHz, CDCl₃) 7.61-7.52 (4H, m, Ar CH), 7.33-7.20 (6H, m, Ar CH), 3.85 (2H, $^3J_{\text{H,H}}$ 7, CH₂), 2.49 (2H, $^3J_{\text{H,H}}$ 7, CH₂), 1.05 (9H, s, CH₃); δ_{C} (75.5 MHz, CDCl₃) 166.5 (quat. C), 158.9 (quat. C), 152.6 (quat. C), 140.0 (3 x Ar CH), 132.7 (2 x Ar CH), 128.9 (CH₂), 120.9 (2 x Ar CH), 120.8 (Ar CH), 113.1 (Ar CH), 112.8 (Ar CH), 41.1 (CH₂), 29.7 (quat. C), 24.4 (3 x CH₃); m/z (CI) 329 (M+H⁺, 100), 271 (80), 241 (7), 199 (90).

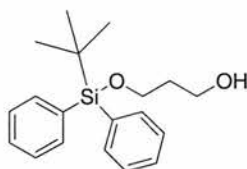
4-(*tert*-Butyl-diphenyl-silyloxy)-butyric acid²¹¹ **202**



A solution of the protected diol **204** (5.90 g, 18 mmol) in DMF (45 ml) was cooled to 0°C under nitrogen and then treated portionwise with pyridinium dichromate (23.6 g, 62 mmol). The resulting mixture was warmed to room temperature and stirred for 16 hours. The reaction mixture was then poured onto water (350 ml) and extracted with diethyl ether (5 x 200 ml). The combined organic layers were dried MgSO₄, reduced *in vacuo* and purified by gradient elution column chromatography (SiO₂, 20:1 hexane:ethyl acetate), followed by (SiO₂, 75:25:0.3 hexane:ethyl acetate:acetic acid), to afford **202** as a colourless solid (3.5 g, 57%): M.p. 107-109°C $\nu_{\max}(\text{KBr})/\text{cm}^{-1}$ 3305, 2918, 2728, 1670, 1452, 1230, 1082, 979, 943, 787, 727; δ_{H} (300 MHz, CDCl₃) 7.8-7.76 (4H, m, Ar CH), 7.55-7.47 (6H, m, Ar CH), 3.82 (2H, t, $^3J_{\text{H,H}}$ 6, CH₂), 2.63 (2H, t, $^3J_{\text{H,H}}$ 8, CH₂), 2.16-1.99 (2H, m, CH₂), 1.17 (9H, s, CH₃); δ_{C} (75.5 MHz, CDCl₃) 180.5 (quat. C), 135.9 (4 x Ar CH), 134.0 (2 x quat. C), 130.0 (2 x Ar CH), 128.1 (4 x Ar CH), 63.2 (CH₂), 31.2 (CH₂), 27.9 (CH₂), 26.8 (3 x CH₃) 19.6 (quat. C); m/z

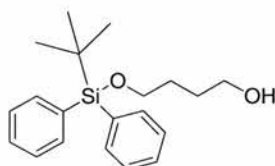
(CI) 343 ($M+H^+$, 100), 285 (10), 265 (14), 207 (5), 187 (22); Found 343.14 [$M+H^+$], $C_{20}H_{27}O_3Si$ requires 343.1365.

3-(*tert*-Butyl-diphenyl-silanyloxy)-propan-1-ol²¹¹ **203**



A solution of 1,3-propanediol (20.0 g, 263 mmol) in dry THF was cooled to $-78^{\circ}C$ under nitrogen. Butyl lithium (5.6 g, 88 mmol) was added dropwise with vigorous stirring. After an additional stir for 5 minutes *tert*-butylchlorodiphenylsilane (TBDPSCI) (24.10 g, 88 mmol) was added dropwise. The resulting mixture was then allowed to warm to room temperature, and stirred for 40 minutes. The reaction mixture was treated with water (50 ml) and sat. NH_4Cl (aq) (50 ml). The aqueous layer was extracted with diethyl ether (3 x 75 ml). The combined organic extracts were, dried, reduced *in vacuo* and purified by column chromatography (SiO_2 , 20:3 hexane:ethyl acetate) to afford **203** as a colourless oil (24.8 g, 90%): $\nu_{max}(KBr)/cm^{-1}$ 3265 (br.), 3069, 2928, 1825, 1739, 1241, 968, 821, 702; δ_H (300 MHz, $CDCl_3$) 7.82-7.72 (4H, m, Ar CH), 7.60-7.49 (6H, m, Ar CH), 3.98-3.92 (4H, m, CH_2), 1.41-1.34 (2H, m, CH_2), 1.25 (9H, s, CH_3); δ_C (75.5 MHz, $CDCl_3$) 135.9 (4 x Ar CH), 133.7 (2 x quat. C), 130.8 (2 x Ar CH), 128.2 (4 x Ar CH), 63.6 (CH_2), 62.3 (CH_2), 34.7 (CH_2), 27.2 (3 x CH_3) 19.5 (quat. C); m/z (CI) 315 ($M+1$, 100%) 257 (20), 199 (10), 91 (39), 73 (27). Found 314.1710 $C_{19}H_{26}O_2Si$ [M^+], requires 314.1702.

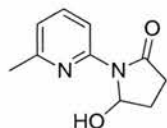
4-(*tert*-Butyl-diphenyl-silanyloxy)-butan-1-ol²¹¹ **204**



A solution of 1,4-butanediol (10.00 g, 101 mmol) in dry THF was cooled to $-78^{\circ}C$ under nitrogen. Butyl lithium (2.17 g, 34 mmol) was added dropwise with vigorous stirring. After an additional stir for 5 minutes *tert*-butylchlorodiphenylsilane (TBDPSCI) (9.34 g, 34 mmol) was added dropwise. The resulting mixture was then allowed to warm to room temperature, and stirred for 40 minutes. The reaction mixture was treated with water (50 ml) and sat. NH_4Cl (aq.) (50 ml). The aqueous layer was extracted with diethyl ether (3 x 50 ml). The combined organic extracts were, dried, reduced *in vacuo* and purified by column chromatography (SiO_2 , 20:3 hexane:ethyl acetate) to afford **204** as a colourless oil (24.8 g,

90%): $\nu_{\max}(\text{KBr})/\text{cm}^{-1}$ 3341, 3070, 2932, 2858, 2739, 1959, 1850, 1427, 1109, 822, 703; δ_{H} (300 MHz, CDCl_3) 7.72-7.62 (4H, m, Ar CH), 7.45-7.32 (6H, m, Ar CH), 3.75-3.63 (4H, m, CH_2), 1.76-1.60 (4H, m, CH_2), 1.08 (9H, s, CH_3); δ_{C} (75.5 MHz, CDCl_3) 135.9 (Ar CH), 134.0 (2 x quat. C) 130.0 (3 x Ar CH), 128.0 (6 x Ar CH), 64.4 (CH_2), 63.1 (CH_2), 30.2 (CH_2), 29.7 (CH_2), 27.2 (3 x CH_3) 19.6 (quat. C); m/z (CI) 329 (M+1, 100%), 271 (14), 257 (20), 199 (5), 91 (42), 73 (27). Found 329.1943 [M+H⁺], $\text{C}_{20}\text{H}_{29}\text{O}_2\text{Si}$ requires 329.1937.

5-Hydroxy-1-(6-methyl-pyridin-2-yl)-pyrrolidin-2-one **208**

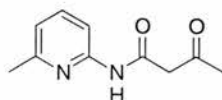


Method A: 4-Hydroxy-*N*-(6-methyl-pyridin-2-yl)-butyramide **196** (400 mg, 2.05 mmol) was added to a stirred solution of pyridinium chlorochromate (660 mg, 3.10 mmol) in dry dichloromethane (30 ml). The reaction was stirred under nitrogen for 2 hours. The crude product was filtered through celite, then reduced *in vacuo* and purified by column chromatography (SiO_2 , 1:1 hexane:ethyl acetate), to afford **208** as a colourless oil (250 mg, 64%):

Method B: To dry dichloromethane (10 ml), oxalyl chloride (200 mg, 1.59 mmol) was added and the solution stirred at -78°C . DMSO (250 mg, 3.19 mmol) was added dropwise over 10 minutes. 4-Hydroxy-*N*-(6-methyl-pyridin-2-yl)-butyramide **196** (280 mg, 1.44 mmol) in dry dichloromethane was added dropwise followed by slow addition of triethylamine (730 mg, 7.2 mmol). This was then left to stir for a further 45 minutes after which time the reaction mixture was allowed to warm to room temperature. The crude product was then reduced *in vacuo* and purified by column chromatography (SiO_2 , 3:2 hexane:ethyl acetate), to afford **208** as a colourless oil (0.15g, 55%):

δ_{H} (300 MHz, CDCl_3) 8.24 (1H, d, $^3J_{\text{H,H}}$ 8, Ar CH), 7.78 (1H, dd, $^3J_{\text{H,H}}$ 8, $^3J_{\text{H,H}}$ 8, Ar CH), 7.06 (1H, d, $^3J_{\text{H,H}}$ 8, Ar CH) 6.17 (1H, dd, $^3J_{\text{H,H}}$ 7, 2, cyclic CH), 3.04-2.95 (1H, m, cyclic CH_2), 2.75-2.63 (1H, m, cyclic CH_2), 2.59 (3H, s, CH_3), 2.51-2.39 (1H, m, cyclic CH_2), 2.27-2.17 (1H, m, cyclic CH_2); δ_{C} (75.5 MHz, CDCl_3) 174.6 (quat. C), 156.9 (quat. C), 151.4 (quat. C), 139.1 (Ar CH), 119.8 (Ar CH), 112.5 (Ar CH), 84.3 (cyclic CH), 31.3 (CH_2), 24.7 (CH_2), 23.1 (CH_3); m/z (CI) 193 (M+H⁺, 100), 175 (28), 58 (50). Found 193.0982 [M+H⁺], $\text{C}_{10}\text{H}_{13}\text{N}_2\text{O}_2$ requires 193.0977.

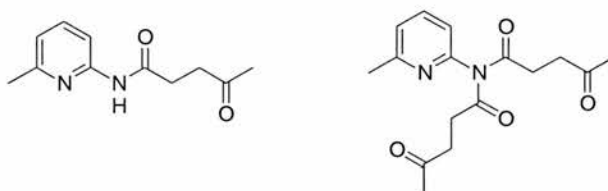
N-(6-Methyl-pyridin-2-yl)-3-oxo-butylamide **211**



2-amino-6-picoline **120** (4.66 g, 43 mmol) was dissolved in methyl acetoacetate **213** (5.00 g, 43.1 mmol) the reaction mixture was stirred and heated to reflux. After 24 hours a colourless precipitate had formed which was isolated by filtration and washed with hexane to afford **211** as a colourless solid (5.23 g, 63%): M.p. 98-100°C; $\nu_{\max}(\text{KBr})/\text{cm}^{-1}$ 3239, 3138, 3069, 1722, 1664, 1553, 1458, 1302, 1151, 796; δ_{H} (300 MHz, CDCl_3) 9.14 (br s, NH), 7.87 (1H, d, $^3J_{\text{H,H}}$ 8, Ar CH), 7.51 (1H, dd, $^3J_{\text{H,H}}$ 8, $^3J_{\text{H,H}}$ 8, Ar CH), 6.82 (1H, d, $^3J_{\text{H,H}}$ 8, Ar CH), 3.53 (2H, s, CH_2), 2.37 (3H, s, CH_3), 2.24 (3H, s, CH_3); δ_{C} (75.5 MHz, CDCl_3) 203.6 (quat. C), 164.4 (quat. C), 157.4 (quat. C), 150.6 (quat. C), 139.0 (Ar CH), 120.0 (Ar CH), 111.4 (Ar CH), 51.4 (CH_2), 31.4 (CH_3), 24.4 (CH_3);

N-(6-Methyl-pyridin-2-yl)-4-oxo-pentanamide **212**

4-Oxo-pentanoic acid (6-methyl-pyridin-2-yl)-(4-oxo-pentanoyl)-amide **215**



β -Phenylhydroxylamine **131** (500 mg, 4.58 mmol) and 4-oxo-pentanoic acid **214** (530 mg, 4.58 mmol) were dissolved in ethyl acetate (10 ml). 2-Amino-6-picoline **120** (500 mg, 4.58 mmol) was added and the reaction mixture stirred for 4 days. A precipitate formed which was filtered and washed with cold ethyl acetate and hexane to afford **215** as a pale yellow solid (180 mg, 13%). Hexane was added to the filtrate to effect the precipitation of **212** which was re-filtered and washed with cold ethyl acetate and hexane to afford **212** as a beige solid (430 mg, 46%):

215: M.p. 63-65°C; $\nu_{\max}(\text{KBr})/\text{cm}^{-1}$ 3296, 2956, 2795, 1705, 1638, 1411, 1298, 1162, 798, 730; δ_{H} (300 MHz, CDCl_3) 7.45 (1H, dd, $^3J_{\text{H,H}}$ 8, $^3J_{\text{H,H}}$ 8, Ar CH), 6.48 (1H, d, $^3J_{\text{H,H}}$ 8, Ar CH), 6.30 (1H, d, $^3J_{\text{H,H}}$ 8, Ar CH), 2.73 (4H, t, $^3J_{\text{H,H}}$ 7, CH_2), 2.66 (4H, t, $^3J_{\text{H,H}}$ 7, CH_2), 2.47 (3H, s, CH_3), 2.20 (6H, s, CH_3); δ_{C} (75.5 MHz, CDCl_3) 208.6 (2xquat. C), 179.1 (2xquat. C), 157.3 (quat. C), 151.5 (quat. C), 141.6 (Ar CH), 112.1 (Ar CH), 108.9 (Ar CH), 39.4 (2 x CH_2), 30.4 (2 x CH_2), 30.3 (CH_3), 20.7 (2 x CH_3); m/z (CI) 287 (M- H_2O , 49%), 255 (25), 219 (10), 203 (100), 117 (40).

212: M.p. 56-58°C; $\nu_{\max}(\text{KBr})/\text{cm}^{-1}$ 3297, 2955, 2795, 1705, 1411, 1298, 1162, 984, 798, 731; δ_{H} (300 MHz, CDCl_3) 7.34 (1H, dd, $^3J_{\text{H,H}}$ 8, $^3J_{\text{H,H}}$ 8, Ar CH), 6.48-6.40 (2H, m, Ar CH), 2.77 (2H, t, $^3J_{\text{H,H}}$ 7, CH_2), 2.60 (2H, t, $^3J_{\text{H,H}}$ 7, CH_2), 2.47 (3H, s, CH_3), 2.21 (3H, s, CH_3); δ_{C} (75.5 MHz, CDCl_3) 208.0 (quat. C), 179.1 (quat. C), 157.5 (quat. C), 152.6 (quat. C), 141.1 (Ar CH), 112.4 (Ar CH), 108.4 (Ar CH), 39.4 (CH_2), 30.3 (CH_2), 30.3 (CH_3), 21.3 (CH_3).

6.8 Data parameters for X-ray crystallography determination

6.8.1 Crystal data and structure refinement for compound 78

Table 6.1 Crystal data and structure refinement for compound 78.

Empirical formula	$C_{17}H_{20}N_6O_5$	
Formula weight	388.39	
Temperature	293(2) K	
Wavelength	0.71073 Å	
Crystal system	Monoclinic	
Space group	P2(1)/c	
Unit cell dimensions	$a = 13.013(4)$ Å	$\alpha = 90^\circ$.
	$b = 17.121(6)$ Å	$\beta = 98.104(7)^\circ$.
	$c = 8.522(3)$ Å	$\gamma = 90^\circ$.
Volume	$1879.8(11)$ Å ³	
Z	4	
Density (calculated)	1.372 Mg/m ³	
Absorption coefficient	0.104 mm ⁻¹	
F(000)	816	
Crystal size	$.1 \times .1 \times .01$ mm ³	
Theta range for data collection	1.58 to 23.32° .	
Index ranges	$-14 \leq h \leq 14$, $-19 \leq k \leq 16$, $-9 \leq l \leq 9$	
Reflections collected	9453	
Independent reflections	2720 [R(int) = 0.6151]	
Completeness to theta = 23.32°	99.8 %	
Absorption correction	Sadabs	
Max. and min. transmission	1.00000 and 0.670412	
Refinement method	Full-matrix least-squares on F ²	
Data / restraints / parameters	2720 / 2 / 122	
Goodness-of-fit on F ²	0.868	
Final R indices [I > 2sigma(I)]	R1 = 0.1166, wR2 = 0.1948	
R indices (all data)	R1 = 0.4064, wR2 = 0.3041	
Extinction coefficient	0.005(2)	
Largest diff. peak and hole	0.273 and -0.277 e.Å ⁻³	

6.8.2 Crystal data and structure refinement for compound 7

Table 6.2 Crystal data and structure refinement for compound 7.

Empirical formula	C ₁₈ H ₂₂ N ₆ O ₅	
Formula weight	402.42	
Temperature	293(2) K	
Wavelength	0.71073 Å	
Crystal system	Orthorhombic	
Space group	Pbca	
Unit cell dimensions	a = 11.054(19) Å	α = 90°.
	b = 8.729(14) Å	β = 90°.
	c = 43.11(7) Å	γ = 90°.
Volume	4160(12) Å ³	
Z	8	
Density (calculated)	1.285 Mg/m ³	
Absorption coefficient	0.096 mm ⁻¹	
F(000)	1696	
Crystal size	.16 x .1 x .01 mm ³	
Theta range for data collection	2.07 to 23.51°.	
Index ranges	-10<=h<=12, -9<=k<=9, -43<=l<=48	
Reflections collected	19723	
Independent reflections	3058 [R(int) = 2.1305]	
Completeness to theta = 23.51°	99.4 %	
Absorption correction	SADABS	
Max. and min. transmission	1.00000 and 0.13582	
Refinement method	Full-matrix least-squares on F ²	
Data / restraints / parameters	3058 / 0 / 106	
Goodness-of-fit on F ²	0.924	
Final R indices [I>2sigma(I)]	R1 = 0.3009, wR2 = 0.5449	
R indices (all data)	R1 = 0.5967, wR2 = 0.7322	
Largest diff. peak and hole	0.428 and -0.368 e.Å ⁻³	

6.8.3 Crystal data and structure refinement for compound 104

Table 6.3 Crystal data and structure refinement for compound 104

Empirical formula	C ₂₀ H ₁₇ N ₃ O ₂	
Formula weight	331.37	
Temperature	293(2) K	
Wavelength	1.54178 Å	
Crystal system	Monoclinic	
Space group	P2(1)/c	
Unit cell dimensions	a = 12.318(3) Å	α = 90°.
	b = 7.467(2) Å	β = 100.774(11)°.
	c = 18.742(5) Å	γ = 90°.
Volume	1693.5(8) Å ³	
Z	4	
Density (calculated)	1.300 Mg/m ³	
Absorption coefficient	0.694 mm ⁻¹	
F(000)	696	
Crystal size	.15 x .1 x .1 mm ³	
Theta range for data collection	3.65 to 73.06°.	
Index ranges	-12 ≤ h ≤ 15, -9 ≤ k ≤ 5, -22 ≤ l ≤ 21	
Reflections collected	12976	
Independent reflections	3141 [R(int) = 0.0824]	
Completeness to theta = 73.06°	92.9 %	
Absorption correction	Multiscan	
Max. and min. transmission	1.00000 and 0.4308	
Refinement method	Full-matrix least-squares on F ²	
Data / restraints / parameters	3141 / 1 / 231	
Goodness-of-fit on F ²	1.086	
Final R indices [I > 2σ(I)]	R1 = 0.0610, wR2 = 0.1525	
R indices (all data)	R1 = 0.0821, wR2 = 0.1644	
Extinction coefficient	0.0026(7)	
Largest diff. peak and hole	0.243 and -0.201 e.Å ⁻³	

6.8.4 Crystal data and structure refinement for compound 113

Table 6.4 Crystal data and structure refinement for compound 113.

Empirical formula	C ₂₀ H ₁₉ N ₃ O ₃	
Formula weight	349.38	
Temperature	293(2) K	
Wavelength	0.71073 Å	
Crystal system	Orthorhombic	
Space group	Pca2(1)	
Unit cell dimensions	a = 12.2690(11) Å	α = 90°.
	b = 12.4891(10) Å	β = 90°.
	c = 22.931(2) Å	γ = 90°.
Volume	3513.7(5) Å ³	
Z	8	
Density (calculated)	1.321 Mg/m ³	
Absorption coefficient	0.091 mm ⁻¹	
F(000)	1472	
Crystal size	.2 x .1 x .06 mm ³	
Theta range for data collection	1.78 to 23.26°.	
Index ranges	-13<=h<=13, -13<=k<=10, -25<=l<=25	
Reflections collected	14342	
Independent reflections	4983 [R(int) = 0.0700]	
Completeness to theta = 23.26°	99.5 %	
Absorption correction	SADABS	
Max. and min. transmission	1.00000 and 0.850993	
Refinement method	Full-matrix least-squares on F ²	
Data / restraints / parameters	4983 / 6 / 456	
Goodness-of-fit on F ²	1.022	
Final R indices [I>2sigma(I)]	R1 = 0.0658, wR2 = 0.1386	
R indices (all data)	R1 = 0.1230, wR2 = 0.1675	
Absolute structure parameter	2(3)	
Extinction coefficient	0.0000(4)	
Largest diff. peak and hole	0.350 and -0.217 e.Å ⁻³	

6.8.5 Crystal data and structure refinement for compound 105

Table 6.5 Crystal data and structure refinement for compound 105.

Empirical formula	C ₂₆ H ₂₂ N ₄ O ₆	
Formula weight	486.48	
Temperature	125(2) K	
Wavelength	0.71073 Å	
Crystal system	Monoclinic	
Space group	P2(1)/c	
Unit cell dimensions	a = 15.5371(18) Å	α = 90°.
	b = 11.4567(14) Å	β = 99.602(2)°.
	c = 12.8018(15) Å	γ = 90°.
Volume	2246.8(5) Å ³	
Z	4	
Density (calculated)	1.438 Mg/m ³	
Absorption coefficient	0.104 mm ⁻¹	
F(000)	1016	
Crystal size	.1 x .1 x .05 mm ³	
Theta range for data collection	2.22 to 23.37°.	
Index ranges	-17<=h<=16, -10<=k<=12, -12<=l<=14	
Reflections collected	9232	
Independent reflections	3149 [R(int) = 0.0729]	
Completeness to theta = 23.37°	96.0 %	
Absorption correction	SADABSe	
Max. and min. transmission	1.00000 and 0.594485	
Refinement method	Full-matrix least-squares on F ²	
Data / restraints / parameters	3149 / 2 / 334	
Goodness-of-fit on F ²	0.935	
Final R indices [I>2sigma(I)]	R1 = 0.0422, wR2 = 0.0929	
R indices (all data)	R1 = 0.0668, wR2 = 0.1012	
Extinction coefficient	0.0077(12)	
Largest diff. peak and hole	0.234 and -0.225 e.Å ⁻³	

6.8.6 Crystal data and structure refinement for compound 148

Table 6.6 Crystal data and structure refinement for compound 148.

Empirical formula	$C_{26}H_{21}BrN_4O_6$	
Formula weight	565.38	
Temperature	293(2) K	
Wavelength	0.71073 Å	
Crystal system	Monoclinic	
Space group	P2(1)/c	
Unit cell dimensions	$a = 9.3487(5)$ Å	$\alpha = 90^\circ$.
	$b = 18.0339(11)$ Å	$\beta = 92.186(2)^\circ$.
	$c = 30.8165(18)$ Å	$\gamma = 90^\circ$.
Volume	$5191.7(5)$ Å ³	
Z	8	
Density (calculated)	1.447 Mg/m ³	
Absorption coefficient	1.631 mm ⁻¹	
F(000)	2304	
Crystal size	.13 x .1 x .1 mm ³	
Theta range for data collection	1.74 to 23.29°.	
Index ranges	$-7 \leq h \leq 10$, $-20 \leq k \leq 19$, $-34 \leq l \leq 27$	
Reflections collected	22388	
Independent reflections	7452 [R(int) = 0.1672]	
Completeness to theta = 23.29°	99.3 %	
Absorption correction	Sadabs	
Max. and min. transmission	1.00000 and 0.857551	
Refinement method	Full-matrix least-squares on F ²	
Data / restraints / parameters	7452 / 4 / 684	
Goodness-of-fit on F ²	0.837	
Final R indices [I > 2sigma(I)]	R1 = 0.0728, wR2 = 0.1607	
R indices (all data)	R1 = 0.2370, wR2 = 0.2077	
Extinction coefficient	0.0015(3)	
Largest diff. peak and hole	1.022 and -0.351 e.Å ⁻³	

7. References

1. Chamberlin, R. T. C., Chamberlin, T. C., *Science*, **1908**, 28, 897.
2. Oparin, A. I., *Origin of life*, Bernal, J. D. (Ed.), Weidenfeld and Nicolson, London, **1967**, 199.
3. Urey, H. C., *Proc. Nat'l Acad. Sci. USA*, **1952**, 38, 351.
4. Sagan, C. C., Chyba, C., *Nature*, **1992**, 355, 125.
5. Eschenmoser, A. K., Kisakurek, M. V., *Helv. Chim. Acta*, **1996**, 79, 1249.
6. Eschenmoser, A. L., Loewenthal, E., *Chem. Soc. Rev.*, **1992**, 21, 1.
7. Haldane, J. B. S., *Origin of life*, Bernal, J. D. (Ed.), Weidenfeld and Nicolson, London, **1967**, 242.
8. Miller, S. L., *Science*, **1953**, 17, 528.
9. Zubay, G., *Origins of Life on Earth and in the Cosmos*, Academic Press, New York, **2000**, 29.
10. Oro, J., *Nature*, **1961**, 191, 1193.
11. Orgel, L. E., *Cold Spring Harbour Symp. Quant. Biol.*, **1987**, 52, 9.
12. Watson, J. D., Crick, F. H. C., *Nature*, **1953**, 171, 964.
13. Gilbert, W., *Nature*, **1986**, 319, 618.
14. Orgel, L. E., Inoue, T., *Sci. Am.*, **1994**, 271, 77.
15. Gesteland, R. F., Atkins, J. A., *The RNA World*, Cold Spring Harbor Laboratory Press, New York, **1993**.
16. Sharp, P. A., *Cell*, **1985**, 42, 397.
17. Pace, N. R., Marsh, T. L., *Origin of Life*, **1985**, 16, 97.
18. Cech, T. R., *Proc. Nat'l Acad. Sci. USA*, **1986**, 83, 4360.
19. Cech, T. R., *Nature*, **1989**, 339, 507.
20. Bridson, P. K., Orgel, L. E., *J. Mol. Biol.*, **1980**, 144, 567.
21. Orgel, L. E., *Nature*, **1992**, 358, 203.
22. Benner, S. A., Ellington, A. D., Taner, A., *Proc. Nat'l Acad. Sci. USA*, **1989**, 86, 7054.
23. Benner, S. A., *Redesigning the molecules of life*, Springer Verlag, Berlin, **1988**, 115.
24. Ferris, J. P., *Nature*, **1995**, 373, 659.
25. Keefe, A. D. N., *Nature*, **1995**, 373, 683.
26. Rode, B. M., *Peptides*, **1999**, 20, 773.
27. Fox, S. W., *Molecular evolution and the origin of life*, Marcel Dekker, New York, **1977**, 1.
28. Lahav, M. J., *Theor. Biol*, **1991**, 151, 531.

29. White, H. B., *J. Mol. Evol.*, **1975**, 7, 101.
30. Eigen, M. S., Schuster, P., *The hypercycle: A Principle of Natural Self-Organisation*, Springer-Verlag, Berlin, **1979**, 1.
31. Cairns-Smith, A. G., *Genetic Takeover and the mineral origins of life*, The Cambridge University Press, Cambridge, **1982**, 1.
32. Ferris, J. P., Hagan, C. H., Hagan, W. J., *Orig. Life Evol. Biosphere*, **1988**, 18, 121.
33. Philp, D., Stoddart, J. F., *Angew. Chem. Int. Ed. Engl.*, **1996**, 35, 1154.
34. Lindsey, J. S., *New J. Chem.*, **1991**, 15, 153.
35. Whitesides, G. M., *Science*, **1995**, 114.
36. Whitesides, G. M., Mathias, J. P., Seto, C. T., *Science*, **1991**, 254, 1312.
37. Sowerby, S. J., Holm, N. G., Petersen, G. B., *Biosystems*, **2001**, 61, 69.
38. Silverman, R. B., *The Organic Chemistry of Enzyme-Catalysed Reactions*, Academic Press, London, **2000**, 1.
39. Wong, C. H., Whitesides, G. M., *Enzymes in Synthetic Organic Chemistry*, London Pitman Publishing, London, **1985**.
40. Dugas, H., *Bioorganic Chemistry*, Springer-Verlag, Berlin, **1989**.
41. Motherwell, W. B., Bingham, M. J., Six, Y., *Tetrahedron*, **2001**, 57, 4663.
42. Page, M. I., *Enzyme Mechanisms*, Royal Society of Chemistry, Cambridge, **1987**, 1.
43. Kirby, A. J., *Adv. Phys. Org. Chem.*, **1980**, 17, 183.
44. Page, M. I., In *The chemistry of enzyme action*, Page, M. I. (Ed.), Elsevier, London, **1984**, 1.
45. Bruice, T. C., Pandit, F. C., *J. Am. Chem. Soc.*, **1960**, 82, 5858.
46. Bruice, T. C., Lightstone, F. C., *J. Am. Chem. Soc.*, **1999**, 118, 2595.
47. Bruice, T. C., Lightstone, F. C., *Acc. Chem. Res.*, **1999**, 32, 127.
48. Lightstone, F. C., Bruice, T. C., *Bioorg. Chem.*, **1998**, 26, 193.
49. Pandit, U. K., Bruice, T. C., *J. Am. Chem. Soc.*, **1960**, 82, 3386.
50. Bruice, T. C., *Annu. Rev. Biochem.*, **1976**, 45, 331.
51. Bruice, T. C., Benkovic, S. J., *Bioorganic mechanism*, Benjamin, New York, **1966**, Chapter 1.
52. Jencks, W. P., *Catalysis in Chemistry and Enzymology*, McGraw Hill, New York, **1969**, Chapter 1.
53. Voet, D., Voet, J. G., *Biochemistry*, John Wiley, New York, **1990**, Chapter 1.
54. Koshland, D. E., *J. Theor. Biol.*, **1962**, 2, 75.
55. Storm, D. R., Koshland, D. E., *J. Am. Chem. Soc.*, **1972**, 94, 5805.
56. Storm, D. R., Koshland, D. E., *Proc. Nat'l Acad. Sci. USA*, **1970**, 65, 445.

57. Dafforn, A., Koshland, D. E., *Proc. Nat'l Acad. Sci. USA*, **1971**, 68, 2463.
58. Bruice, T. C., Brown, A., Harris, D. O., *Proc. Nat'l Acad. Sci. USA*, **1971**, 68, 658.
59. Hoare, D. G., *Nature*, **1972**, 236, 437.
60. Delisi, C., Crothers, D. M., **1973**, 12, 1689.
61. Menger, F. M., Glass, L. E., *J. Am. Chem. Soc.*, **1980**, 102, 5406.
62. Page, M. I., Jencks, W. P., *Proc. Nat'l Acad. Sci. USA*, **1971**, 68, 1678.
63. Menger, F. M., *Acc. Chem. Res.*, **1985**, 18, 128.
64. Bruice, T. C., Lightstone, F. C., *Acc. Chem. Res.*, **1999**, 32, 27.
65. Lightstone, F. C., Bruice, T. C., *J. Am. Chem. Soc.*, **1996**, 118, 2595.
66. Von Kiedrowski, G., Bag, B. G., *Pure Appl. Chem.*, **1996**, 68, 2145.
67. Robertson, A., Sinclair, J. A., Philp, D., *Chem. Soc. Rev.*, **2000**, 29, 141.
68. Anderson, S., Anderson, H. L., Sanders, J. K. M., *Acc. Chem. Res.*, **1993**, 26, 469.
69. Hoss, R., Vogtle, F., *Angew. Chem. Int. Ed. Engl.*, **1994**, 33, 375.
70. Breault, G. A., Hunter, C. A., Mayers, P. C., *Tetrahedron*, **1999**, 55, 5265.
71. Page, M. I., *Phil. Trans. R. Soc. London B*, **1991**, 332, 149.
72. Page, M. I., *Chem. Soc. Rev.* **1973**, 2, 295.
73. Kirby, A. J., *Phil. Trans. R. Soc. London B*, **1993**, 345, 67.
74. Menger, F. M., *Acc. Chem. Res.*, **1993**, 26, 206.
75. Cram, D., *Angew. Chem. Int. Ed. Engl.*, **1988**, 27, 1009.
76. Philp, D., Robertson, A., *Chem. Commun.*, **1998**, 879.
77. Booth, C. A., Philp, D., *Tetrahedron Lett.*, **1998**, 39, 6987.
78. Robertson, A., Philp, D., Spencer, N., *Tetrahedron*, **1999**, 55, 11365.
79. Bennes, R. M., Kariuki, B. M., Harris, D. M., Philp, D., Spencer, N., *Org. Lett.*, **1999**, 1, 1087.
80. Tecilla, P., Hamilton, A. D., *J. Chem. Soc., Chem. Commun.*, **1990**, 1232.
81. Tecilla, P., Jubian, V., Hamilton, A. D., *Tetrahedron*, **1995**, 51, 435.
82. Booth, C. A., Philp, D., *Tetrahedron Lett.*, **1998**, 54, 1759.
83. Booth, C. A., PhD. Thesis, University of Birmingham, **1999**, 83.
84. Chang, S. K., Hamilton, A. D., *J. Am. Chem. Soc.*, **1988**, 10, 18.
85. Chang, S. K., van Engen, D., Fan, E., Hamilton, A. D., *J. Am. Chem. Soc.*, **1991**, 113, 7640.
86. Garcia-Tellado, G. S., Chang, S. K., Geib, S. J., Hamilton, A. D., *J. Am. Chem. Soc.*, **1990**, 112, 7393.
87. Garcia-Tellado, G. S., Albert, J., Hamilton, A. D., *J. Chem. Soc., Chem. Commun.*, **1991**, 1761.

88. Vincent, C., Fan, E., Hamilton, A. D., *Tetrahedron Lett.*, **1992**, 33, 4269.
89. Kelly, T. R., Zhao, C., Bridger, G. J., *J. Am. Chem. Soc.*, **1989**, 111, 3744.
90. Kelly, T. R., Zhao, C., Bridger, G. J., *J. Am. Chem. Soc.*, **1990**, 112, 8024.
91. Schramm, G., Grotzsch, H., Pollman, W., *Angew. Chem. Int. Ed. Engl.*, **1962**, 1, 1.
92. Naylor, R., Gilham, P. T., *Biochemistry*, **1966**, 5, 2722.
93. Orgel, L. E., Zielinski, W. S., *Nature*, **1987**, 327, 346.
94. Orgel, L. E., Wu, T., *J. Am. Chem. Soc.*, **1992**, 114, 317.
95. Orgel, L. E., Inoue, T., Chen, C. B., *J. Mol. Biol.*, **1985**, 181, 271.
96. Orgel, L. E., Inoue, T., *Science*, **1983**, 219, 859.
97. Orgel, L. E., Lohrmann, R., *J. Mol. Biol.*, **1980**, 142, 555.
98. Orgel, L. E., Lohrmann, R., *Acc. Chem. Res.*, **1974**, 7, 368.
99. Orgel, L. E., Inoue, T., Joyce, G. F., Grzeskowiak, K., Brown, J. M., *J. Mol. Biol.*, **1984**, 178, 669.
100. Goodwin, J. T., Lynn, D. G., *J. Am. Chem. Soc.*, **1992**, 114, 9197.
101. Von Kiedrowski, G., *Angew. Chem. Int. Ed. Engl.*, **1986**, 25, 932.
102. Von Kiedrowski, G., Wlotzka, B., Helbing, J., Mazten, M., Jordan, S., *Angew. Chem. Int. Ed. Engl.*, **1991**, 30, 423.
103. Kiedrowski, G., *Bioorg. Chem. Front.*, Vol. 3., **1993**, 113.
104. Li, T., Nicolaou, K. C., *Nature*, **1994**, 369, 218.
105. Yoa, S., Ghosh, I., Reena, Z., Chimielewski, J., *Angew. Chem. Int. Ed.*, **1998**, 37, 478.
106. Yao, S., Ghosh, I., Zutshi, R., Chmielewski, J., *J. Am. Chem. Soc.*, **1997**, 119, 10559.
107. Lee, D. H., Granga, J. R., Martinez, J. A., Severin, K., Ghadiri, M. R., *Nature*, **1996**, 382.
108. Severin, K., Lee, D. H., Martinez, J. A., Ghadiri, M. R., *Chem. Eur. J.*, **1997**, 3, 1017.
109. Dawson, P. E., Muir, T. W., Clark-Lewis, I., Kent, S. B. H., *Science*, **1994**, 266, 776.
110. Rebek, J. Jr., *Chem. Ind.*, **1992**, 171.
111. Rebek, J. Jr., *Sci. Am.*, **1994**, 34.
112. Rebek, J. Jr., *Experientia*, **1991**, 1096.
113. Famulok, M., Nowick, J. S., Rebek, J. Jr., *Acta. Chem. Scand.*, **1992**, 46, 315.
114. Winter, E. A., Rebek, J. Jr., *Acta. Chem. Scand.*, **1996**, 50, 469.
115. Tjivikua, T., Ballester, P., Rebek, J. Jr., *J. Am. Chem. Soc.*, **1990**, 112, 1249.
116. Nowick, J. S., Feng, Q., Tjivikua, T., Ballester, P., Rebek, J. Jr., *J. Am. Chem. Soc.*, **1991**, 113, 8831.
117. Rotello, V., Hong, J.-I., Rebek, J. Jr., *J. Am. Chem. Soc.*, **1991**, 113, 9422.
118. Park, T. K., Schroder, J., Rebek, J. Jr., *Tetrahedron*, **1990**, 47, 2507.

119. Kemp, D. S., Petrakis, K. S., *J. Org. Chem.*, **1981**, *46*, 5140.
120. Menger, F. M., Eliseev, A. E., Khanjin, N. A., *J. Am. Chem. Soc.*, **1994**, *116*, 3613.
121. Menger, F. M., Eliseev, A. E., Khanjin, N. A., *J. Org. Chem.*, **1995**, *60*, 2870.
122. Conn, M. M., Winter, E. A., Rebek, J. Jr., *J. Am. Chem. Soc.*, **1994**, *116*, 8823.
123. Winter, E. A., Rebek, J. Jr., Tsao, B., *J. Org. Chem.*, **1995**, *60*, 7997.
124. Reinhoudt, D. N., Rudkevich, D. M., de Jong, F., *J. Am. Chem. Soc.*, **1996**, *118*, 6880.
125. Hong, J.-I., Feng, Q., Rotello, V., Rebek, J. Jr., *Science*, **1992**, *255*, 848.
126. Park, T. K., Feng, Q., Rebek, J. Jr., *J. Am. Chem. Soc.*, **1992**, *114*, 4529.
127. Winter, E. A., Conn, M. M., Rebek, Jr. J., *J. Am. Chem. Soc.*, **1994**, *116*, 8877.
128. Huc, I., Pieters, R. J., Rebek, J. Jr., *J. Am. Chem. Soc.*, **1994**, *116*, 10296.
129. Conn, M. M., Winter, E. A., Rebek, J. Jr., *Angew. Chem. Int. Ed. Engl.*, **1994**, *33*, 1577.
130. Pieters, R. J., Huc, I., Rebek, J. Jr., *Tetrahedron*, **1995**, *51*, 485.
131. Bag, B.G., von Kiedrowski, G., *Angew. Chem. Int. Ed.*, **1999**, *38*, 3713.
132. Wang, B., Sutherland, I. O., *Chem. Commun.*, **1997**, 1495.
133. Avalos, M., Babiano, R., Cintas, P., Jimenez, J. L., Palacios, J. C., *Chem. Commun.*, **2000**, 887.
134. Soai, K., Niwa, S., *Chem. Rev.*, **1992**, *92*, 833.
135. Alberts, A. H., Wynberg, H., *J. Am. Chem. Soc.*, **1989**, *111*, 7265.
136. Balsells, J., Walsh, P. J., *J. Am. Chem. Soc.*, **2000**, *122*, 1802.
137. Furuno, H., Hanamoto, T., Sugimoto, Y., Inanaga, J., *Org. Lett.*, **2000**, *2*, 49.
138. Crosignani, S., Desimoni, G., Filippone, S., Mortoni, A., *Tetrahedron Lett.*, **1999**, *40*, 7007.
139. Kitamura, M., Suga, S., Oka, H., Noyori, R., *J. Am. Chem. Soc.*, **1998**, *120*, 9800.
140. Shibata, T., Takahashi, T., Konishi, T., Soai, K., *Angew. Chem. Int. Ed. Engl.*, **1997**, *36*, 2458.
141. Shibata, T., Matsumoto, N., Yonekubo, S., Soai, K., *J. Am. Chem. Soc.*, **1998**, *120*, 12157.
142. Shibata, T., Soai, K., *Angew. Chem. Int. Ed.*, **1999**, *38*, 659.
143. Bolm, C., Bienewald, F., Seger, A., *Angew. Chem. Int. Ed. Engl.*, **1996**, *35*, 1657.
144. Soai, K., Hori, H., *J. Chem. Soc., Chem. Commun.*, **1990**, 983.
145. Soai, K., Hayase, T., Shimada, C., Isobe, K., *Tetrahedron Asymm.*, **1994**, *5*, 789.
146. Bolm, C., Harms, K., *Chem. Ber.*, **1992**, *125*, 1191.
147. Li, S., Jiang, Y., Yang, G., Mi, A., *J. Chem. Soc., Perkin Trans. 1*, **1993**, 885.

148. Shibata, T., Choji, K., Tadakatsu, H., Morioka, H., Soai, K., *Chem. Commun.*, **1996**, 751.
149. Shibata, T., Hayase, T., Yamamoto, J., Soai, K., *Tetrahedron Assym.*, **1997**, 8, 1717.
150. Allen, V. C., PhD. Thesis, University of Birmingham, **2000**, 43.
151. Gokel, G., *Crown Ethers and Cryptands*, The Royal Society of Chemistry, Cambridge, **1994**.
152. Kimura, E. S., Yatsunami, T., Kodami, M., *J. Am. Chem. Soc.*, **1981**, 103, 3041.
153. Hosseini, M. W., Lehn, J. M., *J. Am. Chem. Soc.*, **1982**, 104, 3525.
154. Breslow, R., Rajagopalan, R., Schwartz, J., *J. Am. Chem. Soc.*, **1981**, 103, 2905.
155. Rebek, J. Jr., Nemeth, D., Ballaster, P., Lin, F. T., *J. Am. Chem. Soc.*, **1987**, 109, 3474.
156. Tanaka, Y., Kato, Y., Aoyama, Y., *J. Am. Chem. Soc.*, **1990**, 112, 2807.
157. Fan, E., van Arman, S. A., Kincaid, S., Hamilton, A. D., *J. Am. Chem. Soc.*, **1993**, 115, 369.
158. Garcia-Tellado, F., Goswami, S., Chang, S. K., Geib, S., Hamilton, A. D., *J. Am. Chem. Soc.*, **1990**, 112, 7393.
159. Hirst, S. C., Hamilton, A. D., *J. Am. Chem. Soc.*, **1991**, 113, 382.
160. Yang, J., Fan, E., Geib, S., Hamilton, A. D., *J. Am. Chem. Soc.*, **1993**, 115, 5314.
161. Goswami, S., Ghosh, S., Dasgupta, S., *J. Org. Chem.*, **2000**, 65, 1907.
162. Booth, C.A., PhD. Thesis, University of Birmingham, **1999**, 92.
163. Mustafa, A., Abdel., S. M., Zayed, D., Khattab, S., *J. Am. Chem. Soc.*, **1956**, 78, 145.
164. Scriven, E., Turnbull, K., *Chem. Rev.*, **1988**, 88, 351.
165. Huisgen, R., *Angew. Chem., Int. Ed. Engl.*, **1963**, 2, 633.
166. Huisgen, R., *Angew. Chem., Int. Ed. Engl.*, **1963**, 2, 565.
167. Huisgen, R., *J. Org. Chem.*, **1976**, 41, 403.
168. Houk, K. N., Sims, J., Duke, R. E., Strozier, R. W., George, J. K., *J. Am. Chem. Soc.*, **1973**, 95, 7287.
169. Fleming, I., *Frontier Orbitals and Organic Chemical Reactions*, John Wiley and Sons, Bristol, **1976**.
170. Quayle, J. M., Philp, D., Slawin, A., *Tetrahedron Lett.*, **2002**, 43, 7229.
171. Kirby, A. J., *Angew. Chem., Int. Ed. Engl.*, **1996**, 35, 707.
172. Kiedrowski, G., *Angew. Chem., Int. Ed. Engl.*, **1989**, 28, 1235.
173. Kiedrowski, G., Wlotzka, B., Helbing, J., Matzen, M., Jordan, S., *Angew. Chem., Int. Ed. Engl.*, **1991**, 30, 423.
174. Zielinski, W. S., Orgel, L. E., *Nature*, **1987**, 327, 346.
175. Wu, T., Orgel, L. E., *J. Am. Chem. Soc.*, **1992**, 114, 327.

176. Sievers, D., von Kiedrowski, G., *Chem. Eur. J.*, **1998**, *4*, 629.
177. Sinclair, A. J., PhD. Thesis, University of Birmingham, **2000**.
178. Bennes, R. M., PhD. Thesis, University of Birmingham, **2000**.
179. Allen, V. A., Philp, D., *Org. Lett.*, **2001**, *3*, 777.
180. Howell, S., PhD. Thesis, University of St. Andrews, **2001**.
181. Robertson, A., PhD. Thesis, University of Birmingham, **1997**.
182. Dell, C., *J. Chem. Soc., Perkin Trans. 1*, **1998**, 3873.
183. Hisano, T., Harano, K., Matsuoka, T., Watanabe, S., Matsuzaki, T., *Chem. Pharm. Bull.*, **1989**, *37*, 907.
184. Frederikson, M., *Tetrahedron*, **1997**, *53*, 403.
185. Tufariello, J., *Acc. Chem. Res.*, **1979**, *12*, 396.
186. Kiers, D., Moffat, D., Overton, K., *J. Chem. Soc., Chem. Commun.*, **1988**, 654.
187. Vasella, A., Voeffray, R. J., *J. Chem. Soc., Chem. Commun.*, **1981**, 97.
188. Brown, C. W., Marsden, K., Rodgers, M. A. T., Tylor, C. M. B., Wright, R., *Proc. Chem. Soc.*, **1960**, 254.
189. Grashey, R., Huisgen, R., Leitermann, H., *Tetrahedron Lett.*, **1960**, *12*, 9.
190. Delpierre, G. R., Lamchen, M., *Proc. Chem. Soc.*, **1960**, 386.
191. Black, D. S. C., Crozier, F., Davis, V. C., *Synthesis*, **1975**, 205.
192. Huisgen, R., *Angew. Chem. Int. Ed. Engl.*, **1963**, *2*, 565.
193. Huisgen, R., *Angew. Chem. Int. Ed. Engl.*, **1968**, *7*, 321.
194. Huisgen, R., Grashey, R., Sauer, J., *The chemistry of alkenes*, Interscience, New York, **1964**.
195. Al-timari, U., Fisera, L., Ertl, P., Goljer, I., Pronayova, N., *Monatsh. Chem.*, **1992**, *123*, 999.
196. Fleming, I., *Pericyclic Reactions*, Oxford University Press, Oxford, **1999**.
197. Allen, V. A., PhD. Thesis, University of Birmingham, **2000**, 97.
198. March, J., *Advanced Organic Chemistry*, Fifth Edition, John Wiley and Sons, New York, **2001**, 370.
199. Kinderman, M., PhD. Thesis, University of Bochum, **2002**.
200. Bruker Daltonik GmbH **2000** WINNMMR v 6.2.0.0.
201. Kaleidagraph software, Version 3.5, **2000**.
202. Still, W. C., Tempczyk, A., Hawley, R. C., Hendrikson, T., *J. Am. Chem. Soc.*, **1990**, *112*, 6127.
203. Rich, D. H., Gesellchen, P. D., Tong, P. D., *J. Med. Chem.*, **1975**, *18*, 1004.

204. Eliel, E. L., Wilhen, S. H., *Stereochemistry of Organic Compounds*, John Wiley and Sons, New York, **1994**, 665.
205. Cross, L. C., Wilhen, S. H., *Pure Appl. Chem.*, **1976**, 45, 11.
206. Siegl, W. O., *J. Org. Chem.*, **1977**, 42, 1872.
207. Solomon, S., *J. Chem. Soc.*, **1946**, 934.
208. Legge, J., *J. Am. Chem. Soc.*, **1947**, 69, 2079.
209. Peltier, D., Gueguen, M-J., *Bull. Chem. Soc. Jpn.*, **1969**, 264.
210. Bordwell, F. G., Liu, W. Z., *J. Am. Chem. Soc.*, **1996**, 118, 8777.
211. Jacobi, P. A., Murphree, S., Rupprecht, F., Zheng, W., *J. Org. Chem.*, **1996**, 61, 2421.

8. Appendices

8.1 Appendix 1

The command file used in SIMFIT to fit the bimolecular control experimental data for the formation of compound **153**.

```
*=====
* Control data for the reaction between 4-Br-nitrone
* and C1 maleimide ester. Titled 4BrN_ester.
*=====
* 2 constants to be derived

define (1,MAJOR,p,1) scale (3,1)
define (2,MINOR,p,4) scale (3,1)

time (min)

read (4BrN_ester)

doc (4BrN_ester)

choose (exp1)

select (MAJOR, MINOR)

win (0, 1200, 200, 0.1e-3, 0, 10e-3, 2.5e-3, 3e-5)

reaction (A + B --> MAJOR)
reaction (A + B --> MINOR)
reaction (compile)
reaction (show)
reaction (doc)

const (1,50e-4,1,1,100)
const (2,10e-4,2,1,100)

assign (obs, MAJOR = MAJOR)
assign (obs, MINOR = MINOR)
assign (spec, A = #0.025)
assign (spec, B = #0.025)

assign (show)

dim (2)

integ (stiff)

plot

* 10 rounds of Simplex optimiser without screen
* update

simplex (plot)
simplex (plot)

*afterwards newton with screen update

newton (plot)

plot (file)

end
```

The data file obtained in SIMFIT from the fitting of the bimolecular control experimental data for the formation of **153**.

```
*****
SimFit (PB/DLL5.0) 32 bit   V1.0 (20-05-99) (C) 1999 G. v. Kiedrowski *
*****
This version of SimFit comes with 2 GB variable space.
SF32.INI is currently set to:
63 species,63 reactions,24 iteratable rate constants,
31 observables,6 files,4 experiments/file,64 reaction times/experiment.

DEFINE (1,major,p,1)

SCALE (3,1)
major: K1 * FE

DEFINE (2,minor,p,4)

SCALE (3,1)
minor: K1 * FE

TIME (min)

READ (4brn_ester)
4BrN_ester      exp Time[min]      Major      Minor
  1             1         0           0           0           0
  2             1         30      0.000124    0.0000311    0
  3             1         60      0.000237    0.0000593    0
  4             1         90      0.000362    0.0000904    0
  5             1        120      0.000477    0.000119     0
  6             1        150      0.000591    0.000148     0
  7             1        180      0.000706    0.000176     0
  8             1        210      0.000812    0.000203     0
  9             1        240      0.000924    0.000231     0
 10            1        270      0.001053    0.000263     0
 11            1        300      0.001152    0.000288     0
 12            1        330      0.001237    0.000309     0
 13            1        360      0.001369    0.000342     0
 14            1        390      0.00145     0.000362     0
 15            1        420      0.001556    0.000389     0
 16            1        450      0.001656    0.000414     0
 17            1        480      0.001781    0.000445     0
 18            1        510      0.001887    0.000472     0
 19            1        540      0.001994    0.000499     0
 20            1        570      0.002099    0.000525     0
 21            1        600      0.002184    0.000546     0
 22            1        630      0.002294    0.000573     0
 23            1        660      0.002403    0.000601     0
 24            1        690      0.002465    0.000616     0
 25            1        720      0.002548    0.000637     0
 26            1        750      0.002633    0.000658     0
 27            1        780      0.00275     0.000688     0
 28            1        810      0.002835    0.000709     0
 29            1        840      0.002916    0.000729     0
 30            1        870      0.002989    0.000747     0
 31            1        900      0.003091    0.000773     0
 32            1        930      0.003197    0.000799     0
 33            1        960      0.003275    0.000819     0
 34            1        990      0.003377    0.000844     0

DOC (4brn_ester)
documentation file: 4brn_ester.doc

CHOOSE (expl)

SELECT (major,minor)

WIN (0, 1200, 200, 0.1e-3, 0, 10e-3, 2.5e-3,3e-5)

REACTION (a + b --> major)

REACTION (a + b --> minor)

REACTION (compile)

REACTION (show)
-----
```

Reactions:

A + B --> MAJOR k(1) = + .000E+01
 A + B --> MINOR k(2) = + .000E+01

Species found: A B MAJOR MINOR

Rate equations:

$d[A]/dt = -k_1 \cdot [A] \cdot [B] - k_2 \cdot [A] \cdot [B]$
 $d[B]/dt = -k_1 \cdot [A] \cdot [B] - k_2 \cdot [A] \cdot [B]$
 $d[MAJOR]/dt = +k_1 \cdot [A] \cdot [B]$
 $d[MINOR]/dt = +k_2 \cdot [A] \cdot [B]$

Jacobian matrix: NJacobi& = 8 JacobiList& = 20

$d(d[A]/dt)/d[A] = -k_1 \cdot [B] - k_2 \cdot [B]$
 $d(d[A]/dt)/d[B] = -k_1 \cdot [A] - k_2 \cdot [A]$
 $d(d[B]/dt)/d[A] = -k_1 \cdot [B] - k_2 \cdot [B]$
 $d(d[B]/dt)/d[B] = -k_1 \cdot [A] - k_2 \cdot [A]$
 $d(d[MAJOR]/dt)/d[A] = +k_1 \cdot [B]$
 $d(d[MAJOR]/dt)/d[B] = +k_1 \cdot [A]$
 $d(d[MINOR]/dt)/d[A] = +k_2 \cdot [B]$
 $d(d[MINOR]/dt)/d[B] = +k_2 \cdot [A]$

REACTION (doc)

appending to 4brn_ester.doc

CONST (1,50e-4,1,1,100)

CONST (2,10e-4,2,1,100)

ASSIGN (obs,major = major)

ASSIGN (obs,minor = minor)

ASSIGN (spec,a = #0.025)

ASSIGN (spec,b = #0.025)

ASSIGN (show)

MAJOR:= +1.0 x MAJOR
 MINOR:= +1.0 x MINOR
 A:= +0.0 x
 B:= +0.0 x
 MAJOR:=
 MINOR:=

DIM (2)

INTEG (stiff)

PLOT ()

SIMPLEX (plot)

k1_____ k2_____ R.M.S. [%]

initial values:

+ .50E-02 + .10E-02 +864.6362

+ .50E-02 + .12E-02 +864.6362

+ .30E-02 + .13E-02 +716.9067

+ .20E-02 + .18E-02 +648.4491

+ .20E-02 + .18E-02 +648.4491

+ .20E-02 + .18E-02 +648.4491

+ .19E-02 + .72E-03 +628.9587

+ .66E-03 + .45E-03 +375.2409

+ .66E-03 + .45E-03 +375.2409

+ .69E-03 + .31E-03 +366.7839

+ .69E-03 + .31E-03 +366.7839

+ .69E-03 + .31E-03 +366.7839

Minmax constraint was active.

SIMPLEX (plot)

k1_____ k2_____ R.M.S. [%]

initial values:

+ .69E-03 + .31E-03 +366.7839

+ .69E-03 + .31E-03 +366.7839

+ .41E-03 + .40E-03 +308.2608

+ .28E-03 + .32E-03 +252.1788

+ .28E-03 + .32E-03 +252.1788

+ .28E-03 + .32E-03 +252.1788

+ .23E-03 + .21E-03 +177.6058

+ .99E-04 + .98E-04 + 78.9976

+ .56E-04 + .18E-04 + 58.8679

+ .56E-04 + .18E-04 + 58.8679

+ .77E-04 + .26E-04 + 34.0732

+ .77E-04 + .26E-04 + 34.0732

Minmax constraint was active.

NEWTON (plot)

k1_____ k2_____ R.M.S. [%]

Initial values:-----

7.73E-05 2.58E-05 34.0732

± .00E+01 ± .00E+01

1.08E-04 2.63E-05 1.4410

± .11E-06 ± .11E-06

1.09E-04 2.72E-05 0.8485

± .72E-07 ± .66E-07

1.09E-04 2.72E-05 0.8485

± .72E-07 ± .66E-07

sum errors = + .6223E-08

Covariance Matrix:

1.00E+00 1.36E-01

1.36E-01 1.00E+00

The command file used in SIMFIT to fit the recognition-mediated experimental data for the formation of **148**.

```
*=====
* 4BrN_Clacid
* Values for the uncatalysed bimolecular reaction
* are values calculated from ester controls
*=====

define (1,MAJOR,p,1) scale (3,1)
define (2,MINOR,p,4) scale (3,1)

select (MAJOR,MINOR)

doc (4BrN_Clacid)

read (4BrN_Clacid)

time (min)

win (0, 1200, 200, 0.1, 0, 20e-3, 5e-3, 3e-4)

reaction (A + B --> MAJOR)
reaction (A + B --> MINOR)
reaction (A + B + 0.75 MAJOR --> 1.75 MAJOR)
reaction (A + B + 0.5 MINOR --> 1.5 MINOR)
reaction (compile)
reaction (show)

const (1,1.09e-4,0,1,1)
const (2,2.72e-5,0,1,1)
const (3,1e-3,1,1,100)
const (4,1e-3,2,1,100)

assign (obs, MAJOR = MAJOR)
assign (obs, MINOR = MINOR)
assign (spec, A = #25e-3)
assign (spec, B = #25e-3)

choose (expl)

dim (2)

integ (stiff)

plot

* 10 rounds of Simplex optimizer without screen
* update

simplex (plot)
simplex (plot)

* afterwards newton with screen update

newton (plot)

plot
plot (file)
end
```

The data file obtained in SIMFIT from the fitting of the recognition-mediated experimental data for the formation of **148**.

```
*****
* SimFit (PB/DLL5.0) 32 bit  V1.0 (20-05-99) (C) 1999 G. v. Kiedrowski *
*****
This version of SimFit comes with 2 GB variable space.
SF32.INI is currently set to:
63 species,63 reactions,24 iteratable rate constants,
31 observables,6 files,4 experiments/file,64 reaction times/experiment.

DEFINE (1,major,p,1)

SCALE (3,1)
major: K1 * FE

DEFINE (2,minor,p,4)

SCALE (3,1)
minor: K1 * FE

SELECT (major,minor)

DOC (4brn_clacid)
documentation file: 4brn_clacid.doc

READ (4brn_clacid)
4BrN_Clexp  time[min]      Major      Minor
1          1          0          0          0          0
2          1          30          0.000254922  0          0
3          1          60          0.000582354  0.0000850  0
4          1          90          0.001020783  0.000139   0
5          1          120         0.001348727  0.000242771 0
6          1          150         0.001973901  0.000356399 0
7          1          180         0.00254971  0.000446828 0
8          1          210         0.003117875  0.000512996 0
9          1          240         0.0037244   0.000585138 0
10         1          270         0.004358592  0.000656325 0
11         1          300         0.004939431  0.000726832 0
12         1          330         0.005591491  0.000848986 0
13         1          360         0.006217469  0.00091088   0
14         1          390         0.006880286  0.000930384 0
15         1          420         0.007501331  0.000998403 0
16         1          450         0.008081969  0.001065197 0
17         1          480         0.008678366  0.001151631 0
18         1          510         0.009288012  0.001161002 0
19         1          540         0.00982906  0.001189459 0
20         1          570         0.010393177  0.001322637 0
21         1          600         0.010870357  0.001471231 0
22         1          630         0.011358262  0.001448419 0
23         1          660         0.011958981  0.001500528 0
24         1          690         0.012419847  0.001526718 0
25         1          720         0.012790877  0.001737556 0
26         1          750         0.013212173  0.00180962   0
27         1          780         0.013661783  0.001787965 0
28         1          810         0.014039566  0.001810785 0
29         1          840         0.014430993  0.00177159   0
30         1          870         0.014811951  0.001721752 0
31         1          900         0.015135246  0.001782787 0
32         1          930         0.015384615  0.001873556 0
33         1          960         0.01569419  0.001964375 0
34         1          990         0.015971061  0.00190281   0

TIME (min)

WIN (0, 1200, 200, 0.1, 0, 20e-3, 5e-3,3e-4)

REACTION (a + b --> major)

REACTION (a + b --> minor)

REACTION (a + b + 0.75 major --> 1.75 major)

REACTION (a + b + 0.5 minor --> 1.5 minor)
```

REACTION (compile)

REACTION (show)

DGLCODER Version 11.03.93

Reactions:

A + B --> MAJOR k(1) = + .000E+01
A + B --> MINOR k(2) = + .000E+01
A + B + 0.75 MAJOR --> 1.75 MAJOR k(3) = + .000E+01
A + B + 0.5 MINOR --> 1.5 MINOR k(4) = + .000E+01

Species found: A B MAJOR MINOR

Rate equations:

$d[A]/dt = -k_1 \cdot [A] \cdot [B] - k_2 \cdot [A] \cdot [B] - k_3 \cdot [A] \cdot [B] \cdot [MAJOR]^{.75} - k_4 \cdot [A] \cdot [B] \cdot \text{root}[MINOR]$
 $d[B]/dt = -k_1 \cdot [A] \cdot [B] - k_2 \cdot [A] \cdot [B] - k_3 \cdot [A] \cdot [B] \cdot [MAJOR]^{.75} - k_4 \cdot [A] \cdot [B] \cdot \text{root}[MINOR]$
 $d[MAJOR]/dt = +k_1 \cdot [A] \cdot [B] + k_3 \cdot [A] \cdot [B] \cdot [MAJOR]^{.75}$
 $d[MINOR]/dt = +k_2 \cdot [A] \cdot [B] + k_4 \cdot [A] \cdot [B] \cdot \text{root}[MINOR]$

Jacobian matrix: NJacobi& = 14 JacobiList& = 44

$d(d[A]/dt)/d[A] = -k_1 \cdot [B] - k_2 \cdot [B] - k_3 \cdot [B] \cdot [MAJOR]^{0.8} - k_4 \cdot [B] \cdot \text{root}[MINOR]$
 $d(d[A]/dt)/d[B] = -k_1 \cdot [A] - k_2 \cdot [A] - k_3 \cdot [A] \cdot [MAJOR]^{0.8} - k_4 \cdot [A] \cdot \text{root}[MINOR]$
 $d(d[A]/dt)/d[MAJOR] = +-.7500 \cdot k_3 \cdot [A] \cdot [B] \cdot [MAJOR]^{-.3}$
 $d(d[A]/dt)/d[MINOR] = -\frac{1}{2} \cdot k_4 \cdot [A] \cdot [B] \cdot 1/\text{root}[MINOR]$
 $d(d[B]/dt)/d[A] = -k_1 \cdot [B] - k_2 \cdot [B] - k_3 \cdot [B] \cdot [MAJOR]^{0.8} - k_4 \cdot [B] \cdot \text{root}[MINOR]$
 $d(d[B]/dt)/d[B] = -k_1 \cdot [A] - k_2 \cdot [A] - k_3 \cdot [A] \cdot [MAJOR]^{0.8} - k_4 \cdot [A] \cdot \text{root}[MINOR]$
 $d(d[B]/dt)/d[MAJOR] = +-.7500 \cdot k_3 \cdot [A] \cdot [B] \cdot [MAJOR]^{-.3}$
 $d(d[B]/dt)/d[MINOR] = -\frac{1}{2} \cdot k_4 \cdot [A] \cdot [B] \cdot 1/\text{root}[MINOR]$
 $d(d[MAJOR]/dt)/d[A] = +k_1 \cdot [B] + k_3 \cdot [B] \cdot [MAJOR]^{0.8}$
 $d(d[MAJOR]/dt)/d[B] = +k_1 \cdot [A] + k_3 \cdot [A] \cdot [MAJOR]^{0.8}$
 $d(d[MAJOR]/dt)/d[MAJOR] = +0.7500 \cdot k_3 \cdot [A] \cdot [B] \cdot [MAJOR]^{-.3}$
 $d(d[MINOR]/dt)/d[A] = +k_2 \cdot [B] + k_4 \cdot [B] \cdot \text{root}[MINOR]$
 $d(d[MINOR]/dt)/d[B] = +k_2 \cdot [A] + k_4 \cdot [A] \cdot \text{root}[MINOR]$
 $d(d[MINOR]/dt)/d[MINOR] = +\frac{1}{2} \cdot k_4 \cdot [A] \cdot [B] \cdot 1/\text{root}[MINOR]$

CONST (1,1.09e-4,0,1,1)

CONST (2,2.72e-5,0,1,1)

CONST (3,1e-3,1,1,100)

CONST (4,1e-3,2,1,100)

ASSIGN (obs,major = major)

ASSIGN (obs,minor = minor)

ASSIGN (spec,a = #25e-3)

ASSIGN (spec,b = #25e-3)

CHOOSE (expl)

DIM (2)

INTEG (stiff)

PLOT ()

SIMPLEX (plot)

k1_____ k2_____ R.M.S. [%]

initial values:

+ .10E-02 + .10E-02 +112.5327

+ .12E-02 + .10E-02 +112.5327

+ .13E-02 + .60E-03 +112.2597

+ .18E-02 + .40E-03 +111.4459

+ .22E-02 + .50E-03 +110.7093

+ .33E-02 + .15E-03 +108.6061

```

+ .47E-02 + .18E-03 +105.8788
+ .76E-02 + .51E-03 + 99.8596
+ .12E-01 + .73E-03 + 90.0933
+ .20E-01 + .15E-02 + 70.5570
+ .32E-01 + .23E-02 + 39.1480
+ .55E-01 + .43E-02 + 7.4482

```

Minmax constraint was active.

SIMPLEX (plot)

```

k1_____ k2_____ R.M.S. [%]
initial values:
+ .55E-01 + .43E-02 + 7.4482

```

```

+ .55E-01 + .43E-02 + 7.4482
+ .55E-01 + .43E-02 + 7.4482
+ .55E-01 + .43E-02 + 7.4482
+ .55E-01 + .43E-02 + 7.4482
+ .51E-01 + .34E-02 + 3.1006
+ .51E-01 + .34E-02 + 3.1006
+ .51E-01 + .34E-02 + 3.1006
+ .51E-01 + .34E-02 + 3.1006
+ .51E-01 + .34E-02 + 3.1006
+ .51E-01 + .34E-02 + 3.1006
+ .51E-01 + .34E-02 + 3.1006
+ .51E-01 + .36E-02 + 3.0762

```

NEWTON (plot)

```

k1_____ k2_____ R.M.S. [%]
Initial values:-----
5.06E-02 3.56E-03 3.0762
± .00E+01 ± .00E+01

```

```

-----
5.04E-02 3.45E-03 3.0295
± .16E-03 ± .52E-04

```

```

5.04E-02 3.45E-03 3.0295
± .16E-03 ± .53E-04

```

```

5.04E-02 3.45E-03 3.0295
± .16E-03 ± .53E-04

```

sum errors = + .1496E-05

Covariance Matrix:

```

1.00E+00 6.46E-01
6.46E-01 1.00E+00

```

8.2 Appendix 2

Table 8.1 The percentage completion values for the recognition-mediated reactions between all the nitrones and maleimide **77**. The values presented are the relative percentages at 1000 minutes.

	Percentage completion at 1000 minutes
3-Nitron 104	66 %
3-Bromo nitron 109	51 %
3-Chloro nitron 110	43 %
3-Methyl nitron 110	63 %
3- <i>tert</i> -Butyl nitron 112	54 %
4-Nitron 113	76 %
4-Bromo nitron 114	71 %
4-Chloro nitron 115	66 %
4-Methyl nitron 116	73 %
4- <i>tert</i> -Butyl nitron 117	54 %

Table 8.2 The d.e. values for the reactions between the nitrones and maleimide **77**, maleimide ester **79** and the addition of 10 mol%. The differences in d.e. are calculated relative to the bimolecular control reaction in both cases. All the data presented are the relative values at 1000 minutes.

	d.e. of bimolecular control reaction (+ 79)	d.e. of recognition-mediated reaction (+ 77)	Δ d.e.	d.e. with template (+ 77 +10mol% template)	Δ d.e.
3-Nitron 104	67 %	69 %	2 %	76 %	9 %
3-Bromo nitron 109	50 %	61 %	11 %	56 %	6 %
3-Chloro nitron 110	53 %	64 %	11 %	68 %	15 %
3-Methyl nitron 111	63 %	65 %	2 %	67 %	4 %
3- <i>tert</i> -Butyl nitron 112	50 %	78 %	28 %	66 %	16 %
4-Nitron 113	64 %	85 %	21 %	89 %	25 %
4-Bromo nitron 114	60 %	79 %	19 %	86 %	26 %
4-Chloro nitron 115	60 %	86 %	26 %	86 %	26 %
4-Methyl nitron 116	59 %	86 %	27 %	89 %	30 %
4- <i>tert</i> -Butyl nitron 117	55 %	78 %	23 %	85 %	30 %